



UNIVERSITAT DE
BARCELONA

Nitrate salt-based nanofluids for thermal energy storage

Adela Svobodova

ADVERTIMENT. La consulta d'aquesta tesi queda condicionada a l'acceptació de les següents condicions d'ús: La difusió d'aquesta tesi per mitjà del servei TDX (www.tdx.cat) i a través del Dipòsit Digital de la UB (diposit.ub.edu) ha estat autoritzada pels titulars dels drets de propietat intel·lectual únicament per a usos privats emmarcats en activitats d'investigació i docència. No s'autoritza la seva reproducció amb finalitats de lucre ni la seva difusió i posada a disposició des d'un lloc aliè al servei TDX ni al Dipòsit Digital de la UB. No s'autoritza la presentació del seu contingut en una finestra o marc aliè a TDX o al Dipòsit Digital de la UB (framing). Aquesta reserva de drets afecta tant al resum de presentació de la tesi com als seus continguts. En la utilització o cita de parts de la tesi és obligat indicar el nom de la persona autora.

ADVERTENCIA. La consulta de esta tesis queda condicionada a la aceptación de las siguientes condiciones de uso: La difusión de esta tesis por medio del servicio TDR (www.tdx.cat) y a través del Repositorio Digital de la UB (diposit.ub.edu) ha sido autorizada por los titulares de los derechos de propiedad intelectual únicamente para usos privados enmarcados en actividades de investigación y docencia. No se autoriza su reproducción con finalidades de lucro ni su difusión y puesta a disposición desde un sitio ajeno al servicio TDR o al Repositorio Digital de la UB. No se autoriza la presentación de su contenido en una ventana o marco ajeno a TDR o al Repositorio Digital de la UB (framing). Esta reserva de derechos afecta tanto al resumen de presentación de la tesis como a sus contenidos. En la utilización o cita de partes de la tesis es obligado indicar el nombre de la persona autora.

WARNING. On having consulted this thesis you're accepting the following use conditions: Spreading this thesis by the TDX (www.tdx.cat) service and by the UB Digital Repository (diposit.ub.edu) has been authorized by the titular of the intellectual property rights only for private uses placed in investigation and teaching activities. Reproduction with lucrative aims is not authorized nor its spreading and availability from a site foreign to the TDX service or to the UB Digital Repository. Introducing its content in a window or frame foreign to the TDX service or to the UB Digital Repository is not authorized (framing). Those rights affect to the presentation summary of the thesis as well as to its contents. In the using or citation of parts of the thesis it's obliged to indicate the name of the author.



Nitrate salt-based nanofluids for thermal energy storage

Adela Svobodova Sedlackova
PhD Thesis



UNIVERSITAT DE
BARCELONA

Nitrate salt-based nanofluids for thermal energy storage

Author

Adela Svobodova Sedlackova



**UNIVERSITAT DE
BARCELONA**

Materials Science and Physical Chemistry Department

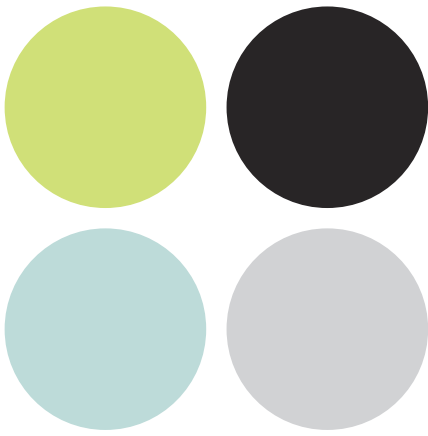
UNIVERSITAT DE BARCELONA

A dissertation submitted to the University of Barcelona in accordance with the requirements of the degree of Doctor of Philosophy in Engineering and Applied Sciences program

Supervisors

**Dra. A. Inés Fernández Renna
Dr. Pablo Gamallo Belmonte**

2022



Why this PhD thesis?

Motivation

Since I was a child, I have admired the advances in science, and I have wondered how we have come to achieve them. The first time I felt that feeling was when I was seven years old, discovering the blades of an imposing wind turbine through the rear window of a car. Since then, that curiosity about human ingenuity and renewable energies has not stopped growing. This curiosity led me to show that there is still much to be done and that this thesis is a small contribution to be part of an enormous milestone. I would like to let it be more significant than a career or an individual achievement. Perhaps that is the secret of my work, wanting to be part of something bigger than me.

Acknowledgements

Agradecimientos

Siempre he creído que para llegar lejos es necesario estar bien acompañado. Y si he llegado hasta aquí ha sido gracias al talento, el ánimo y la dedicación de muchas personas que me han ayudado. Este camino no lo hubiese podido hacer sin todos ellos y ahora que estoy al final de esta tesis doctoral me gustaría empezar agradeciendo:

A los profesores que tuve en mi educación primaria y secundaria, en especial, a la profesora Teresa Llorens, y a los profesores Jaume Puig y Juan Antonio Torres, gracias a los cuales aprendí a pensar y descubrí mi motivación por la ciencia.

A la Dra. Inés Fernández y al Dr. Pablo Gamallo, porque han confiado en mí desde el principio. Por todo el tiempo que me han dedicado, por transmitirme toda su experiencia sin limitar mi creatividad. Por ser un referente y no únicamente en lo profesional sino también en lo personal.

A la Dra. Camila Barreneche, que ha sido como una directora más en mi tesis; por estar siempre dispuesta a ayudarme y darme ese plus de motivación cuando más lo necesitaba. Al Dr. Alejandro por su generosidad, por sus consejos, y por esas largas conversaciones llenas de ideas, divagaciones y mucho humor.

A mis compañeros y amigos: Sergio, Pol y Alex. Por nuestras aventuras, las que hemos vivido y las que están por llegar, porque sin vosotros esto no habría sido lo mismo.

A todos los compañeros de laboratorio por apoyarme y hacer el día a día más fácil: Rebeca, Jofre, Joana, Jaume, Marc, Anna. Y a todos los que se han incorporado recientemente, pero que de igual manera forman un grupo increíble: Eli, JJ, Naiara, Adrià, Quim, Marc, Alejandro, Carla y Camilo. Gracias por hacer que venir a trabajar sea más ameno y divertido. En especial, gracias a Rebeca, por estar siempre allí. Y también sin olvidarme, gracias a Gerard y Héctor por su ayuda.

Quiero agradecer a todo el grupo DIOPMA, cuyos profesores ahora son mis compañeros. Gracias por todo lo que he podido aprender de vosotros y con vosotros, es un gran placer haberme podido rodear con TODOS y cada uno de vosotros; Dr. J.M. Chimenos, Dr. Mònica Martínez, Dr. Mercè Segarra, Dra. Elena Xurriquerria, Dr. Joan Formosa, Dra. Jessica Giró, Dr. J.A. Padilla y Esther Galindo. Gracias por todos estos años, por vuestra ayuda y empatía.

También quería acordarme del grupo de solar del IREC donde descubrí la pasión por la investigación y cómo enfrentarme a la investigación. Y por supuesto, quería agradecer al Dr. Xavier Alcobé por toda la dedicación, confianza y por todo el conocimiento que me ha transmitido.

Y seguramente me deje a alguien. Pues a ti también.

Y finalmente, a mi familia y amigos por haber estado conmigo no solo ahora sino desde mucho antes. Sobre todo, a mi familia porque vuestro apoyo y cariño son infinitos. Y gracias, Dani, por confiar en mí y apoyarme en todo momento.

Sin todos vosotros no hubiese sido posible,

Gracias de corazón.

Abstract

For the development of more compact and efficient thermal systems, nanofluids are presented as a promising option to replace conventional heat transfer fluids. Nanofluids are a suspension of low concentration of nanoparticles (1-100 nm) in a liquid medium. Since nanofluids' discovery in 1995, a veritable science has been created around this concept with an infinity of new applications such as electronics, biomedicine, machining, and renewable energies. The scientific interest in nanofluids is due to the improvement of the base fluid's thermophysical and chemical properties. One of the phenomena that have attracted the interest of the scientific community is the anomalous variation in heat capacity, with increases of up to 40% in different liquid media such as water, thermal oils, paraffin, or molten salt. However, despite many efforts and significant advances, there is still no robust theoretical framework that explains the observed phenomena. Therefore, there is a lack of understanding of the behaviour of nanofluids and their properties.

Among the different types of heat transfer fluids, molten salt-based nanofluids (MSBNFs) show exceptional properties with the incorporation of nanoparticles. For this reason, one of the potential applications is in thermal storage systems (TES) for concentrated solar power plants (CSP) that use nitrate salts (eutectic mixture of NaNO_3 (60%)- KNO_3 (40%)) as a TES medium and heat transfer fluid (HTF). MSBNFs with higher energy density than conventional salts would allow the design of more compact TES systems and therefore improve the overall efficiency of CSP plants and reduce their Levelized Cost of Energy (LCOE). Economically competitive CSP technology is essential for the energy transition and solving renewable energy intermittency by storing solar energy during the day and dispatching it at night. In addition, these plants are an ideal complement to PV technology, resolving the imbalance between

maximum demand and renewable production. However, for the scalability of nanofluids to higher Technology Readiness Level (TRLs), many scientific and economical barriers still must be overcome.

In this thesis, through a review of the state-of-the-art and a bibliometric study, this field of research's social and scientific impact has been shown, identifying the main limitations and obstacles that the scientific community is subjected to. Throughout the chapters, answers to each of the key points that limit the development of nanofluids and especially nanofluids based on nitrate salts, are given from a computational, statistical and experimental point of view.

The main result of the thesis is the identification of the main mechanisms involved in the variation of the heat capacity that respond to the contradictory results of the literature. It has been determined that nanofluids based on nitrate salts behave as a biphasic system due to the formation of nanostructures with a high specific area around the surfaces of the nanoparticles, demonstrating the layering phenomenon observed computationally. Furthermore, the formation of the nanostructured phase with a heat capacity higher than 100% with respect to the nitrate salt is very susceptible to the concentration and dispersion of the nanoparticles. Therefore, these variables play a fundamental role in the value of the heat capacity of the system, where slight variations have a significant impact on the variation of C_p .

Additionally, the last chapter of this thesis shows the potential of the Small Angle X-ray Scattering (SAXS) technique to characterize nanofluids as a function of temperature, offering relevant structural information to understand their thermal behaviour.

Finally, without pointing out the final application, this thesis shows the potential of nitrate salt-based nanofluids as a TES medium for improving thermal efficiency and the possible reduction of the volume of storage tanks, consequently reducing storage costs.

Resumen

Para el desarrollo de sistemas térmicos más compactos y eficientes los nanofluidos se presentan como una opción prometedora para la sustitución de los fluidos de transferencia térmica convencionales. Los nanofluidos son una suspensión de nanopartículas de 1-100 nm en bajas concentraciones en un medio líquido. Desde su descubrimiento en 1995, se ha creado una verdadera ciencia entorno a este concepto y se han abierto las puertas a un gran número de nuevas aplicaciones en electrónica, bio-medicina, mecanizado y en energías renovables, entre otras. El interés científico de los nanofluidos se debe a la mejora de las propiedades tanto termo-físicas como químicas del fluido base. Uno de los fenómenos que más han llamado la atención a la comunidad científica es la variación anómala de la capacidad calorífica, con incrementos de hasta el 40% en diferentes medios líquidos como el agua, aceites térmicos, parafinas o sales fundidas. A pesar de muchos esfuerzos y grandes avances, todavía no existe un marco teórico robusto que dé explicación a los fenómenos observados y, por tanto, hay una falta de comprensión del comportamiento de los nanofluidos y sus propiedades.

Entre los diferentes tipos de fluidos de transferencia térmica, los nanofluidos basados en sales fundidas (MSBNFs) muestran unas propiedades excepcionales con la incorporación de nanopartículas. Es por ello, que una de las aplicaciones de mayor potencial son los sistemas de almacenamiento térmico (TES) para plantas de concentración solar (CSP) que emplean sales de nitrato (mezcla eutéctica de NaNO_3 (60%)- KNO_3 (40%)) como fluido TES. Los MSBNFs con una mayor densidad energética que las sales convencionales permitirían diseñar sistemas TES más compactos y con ello, mejorar la eficiencia general de las plantas CSP y reducir su Coste Nivelado de Energía (LCOE de sus ingles en inglés). Tecnología CSP económicamente más competitiva es imprescindible para la transición energética y solventar la intermitencia de las energías renovables

almacenando energía solar durante el día y despachando durante la noche. Además, estas centrales son un complemento ideal de la tecnología PV solventando el desequilibrio entre la demanda máxima y la producción de renovables. Pero para la escalabilidad de los nanofluidos a mayores Niveles de Preparación Tecnológica (TRLs de sus siglas en inglés) todavía se han de solventar números obstáculos científicos como barreras económicas.

En esta tesis mediante una revisión del estado-del-arte y mediante un estudio bibliométrico de la literatura se ha mostrado el impacto tanto social como científico de este campo de investigación identificándose las principales limitaciones y obstáculos a los que se ve sometida la comunidad científica. A lo largo de los capítulos se van dando respuesta desde un punto de vista tanto computacional, como estadístico y experimental, a cada uno de los puntos clave que limitan el desarrollo de los nanofluidos y especialmente de los nanofluidos basados en sales de nitrato.

El principal resultado de la tesis es la identificación de los principales mecanismos involucrados en la variación de la capacidad calorífica que dan respuesta a los resultados contradictorios de la literatura. Se ha determinado que los nanofluidos basados en sales de nitrato se comportan como un sistema bifásico debido a la formación de nanoestructuras de alta área específica alrededor de las superficies de las nanopartículas, demostrando experimentalmente el fenómeno de formación de una capa (*layering phenomenon*) observado computacionalmente. La formación de la fase nanoestructurada con una capacidad calorífica superior al 100% respecto a la sal de nitrato es muy susceptible a la concentración y dispersión de las nanopartículas. Por tanto, estas variables juegan un papel fundamental en el valor de la capacidad calorífica del sistema, donde pequeñas variaciones tienen un gran impacto en la variación de la C_p .

Adicionalmente, el último capítulo de esta tesis muestra el potencial de la técnica de Dispersión de rayos-X de Ángulo Pequeño (SAXS de sus siglas en inglés) para caracterizar nanofluidos en función de la temperatura ofreciendo información estructural relevante para comprender su comportamiento térmico.

Finalmente, sin perder de vista la aplicación final, esta tesis muestra el potencial del uso de nanofluidos basados en sales de nitrato como medio TES, para la mejora de la eficiencia térmica, la posible disminución del volumen de los tanques de almacenamiento y consecuentemente, la reducción de los costes de almacenamiento.

Table of contents

Glossary.....	vi
List of Figures.....	ix
List of Tables.....	xv
Chapter 1	1
1 Preface.....	3
1.1 From the beginning of scientific thinking to a new era: nanoscience	3
1.2 Revolutions and climate change.....	4
1.2.1 Climate change in the last decades.....	7
1.3 Kaya Identity.....	9
1.4 Climate change mitigation	10
1.4.1 Share of renewable energy in final energy consumption.....	10
1.5 Thermal energy storage, the key to decarbonisation.....	11
1.6 Concentrated Solar Power Plants: future Trends.....	13
Chapter 2	17
2 Introduction to nanofluids state-of-the-art.....	19
2.1 Nanofluid concept.....	19
2.2 Introduction to nanofluids.....	20
2.2.1 Types of nanofluids.....	22
2.2.2 Properties	24
2.2.3 Factors influencing the thermophysical properties of nanofluids.....	30

2.2.4	Preparation of nanofluids	31
2.2.5	Applications	35
2.3	Challenges and limitations	35
Chapter 3		37
3	Objectives	39
Chapter 4		41
4	Thesis structure	42
Chapter 5		45
5	Nanofluids for TES	46
5.1	Introduction.....	46
5.2	CSP technology and TES systems: an overview	46
5.2.1	Materials TES requirements.....	55
5.3	Molten salt-based nanofluids: state-of-the art	56
5.4	Nanofluids specific heat capacity	63
5.4.1	Theoretical framework.....	63
5.5	Challenges and limitations: key points.....	68
Chapter 6		73
6	Past, actual and future trends of nanofluids research	74
6.1	Introduction.....	74
6.1.1	Relevance	75
6.1.2	Objectives	76
6.2	Paper 1	77
6.2.1	Graphical Abstract.....	78
6.2.2	Contribution to the state-of-the-art	79
6.2.3	Publication	81
6.3	A Particular Case – Nanofluids for Energy Systems.....	120
6.3.1	Heat transfer and thermal storage materials	124

6.3.2	Nanofluids synthesis, characterization, and modelling.....	127
6.3.3	European Union Research	129
Chapter 7		133
7	Statistical approach to nanofluids.....	134
7.1	Introduction.....	134
7.1.1	Relevance.....	135
7.1.2	Objectives	135
7.2	Paper 2	136
7.2.1	Graphical abstract	137
7.2.2	Contribution to the state-of-the-art	138
7.2.3	Publication	139
7.3	Paper 3	176
7.3.1	Graphical Abstract.....	177
7.3.2	Contribution to the state-of-the-art	178
7.3.3	Publication	179
Chapter 8		193
8	Computational approach to nitrate salt-based nanofluids.....	194
8.1	Introduction.....	194
8.1.1	Relevance.....	195
8.1.2	Objectives	196
8.2	Paper 4	197
8.2.1	Graphical Abstract.....	198
8.2.2	Contribution to the state of the art.....	199
8.2.3	Publication	202
Chapter 9		215
9	Abnormal specific heat capacity in nitrate salt-based nanofluids	216
9.1	Introduction.....	216
9.1.1	Relevance.....	217

9.1.2	Objectives	218
9.2	Paper 5	219
9.2.1	Graphical Abstract.....	220
9.2.2	Contribution to the state of the art	221
9.2.3	Publication	225
Chapter 10		236
10	Thermal stability of nitrate sant-based nanofluids	238
10.1	Introduction.....	238
10.1.1	Relevance	239
10.1.2	Objectives.....	239
10.2	Paper 6	240
10.2.1	Graphical Abstract	241
10.2.2	Contribution to the state of the art.....	242
10.2.3	Publication	243
Chapter 11		262
11	New approach to nanofluids characterization.....	264
11.1	Introduction.....	264
11.1.1	Relevance	265
11.1.2	Objectives.....	265
11.2	What is SAXS?	265
11.3	Small angle X-ray scattering (SAXS/WAXS) experiments on a PANalytical X'Pert PRO MPD θ/θ	267
11.3.1	PANalytical X'Pert PRO MPD θ/θ characteristics.....	268
11.3.2	SAXS geometry.....	268
11.3.3	SAXS measurements validation	272
11.3.4	Conclusions	280
11.4	SAXS for MSBNFs characterization.....	281
11.4.1	Methodology and samples preparation	282
11.4.2	Results.....	282

11.4.3	Contribution to the state of the art.....	286
Chapter 12.....		288
12	Results summary	289
Chapter 13.....		292
13	Conclusions and future work	294
13.1	General conclusions.....	294
13.2	Future work	296
References		300
A1	Appendix 1	334
A1.1	Database values	334
A2	Appendix 2	338
A2.1	MD simulations – LAMMPS codes.....	338
A3	Appendix 3	342
A2.1	Contributions in conferences.....	342
A2.2	Contributions in training schools.....	347
A2.3	Contribution in WorkShops	349
A2.4	Participation in COST Action	350
A2.5	International collaborations	351
A2.6	Other publications derived from the PhD thesis.....	352

Glossary

A

ASNSS Arc spray nanofluid system

C

CO₂ Carbon Dioxide

CO₂/E Carbon intensity of the global energy mix

CSP Concentrating solar power

D

DMT Dual-media thermocline

DSC Differential scanning calorimetry

E

E Global primary energy consumption

E/GDP Energy intensity

EDS Energy dispersive x-ray spectroscopy

EEW Electrical explosion of wire

F

FF Force field

FTIR Fourier transform infrared



GA Gum Arabic

— **GDP** Gross domestic product

GHG Greenhouse gas



— **HITEC** High temperature eutectic

HTF Heat transfer fluid



— **IEP** Isoelectric point

IPCC Intergovernmental Panel on Climate Change



— **LCOE** Levelized cost of energy (US\$/kWh)

LFR Linear Fresnel Reflector



MENA Middle East and North Africa countries

— **MD** Molecular dynamics

MMT Montmorillonite







MSBNF Molten salt-based



NF Nanofluid

— **NMSBNF** Nitrate salt-based nanofluid

NP Nanoparticle

P Population		
PCM Phase change material		
PDS Parabolic Dish System		
PR Performance ratio		
Pr Productivity	—	
PTSC Parabolic Trough Solar Collectors		
PV Photovoltaic		
PVT Photovoltaic thermal		
R Repetition		
R&D research and development	—	
S Sample		
S/V Surface-to-volume ratio		
SANSS Submerged arc nanofluid system		
SAXS Small angle x-ray scattering		
SDBS Sodium dodecylbenzene sulfonate		
SDS Sodium dodecyl sulfate		
SEM Scanning electron microscope	—	
SHS Sensible heat storage		
SJR Scimago Journal & Country rank		
SMT Single medium thermocline		
SPT Solar Power Tower		
SS Solar salt		
SSBNF Solar salt-based nanofluid		
ST Shell-and -tube		
T Temperature	—	
TES Thermal energy storage		
TGA Thermogravimetric analysis		
TOE Tons of Oil Equivalent		
UV-vis Ultraviolet–visible spectroscopy	—	
XRD X-Ray powder Diffraction	—	

List of figures

Figure 1.1. Timeline of scientific knowledge evolution.	5
Figure 1.2. Timeline of climate change related events.	6
Figure 1.3. Earth's gradient of temperatures (warming stripes) from 1850 to 2020	7
Figure 1.4. a) Evolution of the temperature increase on Earth from 1850 to 2021, and b) prediction of precipitations variation	8
Figure 1.5. Atmospheric CO ₂ concentration evolution from 1960 to 2020 . The red line represents the monthly mean value and the black line represents the monthly mean value of the average seasonal cycle.	8
Figure 1.6. The estimated renewable share in the total final energy consumption, at 2009 and 2019.....	12
Figure 1.7. CSP projects status and total capacity per country; operational, under construction and in development around the world.	14
Figure 2.1. A brief timeline of some of the most relevant discoveries about	20
Figure 2.2. Nanofluids classification as a function of nanoparticles and base fluids.	23
Figure 2.3. Schematic representation of the main factors influencing nanofluids' thermophysical properties.	31
Figure 2.4. Schematic simplified diagram of the two main techniques for preparing ionic-nanofluids by one-step (top) and two-step (bottom) methods.	32

Figure 2.5. Summary of advantages and drawbacks of nanofluids preparation methods.....	33
Figure 2.6. Main techniques employed in the one-step method and two-step methods to produce nanofluids.....	34
Figure 4.1. PhD thesis structure.	43
Figure 5.1. Leading available technologies; a) thermo-solar technologies, and b)thermal energy storage technologies.....	47
Figure 5.2. TES materials requirements for CSP.....	55
Figure 5.3. Top-5 of the main authors, countries, journals, funding’s agencies and research areas involved in MSBNFs research.	58
Figure 5.4. Molten salts-based nanofluids’ main research topics and current state, challenges, and limitations	59
Figure 6.1. Article accepted for publication entitled “A Bibliometric Analysis of Research and Development of Nanofluids” in the Journal of Nanofluids by American Scientific Publishers.	77
Figure 6.2. Graphical abstract of the article “A Bibliometric Analysis of Research and Development of Nanofluids”	78
Figure 6.3. Number of publications and citations related to nanofluids for energy systems applications from 2010 to 2019.....	120
Figure 6.4. a) Top 10 countries/regions with the highest number of publications related to nanofluids application topic in the last decade. b) Number of publications per year for the top 10 countries/regions.....	121
Figure 6.5. Top 15 authors with the highest number of citations on nanofluids application topic.....	123
Figure 6.6. Top 20 countries with the highest number of publications on nanofluids application topic and the collaborations among them.	124
Figure 6.7. Top 10 countries/regions with the highest number of publications on nanofluids application topic as a) heat transfer fluid and b) thermal energy storage medium.	125

Figure 6.8. Top 10 countries/regions with the highest number of publications over the last decade on nanofluids application topic as a) HTF and b) TES materials.....	126
Figure 6.9. Top 10 countries/regions with the highest number of publications in the last 20 years on a) characterization, b) synthesis and c) modelling of nanofluids.	128
Figure 6.10. European Union Nanofluids research were p. = number of publications, PR = performance ratio (num. cites/num. articles), r. = number of researchers, and Pr. = productivity (num. authors/num. articles), at the end of 2020.	130
Figure 7.1. Submitted article entitled “Using statistical analysis to create a new database of Nanofluids specific heat capacity”	136
Figure 7.2. Graphical abstract of the submitted article: “Using statistical analysis to create a new database of Nanofluids’ specific heat capacity”	137
Figure 7.3. Specific Heat capacity variation (%) as a function of the concentration/size quotient (l_c/s index) classified as fluid base family.	139
Figure 7.4. Article published in the Journal of Molecular liquids in 2022, entitled “Novel sampling procedure and statistical analysis for the thermal characterization of ionic nanofluids”	176
Figure 7.5. Graphical abstract of the article entitled “Novel Sampling procedure and statistical analysis for the thermal characterization of ionic nanofluids”	177
Figure 7.6. Specific heat capacity variation (%) as a function of temperature from nitrate salt-based nanofluids with, a) SiO_2 nanoparticles, b) Al_2O_3 nanoparticles, and c) MMT nanoparticles.	179
Figure 7.7. Measurement’s recommendations of thermophysical properties for ionic-nanofluids.....	179
Figure 8.1. Article published in the Renewable Energy journal in 2020, entitled “Effect of nanoparticles in molten salts- MD simulations and experimental study”	197

Figure 8.2. Graphical abstract of the article entitled “Effect of nanoparticles in molten salts- MD simulations and experimental study”	198
Figure 8.3. Scheme of the effect of nanoparticle concentrations and size on nanofluids specific heat capacity.....	199
Figure 8.4. Specific heat capacity variation as a function of nanoparticles concentration, obtained from MD simulations and DSC.....	200
Figure 8.5. Specific heat capacity variation as a function of nanoparticles concentration for flexible and rigid nanoparticles.	201
Figure 8.6. Radial pair distribution of Na-O atoms (O from the nanoparticle surface) at 293 K, 598 K, and 773 K.....	201
Figure 9.1. Article published in the Scientific Reports journal in 2021, entitled “Understanding the abnormal thermal behaviour of nanofluids through Infrared thermography and thermophysical characterization”[2].	219
Figure 9.2. Graphical Abstract of the article entitled “Understanding the abnormal thermal behaviour of nanofluids through Infrared thermography and thermos-physical characterization”	220
Figure 9.3. Infrared thermography’s during the heating process of the nanofluid sample, NF (left, $\text{NaNO}_3 + 1 \text{ wt}\% \text{ SiO}_2$) and the fluid sample (right, NaNO_3).....	222
Figure 9.4. Specific heat capacity of Foamy-like white semisolid layer on top of NF sample and schematic representation of nanofluid phases and interphases.....	223
Figure 10.1. Article accepted in nanomaterials journal (MPDI), entitled “Effect of nanoparticles on the thermal stability and reaction kinetics in ionic nanofluids”	240
Figure 10.2. Graphical Abstract of the article entitled “Effect of nanoparticles on the thermal stability and reaction kinetic of nitrate molten salt-based nanofluids”	241
Figure 10.3. Nitrite concentration as a function of temperature for pure NaNO_3 and Nitrate-based nanofluids with 1 wt% of SiO_2 and Al_2O_3 nanoparticles.....	242

Figure 10.4. TGA measurement from 100 to 900°C of NaNO ₃ , and NaNO ₃ /SiO ₂ , NaNO ₃ /Al ₂ O ₃ NFs with 1 wt% of NPs: a) weight loss as a function of temperature and, b) weight derivative as a function of time.....	243
Figure 11.1. X-Ray beam in SAXS configuration.....	266
Figure 11.2. Guinier and Porod Plot.....	267
Figure 11.3. PANalytical X’Pert PRO MPD configurationsa) Bragg-Brentano geometry (reflection geometry), b) transmission geometry with capillary sample holder, and c) transmission geometry with flat transparent sample holder.	269
Figure 11.4. PANalytical X’Pert PRO MPD q / q ₀ with parallel optics configuration.....	271
Figure 11.5. EasySaxs results for ZnO 41075, TiO ₂ 41508, and TiO ₂ 11210 patterns.....	274
Figure 11.6. Phase and microstructural fit of ZnO 41075 pattern.	275
Figure 11.7. Phase and microstructural fit of TiO ₂ 41508 pattern.	276
Figure 11.8. Phase and microstructural fit of TiO ₂ 11210 pattern.	277
Figure 11.9. TEM images.....	278
Figure 11.10. NSBNF-1 wt% SiO ₂ nanoparticles scattering curves as a function of temperature.	283
Figure 11.11. Nanoparticles form factor.	284
Figure 11.12. Radial distribution per volume at a function of temperature and surface-to-volume values of NMSBNF- 1wt% SiO ₂ nanoparticles.....	285
Figure 12.1. Results summary.....	290
Figure A3.1. Certificate of oral presentation at Iberian Meeting on Materials Science (CNMAT 2018) and XV Congreso Nacional de Materiales.....	342
Figure A3.2. Certificate of oral presentation at Eurotherm Seminar #112. Advances in Thermal Energy Storage.....	343

Figure A3.3. Certificate of oral presentation at 1st International Conference on Nanofluids (ICNF2019) and 2nd European Symposium on Nanofluids (ESNF2019)..... 344

Figure A3.4. Certificate of oral presentation at Enerstock 2021. 15th International Virtual Conference on Energy Storage..... 345

Figure A3.5. Certificate of oral presentation at 3rd European Symposium on Nanofluids (ESNF) in the frame of COST CIG action NanoConvex..... 346

Figure A3.6. Certificate of oral poster presentation at the SolarPACES 2021. the online conferences on Concentrating Solar Power and Chemical Energy Systems..... 347

Figure A3.7. Certificate of oral presentation at the Computational Modeling of Materials school. 347

Figure A3.8. Certificate of participation in the Materials for thermal energy storage- Materials selection, optimization & characterization school..... 348

Figure A3.9. Graphical abstract of the main results obtained in the Birmingham Centre for Energy Storage..... 352

List of tables

Table 2.1. Some selected studies about nanofluids thermal conductivity for different base fluid/nanoparticle systems.....	25
Table 2.2. Some selected studies about nanofluids viscosity for different base fluid/nanoparticles systems.	27
Table 2.3. Some selected studies about nanofluids specific heat capacity for different base fluid/nanoparticles systems.....	28
Table 2.4. Summary of some potential applications of nanofluids reported in the literature in the last years.	36
Table 5.1. CSP projects worldwide with two-tank storage system (last update in February 2022).	49
Table 5.2. CSP projects worldwide with alternative TES systems (last update in February 2022).	53
Table 5.3. Thermophysical properties of sensible heat storage materials (SHS).....	54
Table 5.4. Specific heat capacity of selected molten salt-based nanofluids investigations.	61
Table 5.5. Proposed mathematical models to predict nanofluids specific heat capacity.....	67
Table 6.1. Top 10 authors with the highest number of publications on nanofluids application topic and some quality indexes.....	122
Table 6.2. Top 10 scientific journals with the highest number of publications on nanofluids application topic and some quality indexes, in the last 20 years.	123

Table 6.3. Top 10 authors with the highest number of publications on nanofluids application topic on HTF and some quality indexes, in the last 20 years.....	127
Table 6.4. Top 10 authors with the highest number of publications on nanofluids application topic on TES and some quality indexes, in the last 20 years.....	127
Table 7.1. Statistical data of techniques, methods, and sampling of nanofluids for thermal energy storage.	139
Table 9.1. Structural cell parameters of foamy-like layer, NaNO ₃ -1 wt% SiO ₂ nanofluid and pure NaNO ₃ after thermal treatment of 500°C.	225
Table 11.1. Patterns Average particles size (nm) and form.....	277
Table 11.2. SAXS patterns BET analysis.	279
Table 11.3. Patterns characterization results summary by BET, SAXS, TEM, Rietveld, and PANalytical references values.	279
Table 11.4. Summary of published articles about nanofluids characterization by SAXS technique.	281

From scientific
revolution to
renewable energies

Preface



1. Preface

Voici mon secret: seulement avec le cœur que l'on peut voir à juste titre ce qui est essentiel est invisible pour les yeux. Adapted from Le Petit Prince, Antoine de Saint-Exupéry

1.1 From the beginning of scientific thinking to a new era: nanoscience

The history of the world is told through significant milestones, key events where human progress is reflected: the invention of fire in pre-history, the use of the wheel in ancient times, the creation of the printing press in the medieval age, the steam engine in the modern age or internet in the last decades. The evolution of the human being is marked by great triumphs of thought that bring with them great revolutions. But great revolutions are made of small things, imperceptible events that are a consequence of something bigger. Because

behind a great advance, many attempts, errors, discoveries, or coincidences lead us to success, and all those events help to change the world. When that happens, we recognize them as a revolution, and we mark them as an important event in the calendar. Still, in the evolution of scientific thought, there have been many situations that have gone unnoticed. Imagine one pre-historic tribe that discovered bronze, who thought that there was something better than copper? Or how many materials did they test before you found the suitable alloy? Considering Classical Greece, the cradle of Philosophy, what made them put aside superstition to explain any phenomenon? And if we go a little further, in the

Renaissance, what aroused the curiosity of that generation of inventors, scientists, artists...? Many of these questions do not have easy answers; we can know when Isaac Newton wrote his "Principia Mathematica", but not how many apples had to fall to find the famous gravity's law.

We know all that the history of knowledge has transmitted to us, but not everything that has been hidden in the process. However, thanks to the Scientific Revolution, we began to observe the world more closely. Not only because Zacharias Janssen invented the microscope, but also because modern scientific thinking brought us closer to the way to explain the world. Since the beginning of the 17th century, humanity experienced a period of splendour that continues today. The way of observing the universe, measuring time, controlling energy, and understanding the phenomena surrounding us was revolutionized. We went from a poor and gloomy world to an era of enlightenment where scientific laws were proposed, and the great names of science were born. This development has led us to get closer to the world, to look at it more closely with greater attention. From the creation of the basic sciences to relativity and quantum physics discoveries, we

have come closer to knowledge. As I said, every revolution is made up of units, many times, invisible to the human eye. For this reason, now, at the doors of a new revolution called Nanoscience, it is the best moment to swim deeply into nano-knowledge.

Figure 1.1 shows, in a timeline, some of the most relevant events from the beginning of human thought to the present day with the irruption of nanotechnology.

1.2 Revolutions and climate change

The scientific revolution played a relevant role in giving rise to the industrial revolution of 1760. The industrial revolution supposed first, a change around the world in the social and technological paradigm and second, a large-scale coal consumption. From this point, the world population began to experience unprecedented growth, going from 600 million in 1700 to 990 million in 1800 and reaching 9 billion at the end of 2020. These events led to unprecedented socioeconomic changes that has evolved into the current economic model and consumption habits. But the impact this social change would have on our health and the planet's ecosystems was unknown.

History of Scientific Knowledge

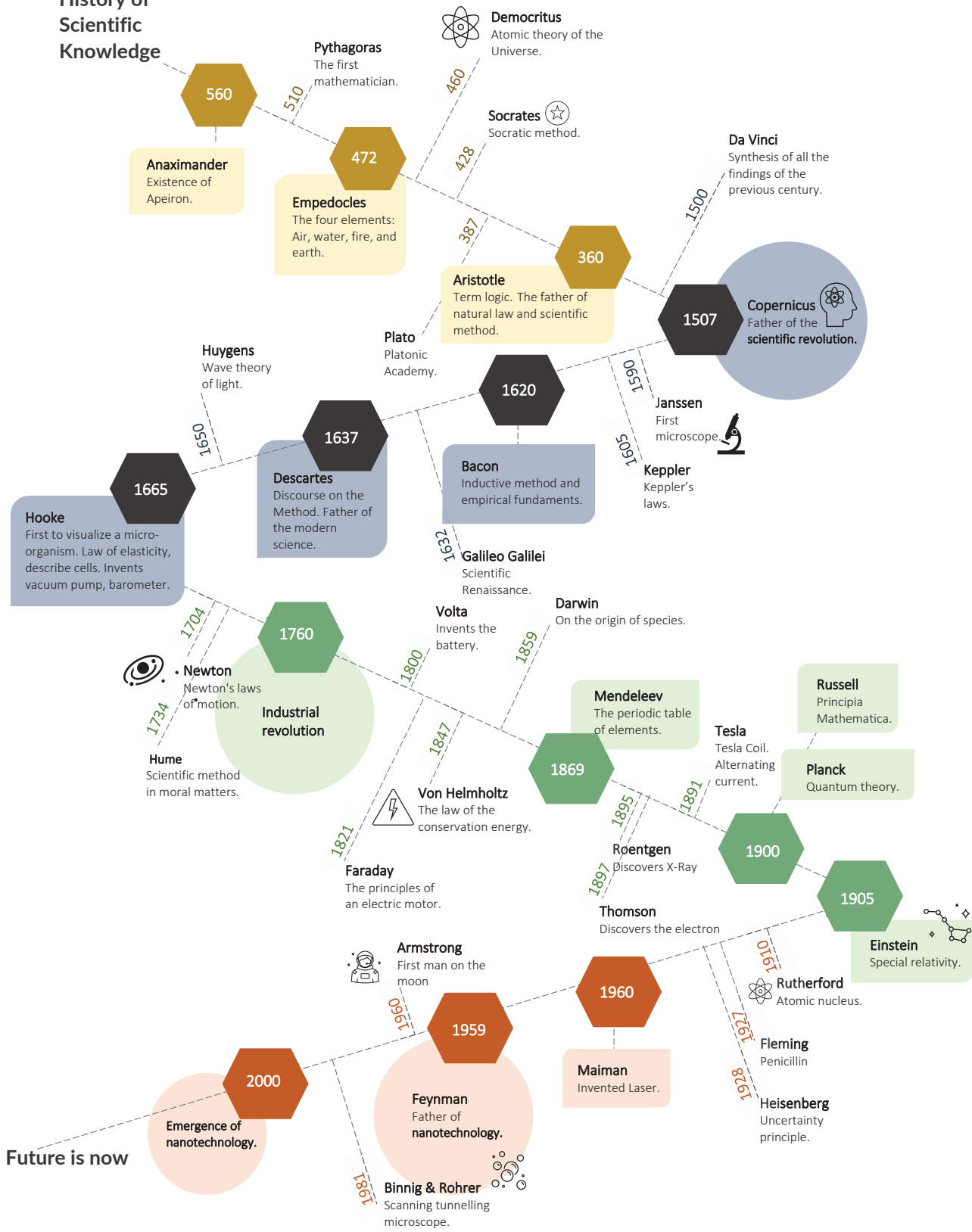


Figure 1.1. Timeline of scientific knowledge evolution.

It was not until the 1960s that these issues began to have a public-political interest when the scientific community began to develop exhaustive studies on the concepts of climate change, greenhouse gases, or global warming, generated mainly by fossil fuels burning. This growing interest was motivated by different pioneering studies that established the bases and the importance of human activity on climate. One of the most relevant studies was carried out by Joseph Fourier in 1824, who studied the phenomena of natural climate change for the first time. Otherwise, the beginning of systematic measurements of atmospheric CO₂ content by David Keeling in 1958 and the creation of the Manua Loa observatory gave for the first time quantifiable human impact on the ecosystem (currently, this observatory is still active, providing reference measurements of the concentrations of greenhouse gases in the Earth's atmosphere)¹. Since then, there has been remarkable progress. **Figure 1.2** briefly summarises in a timeline some of the most relevant events in terms of climate change, up to now, such as the creation of the Intergovernmental Panel on Climate Change (IPCC)² or

the Paris agreement [1]. In the last century, global warming has had a relevant impact on the planet and on our lives due to the increase in greenhouse gases caused by burning fossil fuels.

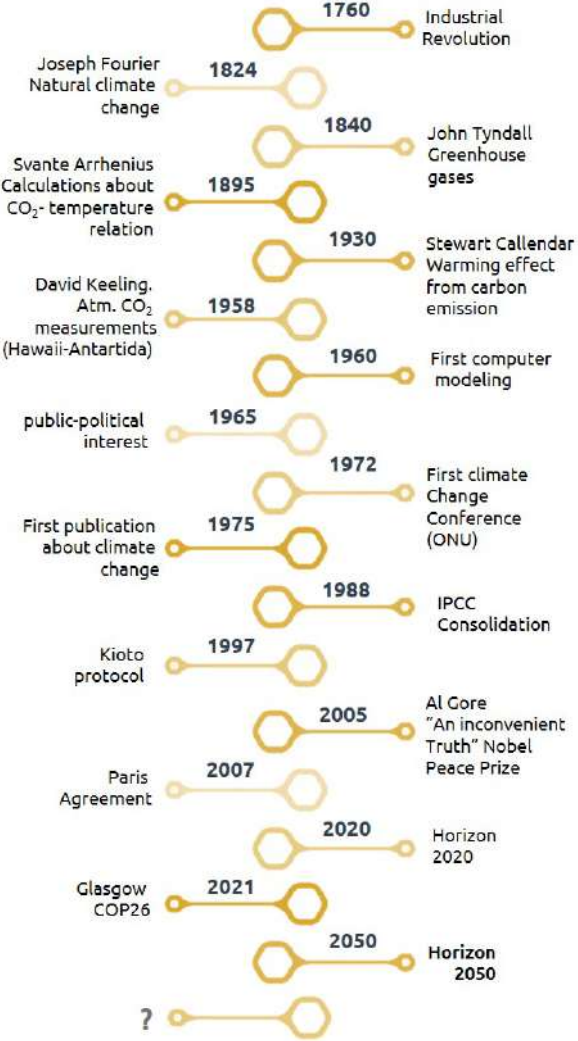


Figure 1.2. Timeline of climate change related events.

¹ Global monitoring Laboratory NOAA (www.gml.noaa.gov).

² IPCC, Intergovernmental Panel on Climate Change (www.ipcc.ch).

Therefore, the scientific community was coined the term "anthropogenic climate change" to differentiate it from the natural climate change. Due to the high impact that human activities are generating on terrestrial ecosystems, the scientific community has proposed a new geological era: **the Anthropocene**.

1.2.1 Climate change in the last decades

*"A picture is worth a thousand words."
Adapted from Henrik Ibsen*



Figure 1.3. Earth's gradient of temperatures (warming stripes) from 1850 to 2020³.

As Henrik Ibsen said, "A picture is worth a thousand words". **Figure 1.3** shows the gradient of the average earth temperature from 1850 to 2020. The redshift observed in the recent years is alarming, reaching an average increment of 1°C on the planet. This value may seem insignificant, but its impact on the Earth is not at all. On the contrary, the average temperature increase has a direct effect on the melting, of the polar caps, with the conse-

quent rise in the sea level and the desertification of the territories, modifying the meteorological phenomena, fauna, vegetation, and therefore human life, as illustrated in **Figure 1.4a-b**. The increase in temperature is mainly due to greenhouse gases in the atmosphere, such as CO₂, which causes the acceleration of climate change, although we cannot forget about CH₄ and H₂O, other species with greenhouse effect even higher than CO₂. The rise in pollution due to human activity, especially by hydrocarbons consumption (coal, oil and gas) has gener-

ated this unprecedented climatic scenario. **Figure 1.5** shows the atmospheric CO₂ concentration (ppm) from the Mauna Loa observatory (Hawaii) from 1960 up to 2020¹. The increase of over 21.5% in the last 40 years is alarming, exceeding 400 ppm after 2015. These values are the highest ever recorded for more than three million years. This fact implies a lack of precedents on its effect on the environment and much less on human health. The fast economic growth can explain this variability in the 20th century after the Second World War.

³ Figure from <https://showyourstripes.info>

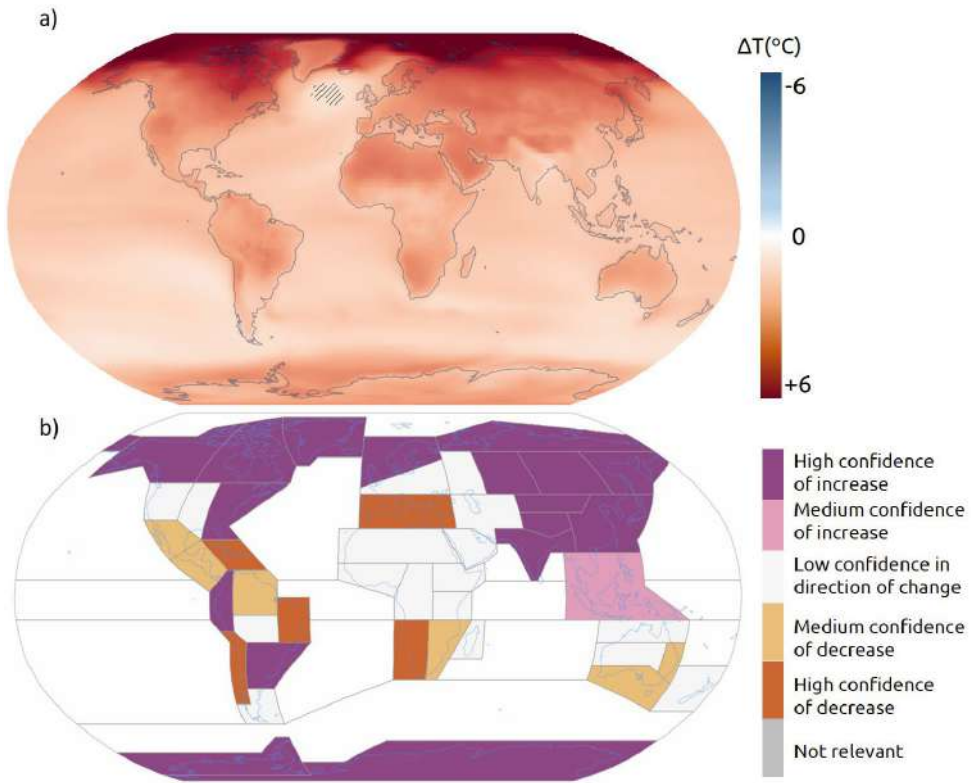


Figure 1.4. a) Evolution of the temperature increase on Earth from 1850 to 2021, and b) prediction of precipitations variation⁴.

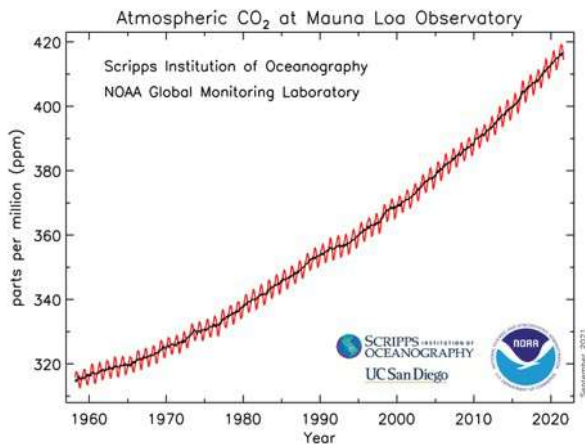


Figure 1.5. Atmospheric CO₂ concentration evolution from 1960 to 2020⁵. The red line represents the monthly mean value and the black line represents the monthly mean value of the average seasonal cycle.

⁴ Figures from IPCC- The Intergovernmental Panel on Climate Change, (<https://www.ipcc.ch/>).

⁵ Figures obtained from the Global monitoring Laboratory NOAA (<https://gml.noaa.gov>).

1.3 Kaya identity

Various factors are directly and indirectly involved in anthropogenic CO₂ emissions. In 1993, the economist Yoichi Kaya [2] introduced the mathematical expression that relates the different terms that have relevant impact on the generation of CO₂ emissions, proposing possible solutions to reduce global warming, **eq. 1.1**:

$$CO_2 = P \cdot \left(\frac{GDP}{P}\right) \cdot \left(\frac{E}{GDP}\right) \cdot \left(\frac{CO_2}{E}\right) \quad (1.1)$$

where **CO₂**= carbon dioxide emissions produced by human activity, **GDP** = gross domestic product, **E**= Global primary energy consumption in TOE (Tons of Oil Equivalent), and the **P**= world population in billions.

Kaya's identity allows us to have a global approach to CO₂ emissions related to human activities. From the different parameters of this identity, it is evident that the population (P) and the standard of living (GDP) will not decrease. On the opposite, it is expected 2.2% annual growth of the GDP together with an increment of CO₂ emissions. For this reason, the first two terms will hardly decrease. GDP is one of the main indicators since it is directly linked to primary energy consumption. Despite this, it is expected that given

the growing energy demand and growth of emerging countries such as China or India, there will be a decoupling of GDP and energy consumption.

On the other hand, it is possible to modify the last two terms. The E/GDP coefficient (**eq.1.1**) is the energy intensity and represents the necessary energy (kWh) to manufacture a product or service. The last term is the coefficient between CO₂ and energy (CO₂/E), which means the carbon intensity of the global energy mix. These two final coefficients can be directly influenced by promoting energy efficiency and incorporating low-carbon technologies and materials. These strategies also have implicit critical factors for sustainable development: recycling, circular economy, and renewable resources.

This last point is relevant since conventional resources based on hydrocarbons are finite resources, not guaranteeing their availability in the future. For this reason, **renewable energies** take a chief role to reduce global CO₂ emissions.

1.4 Climate change mitigation

In the last years, governments have been making great efforts in the energy transition towards low-carbon technologies, to reduce the environmental impact. The Paris agreement is an example of these efforts. The Paris Agreement is a United Nations framework agreement on climate change active from 2016, which establishes a series of strategies and measures for greenhouse gas (GHG) reduction. The agreement seeks to keep the average global temperature increase below 2°C above pre-industrial levels and pursue efforts to limit the rise to 1.5°C, recognising that this would significantly reduce the risks and effects of climate change.

With the government's initiatives, despite not reaching the initial objectives set out in the Paris agreement by the end of 2020; there was a positive balance at the global level, which can be summarised in the following points [3,4]:

- -2.1 Gt reduction in carbon emissions, with the lowest CO₂ emissions since 2011.
- The largest decline in oil consumption of -9.3%.

- The largest increase in renewable power generation of 358 TWh.
- 238 GW increase in wind and solar capacity, 50% larger than any increase in history.

The following set of goals for 2030 are based on [3,4]:

- At least 40% savings in greenhouse gas emissions (from 1990 levels).
- At least 32% share for renewable energy.
- At least 32.5% improvement in energy efficiency.

1.4.1 Share of renewable energy in final energy consumption

At the end of 2019, our energy mix depends on fossil fuels at 80. % and renewable energies over 11.2%, representing around 43 EJ produced by non-conventional sources [5], as illustrated in **Figure 1.6**. This percentage includes modern renewable energies: solar, wind, biomass, geothermal, maritime, hydrothermal energy, and biofuels. Moreover, the category "Others", which includes nuclear energy, shows a 2.3% decrease, motivated by switching nuclear power plants off after Fukushima's incident in 2011. Although the share of fossil fuels in the final energy

demand has not changed significantly, the increase in energy demand is being covered with renewable energies. China's economic growth contributes around 8% in the worldwide energy demand. Despite being the country with the highest installation of new renewable capacity, coal is their principal energy resource. This fact can justify the low change in the fossil fuels share in the final energy demand.

There are three final energy consumption categories: heat (50%), transport (30%), and electric power (20%). Electricity is the sector in which decarbonisation seems easy enough through renewable technologies. 75% of new power plants around the world were already renewable in 2018, and this fraction increases year by year. However, renewables represent in 2019 only 25% of the share of power generation. Despite the efforts to incorporate renewable energies into our energy system share, there are certain limitations, such as the security in the supply chain due to the intermittence of renewable energies. Therefore, the coupling of energy storage systems is key to achieve renewable energies'

goals. In addition to renewable energies, the transition to hydrogen as an energy vector and the improvement of energy efficiency in industrial processes are essential factors to achieve climate objectives and avoid global warming of more than 1.5°C since emissions would have to be reduced up to three parts worldwide.

1.5 Thermal energy storage, the key to decarbonisation

Photovoltaic and wind energy predominate in the current renewable energy market (besides hydroelectricity). Around 139 GW of solar PV was added by the end of 2020, which is equivalent to more than half of the added capacity of all renewables (256 GW), while the 93 GW added of wind power accounted for 36% [5,6]. However, despite their high energy mix share and cost reductions (LCOE⁶), these technologies are limited by their low energy storage capacity and high battery costs.

The decarbonisation of the network and, therefore, the substitution of conventional resources requires designing

⁶ LCOE: levelized cost of energy (US\$/kWh).

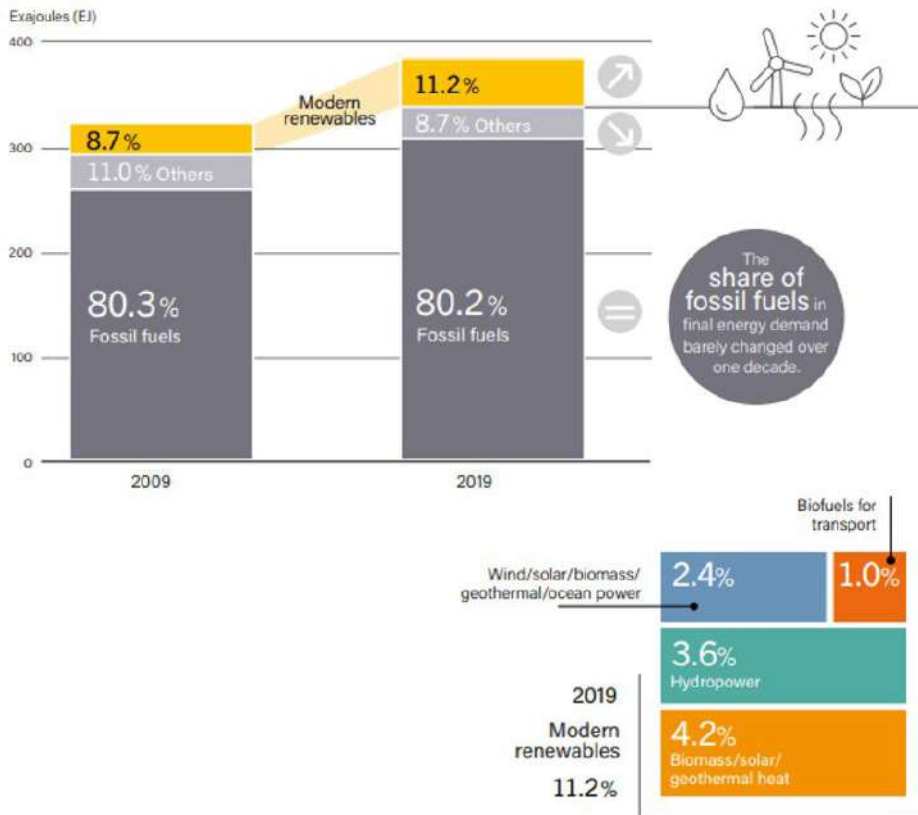


Figure 1.6. The estimated renewable share in the total final energy consumption, at 2009 and 2019[5].

an energy network based on optimising the cost and efficiency between generation and storage. This new network must always satisfy the demand and ensure the stability and security of the energy network. The main concern about the network regulators with renewables is always to guarantee the supply chain. Specifically, the main concern is to meet demand peaks since one of the main problems with renewable energies is to provide energy instantly and without interruptions. And

this is where concentrating solar power plants (CSPs) with thermal storage systems (TES) come into play [7,8].

At the end of 2020, approximately 21 GWh of thermal storage systems were incorporated in CSP plants in operation. This value represented 1.8% of all operational stored energy capacity worldwide (about 2.9 GW). All the installed TES capacity represents a significant proportion of non-pumped hydropower energy storage capacity [9]. Even though photovoltaic (PV) power

installed is 100 times higher than CSP, installed TES capacity in CSP plants is more than twice the capacity of utility-scale batteries [4].

Thanks to thermal storage systems, CSP plants have the potential to produce 24/7 baseload and/or peak electric power. In this way, CSP plants can store solar energy during the day and dispatch electricity from the last hours of the afternoon [10]. These power plants can also, for example, run overnight until the storage ends by avoiding the combined-cycle-gas backup, which has both high cost and environmental damage.

Thus, CSP technology is one of the most promising options to complement solar PV technology and overcome the "photovoltaic duck curve effect" at the end of the day. Moreover, CSP plants will allow to achieve the objectives of decarbonisation of the sector with more ambitious participation of renewable energies by 2030 [11,12]. Therefore, CSP plants allow greater integration of other variable renewable energies in the system, providing stability to the network and security to the supply chain. To achieve the net

zero power generation targets, a contribution of 204 TWh from CSP technology is necessary, representing an annual average generation growth of 31% from 2020 to 2029 (6.7 GW of new capacity per year).

Currently, CSP growth is not aligned with these goals. To achieve these goals, it is necessary to support R&D, recognise CSP's storage and flexibility capabilities, reduce its costs and increase the scale of the industry [5]. **Figure 1.7** shows CSP installed capacity (green), under construction (yellow), and in development (grey) around the world. The sector is dominated by Spain, the United States, and MENA⁷. Moreover, a total of 148 CSP projects are operating and 45.1% of the total installed capacity are equipped with TES⁸. In addition, 95.6% of them use liquid sensible heat storage (SHS) media (mainly solar salts) due to their reliability and lower cost [10].

1.6 Concentrated solar power plants: future trends

The overall cost and performance of a TES system, have a strong influence on the nominal kWh of the CSP plant

⁷ MENA: Middle East and North Africa countries (Algeria, Bahrain, Egypt, Iran, Iraq, Israel, Jordan, Kuwait, Lebanon, Libya, Morocco, Oman, Qatar, Saudi Arabia, Syria, Tunisia, United Arab Emirates, and Yemen).

⁸ Data from SolarPACES is available on www.solarpaces.org (last actualization feb-2022).

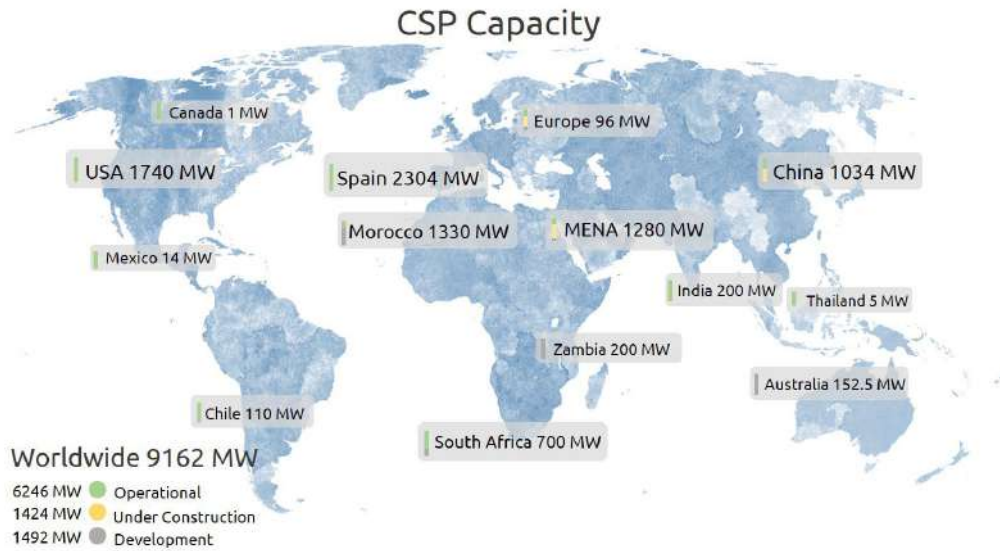


Figure 1.7. CSP projects status and total capacity per country; operational, under construction and in development around the world⁹.

[13-15]. Therefore, to be economically competitive in the future, the storage cost must be reduced considerably [7].

The LCOE of CSP technology has decreased by 68% in the last decade (2010-2020) from 0.340 USD/kWh to 0.108 per USD/kWh. This decrease is motivated by the technological improvement of storage systems by increasing their capacity factors. Even so, the LCOE still must decrease further to be competitive with other energy sources such as PV (0.057 USD/kWh), offshore wind power (0.084 USD/kWh), or onshore wind power

(0.039 USD/kWh) (LCOE at the end of 2020) [5].

The highly utilised configuration in CSP plants is the two-tank with molten salts, concretely with solar salts, which are a eutectic mixture of sodium and potassium nitrates. This TES technology is the most commercially implemented; therefore, it is feasible to deduce that an improvement in TES technology will directly influence the energy generation market [16].

Furthermore, it has been shown that environmental and health impacts also

⁹ Data from solarPACes and the National Renewable Energy Laboratory (NREL), www.nrel.gov/csp/solarpaces/.

limit the two-tank molten salts storage, by reducing the amount of molten salts is required in TES.

Therefore, to achieve proper cost and to reduce the environmental impact requires alternative TES Systems [17,18]. In recent years, big efforts have been done to improve TES efficiency, and to decrease costs.

To achieve this reduction in cost one strategy is the use of nanofluids, specifically nano-salts. Nano-salts, based on preparing a stable suspension of nanoparticles inside solar salt, exhibit improved thermophysical properties (e.g., the heat capacity increase by 30%) [19]. These fluids with high energy density have high potential to improve storage and heat transfer capacity [20]. Therefore, nanofluids can make more compact the storage tanks (lower volume) because less amount of TES material is required to store the same amount of energy. This fact directly decreases the LCOE and transform the system in a more competitive technology for the future.

02

Introduction
to nanofluids

State-of-the-art



2. Introduction to nanofluids

State-of-the-Art

2.1 Nanofluid concept

"...new class of heat transfer fluids can be engineered by suspending metallic nanoparticles in conventional heat transfer fluids..."[1]

"Nanofluids are engineered colloids made of a base fluid and nanoparticles (1–100 nm)..." [2]

"...If nanometer-sized particles could be suspended in traditional heat transfer fluids, a new class of engineered fluids with high thermal conductivity could be produced. These so-called "nanofluids" are..."[3]

"...Nanofluids are engineered by suspending ultrafine metallic or nonmetallic particles of nanometer dimensions in traditional heat transfer fluids such as water, engine oil, and ethylene glycol..."[4]

"...thermal conductivities of a fluid is to suspend metallic nanoparticles within it. The resulting mixture referred to as a nanofluid possesses..."[5]

Definition from the top-5 most cited articles (web of Science core collection) related to nanofluids: According to these definitions:

Nanofluids are engineered stable suspension of nanoparticles in a base fluid.

This term was coined for the first time in 1995 by S. U. Choi and S. Stephan from the Argonne National Laboratory (Massachusetts, USA).

2.2 Introduction to nanofluids

Nanoscience and nanotechnology have been scientific, technological, and social revolutions. This revolution is due to the exceptional properties and behaviour that materials exhibit at the nanoscale. Then, most of the physical, chemical, and biological properties are modified by reducing their scale, describing new phenomena

and behaviour of matter. Apart from facilitating miniaturization, the modification or description of new phenomena of some properties such as electrical and thermal conductivity, magnetic and mechanical properties, reactivity or reaction rates favours the design of new systems and materials [6,7]. Therefore, the use of nanomaterials impacts a wide variety of industrial, technological, or medical applications, among others.

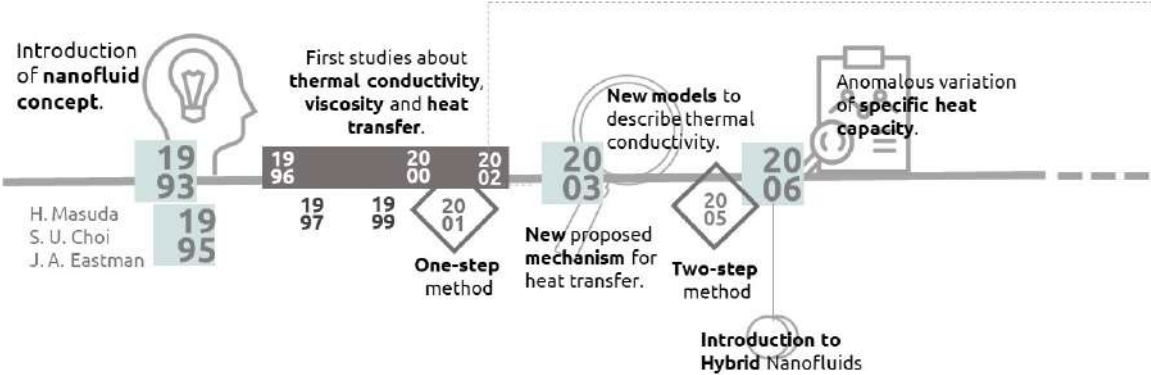


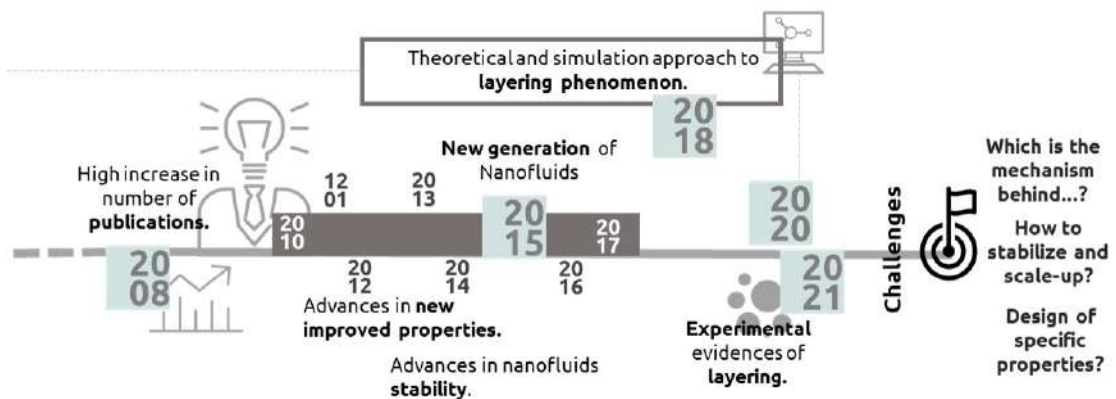
Figure 2.1. A brief timeline of some of the most relevant discoveries about

Nowadays, heat transfer is one of the main branches of study in many engineering discipline. The importance of studying the heat transfer is evidenced by the high number of applications involved, such as electronics, power generation plants, refrigeration, renewable energies, or the petrochemical industry, where various thermal media are used in both boilers and evaporators, heat exchangers, or radiators.

Nanomaterials and the consequent boost of nanofluids win potential together with the desire of developing efficient and compact systems within the context of sustainability and economy. Several studies have been performed regarding methods to increase the heat transfer rate in various systems in recent years. Considering the significant properties of nanoparticles, nanofluids are one of the most suitable

and effective choices in heat transfer enhancement.

Studies such as the one developed by H. Masuda et al., [8] in 1993 were motivated by the previous one study by H. H. Akoh et al., [9] in 1978 and also by the mathematical models developed by Hamilton and Crosser in 1962 on solid-liquid mixtures [10], and tried to improve the thermal properties of conventional heat transfer fluids. Their strategy, mainly focusing on thermal conductivity, was the dispersion of fine solid particles within a fluid. However, despite the theoretical potential of this technique, it did not turn out to be useful due to the high sedimentation of the particles, the increased erosion caused in the systems, and the energy increase associated to the high power-pumping that these fluids need.



nanofluids from 1993 to 2021.

In 1995-1999, two new key publications emerged, by S. U. Choi and J. A. Eastman [4,6]. In the first publication, they suggested following the H. Masuda's [8] particle dispersion strategy, but in this case, decreasing to the nanometric scale [6]. With this procedure, they theoretically determined the influence of nanoparticles on thermal conductivity. This publication first coined the term "Nanofluid" and it is considered one of the first publication in this new field of research. Moreover, the second study published in 1999 they demonstrated their theories experimentally in systems based on water and ethylene glycol with CuO and Al₂O₃ nanoparticles [4]. Therefore, the potential of this strategy resulted in the following main points [11]:

- Reduction of the corrosion, pressure drop, etc.
- Fluid is more stable in comparison to micro or larger particles.
- Influence of the nanoparticles in the thermophysical properties of the base fluid.

The modification of the thermophysical properties of the base fluid resulted to be quite a discovery and to be the main engine of the advance in the investigation of these new kinds of fluid and it drove to the great interest

by the scientific community in recent years.

Figure 2.1 shows a brief timeline with some of the most relevant events from discovering nanofluids to the present day.

In the following section, we will summarize the key points in the nanofluids science and technology, such as introducing the types of nanofluids, the synthesis methodologies, the most relevant properties, and their applications, among others.

2.2.1 Types of nanofluids

There are many different types of nanofluids depending on the base fluid and the type of nanoparticles. One of the most used classification is by nanoparticle type. The following **Figure 2.2** summarizes the most studied nanoparticle and base fluid families. Thus, nanofluids can classify into four main families: ceramic nanofluids, metallic nanofluids, carbon-based nanofluids, and hybrid nanofluids. In the case of hybrid nanofluids, more than 1 type of nanoparticles is used simultaneously as a synergistic strategy to improve their properties, as well see in the following section.

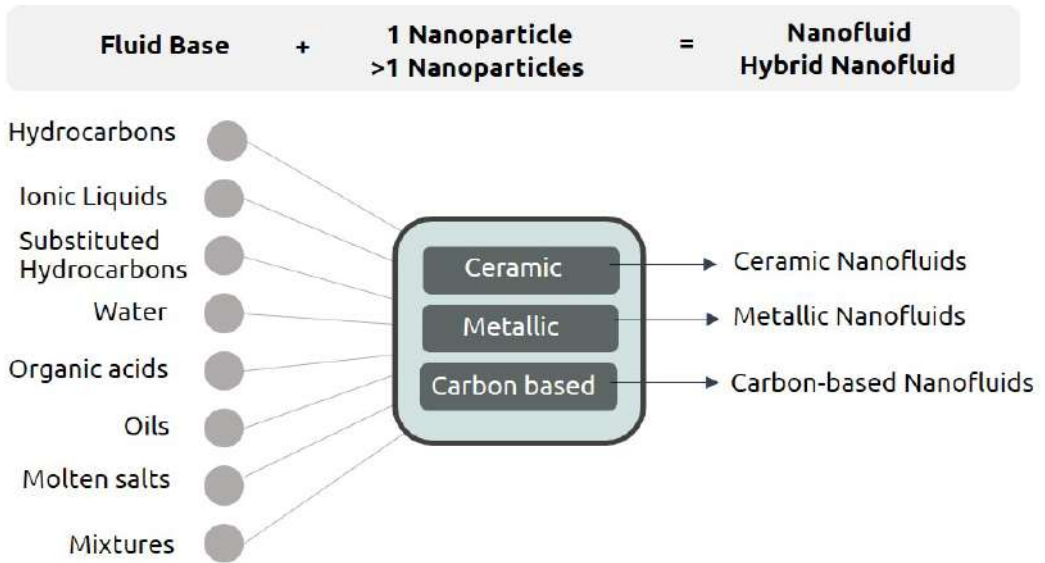


Figure 2.2. Nanofluids classification as a function of nanoparticles and base fluids.

Ceramic nanofluids include oxides, non-oxides, and composites (oxides/non-oxides). Within the oxide nanoparticles, one can find CuO [12,13], SiO₂ [14,15], Al₂O₃ [16,17], TiO₂ [18,19], ZnO [20,21], or Fe₃O₄/Fe₂O₃ [22-24] nanoparticles. Among the pure metals, some of the most studied nanoparticles have been Ag [25,26], Cu [27,28], or Fe [29] nanoparticles. Also, it can find different types of carbides such as SiC [30,31] or nitrides such as AlN [32]. Finally, carbon compounds such as diamond [33-35], graphite [36], and singles/multiwalled carbon nanotubes [37,38]. Ceramic nanoparticles have been among the most studied due to

their easy production, chemical stability, and resistance to oxidation [39-42].

All these kinds of nanoparticles combined with different base fluids like water, ethylene glycol or engine oil produce nanofluids with a wide variety of properties. As seen in the following section, these properties have a strong dependency on some nanoparticle's parameters such as type, size, shape or concentration and the thermal properties of the base fluid.

2.2.2 Properties

The incorporation of nanoparticles into different heat transfer media causes changes in their thermal properties, as seen in the previous section. This causes a considerable impact on the heat transfer efficiency of the fluid, and therefore, on its potential applications [43]. The most studied properties due to their direct relationship with heat transfer capacity are thermal conductivity (more than 11018 publications from 1995)¹, viscosity (more than 7655 publications from 2000)¹, and heat capacity (more than 617 publications from 2003)¹⁰. The interest and the main published results are summarized below.

Thermal conductivity, k:

Thermal conductivity, together with viscosity, has been the first studied property since the beginning of this research field. Its interest falls in its direct influence on the Nusselt number and the Prandtl number, which are two of the most significant parameters in the thermal transfer capacity of the fluid. Therefore, thermal conductivity directly impacts to the convective heat transfer coefficient [42].

Many authors have studied the thermal conductivity in recent years for various nanofluids systems, as summarized in **Table 2.1** (More than 330 values are available in **Appendix 1**). In general, the results show that incorporating low concentrations of nanoparticles in different liquid media increases the thermal conductivity of the system. Other studies reported high increases in the thermal conductivity of water with Al₂Cu (96%), ZrO₂ (60%) [44] and MWCNT (79%) [45] nanoparticles, with concentrations of 1.5 wt%, 1.1 wt%, and 0.3 wt%, respectively. Another relevant result is the 200% increase described in the study by G. Paul et al., [44] after incorporating ZrO₂ nanoparticles in ethylene glycol.

Contrarily, a decrease in conductivity is observed in the study by N. Navarrete et al., [46] with hybrid nanofluids based on solar salt with metallic Al-Cu nanoparticles. Their results indicated a dependency between the thermal conductivity worsening and nanoparticles concentration: from 6% with a concentration of 0.5% to -36.3% at 10% wt. S. Akilu et al., [47] also reported a worsening of conductivity as a function of concentration, but vice versa, improv-

¹⁰ Data from web of science core collection, January 2022, (www.webofscience.com).

ing conductivity with higher concentrations. Similar results were reported by P. D. Myers et al., [48] with CuO nanoparticles in solar salt. Other systems did not present significant modifications with the incorporation of nanoparticles, such as the cases of nanofluids based on: kapok oil/MWCNT [49] or water/SiO₂ [50,51,52]. J. Seo et al., [53] also studied the effect of nanoparticle size in molten LiNO₃-NaNO₃-KNO₃ salts with silica nanoparticles ranging

in size from 5 to 60 nm, where they found no significant effect of nanoparticle size on conductivity. Despite the potential of hybrid nanofluids, the literature reports contradictory results. For example, EG-based nanofluids with MWCNT-ZnO [69] and ZnO-DWCNT [59] did not present significant alterations. In contrast, in solar salt nanofluids with SiO₂-Al₂O₃ hybrid nanoparticles, increases of up to 22% were obtained [70].

Table 2.1. Some selected studies about nanofluids thermal conductivity for different base fluid/nanoparticle systems.

Base Fluid	Nanoparticle	Average Concentration (wt%)	Average Size (nm)	Average Temperature (°C)	Δk (%)	Reference
Water	Al ₂ O ₃	1 vol%	11	70	14.8	[54]
		5 vol%	40	25	10	[55]
	CuO	3.4 vol%	23.6	25	12	[4]
	Ag	0.3	100	70	30	[56]
	ZrO ₂	11	20	25	60	[44]
	Graphene	0.1	Lamellar	0.2	25.5	[50]
	SiO ₂ -SDBS	0.1	70	0.1	0.9	[50]
EG	Zn-Ag	1	40	50	16.2	[57]
	Ag	0.55 vol%	300	130	18	[58]
	SiO ₂	1	17.5	30	-0.8/-1.02	[47]
	ZnO-DWCNT	0.3	-	50	1.08	[59]
Solar salt	MgO	5	-	25	40.6	[60]
	SiO ₂	1	30	300	21	[61]
	MWCNT	1	-	250	-1.9	[38]
	Al-Cu	1	-	300	1.8	[46]
Kapok	SiO ₂ -Al ₂ O ₃	1	41	396	30	[62]
	MWCNT	0.4	-	65	536	[49]
Li ₂ CO ₃ -K ₂ CO ₃	Al ₂ O ₃	1	10	540	32	[63]
	SiO ₂	1	37	540	21.5	[64]
	MWCNT	1	20	400	6	[65]
EG/Water	AlN	0.5	50	-	8	[44]
	Al ₂ Cu	1.5	31	25	96	[44]
	Al ₂ O ₃	5	60.4	25	26	[66]
	MgO	1	0.4	35	0.35	[67]
Glycol	SiO ₂	2	17.5	60	5.4	[68]

According to the results from the literature, it is evident that there is a wide variety of factors that directly and indirectly influence the thermal conductivity of nanofluids, such as the relationship between the fluid medium and the nature of the nanoparticles, temperature, morphology, size, and concentration. Despite the specific cases described many systems such as E.G., glycol, molten salts, water, or oils under conditions (sizes and concentrations of nanoparticles), show increases in the range between 10-40%.

Viscosity, ν :

Viscosity is an essential parameter for all thermal applications that work with fluids. Parameters such as pressure-drop or pumping power, the energy density of a system, or the convective heat transfer coefficient show a dependence on viscosity. Therefore, viscosity has a crucial impact on heat transfer.

Similarly, **Table 2.2** includes some selected viscosity values for different nanofluids systems (an extended table can be found in **Annex 1** with a total of 113 values).

Most researchers reported increases in the viscosity of different nanofluid systems. In the case of viscosity, there seems to be a clear trend of increasing

with increasing nanoparticles concentration, as shown by S. Akilu et al., [47], Z. Jiang et al. [71] or R. Vajjha et al., [72]. One of the most significant values of 2300% were reported by W. Yu et al., [73], through the incorporation of Cu nanoparticles in ethylene glycol, or other studies like the reported by M. J. Pastoriza-Gallego et al., [74] with CuO nanoparticles in water. Despite these extraordinary values, most published results report increases ranging from 10% to 90%, depending mainly on the system and the concentration of nanoparticles. An example is the case of the study by L. Godson et al., [56], where they described variations of 14%, 30%, and 40% at concentrations of 0.3 vol%, 0.6 vol% , and 0.9 vol%, respectively, with Ag nanoparticles in water. S. Akilu et al., [47] also studied the effect of concentration and temperature in the EG-SiO₂ system. They reported an increase in viscosity with both temperature and concentration.

Other studies have also reported the effect of nanoparticles size with contradictory results. The studies by R. Prasher et al., [75] and M. J. Pastoriza-Gallego et al., [76] show a viscosity decline with the increase of the size of the nanoparticles. On the contrary, the studies of C. T. Nguyen et al., [77] and

S. K. Verma et al., [78] reported opposite trends with water/Al₂O₃ nanofluids, where the viscosity went up from 276% to 547%, with nanoparticles of 47 nm and 37 nm (with the same concentration), respectively. An interesting result is the one reported by H. Zhu et al., [79]. In this study, they observe a decrease in the viscosity of water with CaCO₃ nanoparticles, being one of the few results that show this type of behaviour.

Specific Heat Capacity, Cp:

The heat capacity is linked directly to the fluid's ability to store heat. Consequently, fluids with high heat capacity

are required for both refrigeration systems and thermal storage systems. The formers because they need to remove a certain amount of heat and the storage tanks due to they need to store the highest amount of heat.

Therefore, the heat storage and transfer capacity of these types of systems will be limited by the heat capacity of the fluid.

As the thermal conductivity, heat capacity has contradictory values and unclear trends.

Table 2.2. Some selected studies about nanofluids viscosity for different base fluid/nanoparticles systems.

Base Fluid	Nanoparticle	Average Concentration (wt%)	Average Size (nm)	Average Temperature (°C)	Variation ΔViscosity (%)	References
Water	Ag	0.6 vol%	100	70	30	[56]
	Al ₂ O ₃	0.15 vol%	30	30	2.9	[80]
		0.5 vol%	43	25	136	[81]
		12 vol%	36	25	276	[77]
	CaCO ₃	4.1 vol%	50	25	-31	[79]
	SiC	4 vol%	51	50	80	[82]
	TiO ₂	3 vol%	21	25	135	[83]
EG	AlN	5.5	50	60	38.7	[84]
	Cu	2	200	25	2300	[73]
	Nano-Diamond	1	7.5	60	1	[35]
	SiO ₂	1	17.5	55	30	[47]
E.G./water	Al ₂ O ₃	6	28	-	86	[85]
	CuO	3.5	29	50	300	[75]
Oil	CuO	1.5	40	-	300	[86]
Solar salt	SiO ₂	0.5	102.5	450	2.41	[71]
		1	102.5	450	104.7	[71]
Ethanol	SiO ₂	6	190	50	44	[87]
PG	Al ₂ O ₃	3	40	50	26	[75]

For example, many investigators reported increases in heat capacity [33,34,63,88–91], as other investigators reported the opposite effect, a worsening of heat capacity through the addition of nanoparticles [36,37], [92]–[96]. The heat capacity results from some selected studies are collected in **Table 2.3** (More than 380 values are available in **Appendix 1**). Although the study of heat capacity on nanofluids began years later than thermal conductivity or viscosity, the number of publications about this property has grown in recent years. In early years, researchers believed that density and heat capacity obeyed simples'

mixture laws, and its behaviour has been overlooked. These facts are reflected in publications such as that by J. Lee [106], which shows a worsening of the heat capacity when assuming the mixture models. But from different studies such as the one carried out by S. Murshed et al., [107] in 2006, based on the thermal diffusivity in various nanofluids with TiO₂, Al₂O₃, and Al nanoparticles in ethylene glycol and engine oil, indirectly observed that the heat capacity value did not satisfy the common mixing law used until now [108,109].

Table 2.3. Some selected studies about nanofluids specific heat capacity for different base fluid/nanoparticles systems.

Base Fluid	Nanoparticle	Average Concentration (wt%)	Average Size (nm)	Average Temperature (°C)	ΔCp (%)	References
Water	Al ₂ O ₃	2.06	13	27	-1.69	[97]
		21.7	45	27	-46	[78,98]
	TiO ₂	2.1	27	27	-1.7	[34,97]
EG	SiO ₂	1	17.5	30	-0.7	[68,47]
	CuO	0.15	50	100	6.5	[78],[36]
E.G./Water	Al ₂ O ₃	6	44	64.5	-12.2	[99]
PAO	xGnP	0.45	20x100	75	50	[88]
Heat transfer oil	MWCNT	0.25	12.5	328	-31	[78,36,34]
Engine oil	Nanodiamond	1.1	100	88	18.5	[33,34]
Solar salt	SiO ₂	1	12	223	25	[100,101]
		1	5	266	19	[100]
		1	102	400	6.6	[71]
	SiO ₂ -Al ₂ O ₃	1.5	101	118	34.8	[93]
	Al-Cu	1.5	160	300	1.5	[46]
	Nano-Mg	10.4	102.5	180	168.1	[102]
ACaSEu	SiO ₂	1	10	500	32	[103]
EHS	TiO ₂	0.5	25	56	16.5	[104]
Ionic Liquid	Graphene	0.045	-	120	-2.25	[105]

From that moment, the interest in heat capacity grew notably. From the data reported, it is possible to identify the influence of the base fluid nature on the specific heat capacity. In the case of water-based nanofluids, many researchers reported a reduction of C_p , with different types of nanoparticles; up to -33% like in the study reported by I. M. Shahrlul et al., [34] in water/ Al_2O_3 system or even -169% with metallic Cu nanoparticles [110]. Similar results were reported with [92,97,98], CuO [111], TiO_2 [97] or SiO_2 [34,72,99] nanoparticles. Furthermore, similar trends were reported for EG-based [13,36] and paraffin-based nanofluids [28]. Contrarily, studies on molten salts-based nanofluids show the highest increases in the specific heat capacity. B. Dudda et al., [112] reported an increase up to 28% with 1 wt% of SiO_2 nanoparticles in solar salt. Similar results were reported for Al_2O_3 (30% [90]) TiO_2 (7.5% [113]), Mg (168% [102]), and Fe_2O_3 (10.5% [114]) nanoparticles or in hybrid nanoparticles like CuO- TiO_2 (10.5% [115]) or SiO_2 - Al_2O_3 (30% [62]).

Other molten salts, such as those based on carbonates, Li_2CO_3 - K_2CO_3 , showed increases up to 124% with SiO_2 nanoparticles [116] or up to 105% with graphite [117]. Other oil-based

nanofluids also showed anomalous behaviour in heat capacity. S. Toghyani et al., [118] studied Therminol-55 with different types of nanoparticles (i.e., TiO_2 , SiO_2 , Al_2O_3 , and CuO), reporting increases in C_p of 73%. Despite these extraordinary values, the variation of C_p is generally between $\pm 20\%$ for the different nanofluids studied. In addition, several publications focused on the effect of concentration, confirming that the increase in concentration causes a decrease in the heat capacity and finding that an optimal concentration of around 1% of nanoparticles maximizes the heat capacity value [41]. Similarly, various research papers studied the effect of nanoparticles morphology (size and shape) and temperature [100,119,120], reporting contradictory trends. In the same way as thermal conductivity, the specific heat of nanofluids exhibit contradictory trends and a strong dependency on nature, shape, concentration and nanoparticles size.

However, the interest in nanofluids is not based solely on these three properties. Thus, remarkable modifications of other properties have been reported over the years, being the most notable ones the following:

- Reduction and/or inhibition of corrosion [121,122].

- Variation of wettability [123,124].
- Variation of the absorption factor [125,126].
- Variation of magnetic properties [22,127].
- Variation of electrical conductivity [128,129].
- Variation of density [76,130].

2.2.3 Factors influencing the thermophysical properties of nanofluids

As above-mentioned with the increasing number of available publications, some discrepancies in the measured properties have appeared, allowing to identify the factors that contribute to these differences. The following **Figure 2.3** summarizes some of the parameters that have been identified. Some of the most studied factors are the size, concentration, morphology of the nanoparticles, stability, temperature, and pH of the nanofluid. A brief description of the general trends observed for each one is described below:

- Nanoparticle size: thermal conductivity and heat capacity increase with decreasing particle size [53,54,74,131–133].

- Morphology: higher aspect ratio increases thermal conductivity, viscosity and heat capacity. Therefore, nanoparticles with higher aspect ratio transports heat more efficiently [49,100,119].
- Concentration: an increase in nanoparticle concentration produces an increase in thermal conductivity and viscosity whereas a decrease in nanoparticle concentration drives to an increase in the heat capacity [72,134–136]. Nevertheless, the increase of concentration tends to agglomerate the nanoparticles, causing their sedimentation, thus, decreasing the nanofluid stability.
- Temperature: the literature reports a high increase in thermal conductivity and viscosity with temperature. In contrast, no clear trends are found in effect of temperature in the heat capacity [54,72,137–139].

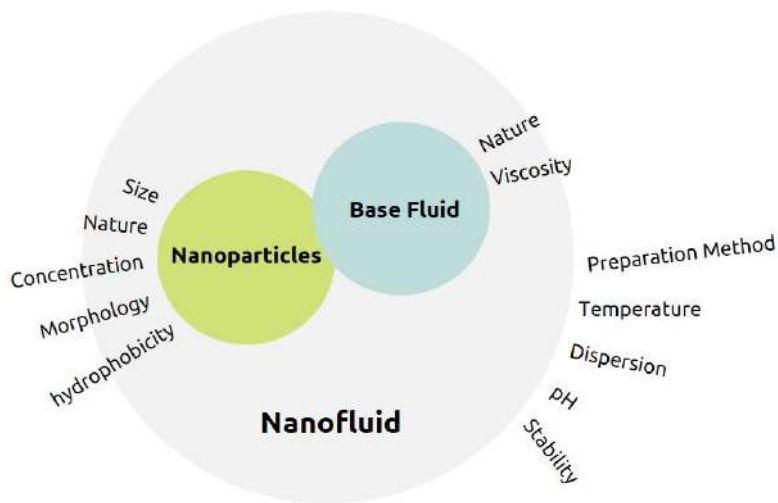


Figure 2.3. Schematic representation of the main factors influencing nanofluids' thermophysical properties.

- **pH:** the pH of nanofluids appears to influence thermophysical properties strongly. Some studies suggest that an optimal pH allows obtaining nanofluids with low viscosity and high thermal conductivity. In addition, some studies indicate a strong influence of pH on stability [140,141].
- **Stability:** the stability of nanoparticles suspension strongly affects the thermophysical properties of the resultant nanofluid. It is evident that researchers are focused on obtaining long stable nanofluid although according to G. Yildiz et al., [142] or A. Sofiah et al., [143] some factors influence the stability (e.g., ultrasonication and agita-

tion duration, presence of surfactants, pH of the mixture, surface charge density, grain size, morphology, concentration and density of nanoparticles).

2.2.4 Preparation of nanofluids

The synthesis of nanofluids is focused on preparing a stable suspension of nanoparticles inside a base fluid with the inhibition of sedimentation. Nowadays, there are two main synthesis paths to prepare nanofluids: one-step method and two-step method [144,145,146].

A schematic representation of the two techniques is depicted in **Figure 2.4**. As the name indicates, the one-step

method involves a unique step to prepare nanofluids, so the nanoparticles are directly synthesized and dispersed in the base fluid using a single or different precursors (bulk materials).

In the two-step method, the nanoparticles are synthesized separately from the base material, thus involve use of pre-synthesized nanopowders. Nanoparticles, nanofibres or any other nanomaterial are initially a crushed dry powder, synthesized by either physical or chemical method and then dispersed in the base fluid. **Figure 2.5** summarizes the main advantages and drawbacks between the two methods.

The most remarkable point is that despite the numerous benefits of the one-step method, such as reducing the nanoparticle’s agglomeration and the increase in the stability of the

nanofluid, it has some clear disadvantages. For example, it does not facilitate the scalability of the process, it has a higher economic cost, and it enhances the presence of impurities. Thus, although the two-step method has more limitations and disadvantages regarding the dispersion and stability of the nanoparticles, it is one of the most used methods since it facilitates its scalability at a lower cost [147–149].

According to these facts, and to develop more efficient synthetic methodologies and more stable and homogeneous nanofluids, various techniques have been developed in the last years, based on one-step and two-step methods (**Figure 2.6**).

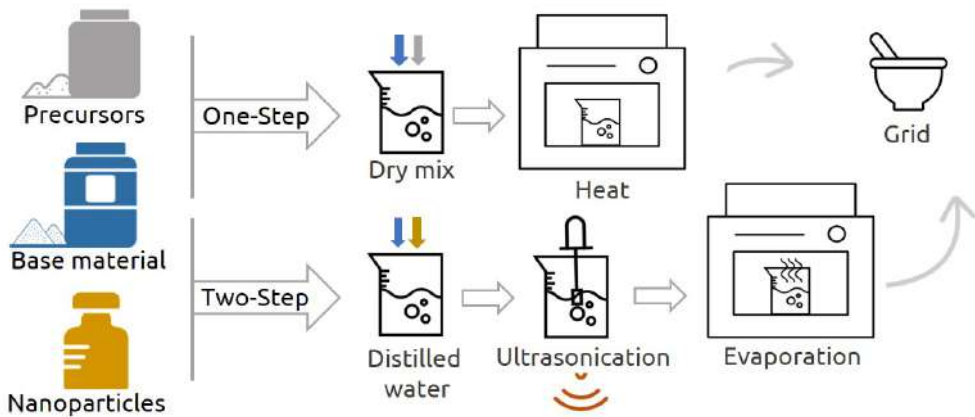


Figure 2.4. Schematic simplified diagram of the two main techniques for preparing ionic-nanofluids by one-step (top) and two-step (bottom) methods.

One-step method involves techniques like vapour deposition (VP) [103,152], laser ablation [153,154], submerged arc nanofluid system (SANSS) [155,156], arc spray nanofluid system (ASNSS) [157,158], microwave irradiation [159,160], electrical explosion of

wire (EEW) [25,161] or thermal decomposition [162,163].

On the contrary, in the two-step method, the nanoparticles can be synthesized by several well-established methods [164,165] and then dispersed in the base fluid.

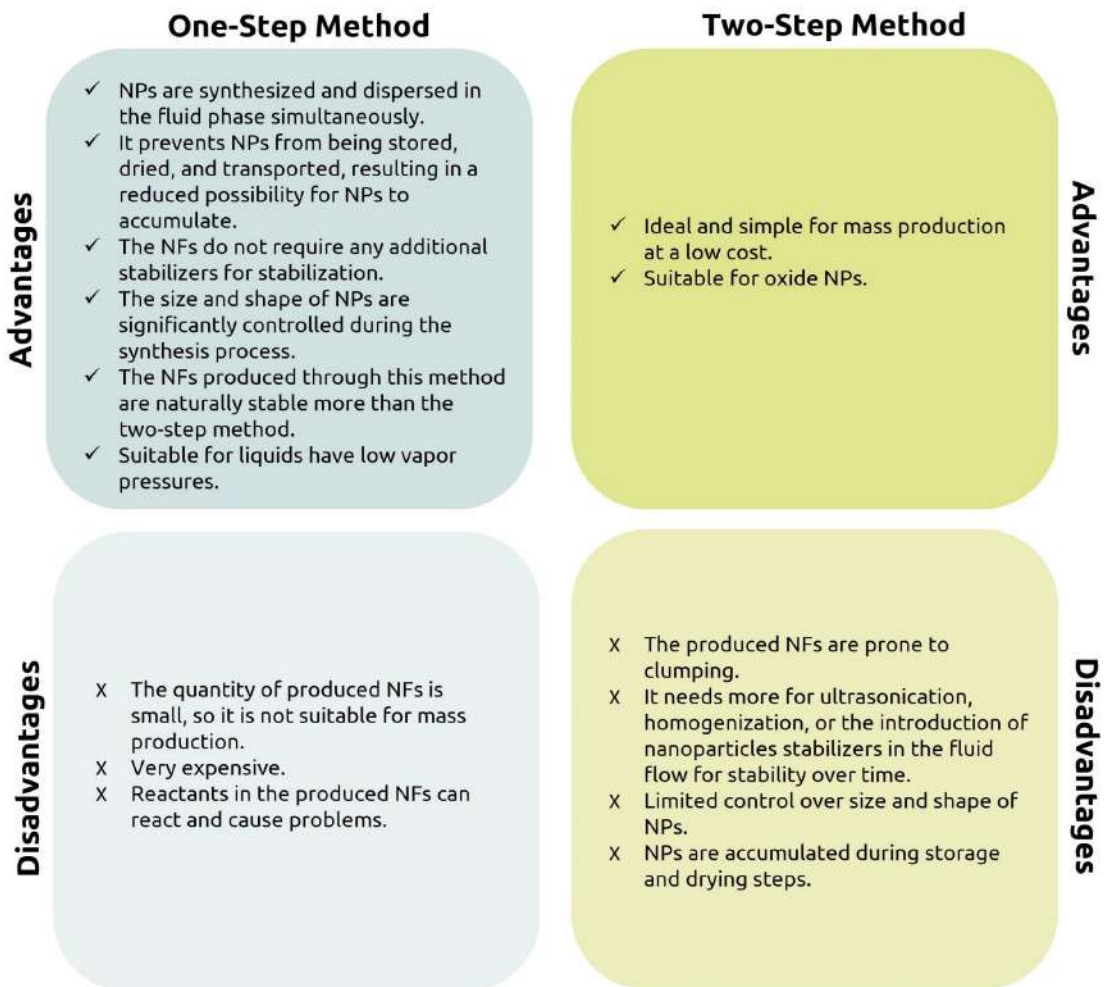


Figure 2.5. Summary of advantages and drawbacks of nanofluids preparation methods[150].

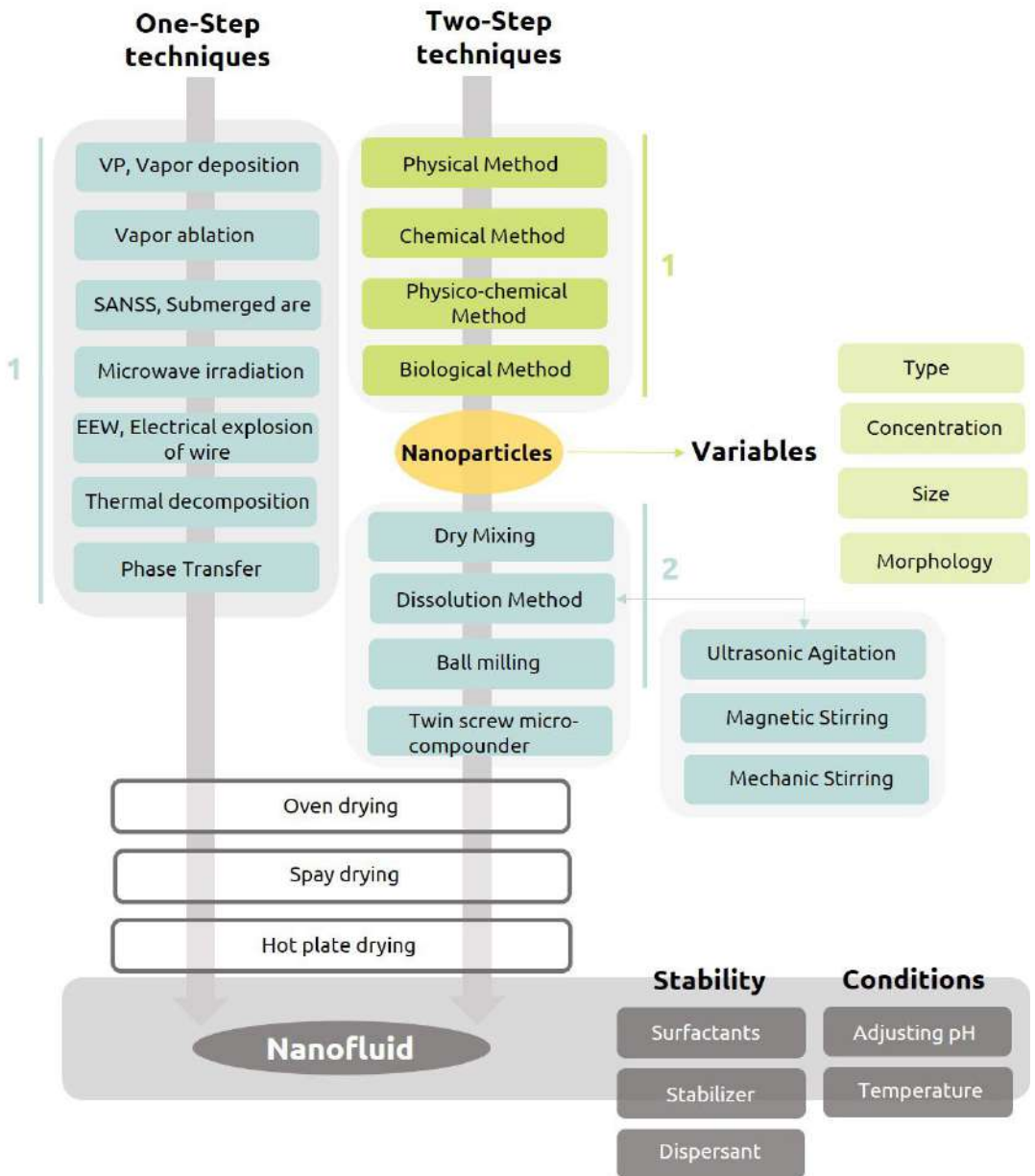


Figure 2.6. Main techniques employed in the one-step method and two-step methods to produce nanofluids [147,150,151].

This last step can be performed through several processes such as dry mixing, dissolution method, ball milling or twin-screw micro compounder

[146,166,167]. To obtain the final nanofluid, most of these techniques end with a drying process such as oven drying, spray drying, or a hot plate and

the melting and/or grinding of the resulting powder.

In addition, nanofluids, mainly synthesized by the two-step method, require the incorporation of stabilizing and/or dispersing agents. Therefore, one of the main challenges is to develop strategies to obtain stable nanofluids. Some of the proposed methods are based on ultrasounds, ultrasonic agitation, magnetic or mechanical agitation, altering the pH of the suspension, or through the addition of surface activators or dispersants. The complexity of this step becomes even more evident in nanofluids for high-temperature applications, such as nanofluids based on molten salts, due to the lack of dispersants or activators that can work at high temperatures (up to 400°C).

Several studies have reported that the different methodologies and processes paths have a strong influence on the properties of nanofluids, that stimulates the research for a method that optimizes the nanofluids properties [89,168,169].

2.2.5 Applications

Nowadays, more and more potential applications are under study due to the exceptional properties exhibited by nanofluids compared to conventional

fluids. These applications belong to sectors such as the medical and pharmaceutical, the automotive industry, electronic compound and the energy one.

Table 2.4. summarizes some of the applications that have been reported in the recent years [170].

2.3 Challenges and limitations

Despite the nanofluid's potential due to their improved thermophysical properties, they must overcome some challenges and obstacles for their scalability. Stability is one of the weak points, and therefore achieving stable nanofluids, especially at high temperatures, is one of the main challenges to face. The poor stability causes a high agglomeration of the nanoparticles, which is aggravated with temperature, causing a decrease in thermal conductivity and heat capacity, and consequently, in the heat transfer capacity. On the other hand, the lack of stability causes the sedimentation of the nanoparticles, which, among other things, also has a high impact in the absorption properties of the nanofluid. In addition, in different systems, agglomeration leads to an increase in corrosion and erosion of the systems and a high-

power-pumping due to the rise of viscosity [199].

Another obstacle to face is the high dispersion of results published in the literature and, therefore, the lack of clear trends and methodologies on the thermal behaviour of nanofluids and their correct characterization. This problem is caused by the lack of a robust theoretical framework that explains the phenomenology of nanofluids.

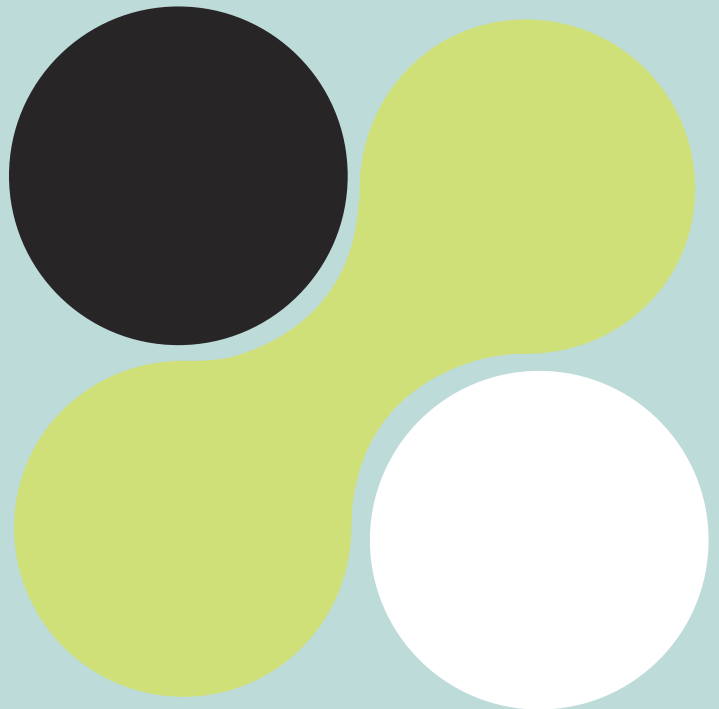
Last but not least, one of the enormous challenges to which nanofluids are exposed for their scalability is the reduction of costs and the environmental impact they have. The high cost and environmental impact are reflected mainly in nanoparticles' precursors and production processes. Therefore, the cost of preparing stable nanoparticles and nanofluids must be balanced against the cost saved by fluid substitution.

Table 2.4. Summary of some potential applications of nanofluids reported in the literature in the last years.

Machining processes and metal quenching (i.e., lubricants, cutting fluids, coolants)	[20,124,171,172]
Automobile sector (i.e., heat exchangers, car radiators, jet cooling system, diesel engines)	[17,173,174]
Cooling systems and chillers (i.e., in domestic and industrial applications: cooling fluids, engine cooling, radiant fluid, lubricating oil, lubricants, heat exchangers)	[40,142,173,175–177]
Electronic devices (i.e., cooling electrical engines)	[151,178,179]
Heat pipes (i.e., air-conditioning, electronic, fans)	[180–182]
Solar systems (i.e., solar collectors, photovoltaic solar systems, solar parabolic collectors, TES, solar water desalination)	[183–190]
Fuel cells	[191,192]
Aerospace	[193]
Geothermal energy	[194]
Oil recovery	[195,196]
Nuclear industry	[197]
Construction industry	[198]

03

Objectives



3. Objectives

The main objective of this PhD thesis is to study and understand the thermo-physical behaviour of nitrate salt-based nanofluids, with particular attention to the anomalous behaviour of specific heat capacity.

To this end, it is desired to address this thesis from a theoretical, statistical, and experimental point of view.

The following specific objectives are proposed to accomplish the general goal:

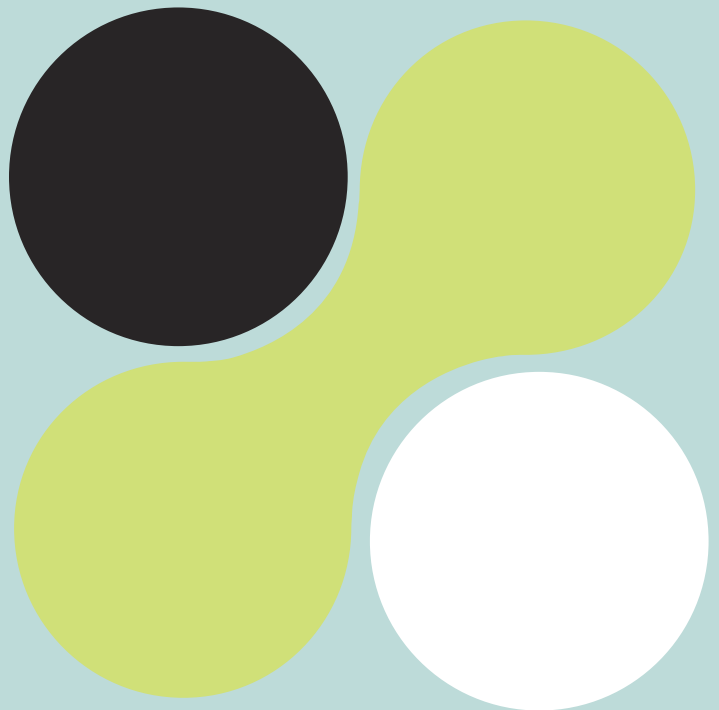
1. Contextualization of the research field: Bibliographical study of the relevance and state of nanofluid research.
2. Identification of the main gaps in the nanofluids research based on

molten salts to design original experiments aligned with the needs for the nanofluids research development.

3. Study and evaluate the possible sources of error and discrepancy of the results published in the bibliography to develop an appropriate methodology to characterize nanofluids and understand their properties.
4. Study the mechanisms involved in the heat capacity and proposal of a theoretical framework.
5. Finally, a feasibility study to employ nanofluids as TES material in concentrating solar power plants (CSP).

04

Thesis structure



4. Thesis structure

The PhD thesis has been presented in the form of a compendium of publications, which have been published, accepted, or submitted in different high-quality scientific journals. The dissertation is divided into 12 chapters with 6 publications, and its correlation as shown in **Figure 4.1**.

This thesis will begin with a preface (**Chapter 1**) and a general introduction (**Chapter 2**) that will help to contextualize the reason and relevance of this thesis and the application of the presented results. **Chapter 5** will specifically introduce the state of the art of molten salt-based nanofluids, identifying the main limitations to which the research is currently subjected. Will select the most relevant ones to respond to the objectives set out in this thesis and be grouped into **Key point 1, Key**

point 2, Key point 3, Key point 4, Key point 5 and Key point 6.

The following chapters will be guided through the key points where a contribution to each of the gaps will be presented to contribute to the advancement of the investigation. In **Chapter 6**, nanofluids research relevance will be contextualized in social and scientific terms, focusing on the molten salt-based nanofluids' relevance.

Each of the chapters in which results are presented in the form of an article (**Chapter 6, Chapter 7, Chapter 8, Chapter 9 and Chapter 10**) will have the following structure: introduction, relevance and objectives, followed by a graphical abstract of the article, the article published/accepted or in the process of review and finally a section with the contribution to state of the art.

These chapters will not have a methodology section or specific conclusions; they can be found in the publication. Finally, **Chapter 11** will be the only chapter of results that will not be presented in article format, and therefore there will be a methodology section and conclusions. This section will finish

with **Chapter 12** with a brief results summary.

Finally, the thesis will conclude in **Chapter 13** with the general conclusions that englobes all the results and the future works derived from the thesis.

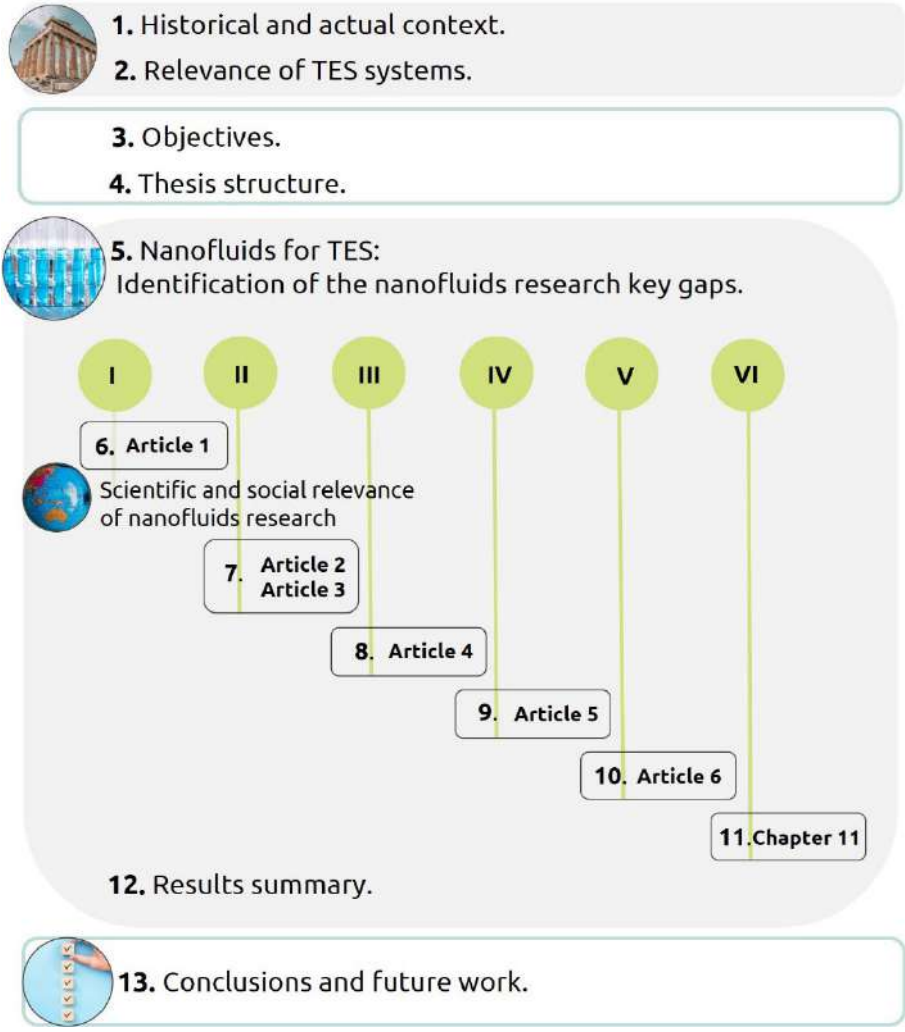
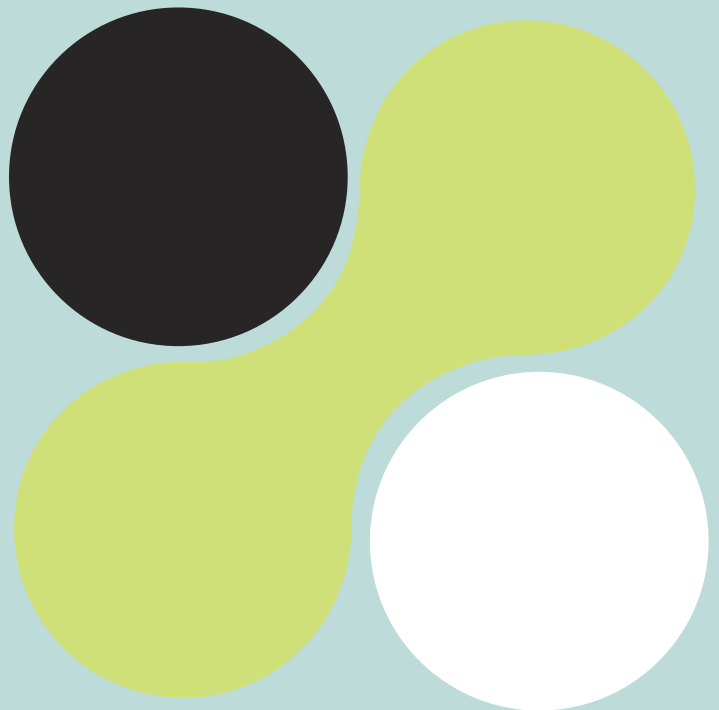


Figure 4.1. PhD thesis structure.

Nanofluids for
thermal energy
storage

Key Points



5. Nanofluids for TES

Key Points

5.1 Introduction

The preface highlighted the potential of CSP technology with integrated TES systems for sustainable development. In this chapter, the most relevant parameters regarding CSP technology and particularly TES systems, will be introduced. In addition, it will identify the most relevant factors to design highly efficient TES systems, where the potential that nanofluids have in this sector and which are the most relevant thermophysical properties will be evidenced. Accordingly, to the scientific relevance seen in the introduction, it will present the most relevant results and research of nanofluids for thermal energy storage.

Finally, this chapter will analyse the case of heat capacity, the focus of this

thesis and outline the main key points and limitations of the state-of-the-art of nanofluids based on molten salts for TES, which will guide the following chapters.

5.2 CSP technology and TES systems: an overview

Nowadays, there are different CSP and TES technologies; the main ones are summarised in **Figure 5.1**. As for CSP technologies, there are 4 well-differentiated [1]: (1) Parabolic Trough Solar Collectors (PTSC), (2) Solar Power Tower (SPT), (3) Linear Fresnel Reflector (LFR), and (4) Parabolic Dish System (PDS). Each one differs by the type of panels they use to collect/concentrate solar radiation, as outlined in **Figure 2.1-a**.

On the other hand, thermal storage is classified into three types based on the way of storing heat: (1) sensible heat storage, which can use solid and/or liquid media, (2) latent heat storage, which use phase change materials, and (3) Thermochemical storage, which use thermochemical reversible reactions [2,3].

The most mature and established technology is based on sensible heat storage; although thermochemical storage can store the highest energy density, however, it is an immature technology. Within sensible storage, there are different configurations for CSP such as

2-Tank molten salts technology, single medium thermocline tank (SMT), Dual-media thermocline tank (DMT), and Shell-and -tube tank (with and without embedded pipes) (ST), as shown in **Figure 5.1-b**. Two-tank TES systems are the most mature technology used since its first start-up in 1984 in the pilot plant of the Solar Electric Generating Station I (SEGS I) project in the USA. CSP with 2-tank storage technology accounts for approximately 48% of all CSPs installed and under development globally. As of 2015, no new facility has been developed without a TES system.

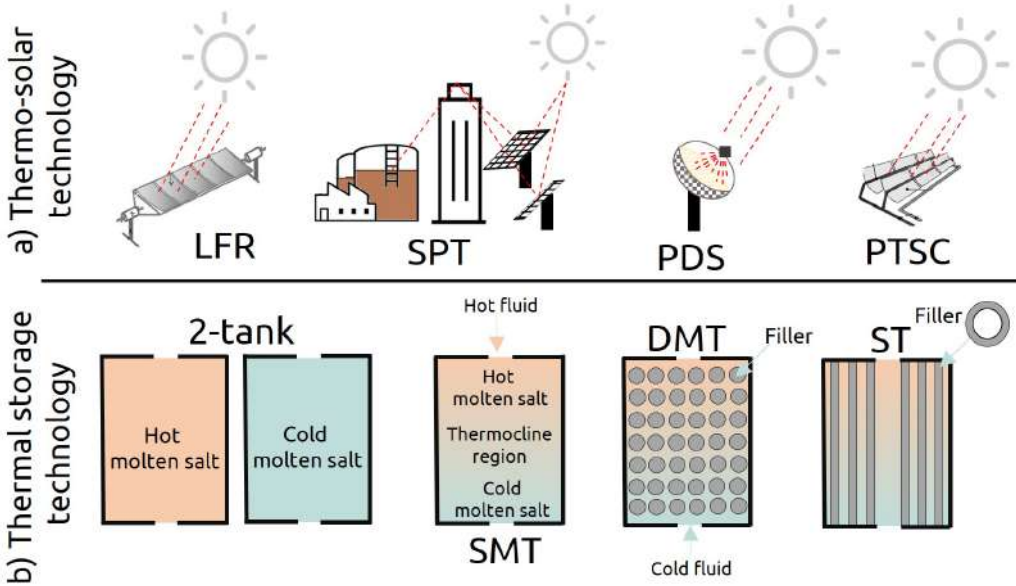


Figure 5.1. Leading available technologies; a) thermo-solar technologies, and b) thermal energy storage technologies [4].

Also, the PTSC system is the technology with the highest installed power around the world. Although, currently, the market is changed, and almost all new projects are based on SPT technology due to its higher potential.

Table 5.1 summarises the CSP projects worldwide that incorporate sensitive two-tank storage systems. We can find the name of the project and the country, its status, use of the facilities, the installed capacity (MWe), the type of collectors, HTF, the kind of TES system and its storage material, the hours of storage, and finally the year of start-up. It is remarkable that approximately 8% of the plants worldwide employ different TES technology.

Table 5.2 summarises these projects specifying the implemented storage technology, the status, and the project's purpose. Only two projects are in the operational phase and with commercial use, which is the case of the Redstone Solar Thermal Power Plant project in South Africa and the Puerto Errado 2 Thermosolar Power Plant in Spain, but with neither of these two technologies reaches a storage time of more than 2 hours. On the other hand, the project of 50 MWe in China with 14 hours of Cement storage are promising. One of the leading indicators to assess the economic viability of this type

of installation is the LCOE (US\$/kWh); as we could see in previous sections, this value represents the average income of electricity generated that would be required to recover the costs of plant lifespan. Currently, the LCOE with a storage system of about 6 h varies between 0.124-0.155 US\$/kWh for PTC technology and between 0.118-0.129 US\$/kWh for SPT technology.

This difference is mainly due to the high operating temperatures reached by SPT systems, which allows a higher differential temperature in the storage system and therefore reduces the amount of TES material needed. That is why the most significant technological interest of this type of installation.

Different studies, such as the one carried out by O. Achkari et al., [5], show that the LCOE of CSP technology depends mainly on the TES system and the amount of energy stored; therefore, to be a more competitive technology must reduce storage costs considerably.

In **Table 5.1** can identify the main fluids used both as HTF and TES. In the analysed projects, TES systems use molten salt technology [6].

Table 5.1. CSP projects worldwide with two-tank storage system (last update in February 2022).

Project	Country	Status	Project Type	Installed Capacity (Mwe)	Type of panels	Type of HTF	Energy Storage system	Storage capacity (hr)	Commissioned date
Solar Electric Generating Station I (SEGS I)	US	NO	PP	13.8	PTC	Molten salts	2-tank direct (molten salts)	3	1984
Andasol-1 (AS-1)	Spain	O	C	50	PTC	Dowtherm A	2-tank indirect (molten salts)	7.5	2008
Andasol-2 (AS-2)	Spain	O	C	50	PTC	Dowtherm A	2-tank indirect (molten salts)	7.5	2009
Archimede	Italy	O	NA	5	PTC	Molten salts	2-tank direct (molten salts)	8	2010
Extresol-1 (EX-1)	Spain	O	C	50	PTC	Diphenyl/Biphenyl Oxide	2-tank indirect (molten salts)	7.5	2010
Extresol-2 (EX2)	Spain	O	C	49.9	PTC	Diphenyl/Biphenyl Oxide	2-tank indirect (molten salts)	7.5	2010
La Florida	Spain	O	NA	50	PTC	Diphenyl/Biphenyl Oxide	2-tank indirect (molten salts)	7.5	2010
Andasol-3 (AS-3)	Spain	O	NA	50	PTC	Thermal Oil	2-tank indirect (molten salts)	7.5	2011
Arcosol 50 (Valle 1)	Spain	O	NA	49.9	PTC	Diphenyl/Diphenyl Oxide	2-tank indirect (molten salts)	7.5	2011
Gemasolar Therosolar Plant (Gemasolar)	Spain	O	NA	19.9	SPT	Molten salts	2-tank direct (molten salts)	15	2011
La Dehesa	Spain	O	NA	49.9	PTC	Diphenyl/Biphenyl Oxide	2-tank indirect (molten salts)	7.5	2011
Manchasol-1 (MS-1)	Spain	O	C	49.9	PTC	Diphenyl/Biphenyl Oxide	2-tank indirect (molten salts)	7.5	2011
Manchasol-2 (MS-2)	Spain	O	C	50	PTC	Diphenyl/Biphenyl Oxide	2-tank indirect (molten salts)	7.5	2011
Termesol 50 (Valle 2)	Spain	O	NA	49.9	PTC	Diphenyl/Diphenyl Oxide	2-tank indirect (molten salts)	7.5	2011
Aste 1A	Spain	O	C	50	PTC	Dowtherm A	2-tank indirect (molten salts)	8	2012
Aste 1B	Spain	O	C	50	PTC	Dowtherm A	2-tank indirect (molten salts)	8	2012
Astexol II	Spain	O	C	50	PTC	Thermal Oil	2-tank indirect (molten salts)	8	2012

Extresol-3 (EX3)	Spain	O	C	50	PTC	Diphenyl/Biphenyl Oxide	2-tank indirect (molten salts)	7.5	2012
La Africana	Spain	O	C	50	PTC	NA	2-tank indirect (molten salts)	7.5	2012
Solana Generating Station (Solana)	US	O	C	280	PTC	Therminol VP-1/Xceltherm MK1	2-tank indirect (molten salts)	6	2013
SUPCON Delingha 10 MW Tower	China	O	-	10	SPT	Molten salts	2-tank direct (molten salts)	2	2013
ASE Demo Plant	Italy	O	D	0.35	PTC	Molten salts	2-tank direct (molten salts)	-	2013
DEWA CSP Trough project	UAE	UD	UD	600	PTC	Thermal Oil	2-tank indirect (molten salts)	11.3	2013
Arenales	Spain	O	C	50	PTC	Diphyl	2-tank indirect (molten salts)	7	2013
Casablanca	Spain	O	C	50	PTC	Diphenyl/Biphenyl Oxide	2-tank indirect (molten salts)	7.5	2013
Termosol 1	Spain	O	C	50	PTC	Thermal Oil	2-tank indirect (molten salts)	9	2013
Termosol 2	Spain	O	C	50	PTC	Thermal Oil	2-tank indirect (molten salts)	9	2013
Noor I Ouarzazate CSP Power Station (OSPS)	Morocco	O	C	160	PTC	Synthetic oil (Dowtherm A)	2-tank indirect (molten salts)	3	2015
KaXu Solar One	South Africa	O	C	100	PTC	Thermal Oil	2-tank indirect (molten salts)	2.5	2015
Crescent Dunes Solar Energy Project (Tonopah)	US	O	C	110	SPT	Molten salts	2-tank direct (molten salts)	10	2015
Shouhang Dunhuang 10 MW Phase I	China	O	C	10	SPT	Molten Salts	2-tank direct (molten salts)	15	2016
Bokpoort	South Africa	O	C	55	PTC	Dowtherm A	2-tank indirect (molten salts)	9.3	2016
Noor II Ouarzazate CSP Power Station (OSPS)	Morocco	O	C	200	PTC	Synthetic oil	2-tank indirect (molten salts)	7	2018
Delingha 50 MW Thermal Oil Parabolic Trough project	China	O	C	50	PTC	Thermal Oil	2-tank indirect (molten salts)	9	2018
Shouhang Dunhuang 100 MW Phase II	China	O	C	100	SPT	Molten salts	2-tank direct (molten salts)	11	2018
SUPCON Delingha 50 MW Tower	China	O	C	50	SPT	Molten salts	2-tank direct (molten salts)	7	2018
Ilanga I	South Africa	O	C	100	PTC	Thermal Oil	2-tank indirect (molten salts)	4.5	2018
Xina Solar One	South Africa	O	NA	100	PTC	Thermal Oil	2-tank indirect (molten salts)	5	2018

Kathu Solar Park	South Africa	O	C	100	PTC	Thermal Oil	2-tank indirect (molten salts)	4.5	2019
Noor III Ouarzazate CSP Power Station (OSPs)	Morocco	UD	C	150	SPT	Molten salts	2-tank direct (molten salts)	7	-
Aurora Solar Energy Project	Australia	UD	UD	150	SPT	Molten salts	2-tank direct (molten salts)	8	-
Atacama-1	Chile	UD	UD	110	SPT	Molten salts	2-tank direct (molten salts)	17.5	-
Copiapó	Chile	UD	UD	260	SPT	Molten salts	2-tank direct (molten salts)	14	-
Likana Solar Energy Project	Chile	UD	UD	390	SPT	Molten salts	2-tank direct (molten salts)	13	-
Tamarugal Solar Energy Project	Chile	UD	UD	450	SPT	Molten salts	2-tank direct (molten salts)	13	-
Chabei 64 MW Molten Salt Parabolic Trough project	China	UD	UD	64	PTC	Molten salts	2-tank direct (molten salts)	16	-
Dacheng Dunhuang 50 MW Molten Salt Fresnel project	China	UD	UD	50	LFR	Molten salts	2-tank direct (molten salts)	13	-
Gansu Akesai 50 MW Molten Salt Trough project	China	UD	UD	50	PTC	Molten salts	2-tank direct (molten salts)	15	-
Golden Tower 100 MW Molten Salts project Golimud	China	UD	UD	100	SPT	Molten salts	2-tank direct (molten salts)	8	-
Gulang 100 MW Thermal Oil Parabolic Trough project	China	UD	UD	100	PTC	Thermal Oil	2-tank indirect (molten salts)	7	-
Hami 50 MW CSP Project	China	UD	UD	50	SPT	Molten salts	2-tank direct (molten salts)	8	-
Luneng Haixi 50 MW Molten Salt Tower	China	UD	UD	50	SPT	Molten salts	2-tank direct (molten salts)	12	-
Qinghai Conhe 50 MW CSP Plant	China	UD	UD	50	SPT	Molten salts	2-tank direct (molten salts)	6	-
Rayspower Yumen 50 MW thermal Oil Trough project	China	UD	UD	50	PTC	Thermal Oil	2-tank indirect (molten salts)	7	-
Shangyu 50 MW DSG Tower CSP Project	China	UD	UD	50	SPT	Steamy/water	2-tank indirect (molten salts)	4	-
Urat 50 MW Fresnel CSP project	China	NO	D	50	LFR	Thermal Oil	2-tank indirect (molten salts)	6	-
Urat Middle Banner 100 MW Thermal Oil Parabolic Trough project	China	UD	UD	100	PTC	Thermal Oil	2-tank indirect (molten salts)	4	-
Yumen 100 MW Molten Salt Tower CSP Project	China	NO	D	100	SPT	Molten salts	2-tank direct (molten salts)	10	-
Yumen 50 MW Molten Slat Tower CSP Project	China	UD	PP	50	SPT	Molten salts	2-tank direct (molten salts)	6	-

Yumen MW Thermal Oil Trough CSP Project	China	UD	UD	50	PTC	Thermal Oil	2-tank indirect (molten salts)	7	-
MINOS	Greece	UD	C	52	SPT	NA	2-tank indirect (molten salts)	5	-
Diwakar	India	UD	C	100	PTC	Synthetic Oil	2-tank indirect (molten salts)	4	-
Gujarat Solar One	India	UD	UD	28	PTC	Diphyl	2-tank indirect (molten salts)	9	-
kvk Energy Solar Project	India	UD	C	100	PTC	Synthetic Oil	2-tank indirect (molten salts)	4	-
Shagaya CSP Project	Kuwait	UD	UD	50	PTC	NA	2-tank indirect (molten salts)	10	-
Redstone Solar Thermal Power Plant	South Africa	UD	C	100	SPT	Molten salts	2-tank direct (molten salts)	12	-
DEWA CSP Tower Project	UAE	UD	UD	100	SPT	Molten salts	2-tank direct (molten salts)	15	-

NA: Not available, C: Commercial, UD: Under Construction, PP: Pilot Plant, NO: Non-Operational, O: Operational and D: demonstration. Adapted from [1] and SolarPaces (<https://solarpaces.nrel.gov/>).

Molten salts can be used both as HTF and TES; therefore, they can differentiate into two configurations: (1) 2-tank direct and (2) 2-tank indirect. In the first, the HTF and the TES are the same fluid, and in the case of indirect configuration, the two media are dissimilar. On the contrary, the HTF media most used in the numbered projects, apart from molten salts, are synthetic oils such as eutectic mixtures of diphenyl-diphenyl oxide (commercially Dowtherm A), biphenyl-biphenyl oxide (commercially Therminol, VP-1) or phe-

nyl ether-biphenyl (commercially Diphyl). The most used commercially within the molten salts are those based on nitrates. Nitrate salts such as solar salt or HITEC are the most used due to their low melting and stability at high temperatures.

Specifically, solar salt is the salt most commercially employed as TES and HTF in CSP due to its excellent thermo-physical properties: good chemical stability, low cost, work temperature between 290-588°C, and high thermal transfer efficiency.

Table 5.2. CSP projects worldwide with alternative TES systems (last update in February 2022).

Project	Country	Status	Type	Installed Capacity (Mwe)	Type of panels	Energy Storage system	Storage capacity (hr)	Year
ECare Solar Thermal Project	Morocco	NO	D	1	LFR	Steam Drum	2	-
Airlight Energy Ait-Baha	Morocco	O	PP	3	LFR	Packed-bed of Rocks	5	2014
Lake cargalligo	Australia	NO	D	1	LFR	Core graphite	-	2011
Zhangbei 50 MW CSG Fresnel Project	China	NO	D	50	LFR	Solid State Formulated concrete	14	-
Zhangjiakou 50 MW CSG Fresnel project	China	UD	UD	50	LFR	Solid State Formulated concrete	14	-
ELLO solar thermal Project	France	UD	C	9	LFR	Steam Drum	4	-
Jülich Solar Tower	Germany	O	D	1.5	SPT	Ceramic heat Sink	1.5	2008
Redstone Solar Thermal Power Plant	South Africa	O	C	50	SPT	Saturated Steam	2	2016
Greenway CSP Mersin Tower Plant	Turkey	O	D	1.4	SPT	Molten salt.Single 3-phase tank	-	2012
Puerto Errado 1 Thermsolar Power Plant	Spain	O	D	1.4	LFR	Single-tank thermocline (Ruths tank)	-	2009
Puerto Errado 2 Thermsolar Power Plant	Spain	O	C	30	LFR	Single-tank thermocline (Ruths tank)	0.5	2012

Other salts with high potentials are HITEC due to their lower melting temperature (142°C) and high thermal stability (525°C) or HITEC-XL with a melting point of 120°C. However, their high viscosities limit their applicability. There are also the LiNO₃ salts (KNO₂-NaNO₃-LiNaNO₃), which have the highest heat capacity and the lowest melting points. On the other hand, there are salts based on carbonates; due to their high solidification point (above 350°C), their use in CSP is limited. Finally, there are those based on chlorides. This type of salt is one of the most promising salts for TES and HTF for CSP due to its high thermal stability (above 800°C), high thermal conductivity, low cost, and abundance, although

it exhibits high corrosion limiting its applicability in CSP. **Table 5.3** summarises the main properties of some of the most relevant SHS materials [5,7,8].

Despite their good properties and technological maturity, Molten salt-based systems are limited by environmental and health issues and relatively low heat capacity and thermal stability. Therefore, reducing the amount of salt in TES is a priority for developing this technology. Two main ways to influence this point are (1) improvement of the thermal properties of the TES material and (2) improvement of the storage technology, such as through the SMT, DMT and ST configurations, as mentioned in **Figure 2.1-b**.

Table 5.3. Thermophysical properties of sensible heat storage materials (SHS).

Material	Density (g/cm ³)	Melting Point (°C)	Stability Limit (°C)	Viscosity (mPa·s)	Specific heat (J/kg·K)	Thermal conductivity (W·m/K)	Energy density (kJ/m ³ ·K)
High alumina concrete	2.4	1600	1450	-	980	0.2	2352
Silicone Carbide ceramics	3.5	2730	-	-	866	1.4	3031
Graphite	2.3	3600	3000	-	610	155	1378
Synthetic Oil	0.9				2300	0.1	2070
Therminol, VP-1	9.1-6.6		400	0.36-0.13	2.1-2.7	0.11-0.07	18700
Water	1				4187	0.6	4174
Molten Salts							
Solar salt, NaNO ₃ -KNO ₃	1800	220	600	1.03	1495	0.55	2825
HITEC, KNO ₃ -NaNO ₂ -NaNO ₃	1.75	142	530	3.16	1550	0.5	2760
HITEC XL, Ca(NO ₃) ₂ -KNO ₃ -NaNO ₃	1.92	130	500	6.37	1450	0.52	2730
Li ₂ CO ₃ -Na ₂ CO ₃ -K ₂ CO ₃	1.85	400	850	4.3	1.4-1.5	0.49	2683
KNO ₃ -NaNO ₃ -LiNO ₃	1.8	120	600	1.5	1.63	0.3	2934
Sodium chloride	2.2	801	550	-	860	7	1861

5.2.1 Materials TES requirements

As we have seen, one of the critical elements of CSP technology is molten salt, which can be used as thermal energy storage (TES) to absorb and store thermal energy from the sun and as a heat transfer medium (HTF) to transfer the stored thermal energy to a steam generator for the production of electrical power.

Therefore, to improve the overall efficiency of CSP plants and thus decrease the LCOE of the storage systems (70% of the cost is given by the cost of the materials of the TES system), the thermal capacity, the transfer characteristics temperature and the stability of

the molten salts are the main parameters that have to be optimised to obtain an optimal behaviour of the plant

Salts with high thermal stability (> 800°C) are required since they facilitate their use in CSP with a Brayton cycle of supercritical CO₂ higher than 50%. Nitrate salts decompose around 600°C, and therefore, higher stability temperatures are necessary to develop the new generation of high-efficiency CSP plants [9]. On the contrary, one of the main limitations of the use of molten salts is their high corrosion of the installation materials at high temperatures, and this factor is even more accentuated with chlorides. The following **Figure 5.2**. TES materials requirements for CSP summarises the main requirements for TES material.

TES Requirements

- ✓ High operational temperature range: Low melting/solidification temperature and high temperature stability.
- ✓ High and uniform specific heat capacity with temperature.
- ✓ High thermal conductivity (quick charging-discharging cycles).
- ✓ Minimal supercooling.
- ✓ Low price and widely available.
- ✓ High thermal, chemical and cyclic stability.
- ✓ Non-flammable, non-toxic, and non-corrosives and low vapour pressure.

Figure 5.2. TES materials requirements for CSP.

Therefore, the maximum and minimum working temperature, thermal conductivity and diffusivity, vapour pressure, heat transfer coefficient, chemical stability, compatibility with different materials, area-volume relation, and costs are also essential properties to be considered [9]. However, the most important properties of the storage medium are the density and the specific heat since it determines the energy density [10]. The heat capacity has a direct effect on the storage capacity of the system and its heat transfer efficiency, which can be easily seen with the **equations (5.1) and (5.2)** [4,11].

Where Q: is the amount of heat, ρ : density, C_p : specific heat capacity, V: storage tank volume, T: temperature. The suffixes TES: the storage material, molten salts, HTF: heat transfer fluid, hot: cold tank temperature, and hot: hot tank temperature.

A high C_p increases the storage time and, therefore, the capacity of the TES system, helping to reduce the volume

of storage tanks for the same amount of energy, which also helps reduce the environmental and health impact generated by a large amount of salt used in the tanks. Therefore, three main key points are the research hotspots in the field of medium and high-temperature storage in recent years: (1) reducing the melting point, (2) increasing the thermal stability limit, and (3) enhancing the specific heat capacity of molten salt

5.3 Molten salt-based nanofluids: state-of-the art

It is precisely in the quest to improve the properties of molten salts that nanofluids come into play, specifically molten salt-based nanofluids (MSBNFs).

Research into these systems has increased since the first pilot plant in 1984 and the first commercial plant in 2008 with molten salt technology.

$$\text{Storage effectiveness} = \frac{\dot{Q}_{\text{TES,stored}} - \dot{Q}_{\text{TES,discharged}}}{\rho_{\text{TES}} C_{p,\text{TES}} V_{\text{TES}} (T_{\text{hot}} - T_{\text{cold}})} \quad (5.1)$$

$$V_{\text{TES}} = \frac{Q_{\text{TES}}}{\varepsilon \rho_{\text{HTF}} C_{p,\text{HTF}} (T_{\text{hot}} - T_{\text{cold}}) + (1 - \varepsilon) \rho_{\text{TES}} C_{p,\text{TES}} (T_{\text{hot}} - T_{\text{cold}})} \quad (5.2)$$

The strategy of improving properties through the incorporation of nanoparticles is presented as one of the most promising options to strengthen the thermophysical properties of MSBNFs and to be able to develop high energy density TES systems.

Over 250 publications from 2009 to the end of 2021 have been published on solar salt-based nanofluids (web of science core collection). One of the first publications was performed by D. Banerjee et al., [12]. Their results show a 14.6% increase in sensible heat capacity after incorporating SiO₂ nanoparticles into LiCO₃-K₂CO₃. Currently, the MSBNFs research field is led by Shin, D and Banerjee, D. from Texas A&M University (USA) and Ding, Y. from the University of Birmingham (UK).

Likewise, the publication by M. Chieruzzi et al., [13] entitled "*Effect of nanoparticles on the heat capacity of nanofluids based on molten salts as PCM for thermal energy storage*" is one of the most cited publications, along with those by D. H. Shin et al., [14] "*Enhanced Specific heat of Silica nanofluids*", H. Tiznobaik et al., [15] "*Enhanced specific heat capacity of high-temperature molten salt-based nanofluids*", de , C. Castro et al., [16] "*Thermal Properties of Ionic Liquids and IoNanofluids of Imidazolium and Pyrrolidinium Liquids*", and

B. Dudda et al., [17] "*Effect of nanoparticle dispersion on specific heat capacity of a binary nitrate salt eutectic for concentrated solar power applications*", are the 5 most cited publications in this field of research.

Figure 5.3 shows the Top-5 of some of the most relevant metrics: authors, countries, journals, funding agencies and research areas (according to the web of science, core collection Feb-2022).

The research areas give an idea of the research carried out and the engineering application of nanofluids based on molten salts.

The one that can be more striking is that the physics area is in second place. But it is not surprising; it reflects where part of the efforts of scientists focuses on fundamental understanding aspects of the behaviour of nanofluids and developing a theoretical framework.

The main research goals in developing MSBNFs are a high heat capacity for the HTF medium to capture as much thermal energy as possible and store the largest amounts of heat in the TES.



Figure 5.3. Top-5 of the main authors, countries, journals, funding's agencies and research areas involved in MSBNFs research.

In addition, a low melting temperature is required to prevent freezing of nanofluids in pipes, low viscosity to decrease pumping energy, low corrosion and high decomposition temperature to maximise operating temperature to increase overall efficiency and reduce costs of CSP plants [18].

Under this context, in **Figure 5.4** the key results and research state in MSBNFs are outlined. In recent years,

the research has made significant progress on MSBNFs.

These advances come hand in hand with the advancements and state of the art in the general line of nanofluids seen in the introduction. Some of the most studied parameters that have a high incidence on the final properties of MSBNFs are related to the nanoparticles (size, shape and concentration) and the preparation method.

Molten Salt – based nanofluids

Research State

Parameters

- NPs size, shape and concentration
- Preparation method

Corrosion

- ✓ NPs forms a protective layer that acts as barrier and reduces the corrosion rates.

- Optimum concentration 1 wt%
- Variation of melting and enthalpy point
- ✓ Enhanced thermal stability
- ✓ Reduction solidification time
- ✓ Enhanced Specific Heat
- ✓ Thermal conductivity enhancement
- ✓ Higher discharge rates
- ✓ Enhanced Nussel Number
- ✓ Enhanced heat transfer coefficient
- x Thermal cycling decreases properties

Main studied systems

Nitrates:

- Solar salt
- CaNaK Nitrates
- LiNaKCa Nitrates
- Kca Nitrate
- KNO₃
- NaK Nitrates
- HITEC

Carbonates:

- LiNaK carbonates
- LiK carbonate

Chlorides:

- NaCaMg Chloride
- BaCaLiNa Chloride

Bromides:

- LiNaKCa Bromide

Stability

- x Low nanoparticles stability
- Causes:
 - x Brownian motion
 - x Sonication time
 - x Particle-Particle and Particle-Fluid interaction
- Enhancement methods:
 - Surfactants
 - pH control
 - Ultrasonic agitation

Characterization techniques

- SEM
- DRX
- EDS
- FT-IR
- DSC
- Rheometer
- TGA
- Zeta Potential

Theoretical Framework

- ? Layering phenomenon
- ? Relation between NPs effects and Coulombic potential energy
- ? Ionic exchange between NPs and salts
- ? Dendritic nanostructures
- ? Mathematical Model I – Model II

Challenges and limitations

- Inconsistent finding for similar molten salts and nanoparticles.
- Lack of a strong theoretical framework and clear tendencies about its behaviour.
- Non-suitable preparation method for large scale production.
- Needed to develop more cost-effective methods to produce NPs and stable MSBN.
- Needed to develop suitable measurement methodologies and characterization techniques.
- Needed to develop strategies to obtain stable and homogeneous MSBN.

Figure 5.4. Molten salts-based nanofluids' main research topics and current state, challenges, and limitations.

In this last point, the wet preparation method has been the most used and with which the best thermophysical properties are reported, despite its long preparation times to disperse the nanoparticles and, therefore, its low scalability in terms of costs, as shown in the study performed by Y. Grosu et al., [19]. Regarding the concentration of nanoparticles, an optimal concentration of around 1 wt% has been reported in various studies for different sizes of nanoparticles. Thus, many of the published results employ MSBNFs in this range of concentrations. In **Table 5.4**, some of the best and worst values reported in the literature have been selected. Furthermore, in **Appendix 1** 270 Cp values are compiled for different MSBNFs systems. In the introduction, we could see the high discrepancy of results, and the case of the MSBNFs is not an exception.

Although the results in **Table 5.4** may indicate that carbonate and lithium-based salts exhibit the best properties, these values can be misleading, for example, in the case of the $\text{Li}_2\text{CO}_3\text{-K}_2\text{CO}_3$ system with 1.5 wt% SiO_2 , an increase of 121% of the Cp [20] was reported, but other studies reported much lower variations of 26% in the same systems. Or, as is the case of solar salt, where one of the worst results of Cp of -

19.3% was reported incorporating 0.5% of SiO_2 nanoparticles, other studies under similar conditions reported 3.4% [20,21], 4.9% [22] or 25% [20,21].

In addition, although the literature indicates that the increase in Cp is due to low concentrations of nanoparticles, there are no clear trends in its effect or the effect of the shape or nature of the nanoparticles. An example are the results published by Y. Huang et al., [23], which reported an increase in Cp of 168% with concentrations of 10.4 wt%.

Furthermore, a lack of homogeneity regarding the effect of temperature has also been identified, with contradictory results being reported. **This indicates one of the first obstacles in developing MSBNs, the dispersion and lack of homogeneity of the results**

Another of the most relevant aspects of MSBNFs is their thermal stability, their enthalpy values and melting temperature or degradation temperature. In the same way as the Cp values, the results are contradictory [24–28]. For example, the studies by X. Qiangzhi et al., [29] show a decrease in melting temperature, and those of Y. Luo et al., do not show an increased melting temperature [27].

Table 5.4. Specific heat capacity of selected molten salt-based nanofluids investigations.

Molten Salt	NPs	Avg. Concentration (wt%)	Avg. Size (nm)	Avg. Temperature (°C)	Cp variation (ΔC_p)	Ref.
Selected values of ΔC_p enhancements						
NaNO ₃ -KNO ₃ (60:40)	Nano-Mg	10.4	102.5	180	168.1	[23]
Li ₂ CO ₃ -K ₂ CO ₃	SiO ₂	1.5	11	360	121	[20]
NaNO ₃ -KNO ₃ (60:40)	Nano-Mg	14.8	102.5	180	118.6	[23]
K ₂ CO ₃ -LiCO ₃ -NaNO ₃	SiO ₂	1	20	540	113.66	[38]
K ₂ CO ₃ -LiCO ₃ -NaNO ₃	SiO ₂	1	20	540	108.70	[38]
K ₂ CO ₃ -LiCO ₃ -NaNO ₃	SiO ₂	1	20	520	92.12	[38]
ACaSEu (Alkali Chloride Salt Eutectic)	SiO ₂	1.5	10.5	540	87.5	[39]
K ₂ CO ₃ -LiCO ₃ -NaNO ₃	SiO ₂	1	20	520	80.61	[38]
K ₂ CO ₃ -LiCO ₃ -NaNO ₃	SiO ₂	1	20	500	79.88	[38]
K ₂ CO ₃ -LiCO ₃ -NaNO ₃	SiO ₂	1	20	500	70.12	[38]
NaNO ₃ -KNO ₃ (60:40)	SiO ₂ - Al ₂ O ₃	1	101	125	57.7	[20]
K ₂ CO ₃ -LiCO ₃ -NaNO ₃	SiO ₂	1	20	360	42.4	[38]
K ₂ CO ₃ -LiCO ₃ -NaNO ₃	SiO ₂	1	20	360	36.8	[38]
K ₂ CO ₃ -LiCO ₃ -NaNO ₃	SiO ₂	1	20	340	35.43	[38]
K ₂ CO ₃ -LiCO ₃ -NaNO ₃	SiO ₂	1	20	360	35.2	[38]
NaNO ₃ -KNO ₃ (60:40)	SiO ₂ - Al ₂ O ₃	1.5	101	118	34.8	[20]
Li ₂ CO ₃ -K ₂ CO ₃	Al ₂ O ₃	1	10	540	33	
K ₂ CO ₃ -LiCO ₃ -NaNO ₃	SiO ₂	1	20	500	32.93	[38]
ACaSEu (Alkali Chloride Salt Eutectic)	Al ₂ O ₃	1	10	500	32	[39]
Li ₂ CO ₃ -K ₂ CO ₃	Al ₂ O ₃	1	10	540	32	[40]
Selected values of ΔC_p worsening						
NaNO ₃ -KNO ₃ (60:40)	Al-Cu	10	160	400	-6.39	[41]
BaCl ₂ -H ₂ O	TiO ₂	0.6485	20	300	-7.25	[42]
BaCl ₂ -H ₂ O	TiO ₂	0.6485	20	45	-7.35	[39]
LiNO ₃ -NaNO ₃ -KNO ₃	SiO ₂	0.5	102.5	40	-7.42	[40]
NaNO ₃ -KNO ₃ (60:40)	SiO ₂ - Al ₂ O ₃	0.5	101	183	-7.5	[20]
NaNO ₃ -KNO ₃ (60:40)	Al ₂ O ₃	0.5	13	125	-7.6	[20]
NaNO ₃ -KNO ₃ (60:40)	Al ₂ O ₃	0.5	13	183	-7.6	[20]
KNO ₃	SiO ₂ -Al ₂ O ₃	1	10	275	-7.8	[40]
KNO ₃	Al ₂ O ₃	1	13	370	-7.8	[26]
NaNO ₃ -KNO ₃ (60:40)	Al ₂ O ₃	4.6	9	208	-8.1	[20]
NaNO ₃ -KNO ₃ (60:40)	TiO ₂	0.5	50	350	-8.76	[24]
KNO ₃	TiO ₂	0.5	50	258	-9.09	[24]
NaNO ₃ -KNO ₃ (60:40)	Al ₂ O ₃	2.7	13	208	-9.4	[20]
NaNO ₃ -KNO ₃ (60:40)	TiO ₂	1.5	20	125	-10.7	[20]
NaNO ₃ -KNO ₃ (60:40)	TiO ₂	1.5	20	183	-11.8	[20]
NaNO ₃ -KNO ₃ (60:40)	Al ₂ O ₃	4.6	13	208	-12.5	[20]
NaNO ₃ -KNO ₃ (60:40)	TiO ₂	0.5	20	125	-14.4	[20]
NaNO ₃ -KNO ₃ (60:40)	TiO ₂	1.5	50	350	-14.6	[24]
NaNO ₃ -KNO ₃ (60:40)	TiO ₂	0.5	20	183	-15.6	[20]
NaNO ₃ -KNO ₃ (60:40)	SiO ₂	0.5	7	183	-19.3	[20]

The same happens with enthalpy values, or thermal stability temperatures [27,30–34]. For example, Pramod et al., [35] showed that incorporating nanoparticles in solar salt increased the thermal stability of nanofluids, in contrast to the studies carried out by Myers et al., [36] or P. Andreu-Cabedo et al., [37] did not observe significant variations. This point indicates the second main obstacle to which MSBNFs are subjected: the lack of clear trends on the behaviour of MSBNFs-

In recent years, some articles have been studying the corrosion rate of MSBNFs. The high corrosion of molten salts, especially at high temperatures, in CSP plants is one of the biggest obstacles facing researchers.

Some studies show that incorporating nanoparticles in molten salts is a possible strategy to reduce corrosion rates [18]. Studies such as the one carried out by A. Fernández et al., [43] observed a decrease in corrosion rates with the addition of 1wt% of SiO₂ nanoparticles in solar salt. They described that this decrease is due to the incorporation of nanoparticles in the salt-wall interfaces, generating a protective layer. On the contrary, other studies, such as the one carried out by J. Piquot et al., [44] showed that nano-

particles considerably increase the corrosion rates of metallic components. Some research indicates that these two contradictory effects are due to the formation of microbubbles between the nanoparticles; reducing it, the formation of the protective layer prevails, and the corrosion rates are mitigated [45].

Other relevant advances in MSBNFs are those related to the stability of nanoparticles in molten salts. The main strategies followed have been:

1. The use of surfactants modifying the surface properties of hydrophobicity of the nanoparticles. Some of the surfactants studied for high temperatures have been sodium dodecylbenzene sulfonate (SDBS) [46], sodium dodecyl sulfate (SDS) [46,47], and Gum Arabic (GA) [48,49].
2. Controlling the time and power of sonication [50,51].
3. Through nanoparticles' surface modifications to reduce the surface energy [52].
4. Controlling the pH, where the stability of the MSBNFs decreases when the pH value tends to equal the isoelectric point (IEP) value [53,54].

Apart from studying the properties and behaviour of MSBNs, A. Alashkar et al., [55] carried out a thermo-economic study of the use of nanofluids in a PTSC system with incorporated TES. Their results show that the substitution of conventional HTF and TES materials increases the power output and the net saving, reducing the LCOE. Therefore, nanofluids have the potential to improve the performance and cost parameters.

Another relevant aspect that we can see in **Figure 5.4** are the characterisation techniques. Despite the number of characterisation techniques used, such as SEM, TEM, XRD or FTIR, they present a limitation: they are performed at room temperature or low temperatures. Therefore, there is a lack of techniques for characterising MSBNFs in a liquid state and therefore at high temperature, which helps us have relevant information to understand the thermophysical behaviour of nanofluids and the particle-liquid interaction.

Finally, it is the research in the development of a theoretical framework to explain the behaviour of nanofluids and specifically of the mechanisms involved in the abnormal behaviour of the C_p of MSBNFs, which has the most relevance to be able to respond to all

the discrepancies and develop nanofluids with specific properties.

5.4 Nanofluids specific heat capacity

As seen in the previous sections, heat capacity is one of the most relevant properties for developing high energy density TES systems. And it is precisely the heat capacity, along with thermal conductivity and viscosity, which are three of the most interesting nanofluids properties, as described in the introduction.

5.4.1 Theoretical framework

Many studies have reported increases in thermal conductivity and models to predict and explain these values. One of those main models is based on the aggregation effects of nanoparticles. Suspended nanoparticles tend to cluster in fractal-like structures due to Brownian motion, which creates a preferential pathway for heat conduction and explains the increase in thermal conductivity [56]. Currently, the 4 most considered mechanisms to explain thermal conductivity are (1) the nature of heat transfer in the nanoparticles, (2) the Brownian motion, (3) liquid layering at the nanoparticle's interfaces, and finally (4) clustering of the

nanoparticles. Despite this, the mechanisms involved are still not well understood due to the lack of reliable results to support these theories. As for heat capacity, we find ourselves in the same situation, with the addition that there is much less research. Furthermore, some of the mechanisms proposed for conductivity cannot be applied to explain the reported controversial values of heat capacity. This is because the heat capacity, as we have seen, is directly related to the physical structure; therefore, the low concentration in nanoparticles supposedly cannot be modified the systems' structure and therefore has a negligible effect on the heat capacity.

In the next point, the main theories and models developed to describe nanofluids' heat capacity and behaviour are described.

5.4.1.1 Main proposed mechanisms:

Initially, in 2011, Shin, D. and Banerjee, D. [57] compiled the three main possible mechanisms that could explain the abnormal increase in heat capacity. These three modes are as follows:

Mechanism 1: Higher specific heat capacity of nanoparticles than bulk.

Different studies show an increase in the heat capacity of nanoparticle compared to bulk materials. Therefore, they indicate that the heat capacity increases with the decrease in particle size [58,59]. Thus, the variation of C_p would be linked to the augmentation of the specific surface areas [60].

Mechanism II: Solid-Liquid interaction energy.

This mechanism depends on the high specific surface area of the nanoparticles within the molten salts. One of the proposals maintains that the particle-liquid interface has an abnormally high resistance, hypothesizing that the high interfacial resistance acts as a mechanism for thermal energy storage. However, this theory has little support in the literature, both experimentally and theoretically [61,62].

Mechanism II: Layering of liquid molecules at the surface to form a semi-solid layer.

This mechanism describes a clustering of liquid surface molecules around nanoparticles to form a semi-solid layer. The presence of a dense semi-solid layer of liquid particles on the surface of the nanoparticles is thought to contribute to the increased heat capacity of the nanofluid. This effect is attributed to the thermal properties of

this layer. However, because the heat capacity of salt in the solid state is less than that in the liquid state, there is little reason to believe that a semi-solid phase of salt would have a higher C_p than either phase [61,63–66]. Some of the main contributions of recent years are summarised below, both based on these mechanisms and new contributions from an experimental and computational approach to developing the MSBNFs heat capacity theory.

Sin, D. and Banerjee, D. in **2011** observed a formation of **percolation networks** forming **fractal-like fluid nanostructures** by nanoparticles aggregation through SEM in lithium carbonate and potassium carbonate molten salts doped with SiO_2 nanoparticles (1 wt%) [14], and in alkali metal chloride-salts eutectics with the same nanoparticles type and concentration [61]. They proposed the explanation of specific heat capacity enhancement due to the high specific surface energies associated with the high specific surface area of the nanoparticles, its distinct thermophysical properties to molten salt's heat capacity enhancement.

Additionally, various studies report similar nanostructures, like Tiznobaik, H. and Shin, D. [15] in **2012** who observed similar formations of **needle-**

like structure with high specific heat capacity in lithium carbonate and potassium carbonate with SiO_2 nanoparticles of dissimilar nominal diameters and the same concentration (1 wt%) Or the study performed in 2018 by W. Song et al., [55] in quaternary nitrate salts with 15 wt% of SiO_2 nanoparticles. Despite this, such as the one carried out by M. Chieruzzi et al., [13] in **2013** with a similar system does not observe these nanostructures.

Other studies, such as the one carried out by C. De Castro et al., [16] in 2010, suggest the existence of the formation of **nanoclusters** and preferred paths for heat transfer and storage. Furthermore, in 2015 H. Tiznobaik et al., [68] identified that the formation of nanostructures during the formation of the **semi-solid layer** continues to grow until forming **long-range dendritic nanostructures** larger than nanoparticles with a high specific area and surface energy that increase C_p [69].

Nanolayer formation: semi-solid nanolayer around nanoparticles is suggested sometimes as the responsible for nanofluids thermophysical properties enhancement. Through molecular dynamics simulations, various authors studied the formation of a semi-solid layer, known as the **layering phenome-**

non (mechanism III), to explain the increase in heat capacity, such as the study by B. Jo et al., [70] in 2014. This mechanism has been extensively studied to explain the thermal conductivity behaviour.

MD simulations and simple liquid-solid interfaces, demonstrates that the layering of the liquid atoms at the liquid-solid interfaces does not have any significant effect on thermal transport properties such as thermal conductivity [62]. Otherwise, other studies, such as the performed by L. Li et al., [64] by tracking the movement of the solid nanoparticles and the liquid atoms, found that a solid-like thin liquid layer is formed at the interface between the nanoparticles and liquid. This layer moves with the Brownian motion of the nanoparticles, and this layer contributes to the significant enhancement of the nanofluids thermal conductivity.

Other computational studies also explain the variation of thermal conductivity upon confinement of liquids at the nanoscale. Nonetheless, only a few studies are related to modelling the effect of a nanolayer on the specific heat capacity of [63,73]. They observed a **relationship between layering and** the increase in **Cp**. On the contrary, the study carried out by A. Zabalegui et al., [64]

reported that in the case of PCMs, the interfacial liquid layering could not explain the behaviour of nanofluids, and what the **nanoparticles clustering** has the most significant influences in the **Cp**.

The layering theory makes more sense when the formation of nanostructures is described since these structures can modify the structure of the molten salts, altering the heat capacity [69].

5.4.1.2 *Mathematical models: Heat capacity prediction*

Different mathematical models developed from the mechanisms described above to determine the heat capacity of nanofluids are shown in **Table 5.5**.

Model I, **eq. 6.3**, was developed by Pak and Cho et al., [74] and is based on the liquid-particles mixture theory and the dependency of the particle concentration. However, this model is approximately valid for dilute suspensions when small density differences exist between base fluid and nanoparticles. Xuan and Roetzel et al., [75] modified this correlation by assuming thermal equilibrium between the nanoscale solid particles and the liquid phase, including the density, Model II, **eq.6.4**.

Nevertheless, the literature showed a large gap between the expected values and the values obtained experimentally [12,76].

Finally, Dudda and Shin adapted these models in **eq.6.5**, considering the nanostructure's mass and heat capacity, and in **eq.6.6**, considering the layering phenomenon [56,77,78]. Despite this, these equations are only theoretical. They cannot be empirically demon-

strated since the nanostructures' properties and the nanolayer are unknown and only estimated using simulation tools such as MD simulations. Therefore, no robust model is available in the literature that explains the anomalous behaviour of molten salt-based nanofluids—indicating that more experimental and theoretical studies are required.

Table 5.5. Proposed mathematical models to predict nanofluids specific heat capacity.

Model I	$C_{p,nf} = \phi \cdot C_{p,s} + (1 - \phi) \cdot C_{p,bf} \quad (6.3)$ <p>$C_{p,nf}$ = specific heat capacity of the nanofluid. $C_{p,s}$ = solid particle specific heat capacity. ϕ = particle volumetric concentration and $C_{p,bf}$ = base fluid specific heat.</p>
Model II	$C_{p,nf} = \frac{\phi \cdot \rho_s \cdot C_{p,s} + (1 - \phi) \cdot \phi \cdot \rho_{bf} \cdot C_{p,bf}}{\rho_{nf}} \quad (6.4)$ <p>ρ_s = solid particles density. ρ_{bf} = base fluid density and ρ_{nf} = nanofluid density.</p>
Nanostructures	$C_{p,nf} = \frac{m_s \cdot C_{p,s} + m_{bf} \cdot C_{p,bf} + m_{ns} \cdot C_{p,ns}}{m_s + m_{nf} + m_{ns}} \quad (6.5)$
Nanolayer	$C_{p,nf} = \frac{C_{p,s} \cdot W_p + C_{p,nanolayer} \cdot W_{nanolayer} + C_{p,f}(W_f - W_{nanolayer})}{W_f + W_p} \quad (6.6)$
	W=weight

5.5 Challenges and drawbacks: key points

sodium nitrate salt (NaNO_3) to reduce the number of variables.

Despite the MSBNFs potential, there are some limitations of using MSBNFs in CSP, such as the high cost of nanoparticles and preparation techniques, the increase in the pressure drop and the aggregation of the nanoparticles, hindering maintaining long-term properties [18].

Therefore, the low stability, agglomeration, and preparation methods and the lack of a solid theoretical framework make the advances in MSBNFs research and implementation difficult.

Therefore, the review of state of the art in MSBNFs has pointed out the different key points that have to be solved for the advancement in nanofluid research. The main key points that have been selected to study in this thesis are summarised below.

The following chapters will be guided through these key points, providing the developed research to contribute to the state of the art and progress in nanofluids science.

The studies that will be presented will be based on mono-component salts:

Relevance

The high number of publications point out a lack of general overview of nanofluids' past, current, and future research state and their social relevance.

**Key
point 2**

Nanoparticles

No clear tendencies about nanoparticles' effect.

Literature suggests:

Maximum specific heat capacity enhancement around 1 wt% of nanoparticle concentration.

Effect of nanoparticles size, concentration, temperature.

**Key
point 4**

Thermal Stability

There are no clear trends in the effect of nanoparticles on the thermal stability of MSBNFs.

Lack of information on the stability of the properties under working conditions in CSP.

**Key
point 6**

**Key
point 1**

The literature shows a high discrepancy and contradictory results between similar systems and experimental conditions.

No clear trends on the thermo-physical properties of MSBNFs.

Discrepancies

**Key
point 3**

Lack of a robust theoretical framework to explain the abnormal thermal behaviour of nanofluids.

Main proposed mechanism: Formation of a semi-solid layer and nanostructures in log-range terms with high specific surface areas.

There are no clear experimental demonstrations of the formation of nanostructured semi-solid layer and their properties.

Framework

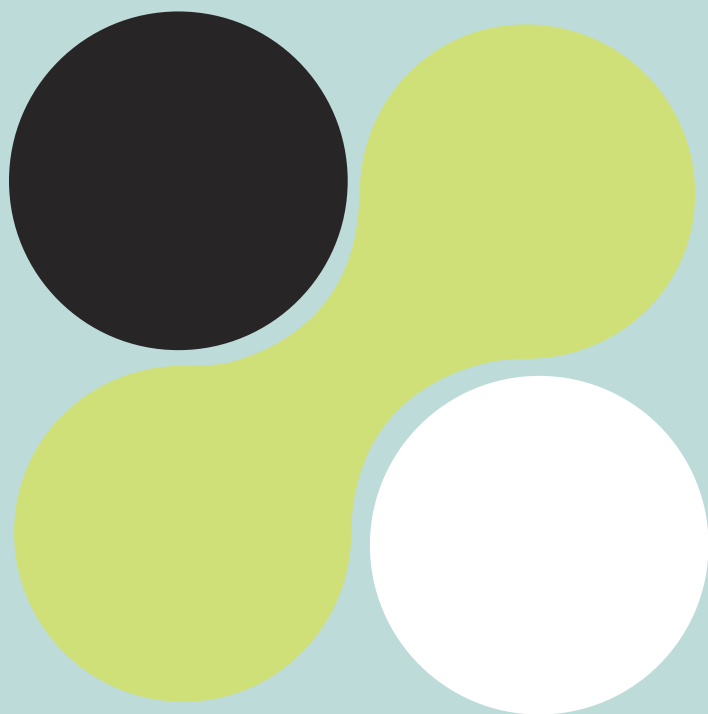
**Key
point 5**

Lack of techniques to characterize MSBNFs in a liquid state at high temperature.

Characterization

Past, actual and
future trends of
nanofluids research

Paper 1





Key point 1
Relevance

6. Past, actual and future trends of nanofluids research

Bibliometric study

6.1 Introduction

In the previous chapter, an overview of nanofluids' state of the art was summarized from a scientific point of view. Despite this, given the high number of publications, the impact and scope of this research is also important. Therefore, questions such as current or future trends, the main countries publishing in the topic, researchers/authors, or institutions involved in that field, the main journals used by the scientific community to report the main advances in the state of the art, or the available funding for the research, are questions that need to be known.

In addition, another relevant aspect is the lack of a global and unified vision on this research field.

This chapter address these key points and contextualize the research and highlight its impact on society.

One of the ways to analyse the bibliography is through a bibliometric analysis. A bibliometric is a quantitative analysis of publications to study and analyse scientific activity. Through mathematical and statistical methods, publications are analysed to assess the impact and evolution of scientific research using various indicators. Therefore, the potential of this type of study is to offer a broad perspective on the

past, current, and future of nanofluids research. For example, for researchers, these indicators are relevant because they offer value on the dissemination and impact of publications among the scientific community. Furthermore, helps researchers to select the most appropriate journals to disseminate their results, the topic to start a new project/PhD, to find researchers with common fields, or to find new collaboration around the world. Therefore, this type of analysis facilitates national and international collaborations, and has perspectives outside your work cluster. On the contrary, it has relevance not only for researchers but also for organizations because it allows obtaining objective measurements of the quality of the research, researchers, or groups. Also, it allows identifying the regions/countries that have the most impact on research, its growth, and potential applications [1–4].

6.1.1 Relevance

In recent years the field of nanofluids has aroused high interest in the scientific community around the world. Consequently, many authors have been involved in this research, generating a high number of scientific publi-

cations. This fact means that it is increasingly difficult to have a general and objective point of view of new advances and future trends. In addition, investigations are more and more specialized and technical. In this sense, review articles play a relevant key point to summarize the research. Despite this, there is a lack of information on social, economic, or demographic aspects to understand the relevance and status of the research.

Therefore, contextualizing the research field helps us to have general overview. Thus, offer some key points to understand the social benefit, therefore, its incidence in society, being this the final objective of any research.

To this end, a bibliometric study helps to contextualize a research field, identify the most relevant or specialized researchers, and quantitatively analyse the relevance of the research field in a global context. And most importantly, it helps us identify future trends. Finally, the most relevant issue is that is the first time that nanofluids literature is analysed through a bibliometric analysis, offering original data.

6.1.2 Objectives

The main objective of this research is to understand the nanofluid's context, know the main applications and identify the past, present, and future trends.

This study has been approached from two points of view: (1) an overview of the nanofluids field; identifying future trends, main applications, and main authors, among other parameters. (2) The analysis of a particular case of nanofluids for energy sector, mainly in renewable energy applications. Finally, (3) to know the nanofluid research state in the European Union.

Specifically, this study has a particular objective for this thesis to highlight its scientific and social relevance (**Key point I**).

6.2 Paper 1

Development of Nanofluids” since 17th March 2022, as shown in **Figure 6.1**.

The complete study is accepted in the *Journal of Nanofluids*, under the title: "A Bibliometric Analysis of Research and

ACTION	STATUS	ID	TITLE	SUBMITTED	DECISIONED
	ADM: Chamkha, Ali	JON-2021-0023.R2	A Bibliometric Analysis of Research and Development of Nanofluids	14-Mar-2022	17-Mar-2022
	<ul style="list-style-type: none"> Accept (17-Mar-2022) Awaiting Production Checklist 		View Submission		
	view decision letter Contact Journal				

2
3
4
5
6
7
8
9
10
11
12
13
14
15
16
17
18
19
20
21
22
23
24
25
26
27
28
29
30
31
32
33
34
35
36
37
38
39
40
41
42
43
44
45
46
47
48
49
50
--

A Bibliometric Analysis of Research and Development of Nanofluids

Adela Svobodova-Sedlackova^{1,2}, Alejandro Calderón¹, Camila Barreneche¹, Rebeca Salgado-Pizarro¹, Pablo Gamallo^{1,2} and A. Inés Fernández^{1,*}

¹ *Departament de Ciència de Materials i Química Física, Universitat de Barcelona, C/Martí i Franqués 1, 08028, Barcelona, Spain*
² *Institut de Química Teòrica i Computacional, IQTCUB, Universitat de Barcelona, C/Martí i Franqués 1, 08028, Barcelona, Spain*

*Correspondence: A. Inés Fernández, ana_inesfernandez@ub.edu

Submitted/Received: 12-1-2021/ Revised/Accepted: 03-14-2022/

Abstract

Nanofluid concept was defined over 28 years ago. Since then, a veritable science has been developed around this concept. From 1993 until 2020, up to 18021 articles were published in high-quality journals worldwide. The high scientific interest in nanofluids lies in their exceptional thermophysical properties and their possibilities to design more efficient processes and systems. Although the numerous articles, there is a lack of information on the scope, its social and economic impact, or its future trends. This study provides an overview through bibliometric methods that allow better knowledge of the research field. The main goal is to offer a more generalized and strategic vision to help those researchers interested in this topic with accurate information on its impact. In addition, this study helps to maximize international collaborations and provide relevant information to decision-makers. The analysis reveals that research in nanofluids in the last decade has experienced a great specialization in a wide variety of new applications, reaching more new sectors. The main research communities, the most productive authors, or the most relevant journals are some of the analyzed metrics that provide key parameters for contextualization, allowing a clear vision of the current state of the nanofluids research field.

Keywords: Nanofluids; Heat Transfer Fluid, Thermal Energy Storage, Working Fluid, Bibliometric Analysis

Figure 6.1. Article accepted for publication entitled “A Bibliometric Analysis of Research and Development of Nanofluids” in the *Journal of Nanofluids* by American Scientific Publishers.

6.2.1 Graphical Abstract

Figure 6.2 summarizes the most relevant results.

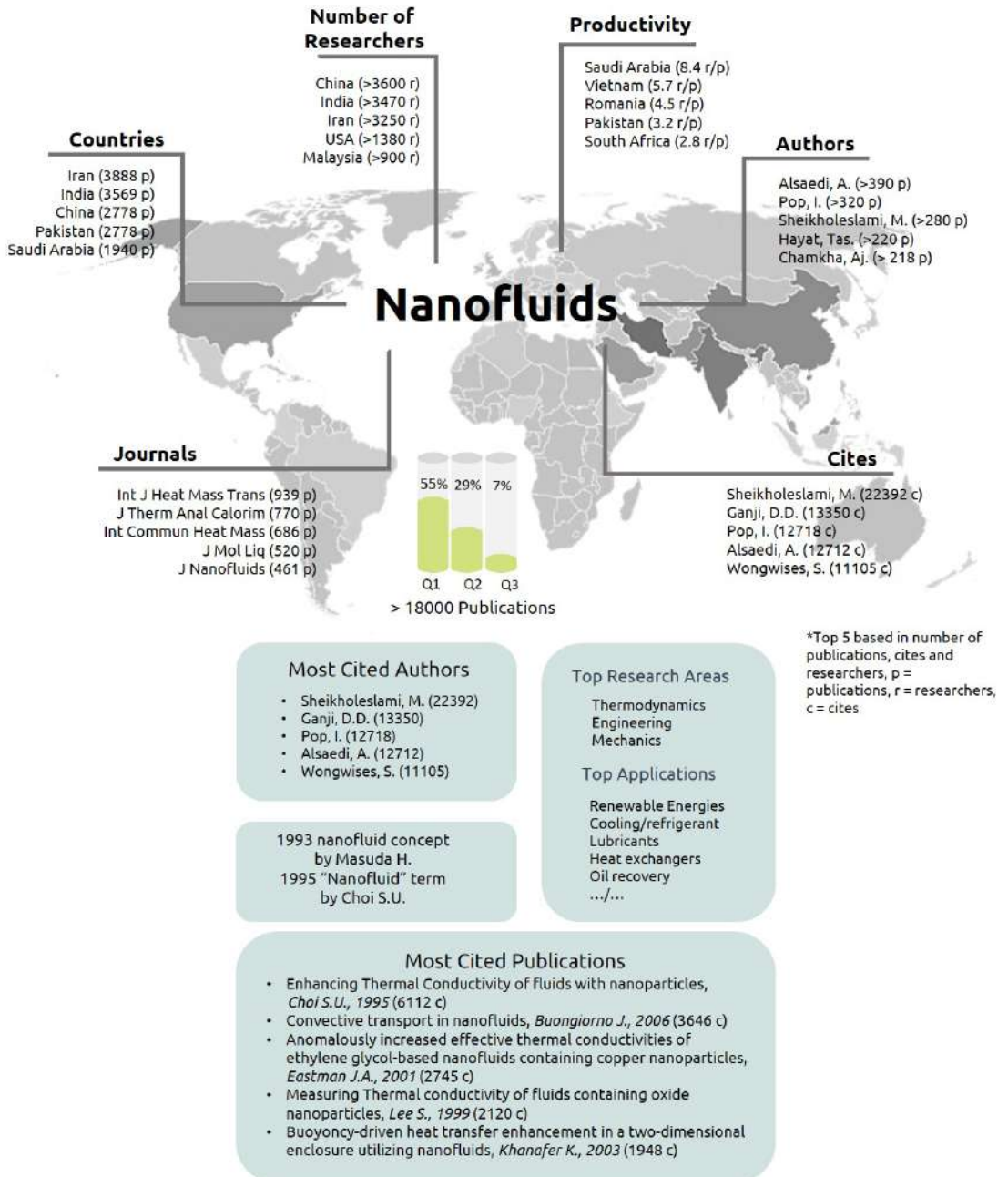


Figure 6.2. Graphical abstract of the article "A Bibliometric Analysis of Research and Development of Nanofluids".

6.2.2 Contribution to the state-of-the-art

A graphic consisting of a light blue rounded rectangle. Inside it is a green circle with a white border. The text 'Key point 1 Relevance' is centered within the green circle.

Key point 1 Relevance

The high number of publications point out a **lack of general overview** of nanofluids' past, current, and future research state and their social relevance.

- ✓ Thanks to the exhaustive bibliometric analysis, it has been possible to obtain a more realistic and unified overview.
- ✓ The vision that we have may be biased and delimited due to the little information on the state of this research outside our usual work cluster, which means that researchers are unaware of much of the progress. In part, this is a consequence of the growth and greater scope of research since efforts to unify and review the entire bibliography are practically impossible. Accordingly, besides the reviews on the state-of-the-art, this type of quantitative analysis of the publications offers us this general vision of the research progress, so necessary for adequate progress and to reach higher TLRs.
- ✓ Therefore, this study helps those interested in this research field a nanofluids overview impact from different points of view. In the first place, it gives a quantitative value of the number of publications, authors, journals, and countries involved. And secondly, it offers the top-10 of these parameters. On the other hand, the analysis highlights the need for greater collaboration, especially international, since there is

little collaboration between the principal researcher's nodes that lead scientific production. This means that there is low unification and cooperation between the main authors and/or research groups.

- Through the various metrics that have been used in this analysis, we can highlight the following relevant points that can help in the consolidation and advancement of this research:
- The identification of the main authors and work clusters encourages collaboration, in addition to helping to identify possible collaborators to request international projects and funding.
- The identification of the main journals helps, on the one hand, researchers to find the most suitable journals to publish their research, and on the other hand, it makes it easier for those interested in the subject where to find relevant information. Similarly, highlighting the most relevant and most cited publications helps identify the focus of research interest.
- The identification of the main countries shows us the interest of the regions in a particular field, and therefore, of their needs and interests. In addition, if financing and applications are analysed, it helps to understand the real socio-economic impact.
- Finally, analysing the research trends, from the point of view of applications and keywords, gives us an idea of the maturity and specialization of the research.

- ✓ In the case of this thesis, the analysis has contributed to having a much more solid context and impact values. Additionally, the identification of the most relevant publications and authors has helped to provide relevant information and different points of view in terms of applications, technological maturity, and advances, as well as the difficulties to which researchers are subjected. This last point has been key to devising new research strategies and responding to existing limitations to nanofluids' research progress.

6.2.3 Publication

The article is attached below.

A Bibliometric Analysis of Research and Development of Nanofluids

Adela Svobodova-Sedlackova^{1,2}, Alejandro Calderón¹, Camila Barreneche¹, Rebeca Salgado-Pizarro¹, Pablo Gamallo^{1,2} and A. Inés Fernández^{1,*}

¹ *Departament de Ciència de Materials i Química Física, Universitat de Barcelona, C/Martí i Franqués 1, 08028, Barcelona, Spain*

² *Institut de Química Teòrica i Computacional, IQTCUB, Universitat de Barcelona, C/Martí i Franqués 1, 08028, Barcelona, Spain*

*Correspondence: A. Inés Fernandez, ana_inesfernandez@ub.edu

Abstract

Nanofluid concept was defined over 28 years ago. Since then, a veritable science has been developed around this concept. From 1993 until 2020, up to 18021 articles were published in high-quality journals worldwide. The high scientific interest in nanofluids lies in their exceptional thermophysical properties and their possibilities to design more efficient processes and systems. Although the numerous articles, there is a lack of information on the scope, its social and economic impact, or its future trends. This study provides an overview through bibliometric methods that allow better knowledge of the research field. The main goal is to offer a more generalized and strategic vision to help those researchers interested in this topic with accurate information on its impact. In addition, this study helps to maximize international collaborations and provide relevant information to decision-makers. The analysis reveals that research in nanofluids in the last decade has experienced a great specialization in a wide variety of new applications, reaching more new sectors. The main research communities, the most productive authors, or the most relevant journals are some of the analyzed metrics that provide key parameters for contextualization, allowing a clear vision of the current state of the nanofluids research field.

Keywords: Nanofluids; Heat Transfer Fluid, Thermal Energy Storage, Working Fluid, Bibliometric Analysis

1. Introduction

Materials science and technology are essentials for the development and improvement of wide types of applications, and therefore, it has a relevant impact into the efficiency of many productive systems. Depending on the application, new advanced materials require high-performance properties such as enhanced thermal properties, thermal stability, or high electrical and optical properties. In the last decade, one of the sectors where materials improvement has taken high relevance is the energy sector [1–4]. For example, technologies based on renewable energies (RE) are fundamental for the energy transition in a world where decarbonizing energy systems is mandatory to reduce greenhouse emissions and fossil fuels dependency [5]. However, RE are not the only sector that needs high-performance materials. Thus, demand of these materials has become essential in a high variety of industrial sectors such as chemical industry [6,7], manufacturing [8,9], construction [10,11], batteries [12], automation [13,14], cooling [15,16], and nuclear power-plants [2,17]. In addition, several emerging potential applications are currently under research, such as drug delivery and cancer treatments in medical and bio-medical sectors [18–21] or porous media [22–25], expanding the field of interest of nanofluids considerably. These applications usually have in common the use of thermal energy storage materials and/or heat transfer fluids. The conventional working fluids are commonly water, mineral oils, ethylene glycol, engine oils, or molten salts, among others.

Over the last years, nanoscience and nanotechnology have allowed the improvement of the thermophysical properties of these working fluids achieving high technological advances and high-efficiency systems. New promising applications have emerged with the use of nanofluids [26,27]. Nanofluids are engineered by the incorporation of nanometer-sized particles in a base fluid [28–31]. These fluids have attracted the scientific community's interest due to their exceptional thermal behavior [32]. Thus, the literature suggests that the incorporation of nanoparticles at low concentrations enhances the thermophysical properties (i.e., specific heat capacity, thermal conductivity, viscosity, heat transfer coefficient [11,33,34]), therefore, the heat transfer capacity. Some studies report enhanced properties in diverse base fluids like molten salts [35–39], water [40–42], or oils [43–45], among others. This fact makes that nanofluids exhibit unique properties. Nanofluids are subjected to several limitations for achieving industrial scalability despite its potential. First, there is a lack of consensus in the theoretical explanation describing the exceptional behavior of their properties. This fact limits the design of nanofluids with specific properties and the theoretical prediction of their behavior at operative conditions. Second, there is a

huge discrepancy among the published thermophysical values [46–53]. One of the most relevant discrepancies are those caused by negative variations after the incorporation of nanoparticles. Therefore, there is a worsening in the thermo-physical properties with respect to the base fluid on many occasions. For example, some studies reports a worsening in specific heat capacity in water-based systems [54,55] or oil-based systems [56,57]. Thus, despite the higher interest of the scientific community and a large number of publications, it is very difficult to determine tendencies about thermo-physical properties and to compare and validate results. Consequently, the results obtained have low reproducibility. Furthermore, there is no clear methodology to characterize nanofluids. These two main limitations hinder the advances of this promising new technology in its industrial applications, as many issues remain to be addressed.

The growing interest in nanofluids is being reflected in the large number of publications and researchers involved over the last years. This fact implies that more applications and fields of study are being addressed, reaching a high technical and specialized level. Consequently, it becomes more difficult to have a general overview of the state of the research, its progress, limitations, and drawbacks. Various specialized reviews about nanofluids' state of the art can be found in the literature [15,32,58,59]. Some aspects like applications or thermal properties are analyzed in these review papers. Nonetheless, there is a lack of information on the scope, general overview, social and economic impact, or future trends. These parameters are of high interest to address the impact on the scientific community and to analyze the current state and future trends in this research field.

Bibliometric studies become a powerful tool to analyze these relevant aspects due to its relevance of management of knowledge and monitoring information. Bibliometrics has become a methodology in which written publications in a particular research field are studied by using statistical analysis [60,61]. Bibliometric studies have proved to be useful for impact evaluation of scientific output by using several metrics in order to establish scientific relevance [62,63]. In the last decades, scientific output has been doubled every 15 years. Annual overall scientific output has reached near 3 million of publications [64]. Under these conditions, bibliometrics has proved useful in several research areas, such as management, econometrics, data envelopment, gray systems, innovation, health economics, marketing, statistics, ecology, production management, renewable energies, thermal energy storage technologies, and concentrating solar power, among others [65–67].

The main objective of this study is to provide a relevant overview of nanofluids research field through bibliometric methods from 1993 until 2020. For this purpose, different

issues such as regional particularities, the author's interactions, or economic aspects are analyzed. This study will help to understand the scope, relevance, and potential of nanofluids. It will also allow authors to identify areas of knowledge, gaps, and establish future relationships to advance nanofluids research.

2. Materials and Methods

The methodology used was established in a previous study [67], and it consists in a multi-stage step well defined for obtaining significant and reliable results, Figure 1.

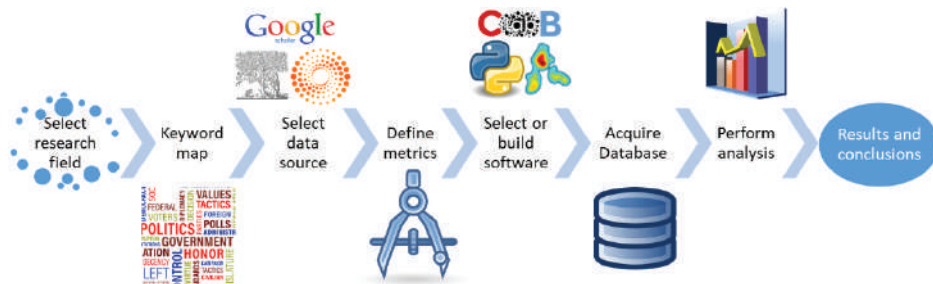


Figure 1. Methodology stages for performing a bibliometric study [67].

The search field under study is nanofluids; however, it is necessary to define this term. Nanofluids are colloids of nanoparticles inside a liquid medium with specific thermophysical properties [29]. Therefore, the bibliometric analysis was based in this definition. To be more specific in the searching process some other fields such as nanofluidics, or photoelectrodes have been excluded since they do not really belong to the main research field.

Once the search field is correctly delimited, and restrictions are defined, a keyword map was built to prepare a search string which was used for acquiring the database. Table 1 shows several phrases that are used in the mentioned keyword map. Each row represents a search queue; the main phrase represents the phrase that must be present for getting a positive match. However, it must also contain one or more of the complement phrases unless there is none defined. Exclusions phrases will discard any paper in which one or more of these terms are found. In this case, the four exclusions phrases are used for all the rows. As a result of the keyword map, the following logical search string was defined: `((("Nanofluid**") NOT ("nanofluidic* "OR" nanoemulsion* "OR" ferromagnetic") OR ("nanoliquid**" AND ("enhanced" OR "nanoparticle**" OR "effect" OR "suspension**" OR "dispersion")) NOT ("nanofluidic*" OR "nanoemulsion**" OR "ferrofluid**`

OR "ferromagnetic") OR ("nano-fluid*") NOT ("nanofluidic*" OR "nanoemulsion*" OR "ferrofluid*" OR "ferromagnetic").

Table 1. Nanofluids research field keyword map.

Exclusion phrases	Main phrases	Complement phrases
nanofluidics	nanofluid	
nanoemulsion	nanoliquid	Enhanced nanoparticle effect suspension dispersion
ferromagnetic	nanofluid	

The data sources for this bibliometric study included scientific journals, conference proceedings, books, book chapters, etc. These sources (i.e., metadata) are usually used for scientific studies searching but also can be useful for performing bibliometric analyses. This data is available in many platforms such as Web of Science, Scopus, Google Scholar, among others. For this study Web of Science Core Collection was selected as the main source since it has detailed metadata (which is adequate for the desired metrics) and includes more than 64 million high-quality publications. The available data in the metadata was: title, abstract, author's keywords, authors, year, number of citations, affiliations, and journals.

The next step was to select the metrics to be calculated and extracted from the database. Table 2 shows a complete list of the metrics reported in the current study, the software tools used, and if the metric was used. For obtaining these metrics Python programming, and CLab complexity network in Python and JavaScript were used. Also, Origin from OriginLabs®, VOS Viewer from Centre for Science and Technology Studies (CWTS) in Leiden University, and Microsoft® Excel were used for data visualization.

The main metrics are defined as: (1) the publications correspond to the number of publications in peer-reviewed journals. (2) Journal impact factor is calculated as the average number of citations per paper during the two last years. (3) H-index measures the productivity and impact of a researcher by the number of publications and its citations.

During data acquisition from WOS Core Collection data source 20095 papers were selected. Search was limited to articles, reviews, book chapters, and books. Additionally, the search string was looked up by subject. These includes searching in title, abstract, author keywords and Keywords Plus®. This last is defined by WOS and is not under control of the authors.

Table 2. Metrics used during the study.

Metric	Software
Total publications evolution	Python, Origin
Total citations per year	Python, Origin
Total publications per country	Python, Origin, Ms Excel
Country and EU evolution	Python, Origin
EU countries evolution	Python, Origin
Country and EU increment per year	Python
Country and EU co-citation interaction	Python, VOS viewer
Journals with h-index and performance ratio	Python
Top authors evolution	Python, Origin
Top authors with h-index	Python
Author communities	Python, CLab
Author co-citation evolution	VOS Viewer
Research areas evolution	Python, Origin
Funding evolution analysis	Python, Origin
Countries Journals quartile publications (%)	Python
Author's quartile publications (%)	Python

When analysing the database obtained from WOS Core Collection, incorrect Keywords Plus® delimitation was discovered since the term “nanofluid” was included by WOS on papers not related to this research area. Since WOS subject search doesn't allow exclusion of Keywords Plus® a filter was applied to the extracted database by using Python with the same search restrictions, but excluding Keywords Plus®, obtaining 17997 papers for the study.

3. Results

3.1. Nanofluids worldwide research production

Based on the bibliometric database, a wide collection of publications related to the nanofluids field was obtained. Under this specified bibliometric search (web of science core collection), nanofluids published research began in 1997. Denote that, if a more exhaustive search is done, outside of this database, it is found that the origin of this research field was in 1993, introduced by Masuda H. from the Tohoku University. His publication “Alteration of Thermal Conductivity and Viscosity of Liquid by Dispersing Ultra-Fine Particles” [68] is the

first study about the concept of incorporating fine particles into fluids to improve its thermo-physical properties.

Figure 2 shows the nanofluid's scientific production; Figure 2a) show the total worldwide production in the last decade, and Figure 2b) the evolution over the years from 1997 to 2020 of the number of publications in this field.

Research production stage: Prince et al. [69] describes in their work three stages in the growth of knowledge: a) a preliminary phase with slight increments; b) a phase of exponential growth; c) a period of inalterable development, where effective saturation starts. According to this description and the obtained curve of the evolution over time of the number of publications (Figure 2b), nanofluids research field is actually in phase b) with exponential growth of the research production. Moreover, Prince indicates that the inflection point, in which the saturation starts, is usually after 30 years. Therefore, there are approximately 20 years of accelerated growth left.

After the study by Masuda H. introducing this research area, Choi, S.U. from the Argonne National Laboratory, coined for the first time the term "nanofluid" in 1995. Becoming their study: "Enhancing thermal conductivity of fluids with nanoparticles" [28], the first publication to use the term "nanofluid" with the particles reduction to the nanoscale (denote that this publication is not indexed in web of science). From these studies, and the exceptional properties of nanoparticles, an increase of scientific interest in the nanofluids topic was noticed and the way of naming these fluids was consolidated. It is interesting to remark, that, between the firsts publications in the database (for example "Quasi Hydrodynamics of nanofluid mixtures" [70] by Pozhar, L. et al., 1997) appears the term "nanofluids" with a different meaning. During the research field early years, it seemed that the term nanofluids was used ambiguously for different fields, for example, in nanofluidics (fluids confined at the nano-scale) and for the nanofluids here described. Nonetheless, even today there is no unanimity on a strict definition of nanofluid, causing controversy between the researchers. On the other hand, several years had to pass before this field began to grow at present rates. Since 2003, it was observed a growth in the number of publications, reaching 2915 publications at the end of 2020: with a total of 18021 articles about nanofluids. Furthermore, it was observed that from 2018 to 2019, there was the highest annual increase of the number of publications. This advance in nanofluids research in the last decade has been motivated by the high technological and scientific interest that falls on these fluids due to their improved thermophysical properties. In particular, the field of nanofluids has taken a great step forward, from basic science publications to a wide variety of industrial

applications. On the other hand, it can be observed from Figure 2a) that Iran is the country with larger production, with a total of 3891 articles, followed by India (3574 articles), and China (2779 articles). Figure 2b), represents (by a black dashed line) the number of cites per year and the total number of publications. For the year 2016 a peak can be observed in the number of citations with more than 39000. These can be explained because more recent publications still are not so cited, however it can be expected that recent publications will significantly increase their citations.

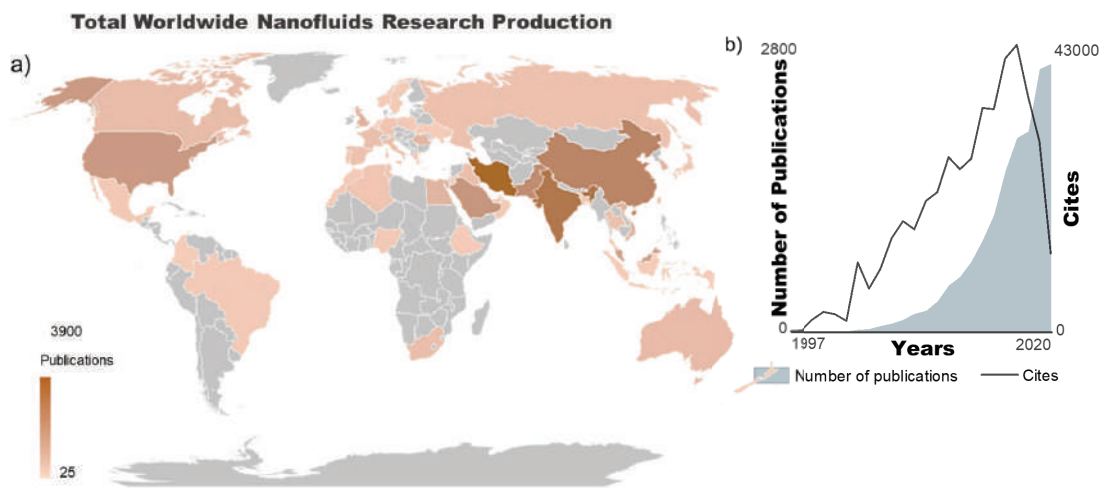


Figure 2. Total Worldwide nanofluids research production from 1997 to 2020: a) Nanofluids total accumulated publications per country. b) Evolution of the number of publications and number of cites per year.

For the analysis of cites, it is interesting to analyze the co-citation of the publications. Figure 3 shows the co-citation of the top ten publications, where size of the circles is proportional to the number of publications and the thickness of the lines connecting them is proportional to the number of interactions (co-citations). This allows us to identify the pillar research efforts for the development of nanofluids research field. Two more co-cited articles are found published before 1993-1995 (year of the first publications related to nanofluids); by Hamilton, R.J et al. (1962, "Thermal Conductivity of Heterogeneous Two-Component Systems" [71]), and Brinkman, H.C et al. (1952," The Viscosity of concentrated Suspensions" [72]). Notice that these two publications were related to the behavior of

thermophysical properties (i.e., thermal conductivity and viscosity). Therefore, these publications can represent the previous step to develop nanofluid field. On the other hand, it is possible to identify two main articles co-citation clusters (represented by yellow and blue circles). The works performed by Buongiorno, J. (2006), and Eastman, J.A. (2001) are the two most co-cited articles. Furthermore, notice that Choi, S.U, East-man J.A., and Lee, S. form part of the same working group.

In addition, Table 3 describes the ten most cited articles by the end of 2020; being the work "Enhancing thermal conductivity of fluids with nanoparticles" by Choi, S.U. and Eastman J.A. [28] is the most cited article (6112 cites (2021)). Despite not being one of the countries with the highest number of published papers (India, Iran, and China), USA leads the three most cited nanofluids publications.

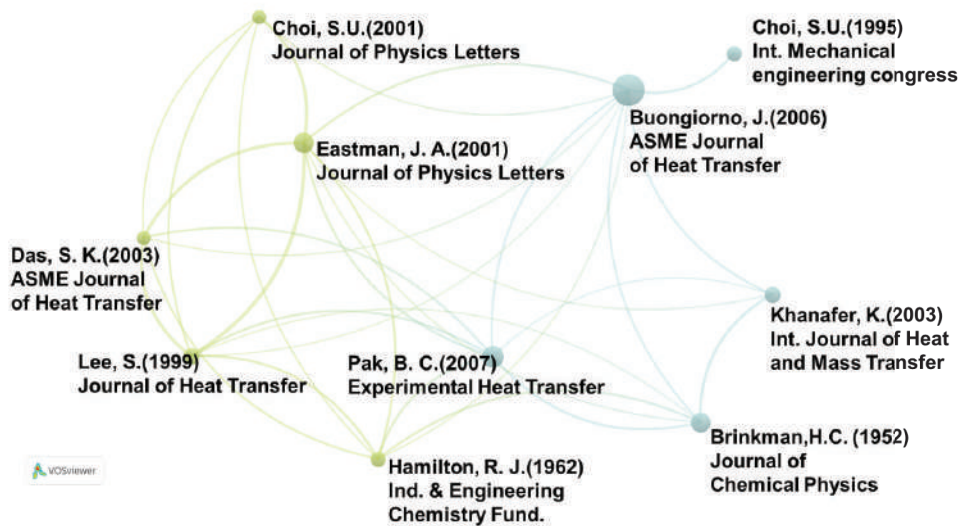


Figure 3. Co-citation interactions of the top ten most co-cited articles in nanofluids research field. Each circle indicates the main author's name, year of the publication and journal.

Table 3. Author's name, article title, journal, number of cites, year of publication, country, and affiliation of the authors of the top ten most cited articles in nanofluids field from 1999 to 2020.

Authors	Title	Journal	Cites	Year	Country	Affiliation	Ref.
Choi S.U et al.	Enhancing thermal conductivity of fluids with nanoparticles	International mechanical engineering congress and exhibition	6112	1995	USA	Argonne Natl Lab.	[22]
Buongiorno J.	Convective transport in nanofluids	Journal of Heat transfer-Transactions of the ASME	3646	2006	USA	MIT	[23]
Eastman JA., et al.	Anomalous increased effective thermal conductivities of ethylene glycol-based nanofluids containing copper nanoparticles	Applied physics letters	2745	2001	USA	Argonne Natl Lab.	[24]
Lee S. Et al.	Measuring thermal conductivity of fluids containing oxide nanoparticles	Journal of Heat transfer- transactions of the ASME	2120	1999	USA, South Korea	Kyonggi Univ., Argonne Natl Lab.	[64]
Khanafer K. et al.	Buoyancy-driven heat transfer enhancement in a two-dimensional enclosure utilizing nanofluids	International Journal of heat and mass transfer	1984	2003	Canada, USA	Univ. Calif. Riverside, McMaster Univ.	[25]
Wang X.-Q. et al.	Heat transfer characteristics of nanofluids: a review	International Journal of thermal sciences	1810	2007	Singapore	Natl Univ Singapore	[65]
Xuan Y, et al.	Heat transfer enhancement of nanofluids	International Journal of heat and fluid flow	1741	2000	China	Nanjing Univ. Sci. & Technol.	[66]
Das Sk. Et al.	Temperature dependence of thermal conductivity enhancement for nanofluids	Journal of Heat transfer- transactions of the ASME	1685	2003	India, Germany	Indian Inst Technol, Univ. Bundeswehr Hamburg	[67]
Xuan Y. et al.	Conceptions for heat transfer correlation of nanofluids	International Journal of heat and mass transfer	1660	2000	Germany, China	Nanjing Univ. Sci. & Technol. and Univ. Bundeswehr Hamburg	[68]
Keblinski P. et al.	Mechanisms of heat flow in suspensions of nano-sized particles (nanofluids)	International Journal of heat and mass transfer	1598	2002	USA	Rensselaer Polytech Inst. and Argonne Natl Lab.	[69]

Obsolescence: The law of aging or obsolescence of scientific literature is another important factor to evaluate the time when a topic loses scientific relevance. To evaluate obsolescence Burton and Kebler et al. [73], define the concept of semi-period, which refers to the time in which half of the referenced literature within a scientific discipline has been published; in the case of nanofluids topic the semi-period is over seven years. Therefore, almost all the available bibliography remains relevant.

Countries evolution: Figure 4 shows in detail the evolution from 2000 to 2020 of the number of publications of the ten most productive countries and EU. The papers had been metered based on the affiliation of the authors when published. An annual increase is observed for all countries. From the first publication in 1995 from USA, in 2000, only China (two articles), Germany (one article), Ukraine (one article), and United Kingdom (one article) published studies related to nanofluids. Nonetheless, since 2007 the increase in publications becomes more evident. USA is a pioneer in this sector and led the number of published papers up to 2011. Over the next years, the number of publications remained stable compared to the growth by other entities. In contrast, in countries like Iran, India, and China, a potential interest grew in the nanofluids field since 2006, 2003, and 2002 respectively; and the number of contributions had increased notably, causing them to lead the countries with a larger number of published papers during recent years (first, second and third position, respectively). An interesting case is Vietnam, which nowadays is among the top ten countries in publications related to nanofluids, despite the first contribution was published in 2014. Also, countries with similar trends were Malaysia (starting at 2009), Saudi Arabia (starting at 2010), and Pakistan (starting at 2010). Because of the lower individual contribution of the countries belonging to the European Union, all of them are grouped in Figure 4a) and disaggregated in Figure 4b). Figure 4b shows that, within the European Union, Romania is the main contributor, followed by Spain, France, and Italy. Despite this, until 2005 Germany led the region. Apart from the top ten countries, a total of 117 countries around the world and over 26115 different authors had contributed until the end of 2020 to the nanofluids research. Being Asia the continent with the highest number of publications.

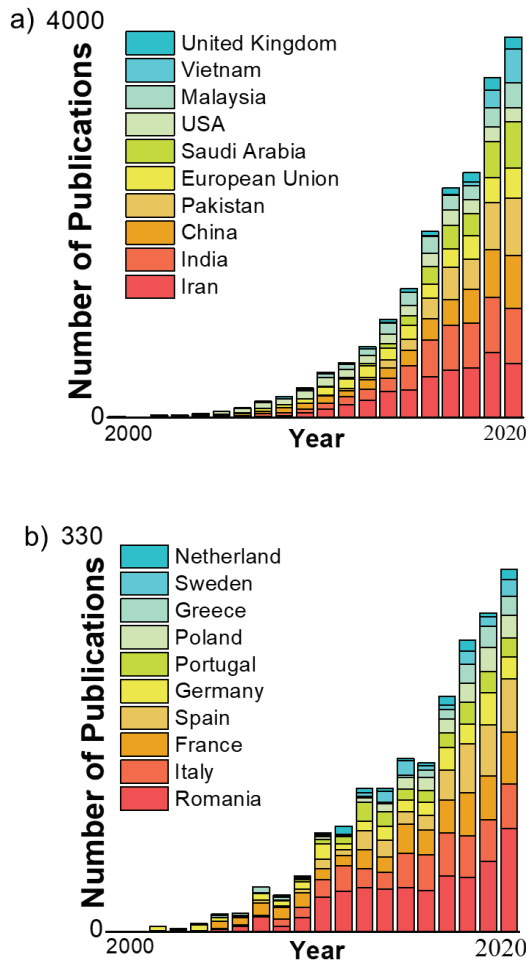


Figure 4. Evolution of the number of publications on nanofluids field over the last two decades for the top ten countries/regions a) in the world and b) in the European Union.

Finally, one of the most relevant results on this metric is the analysis of the interactions between countries. This analysis is helpful to visualize the collaborations among countries and research groups. Figure 5 shows the different collaborations among the top 20 countries and EU. First, it is observed the formation of four main countries clusters; (1, Orange) led by Pakistan and Arabia Saudi: Pakistan, Arabia Saudi, Egypt, and United Arab Emirates. (2, Blue) led by India and China: India, China, EU, USA, UK, Canada, South

Korea, and South Africa (3, Yellow) led by Iran: Iran, Malaysia, Vietnam, Iraq, and Australia. And finally, (4, red) led by European Union: European Union, Turkey, Taiwan, and Thailand. It is possible to observe the large number of interactions that exist among most of the countries/regions; in outstands that there is high collaboration in the field of nanofluids worldwide. Specifically, the highest number of collaborations occur between Pakistan and Saudi Arabia. On the other hand, Iran, that leads the field of nanofluids, has many interactions with different countries such as China, Vietnam, Malaysia, and USA. In addition, it is interesting to note that there is relatively little interaction between India and China, two of the leading countries.

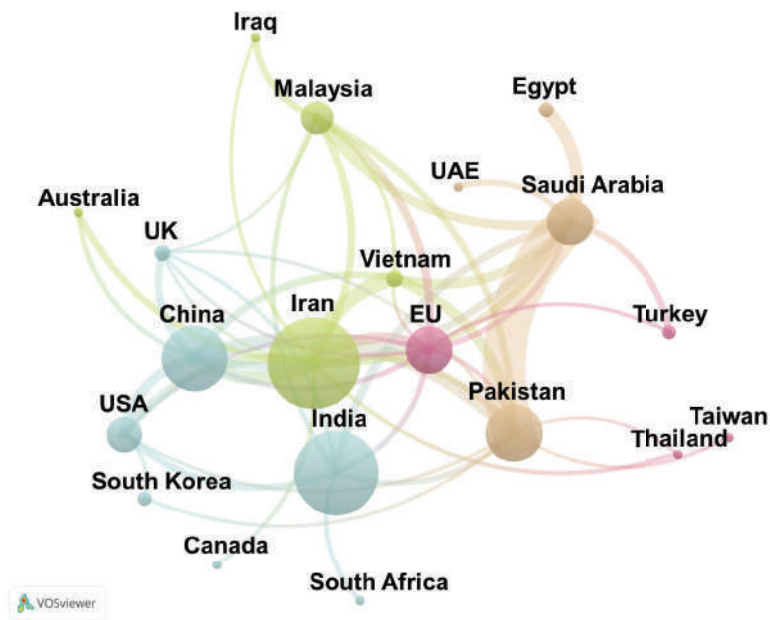


Figure 5. Top 20 affiliations (countries/regions) of the main authors publishing on nanofluids field, and the four main interaction clusters (1) yellow, (2) blue, (3) Orange, and (4) pink.

More in detail, these interactions can be analyzed by institutions. The country cluster derives in four institutions clusters: 1) Islamic Azad University (Iran), Ferdowsi University Mashhad (Iran), King Mongkut's University of Technology Thonburi (Thailand), and Universiti Malaya (Malaysia) (2), Argonne National Laboratory (USA), Massachusetts Institute of Technology (USA), and Indian Institute of Technology (India), (3) Quaid-i-Azam

University Islamabad (Pakistan), and King Abdulaziz University (Saudi Arabia), and 4) Babol Noshirvani University of Technology (Iran).

Countries productivity: a good estimation of the countries performance of research production is to assess the number of researchers and the number of publications of each country. After identifying the affiliation of 78 % of all the authors, the productivity index (amount of researchers/number of publications) of the 20 countries with the highest number of publications has been determined in Table 4. In addition, the percentage of publications was analyzed according to the quartile of the journals (from Q1 to Q4). From this analysis, the most productive country is Saudi Arabia with an index productivity of 8.4, which indicates that on average each author published over eight articles. Thus, it offers an idea of the authors' degree of specialization in nanofluids. In contrast, China shows the lowest productivity index (0.8) of the top 20 countries. It stands out that, despite being the lowest index, it is a relatively high average value, and shows the good performance of all the top 20 countries. The journal interquartile rang is a good indicator of the publication's quality and impact on the scientific community. Of the 20 countries with more publications, Australia (68.81 %), Italy (64.61 %), and France (64.21 %) have the highest ratio of publications published in high-impact journals (Q1). In opposite, Pakistan (37.47 %) and India (39.67 %) are the ones that published mainly in Q2 journals. From all the worldwide countries that published more than 100 publications, Spain presented the highest publications Q1 coverage (72.50 %) publications at the end of 2020. Finally, is possible to observe that most of the research was published in high-impact journals, an indicate the nanofluids research quality.

Table 4. Index country productivity (amount of researchers/number of publications) of the top 20 countries with the highest number of publications.

Country	Researchers	Publications	Productivity	Q1	Q2	Q3	Q4
Iran	3259	3891	1.2	58.33%	31.94%	7.64%	1.52%
India	3477	3574	1.0	39.67%	42.48%	13.67%	3.31%
China	3602	2779	0.8	61.23%	27.25%	7.52%	3.20%
Pakistan	752	2421	3.2	37.47%	47.31%	11.46%	3.35%
Saudi Arabia	231	1943	8.4	45.15%	41.80%	9.38%	3.40%
USA	1380	1543	1.1	63.22%	28.91%	4.87%	1.88%
Malaysia	909	1422	1.6	55.49%	27.92%	9.99%	5.34%

Vietnam	130	748	5.7	53.86%	36.44%	4.39%	5.32%
UK	312	699	2.2	64.38%	27.18%	4.58%	3.00%
Egypt	349	634	1.8	43.69%	39.59%	11.20%	4.73%
Turkey	356	629	1.8	50.64%	29.62%	15.45%	2.71%
South Korea	640	618	1.0	54.13%	33.71%	5.67%	5.83%
Romania	117	526	4.5	53.80%	28.90%	12.17%	4.37%
Australia	205	420	2.0	68.81%	22.38%	5.48%	1.43%
Canada	241	391	1.6	60.51%	32.82%	4.10%	1.79%
Taiwan	330	368	1.1	57.34%	28.80%	6.79%	6.25%
Iraq	133	356	2.7	61.52%	25.84%	8.43%	3.09%
South Africa	117	326	2.8	47.08%	37.23%	11.38%	4.00%
Italy	312	308	1.0	64.61%	23.05%	9.42%	1.62%
France	193	299	1.5	64.21%	22.41%	9.70%	3.68%

3.2. Authorship evolution

The cumulative author evolution by number of publications and citations is shown in Figure 6. The main authors from 2010 to 2020 are Alsaehdi, A. (Saudi Arabia, King Abdulaziz University), with more than 397 articles related to nanofluids field and 12712 accumulated cites (h-index 63) and followed by Pop, I. (Romania, University of Cluj) with more than 238 accumulated publications, and 9795 cites (h-index 59). Since 2014 it can be observed the high increase in the number of publications by various authors such as Ganji, D. D. with 213 articles and 13374 cites (h-index = 67). Also, it is interesting the high growth of some authors, such as the case of Sheikholeslami, M. or Hayat, T., since 2017-2018. Likewise, Khan, M., despite starting to publish in the field of nanofluids in 2016, is among the top ten authors list. With more than 197 articles and 5351 accumulated cites (h-index 43). From this analysis, it can be seen the high impact of the nanofluids researchers in the scientific community with high productivity authors. Moreover, another relevant parameter to identify the research quality is the quartile of the journals where the investigation is published. Sheikholesami, M. (66.1 %) and Oztop, H.F. (67.3 %) are the two authors with highest percentage of their publications in Q1 journals. However, from all the nanofluids researchers, is the author Afrand, M. from the Islamic Azad University, who presents the highest coverage (69.3 %) of their publications in Q1 journals.

Top 10 Nanofluids Authors

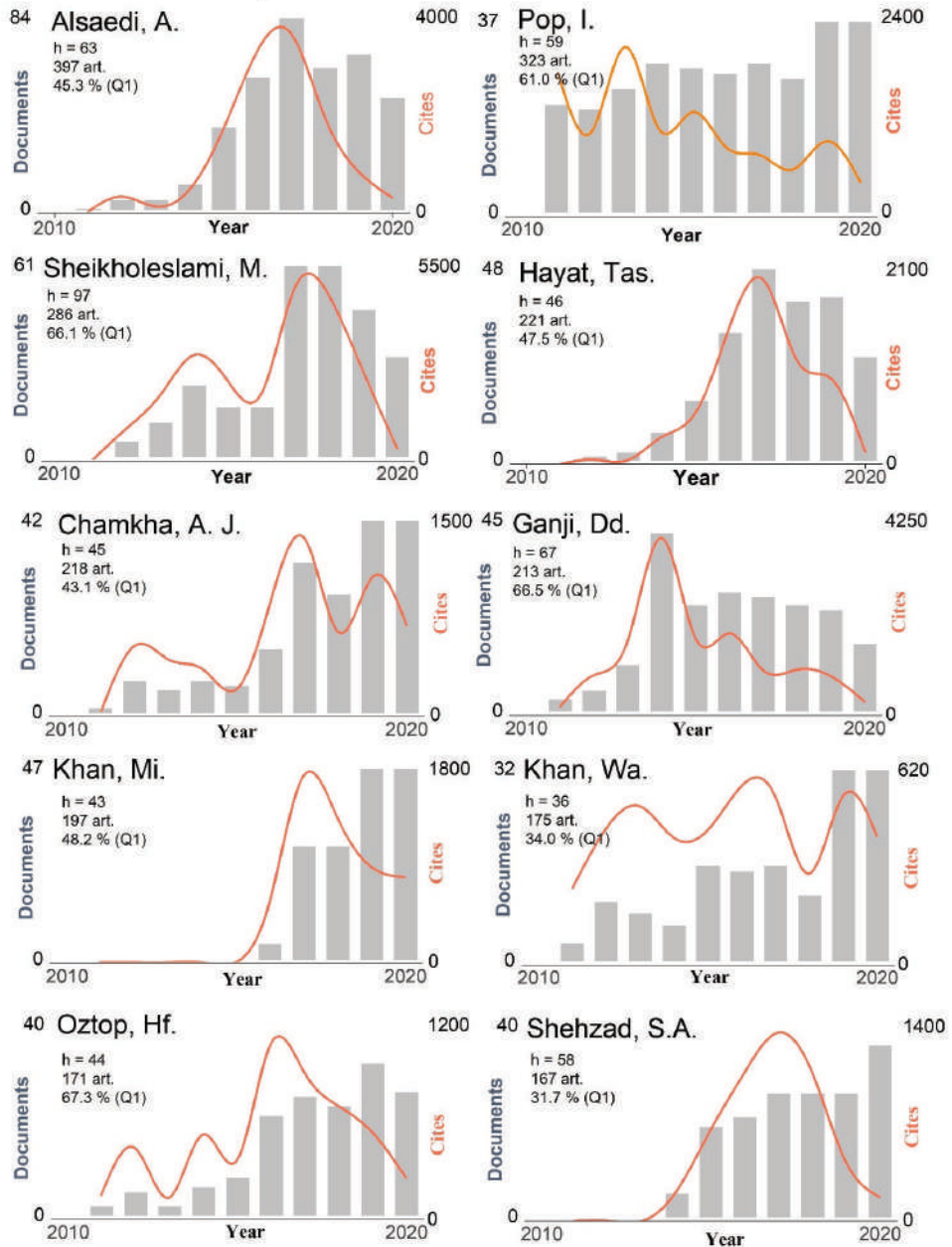


Figure 6. Top ten authors with the highest number of publications in nanofluids field during last decade.

Furthermore, Figure 7 shows the authorship communities within the top 50 authors in the nanofluid field. The main authors of each community have been identified, including the top ten authors analyzed in Figure 6. The list of publications in the database was analyzed with CLab software tool to define the attractions forces among the authors (represented by circles) to identify the communities they belong to. Size of the circles are proportional to the number of publications for each author, while attractions are calculated according to the number of co-authorships between authors. There are seven main communities of authors in the nanofluids field: (1) led by Chamkha, A.J. and Sheikholeslami, M., (2) led by Alsaedi, A. and Hayat, T., (3) led by Saidur, R., (4) led by Ganji, D.d., (5) led by Oztop H.F., (6) led by Pop,I. and Wongwises, S., and finally community (7) formed by a single author, Sibanda, P. Also, it is of interest that three of the main authors (Khan, M., Alsaedi, A. and Hayat, T.) are part of the same community (2). The identified nanofluids communities shown a high interrelation among them (especially between (1) and (2)), forming very strong and interconnected communities (grey lines), except community (7). This community did not show any interaction between the other main communities and authors.

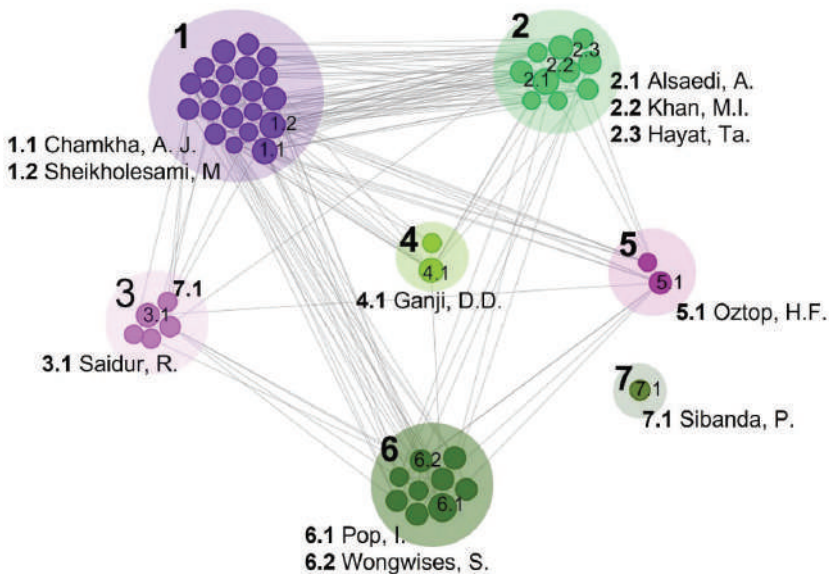


Figure 7. Authorship communities publishing on nanofluids field (the top ten most relevant authors are indicated).

Therefore, these numerous interactions give rise to a great transfer of knowledge and generate well-established groups of researchers in the field of nanofluids, allowing stronger advancement in nanofluids science.

Additionally, the most co-cited authors (interaction between the authors by the number of citations between them) until the end of 2020 had been Alseadi, A. and Pop, I. Among them, Choi, S. is one of the most co-cited authors for publishing the first study on nanofluids and is widely cited by many of the leading authors. Other authors such as Saidur R. or Ding, Y., despite they don't appear in the top ten by number of articles, they generate high scientific interest based in the number of citations (over 8541 and 8686 citations, respectively). Therefore, the authors with higher number of publications are not the same as the most cited ones.

In addition, three main authors' clusters were identified: 1 (orange), 2 (blue) and the last (3) yellow. The highest interaction is observed between cluster (1) and (2). Specifically, it is noticeable a strong interaction inside the cluster (1) between Sheikholeslami, M., and Ganji, D.d. both from the Babol Noshirvani University of Technology, Iran. The same happens inside the cluster (3) between Alsaedi, A. and Hayat, T. from King Abdulaziz University (Saudi Arabia) and Quaid-i-Azam University (Pakistan), respectively.

3.3. Journals analysis

The Top ten journals where nanofluids research is published were analyzed. Several parameters such as the number of articles and citations, the h-index calculated for this research area, the SJR number (2020), the journal's quartile (Q1, Q2, Q3, ...), and finally, the two main countries that published in each journal are listed in Table 5. Moreover, the performance ratio (PR) is also included, this parameter is obtained by dividing the number of citations by the total number of nanofluid articles published in each journal in the last 20 years.

The journal with more publications until 2020 is the International Journal of Heat and Mass Transfer, classified as Q1 by SJR (Scimago Journal & Country Rank), with a total of 940 articles, more than 70306 citations and one of the largest PR. In addition, the specialized nanofluids journal (Journal of Nanofluids, Q2), occupies the 5th place with a total of 463 publications and more than 2568 citations, but with the lowest PR. In contrast, the International Journal of Thermal Sciences had the higher PR (82.35). Instead, this publisher nucleus is from UK, Netherlands, United States, Germany, and France, and the main

editorial is Elsevier, followed by Springer. Furthermore, it is remarkable that more than half (57.2 %) of the literature published about nanofluids is included in Q1-Journals. These data denote the good quality and scientific relevance of the nanofluids publications. Moreover, the first journal in publishing an article about nanofluids was the Journal of Heat Transfer-transactions of the ASME. In the last two years (2019-2020), the journal that published more nanofluids articles was the Journal of Thermal Analysis and Calorimetry. The increase in publications in Q3 may be due to the large annual volume of publications. In addition, Iran has published in all the journals that include nanofluids in their publications with the exception of the International Journal of Heat and Mass Transfer based in United Kingdom where China and USA are the countries with more publications.

Table 5. Top ten of the journals that publish nanofluids research: Journal name, number of articles, number of citations, performance ratio, nanofluids h-index, SJR 2020, quartile score, and main countries and number of publications of two main countries that publish in each journal.

Journal	Nanofluids Articles	Nanofluids Citations	Performance Ratio	h-index	SJR 2020	Quartile Scores	Main Countries
International Journal of Heat and Mass Transfer	940	70306	74.79	121	1.65	Q1	China (233), USA (155)
Journal of Thermal Analysis and Calorimetry	770	11031	14.33	51	0.42	Q3	Iran (375), Saudi Arabia (137)
International Communications in Heat and Mass Transfer	686	28089	40.95	87	1.41	Q1	Iran (270), Malaysia(144)
Journal of Molecular Liquids	520	18355	35.30	70	0.88	Q1	Iran (224), Pakistan (125)
Journal of Nanofluids	463	2568	5.55	20	0.34	Q2	India (303), USA (48)
Applied Thermal Engineering	432	17672	40.90	68	1.78	Q1	Iran (143), China (86)
International Journal of Numerical Methods for Heat & Fluid Flow	321	4478	13.95	32	0.51	Q2	Iran (98), Saudi Arabia (85)
Powder Technology	274	11013	40.19	59	1.00	Q1	Iran (124), India (58)
International Journal of Thermal Sciences	273	22482	82.35	80	1.26	Q1	Iran (73), USA (34)
Heat and Mass Transfer	269	4399	16.53	30	0.57	Q2	Iran (101), China (65)

These ten journals represent the 0.8 % of all the journals (1129 total journals), and the 27.5 % of all the publications (and 37.4 % of all cites). Moreover, only the 2.4 % of the journals (top 30) represents over the 45 % of the publications. Other important aspect is the number of authors per article. After studying the literature, the largest number of publications, 26.8 %, had three authors. Being the average between 2-5 authors per article. Otherwise, only the 4.4 % of the publications had one author. The round-robin or benchmark study entitled "A benchmark study on the thermal conductivity of nanofluids" [74] with 71 authors from 31 institutions, was the article with the highest number of authors and institutions. This article is an example of the high interaction and collaborations between communities.

Bibliometrics Laws: A relevant way to analyze journals and authors of a particular subject is through the empirical laws of Bradford, Lotka, and Zipf distributions. For the correct analysis of the bibliography through these distributions, certain conditions must be satisfied: (1) the subject of the bibliography, in this case the nanofluid concept, must be well defined. (2) all relevant papers and journal must be included, and (3) the bibliography must be of limited time span so that all contributing journals have the same opportunity of contributing papers [75]. The Bradford distribution, show that there are few papers grouped in a small number of journals called "nucleus", which determine the Bradford Law [76,77]. This law groups journals and articles to identify the number of items relevant to a particular subject; is based on the total of articles published by journals in a particular area which determines the percentage of total coverage by various number of journals. This distribution is explained by $R(n) = N \cdot \ln(n/s)$ ($1 \leq n \leq N$) [75,78] where $R(n)$ is the total number of journals publishing n articles, N the total number of journals and s is a particular constant for the specific field. In Figure 8 $R(n)$ is presented as a function of $\ln(n)$. From this representation it was obtained: a) the specific constant for nanofluids field, s , b) the stage of production/obsolescence, c) the identification of the nucleus, d) the evolution over the years of the number of publications as a function of the number of journals (from 1997 to 2021), and finally, e) the completeness or incompleteness of the literature [79,80].

Since 1997, the accumulated number of articles grew remarkably, especially in 2018. At the same time, the number of articles grew from >100 to 1230 (from 2005 to 2021). The nanofluids characteristic constant literature, s , can be extracted from Figure 8, as an extrapolation of the linear area to the x-axis. In nanofluids research field at the end of 2021, the constant is $s \approx 1.6$. This indicate that to cover half the output of papers, it is necessary to take only the 45 most productive journals, according to equation $s(N/s)^{1/2}$ [75]. Generally,

this term is not independent, it increases with time if the bibliography remains > 5 years. Additionally, a value above $s=1$, suggests that the bibliography becomes more breadth. Therefore, we can consider that the nanofluids field of knowledge is expanding and branches out into new applications and investigations [75].

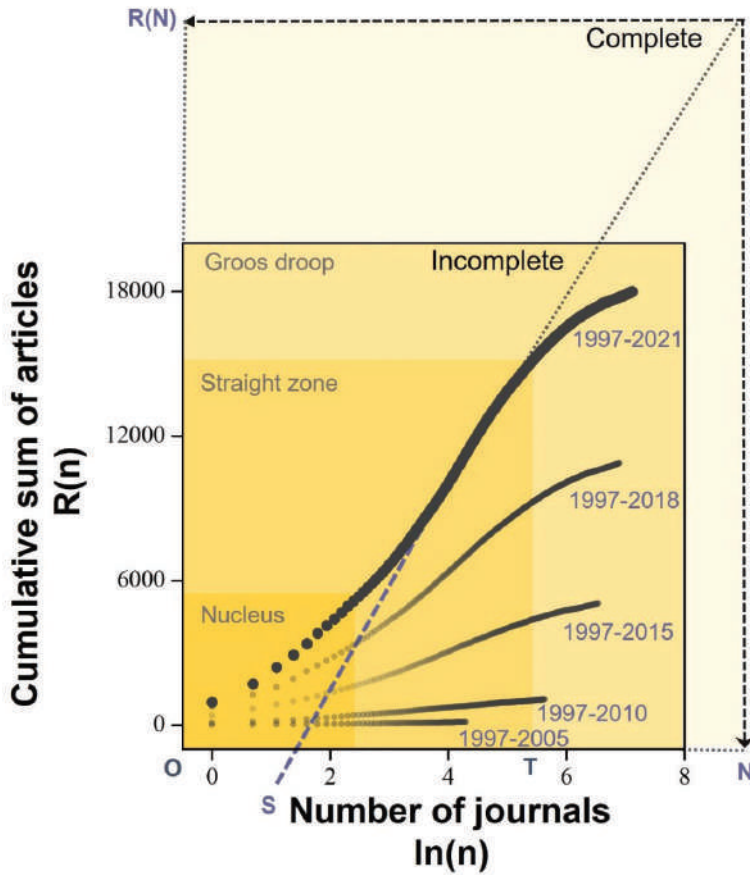


Figure 8. Evolution of the cumulative sum of nanofluids articles as a function of the number of journals, n , in $\ln(n)$ from 1997 to 2021.

Note that in the curves of 1997-2005 and 1997-2010 is not observed the end “droop” of the curve. This can indicate a change in the nanofluids research (i.e., study of new applications, properties, etc.). From equation (1) and the constant value is possible to determine the percentage coverage of articles by a certain number of journals. Brandford defines the nucleus as the points in the distribution, ($\ln(\text{journals})$), before the linear part

(straight zone) [75]. Therefore, the nucleus represents the minimum number of journals to have a representative number of articles about a certain topic. According to Figure 8, to cover the 20 % (3600 articles) of the total number of articles, approximately six journals are needed, which represents the < 0.57 % of the number of journals by the end of 2020. The results from the Bradford distribution were considered according to the experimental value obtained directly from the database (six most productive journals produce the 21.2 % of the publications). Due to the great coverage of articles in these six journals, the nucleus can be defined with the most productive journals [81]. Therefore, the determined constant was a good representative value of nanofluids research field.

Moreover, incompleteness of the literature can be estimated from the deviation of the linearity of the straight zone, the so-called “groos droop” zone. Furthermore, the droop at the end of curve, generally indicates that the bibliography is not complete, in the sense in which the technique requires. From the Figure 8, it can be estimated the expected N sources to contribute to the total bibliography according to: $N = \frac{R(p) \cdot OT}{3 \cdot SM}$, [76] where R(p) is the number of items corresponding to point P and where the lengths OT and SN were extracted graphically. According to the last equations and Figure 8, the total number of journals N, is determined by $(\ln(N) = 8.7)$ where N= 6000 journals. Finally, when N is known is possible to determine exactly the expected accumulated final articles (R (N)) according to: $R(N) = N \cdot \ln\left(\frac{N}{s}\right) = 49014$ articles. Therefore, according to the Bradford distribution the nanofluid research field is approximately at 37 % of a complete development and is expected to reach more than 49000 articles.

Lotka’s distribution [76,77], with the inverse square law, evaluate the author’s productivity in a specific research field. The distribution shows that the number of authors writing n papers is $1/n^2$ of the number of authors writing one paper: $A(R) = \frac{A(1)}{R^{1.6}}$, where A(R) is the number of authors that publish R articles, R is the number of articles that an author publishes, and A(1) is the number of authors that publish only one work [82,83]. Finally, the exponent (1.6) is related to the productivity by a scientific community (Lotka exponent, s) and is related to the constant obtained from the Bradford distribution in Figure 8. In the nanofluids research field at the end of 2020 a total of 17037 authors published only one work. If we assume that R is for example R= 100, hence, according to equation (4), $A(R) = 10.7$ for nanofluids research field, meaning that for publishing 100 articles 10.7 authors are needed. Therefore, nanofluids field presents, also in this metric, high authors’ productivity.

On the other hand, the number of authors with one article represent, at the end of 2020, the 65.2 % of all the authors (26114 in total). Authors with 2-10 articles represent the 31.7 %. The 1.7 % of the authors publish between 11-20 articles, the 0.94 % publish between 11-50 articles, and only the 0.3 % of the authors was publishes more than 51 articles. The top ten authors from Figure 6 were included in this minority group of authors (0.3 %).

3.4. Keywords evolution

The field of nanofluids is a very broad topic, studying the main keywords used by authors to identify their work allows us to better understand this area, its development, and potential applications. Figure 9 shows the evolution over the last 21 years of the 200 most repeated keywords in nanofluids articles. The keyword most used is “nanofluid” and “nanofluids”, indicating that most of the articles include these words within the keywords. This reflects that today the term nanofluids has been well defined and identified by the research community. Furthermore, three main stages were identified over the years, which are represented with purple, blue, green, and yellow. The keyword map shows a clear evolution over the research topics and the research of very specific properties. During early years, the nanofluids publications were related to the study of basic thermophysical properties such as “thermal conductivity” or “flow” and “transport” characteristics (purple). The second group incorporated terms such as “nanoparticles”, “surface effects” or “transfer enhancement” (blue). After 2010, the research was focused on the study of “natural-convection” and “forced-convection”, the study of the “stability”, “nanofluids performance”, and “pressure drop” (dark green). This indicates an increased interest on nanofluids, their behavior, and issues related to industrial applications. From 2010 to 2020, there was the greatest evolution of keywords. Appears terms such as “boundary-layer flow”, “surfactants”, “porous medium” or the study of “rheological behavior” (yellow). Finally, the most employed keyword at the end of 2020 is “entropy generation” and “thermal-radiation”. Therefore, the keyword evolution shows that the science of nanofluids covers a large number of research areas and that has been consolidated over the years.

Science & Ecology, Optical, or Metallurgy & Metallurgical Engineering. However, it is not proportional to the decrease observed in the other areas (not visible in Figure 10). No clear reason was identified for 2018 decrease.

Additionally, the five main research areas of the three main countries with more publications (Iran, India, and China) were identified. Mainly, the three countries publish in similar research areas (in decreasing order): (1) Iran: thermodynamics, engineering, mechanics, chemistry, and physics. (2) India: engineering, thermodynamics, science technology, mechanics, and physics. (3) China: engineering, thermodynamics, mechanics, physics, and energy fuels. Iran seems to be more geared towards research about basic science (i.e., the study of thermophysical properties), while India and China seem to be more focused in applications. Specifically, it can be seen that China research areas area focused on energy fuels.

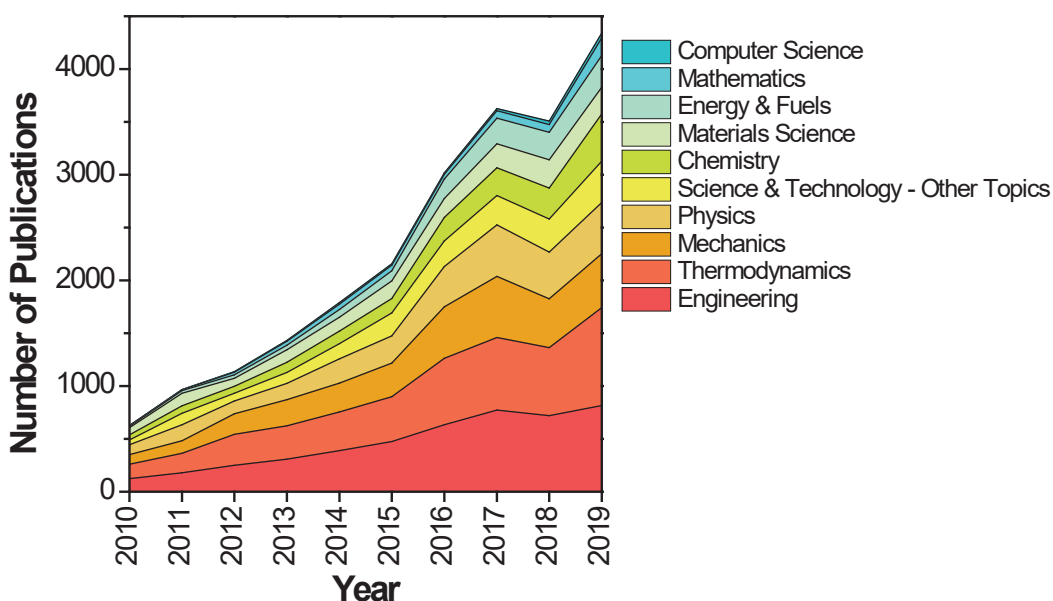


Figure 10. Top ten most relevant nanofluids research areas during the last decade.

3.6. Applications

The advance in nanofluids research in the last decade has been motivated by the high technological and scientific interest that falls on these fluids due to their enhanced thermophysical properties. In particular, the field of nanofluids has taken a great step forward

from basic science publications to a wide variety of industrial applications, as observed in the research areas evolution. Due to the high number of publications, is necessary to determine the current focus of interest in the nanofluids research. For this propose, all publications from 2020 and part of 2021 from the three main countries were analyzed. Table 6 summarizes the main research topics in Iran, India, and China; classified as applications and materials science (i.e., thermophysical properties). Two main research nanofluids applications are identified: heat exchangers and renewable energies (i.e., solar collectors or PV-T). The three countries, but specially India and China, investigate about the use of nanofluids as cutting fluids/lubricants for the metallurgical sector. This application seems to be gaining ground and relevance in nanofluids research.

Table 6. Main research topics about nanofluids field of the three main productive countries (Iran, India, and China) in 2020 and 2021. The topics are classified as applications and materials science.

COUNTRY	RESEARCH TOPICS	
	Applications	Materials Science
IRAN	Air dehumidification, desalination, electroosmotic, medical applications (dental, drug delivery in blood circulation), heat exchangers (gas refineries, gasoline sector, oil recovery , coolant (electronic, batteries, fuel cells, coil, automotive), heat pumps, radiators, antifreeze, refrigerants, lubricants, porous media, heat sink, emulsions, helical tubes, CO ₂ absorption/capture, quantum dots, renewable energy (CSP, PV-T, PV, biomass, geothermal, solar collector).	Specific heat capacity, thermal conductivity, thermal behavior, convection (natural/free/forced), heat transfer , entropy generation, hydrothermal, viscosity, solidification, pressure drop.

INDIA	Heat transfer dissipation/cooling/insulation (electronics, fuel cells, battery, automotive), heat exchangers , heat pipe, heat sink, vertical plate, CO ₂ capture/absorption, renewable energy (PV-T, solar collectors, solar heating) , lubricants, metallurgical sector (lubricants, cutting fluids) , quantum dots, biosurfactants, biomedical (blood, circulating system), oil field (oil recovery, biofuels, biodiesel, diesel, gasoline), radiators, porous media	Interfacial layer, hydrodynamics, thermal performance, convection (bioconvection/natural/free), thermal radiation , heat generation/absorption, heat transfer , diffusion, entropy generation, viscosity, boiling heat, ohmic heat, biomagnetic, subcooling, osmotic flow, mass transfer, biomimetic, photothermal conversion, pool boiling, thermal energy storage, synthesis
CHINA	Oil field (engine oil/ oil recovery/diesel/petroleum/reservoirs wettability), CO ₂ capture, removal SO ₂ , heat sink, heat pipe, heat exchanger , nanocomposites, renewable energy (geothermal, solar still, solar collector, PV-T), steam production, cooling/refrigerant (electronics, fuel cells, domestic refrigerators, automotive), electric heaters, air purification, metallurgical sector/machining/ tribological behavior (lubricants), biotechnological, surfactants, optoelectronic, building	Interfacial layer/interfaces, convection (bioconvection), thermal transfer (thermal performance), mass/heat transfer, entropy generation, rheology, hydrothermal, thermal conductivity, stability, thermal radiation, thermal energy storage , evaporation, phase change materials , heat conduction, adsorption/absorption, wettability

Also, other potential application is the heat dissipation for electronic devices. Another emerging nanofluids applications identified are the use for CO₂ capture, air dehumidification, desalination, quantum dots, or biomedical sector. In particular, most of the publications in India are focused on sustainability and the environment. Finally, an important number of publications were focused on to the oil sector (i.e., oil recovery, gasoil, or reservoir wettability). Also, it was also associated to materials science by studying the properties related to the applications described above. The most studied property related subject in 2020-2021 was heat transfer behaviour or thermal transfer and convection. Finally, it can be observed that properties related to thermal energy storage and phase change materials have gained relevance (mainly due to the relevance of renewable energies).

3.7. Funding and social impact

Another key metric of interest is the funding reported in the published papers of this area. According to Figure 11, despite the reported funding in nanofluids has grown over the years, still almost half of the publications does not report funding. On the other hand, the main part of reported funding in the nanofluids area during the last years comes from EU's projects: COST Action (CA15119) - Overcoming Barriers to Nanofluids Market Uptake – NANOUPTAKE [84], which was active since 2016 to July 2020. This COST ACTION program organized the 1st International Nanofluid Congress in 2019, promoting knowledge, sharing results, and starting new collaborations and links among researchers from the EU in the nanofluids field. Initiatives like this had generated a growing community in Europe and had increased the scientific interest in this topic.

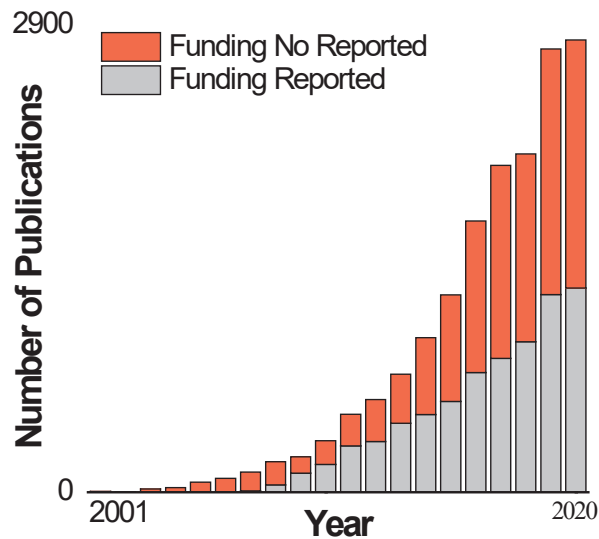


Figure 11. Evolution of the publications on nanofluids funded or not from 2000 to 2019.

The three main funding efforts of the three countries with more publications were analyzed. (1) Iran: national natural Science Foundation of China (NSFC), Thailand research foundation (TRF), and Iran national Science foundation (INSF). (2) India: Department of science technology India, University grants commission India, and Council of scientific industrial research India (CSIR). Finally, (3) China: National Natural Science Foundation of

China (NSFC), Fundamental research foundation for the central universities, and China postdoctoral science foundation. The case of Iran is noteworthy since two of the funding agencies are from foreign countries. Therefore, an important part of Iran nanofluids research is supported by China and Thailand. This fact may be motivated by the formation of the "Belt and Road Initiative" [85] adopted by the Chinese government in 2013 for the global infrastructure and development strategy, and specifically by the strategic partnership agreement on energy issues between China and Iran. On the other hand, the most important funding's agencies from India and China are national agencies. Finally, the main agency that invest in nanofluids research is the National Natural Science foundation of China (NSFC).

4. Conclusions

The analysis presented in this work is essential to understand the relevance and the global research status in the nanofluids field. Nowadays, according to the number of publications, Iran, India, and China leads the nanofluids research. Nonetheless, countries like Australia, Italy, and France, lead in high-impact research metrics. The nanofluid field has been experiencing rapid growth during the last two decades due to its promising potential for several applications. Its interest and impact are corroborated by more than half of publications in high-quality journals (Q1), researchers and countries involved, and its expansion to new applications and sectors. Topics such as heat exchangers or cooling fluids continue to be among the most studied during 2020-2021. Moreover, during recent years new applications like entropy generation, CO₂ absorption, biomedicine, or quantum dots had emerged. The bibliometric analysis reveals that there are four main researcher clusters performing studies about nanofluids. It should be highlighted that there is low interaction between them. By summarizing the most relevant authors and contributions around the world, this study helps researchers and institutions to find high-quality investigations and research groups driving the research outside their cluster. This fact helps to strengthen and progress towards a robust, coherent, and homogeneous research field. Finally, based on the funding analysis, nanofluids became during the recent years in a strategic priority for technological development by many governments due to their financing efforts reported. This interest rest in the need to develop more efficient processes and systems, as well the need to decrease environmental impact in terms of CO₂ emissions and energy efficiency.

Conflict of interest

The authors declare no conflicts of interest.

Acknowledgments

This research was funded by the Spanish government RTI2018-093849-B-C32, RTI2018-094757-BI00, MDM-2017-0767, MCIU/AEI/FEDER, UE. The authors would like to thank the Catalan Government for the quality accreditation given to their research groups DIOPMA (2017 SGR 118) and CMSL (2017 SGR 13). A.S thanks to Generalitat de Catalunya, AGAUR, for her Grant FI-DGR 2018. P.G. thanks Generalitat de Catalunya for his Serra Hünter Associate Professor ship. Finally, R.S. is grateful to the grant PRE2019-087336 funded by MCIN/AEI/ 10.13039/501100011033 and by “ESF Investing in your future”.

References

- [1] Fabre,E. and Murshed,S. M. S. **2021**.A comprehensive review of thermophysical properties and prospects of ionanocolloids in thermal energy applications.*Renewable and Sustainable Energy Reviews*.vol. 151, no. August.p. 111593. doi: 10.1016/j.rser.2021.111593.
- [2] Wahab,A.,Hassan,A.,Qasim,M. A.,Ali,H. M.,Babar,H.,and Sajid,M. U. **2019**.Solar energy systems – Potential of nanofluids.*Journal of Molecular Liquids*.vol. 289. doi: 10.1016/j.molliq.2019.111049.
- [3] Bretado-de los Rios,M. S.,Rivera-Solorio,C. I.,and Nigam,K. D. P. **2021**.An overview of sustainability of heat exchangers and solar thermal applications with nanofluids: A review.*Renewable and Sustainable Energy Reviews*.vol. 142, no. March.p. 110855. doi: 10.1016/j.rser.2021.110855.
- [4] Alirezaie,A.,Hajmohammad,M. H.,and Alipour,A. **2018**.Do nanofluids affect the future of heat transfer?"A benchmark study on the efficiency of nanofluids"*Energy*.vol. 157. doi: 10.1016/J.ENERGY.2018.05.060.
- [5]. **2019**.*Renewables 2019 Analysis and forecast to 2024*. iea, International Energy Agency.
- [6] Eltoun,H.,Yang,Y. L.,and Hou,J. R. **2021**.The effect of nanoparticles on reservoir wettability alteration: a critical review.*Petroleum Science*.vol. 18, no. 1.pp. 136–153.

doi: 10.1007/s12182-020-00496-0.

- [7] Yakasai,F.,Jaafar,M. Z.,Bandyopadhyay,S.,and Agi,A. **2021**.Current developments and future outlook in nanofluid flooding: A comprehensive review of various parameters influencing oil recovery mechanisms.*Journal of Industrial and Engineering Chemistry*.vol. 93.pp. 138–162. doi: 10.1016/j.jiec.2020.10.017.
- [8] Hemmat Esfe,M.,Bahiraei,M.,and Mir,A. **2020**.Application of conventional and hybrid nanofluids in different machining processes: A critical review.*Advances in Colloid and Interface Science*.vol. 282.p. 102199. doi: 10.1016/j.cis.2020.102199.
- [9] Han,X.,Thrush,S. J.,Zhang,Z.,Barber,G. C.,and Qu,H. **2021**.Tribological characterization of ZnO nanofluids as fastener lubricants.*Wear*.vol. 468–469, no. December 2020.p. 203592. doi: 10.1016/j.wear.2020.203592.
- [10] Kulkarni,D. P.,Das,D. K.,and Vajjha,R. S. **2009**.Application of nanofluids in heating buildings and reducing pollution.*Applied Energy*.vol. 86, no. 12.pp. 2566–2573. doi: 10.1016/j.apenergy.2009.03.021.
- [11] Nasiri,A.,Rashidi,A.,Shariaty-Niasar,M.,and Soltanian,H. **2014**.Preparation and application of carbon nanotube nanofluid as a reinforcement of cement slurry.*Advances in Cement Research*.vol. 26, no. 3.pp. 177–184. doi: 10.1680/adcr.13.00007.
- [12] Kim,J. and Park,H. **2021**.Enhanced mass transfer in nanofluid electrolytes for aqueous flow batteries: The mechanism of nanoparticles as catalysts for redox reactions.*Journal of Energy Storage*.vol. 38, no. March.p. 102529. doi: 10.1016/j.est.2021.102529.
- [13] Bigdeli,M. B.,Fasano,M.,Cardellini,A.,Chiavazzo,E.,and Asinari,P. **2016**.A review on the heat and mass transfer phenomena in nanofluid coolants with special focus on automotive applications.*Renewable and Sustainable Energy Reviews*.vol. 60.pp. 1615–1633. doi: 10.1016/j.rser.2016.03.027.
- [14] Xian,H. W.,Sidik,N. A. C.,and Najafi,G. **2019**.Recent state of nanofluid in automobile cooling systems.*Journal of Thermal Analysis and Calorimetry*.vol. 135, no. 2.pp. 981–1008. doi: 10.1007/s10973-018-7477-3.
- [15] Aglawe,K. R.,Yadav,R. K.,and Thool,S. B. **2020**.Preparation, applications and challenges of nanofluids in electronic cooling: A systematic review.*Materials Today: Proceedings*.vol. 43.pp. 366–372. doi: 10.1016/j.matpr.2020.11.679.
- [16] Siricharoenpanich,A.,Wiriyasart,S.,and Naphon,P. **2021**.Study on the thermal

dissipation performance of GPU cooling system with nanofluid as coolant. *Case Studies in Thermal Engineering*. vol. 25, no. April 2020. p. 100904. doi: 10.1016/j.csite.2021.100904.

- [17] Hameed, A. *et al.* **2019**. Experimental investigation on synthesis, characterization, stability, thermo-physical properties and rheological behavior of MWCNTs-kapok seed oil based nanofluid. *Journal of Molecular Liquids*. vol. 277. pp. 812–824. doi: 10.1016/j.molliq.2019.01.012.
- [18] Krishna, M. V. and Chamkha, A. J. **2020**. Hall and ion slip effects on Unsteady MHD Convective Rotating flow of Nanofluids—Application in Biomedical Engineering. *Journal of the Egyptian Mathematical Society*. vol. 28, no. 1. pp. 1–15. doi: 10.1186/s42787-019-0065-2.
- [19] Sridhar, V. and Ramesh, K. **2022**. Peristaltic activity of thermally radiative magneto-nanofluid with electroosmosis and entropy analysis. *Heat Transfer*. vol. 51, no. 2. pp. 1668–1690. doi: 10.1002/htj.22369.
- [20] Mansour, M. A., Ahmed, S. E., Hady, F. M., Ibrahim, F. S., and Ismaeel, A. M. **2022**. Numerical simulation for nanofluid leakage from a single 2D blood vessel. *Alexandria Engineering Journal*. vol. 61, no. 5. pp. 3999–4010. doi: 10.1016/j.aej.2021.09.029.
- [21] Hamad, E. M. *et al.* **2021**. Review of Nanofluids and Their Biomedical Applications. *Journal of Nanofluids*. vol. 10, no. 4. pp. 463–477. doi: 10.1166/jon.2021.1806.
- [22] Krishna, M. V. and Chamkha, A. J. **2019**. Hall effects on MHD squeezing flow of a water-based nanofluid between two parallel disks. *Journal of Porous Media*. vol. 22, no. 2. pp. 209–223. doi: 10.1615/JPorMedia.2018028721.
- [23] Veera Krishna, M., Bharathi, K., and Chamkha, A. J. **2018**. Hall effects on mhd peristaltic flow of Jeffrey fluid through porous medium in a vertical stratum. *Interfacial Phenomena and Heat Transfer*. vol. 6, no. 3. pp. 253–268. doi: 10.1615/InterfacPhenomHeatTransfer.2019030215.
- [24] Veera Krishna, M. and Chamkha, A. J. **2019**. Hall and ion slip effects on MHD rotating boundary layer flow of nanofluid past an infinite vertical plate embedded in a porous medium. *Results in Physics*. vol. 15, no. April. doi: 10.1016/j.rinp.2019.102652.
- [25] Krishna, M. V. and Chamkha, A. J. **2020**. Hall and ion slip effects on MHD rotating flow of elastico-viscous fluid through porous medium. *International Communications in*

Heat and Mass Transfer.vol. 113, no. February.p. 104494. doi: 10.1016/j.icheatmasstransfer.2020.104494.

- [26] Ghazvini,M.,Akhavan-Behabadi,M. A.,Rasouli,E.,and Raisee,M. **2012**.Heat transfer properties of nanodiamond-engine oil nanofluid in laminar flow.*Heat Transfer Engineering*.vol. 33, no. 6.pp. 525–532. doi: 10.1080/01457632.2012.624858.
- [27] Bazri,S.,Badruddin,I. A.,Naghavi,M. S.,and Bahiraei,M. **2018**.A review of numerical studies on solar collectors integrated with latent heat storage systems employing fins or nanoparticles.*Renewable Energy*.vol. 118.pp. 761–778. doi: 10.1016/j.renene.2017.11.030.
- [28] Choi,S. U. S. **1995**.Enhancing thermal conductivity of fluids with nanoparticles.*American Society of Mechanical Engineers, Fluids Engineering Division (Publication) FED*.vol. 231, no. January 1995.pp. 99–105.
- [29] Buongiorno,J. **2006**.Convective transport in nanofluids.*Journal of Heat Transfer*.vol. 128, no. 3.pp. 240–250. doi: 10.1115/1.2150834.
- [30] Eastman,J. A.,Choi,S. U. S.,Li,S.,Yu,W.,and Thompson,L. J. **2001**.Anomalously increased effective thermal conductivities of ethylene glycol-based nanofluids containing copper nanoparticles.*Applied Physics Letters*.vol. 78, no. 6.pp. 718–720. doi: 10.1063/1.1341218.
- [31] Khanafer,K.,Vafai,K.,and Lightstone,M. **2003**.Buoyancy-driven heat transfer enhancement in a two-dimensional enclosure utilizing nanofluids.*International Journal of Heat and Mass Transfer*.vol. 46, no. 19.pp. 3639–3653. doi: 10.1016/S0017-9310(03)00156-X.
- [32] Sezer,N.,Atieh,M. A.,and Koc,M. **2018**.A comprehensive review on synthesis, stability, thermophysical properties, and characterization of nanofluids.*Powder Technology*.vol. 344.pp. 404–431. doi: 10.1016/j.powtec.2018.12.016.
- [33] Coccia,G.,Tomassetti,S.,and Di Nicola,G. **2021**.Thermal conductivity of nanofluids: A review of the existing correlations and a scaled semi-empirical equation.*Renewable and Sustainable Energy Reviews*.vol. 151, no. August.p. 111573. doi: 10.1016/j.rser.2021.111573.
- [34] Hajatzadeh,A. *et al.* **2021**.Nanofluids : Physical phenomena , applications in thermal systems and the environment effects- a critical review.*Journal of Cleaner Production*.vol. 320, no. July.p. 128573. doi: 10.1016/j.jclepro.2021.128573.
- [35] Huang,Y.,Cheng,X.,Li,Y.,Yu,G.,Xu,K.,and Li,G. **2018**.Effect of in-situ synthesized

- nano-MgO on thermal properties of NaNO₃-KNO₃. *Solar Energy*. vol. 160, no. December 2017. pp. 208–215. doi: 10.1016/j.solener.2017.11.077.
- [36] Chieruzzi, M., Cerritelli, G. F., Miliozzi, A., Kenny, J. M., and Torre, L. **2017**. Heat capacity of nanofluids for solar energy storage produced by dispersing oxide nanoparticles in nitrate salt mixture directly at high temperature. *Solar Energy Materials and Solar Cells*. vol. 167, no. December 2016. pp. 60–69. doi: 10.1016/j.solmat.2017.04.011.
- [37] Muñoz-Sánchez, B., Nieto-Maestre, J., Imbuluzqueta, G., Marañón, I., Iparraguirre-Torres, I., and García-Romero, A. **2017**. A precise method to measure the specific heat of solar salt-based nanofluids. *Journal of Thermal Analysis and Calorimetry*. vol. 129, no. 2. pp. 905–914. doi: 10.1007/s10973-017-6272-x.
- [38] Nithiyantham, U., Zaki, A., Grosu, Y., González-Fernández, L., Igartua, J. M., and Faik, A. **2019**. SiO₂@Al₂O₃ core-shell nanoparticles based molten salts nanofluids for thermal energy storage applications. *Journal of Energy Storage*. vol. 26, no. August. p. 101033. doi: 10.1016/j.est.2019.101033.
- [39] Svobodova-Sedlackova, A., Calderón, A., Barreneche, C., Gamallo, P., and Fernández, A. I. **2021**. Understanding the abnormal thermal behavior of nanofluids through infrared thermography and thermo - physical characterization. *Scientific Reports*. no. 0123456789. pp. 1–10. doi: 10.1038/s41598-021-84292-9.
- [40] Carrillo-Berdugo, I. *et al.* **2019**. Interface-inspired formulation and molecular-level perspectives on heat conduction and energy storage of nanofluids. *Scientific Reports*. vol. 9, no. 1. pp. 1–13. doi: 10.1038/s41598-019-44054-0.
- [41] Singh, D. *et al.* **2009**. An investigation of silicon carbide-water nanofluid for heat transfer applications. *Journal of Applied Physics*. vol. 105, no. 6. doi: 10.1063/1.3082094.
- [42] Pastoriza-Gallego, M. J., Casanova, C., Páramo, R., Barbs, B., Legido, J. L., and Piñeiro, M. M. **2009**. A study on stability and thermophysical properties (density and viscosity) of Al₂O₃ in water nanofluid. *Journal of Applied Physics*. vol. 106, no. 6. doi: 10.1063/1.3187732.
- [43] Starace, A. K., Gomez, J. C., Wang, J., Pradhan, S., and Glatzmaier, G. C. **2011**. Nanofluid heat capacities. *Journal of Applied Physics*. vol. 110, no. 12. doi: 10.1063/1.3672685.
- [44] Saeedinia, M., Akhavan-Behabadi, M. A., and Razi, P. **2012**. Thermal and rheological characteristics of CuO-Base oil nanofluid flow inside a circular tube. *International*

Communications in Heat and Mass Transfer.vol. 39, no. 1.pp. 152–159. doi: 10.1016/j.icheatmasstransfer.2011.08.001.

- [45] Rehman,W. U. *et al.* **2019**.Synthesis, characterization, stability and thermal conductivity of multi-walled carbon nanotubes (MWCNTs) and eco-friendly jatropha seed oil based nanofluid: An experimental investigation and modeling approach.*Journal of Molecular Liquids*.vol. 293. doi: 10.1016/j.molliq.2019.111534.
- [46] Shin,D. and Banerjee,D. **2011**.Enhancement of specific heat capacity of high-temperature silica-nanofluids synthesized in alkali chloride salt eutectics for solar thermal-energy storage applications.*International Journal of Heat and Mass Transfer*.vol. 54, no. 5–6.pp. 1064–1070. doi: 10.1016/j.ijheatmasstransfer.2010.11.017.
- [47] Verma,S. K. and Tiwari,A. K. **2015**.Progress of nanofluid application in solar collectors: A review.*Energy Conversion and Management*.vol. 100.pp. 324–346. doi: 10.1016/j.enconman.2015.04.071.
- [48] Shahrul,I. M.,Mahbubul,I. M.,Khaleduzzaman,S. S.,Saidur,R.,and Sabri,M. F. M. **2014**.A comparative review on the specific heat of nanofluids for energy perspective.*Renewable and Sustainable Energy Reviews*.vol. 38.pp. 88–98. doi: 10.1016/j.rser.2014.05.081.
- [49] Yang,L.,Xu,J.,Du,K.,and Zhang,X. **2017**.Recent developments on viscosity and thermal conductivity of nanofluids.*Powder Technology*.vol. 317.pp. 348–369. doi: 10.1016/j.powtec.2017.04.061.
- [50] Murshed,S. M. S. and Estellé,P. **2017**.A state of the art review on viscosity of nanofluids.*Renewable and Sustainable Energy Reviews*.vol. 76, no. August 2016.pp. 1134–1152. doi: 10.1016/j.rser.2017.03.113.
- [51] Kumar,L. H.,Kazi,S. N.,Masjuki,H. H.,and Zubir,M. N. M. **2022**.A review of recent advances in green nanofluids and their application in thermal systems.*Chemical Engineering Journal*.vol. 429, no. September 2021.p. 132321. doi: 10.1016/j.cej.2021.132321.
- [52] Ahmadi,M. H.,Mirlohi,A.,Alhuyi Nazari,M.,and Ghasempour,R. **2018**.A review of thermal conductivity of various nanofluids.*Journal of Molecular Liquids*.vol. 265.pp. 181–188. doi: 10.1016/j.molliq.2018.05.124.
- [53] Sofiah,A. G. N.,Samyano,M.,Pandey,A. K.,Kadrigama,K.,Sharma,K.,and Saidur,R. **2021**.Immense impact from small particles: Review on stability and thermophysical

properties of nanofluids. *Sustainable Energy Technologies and Assessments*. vol. 48, no. 5. p. 101635. doi: 10.1016/j.seta.2021.101635.

- [54] Pandey, S. D. and Nema, V. K. **2012**. Experimental analysis of heat transfer and friction factor of nanofluid as a coolant in a corrugated plate heat exchanger. *Experimental Thermal and Fluid Science*. vol. 38. pp. 248–256. doi: 10.1016/j.expthermflusci.2011.12.013.
- [55] Vajjha, R. S. and Das, D. K. **2009**. Specific heat measurement of three nanofluids and development of new correlations. *Journal of Heat Transfer*. vol. 131, no. 7. pp. 1–7. doi: 10.1115/1.3090813.
- [56] Fakoor Pakdaman, M., Akhavan-Behabadi, M. A., and Razi, P. **2012**. An experimental investigation on thermo-physical properties and overall performance of MWCNT/heat transfer oil nanofluid flow inside vertical helically coiled tubes. *Experimental Thermal and Fluid Science*. vol. 40. pp. 103–111. doi: 10.1016/j.expthermflusci.2012.02.005.
- [57] Murshed, S. M. S. **2011**. Determination of effective specific heat of nanofluids. *Journal of Experimental Nanoscience*. vol. 6, no. 5. pp. 539–546. doi: 10.1080/17458080.2010.498838.
- [58] Angayarkanni, S. A. and Philip, J. **2015**. Review on thermal properties of nanofluids: Recent developments. *Advances in Colloid and Interface Science*. vol. 225. pp. 146–176. doi: 10.1016/j.cis.2015.08.014.
- [59] Che Sidik, N. A., Mahmud Jamil, M., Aziz Japar, W. M. A., and Muhammad Adamu, I. **2017**. A review on preparation methods, stability and applications of hybrid nanofluids. *Renewable and Sustainable Energy Reviews*. vol. 80, no. May. pp. 1112–1122. doi: 10.1016/j.rser.2017.05.221.
- [60] PRITCHARD, A. **1969**. Statistical bibliography or bibliometrics. *Journal of Documentation*. vol. 25. p. 348.
- [61] Belter, C. W. **2015**. Bibliometric indicators: Opportunities and limits. *Journal of the Medical Library Association*. vol. 103, no. 4. pp. 219–221. doi: 10.3163/1536-5050.103.4.014.
- [62] Roemer, C. R. and Borchardt, R. **2015**. *Meaningful Metrics. A 21st-Century Librarian's Guide to Bibliometrics, Altmetrics, and research Impact*.
- [63] Szomszor, M. et al. **2021**. Interpreting Bibliometric Data. *Frontiers in Research Metrics and Analytics*. vol. 5, no. February. pp. 1–20. doi: 10.3389/frma.2020.628703.
- [64] Andrés, A. **2009**. *Measuring Academic Research: How to Undertake a Bibliometric*

Study. Oxford: Chandos Publishing. doi: 10.1533/9781780630182.

- [65] Merigó, J. M., Gil-Lafuente, A. M., and Yager, R. R. **2015**. An overview of fuzzy research with bibliometric indicators. *Applied Soft Computing Journal*. vol. 27. pp. 420–433. doi: 10.1016/j.asoc.2014.10.035.
- [66] Calderón, A., Barreneche, C., Hernández-Valle, K., Galindo, E., Segarra, M., and Fernández, A. I. **2019**. Where is Thermal Energy Storage (TES) research going? – A bibliometric analysis. *Solar Energy*. doi: <https://doi.org/10.1016/j.solener.2019.01.050>.
- [67] Calderón, A. **2019**. Study of solid particle materials as high temperature Thermal Energy Storage and Heat Transfer Fluid for Concentrating Solar Power, Universitat de Barcelona. doi: <http://hdl.handle.net/2445/144858>.
- [68] Masuda, H., Ebata, A., Teramae, K., and Hishinuma, N. **1993**. Alteration of Thermal Conductivity and Viscosity of Liquid by Dispersing Ultra-Fine Particles. Dispersion of Al₂O₃, SiO₂ and TiO₂ Ultra-Fine Particles. *Netsu Bussei*. vol. 7, no. 4. pp. 227–233. doi: 10.2963/jjtp.7.227.
- [69] de Solla Price, D. J. **1976**. A General Theory of Bibliometric and Other Cumulative Advantage Processes. *Journal of the American Society for Information Science*. vol. 27, no. 5–6. pp. 292–306.
- [70] Pozhar, L. A. and Gubbins, K. E. **1997**. Quasihydrodynamics of nanofluid mixtures. *Physical Review E - Statistical Physics, Plasmas, Fluids, and Related Interdisciplinary Topics*. vol. 56, no. 5. pp. 5367–5396. doi: 10.1103/PhysRevE.56.5367.
- [71] Hamilton, R. L. and Crosser, O. K. **1962**. Thermal conductivity of heterogeneous TWO-COMPONENT SYSTEMS. no. 3. pp. 1–5.
- [72] Brinkman, H. C. **1952**. The Viscosity of Concentrated Suspensions. *Journal of Chemical Physics*. vol. 20, no. 4. pp. 571–583. doi: 10.1122/1.549141.
- [73] Burton, R. E. and Webler, R. W. **1960**. The "half-life" of some scientific and technical literatures. *American Documentation*. vol. XI. pp. 18–22.
- [74] Buongiorno, J. *et al.* **2009**. A benchmark study on the thermal conductivity of nanofluids. *Journal of Applied Physics*. vol. 106, no. 9. doi: 10.1063/1.3245330.
- [75] Brookes, B. C. **1969**. Bradford's law and the bibliography of science. *Nature*. vol. 224, no. 5223. pp. 953–956. doi: 10.1038/224953a0.
- [76] Brookes, B. **1973**. Numerical Methods of Bibliographic Analysis. *Library Trends*. vol.

22.pp. 18–43.

- [77] O'Connor,D. O. and Voos,H. **1981**.Empirical laws, theory construction and bibliometrics.*Library Trends*.vol. 30, no. 1.pp. 9–20.
- [78] Bradford,S. C. **1985**.Sources of information on specific subjects.*Journal of Information Science*.vol. 10, no. 4.pp. 173–175. doi: 10.1177/016555158501000406.
- [79] Martín-Del-río,B.,Neipp,M. C.,García-Selva,A.,and Solanes-Puchol,A. **2021**.Positive organizational psychology: A bibliometric review and science mapping analysis.*International Journal of Environmental Research and Public Health*.vol. 18, no. 10. doi: 10.3390/ijerph18105222.
- [80] Zeng,L.,Li,R. Y. M.,Nuttapong,J.,Sun,J.,and Mao,Y. **2022**.Economic Development and Mountain Tourism Research from 2010 to 2020: Bibliometric Analysis and Science Mapping Approach.*Sustainability (Switzerland)*.vol. 14, no. 1. doi: 10.3390/su14010562.
- [81] Bailón-Moreno,R.,Jurado-Alameda,E.,Ruiz-Baños,R.,and Courtial,J. P. **2005**.Bibliometric laws: Empirical flaws of fit.*Scientometrics*.vol. 63, no. 2.pp. 209–229. doi: 10.1007/s11192-005-0211-5.
- [82] Ahmi,A.,Saidin,S. Z.,Mohd Nasir,M. H.,and Ismail,Z. **2020**.Applicability of lotka's law in extensible business reporting language (XBRL) studies.*International Journal of Advanced Science and Technology*.vol. 29, no. 6.pp. 282–289.
- [83] Kushairi,N. and Ahmi,A. **2021**.Flipped classroom in the second decade of the Millenia: a Bibliometrics analysis with Lotka's law.*Education and Information Technologies*.vol. 26, no. 4.pp. 4401–4431. doi: 10.1007/s10639-021-10457-8.
- [84] European Cooperation in science & technology. **2021**.COST Association, CA15119-Overcoming barriers to Nanofluids Market Uptake. www.cost.eu/actions/CA15119 (accessed Sep. 02, 2021).
- [85] State Information Center.Belt and road portal. <https://eng.yidaiyilu.gov.cn> (accessed Sep. 02, 2021).

6.3 A Particular Case – Nanofluids for Energy Systems

With the previous study, it has been identified that one of the main applications of nanofluids is related to energy systems and mainly focused on renewable energies, where TES systems are included, which is the focus of this thesis. Using the same methodology, the analysis of the following keywords was carried out (in the same database): “collector, csp, steam accumulator, cooling, nuclear, geothermal, automotive, electronics, heat exchanger, pipe, exchanger, compressed, oil recovery, photovoltaic-thermal, photothermalelectric, photovoltaic thermal, pvt, concentrated solar, Fresnel”.

Figure 6.3 shows the evolution during the last decade of the number of publications and citations related to the different technologies that use working fluids. It is observed that, as in the general case, there is an exponential growth in the number of publications over the years, accumulating a total of 3134 publications at the end of 2019, representing more than 20% of the total nanofluids publications.

Figure 6.4-a shows the top 10 countries/regions with the highest number of publications on nanofluids applications that require working fluids in the last decade. As in the general case, Iran, India, and China are the top three countries.

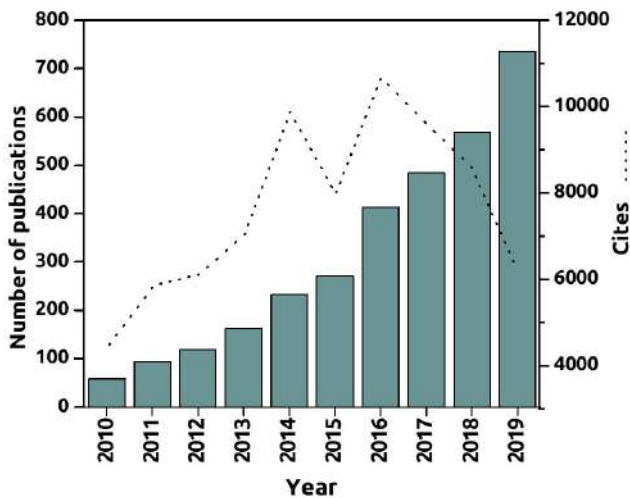


Figure 6.3. Number of publications and citations related to nanofluids for energy systems applications from 2010 to 2019.

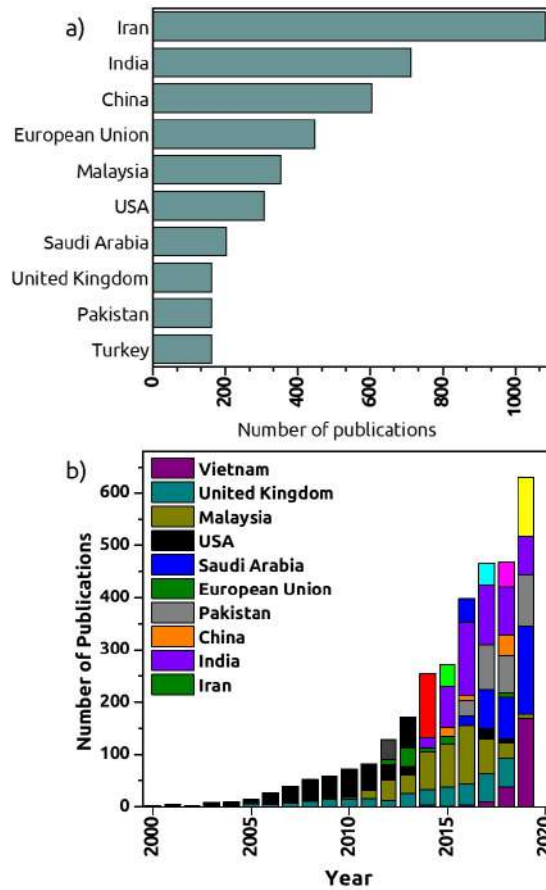


Figure 6.4. a) Top 10 countries/regions with the highest number of publications related to nanofluids application topic in the last decade. b) Number of publications per year for the top 10 countries/regions.

Figure 6.4-b details the temporal evolution of those publications and countries/regions in the last decade. During this period and year by year all countries/regions have increased the number of articles related to this topic. At the end of 2019, Iran followed by India are the countries that most contributed in the nanofluids applications field.

In addition, Table 6.1 shows the top 10 authors with the highest number of publications on nanofluids applications in the last decade. On this field, the top author at the end of 2019 is Saidur, R. with 67 publications and more than 3000 citations. On the other hand, the author Sarafray, M. M. has 37 publications and has more than 3000 citations.

It is interesting to note that there are not Chinese affiliated authors among the top 10 authors, despite being one of the top contributing countries. As previously done, it is interesting to analyse which authors are most cited and their interactions in the field of nanofluids applications (Figure 6.5). There are two main authors' clusters, the first formed mainly by Choi, S. and Xuan, Y. and the second led by Sheikholeslami, M. On the other hand, Table 6.2 lists the main journals where the authors published papers about applications of nanofluids. The main journal on this subject is Applied Thermal Engineering, with a total of 241 articles and 8285 citations, at the end of

2019. Despite this, journals such as International Communications in Heat and Mass Transfer or Energy Conversion and Management presented an improved PR. Furthermore, note that most of the journals are in the Q1 quartile. Additionally, in the Journal of Thermal Analysis and Calorimetry (Q3) from Netherlands, more than 50% of the publications come from Iran. To conclude this sub-category, the interaction among the different affiliation countries/regions was analysed. Figure 6.6 shows the interactions among the top 20 countries/regions according to their number of publications. The most relevant result is the high collaboration that Saudi Arabia has with countries such as Pakistan, Egypt, or Iran.

Table 6.1. Top 10 authors with the highest number of publications on nanofluids application topic and some quality indexes.

Author	Number of publications	h-index	Number of citations	Affiliation
Saidur, Rahman	67	36	3062	Sunway University, Malaysia
Wongwises, Somchai	51	28	3114	King Mongkut's University of Technology Thonburi, Thailand
Bahiraee, Mehdi	46	23	1062	Duy Tan University, Vietnam
Kazi, Salim Newaz	38	16	1111	University of Malaysia, Malaysia
Sarafraz, Mohammad Mohsen	37	36	3062	Deakin University, Australia
Hormozi, Faramarz	37	23	1405	Semnan University, Iran
Toghraie, Davood	34	16	898	Khomeinishahr Azad University, Iran
Sheikholeslami, Mohsen	32	19	1609	Babol Noshirvani University of Technology, Iran
Afrand, Masoud	31	15	1125	Islamic Azad University, Najafabad Branch, Iran
Sozen, Adnan	31	12	307	Gazi Üniversitesi, Turkey

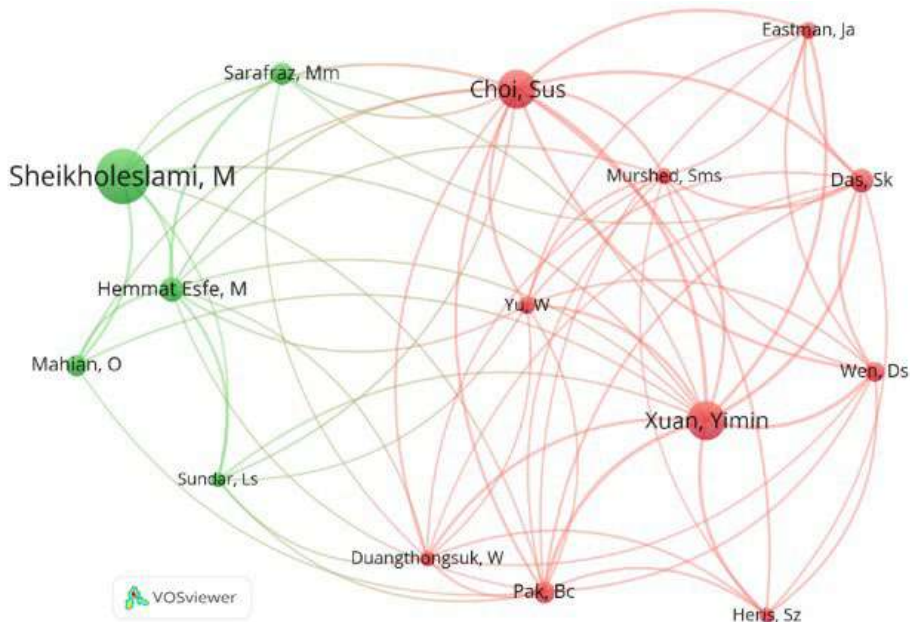


Figure 6.5. Top 15 authors with the highest number of citations on nanofluids application topic.

Table 6.2. Top 10 scientific journals with the highest number of publications on nanofluids application topic and some quality indexes, in the last 20 years.

Journal	Total articles	Total citations	Performance Ratio	h-index	SJR 2019	Quartile Scores	Main countries
Applied Thermal Engineering	241	8285	34.4	50	1.78	Q1	Iran (80) China (48)
International Journal of Heat and Mass Transfer	229	12558	54.8	58	1.65	Q1	China (64) USA (30)
Journal of Thermal Analysis and Calorimetry	204	1747	8.6	23	0.42	Q3	Iran (106) India (33)
International Communications in Heat and Mass Transfer	181	6461	35.7	47	1.41	Q1	Iran (65) Malaysia (54)
Energy Conversion and Management	135	5435	40.3	47	2.92	Q1	Iran (47) China (29)
Heat and Mass Transfer	95	981	10.3	14	0.57	Q2	Iran (35) India (23)
Solar Energy	88	2773	31.5	31	1.54	Q1	China (19), Iran (17)
Renewable Energy	86	2543	29.6	29	2.05	Q1	Iran (22), India (14)
Experimental Thermal and Fluid Science	79	4306	54.5	41	1.39	Q1	Iran (28), India (19)
Journal of Molecular Liquids	75	1597	21.3	23	0.88	Q1	Iran (40), China (14)

Also, it is noted the strong interaction that the United States has with China and Iran. In addition, India despite being the second country with the highest number of publications, does not have strong interactions with any country.

6.3.1 Heat transfer and thermal storage materials

Working fluids are classified as heat transfer fluids (HTF) or thermal energy storage (TES) media. In this section, the bibliometric analyses of these two categories are presented. **Figure 6.7** com-

pare for both cases the top 10 countries/regions with the highest number of publications in both topics. In the case of HTFs, **Figure 6.7-a** shows that the main regions publishing in this topic are the European Union followed by India, with more than 100 of publications at the end of 2019.

On the other hand, in the field of TES (**Figure 6.7-b**) the two main countries that contribute are Iran followed by India with more than 1000 publications. Therefore, in general trends, nanofluids for TES are more studied than for heat transfer fluids.

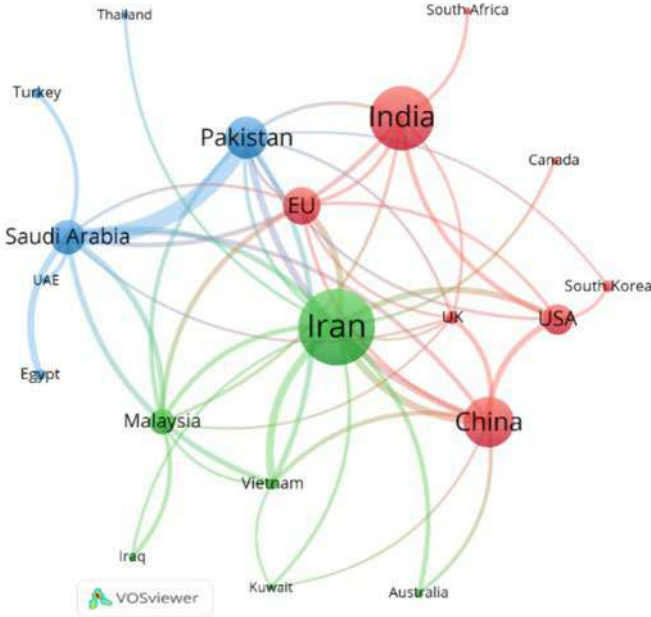


Figure 6.6. Top 20 countries with the highest number of publications on nanofluids application topic and the collaborations among them.

Moreover, the evolution over the last 10 year of the top 10 countries publishing in these sub-topics is analysed in **Figure 6.8** where it is disclosed the HTF and TES evolution during the last decade. For the HTF case, (**Figure 6.8-a**), a stagnation of the number of publications is observed in the years 2012 and 2015. The reduction in 2012 was caused mainly by the decrease of publications from China and United Kingdom and the decrement in 2015 was mainly due to the decrease in the number of EU publications. Since 2016 and up to 2019 the number of publications has increased, reaching almost 90 publications per year

Thereby, TES field is growing the number of publications year by year as **Figure 6.8-b** shows. Furthermore, a high increase in the number of publications during 2019 is observed. This fact indicates that during the last year this sector has taken a higher scientific interest for all the countries/regions plotted and denoting the potential for the use of nanofluids as TES medium.

Table 6.3 and **Table 6.4** shows the top 10 main authors in these two topics. The main HTF author was Navas, J. with 18 publications.

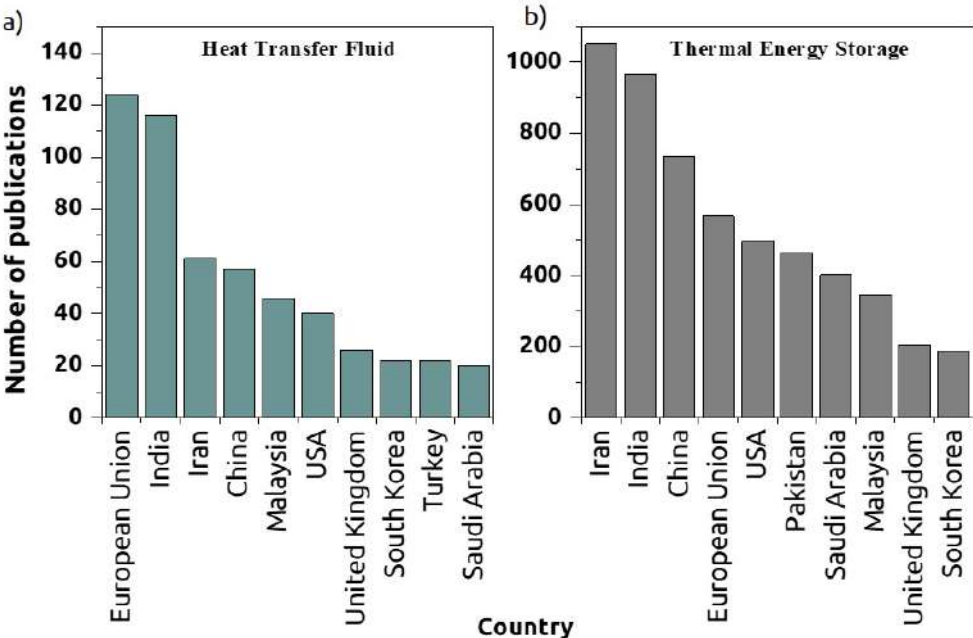


Figure 6.7. Top 10 countries/regions with the highest number of publications on nanofluids application topic as a) heat transfer fluid and b) thermal energy storage medium.

Although, all HTF authors have approximately the same order of magnitude in number of publications, **Table 6.3**. It is important to note that predominate authors from Spanish institutions, except for Saidur, R. from Malaysia. On the other hand, on the TES sub-topic, the main author is Alsaedi, A., with 91 publications. The top 10 authors of this sub-topic are listed in **Table 6.4**, being the most cited author Sheikholeslami, M. with 4.436 cites. Notice that some

of the authors listed are also those that published a higher number of publications about nanofluids in the general analysis (e.g., Alsaedi, A., Pop, I. or Sheikholeslami, M. Again, this fact indicates the relevance of the TES topic in the nanofluids field.

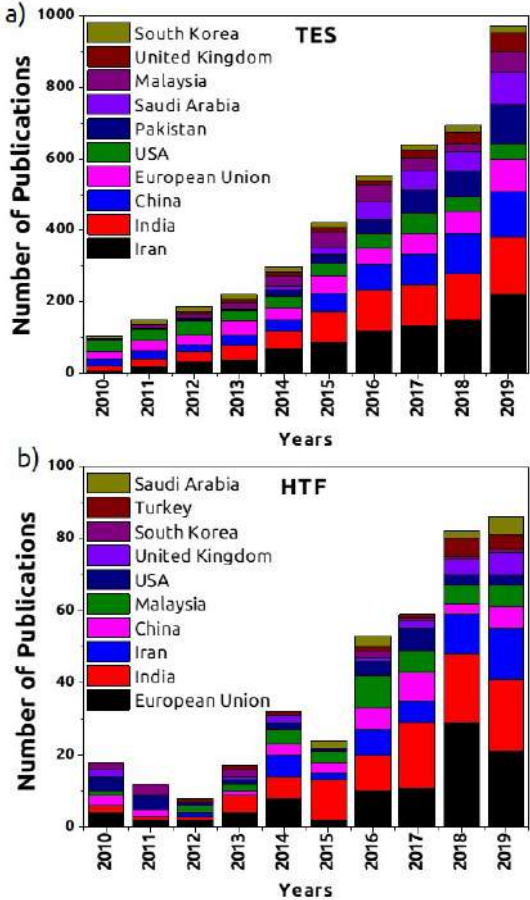


Figure 6.8. Top 10 countries/regions with the highest number of publications over the last decade on nanofluids application topic as a) HTF and b) TES materials

Table 6.3. Top 10 authors with the highest number of publications on nanofluids application topic on HTF and some quality indexes, in the last 20 years.

Author	Number of publications	h-index	Number of citations	Affiliation
Navas, Javier	18	7	169	Universidad de Cadiz, Spain
Saidur, Rahman	17	11	710	Sunway University, Malaysia
Alcantara, Rodrigo	16	6	144	Universidad de Cadiz, Spain
Gomez-villarejo, Roberto	14	6	134	Universidad de Cadiz, Spain
Aguilar, Teresa	13	6	155	CIC energigune, Spain
Fernandez-lorenzo, Concha	12	6	137	Universidad de Cadiz, Spain
Sanchez-coronilla, Antonio	12	6	134	University of Seville, Spain
Martin, Elisa i.	11	6	133	University of Seville, Spain
Kazi, Salim Newaz	10	8	635	University of Malaysia, Malaysia
Jesus Gallardo, Juan	9	5	122	Universidad de Cadiz, Spain

Table 6.4. Top 10 authors with the highest number of publications on nanofluids application topic on TES and some quality indexes, in the last 20 years.

Author	Number of Publications	h-index	Number of citations	Affiliation
Alsaedi, Ahmed	91	27	2323	King Abdulaziz University, S. Arabia
Chamkha, Ali j.	67	24	1639	Prince M. Bin Fahd Univ., S. Arabia
Ganji, Davood Domiri	65	33	3816	Babol Noshirvani Univ. of Tech., Iran
Pop, Ioan	63	25	2873	Univ, Babes-Bolyai din Cluj-Napoca, Romania
Hayat, Tasawar	57	22	1137	Quaid-i-Azam University, Pakistan
Sheikholeslami, Mohsen	54	30	4436	Babol Noshirvani Univ. of Tech., Iran
Bahiraee, Mehdi	52	24	1113	Duy Tan University, Vietnam
Wongwises, Somchai	51	26	2373	King Mongkut's Univ. of Tech. Thonburi, Thailand
Afrand, Masoud	49	26	1719	Islamic Azad Univ., Najafabad Branch, Iran
Hayat, Tanzila	49	23	1742	Quaid-i-Azam Univ., Pakistan

6.3.2 Nanofluids synthesis, characterization, and modelling

The last analysis performed divides the publications about nanofluids in three

categories: characterization, preparation, and modelling techniques. Analysing these topics can help understand what the investigations are primarily based on and better define the investigation. **Figure 6.9** shows the top

10 of the countries/regions that published in each category (in the last 20 years). The characterization one contains the main properties to characterize nanofluids and their behaviour, these include properties such as the specific heat capacity, thermal conductivity, viscosity, convective heat transfer, pressure drop, thermal transport or contact angle. **Figure 6.9-a** shows that Iran followed by India are the main

countries, with up to 3000 publications. Denote that, the total number of publications in this category represented the higher percentage, more than 95%, of the total publications in nanofluids field. This result indicates an important point; currently, the focus of nanofluids topic is on the nanofluids characterization and the understanding of their properties.

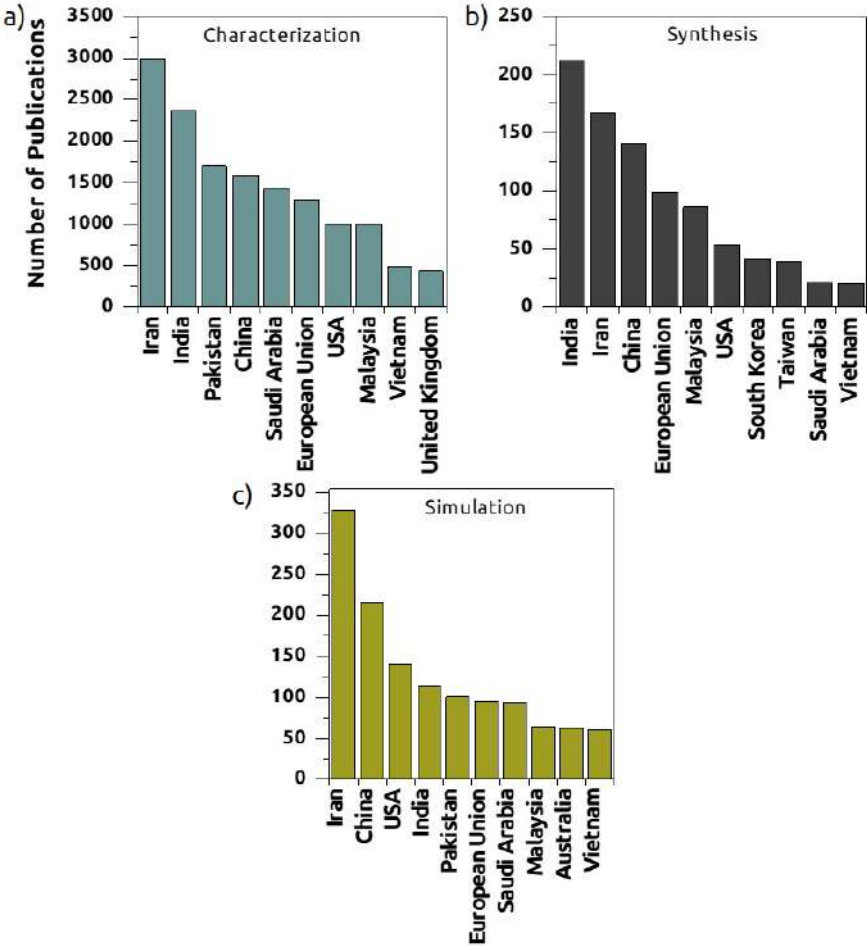


Figure 6.9. Top 10 countries/regions with the highest number of publications in the last 20 years on a) characterization, b) synthesis and c) modelling of nanofluids.

On the other hand, **Figure 6.9-b** shows that India and China are again the main countries publishing in the synthesis category. In the last years, the synthesis methods have been demonstrated as one of the main parameters affecting the final properties of nanofluids when comparing results between different experiments, as seen in **Chapter 2**. Nonetheless, it is important to remark the low number of publications that describes the synthesis method.

Finally, in **Figure 6.9-c** Iran and China are the most representative countries in the modelling field. Notice that in this category are included techniques such as quantum mechanics, mesoscale simulations, or finite element method (fem) simulations

6.3.3 European Union research

Until now, we have seen a global context of nanofluids research. In these last analysed topics, especially in HTF and TES systems, the European Union is positioned as one of the regions that leads these applications. With a focus on Spain and Middle Eastern countries, such as Iran and Saudi Arabia. This interest is reflected in the presence of CSP technology in these regions, as we

previously saw in **Figure 1.7** in the preface section.

Highlighting the high contribution by Spain, specifically by the University of Seville, that is motivated by Abengoa's facilities in this region, with the most mature technology and capacity installed around the world.

The following **Figure 6.10** shows the scientific production state in the European Union on nanofluids. Romania has the highest interest in nanofluids in terms of the number of publications and citations. On the contrary, Spain has the largest number of researchers contributing to this area. On the other hand, Netherland together with Spain leads the sector in terms of the number of publications in high-impact journals (Q1). Additionally, the global publications' average (%) in Q1 is over 11% larger than the world average.

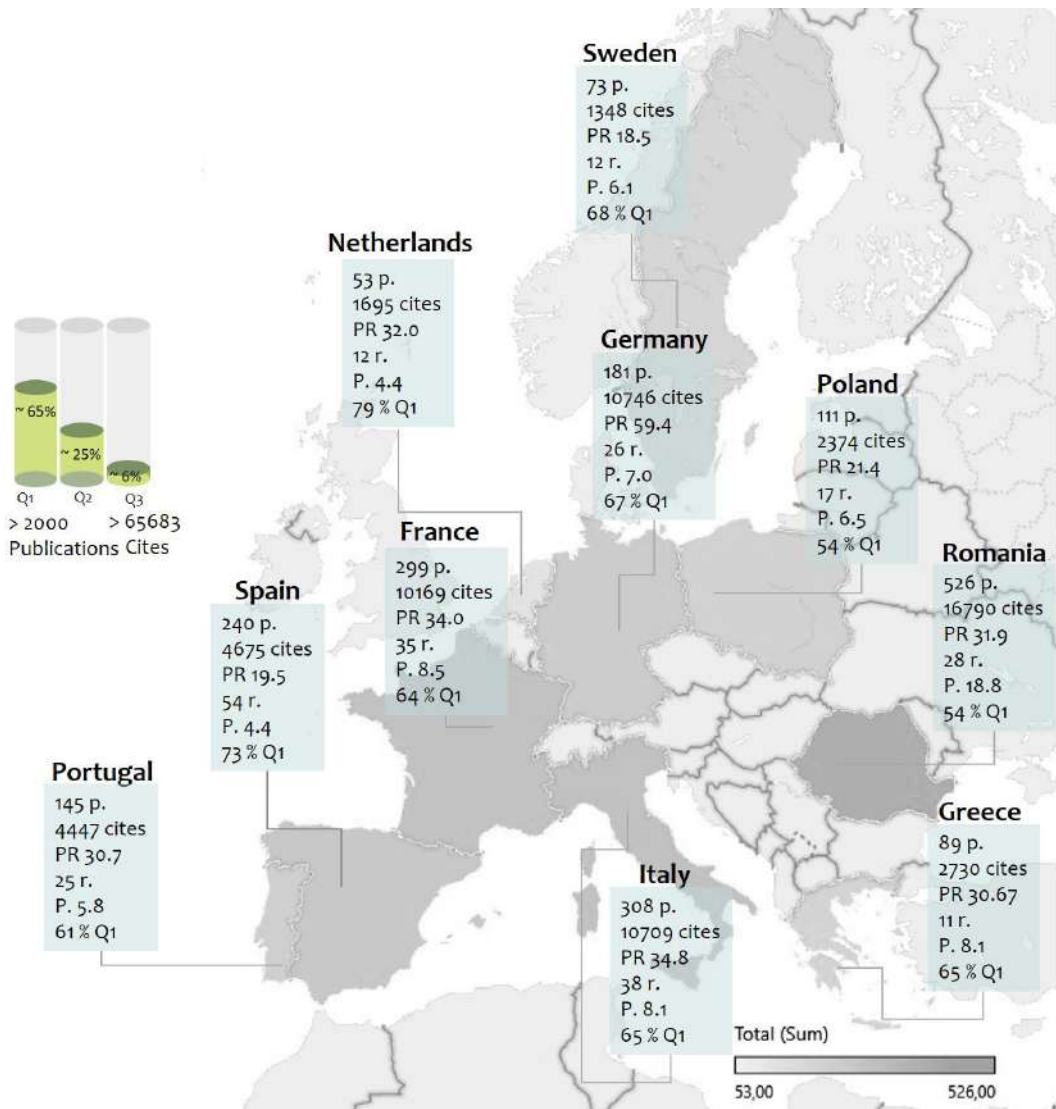
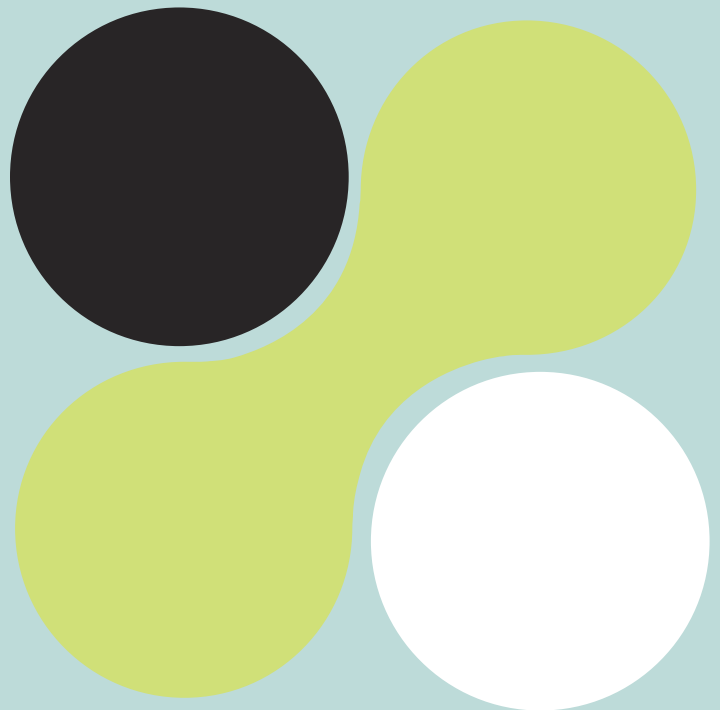


Figure 6.10. European Union Nanofluids research were p. = number of publications, PR = performance ratio (num. cites/num. articles), r. = number of researchers, and Pr. = productivity (num. authors/num. articles), at the end of 2020.

Statistical
approach
to nanofluids

Paper 2 & 3





Key point 2
Discrepancies

7. Statistical approach to nanofluids

Statistical tools for characterising and analysing the thermophysical properties

7.1 Introduction

Through the previous chapters, we have obtained a general idea about the state of this research and its relevance. This review indicated that there is still a long way to go and many obstacles to overcome to understand the science behind nanofluids. Therefore, developing a robust theoretical framework is essential to reach this milestone. Thus, the need to solve fundamental aspects, such as the lack of homogeneity of the published results, becomes even more evident. This fact implies a lack of knowledge of the

nanofluids thermophysical properties or thermal behaviour. These gaps are hindering its development and industrial application. In addition, there is also evidence of a lack of an appropriate methodology both to measure the properties and to analyse the results. Before starting any research and designing new experiments, it is essential to know and understand what the researchers are doing, and the results reported in the literature. For this reason, having a wide range of experimental results and procedures will make it easier to have a straightforward approach on how to address this

issue and contribute to its development with original and innovative experiments. It is precisely in these aspects that this chapter intends to influence through two points of view: (1) determine trends and limitations based on published results in the literature, and (2) corroborate the trends experimentally through a statistical analysis.

7.1.1 Relevance

The relevance of the two studies presented in this chapter lies in the novelty of analysing the bibliography and the published thermophysical properties from a statistical point of view, offering much clearer trends to researchers. Furthermore, these studies are of great help in selecting and synthesizing nanofluids with specific properties. On the other hand, this analysis allows us to identify the limitations and main errors made in reporting the data and measuring the nanofluids properties.

Additionally, the second study offers a statistical and sampling procedure to measure experimentally and present nanofluids' thermo-physical properties properly. Therefore, the ultimate purpose of this chapter is to contribute to **Key point 2**, helping to solve the controversial reported results.

7.1.2 Objectives

PART A:

- A critical review of publications related to nanofluids for TES.
- Collection of heat capacity values. Along with the values of base fluid, type of nanoparticles, concentration and size of nanoparticles and temperature.
- Identification of the methodologies and measurement equipment used.
- Identification of the sampling and statistics performed on the published results.
- Creation of a database with the Ansys CES Granta Selector software.
- Identification of sources of error and discrepancy between results.

PART B:

- Carry out a statistical sampling study in the case of NSBNFs.
- Determine the influence of nanoparticles on the melting temperature, melting enthalpy, heat capacity and their behaviour as a function of temperature.
- Determine the influence of the synthesis method on the final properties.

- Experimental determination of an appropriate methodology for characterizing nanofluids to minimize the standard deviation.

new database of Nanofluids' specific heat capacity", on 10 March 2022, as shown in **Figure 7.1**

7.2 Paper 2

The complete study is submitted in the Journal of Applied Energy entitled: "*Using statistical analysis to create a*

Using statistical analysis to create a new database of Nanofluids' specific heat capacity.

Adela Svobodova-Sedlackova^{1,2}, Alejandro Calderón^{1,3}, Xavier Sanuy Morell⁴, Marc Majó¹, Camila Barreneche¹, Pablo Gamallo^{1,2} and A. Inés Fernández^{1*}

¹*Departament de Ciència de Materials i Química Física, Universitat de Barcelona, C/Martí i Franqués 1, 08028, Barcelona, Spain.*

²*Institut de Química Teòrica i Computacional, IQTCUB, Universitat de Barcelona, C/Martí i Franqués 1, 08028, Barcelona, Spain.*

³*Departament d'Enginyeria Mecànica, Universitat Rovira i Virgili, Av. Paisos Catalans 26, 43007 Tarragona, Spain*

⁴*Department of Materials Science and Engineering, the University of Sheffield, Sir Robert Hadfield Building, Mappin St, S1 3JD, Sheffield, UK*

*Correspondance: ana_inesfernandez@ub.edu

Submitted/Received:

Revised/Accepted:

Abstract

Nowadays, heat transfer fluids (HTFs) with high thermal properties are needed to develop more efficient and compact energy systems to achieve sustainable development goals. Nanofluids (NFs), through the incorporation of nanoparticles in conventional HTFs, become one of the most suitable techniques to improve their thermophysical properties. However, despite its potential industrial applications, there is not only a lack of a theoretical framework but also a clear trend about its behavior. Therefore, this work aims to perform a critical review and statistical analysis to understand the NFs heat capacity (C_p). To this end, a wide variety of NFs from the literature was processed using Principal Component Analysis (PCA) and Response Surface Methodology (RSM). Finally, a database with Ansys Granta Constructor 2021 software was created and an analysis with Ansys Granta Selector 2021 was performed. As a result, the key parameters that impact the C_p of several nanofluids are obtained as well as: their high-temperature dependence, the nature of the liquid medium, and the type of nanoparticles. In addition, the results allow to identify and design nanofluids with specific properties for specific working conditions.

Figure 7.1. Submitted article entitled "Using statistical analysis to create a new database of Nanofluids specific heat capacity".

7.2.1 Graphical abstract

Figure 7.2 summarizes the most relevant results.

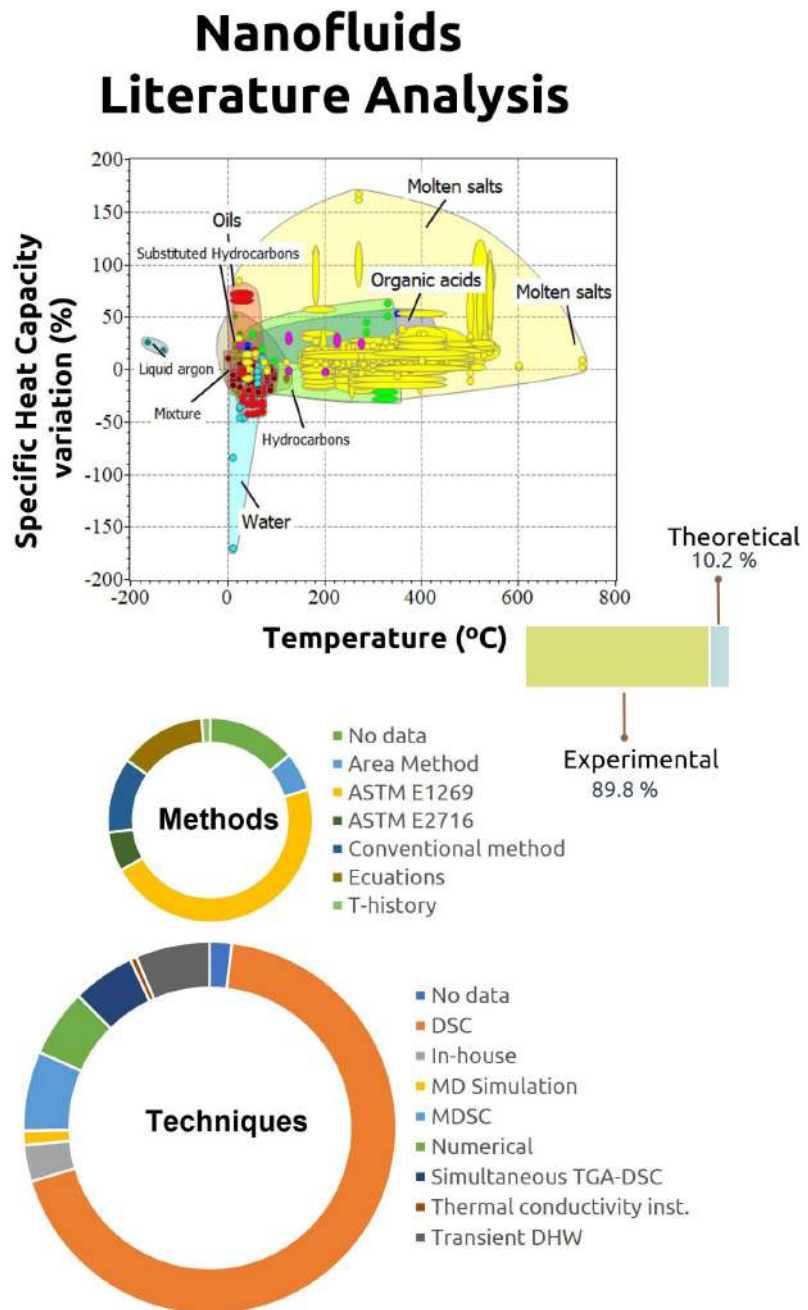
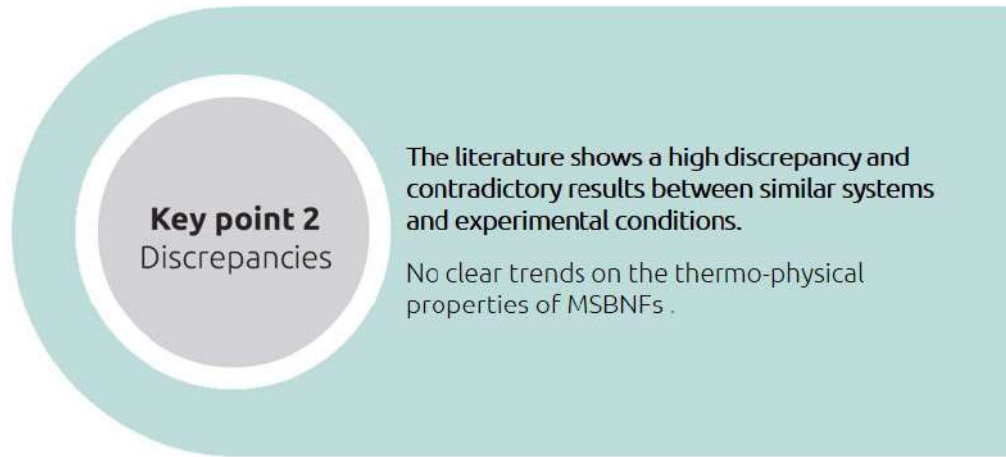


Figure 7.2. Graphical abstract of the submitted article: "Using statistical analysis to create a new database of Nanofluids' specific heat capacity".

7.2.2 Contribution to the state-of-the-art



Key point 2
Discrepancies

The literature shows a high discrepancy and contradictory results between similar systems and experimental conditions.

No clear trends on the thermo-physical properties of MSBNFs .

- ✓ Through the creation of a database, despite the high discrepancy regarding the specific heat capacity, some trends' can be found:
 - Inorganic base fluids show higher enhancements than organic base fluids. Specifically, molten salts show a higher potential to enhance their Cp. In contrast, water-based nanofluids show low enhancements and a Cp worsening in general trends.
 - Metal oxides and carbon-based nanoparticles show better performance. In contrast, metallic nanoparticles affect negatively in the Cp values.
 - The results shows and optimal relationship between nanoparticles concentration and size: (concentration (wt%)/size(nm) between 0.02 and 0.1 wt%·nm⁻¹ as depicts **Figure 7.3**.

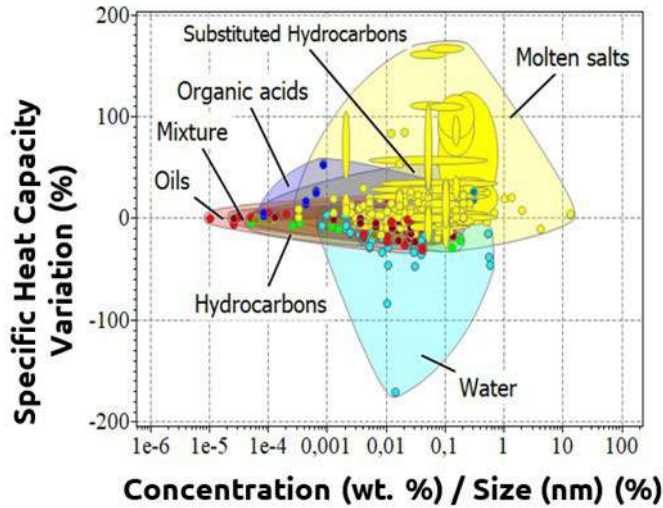


Figure 7.3. Specific Heat capacity variation (%) as a function of the concentration/size quotient ($1c/s$ index) classified as fluid base family.

- The literature analysis from the point of view of methodological procedures helps to highlight the lack of standard procedures to characterize nanofluids. Moreover, the results show low sampling and repeatability in the published literature. Some of these facts contribute to the impossibility to compare results. Table 7.1 shows some of the obtained statistical values.

Table 7.1. Statistical data of techniques, methods, and sampling of nanofluids for thermal energy storage.

Techniques	Methods	Sampling-statistics
No data: 14.0 %	No data: 1.9 %	No data: 29.0 %
Area Method: 6.1 %	DSC: 68.4 %	1 S, 1 R: 4.4 %
ASTM E1269: 46.7%	Hand Made: 3.2 %	> 1 S, 1 R: 15.8 %
ASTM E2716: 6.2%	MD Simulation: 1.2 %	1 S, >1 R: 36.3 %
Conventional method: 11.9 %	MDSC: 6.9 %	> 1 S, >1 R: 14.6 %
Ecuations: 13.7%	Numerical: 5.9 %	
T-history: 1.4%	Simultaneous TGA-DSC: 5.4 %	
	Thermal conductivity inst.: 0.6 %	
	Transient DHW: 6.4 %	

7.2.3 Publication

The article is attached below.

Using statistical analysis to create a new database of Nanofluids' specific heat capacity

Adela Svobodova-Sedlackova^{1,2}, Alejandro Calderón^{1,3}, Xavier Sanuy Morell⁴, Marc Neira-Viñas¹, Marc Majó¹, Camila Barreneche¹, Pablo Gamallo^{1,2} and A. Inés Fernandez^{1*}

¹*Departament de Ciència de Materials i Química Física, Universitat de Barcelona, C/Martí i Franqués 1, 08028, Barcelona, Spain.*

²*Institut de Química Teòrica i Computacional, IQTCUB, Universitat de Barcelona, C/Martí i Franqués 1, 08028, Barcelona, Spain.*

³*Departament d'Enginyeria Mecànica, Universitat Rovira i Virgili, Av. Paisos Catalans 26, 43007 Tarragona, Spain*

⁴*Department of Materials Science and Engineering, the University of Sheffield, Sir Robert Hadfield Building, Mappin St, S1 3JD, Sheffield, UK*

*Corresponding author: ana_inesfernandez@ub.edu

Abstract

Nowadays, heat transfer fluids (HTFs) with high thermal properties are needed to develop more efficient and compact energy systems to achieve sustainable development goals. Nanofluids (NFs), through the incorporation of nanoparticles in conventional HTFs, become one of the most suitable techniques to improve their thermophysical properties. However, despite its potential industrial applications, there is not only a lack of a theoretical framework but also a clear trend about its behavior. Therefore, this work aims to perform a critical review and statistical analysis to understand the NFs heat capacity (C_p). To this end, a wide variety of NFs from the literature was processed using Principal Component Analysis (PCA) and Response Surface Methodology (RSM). Finally, a database with Ansys Granta Constructor 2021 software was created and an analysis with Ansys Granta Selector 2021 was performed. As a result, the key parameters that impact the C_p of several nanofluids are obtained as well as: their high-temperature dependence, the nature of the liquid medium, and the type of nanoparticles. In addition, the results allow to identify and design nanofluids with specific properties for specific working conditions.

Keywords: Nanofluids; Concentrated Solar Power (CSP); Thermal Energy Storage (TES); nanoparticles; Principal Component Analysis (PCA); Response Surface Methodology (RSM)

1. Introduction

Energy is an essential resource for humanity, and its storage is one of the fundamental points for industrial development. Energy storage is considered a key enabling technology for fully implementing renewable energies (RE), solving their main drawback, and facilitating sustainable development goals. Therefore, incorporating a storage system allows to implement more efficient, safe, and flexible systems [1,2]. In Particular, concentrated solar power (CSP) plants that incorporate thermal energy storage (TES) facilities have become one of the most promising renewable solar technologies due to their cost-efficiency relation [3,4]. Several parameters of working fluids must be considered to design more efficient systems. Usually, these working fluids are simultaneously used as TES material and/or as heat transfer fluid (HTF). Therefore, the design, development, and improvement of TES and HTF fluids are essential for developing high-efficiency and optimal systems [5].

In the last years, researchers in diverse fields have been interested in the improvement of thermophysical properties across the addition of nanoparticles (NPs) into fluids (*i.e.*, oils [6], polyethylene glycol [7], molten salts [8], water [9]). This fact encourage to develop a new class of fluids known as nanofluids (NFs), studied for the first time in 1995 by Choi S. *et al.* [10]. NFs are engineered by suspending nanoparticles (NPs) (1–100 nm) in a base fluid. The NPs materials can be metallic, non-metallic, oxides, carbides, ceramics, carbon, a mixture of different NPs (hybrid NFs), and even nanoscale liquid droplets [11–14]. The NFs show improved thermophysical properties such as heat and mass transfer, thermal conductivity (κ), or specific heat capacity (C_p) compared to the base fluid [15–17]. Furthermore, a large variety of new potential applications of NFs have emerged over time, such as: lubricants [18], desalination [19], CO₂ absorption/capture [20], batteries [21], industrial cooling [22], or heat exchangers [23]. Specifically, NFs attracted the scientific community's attention due to their anomalous C_p improvement, reaching enhancements up to 30-40 % with the addition of low NPs concentrations (*i.e.*, 1 wt.%) [24]. Several studies have been carried out in recent years to investigate the NFs C_p enhancement, and great advances have been made to understand the phenomenon [25]. Moreover, the main parameters and properties that influence the C_p variation have been identified in the last years: NPs parameters (*i.e.*, concentration, size, shape, or nature), temperature, and pH, among others [16,26] Nevertheless, to achieve its scalability and understand its full potential, further investigations are required in order to develop a strong theoretical framework. Despite this, no studies have been found in which a clear trend in C_p values is showed

[16]. There is a high dispersion on the experimental-measured data reported in the literature: experiments under the same experimental conditions show different C_p values and performance. Furthermore, the results are contradictory in many cases, with unclear trend on their behavior [27–32]. Therefore, there are not clear tendencies on how the incorporation of NPs affects C_p . Another difficulty seen in the literature is the few specifications and non-accurate descriptions of the measurements and calculation methods. For example, there is no information that indicate at which temperature thermal values were obtained, or which methodology was followed. As a result, there does not seem to be a clear specification or protocol for properly measuring NFs. These facts make the comparison of results and the comprehension of their thermal performance under real conditions a challenging task.

This study aims to perform a critical review and analysis to understand the NFs C_p experimental reported data. For this purpose, several parameters from NFs employed in energy storage applications were collected from the literature: base fluid and NPs material, size, and concentration of the NPs, temperature, C_p enhancement, sampling, and experimental procedure (*i.e.*, equipment and methodology). Furthermore, a principal component analysis (PCA), ANOVA test, and response surface methodology (RSM) were employed to determine the main parameters affecting the C_p and their behavior and develop a mathematical model. The Ansys Granta Constructor 2021 tool was used to create a database which was analyzed using Ansys Granta Selector 2021 to select NFs with specific properties and observe their behavior. The main goal of this study is to unify C_p values and to identify clear trends to design NFs for applications with specific thermal requirements.

2. Methodology

Data acquisition: The data source for this study groups scientific journals and conference proceedings from Scopus database. The search was effectuated under the following keywords: "Nanofluids" and "Energy Storage." There were 301 publications associated with this research topic at the end of 2020, and 111 articles included C_p values. A total of 884 C_p values and their measurement specifications were extracted.

Principal component analysis (PCA): the database was standardized by the StandardScaler Sklearn function to make an equal comparison between each value [33]. Afterward, the database was transformed by a principal component analysis (PCA) defined by Sklearn [33]. PCA is a statistical method used for dimensionality reduction, features extraction, or data visualization by an orthogonal transformation of the dataset into a new subspace, with new axes called principal components (PCs) [34–36].

Statistical analysis-response surface methodology (RSM): The data were evaluated by the ANOVA statistical analysis (analysis of the variance) to fit the data to a mathematical model and predict values. To this end, the dependent variable (response) was the specific heat capacity, and the independent variables, the nanoparticles' size, concentration, and temperature. In this manner, with the help of the design of experiments software (Stat-Ease) and the obtained equations, a response surface was analyzed. As a result, the developed models using the experimental responses exhibited p-values below 0.0001, implying that the proposed models are relevant considering the factor relations presented for each response or equation.

Ansys Granta 2021 Constructor/Selector database: The database was created with the Constructor software from Ansys, employing the data obtained from the literature. The general organization of the database was divided into inorganic, organic, and mixtures and then arranged depending on the base fluid or the type of nanoparticles. The base fluids considered were hydrocarbons, substituted hydrocarbons, ionic liquids, molten salts, oils, organic acids, water, and mixtures. And the nanoparticles treated were metal oxides, metals, nitrides, and carbon-based nanoparticles. **Figure 1** depicts the arrangement of nanofluids, and the nanoparticles used in each base fluid.

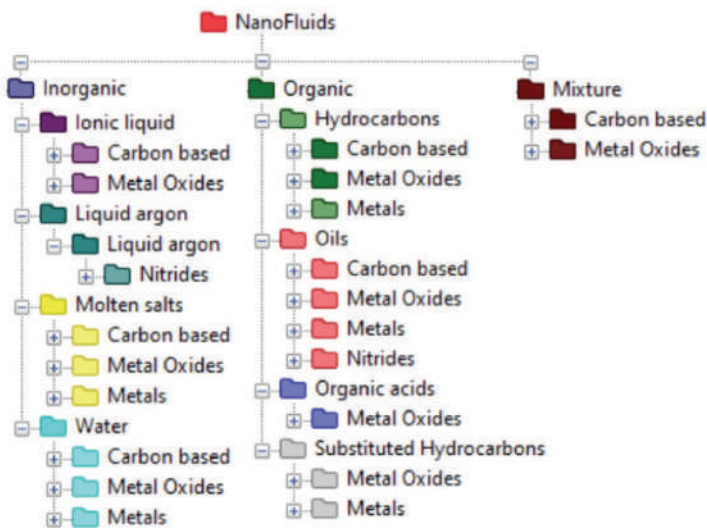


Figure 1. Arrangement of nanofluids in the nanofluids database.

3. Results

NFs were studied for diverse applications as HTS or TES material. These applications can be classified as high, medium, or low temperature [37]. Therefore, each application needs different thermal requirements. For this reason, a great variety of base fluid materials were found in the literature research. More in detail, **Table 1** summarizes the obtained 36 base fluids, with their corresponding references. Point out that solar salt ($\text{NaNO}_3 - \text{KNO}_3$ (60:40)) and water were the most studied systems and from which more C_p values were obtained.

Table 1. Summary of nanofluids base materials collected from the literature and their corresponding references.

Base material	References
Distilled Water (DW)	[45][46]
Methoxyperfluorobutane (HFE 7100)	[70]
Water	[70][71][72][73][74][75][76][77][78] [79][80][81][47][82][48][83][84] [85]
Propylene glycol (PG)	[53]
Capric acid (CA)	[86]
Myristic acid-capric acid eutectic (MA-CA)	[86]
Paraffin	[87][88][89]
n-octadecane	[49]
Polyalphaolefein (PAO)	[90][91]
Engine oil	[92][93][46][94]
Heat transfer oil	[95]
Mineral oil	[90]
Therminol-55	[96]
Oleic acid-(DL-menthol)	[97]
ethylene glycol (EG)	[51][50][98][94][46][84][90][99]
Glycerol	[99]
EG/Water	[100][101][102][103][72][90][104] [105][106][45][107][108]
KNO_3	[109][110][111]
NaNO_3	[4] [25] [59]
$\text{NaNO}_3 - \text{KNO}_3$ (60:40)	[112][113][114][28][115][30][116][117][29][118][119][120][121][122][123][124][125][126][127][128][129][1 30][131] [132][133][27][134][135][60][61] [110][136][62]
$\text{BaCl}_2 - \text{H}_2\text{O}$	[137]
$\text{NaCl} - \text{CaCl}_2$	[138]
$\text{BaCl}_2 - \text{NaCl} - \text{CaCl}_2 - \text{LiCl}$	[139]
$\text{Ca}(\text{NO}_3)_2 \cdot 4\text{H}_2\text{O} - \text{NaNO}_3 - \text{KNO}_3 - \text{LiNO}_3$	[30]
$\text{Ca}(\text{NO}_3)_2 - \text{KNO}_3 - \text{NaNO}_3 - \text{LiNO}_3$	[140][141][32]
$\text{Na}_2\text{CO}_3 \cdot 10\text{H}_2\text{O} - \text{Na}_2\text{HPO}_4 \cdot 12\text{H}_2\text{O}$ EHS (Eutectic Hydrate salt)	[142]
$\text{KNO}_3 - \text{NaNO}_2 - \text{NaNO}_3$ (53:40:7 mol. %) (MHS)	[143]

K ₂ CO ₃ -LiCO ₃ -Na ₂ CO ₃	[144]
Li ₂ CO ₃ -K ₂ CO ₃	[145][146][147][148][63][64][65] [66][67][68][69][149]
LiNO ₃ -NaNO ₃ -KNO ₃	[30][150][151]
Aviation turbine fuel	[152]
Ionic liquid [C4mim][PF6]	[153]
Ionic liquid ([HMIM]BF ₄)	[154]
Ionic liquid (C4mim)[NTf ₂]	[155]
Ionic liquid [C4mpyrr][NTf ₂]	[155]
Liquid argon	[156]

For each scientific article, the obtained information was: base fluid type (BF), density base fluid (ρ (BF), kg·m³), NPs type, NPs morphology (form factor), NPs concentration (wt. % and/or v. %), NPs density (ρ (NPs), kg·m³), NPs size (S, nm), temperature (T, °C) at was measured the C_p , C_p of BF (J·K⁻¹), C_p of NF (J·K⁻¹), NFs C_p variation (ΔC_p ,%), measurement conditions and procedures. Measurement conditions and procedures include the measurement methods, measurement techniques, sampling, and measurement conditions (*i.e.*, whether the first measurement was discarded or not). These variables are critical to analyzing C_p measurement methodology to compare values and develop standard methods for characterizing NFs.

3.1. Specific Heat capacity methodology and procedures

Instrumental and methodological analysis: Several techniques were found in the literature review to measure the C_p . These can be classified as theoretical (10.18 %) and experimental (89.82 %) techniques. The experimental techniques include a Transient double hot-wire (DHW), thermal conductivity instrument, simultaneous Thermogravimetry Analysis-Differential Scanning Calorimetry (TGA-DSC), Modulated Differential Scanning Calorimetry (MDSC), Handmade setups, and Differential Scanning calorimetry (DSC). Otherwise, theoretical techniques include numerical procedures and simulations (*i.e.*, molecular Dynamics Simulations (MD)). **Figure 2** shows a pie chart of the different techniques. The most used equipment was DSC, accounting more than 68 % of data measured through this technique. The rest of the techniques represent the 30.1 %: Transient DHW (6.4 %), Thermal conductivity instrument (0.6 %), Simultaneous TGA-DSC (5.4 %), Numerical techniques (5.9 %), MDSC (6.9 %), MD Simulations (1.2 %) and In-house devices (3.2 %). However, an important remark is that 1.9 % of the data do not describe the technique used to measure the thermophysical properties. Although this is a small proportion, it creates a gap in the methodological procedure since this parameter has to be described in the papers to reproduce the experiments under the same conditions. In fact, it is not surprising that the DSC was the most employed

technique because it is the most precise and suitable instrument to determine thermal properties (*i.e.*, melting temperature, melting enthalpy, or C_p) [38,39]. More in detail, the most used calorimetry instruments (DSC) were manufactured by Mettler Toledo© (26.5 %) and TA Instruments© (22.7 %), representing almost 50 % of the data, followed by Netzsch-Gruppe© (15.2), PerkinElmer®, Inc. (8.6 %) and finally Setaram kep technologies, Inc. ® (5.2 %).

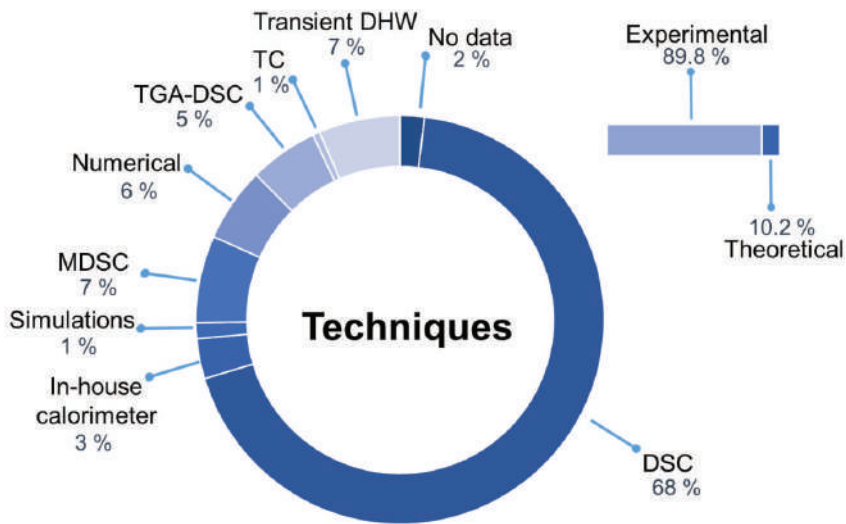


Figure 2. A pie chart of techniques used to determine the specific heat capacity: Transient DHW, TC (thermal conductivity instrument), Simultaneous TGA-DSC, Numerical techniques, MDSC (Modulated Differential scanning calorimeter), Simulations, In-house calorimeters, DSC, and percentage of no data. On the right is the rate of experimental and theoretical C_p determinations.

Otherwise, the analysis of the measurement methods by each instrumental technique is another important characteristic to consider. Six different methods were identified and categorized into three main groups according to the technique. The pie chart shown in **Figure 3** presents the ratio (%) of data measured following each method: (1) Transient DHW: T-history (1.4 %). (2) Thermal conductivity instrument, numerical, MD simulations and in-house setups equations (13.7 %). (3) TGA-DSC, MDSC and DSC techniques: Direct method (11.9 %), ASTM E2716 (6.2 %), ASTM E1269 (46.7 %) and Area method (6.1 %). Finally, a total of 124 C_p values (14 %) does not indicate the methodology used. In this case, it is remarkable that the lack of information is higher than the ones for the instrumental section.

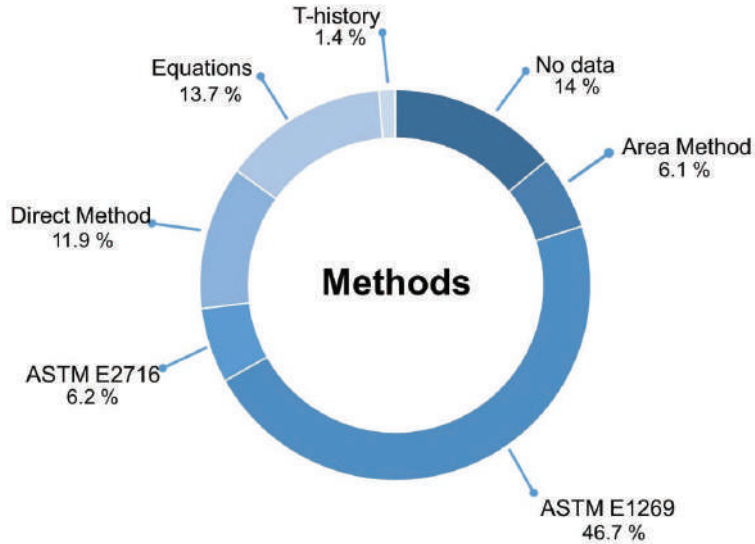


Figure 3. A pie chart of methods to determine the specific heat capacity: ASTM E1269, No data, equations, direct Method, ASTM E2716, Area Method, and T-History.

This fact generates uncertainty in the data and an incomplete methodological description because the results cannot be replicated.

Despite this, the most applied methodology is a standard procedure, "*Standard Test Method for Determining Specific Heat Capacity by Differential Scanning Calorimetry*" [40] by ASTM International. Therefore, following standardized procedures helps to compare results with each other. Otherwise, the second main group corresponds to the C_p determination through equations (13.7 %), followed by the direct method in DSC (11.9 %). Moreover, the area method (6.1 %) and standard methodology ASTM E2716 "Standard Test Method for Determining Specific Heat Capacity by Sinusoidal Modulated Temperature Differential Scanning Calorimetry" [41] (6.2 %) shows a similar ratio. Lastly, the less-used method is the T-history (1.4%) which has been used in the transient DHW technique. In addition, **Table 2** summarizes the relevant equations used to determine C_p for all the described methods.

Table 2. Equation's description of specific heat capacity methods: Model I, Model II, In-house calorimeter, Diffusivity, effective volumetric specific heat, effective specific heat, simulations, Debye theory, ASTM E1269, ASTM E2716.

Method	Formula
Model I	$C_{p,nf} = \phi \cdot C_{p,s} + (1 - \phi) \cdot C_{p,bf} \quad (eq.1)$ <p>$C_{p,nf}$= specific heat capacity of the nanofluid. $C_{p,s}$= solid particle specific heat capacity. ϕ = particle volumetric concentration and $C_{p,bf}$= base fluid specific heat.</p>
Model II	$C_{p,nf} = \frac{\phi \cdot \rho_s \cdot C_{p,s} + (1 - \phi) \cdot \phi \cdot \rho_{bf} \cdot C_{p,bf}}{\rho_{nf}} \quad (eq.2)$ <p>ρ_s=solid particles density. ρ_{bf} =base fluid density and ρ_{nf} =nanofluid density.</p>
Effective volumetric specific heat	$(\rho C_p)_{nf} = [\phi_p \cdot \rho_p \cdot C_{p-p} + (1 - \phi_p) \cdot \rho_f \cdot C_{p-f}] \quad (eq.3)$ <p>ϕ= particle volumetric concentration and subscript <i>nf</i> indicate the nanofluid, <i>p</i> the nanoparticle, and <i>f</i> the base fluid.</p>
Effective specific heat	$C_{p-nf} = \frac{[\phi_p \cdot \rho_p \cdot C_{p-p} + (1 - \phi_p) \cdot \rho_f \cdot C_{p-f}]}{\phi_p \cdot \rho_p + (1 - \phi_p) \cdot \rho_f} \quad (eq.4)$ <p>ϕ= particle volumetric concentration and subscript <i>nf</i> indicate the nanofluid, <i>p</i> the nanoparticle, and <i>f</i> the base fluid.</p>
In-house calorimeter	$C_{p,nf} = \frac{\dot{Q} \cdot \Delta t - m_c \cdot C_{pc} \cdot \Delta T_c - m_{co} \cdot C_{p,co} \cdot \Delta T_{co} - m_{IN} \cdot C_{p,IN} \cdot \Delta T_{IN} - \dot{q}_L \cdot \Delta t}{m_{nf} \cdot \Delta T_{nf}} \quad (eq.5)$ <p>\dot{Q}= heat applied, Δt = interval time (s), ΔT= temperature rise (K), m= mass (kg), C_p= specific heat capacity, \dot{q}_L= heat transfer to the environment, and the subscripts <i>C</i> indicates the container, <i>CO</i> the heating coil, and <i>IN</i> the insulation.</p>
Diffusivity	$C_{p-nf} = \frac{k_{nf}}{\alpha_{nf} \cdot \rho_{nf}} \quad (eq.6)$ $\rho_{nf} = \phi \cdot \rho_p + (1 - \phi_p) \cdot \rho_f \quad (eq.7)$ <p>k_{nf}= thermal conductivity, α_{nf}= thermal diffusivity, ρ_{nf} = nanofluid density, ϕ= particle volumetric concentration, ρ_p= particles density and ρ_f= fluid density.</p>
Simulations	$C_p = \left(\frac{\partial E}{\partial T}\right)_p = \frac{\langle \delta E^2 \rangle_{NPT}}{k_B \cdot T^2} \quad (eq.8)$ <p>k_B= Boltzmann constant, T= temperature, E= total internal energy and C_p= specific heat capacity.</p>

Debye theory (Phonon heat capacity)	$C_v = \frac{1}{\rho V K_B T^2} \sum_{\vec{q},p} \frac{(\hbar\omega_{\vec{q},p})^2 e^{\frac{\hbar\omega_{\vec{q},p}}{K_B T}}}{(e^{\frac{\hbar\omega_{\vec{q},p}}{K_B T}} - 1)^2} \quad (eq. 9)$ <p>C_v = specific heat capacity at constant volume, k_B = Boltzmann constant, T = temperature, $\hbar\omega_{\vec{q},p}$ = phonon energy, ρ = density and V = volume.</p>
ASTM E1269	$C_p = C_{p,sapphire} \cdot \frac{\Delta q_s \cdot m_{sapphire}}{\Delta q_{sapphire} \cdot m_s} = C_{p,sapphire} \cdot \frac{(q_s - q_o) \cdot m_{sapphire}}{(q_{sapphire} - q_o) \cdot m_s} \quad (eq. 10)$ <p>C_p = specific heat capacity, q = heat flow, m = mass, and subscript s indicates samples (pure mixtures or nanomaterials) and st the standard materials.</p>
ASTM E2716	$C_{p,rev} = \frac{A_{mhf}}{W_s \cdot A_{mrh}} \quad (eq. 11)$ $T = T_o + \beta \cdot T + A_{mhr} \cdot \sin(\omega t) \quad (eq. 12)$ $C_{p,non} = \frac{\langle P \rangle}{W_s \cdot \beta} - C_{p,rev} \quad (eq. 13)$ <p>$C_{p,rev}$ = reversing component of the apparent specific heat, A_{mhf} = amplitude of the first harmonic of the heat flow, A_{mrh} = amplitude of the applied heating rate, W_s = mass sample, β = heating rate, A_{mhr} = amplitude of the perturbation, ω = frequency of the perturbation, T = sample temperature, t = time, $\langle P \rangle$ = average heat flow, and $C_{p,non}$ = non-reversing specific heat.</p>
Areas Method	$C_{p,m} = \frac{C_{p,s} \cdot A_m}{A_s} \quad (eq. 14)$ $A_s = \frac{\dot{Q}_s}{m_s} = C_{p,s} \cdot \beta \quad (eq. 15)$ $A_s = \frac{\dot{Q}_m}{m_m} = C_{p,m} \cdot \beta \quad (eq. 16)$ <p>A_s = Integrated peak area for the sapphire curve, A_m = integrated peak area for the material curve, $C_{p,s}$ = sapphire specific heat capacity, m_s = sapphire sample mass, m_m = material sample mass, \dot{Q}_s = the sapphire heat flux signal, \dot{Q}_m = material heat flux signal, and β = heating rate.</p>
Direct method	$\dot{Q} = C_p(T) \cdot \beta \quad (eq. 17)$ <p>\dot{Q} = Heat flux. $C_p(T)$ = specific heat capacity in function of the temperature. β = heating rate.</p>
T-History	$T'_s = \frac{dT_s}{dt} = \frac{h_{air} \cdot A_{surface} \cdot (T_{air} - T_s)}{m_s \cdot C_{p,s}} \quad (eq. 18)$ <p>T_{air} = temperature of furnace air, T_s = sample temperature, m_s = sample mass, $C_{p,s}$ = specific heat capacity sample</p>

The first eight equations of Table 2 have been included in the equation methods group-first, the equations formulated for the NFs; Model I, **eq. 1**, was developed by Pak and Cho et al. [42] and is based on the liquid-particles mixture theory and the dependency of the particle concentration. However, this model is approximately valid for dilute suspensions when small density differences exist between base fluid and nanoparticles. Xuan and Roetzel et al. [43] modified this correlation by assuming thermal equilibrium between the nanoscale solid particles and the liquid phase, including the density (Model II), **eq.2**. Nevertheless, the literature showed a large gap between the expected values and the values experimentally obtained. Therefore, the values obtained through these models tend to present a high standard deviation. Derived from these two models, **eq. 3** and **eq. 4** and from the definition of the nanofluids density [44] were defined the effective volumetric specific heat and the effective specific heat of NFs, respectively. On the other hand, **eq. 3** describes the equation mainly used in the in-house calorimeters, as a function of the temperature, time, mass, and the applied heat flux [45]. Another way to determine C_p was related to its determination through thermal conductivity and thermal diffusivity values, **eq.4.**, **eq. 5** [42,46,47].

Alternatively, thermophysical properties can be determined theoretically from simulations (*i.e.*, Molecular dynamics simulations, MD). These numerical techniques use internal energy terms to predict the C_p , such as the **eq. 8** [48,49]. Finally, the C_p at constant volume can be determined through theoretical models as **eq. 9** describes (Debye theory) [50]. In the same way, **eq.10-17** describe all the methods derived from a calorimetric instrument (*i.e.*, Differential scanning calorimetry technique): direct method, ASTM E2716, ASTM E1269, MDSC, and areas method. The ASTM E1269 is a standard three-step procedure: the baseline heat flux (q_o) was obtained with two empty-pans as the first step analysis. In the second step, the heat flux of a reference sample with a known C_p (*i.e.*, sapphire sample) was measured ($q_{ref/sapphire}$). Finally, in the third step, the sample heat was determined (q_{sample}), and by eq. 10, the C_p is obtained [39]. On the other hand, can be used other two methods to determine C_p with DSC. First, the area method consists of two consecutive isothermal segments without a heating stage and a temperature difference of 1 °C between the isotherms. The signal peak due to the isotherm's temperature differences, see eq.15, is compared with the area of the known reference material, eq.16 (*i.e.*, sapphire), to obtain the C_p by the eq.14 [39]. Otherwise, the conventional method involves the evaluation of the enthalpy curve, measured within a certain temperature range. The area under the enthalpy curve represents the C_p . This is based on the relation between the heat flow rate, the C_p at a constant pressure of the sample inside the sample cell, and the scanning rate β , eq. 17 [39]. Finally, the MDSC

technique (which is a DSC variation technique) applies a sinusoidal heat signal (eq. 12), separating the C_p into reversing, eq. 11, and non-reversing component, eq.13. The reversing component of the heat flow is obtained from the amplitude of the first harmonic of the heat flow A_{mhf} , through a Fourier transform of the data. Then, the reversing component of the apparent C_p , is obtained by dividing the heat flow A_{mhf} by the amplitude of the applied heat rate, A_{mrh} , [51,52]. This technique is useful to separate the kinetic contribution (time-dependent factors). Lastly, a T - history technique determines the C_p according to the eq. 18 [53,54]. This method was first developed by Yinping *et al.* in 1999 [55] and enables to obtain melting point, fusion heat, degree of sub-cooling, thermal conductivity, and specific heat of several samples simultaneously.

Sampling: The high inconsistency about the C_p values in the reviewed and reported literature suggest that one of the possible issues that caused the high discrepancy was the difficult task of obtaining a good representative sample due to the low nanoparticles' concentration. Typically, due to the small amount of sample weight that uses standard calorimetric techniques. For this reason, an analysis of the sampling and statistics followed by researchers was performed. Two main aspects were considered: the number of samples and the number of measurements repetitions per each sample. **Figure 4** summarizes the general trends of the sampling performed in the analyzed literature.

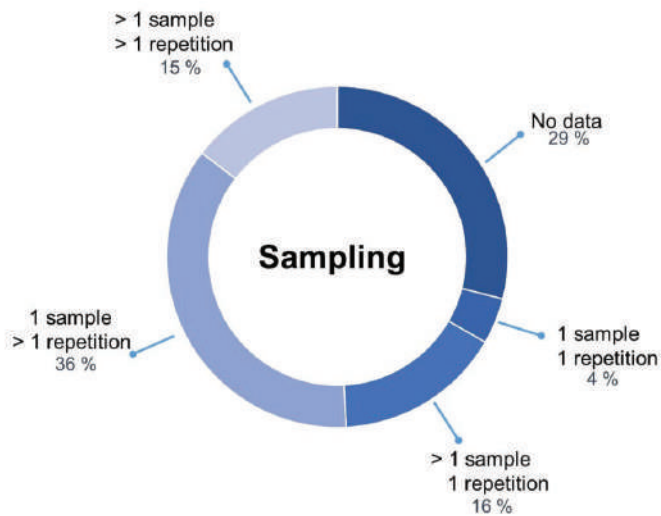


Figure 4. A pie chart of the sampling done in the revised literature to determine specific nanofluids heat capacity values.

Many C_p values were obtained from one sample and more than one measurement repetition (36 %). The choice of this procedure minimizes the effect of non-stability and agglomeration of nanoparticles inside the liquid medium. However, it is not a proper measurement procedure from the point of view of sampling and instrumental error because there is not a representative sample.

The opposite situation is the cases where more than one sample was analyzed but only one repetition for each sample was run. This experimental procedure was used to obtain 15.8 % of the data.

In addition, the most appropriate procedure is the case where more than one sample and more than one repetition is performed and represents 14.6 % of the cases. This last sampling procedure should minimize nanoparticle concentration, stability, and measurement errors. Hence, this procedure is expected to offer high-quality values regarding measurement uncertainty.

Finally, the least desirable procedure is obtained when only one sample and one measurement repetition are performed. This undesirable condition represents only 4.4 % of the data.

Nevertheless, sampling procedure of NFs needs to be carried out in order to reduce measurement errors. Thereby, the first step is to develop a methodology to obtain a good representative sample (*i.e.*, quartering) and determine the minimum number of independent samples to minimize a measurement error due to the inhomogeneity of NFs samples.

As a final fact, a relevant finding is that the 29 % of data presented in the literature does not report how the C_p result was obtained. The lack of that information about experimental procedure is the base to highlight even more that there is significant uncertainty in the reported C_p values.

Likewise, it is well known that the particle size of the samples influences the thermophysical properties (*i.e.*, melting temperature, specific heat capacity). For this reason, it is crucial first to melt the sample to remove the granulometry effects. In addition, it ensures a better contact of the sample with the bottom of the crucible and removes the air within the sample. As a result, values obtained with a single measurement have low-quality from a statistical point of view. To minimize this effect, it is necessary to perform several measurement repetitions and discard the first analysis (first run) to obtain a more reliable value. From the analyzed literature, only 21 % of the data considered this factor and the other 79 % of the data do not specify this information.

These analyses reveal another source of error in the reported C_p values, which influences the lack of homogeneity of the results.

3.2. Principal component analysis (PCA) and Response Surface Methodology (RSM)

Finding correlations between the main parameters involved in the C_p enhancement is crucial to understand their behavior and giving a step forward to synthesize and optimize NFs. In this study, three main parameters were selected: temperature ($^{\circ}\text{C}$), NPs concentration (wt.%), and NPs size (nm). For this purpose, response surface methodology (RSM) was employed to predict the C_p variation (ΔC_p , %) and Principal Component Analysis (PCA) was applied to identify the main variables and quantify its influence on the C_p value.

The analysis of the nanofluids dataset by PCA has shown the variances' values of the three new PCs, representing the full dataset after the transformation (see **Table 3**). One criterion for selecting the number of PCs needed is based on the cumulative percentage of the total variance, which is often considered satisfactory when it lies within the range of 70 - 80 % [56]. All the analyzed data in **Table 2** for PC1 and PC2 presents a cumulative percentage of variance > 70 %, which implies that these PCs can be used to explain the dataset, thus reducing the original dimensionality by one variable. Moreover, PCA transformation has shown the correlation between PCs and the original variables (1 means perfect correlation, -1 inverse correlation, and 0 no correlation). While the initial three parameters (concentration, size, and temperature) show approximately the same values for PC1, in PC2, concentration and size are the predominant features. However, the temperature and size have a higher contribution to PC1 and PC2, respectively.

Table 3. Contribution of the original variables to the PCs, Eigenvalues, percentage of variance, and its accumulative values from the PCA analysis.

	PC1	PC2	PC3
Concentration	0.56951	0.627945	0.530418
Size	0.542798	0.771884	0.331007
Temperature	0.617275	0.099399	0.780443
Eigenvalues	1.180865	0.934924	0.892385
Percentage of variance (%)	39.26%	31.08%	29.67%
Cumulative (%)	39.26%	70.33%	100.00%

On the other hand, RSM is a mathematical and statistical technique useful for modeling and problem analysis, where some variables influence the response. The objective is to optimize this response. In this case, the C_p is a function of $C_p \cong f(T, \phi, S) + \epsilon$, where ϵ represents the noise error observed in the response, T the temperature, ϕ the concentration, and S NPs size. The expected response can be expressed by $E(C_p) = f(T, \phi, S) = \beta$ and the response surface can be represented by: $\beta = f(T, \phi, S)$ [57]. To obtain the response surface, it is first necessary to find an appropriate approximation of the functional relationship between C_p and the independent variables. For this purpose, analysis of variance (ANOVA) was performed. ANOVA provides a statistical test of whether two or more population means are equal and therefore generalizes the t -test beyond two means and is based on the analysis of the p -values to predict an optimal response. Therefore, ANOVA analysis should provide a mathematical function for NPs C_p values. The p -value represents the smallest level of significance that would lead to the rejection of the null hypothesis, in this case < 0.05 (with a confidence level above 95 %), indicating that the controllable factor does not affect the response [58].

For this propose, several scenarios with different data aggrupation were analyzed:

- (1) all the data together,
- (2) experimental values,
- (3) values obtained under E1269 standard methodology,
- (4) values obtained with statistics (sampling and/or repetitions),
- (5) values obtained with sampling (> 1 sample),
- (6) values obtained with measurement repetitions (> 1 repetition).

In the scenarios (1), (2), (3), (4), and (6), no correlations were found. Therefore, no mathematical model was fitted to the data. Nevertheless, a correlation was found only in the scenario (5) where the obtained C_p values is an average of more than one independent sample (sampling procedure).

Figure 5 shows the three-dimensional predicted response surface (right) and the contour plot (left) from the ANOVA analysis for the scenario 5. The best model to fit the data was a quadratic model with < 0.0001 p -values. Moreover, the Model F -value of 6.72 indicates that the model is significant, and the lack of fit F -value of 0.95 implies that the

lack of fit is not significant relative to the pure error. There is only a 0.01 % change that an F-value this large could occur due to noise. Despite this adjustment, the standard deviation of the model is ± 7 . These deviations agree with previous work where nanofluids' thermophysical properties were statistically analyzed by experimental sampling procedure [59]. The factors terms were C_p (response) = $0,3076 - 0,0579 \cdot A$ (temperature) $+ 0,4512 \cdot B$ (Size) $- 1,3651 \cdot C$ (Concentration) $- 0,0004 \cdot AB - 0,0073 \cdot AC + 0,023 \cdot BC + 0,00017 \cdot A^2 - 0,0021 \cdot B^2 - 0,2922 \cdot C^2$. Therefore, this model allows identifying NFs trends. In Figure 5, the predicted C_p response as a function of the NPs size and concentration was depicted with the temperature evolution: a-b) at 50°C, c-d) at 200 °C, e-f) at 350 °C and g-h) at 500 °C. In Figure 5 a-b) at 50 °C, it can be identified four main regions delimited by the contour lines; from red (+30 % C_p variation) to dark blue (-30% C_p variation). Contour lines points to a direction where the C_p is maximized. A curved domain with a maximum C_p improvement of about 20 % was identified between the NPs concentration range 2 to 9 wt. %, and between 65-100 NPs nominal diameter (nm). In contrast, NP concentration increment leads to a C_p variation and NP size decreases, reaching negative values up to -20 %. When the temperature increase (100 - 250 °C), see Figure 5 c-d) and e-f), the contour lines of 10, 0, and -10 shifted towards high NPs size values; disappearing the domain of values higher than 20 % and appearing new domains of negative values (-20 % and -30 %). On the contrary, with the temperature increase, this trend was changed. At higher temperatures (500 °C), see Figure 5 g-h) a domain of maximum C_p variation is shown up to 25 % for NFs with low NPs concentrations and sizes between 0,001 - 1 wt.% and 30 - 90 nm, respectively. Consequently, a strong temperature dependence has been found in the behavior of NFs. This fact is crucial to select the appropriate parameters (*i.e.*, nanoparticles size and concentration) according to their working temperature. These tendencies are consistent with the values obtained from the PCA analysis.

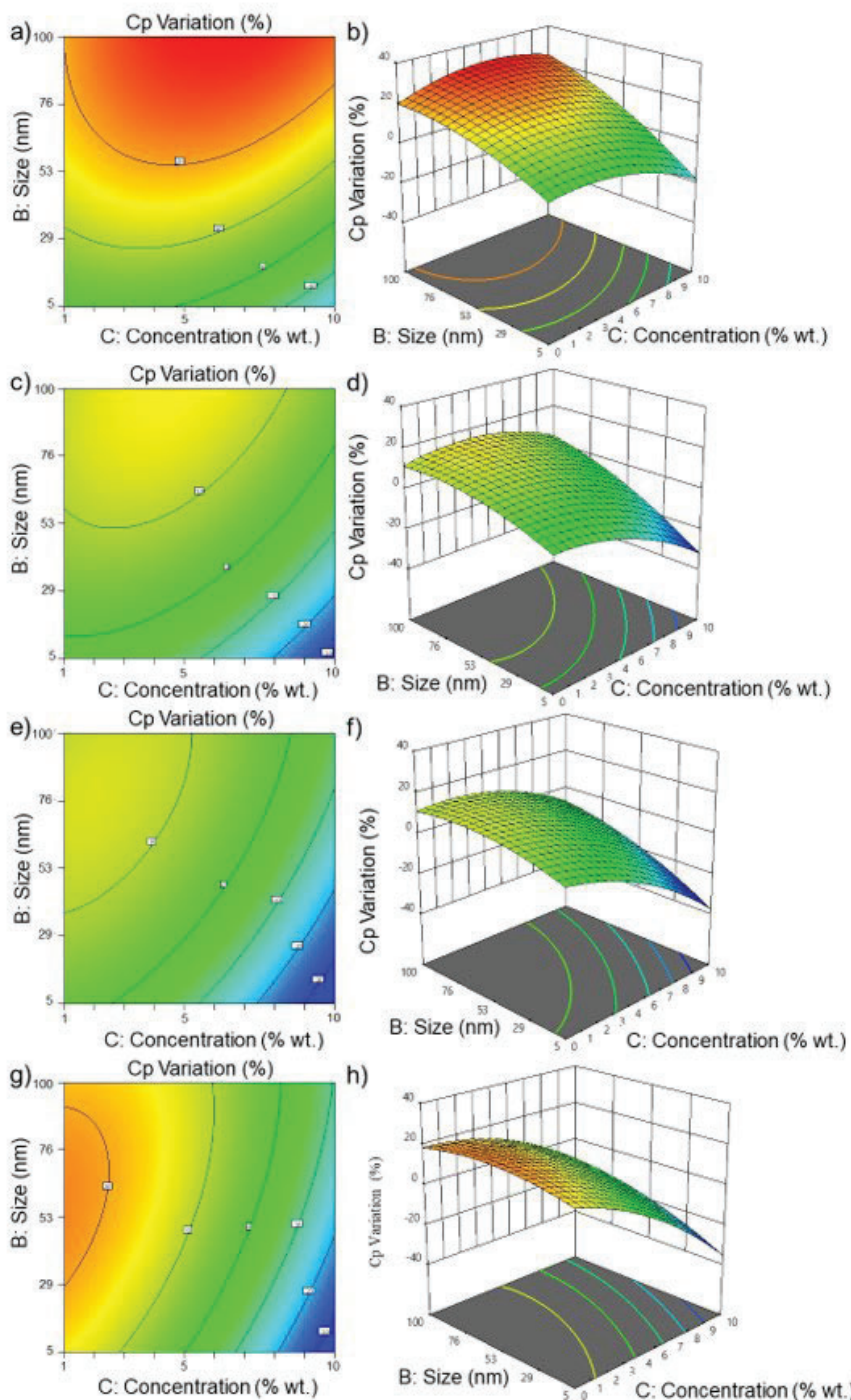


Figure 5. A three-dimensional response surface (right) and contour plot (left) showing the expected specific heat capacity (y) as a function of the size (x_1) and concentration (x_2), at a fixed temperature: a)-b) at 50 °C, c)-d) at 200 °C, e)-f) at 350 °C and g)-h) at 500 °C.

3.3. Nanofluids selector database representation

The relation between the C_p variation regarding the initial value, the size, and concentration of NPs, help to understand the connection between the C_p change and the NPs addition.

Therefore, creating a database is a helpful way to identify the main trends in NF's behavior. Furthermore, the database makes it possible to define the properties and tolerances of NFs for their in-service engineering modelling/simulation. (i.e., as HTF/TES material in CSP facilities). As seen in the previous sections, the concentration and size of NPs are two of the main significant parameters of NFs thermo-physical properties. Accordingly, a quotient between concentration (wt.%) / Size (nm) was defined as an index for NFs: $I^{c/s}$, for better interpretation of the data. In this way, the database makes possible to identify the best parameters for synthesizing NFs with a specific C_p . On the other hand, an evidence of the high dispersion of results is elucidated with this database. This fact is observed in the database figures: the higher the bubble size, the higher the dispersion of the data value.

Figure 6 shows the nanofluids ΔC_p variations as a function of $I^{c/s}$: **a)** by taking the type of NPs into account and **b)** by base fluids. It can be observed that, generally, metal oxide NPs and carbon base NPs give the most significant variation, particularly with enhancements up to 150 % when are combined with a molten salt base fluid. These enhancements occur when the $I^{c/s}$ index is between the range of 0.01 - 0.1 wt.% nm⁻¹, (it is important to emphasize that the graphs presented only include spherical shaped nanoparticles when the size is analyzed; nanowires are also included in the database with length x nominal diameter). On the contrary, NFs based on metallic NPs show the worst behavior with variations up to -50 %. Conversely, hydrocarbons, ionic liquids, mixtures, and oils showed a slight positive variation in many cases. However, a severe decrease prevails in many cases with different types of NPs. It is important to highlight that in general, the water base NFs showed a decrease of C_p . Therefore, incorporating NPs in water systems does not improve its properties. In the case of substituted hydrocarbons or organic acids are registered enhancements up to 50 %.

Furthermore, in general, the literature's highest ΔC_p are obtained with NPs concentrations between 0.1 wt.% up to 2 wt.%. However, some ΔC_p enhancements were reported with higher NPs concentrations, an example are the values reported by Y. Huang et al. [60].

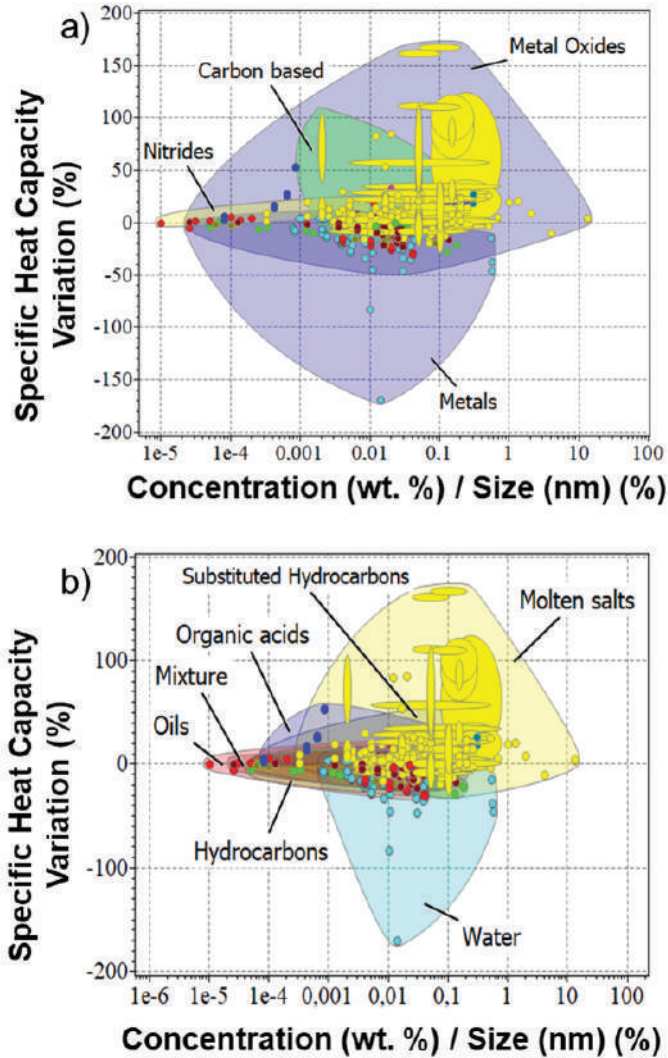


Figure 6. Specific Heat capacity variation (%) as a function of the concentration/size quotient ($I^{c/s}$ index) is classified as the nanoparticle's family (a) and classified as base fluid family (b).

On the other hand, the size of NPs gives a higher ΔC_p enhancement with smaller nominal diameters. For example, from 2 nm to 20 nm of NPs nominal diameter, a significant increase has been observed; whereas, with larger NPs sizes, the increments are less relevant or even negative.

To choose the most suitable NF for a specific application, service temperature is needed to identify the best candidate. **Figure 7** presents the C_p values as a function of temperature. In Figure 7-a) are shown the C_p of the evaluated NFs versus the

measurement temperature. As can be noted, most NFs reported data is in the temperature range between 25 °C and 250 °C. However, molten salts can reach up to 600 °C. Water, oils, and some mixtures present the highest C_p of the treated NFs, but molten salts are the most employed fluid despite their relatively low C_p when working at high temperatures.

For this reason, knowing the C_p of this kind of fluids is of great interest. Also, it is essential to consider the C_p and the variation that can be achieved by adding NPs. Thus, Figures **7-b)** and **7-c)** represent the ΔC_p as a function of temperature, classified as base fluid type, see **7-b)**, and NPs type, see **7-c)**.

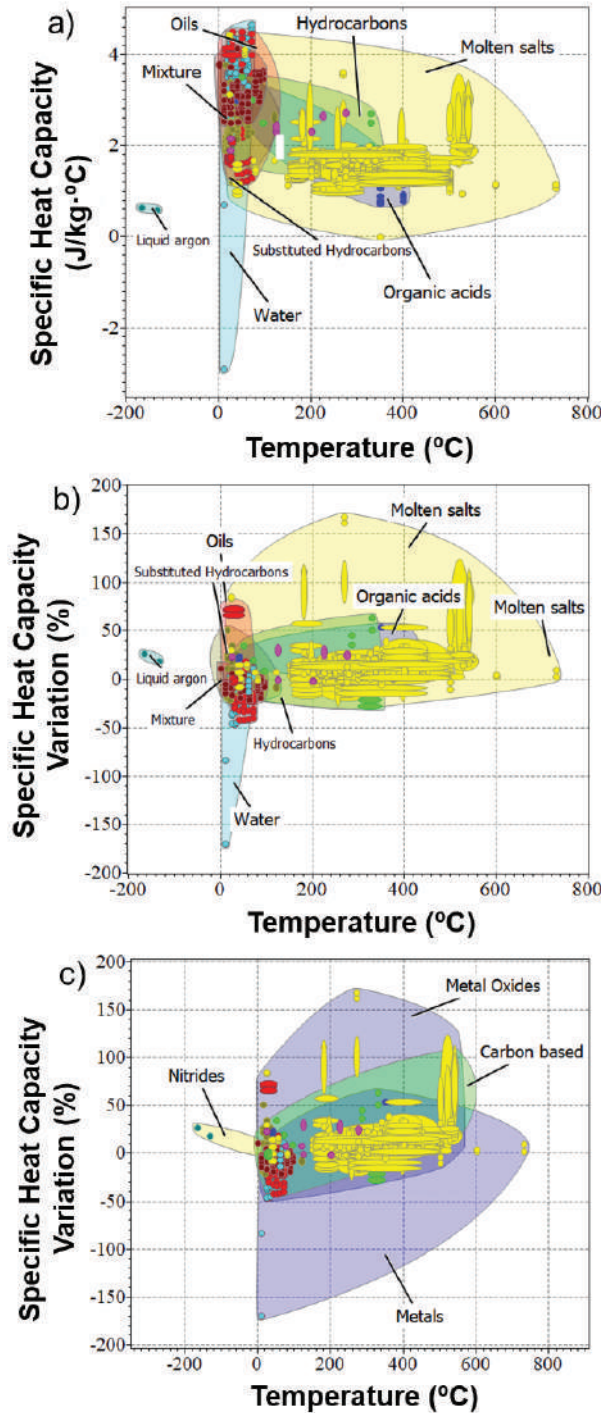


Figure 7. Nanofluids specific heat capacity as a function of the temperature: a) Specific heat capacity (J/kg·°C) of nanofluids families classified as base fluid type, b) Specific Heat capacity variation (%) classified as the base fluid types of family and c) Specific heat capacity variation (%) classified as a nanoparticle's family.

The largest ΔC_p are obtained with molten salts at approximately 300 °C. On the other hand, the second group with higher ΔC_p enhancements were thermal oils, reaching improvements up to 80 % with metal oxide NPs. Despite this, they do not exceed the maximum C_p values of the water in the temperature range between ambient temperature and 90 °C.

Finally, **Figure 8** shows a particular case of molten salts and the type of NPs used, from 1 nm to 200 nm of the nanoparticle size range. It can be observed that carbon-based and metal oxides nanoparticles give a larger C_p enhancement, especially between the range of 0.1 to 2 wt.% of NPs. Higher variation can be noticed in a particular case of NaNO₃-KNO₃ molten salt with MgO as NPs and a concentration of 5, 10, and 15 wt.%, reaching a maximum of C_p variation of 168 % [60]–[62]. Otherwise, Li₂CO₃-K₂CO₃ molten salt with SiO₂ NPs also shows a remarkable C_p enhancement in a range concentration from 0.1 wt.% to 2 wt.%, achieving a variation between 2 % and 124 % in the experimental results [30], [63]–[69].

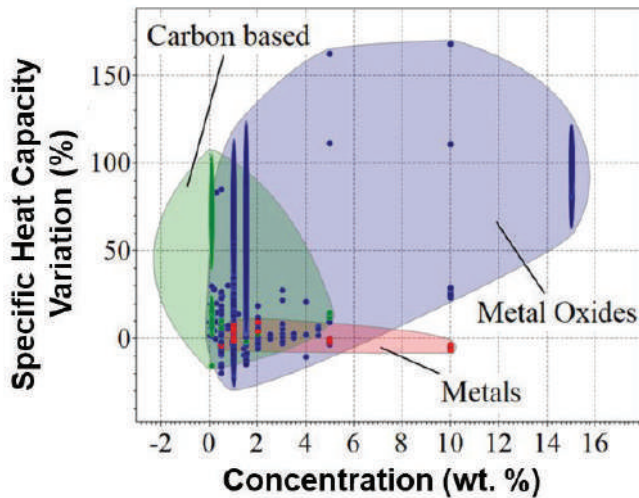


Figure 8. Specific heat capacity variation (%) as a function of concentration (wt.%) of molten salts-based nanofluids is classified as the nanoparticle's family.

4. Conclusions

This paper collected and analyzed 899 values of nanofluids C_p published in the field of thermal energy storage in order to understand their behavior and the effect of incorporating NPs. Thanks to the instrumentation analysis, measurement techniques,

calculation methods, and the sampling used to determine the C_p , the identification of possible sources of errors that cause the large discrepancy in the results presented in the literature have been done. The first identified source of error was the few methodology specifications in the C_p determination. As a result, in a significant part of the reported results there is a gap for a proper methodological procedure for measuring nanofluids thermal properties. The second main source of error was the lack of adequate sampling and statistical analysis. The main conclusions obtained by PCA, RSM methodology, and the database were summarized as the following:

- Temperature, concentration, and NPs size show a similar influence in the C_p value.
- A mathematical correlation was determined only with a group of values statistically obtained through a sampling procedure.
- It has been verified that metal oxides NPs are the best candidates for C_p enhancements and metal NPs the worst ones. Being the MgO NPs, those who provided increments above 100 %.
- Molten salts were the base fluid with larger C_p increments and water with the lowest increment values.
- Higher enhancements were obtained with concentrations from 0.1 wt.% to 2 wt.% and nominal diameter from 2 nm to 20 nm.

The database allows identifying and selecting nanofluids for specific applications.

5. Recommendations

To sum up, some recommendations for future work are proposed:

- (1) To do a statistical sampling procedure and provide a detailed description of this methodology procedure to present a C_p value.
- (2) To provide not only the C_p enhancement but also the nanofluid C_p value and the base fluid C_p value separately.
- (3) To provide information about the C_p measurement temperature since it has important influence in the thermophysical properties determination.

All these recommendations facilitate the comparison, and even more important, the reproducibility of the C_p values obtained as results and identify NFs behavior patterns and their relationship with the type and concentration of NPs.

Conflict of interest

The authors declare no conflicts of interest.

Acknowledgments

The research leading to these results is partially funded by the Spanish government RTI2018-093849-B-C32, RTI2018-094757-BI00, MDM-2017-0767 MCIU/AEI/FEDER, UE. The authors would like to thank the Catalan Government for the quality accreditation given to their research groups DIOPMA (2017 SGR 118) and CMSL (2017 SGR 13). DIOPMA is certified agent TECNIO in the category of technology developers from the Government of Catalonia. AS thanks to Generalitat de Catalunya (AGAUR) for her Grant FI-DGR 2018. Moreover, PG thanks Generalitat de Catalunya for his Serra Hünter Associate Professorship. Finally, XS also gratefully acknowledge the financial support of the Science Foundation Ireland 18/EP SRC-CDT/3584 and the Engineering and Physical Sciences Research Council EP/S022635/1, along with VBC Group, Loughborough, UK.

References

- [1] Peiró, G., Prieto, C., Gasia, J., Jové, A., Miró, L., and Cabeza, L. F. **2018**. Two-tank molten salts thermal energy storage system for solar power plants at pilot plant scale: Lessons learnt and recommendations for its design, start-up and operation. *Renewable Energy*. vol. 121. pp. 236–248. doi: 10.1016/j.renene.2018.01.026.
- [2] Mostafavi Tehrani, S. S., Taylor, R. A., Nithyanandam, K., and Shafiei Ghazani, A. **2017**. Annual comparative performance and cost analysis of high temperature, sensible thermal energy storage systems integrated with a concentrated solar power plant. *Solar Energy*. vol. 153. pp. 153–172. doi: 10.1016/j.solener.2017.05.044.
- [3] Calderón, A., Barreneche, C., Prieto, C., Segarra, M., and Fernández, A. I. **2021**. Concentrating Solar Power Technologies: A Bibliometric Study of Past, Present and Future Trends in Concentrating Solar Power Research. *Frontiers in Mechanical Engineering*. vol. 7, no. June. pp. 1–22. doi: 10.3389/fmech.2021.682592.
- [4] Svobodova-Sedlackova, A., Barreneche, C., Alonso, G., Fernandez, A. I., and Gamallo, P. **2020**. Effect of nanoparticles in molten salts – MD simulations and experimental study. *Renewable Energy*. vol. 152. pp. 208–216. doi: 10.1016/j.renene.2020.01.046.
- [5] Peiró, G., Gasia, J., Miró, L., Prieto, C., and Cabeza, L. F. **2017**. Influence of the heat transfer fluid in a CSP plant molten salts charging process. *Renewable Energy*. vol. 113. pp. 148–158. doi: 10.1016/j.renene.2017.05.083.
- [6] Rubbi, F., Das, L., Habib, K., Aslfattahi, N., Saidur, R., and UI Alam, S. **2021**. A comprehensive review on advances of oil-based nanofluids for concentrating solar thermal collector application. *Journal of Molecular Liquids*. no. xxxx. p. 116771. doi: 10.1016/j.molliq.2021.116771.
- [7] Minea, A. A. **2021**. State of the art in PEG-based heat transfer fluids and their suspensions with nanoparticles. *Nanomaterials*. vol. 11, no. 1. pp. 1–12. doi: 10.3390/nano11010086.

- [8] Wang,W.,Wu,Z.,Li,B.,and Sundén,B. **2019**.A review on molten-salt-based and ionic-liquid-based nanofluids for medium-to-high temperature heat transfer.*Journal of Thermal Analysis and Calorimetry*.vol. 136, no. 3.pp. 1037–1051. doi: 10.1007/s10973-018-7765-y.
- [9] Rubbi,F.,Das,L.,Habib,K.,Aslfattahi,N.,Saidur,R.,and Rahman,M. T. **2021**.State-of-the-art review on water-based nanofluids for low temperature solar thermal collector application.*Solar Energy Materials and Solar Cells*.vol. 230, no. June.p. 111220. doi: 10.1016/j.solmat.2021.111220.
- [10] Choi,S. U. S.,Li,S.,and Eastman,J. A. **1999**.Measuring thermal conductivity of fluids containing oxide nanoparticles.*Journal of Heat Transfer*.vol. 121, no. 2.pp. 280–289. doi: 10.1115/1.2825978.
- [11] Shi,L.,Zhang,S.,Arshad,A.,Hu,Y.,He,Y.,and Yan,Y. **2021**.Thermo-physical properties prediction of carbon-based magnetic nanofluids based on an artificial neural network.*Renewable and Sustainable Energy Reviews*.vol. 149, no. July 2020.p. 111341. doi: 10.1016/j.rser.2021.111341.
- [12] Mukhtar,A. *et al.* **2020**.Experimental and comparative theoretical study of thermal conductivity of MWCNTs-kapok seed oil-based nanofluid.*International Communications in Heat and Mass Transfer*.vol. 110, no. November 2019.p. 104402. doi: 10.1016/j.icheatmasstransfer.2019.104402.
- [13] Xiong,Q.,Hajjar,A.,Alshuraiaan,B.,Izadi,M.,Altnji,S.,and Shehzad,S. A. **2021**.State-of-the-art review of nanofluids in solar collectors: A review based on the type of the dispersed nanoparticles.*Journal of Cleaner Production*.vol. 310, no. March.p. 127528. doi: 10.1016/j.jclepro.2021.127528.
- [14] Akkala,S. R.,Kaviti,A. K.,ArunKumar,T.,and Sikarwar,V. S. **2021**.Progress on suspended nanostructured engineering materials powered solar distillation- a review.*Renewable and Sustainable Energy Reviews*.vol. 143, no. March.p. 110848. doi: 10.1016/j.rser.2021.110848.
- [15] Awais,M.,Bhuiyan,A. A.,Salehin,S.,Ehsan,M. M.,Khan,B.,and Rahman,M. H. **2021**.Synthesis, heat transport mechanisms and thermophysical properties of nanofluids: A critical overview.*International Journal of Thermofluids*.vol. 10.p. 100086. doi: 10.1016/j.ijft.2021.100086.
- [16] Sezer,N.,Atieh,M. A.,and Koc,M. **2018**.A comprehensive review on synthesis, stability, thermophysical properties, and characterization of nanofluids.*Powder Technology*.vol. 344.pp. 404–431. doi: 10.1016/j.powtec.2018.12.016.
- [17] Sharma,A. K.,Tiwari,A. K.,and Dixit,A. R. **2016**.Rheological behaviour of nanofluids: A review.*Renewable and Sustainable Energy Reviews*.vol. 53.pp. 779–791. doi: 10.1016/j.rser.2015.09.033.
- [18] Kumaran,K. **2021**.A comprehensive review on the application of nanofluids in the machining process.*The International Journal of Advanced Manufacturing Technology*.vol. 47. doi: <https://doi.org/10.1007/s00170-021-07316-8>.
- [19] Parmar,H. B. *et al.* **2021**.Nanofluids improve energy efficiency of membrane distillation.*Nano Energy*.vol. 88, no. May.p. 106235. doi: 10.1016/j.nanoen.2021.106235.
- [20] Yu,W.,Wang,T.,Park,A. H. A.,and Fang,M. **2019**.Review of liquid nano-absorbents for enhanced CO₂ capture.*Nanoscale*.vol. 11, no. 37.pp. 17137–17156. doi: 10.1039/c9nr05089b.
- [21] Kim,J. and Park,H. **2021**.Enhanced mass transfer in nanofluid electrolytes for

- aqueous flow batteries: The mechanism of nanoparticles as catalysts for redox reactions. *Journal of Energy Storage*.vol. 38, no. March.p. 102529. doi: 10.1016/j.est.2021.102529.
- [22] Yıldız,G.,Ağbulut,Ü.,and Gürel,A. E. **2021**.A review of stability, thermophysical properties and impact of using nanofluids on the performance of refrigeration systems.*International Journal of Refrigeration*.vol. 129.pp. 342–364. doi: 10.1016/j.ijrefrig.2021.05.016.
- [23] Bretado-de los Rios,M. S.,Rivera-Solorio,C. I.,and Nigam,K. D. P. **2021**.An overview of sustainability of heat exchangers and solar thermal applications with nanofluids: A review.*Renewable and Sustainable Energy Reviews*.vol. 142, no. March.p. 110855. doi: 10.1016/j.rser.2021.110855.
- [24] Nithiyantham,U. *et al.* **2019**.Nanoparticles as a high-temperature anticorrosion additive to molten nitrate salts for concentrated solar power.*Solar Energy Materials and Solar Cells*.vol. 203, no. August.p. 110171. doi: 10.1016/j.solmat.2019.110171.
- [25] Svobodova-Sedlackova,A.,Calderón,A.,Barreneche,C.,Gamallo,P.,and Fernández,A. I. **2021**.Understanding the abnormal thermal behavior of nanofluids through infrared thermography and thermo - physical characterization.*Scientific Reports*.no. 0123456789.pp. 1–10. doi: 10.1038/s41598-021-84292-9.
- [26] Angayarkanni,S. A. and Philip,J. **2015**.Review on thermal properties of nanofluids: Recent developments.*Advances in Colloid and Interface Science*.vol. 225.pp. 146–176. doi: 10.1016/j.cis.2015.08.014.
- [27] Lasfargues,M.,Geng,Q.,Cao,H.,and Ding,Y. **2015**.Mechanical dispersion of nanoparticles and its effect on the specific heat capacity of impure binary nitrate salt mixtures.*Nanomaterials*.vol. 5, no. 3.pp. 1136–1146. doi: 10.3390/nano5031136.
- [28] Li,Y. *et al.* **2019**.Experimental study on the effect of SiO₂ nanoparticle dispersion on the thermophysical properties of binary nitrate molten salt.*Solar Energy*.vol. 183, no. December 2018.pp. 776–781. doi: 10.1016/j.solener.2019.03.036.
- [29] Riazi,H.,Mesgari,S.,Ahmed,N. A.,and Taylor,R. A. **2016**.The effect of nanoparticle morphology on the specific heat of nanosalts.*International Journal of Heat and Mass Transfer*.vol. 94.pp. 254–261. doi: 10.1016/j.ijheatmasstransfer.2015.11.064.
- [30] Jiang,Z. *et al.* **2019**.Novel key parameter for eutectic nitrates based nanofluids selection for concentrating solar power (CSP) system.*Applied Energy*.vol. 235, no. July 2018.pp. 529–542. doi: 10.1016/j.apenergy.2018.10.114.
- [31] Shahrul,I. M.,Mahbulul,I. M.,Khaleduzzaman,S. S.,Saidur,R.,and Sabri,M. F. M. **2014**.A comparative review on the specific heat of nanofluids for energy perspective.*Renewable and Sustainable Energy Reviews*.vol. 38.pp. 88–98. doi: 10.1016/j.rser.2014.05.081.
- [32] Chen,X.,Wu,Y. ting,Zhang,L. di,Wang,X.,and Ma,C. fang. **2019**.Experimental study on thermophysical properties of molten salt nanofluids prepared by high-temperature melting.*Solar Energy Materials and Solar Cells*.vol. 191, no. December 2017.pp. 209–217. doi: 10.1016/j.solmat.2018.11.003.
- [33] Pedregosa, Fabian and Varoquaux, Gael and Gramfort, Alexandre and Michel, Vincent and Thirion, Bertrand and Grisel, Olivier and Blondel, Mathieu and Prettenhofer, Peter and Weiss, Ron and Dubourg, V. and others. **2011**.Scikit-learn:

Machine Learning in Python.*the Journal of machine Learning research*.vol. 12.pp. 2825–2830. doi: 10.1289/EHP4713.

- [34] Jolliffe, I. T. and Cadima, J. **2016**. Principal component analysis: A review and recent developments. *Philosophical Transactions of the Royal Society A: Mathematical, Physical and Engineering Sciences*.vol. 374, no. 2065. doi: 10.1098/rsta.2015.0202.
- [35] Bishop, C. M. **2007**. Pattern Recognition and Machine Learning. *Journal of Electronic Imaging*.vol. 16, no. 4.p. 049901. doi: 10.1117/1.2819119.
- [36] Hotelling, H. **1933**. Analysis of a complex of statistical variables into principal components. *Journal of Educational Psychology*.vol. 24, no. 6.pp. 417–441. doi: 10.1037/h0071325.
- [37] Che Sidik, N. A., Mahmud Jamil, M., Aziz Japar, W. M. A., and Muhammad Adamu, I. **2017**. A review on preparation methods, stability and applications of hybrid nanofluids. *Renewable and Sustainable Energy Reviews*.vol. 80, no. May.pp. 1112–1122. doi: 10.1016/j.rser.2017.05.221.
- [38] Ferrer, G., Barreneche, C., Solé, A., Martorell, I., and Cabeza, L. F. **2017**. New proposed methodology for specific heat capacity determination of materials for thermal energy storage (TES) by DSC. *Journal of Energy Storage*.vol. 11.pp. 1–6. doi: 10.1016/j.est.2017.02.002.
- [39] Mettler Toledo. **1998**. Measuring specific heat capacity. *USER COM*.no. June.pp. 1–20.
- [40]. **2018**. ASTM E1269-11(2018), *Standard Test Method for Determining Specific Heat Capacity by Differential Scanning Calorimetry*. West Conshohocken, PA, www.astm.org. [Online]. Available: www.astm.org
- [41] ASTM International. **2014**. ASTM E2716, *Standard Test Method for Determining Specific Heat Capacity by Sinusoidal Modulated Temperature Differential Scanning Calorimetry*. West Conshohocken, PA, www.astm.org.
- [42] Wang, B. X., Zhou, L. P., Peng, X. F., Du, X. Z., and Yang, Y. P. **2010**. On the specific heat capacity of CuO nanofluid. *Advances in Mechanical Engineering*.vol. 2010. doi: 10.1155/2010/172085.
- [43] Yimin, X. and Wilfried, R. **2000**. Conceptions for heat transfer correlation of nanofluids. *International Journal of Heat and Mass Transfer*.vol. 43, no. 4.pp. 3701–3707. doi: 10.1016/j.ijhmt.2017.01.005.
- [44] Pastoriza-Gallego, M. J., Casanova, C., Páramo, R., Barbs, B., Legido, J. L., and Piñeiro, M. M. **2009**. A study on stability and thermophysical properties (density and viscosity) of Al₂O₃ in water nanofluid. *Journal of Applied Physics*.vol. 106, no. 6. doi: 10.1063/1.3187732.
- [45] Vajjha, R. S. and Das, D. K. **2009**. Specific heat measurement of three nanofluids and development of new correlations. *Journal of Heat Transfer*.vol. 131, no. 7.pp. 1–7. doi: 10.1115/1.3090813.
- [46] Murshed, S. M. S. **2011**. Determination of effective specific heat of nanofluids. *Journal of Experimental Nanoscience*.vol. 6, no. 5.pp. 539–546. doi: 10.1080/17458080.2010.498838.
- [47] Khodadadi, J. M. and Hosseinizadeh, S. F. **2007**. Nanoparticle-enhanced phase change materials (NEPCM) with great potential for improved thermal energy storage. *International Communications in Heat and Mass Transfer*.vol. 34, no.

- 5,pp. 534–543. doi: 10.1016/j.icheatmasstransfer.2007.02.005.
- [48] Rajabpour,A.,Akizi,F.,Heyhat,M.,and Gordiz,K. **2013**.Molecular dynamics simulation of the specific heat capacity of water-Cu nanofluids.*International Nano Letters*.vol. 3, no. 1.p. 58. doi: 10.1186/2228-5326-3-58.
- [49] Li,Q.,Yu,Y.,Liu,Y.,Liu,C.,and Lin,L. **2017**.Thermal properties of the mixed n-octadecane/Cu nanoparticle nanofluids during phase transition: A molecular dynamics study.*Materials*.vol. 10, no. 1. doi: 10.3390/ma10010038.
- [50] Wang,B.-X.,Zhou,L.-P.,and Peng,X.-F. **2006**.Surface and Size Effects on the Specific Heat Capacity of Nanoparticles.*International Journal of Thermophysics*.vol. 27, no. 1.pp. 139–151. doi: 10.1007/s10765-006-0022-9.
- [51] De Robertis,E. *et al.* **2012**.Application of the modulated temperature differential scanning calorimetry technique for the determination of the specific heat of copper nanofluids.*Applied Thermal Engineering*.vol. 41.pp. 10–17. doi: 10.1016/j.applthermaleng.2012.01.003.
- [52] Leonard C. Thomas. **2015**.Modulated DSC Paper #1 Why Modulated DSC®? ; An Overview and Summary of Advantages and Disadvantages Relative to Traditional DSC.*TA Instruments Technical Paper*.vol. 1.pp. 1689–1699.
- [53] Ma,B.,Kumar,N.,Kuchibhotla,A.,and Banerjee,D. **2018**.Experimental Measurement of the Effect of Particle Concentration on the Specific Heat Capacity of Silica Nanofluids.*Proceedings of the 17th InterSociety Conference on Thermal and Thermomechanical Phenomena in Electronic Systems, ITherm 2018*.pp. 246–251. doi: 10.1109/ITHERM.2018.8419554.
- [54] Solé,A.,Miró,L.,Barreneche,C.,Martorell,I.,and Cabeza,L. F. **2013**.Review of the T-history method to determine thermophysical properties of phase change materials (PCM).*Renewable and Sustainable Energy Reviews*.vol. 26.pp. 425–436. doi: 10.1016/j.rser.2013.05.066.
- [55] Li,Y.,Zhang,Y.,Li,M.,and Zhang,D. **2013**.Testing method of phase change temperature and heat of inorganic high temperature phase change materials.*Experimental Thermal and Fluid Science*.vol. 44.pp. 697–707. doi: 10.1016/j.expthermflusci.2012.09.010.
- [56] Jolliffe,I. T. **2002**.Choosing a subset of principal components or variables, chap. 6, Principal component analysis, 2nd edn., Springer-Verlag, Ed. New York, pp. 111– 149.
- [57] Montgomery,D. C. **2013**.*Design and Analysis of Experiments*. John Wiley & Sons, Inc. doi: 10.1002/9783527809080.cataz11063.
- [58] Heumann,C. and Schomaker Shalabh,M. **2002**.*Introduction to Statistics and Data Analysis*, no. 1. Springer Nature. doi: 10.1007/978-3-319-46162-5.
- [59] Svobodova-Sedlackova,A.,Barreneche,C.,Gamallo,P.,and Inés Fernández,A. **2021**.Novel sampling procedure and statistical analysis for the thermal characterization of ionic nanofluids.*Journal of Molecular Liquids*.vol. 347.p. 118316. doi: 10.1016/j.molliq.2021.118316.
- [60] Huang,Y.,Cheng,X.,Li,Y.,Yu,G.,Xu,K.,and Li,G. **2018**.Effect of in-situ synthesized nano-MgO on thermal properties of NaNO₃-KNO₃.*Solar Energy*.vol. 160, no. December 2017.pp. 208–215. doi: 10.1016/j.solener.2017.11.077.
- [61] Navarrete,N. *et al.* **2019**.Improved thermal energy storage of nanoencapsulated phase change materials by atomic layer deposition.*Solar Energy Materials and*

Solar Cells.no. October. doi: 10.1016/j.solmat.2019.110322.

- [62] Wei,X.,Yin,Y.,Qin,B.,Wang,W.,Ding,J.,and Lu,J. **2020**.Preparation and enhanced thermal conductivity of molten salt nanofluids with nearly unaltered viscosity.*Renewable Energy*.vol. 145.pp. 2435–2444. doi: 10.1016/j.renene.2019.04.153.
- [63] Tiznobaik,H. and Shin,D. **2013**.Enhanced specific heat capacity of high-temperature molten salt-based nanofluids.*International Journal of Heat and Mass Transfer*.vol. 57, no. 2.pp. 542–548. doi: 10.1016/j.ijheatmasstransfer.2012.10.062.
- [64] Shin,D. and Banerjee,D. **2011**.Enhanced specific heat of silica nanofluid.*Journal of Heat Transfer*.vol. 133, no. 2.pp. 1–4. doi: 10.1115/1.4002600.
- [65] Shin,D. and Banerjee,D. **2015**.Enhanced thermal properties of SiO₂ nanocomposite for solar thermal energy storage applications.*International Journal of Heat and Mass Transfer*.vol. 84.pp. 898–902. doi: 10.1016/j.ijheatmasstransfer.2015.01.100.
- [66] Tiznobaik,H. and Shin,D. **2013**.Experimental validation of enhanced heat capacity of ionic liquid-based nanomaterial.*Applied Physics Letters*.vol. 102, no. 17.pp. 1–4. doi: 10.1063/1.4801645.
- [67] Tiznobaik,H. and Shin,D. **2012**.Imece2012-87692 Experimental Study of Nanoengineered Molten Salts As Thermal.pp. 1–6.
- [68] Shin,D. and Banerjee,D. **2013**.Enhanced specific heat capacity of nanomaterials synthesized by dispersing silica nanoparticles in eutectic mixtures.*Journal of Heat Transfer*.vol. 135, no. 3.pp. 1–8. doi: 10.1115/1.4005163.
- [69] Shin,D. and Banerjee,D. **2010**.Effects of silica nanoparticles on enhancing the specific heat capacity of carbonate salt eutectic (work in progress).*INTERNATIONAL JOURNAL OF STRUCTURAL CHANGES IN SOLIDS – Mechanics and Applications*.vol. 2, no. November.pp. 25–31. [Online]. Available: <http://journals.tdl.org/ijscs/index.php/ijscs/article/view/2337>
- [70] Lee,J. and Mudawar,I. **2007**.Assessment of the effectiveness of nanofluids for single-phase and two-phase heat transfer in micro-channels.*International Journal of Heat and Mass Transfer*.vol. 50, no. 3–4.pp. 452–463. doi: 10.1016/j.ijheatmasstransfer.2006.08.001.
- [71] Assael,M. J.,Antoniadis,K. D.,Wakeham,W. A.,and Zhang,X. **2019**.Potential applications of nanofluids for heat transfer.*International Journal of Heat and Mass Transfer*.vol. 138.pp. 597–607. doi: 10.1016/j.ijheatmasstransfer.2019.04.086.
- [72] Selvam,C.,Mohan Lal,D.,and Harish,S. **2017**.Thermal conductivity and specific heat capacity of water–ethylene glycol mixture-based nanofluids with graphene nanoplatelets.*Journal of Thermal Analysis and Calorimetry*.vol. 129, no. 2.pp. 947–955. doi: 10.1007/s10973-017-6276-6.
- [73] Ho,C. J.,Huang,J. B.,Tsai,P. S.,and Yang,Y. M. **2011**.Water-based suspensions of Al₂O₃ nanoparticles and MEPCM particles on convection effectiveness in a circular tube.*International Journal of Thermal Sciences*.vol. 50, no. 5.pp. 736–748. doi: 10.1016/j.ijthermalsci.2010.11.015.
- [74] Leela Vinodhan,V.,Suganthi,K. S.,and Rajan,K. S. **2016**.Convective heat transfer performance of CuO-water nanofluids in U-shaped minitube: Potential for improved energy recovery.*Energy Conversion and Management*.vol. 118.pp. 415–425. doi: 10.1016/j.enconman.2016.04.017.

- [75] Bock Choon Pak, Y. I. C. **2013**. Hydrodynamic and Heat Transfer Study of Dispersed Fluids With Submicron Metallic Oxide. *Experimental Heat Transfer: A Journal of , Thermal Energy Transport , Storage , and Conversion*. no. January 2013. pp. 37–41.
- [76] Carrillo-Berdugo, I. *et al.* **2019**. Interface-inspired formulation and molecular-level perspectives on heat conduction and energy storage of nanofluids. *Scientific Reports*. vol. 9, no. 1. pp. 1–13. doi: 10.1038/s41598-019-44054-0.
- [77] Pandey, S. D. and Nema, V. K. **2012**. Experimental analysis of heat transfer and friction factor of nanofluid as a coolant in a corrugated plate heat exchanger. *Experimental Thermal and Fluid Science*. vol. 38. pp. 248–256. doi: 10.1016/j.exptthermflusci.2011.12.013.
- [78] Ajeel, R. K., Salim, W. S. W., and Hasnan, K. **2019**. An experimental investigation of thermal-hydraulic performance of silica nanofluid in corrugated channels. *Advanced Powder Technology*. vol. 30, no. 10. pp. 2262–2275. doi: 10.1016/j.appt.2019.07.006.
- [79] Choi, J. and Zhang, Y. **2012**. Numerical simulation of laminar forced convection heat transfer of Al₂O₃-water nanofluid in a pipe with return bend. *International Journal of Thermal Sciences*. vol. 55. pp. 90–102. doi: 10.1016/j.ijthermalsci.2011.12.017.
- [80] Teng, T. P. and Hung, Y. H. **2014**. Estimation and experimental study of the density and specific heat for alumina nanofluid. *Journal of Experimental Nanoscience*. vol. 9, no. 7. pp. 707–718. doi: 10.1080/17458080.2012.696219.
- [81] Zhou, S. Q. and Ni, R. **2008**. Measurement of the specific heat capacity of water-based Al₂O₃ nanofluid. *Applied Physics Letters*. vol. 92, no. 9. pp. 2006–2009. doi: 10.1063/1.2890431.
- [82] Khanafer, K., Vafai, K., and Lightstone, M. **2003**. Buoyancy-driven heat transfer enhancement in a two-dimensional enclosure utilizing nanofluids. *International Journal of Heat and Mass Transfer*. vol. 46, no. 19. pp. 3639–3653. doi: 10.1016/S0017-9310(03)00156-X.
- [83] Pantzali, M. N., Kanaris, A. G., Antoniadis, K. D., Mouza, A. A., and Paras, S. V. **2009**. Effect of nanofluids on the performance of a miniature plate heat exchanger with modulated surface. *International Journal of Heat and Fluid Flow*. vol. 30, no. 4. pp. 691–699. doi: 10.1016/j.ijheatfluidflow.2009.02.005.
- [84] Barbés, B. *et al.* **2013**. Thermal conductivity and specific heat capacity measurements of Al₂O₃ nanofluids. *Journal of Thermal Analysis and Calorimetry*. vol. 111, no. 2. pp. 1615–1625. doi: 10.1007/s10973-012-2534-9.
- [85] O’Hanley, H., Buongiorno, J., McKrell, T., and Hu, L. W. **2012**. Measurement and model validation of nanofluid specific heat capacity with differential scanning calorimetry. *Advances in Mechanical Engineering*. vol. 2012. doi: 10.1155/2012/181079.
- [86] Martín, M., Villalba, A., Inés Fernández, A., and Barreneche, C. **2019**. Development of new nano-enhanced phase change materials (NEPCM) to improve energy efficiency in buildings: Lab-scale characterization. *Energy and Buildings*. vol. 192. pp. 75–83. doi: 10.1016/j.enbuild.2019.03.029.
- [87] Gunjo, D. G., Jena, S. R., Mahanta, P., and Robi, P. S. **2018**. Melting enhancement of a latent heat storage with dispersed Cu, CuO and Al₂O₃ nanoparticles for solar thermal application. *Renewable Energy*. vol. 121. pp. 652–665. doi:

10.1016/j.renene.2018.01.013.

- [88] Sebti, S. S., Mastiani, M., Mirzaei, H., Dadvand, A., Kashani, S., and Hosseini, S. A. **2013**. Numerical study of the melting of nano-enhanced phase change material in a square cavity. *Journal of Zhejiang University: Science A*. vol. 14, no. 5. pp. 307–316. doi: 10.1631/jzus.A1200208.
- [89] Wu, S., Wang, H., Xiao, S., and Zhu, D. **2012**. Numerical simulation on thermal energy storage behavior of Cu/paraffin nanofluids PCMs. *Procedia Engineering*. vol. 31. pp. 240–244. doi: 10.1016/j.proeng.2012.01.1018.
- [90] Starace, A. K., Gomez, J. C., Wang, J., Pradhan, S., and Glatzmaier, G. C. **2011**. Nanofluid heat capacities. *Journal of Applied Physics*. vol. 110, no. 12. doi: 10.1063/1.3672685.
- [91] Nelson, I. C., Banerjee, D., and Ponnappan, R. **2009**. Flow loop experiments using polyalphaolefin nanofluids. *Journal of Thermophysics and Heat Transfer*. vol. 23, no. 4. pp. 752–761. doi: 10.2514/1.31033.
- [92] Ghazvini, M., Akhavan-Behabadi, M. A., Rasouli, E., and Raisee, M. **2012**. Heat transfer properties of nanodiamond-engine oil nanofluid in laminar flow. *Heat Transfer Engineering*. vol. 33, no. 6. pp. 525–532. doi: 10.1080/01457632.2012.624858.
- [93] Saeedinia, M., Akhavan-Behabadi, M. A., and Razi, P. **2012**. Thermal and rheological characteristics of CuO-Base oil nanofluid flow inside a circular tube. *International Communications in Heat and Mass Transfer*. vol. 39, no. 1. pp. 152–159. doi: 10.1016/j.icheatmasstransfer.2011.08.001.
- [94] Murshed, S. M. S. **2012**. Simultaneous measurement of thermal conductivity, thermal diffusivity, and specific heat of nanofluids. *Heat Transfer Engineering*. vol. 33, no. 8. pp. 722–731. doi: 10.1080/01457632.2011.635986.
- [95] Fakoor Pakdaman, M., Akhavan-Behabadi, M. A., and Razi, P. **2012**. An experimental investigation on thermo-physical properties and overall performance of MWCNT/heat transfer oil nanofluid flow inside vertical helically coiled tubes. *Experimental Thermal and Fluid Science*. vol. 40. pp. 103–111. doi: 10.1016/j.expthermflusci.2012.02.005.
- [96] Toghyani, S., Baniasadi, E., and Afshari, E. **2016**. Thermodynamic analysis and optimization of an integrated Rankine power cycle and nano-fluid based parabolic trough solar collector. *Energy Conversion and Management*. vol. 121. pp. 93–104. doi: 10.1016/j.enconman.2016.05.029.
- [97] Dehury, P., Singh, J., and Banerjee, T. **2018**. Thermophysical and Forced Convection Studies on (Alumina + Menthol)-Based Deep Eutectic Solvents for Their Use as a Heat Transfer Fluid. *ACS Omega*. vol. 3, no. 12. pp. 18016–18027. doi: 10.1021/acsomega.8b02661.
- [98] Wang, B. X., Zhou, L. P., Peng, X. F., Du, X. Z., and Yang, Y. P. **2010**. On the specific heat capacity of CuO nanofluid. *Advances in Mechanical Engineering*. vol. 2010, no. January. doi: 10.1155/2010/172085.
- [99] Akilu, S., Baheta, A. T., Minea, A. A., and Sharma, K. V. **2017**. Rheology and thermal conductivity of non-porous silica (SiO₂) in viscous glycerol and ethylene glycol based nanofluids. *International Communications in Heat and Mass Transfer*. vol. 88, no. October. pp. 245–253. doi: 10.1016/j.icheatmasstransfer.2017.08.001.
- [100] Teng, T. P. and Yu, C. C. **2013**. Heat dissipation performance of MWCNTs nanocoolant for vehicle. *Experimental Thermal and Fluid Science*. vol. 49. pp. 22–30.

doi: 10.1016/j.expthermflusci.2013.03.007.

- [101] Nieh, H. M., Teng, T. P., and Yu, C. C. **2014**. Enhanced heat dissipation of a radiator using oxide nano-coolant. *International Journal of Thermal Sciences*. vol. 77. pp. 252–261. doi: 10.1016/j.ijthermalsci.2013.11.008.
- [102] Kumaresan, V. and Velraj, R. **2012**. Experimental investigation of the thermo-physical properties of water-ethylene glycol mixture based CNT nanofluids. *Thermochimica Acta*. vol. 545. pp. 180–186. doi: 10.1016/j.tca.2012.07.017.
- [103] Kumaresan, V., Mohaideen Abdul Khader, S., Karthikeyan, S., and Velraj, R. **2013**. Convective heat transfer characteristics of CNT nanofluids in a tubular heat exchanger of various lengths for energy efficient cooling/heating system. *International Journal of Heat and Mass Transfer*. vol. 60, no. 1. pp. 413–421. doi: 10.1016/j.ijheatmasstransfer.2013.01.021.
- [104] Nagarajan, F. C., Kannaiyan, S. K., and Boobalan, C. **2020**. Intensification of heat transfer rate using alumina-silica nanocoolant. *International Journal of Heat and Mass Transfer*. vol. 149. doi: 10.1016/j.ijheatmasstransfer.2019.119127.
- [105] Kulkarni, D. P., Vajjha, R. S., Das, D. K., and Oliva, D. **2008**. Application of aluminum oxide nanofluids in diesel electric generator as jacket water coolant. *Applied Thermal Engineering*. vol. 28, no. 14–15. pp. 1774–1781. doi: 10.1016/j.applthermaleng.2007.11.017.
- [106] Vajjha, R. S. and Das, D. K. **2012**. A review and analysis on influence of temperature and concentration of nanofluids on thermophysical properties, heat transfer and pumping power. *International Journal of Heat and Mass Transfer*. vol. 55, no. 15–16. pp. 4063–4078. doi: 10.1016/j.ijheatmasstransfer.2012.03.048.
- [107] P.K., Na., D.P., K., A., D., and D.K., D. **2007**. Experimental investigation of viscosity and specific heat of silicon dioxide nanofluid. *Micro and Nano Letters*. vol. 2, no. 3. pp. 67–71. doi: 10.1049/mnl.
- [108] Elias, M. M. *et al.* **2014**. Experimental investigation on the thermo-physical properties of Al₂O₃ nanoparticles suspended in car radiator coolant. *International Communications in Heat and Mass Transfer*. vol. 54. pp. 48–53. doi: 10.1016/j.icheatmasstransfer.2014.03.005.
- [109] Qiao, G., Lasfargues, M., Alexiadis, A., and Ding, Y. **2017**. Simulation and experimental study of the specific heat capacity of molten salt based nanofluids. *Applied Thermal Engineering*. vol. 111. pp. 1517–1522. doi: 10.1016/j.applthermaleng.2016.07.159.
- [110] Awad, A., Navarro, H., Ding, Y., and Wen, D. **2018**. Thermal-physical properties of nanoparticle-seeded nitrate molten salts. *Renewable Energy*. vol. 120. pp. 275–288. doi: 10.1016/j.renene.2017.12.026.
- [111] Chieruzzi, M., Miliozzi, A., Crescenzi, T., Torre, L., and Kenny, J. M. **2015**. A New Phase Change Material Based on Potassium Nitrate with Silica and Alumina Nanoparticles for Thermal Energy Storage. *Nanoscale Research Letters*. vol. 10, no. 1. doi: 10.1186/s11671-015-0984-2.
- [112] Dudda, B. and Shin, D. **2012**. Imece2012-87707 Investigation of Molten Salt Nanomaterial As Thermal Energy Storage in. pp. 1–6.
- [113] Muñoz-Sánchez, B., Nieto-Maestre, J., Iparraguirre-Torres, I., Julià, J. E., and García-Romero, A. **2017**. Silica and alumina nano-enhanced molten salts for thermal energy storage: A comparison. *AIP Conference Proceedings*. vol. 1850, no. June.

doi: 10.1063/1.4984439.

- [114] Nithiyantham,U.,Grosu,Y.,González-Fernández,L.,Zaki,A.,Igartua,J. M.,and Faik,A. **2019**.Development of molten nitrate salt based nanofluids for thermal energy storage application: High thermal performance and long storage components life-time.*SOLARPACES 2018: International Conference on Concentrating Solar Power and Chemical Energy Systems*.vol. 2126.p. 200025. doi: 10.1063/1.5117740.
- [115] Hu,Y.,Zhang,B.,Tan,K.,He,Y.,and Zhu,J. **2020**.Regulation of natural convection heat transfer for SiO₂–solar salt nanofluids by optimizing rectangular vessels design.*Asia-Pacific Journal of Chemical Engineering*.no. January.pp. 1–15. doi: 10.1002/apj.2409.
- [116] Dudda,B. and Shin,D. **2013**.Effect of nanoparticle dispersion on specific heat capacity of a binary nitrate salt eutectic for concentrated solar power applications.*International Journal of Thermal Sciences*.vol. 69.pp. 37–42. doi: 10.1016/j.ijthermalsci.2013.02.003.
- [117] Andreu-Cabedo,P.,Mondragon,R.,Hernandez,L.,Martinez-Cuenca,R.,Cabedo,L.,and Julia,J. E. **2014**.Increment of specific heat capacity of solar salt with SiO₂ nanoparticles.*Nanoscale Research Letters*.vol. 9, no. 1.pp. 1–11. doi: 10.1186/1556-276X-9-582.
- [118] Navarrete,N.,Hernández,L.,Vela,A.,and Mondragón,R. **2020**.Influence of the production method on the thermophysical properties of high temperature molten salt-based nanofluids.*Journal of Molecular Liquids*.vol. 302.p. 112570. doi: 10.1016/j.molliq.2020.112570.
- [119] Hu,Y.,He,Y.,Gao,H.,and Zhang,Z. **2019**.Forced convective heat transfer characteristics of solar salt-based SiO₂ nanofluids in solar energy applications.*Applied Thermal Engineering*.vol. 155, no. April.pp. 650–659. doi: 10.1016/j.applthermaleng.2019.04.109.
- [120] Chieruzzi,M.,Cerritelli,G. F.,Miliozzi,A.,Kenny,J. M.,and Torre,L. **2017**.Heat capacity of nanofluids for solar energy storage produced by dispersing oxide nanoparticles in nitrate salt mixture directly at high temperature.*Solar Energy Materials and Solar Cells*.vol. 167, no. December 2016.pp. 60–69. doi: 10.1016/j.solmat.2017.04.011.
- [121] Hu,Y.,He,Y.,Zhang,Z.,and Wen,D. **2019**.Enhanced heat capacity of binary nitrate eutectic salt-silica nanofluid for solar energy storage.*Solar Energy Materials and Solar Cells*.vol. 192, no. July 2018.pp. 94–102. doi: 10.1016/j.solmat.2018.12.019.
- [122] Muñoz-Sánchez,B.,Nieto-Maestre,J.,Iparraguirre-Torres,I.,Sánchez-García,J. A.,Julia,J. E.,and García-Romero,A. **2016**.The influence of mixing water on the thermophysical properties of nanofluids based on solar salt and silica nanoparticles.*AIP Conference Proceedings*.vol. 1734, no. May 2016. doi: 10.1063/1.4949129.
- [123] Muñoz-Sánchez,B.,Nieto-Maestre,J.,Guerreiro,L.,Julia,J. E.,Collares-Pereira,M.,and García-Romero,A. **2017**.Molten salt based nanofluids based on solar salt and alumina nanoparticles: An industrial approach.*AIP Conference Proceedings*.vol. 1850, no. June. doi: 10.1063/1.4984437.
- [124] Schuller,M.,Shao,Q.,and Lalk,T. **2015**.Experimental investigation of the specific heat of a nitrate-alumina nanofluid for solar thermal energy storage systems.*International Journal of Thermal Sciences*.vol. 91.pp. 142–145. doi:

10.1016/j.ijthermalsci.2015.01.012.

- [125] Lu, M.-C. and Huang, C.-H. **2013**. Specific heat capacity of molten salt-based alumina nanofluid. *Nanoscale research letters*. vol. 8, no. 1. p. 292. doi: 10.1186/1556-276X-8-292.
- [126] Nithiyantham, U., González-Fernández, L., Grosu, Y., Zaki, A., Igartua, J. M., and Faik, A. **2020**. Shape effect of Al₂O₃ nanoparticles on the thermophysical properties and viscosity of molten salt nanofluids for TES application at CSP plants. *Applied Thermal Engineering*. vol. 169, no. January. p. 114942. doi: 10.1016/j.applthermaleng.2020.114942.
- [127] Chieruzzi, M., Cerritelli, G. F., Miliozzi, A., and Kenny, J. M. **2013**. Effect of nanoparticles on heat capacity of nanofluids based on molten salts as PCM for thermal energy storage. *Nanoscale Research Letters*. vol. 8, no. 1. pp. 1–9. doi: 10.1186/1556-276X-8-448.
- [128] Muñoz-Sánchez, B., Nieto-Maestre, J., Imbuluzqueta, G., Marañón, I., Iparraguirre-Torres, I., and García-Romero, A. **2017**. A precise method to measure the specific heat of solar salt-based nanofluids. *Journal of Thermal Analysis and Calorimetry*. vol. 129, no. 2. pp. 905–914. doi: 10.1007/s10973-017-6272-x.
- [129] Hu, Y., He, Y., Zhang, Z., and Wen, D. **2017**. Effect of Al₂O₃ nanoparticle dispersion on the specific heat capacity of a eutectic binary nitrate salt for solar power applications. *Energy Conversion and Management*. vol. 142. pp. 366–373. doi: 10.1016/j.enconman.2017.03.062.
- [130] Lasfargues, M., Bell, A., and Ding, Y. **2016**. In situ production of titanium dioxide nanoparticles in molten salt phase for thermal energy storage and heat-transfer fluid applications. *Journal of Nanoparticle Research*. vol. 18, no. 6. pp. 1–11. doi: 10.1007/s11051-016-3460-8.
- [131] Navarrete, N., Mondragón, R., Wen, D., Navarro, M. E., Ding, Y., and Juliá, J. E. **2019**. Thermal energy storage of molten salt –based nanofluid containing nano-encapsulated metal alloy phase change materials. *Energy*. vol. 167. pp. 912–920. doi: 10.1016/j.energy.2018.11.037.
- [132] Lasfargues, M., Stead, G., Amjad, M., Ding, Y., and Wen, D. **2017**. In situ production of copper oxide nanoparticles in a binary molten salt for concentrated solar power plant applications. *Materials*. vol. 10, no. 5. pp. 1–10. doi: 10.3390/ma10050537.
- [133] Luo, Y., Du, X., Awad, A., and Wen, D. **2017**. Thermal energy storage enhancement of a binary molten salt via in-situ produced nanoparticles. *International Journal of Heat and Mass Transfer*. vol. 104. pp. 658–664. doi: 10.1016/j.ijheatmasstransfer.2016.09.004.
- [134] Xie, Q., Zhu, Q., and Li, Y. **2016**. Thermal Storage Properties of Molten Nitrate Salt-Based Nanofluids with Graphene Nanoplatelets. *Nanoscale Research Letters*. vol. 11, no. 1. pp. 1–7. doi: 10.1186/s11671-016-1519-1.
- [135] Hamdy, E., Ebrahim, S., Abulfotuh, F., and Soliman, M. **2017**. Effect of multi-walled carbon nanotubes on thermal properties of nitrate molten salts. *Proceedings of 2016 International Renewable and Sustainable Energy Conference, IRSEC 2016*. pp. 317–320. doi: 10.1109/IRSEC.2016.7983997.
- [136] Hassan, M. A. and Banerjee, D. **2019**. A soft computing approach for estimating the specific heat capacity of molten salt-based nanofluids. *Journal of Molecular Liquids*. vol. 281. pp. 365–375. doi: 10.1016/j.molliq.2019.02.106.
- [137] He, Q., Wang, S., Tong, M., and Liu, Y. **2012**. Experimental study on thermophysical

- properties of nanofluids as phase-change material (PCM) in low temperature cool storage. *Energy Conversion and Management*. vol. 64. pp. 199–205. doi: 10.1016/j.enconman.2012.04.010.
- [138] Tian, H. *et al.* **2017**. Enhanced specific heat capacity of binary chloride salt by dissolving magnesium for higher temperature thermal energy storage and transfer. *Journal of Materials Chemistry A*. vol. 5, no. 28. pp. 14811–14818. doi: 10.1039/c7ta04169a.
- [139] Shin, D. and Banerjee, D. **2011**. Enhancement of specific heat capacity of high-temperature silica-nanofluids synthesized in alkali chloride salt eutectics for solar thermal-energy storage applications. *International Journal of Heat and Mass Transfer*. vol. 54, no. 5–6. pp. 1064–1070. doi: 10.1016/j.ijheatmasstransfer.2010.11.017.
- [140] Chen, X., Wu, Y. ting, Zhang, L. di, Wang, X., and Ma, C. fang. **2018**. Experimental study on the specific heat and stability of molten salt nanofluids prepared by high-temperature melting. *Solar Energy Materials and Solar Cells*. vol. 176, no. November 2017. pp. 42–48. doi: 10.1016/j.solmat.2017.11.021.
- [141] Zhang, L. di, Chen, X., Wu, Y. ting, Lu, Y. wei, and Ma, C. fang. **2016**. Effect of nanoparticle dispersion on enhancing the specific heat capacity of quaternary nitrate for solar thermal energy storage application. *Solar Energy Materials and Solar Cells*. vol. 157. pp. 808–813. doi: 10.1016/j.solmat.2016.07.046.
- [142] Liu, Y. and Yang, Y. **2017**. Investigation of specific heat and latent heat enhancement in hydrate salt based TiO₂ nanofluid phase change material. *Applied Thermal Engineering*. vol. 124. pp. 533–538. doi: 10.1016/j.applthermaleng.2017.05.150.
- [143] Ho, M. X. and Pan, C. **2014**. Optimal concentration of alumina nanoparticles in molten hitec salt to maximize its specific heat capacity. *International Journal of Heat and Mass Transfer*. vol. 70. pp. 174–184. doi: 10.1016/j.ijheatmasstransfer.2013.10.078.
- [144] Sang, L., Ai, W., Liu, T., Wu, Y., and Ma, C. **2019**. Insights into the specific heat capacity enhancement of ternary carbonate nanofluids with SiO₂ nanoparticles: the effect of change in the composition ratio. *RSC Advances*. vol. 9, no. 10. pp. 5288–5294. doi: 10.1039/c8ra10318f.
- [145] Shin, D. and Banerjee, D. **2014**. Specific heat of nanofluids synthesized by dispersing alumina nanoparticles in alkali salt eutectic. *International Journal of Heat and Mass Transfer*. vol. 74. pp. 210–214. doi: 10.1016/j.ijheatmasstransfer.2014.02.066.
- [146] Jo, B. and Banerjee, D. **2014**. Enhanced specific heat capacity of molten salt-based nanomaterials: Effects of nanoparticle dispersion and solvent material. *Acta Materialia*. vol. 75. pp. 80–91. doi: 10.1016/j.actamat.2014.05.005.
- [147] Tiznobaik, H., Banerjee, D., and Shin, D. **2015**. Effect of formation of “long range” secondary dendritic nanostructures in molten salt nanofluids on the values of specific heat capacity. *International Journal of Heat and Mass Transfer*. vol. 91. pp. 342–346. doi: 10.1016/j.ijheatmasstransfer.2015.05.072.
- [148] Jo, B. and Banerjee, D. **2015**. Enhanced specific heat capacity of molten salt-based carbon nanotubes nanomaterials. *Journal of Heat Transfer*. vol. 137, no. 9. pp. 1–7. doi: 10.1115/1.4030226.
- [149] Jo, B. and Banerjee, D. **2014**. ENHANCED SPECIFIC HEAT CAPACITY OF

MOLTEN SALTS USING ORGANIC NANOPARTICLES.no. 2011.pp. 1–8.

- [150] Seo,J. and Shin,D. **2014**.Enhancement of specific heat of ternary nitrate (LiNO₃-NaNO₃-KNO₃) salt by doping with SiO₂ nanoparticles for solar thermal energy storage.*Micro and Nano Letters*.vol. 9, no. 11.pp. 817–820. doi: 10.1049/mnl.2014.0407.
- [151] Seo,J. and Shin,D. **2016**.Size effect of nanoparticle on specific heat in a ternary nitrate (LiNO₃-NaNO₃-KNO₃) salt eutectic for thermal energy storage.*Applied Thermal Engineering*.vol. 102.pp. 144–148. doi: 10.1016/j.applthermaleng.2016.03.134.
- [152] Sonawane,S.,Patankar,K.,Fogla,A.,Puranik,B.,Bhandarkar,U.,and Sunil Kumar,S. **2011**.An experimental investigation of thermo-physical properties and heat transfer performance of Al₂O₃-Aviation Turbine Fuel nanofluids.*Applied Thermal Engineering*.vol. 31, no. 14–15.pp. 2841–2849. doi: 10.1016/j.applthermaleng.2011.05.009.
- [153] Nieto De Castro,C. A.,Murshed,S. M. S.,Lourenço,M. J. V.,Santos,F. J. V.,Lopes,M. L. M.,and França,J. M. P. **2012**.Enhanced thermal conductivity and specific heat capacity of carbon nanotubes ionanofluids.*International Journal of Thermal Sciences*.vol. 62.pp. 34–39. doi: 10.1016/j.ijthermalsci.2012.03.010.
- [154] Liu,J.,Wang,F.,Zhang,L.,Fang,X.,and Zhang,Z. **2014**.Thermodynamic properties and thermal stability of ionic liquid-based nanofluids containing graphene as advanced heat transfer fluids for medium-to-high-temperature applications.*Renewable Energy*.vol. 63.pp. 519–523. doi: 10.1016/j.renene.2013.10.002.
- [155] Paul,T. C.,Morshed,A. K. M. M.,and Khan,J. A. **2013**.Nanoparticle Enhanced Ionic Liquids (NEILS) as working fluid for the next generation solar collector.*Procedia Engineering*.vol. 56.pp. 631–636. doi: 10.1016/j.proeng.2013.03.170.
- [156] Mohebbi,A. **2012**.Prediction of specific heat and thermal conductivity of nanofluids by a combined equilibrium and non-equilibrium molecular dynamics simulation.*Journal of Molecular Liquids*.vol. 175.pp. 51–58. doi: 10.1016/j.molliq.2012.08.010.

7.3 Paper 3

The complete study is published in the Journal of Molecular Liquids, entitled "Novel Sampling procedure and statistical analysis for the thermal characterization of ionic nanofluids".

The article is available online in the Elsevier database since the 13th of December 2021, and it was published on volume 347, as shown in **Figure 7.4**.

Besides, a related work was presented at the 27th SolarPACES conference (**SolarPACES 2021**) and the 3rd European Symposium on Nanofluids (**ESNF 2021**), see **Appendix 3**.

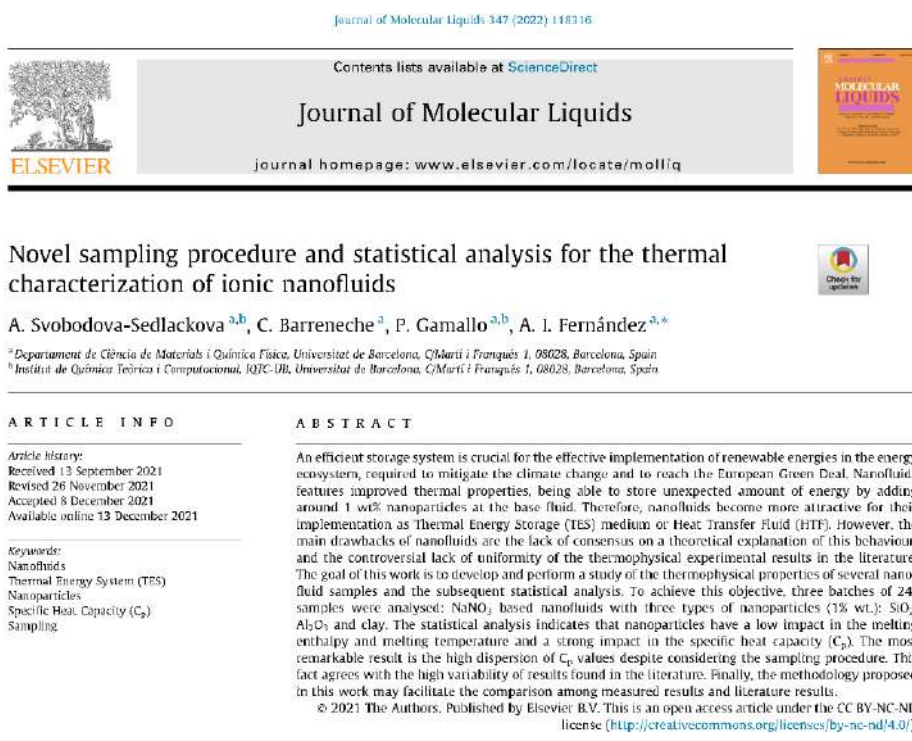


Figure 7.4. Article published in the Journal of Molecular liquids in 2022, entitled "Novel sampling procedure and statistical analysis for the thermal characterization of ionic nanofluids" [1].

7.3.1 Graphical Abstract

Figure 7.5 summarizes the most relevant results.

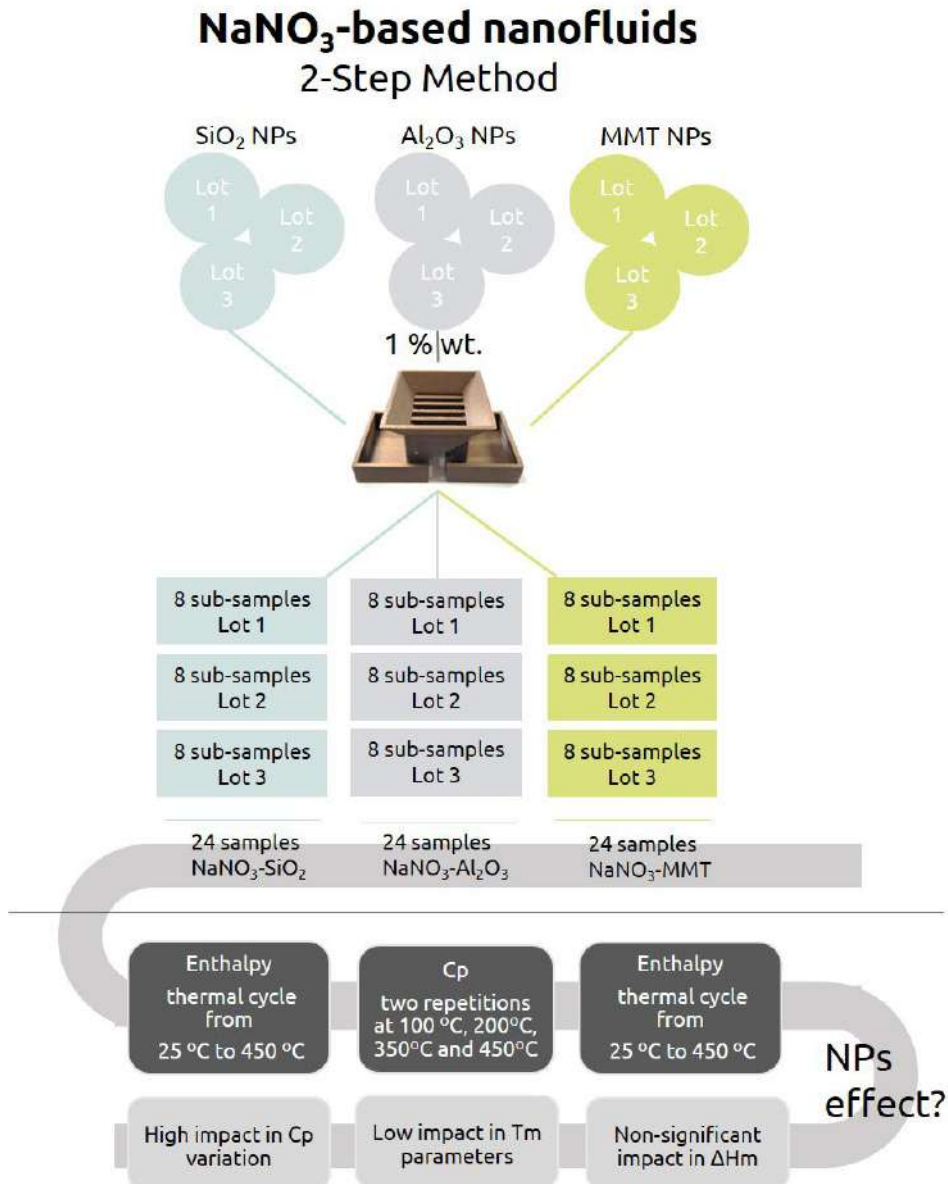
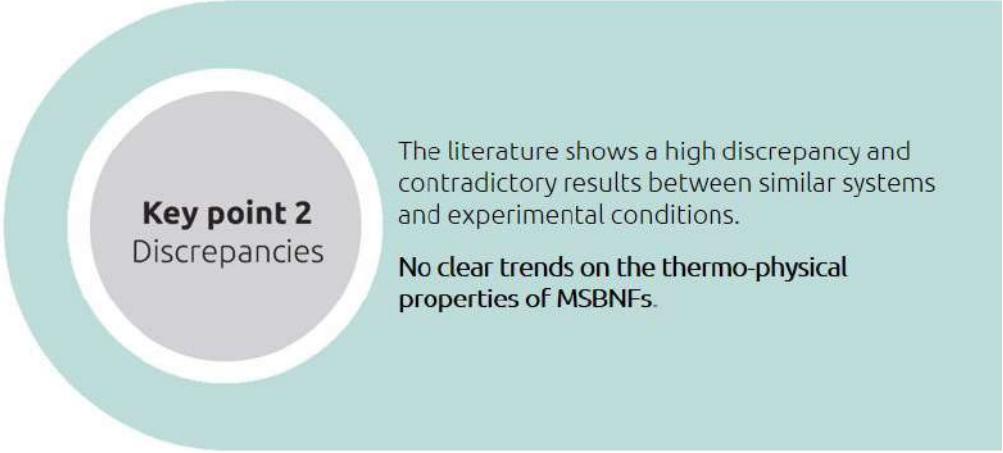


Figure 7.5. Graphical abstract of the article entitled “Novel Sampling procedure and statistical analysis for the thermal characterization of ionic nanofluids” [1].

7.3.2 Contribution to the state-of-the-art



Key point 2
Discrepancies

The literature shows a high discrepancy and contradictory results between similar systems and experimental conditions.

No clear trends on the thermo-physical properties of MSBNFs.

- ✓ Another relevant aspect included in Key point II is the case of MSBNFs. Through the sampling study carried out in this section, the melting temperature, melting enthalpy and heat capacity of sodium nitrate nanofluids with different types of nanoparticles (SiO_2 , Al_2O_3 and MMT) in 1% have been statistically studied. The most relevant results that contribute to state of the art are:
 - Nanofluids complete the melting at lower temperatures than pure NaNO_3 . No significant differences were found in the enthalpy of fusion by adding nanoparticles.
 - Initial DSC measurement must be discarded.
 - It is necessary to include the associated error of the synthesis method in the total C_p error.
 - After performing an accurate sampling, nanofluids show a high variation in C_p values: from 80% to -20, **Figure 7.6.**

- ✓ This last point is relevant since it does not reduce the dispersion in the heat capacity values despite the sampling carried out. This fact may indicate the presence of more complex phenomena and

the lack of an appropriate measurement methodology. In addition, these results corroborate the dispersion of results published in the literature.

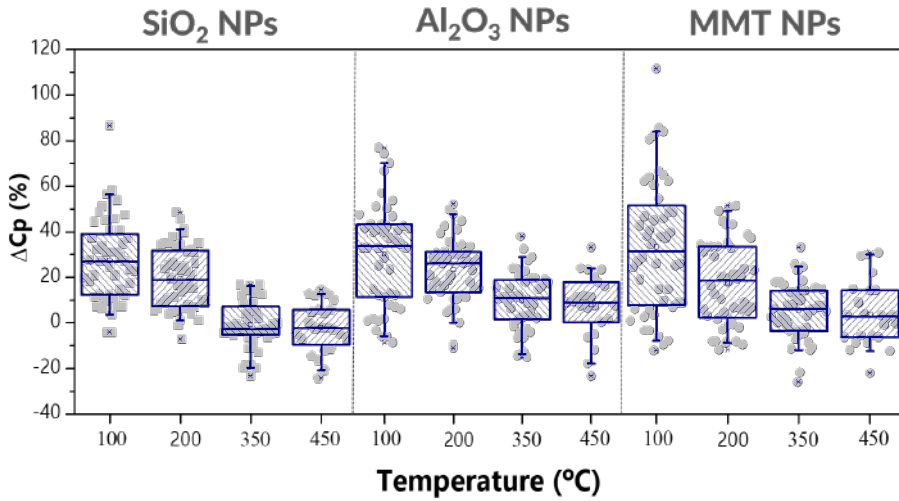


Figure 7.6. Specific heat capacity variation (%) as a function of temperature from nitrate salt-based nanofluids with, a) SiO_2 nanoparticles, b) Al_2O_3 nanoparticles, and c) MMT nanoparticles.

- ✓ Finally, thought this study some measurement recommendations and procedures has been highlighted, **Figure 7.7.**

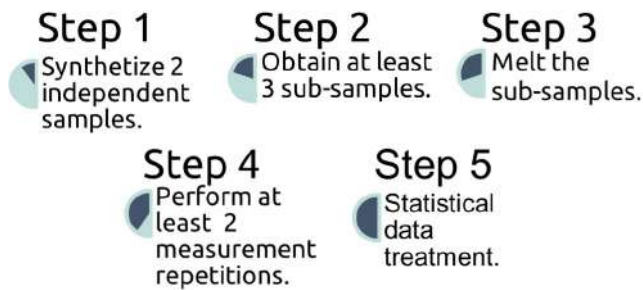


Figure 7.7. Measurement's recommendations of thermophysical properties for ionic-nanofluids.

7.3.3 Publication

The article is attached below (DOI: <https://doi.org/10.1016/j.molliq.2021.118316>).



Novel sampling procedure and statistical analysis for the thermal characterization of ionic nanofluids



A. Svobodova-Sedlackova^{a,b}, C. Barreneche^a, P. Gamallo^{a,b}, A. I. Fernández^{a,*}

^aDepartament de Ciència de Materials i Química Física, Universitat de Barcelona, C/Martí i Franqués 1, 08028, Barcelona, Spain

^bInstitut de Química Tècnica i Computacional, IQTC-UB, Universitat de Barcelona, C/Martí i Franqués 1, 08028, Barcelona, Spain

ARTICLE INFO

Article history:

Received 13 September 2021

Revised 26 November 2021

Accepted 8 December 2021

Available online 13 December 2021

Keywords:

Nanofluids

Thermal Energy Storage (TES)

Nanoparticles

Specific Heat Capacity (C_p)

Sampling

ABSTRACT

An efficient storage system is crucial for the effective implementation of renewable energies in the energy ecosystem, required to mitigate the climate change and to reach the European Green Deal. Nanofluids features improved thermal properties, being able to store unexpected amount of energy by adding around 1 wt% nanoparticles at the base fluid. Therefore, nanofluids become more attractive for their implementation as Thermal Energy Storage (TES) medium or Heat Transfer Fluid (HTF). However, the main drawbacks of nanofluids are the lack of consensus on a theoretical explanation of this behaviour, and the controversial lack of uniformity of the thermophysical experimental results in the literature. The goal of this work is to develop and perform a study of the thermophysical properties of several nanofluid samples and the subsequent statistical analysis. To achieve this objective, three batches of 24-samples were analysed: NaNO_3 based nanofluids with three types of nanoparticles (1% wt.): SiO_2 , Al_2O_3 and clay. The statistical analysis indicates that nanoparticles have a low impact in the melting enthalpy and melting temperature and a strong impact in the specific heat capacity (C_p). The most remarkable result is the high dispersion of C_p values despite considering the sampling procedure. This fact agrees with the high variability of results found in the literature. Finally, the methodology proposed in this work may facilitate the comparison among measured results and literature results.

© 2021 The Authors. Published by Elsevier B.V. This is an open access article under the CC BY-NC-ND license (<http://creativecommons.org/licenses/by-nc-nd/4.0/>).

1. Introduction

Nanofluids (NFs) are a colloidal suspension of nanoparticles (NPs) in a liquid medium that were originally introduced by Choi S.U. et al. in 1995 [1]. Since then and up to 2021, almost eighteen thousand articles related to this field have been published. One of the most studied topic is the enhancement of thermophysical properties of the fluid due to the presence of NPs at low concentrations [2,3,4]. Since the specific heat capacity (C_p) is one of the variables that measures the amount of heat that can be stored by a material, it is the property with highest interest for evaluating thermal energy storage (TES) systems. The reviewed literature shows exceptional C_p values with increments up to 30% when 1% in weight (wt.) of NPs are added to the base fluid [5].

According to this, in the last years NFs have become an interesting TES media to be implemented in concentrate solar power (CSP) plants [6,7] because the presence of NFs may improve the thermal properties of solar salt, used in these plants as TES media and HTF,

which consists in the eutectic mixture of KNO_3 and NaNO_3 [5]. Obviously, the improvement of the base fluid's thermal properties would drive to a more efficient energy storage and consequently, to more efficient CSP plants [8] (e.g., higher thermal capacities would imply the volume reduction of the storage tanks [9]). Besides their use in solar energy applications [10,11], NFs are also being considered as heat transfer fluids [12], lubricants [13], in electronics [14], automotive [15,16], industrial cooling [17], nuclear systems [18], quantum dots [19] or in heating buildings [20,21].

Materials with these properties could significantly improve thermal storage efficiency. Although great advances have been made in this field, there is still a long way to do to fully understand the phenomenon that provokes the C_p enhancement [22]. Moreover, other factors as the influence of the size, concentration and density of nanoparticles, C_p of the base fluid or even the pH and temperature of the sample can have a great influence on the final properties [23]. Another drawback is the high dispersion observed in the published C_p values, under similar or in some cases, the same experimental conditions. Table 1 lists C_p variation, ΔC_p , for different solar salt-based NFs with 1 wt% of different NPs. ΔC_p corresponds to the difference in C_p of NFs and the NaNO_3 - KNO_3 base

* Corresponding author.

E-mail address: ana_inesfernandez@ub.edu (A.I. Fernández).

Table 1
Specific heat capacity variation, ΔC_p , of solar salt nanofluids with 1 wt% of nanoparticles with different sizes.

Base	Nanoparticle	Average Size (nm)	Average Temperature (°C)	ΔC_p (%)	References
NaNO ₃ - KNO ₃ (60:40)	SiO ₂	5	113.3, 266.6, 233.3	8, 19, 10	[27, 50, 51]
		7	183.3	0.8	[50, 51]
		10	113.3, 233.3, 500	12, 13, 13	[50, 27, 52]
		12	223.3	25.03	[50, 28]
		16	200, 250	8.9, 8.9	[50, 52]
		102.5	40, 400	-0.34, 6.65	[52]
		20	200, 200, 350	17.6, -2, 17.6	[50, 52]
		25	400	21.1, 20.3, 9.5, 10.6, 15.82	[53]
		30	266.6, 113.3, 233.3	25, 19, 21	[50, 51, 27]
		60	233.3, 113.3	28, 27	[50, 27]
	Al ₂ O ₃	13	183.3, 125, 125, 230	5.9, 19.9, 5.9, 3	[50, 51, 47, 54]
		50	230	6	[54]
	SiO ₂ - Al ₂ O ₃	7	185, 272.5	28.9, 2.6	[52, 29]
		41	396	30	[55]
		101	183.3, 125	22.5, 57.7	[50, 51]
	TiO ₂	103.5	185, 272.5	14.9, 0.8	[52, 47]
		20	183.3, 125	-6.3, -6	[50, 51]
		50	350, 182.5	-2.19, 1.6	[56]
	Al-Cu	160	300, 350, 400	0.07, -1.34, -3.69	[57]
		29	295	-1.27	[52, 58]
CuO	50	182.5, 350	6.3, -1.97	[56]	
	180	80, 189, 280	0.62, 8.16, 3.99	[59]	
Sn-SiO ₂	180	80	-1.26, 5.69, 5.88	[59]	
Fe ₂ O ₃	30	350, 182.5	2.19, 9.1	[56]	
Sn	180	80, 180, 280	-5.09, 1.79, 2.02	[59]	

fluid. A high dispersion of the ΔC_p is observed ranging from -5% to 22%. Moreover, different methodologies and techniques have been used to measure the C_p value (i.e., standard ASTM E1219[24], ASTM E2716[25] or the Areas Method[26]). In particular, the C_p values have been obtained by dissimilar number of samples and measurement repetitions. For example, B. Dudda et al [27] or Z. Jiang et al. [28] in their studies measured up to 5 samples and 3 measurement repetitions. In opposite, M. Chieruzzi [29] obtained the C_p value by means of 1 sample and 6 measurement repetitions. Therefore, it is evident that there is a lack of a methodological procedure that makes impossible the direct comparison among results. Likewise, in the light of the ΔC_p values in Table 1, there is not a clear tendency about the effect of temperature in the nanofluids behaviour. Similar tendencies and inconsistencies have been found in other base fluids such as molten salts [30–33], water [34–37], ethylene and propylene glycol [38–42] or oils [39,43–45]. This fact points out that there is not a clear trend or specific values about NFs properties [46–49]. Thereby, the difficulties to obtain a representative sample is one of the possible reasons of these discrepancies. Obviously, this fact makes difficult to take a step forward in the NFs implementation and development for industrial applications.

This work aims at obtaining a statistically representative sampling of NFs to ensure accurate thermophysical results after their characterization. The study comprises the evaluation by means of differential scanning calorimetry (DSC) of thermophysical properties of NFs such as specific heat capacity, melting point and melting enthalpy, measuring a high number of samples. Sodium nitrate has been used as fluid along with three different NPs, silica (SiO₂), alumina (Al₂O₃), and montmorillonite (MMT). All the results have been compared with pure NaNO₃ used as a reference at the same experimental conditions. Furthermore, the chemical composition of the samples has been studied via an Inductively Coupled Plasma (ICP) analysis to determine the NP concentration, and to obtain a clear correlation between the NP concentration and the specific heat capacity variation. The statistical procedure used and the proposed methodology can contribute to the field in different ways; first, facilitating the comparison between results and, second, providing a clearer point of view about the thermophysical properties trends of NFs.

2. Experimental procedure and methodology

2.1. Sample preparation

The NFs were synthesized in our laboratories starting from sodium nitrate (Sigma Aldrich, 99.995%) as base fluid and then doped with three types of NPs: 5–15 nm diameter silica (Sigma Aldrich, 99.5%), 13 nm diameter alumina (Sigma Aldrich, 99.995%), and the clay montmorillonite (Nanomer[®] 1.44P, Sigma-Aldrich) with a basal distance between 24 and 26 Å. To prepare the NF samples, a standard dissolution method [60] was followed (see Fig. 1).

1. To prepare 50 g sample (salt + NPs)
2. To dissolve the salt in 30 mL distilled water
3. To sonicate for 10 min for a correct dispersion of the NPs inside the salt
4. To dry the samples in an oven at 105 °C until the total water evaporation and recrystallization of the material
5. To grind the sample in an Agatha mortar

NFs can be synthesized by several methods, and all of them share the same objective of avoiding or reducing the agglomeration of NPs for thus, synthesizing a stable and durable NF. The methods reported in the literature use commercial NPs or synthetic ones although in such a case, they also report the description of the synthetic path.

Nanofluids can be prepared by means of two main paths, the one or the two-step method. In the one step method, the production of NPs and their dispersion are done simultaneously. On the contrary, the two-step method uses commercial or previously synthesized NPs. These paths include different methods such as dry mixing, dry milling, dissolution method, or magnetic stirring [61]. Furthermore, the literature suggests that the synthesis method has a strong influence on the NPs dispersion, and consequently, on the final thermophysical properties of the NFs [53,62,3]. While the influence of the synthesis method on the final properties is covered in the literature there is a lack of information about the reproducibility between different synthesized lots following the same methodology.

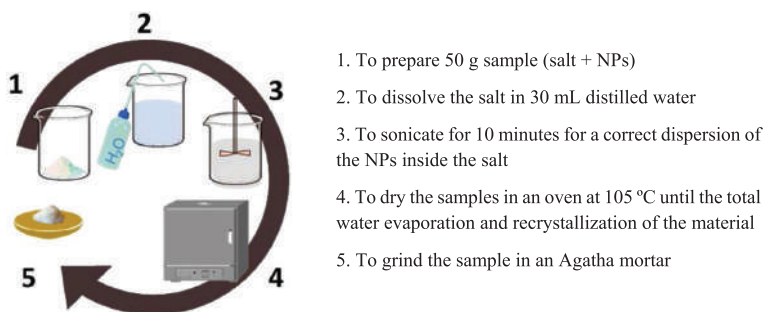


Fig. 1. 1-step nanofluid synthesis scheme.

2.2. Sampling procedure and measurement methodology recommendation

A standard quartering method was applied during the sampling [63]. Since the quantity of sample under study is small (≈ 50 g, see Section 2.1), conventional quartering instruments are not useful. For that reason, an own riffle splitter (Fig. 2) suitable for small samples was designed in Autocad and printed on a Prusa i3, Anycubic 3D printer. Thus, the amount of sample required to be processed was around the amount analysed by the DSC equipment (≈ 10 – 15 mg).

For each type of NF sample, three independent lots of 50 g were synthesized (see section 2.1.), and each lot was quartered in eight batches (sub-samples), obtaining 24 representative samples per NF. In the case of pure NaNO_3 , the 3 lots were subdivided in four batches (12 samples). Therefore, a total amount of 84 samples were obtained. A schematic representation of the sampling procedure followed is depicted in Fig. 3. The thermophysical characterization of each sample was carried out in three steps; (1) thermal cycle from 25 °C to 450 °C for measuring the melting enthalpy and the melting temperature, (2) two consecutive measurement repetitions of C_p at 150 °C, 250 °C, 350 °C and 450 °C, and (3) repetition of the thermal cycle from 25 °C to 450 °C. The full process generated 384 measurements per type of NF and thermophysical property (i.e., 48 measurements for each property). Finally, all the values obtained were statistically analyzed.

2.3. Characterization

2.3.1. Thermophysical characterization

The melting temperature was characterized by three parameters: the onset temperature (T_{on}) when the sample starts the melting process, the peak temperature (T_{peak}) when the sample is half-

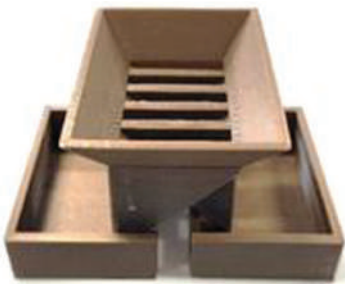


Fig. 2. Mini-riffle splitter system printing in 3D.

melted and the endset temperature (T_{end}) when the sample finishes the melting process. Based on the literature, the reported average melting temperature, T_m , of pure NaNO_3 is 307 °C and the melting enthalpy value, ΔH_m , varies in the range 172–187 J g^{-1} [64]. Nonetheless, the recommended values obtained through differential scanning calorimetry (DSC) are $T_m = 307$ °C and $\Delta H_m = 178$ J g^{-1} [65]. In this work, T_m , ΔH_m and C_p have been analysed by Differential Scanning Calorimetry (DSC 822e from Mettler Toledo). All the measurements were performed at inert atmosphere, under a 50 mL/min N_2 constant flow. T_m and ΔH_m measurements were performed by a dynamic method from 25 °C to 450 °C, using a 0.5 K/min heating rate. The C_p values were measured at 150 °C, 250 °C, 350 °C and 450 °C, and determined through the areas method described by Ferrer et al. [26] which is a method more accurate than both dynamic and step methods. The amount of sample analysed was around 10 mg within a 100 μl pinned aluminium crucible.

Notice that, two consecutive measurements of C_p were run for each sample and that, prior to the measurement each sample was introduced into the oven at 100 °C to avoid humidity in the samples due to the high hygroscopic nature of the species.

In addition, two measurements have been analysed namely first and second runs. This double run method applies because during the first measurement, the samples have undefined contact between the bottom of the crucible and the sample surface.

2.3.2. Chemical characterization

Inductively Coupled Plasma Atomic Emission Spectroscopy (-ICP-AES) analysis was performed with PerkinElmer ELAN 6000. These measurements were performed in order to determine the concentration of NPs in the samples previously analyzed by DSC. The samples were digested in 100 mg aliquots with 1 mL of HNO_3 and 1 mL of HF, and they were kept during 24 h in an oven at 90 °C. Finally, 25 mL deionized H_2O were added. This technique allows to analyze the Si and Al content of SiO_2 , Al_2O_3 and MMT NPs.

2.3.3. Statistics

The statistical analysis of the obtained results was carried out via the independent-sample Student's t -test. This test allows discarding non-repeatable data among the entire population of results. The p -value is the probability that the results from the sample data occurred by chance and it ranges from 0 to 1. Thus, a p -value of 0.01 means there is only a 1% probability that the results from an experiment happened by chance. Low p -values are good, and they indicate that the data did not occur accidentally. In most cases, a p -value of 0.05 is accepted to mean the data is valid. In this study three p -values have been used, $p < 0.05$ (little significant differences), $p < 0.001$ (quite significant differences) and $p < 0.0001$ (highly significant differences).

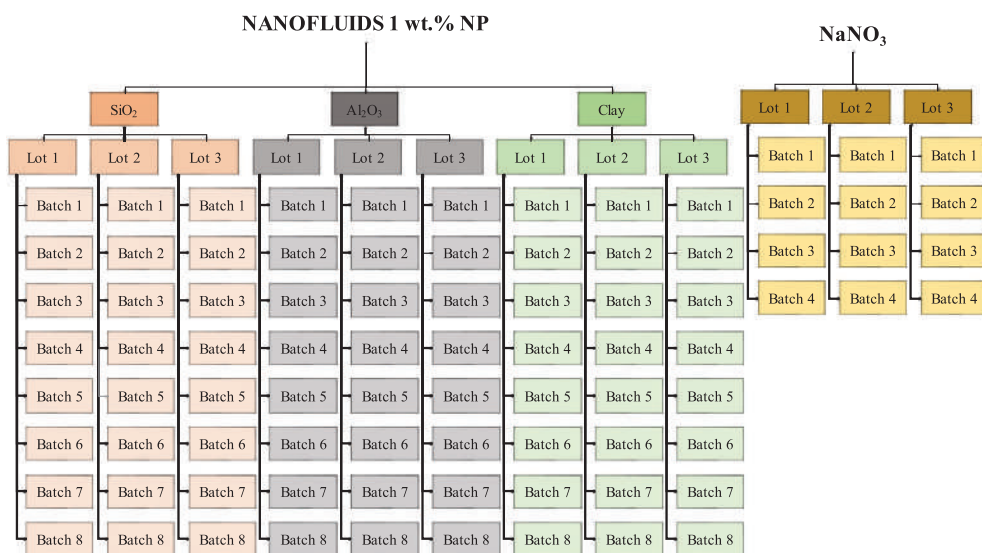


Fig. 3. Schematic representation of the quartering performed for all the samples of the three NFs and also for pure sodium nitrate: NaNO₃-1 wt% SiO₂ NPs (orange), NaNO₃-1 wt% Al₂O₃ NPs (grey), NaNO₃-1 wt% MMT NPs (green) and pure NaNO₃ (yellow).

Additionally, it was taken into account the uncertainty suggested by the DSC manufacturer, Mettler Toledo [66], described in Table 2.

Finally, the total standard deviation was calculated following the equation (1), taking into account the systematic error, equation (2), that considers the four sources of error listed in Table 2, and finally, the random error, equation (3), where σ is the standard deviation, p_c is the confidence level, N is the population size, x_i is the observed value of the sample items, and \bar{x} is the mean value of these observations.

$$\sigma_{\text{total}} = \sqrt{(\sigma_{\text{systematic}})^2 + (\sigma_{\text{random}})^2} \tag{1}$$

$$\begin{aligned} \sigma_{\text{systematic}} &= \sqrt{(0.2)^2 + (0.5)^2 + (1.5)^2 + (3)^2} = \mp 3.4\%(p_c) \\ &= 68\% \end{aligned} \tag{2}$$

$$\sigma_{\text{random}} = \sqrt{\frac{1}{N-1} \hat{A} \cdot \sum_1 (x_i - \bar{x})^2} \tag{3}$$

Table 2
Source and uncertainty of the DSC measurements.

Source	Measurement uncertainty
Mass of the test specimen	± 20 µg (e.g., reproducibility of the balance; if the mass is about 10 mg, this corresponds to ± 0.2%)
Put the sample into the crucible	negligible
Thermal contact with the crucible	± 0.5% (estimate)
Heating rate	negligible negligible, if adjusted under the same conditions
Gas Flow	
Adjustment	± 1.5% (uncertainty of the calibration material)
Integration limits	± 3% (statistics of repeated evaluations)
Baseline type	

3. Results and discussion

The results are presented using box-plot type distributions. Each set of results associated to a property is represented by a box. The box is formed by three horizontal lines; the bottom one that corresponds to the 25% of the results variance (i.e., first quartile, Q1), the upper one to the 75% of the results variance (i.e., third quartile, Q3) and the middle one that corresponds to the median, that is the 50% of the results variance (i.e., second quartile, Q2). Thus, the box itself represents the set of values associated to a variable but excluding the 25% of values furthest away from the median. Vertical lines represent the maximum and minimum values of the variable considering that the maximum value corresponds to 1.5 times the interquartile Q3-Q1 range. The values beyond these vertical lines correspond to atypical or outlier values also included in this study. Finally, the dots and squares inside the boxes represent the mean values [67,68].

3.1. Melting temperature

The values for the melting temperature of NaNO₃ are in good agreement with the values reported in the literature. Fig. 4 shows the box-plot distributions for the melting parameters of the three NFs derived from the DSC: T_{on} (red) that correspond to the intersection point between the baseline before the phase change process starts and the inflectional tangent, T_{peak} (blue) that corresponds to the temperature at the transformation peak, and T_{end} (green) that corresponds to the temperature when the transformation is completed. Moreover, the values for the melting temperature of pure NaNO₃ are also included in Fig. 4 (grey boxes) showing a good agreement with the reported value of $T_m = 306.7 \pm 0.2$ °C [65].

As above-mentioned, for each sample two consecutive measurements (runs) were performed and analysed individually. During the first measurement no significant differences appear regarding the T_{on} of the pure NaNO₃. However, T_{peak} and T_{end} show increments on their values, suggesting a slower melting process.

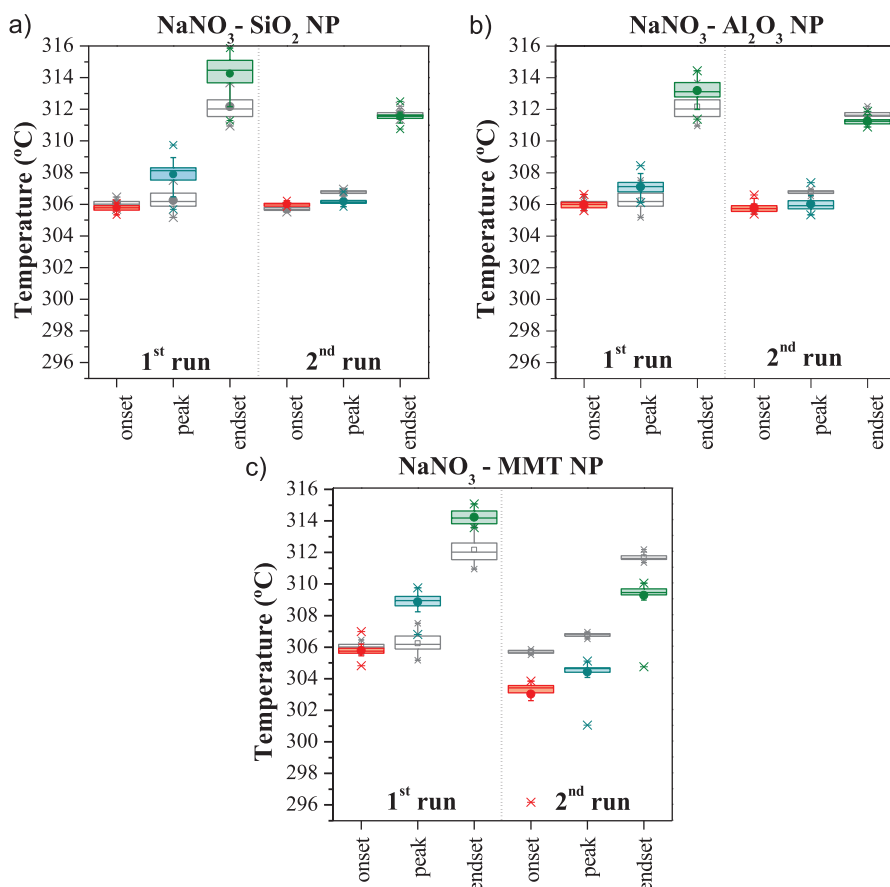


Fig. 4. Box-plot of the melting point values of the NFs over a population of $N = 24$. Onset, endset and peak temperature correspond to orange, green and blue boxes, respectively. The results obtained during the first melting run (left) and at the second melting run (right) are also shown: a) NaNO_3 - 1% wt. SiO_2 NFs, b) NaNO_3 - 1% wt. Al_2O_3 NFs and c) NaNO_3 -1% wt. MMT NFs. Grey boxes stand for pure NaNO_3 with a statistical sampling of $N = 12$.

These differences mainly are due to the effect of the particle size of the NaNO_3 samples. Therefore, to avoid this effect and guarantee the good quality measurement of the thermophysical properties, the first run is absolutely necessary to ensure that the crucible bottom base is completely filled[69]. Indeed, for all the samples (pure NaNO_3 and NFs) the values of the second run were less dispersed and more homogeneous (minor interquartile range, Q1–Q3) than during the first measurement, particularly considering the T_{peak} and the T_{end} .

NaNO_3 based NFs with SiO_2 and Al_2O_3 , Fig. 4-a and Fig. 4-b, respectively, shows a similar T_{on} behaviour than NaNO_3 pure salt with no significant differences ($p > 0.05$) (run 2). On the contrary, the MMT nanofluid shows highly significant differences ($p < 0.0001$) on the T_{on} , Fig. 4-c. Then, only MMT NPs change the NaNO_3 T_{on} (beginning of the melting process).

In general, these trends are not in agreement with already reported data. For example, the results from M. Chieruzzi et al., indicate that T_{on} decreases up to 9.7 °C adding NPs of SiO_2 , Al_2O_3 and $\text{SiO}_2/\text{Al}_2\text{O}_3$ into solar salt [29,70]. Likewise, other studies with the addition of other kind of NPs in molten salts like CuO , TiO_2 or Fe_2O_3 , show a similar T_{on} drop [71,56].

On the other hand, for both Al_2O_3 and MMT NFs (run 2), a slight shift in the T_{peak} was observed, with highly significant differences

($p < 0.0001$) in front of the pure NaNO_3 (i.e., $T_{\text{peak}} < 1$ °C and $T_{\text{peak}} > 2$ °C, respectively). On the contrary, for SiO_2 NFs (Fig. 4-a) there are not significant differences for T_{peak} ($p > 0.05$).

A similar tendency was found in the value of T_{end} ; the addition of NPs decreases the endset temperature (i.e., $T_{\text{end}} < 1$ °C and $T_{\text{end}} < 2$ °C for Al_2O_3 and MMT NFs, respectively). On the contrary, for SiO_2 NFs no significant differences were found ($p > 0.05$). Therefore, with Al_2O_3 and MMT NPs the phase change transformation is completed at lower temperatures. Furthermore, the obtained results show a reduction of the three melting temperatures when adding MMT NPs. This fact agrees with the results obtained by Q. Xie et al. [48] for who the addition of graphene nanoplatelets into solar salts exhibited a reduction of the three temperatures.

It is important to highlight the outlier values in MMT NFs at the second run for the three parameters, (Fig. 4-c) that represent an anomalous data, suggesting a possible measurement error or abnormal behaviour of the sample, as suggested in a previous work[22].

Nonetheless, no important changes were found in the melting performance of the NFs. Notice that the mean values and the standard deviations from Fig. 4 are listed in Table 3.

3.2. Melting enthalpy

The same statistical treatment was performed for the melting enthalpy (ΔH_m) of the three NFs (Fig. 5). As in the case of the melting temperatures, there are differences between the two thermal cycles (runs).

For the first run, the ΔH_m was higher (up to 6%) than in the second run, and this behaviour is observed for all NFs under study as well as for the pure NaNO_3 . In all the cases, during the second run, the mean ΔH_m values decrease up to 7%, nonetheless without statistically significant differences ($p > 0.05$). As in the melting temperature, this is mainly due to grain size effects of the sample [69]. However, only for Al_2O_3 NFs (Fig. 5-b), the ΔH_m decreases with slight significant differences ($p < 0.05$).

Therefore, non-important modification in the latent heat of fusion is obtained with the addition of 1 wt% of NPs into NaNO_3 pure salt. Notice that the outliers for the MMT NFs (Fig. 5-c) correspond to the same outlier samples obtained in the melting temperature measurements (Fig. 4-c). Nevertheless, previous results show different behaviours; thus, M. Lasfargues et al. [72], and Y. Luo et al. [71] determined a decrease in ΔH_m adding 1 wt%. CuO and TiO_2 NPs in molten salts, whereas Y. Li et al. [73], and A. Awad et al. [56] obtained an enhancement of ΔH_m with the incorporation of SiO_2 , Fe_2O_3 , CuO and TiO_2 NPs also in molten salts, in agreement with our results. Otherwise, G. Qiao et al. [74], and P. Myers et al. [75] stated non-significant modifications for the ΔH_m values when SiO_2 or CuO NPs are added into the salt.

Indeed, it is remarkable that all the cited studies, generally, did not use more than three different samples for the measurement of the thermophysical properties. In addition, these previous works sometimes carried out up to five repetition measurements of the same sample and discarded the first run measurement. Based on the previous results we are confident that the methodology described herein reduces the error associated to the ΔH_m determination.

3.3. Specific heat capacity- synthesis method

The C_p analysis among different synthesized lots with identical preparation was performed to analyse the statistical error due to the synthesis procedure. C_p values as a function of temperature are shown in Fig. 6. The C_p results show an increase with temperature, from approximately $0.8 \text{ J g}^{-1} \text{ K}^{-1}$ up to $1.3 \text{ J g}^{-1} \text{ K}^{-1}$. Statistical p-value analysis shows a slight significant difference between the lots of the three formulated NFs.

Thereby, the C_p of the SiO_2 NFs shown in Fig. 6-a, has significant differences ($p < 0.05$) when it is measured at 100°C between lots 1–3 and 2–3. The same is observed between lots 1–3 at 200°C , and lots 1–2 at 350°C ($p < 0.05$). In the case of the Al_2O_3 NFs C_p (Fig. 6-b), there is only a significant difference ($p < 0.05$) between lots 2–3 at 350°C . Finally, in the case of MMT NFs (Fig. 6-c), a slight significant difference between lots 1–3 ($p < 0.05$) is observed.

Table 3

Mean values and standard deviations of the melting parameters; onset, peak, and endset temperatures, for pure NaNO_3 and the three NaNO_3 based nanofluids with 1% wt. of SiO_2 , Al_2O_3 and MMT nanoparticles, during the first and second melting measurements.

System	Cycle	onset ($^\circ\text{C}$)	(\pm)	peak ($^\circ\text{C}$)	(\pm)	endset ($^\circ\text{C}$)	(\pm)
NaNO_3	Run 1	306.0	0.2	306.2	0.8	312.2	0.8
	Run 2	305.7	0.1	306.7	0.2	311.7	0.3
$\text{NaNO}_3\text{-SiO}_2$	Run 1	305.7	0.2	308.1	0.9	314.4	1.2
	Run 2	306.0	0.1	306.1	0.2	311.5	0.3
$\text{NaNO}_3\text{-Al}_2\text{O}_3$	Run 1	305.9	0.3	307.1	0.6	313.0	0.8
	Run 2	305.7	0.3	306.0	0.4	311.2	0.2
$\text{NaNO}_3\text{-MMT}$	Run 1	305.7	0.4	308.8	0.6	314.2	0.5
	Run 2	303.0	1.5	304.5	0.9	309.3	1.0

Therefore, these results highlight that to determine a more precise C_p value, the systematic error associated to the NFs preparation needs to be considered. Accordingly, to determine more precisely the C_p , it is mandatory to average samples from different lots. On the other hand, it is important to highlight that there are differences between lots when these samples are measured at different temperatures, and this fact does not correlate for all the temperature ranked. This effect evidences the presence of uncontrolled physicochemical phenomena that take place at different temperatures.

3.4. Specific heat capacity of NFs

Fig. 7 shows the C_p mean values obtained from all the analysed NF samples. The C_p values as a function of temperature for the three NFs and for the pure NaNO_3 are plotted in Fig. 7-a. The obtained C_p values for the pure NaNO_3 at 100°C , 200°C , 350°C and 450°C are $0.66 \pm 0.07 \text{ J g}^{-1} \text{ K}^{-1}$, $0.85 \pm 0.07 \text{ J g}^{-1} \text{ K}^{-1}$, $1.13 \pm 0.09 \text{ J g}^{-1} \text{ K}^{-1}$ and $1.17 \pm 0.08 \text{ J g}^{-1} \text{ K}^{-1}$, respectively. These values are lower than those reported by T. Bauer et al. [76] which correspond to $1.25 \text{ J g}^{-1} \text{ K}^{-1}$ at 100°C , $1.55 \text{ J g}^{-1} \text{ K}^{-1}$ at 200°C , and around $1.65 \text{ J g}^{-1} \text{ K}^{-1}$ once the samples are at the liquid state.

This deviation of the C_p can be caused both by the presence of impurities in the salt and by the low amount of mass analyzed in the DSC, as demonstrated by B. Muñoz-Sánchez et al. [77]. In solid state ($T < 307^\circ\text{C}$) the three NFs improved their C_p in comparison of the pure NaNO_3 , with significant statistical differences ($p < 0.0001$). Nevertheless, the differences were minor at the liquid state ($T > 307^\circ\text{C}$).

For the case of SiO_2 and MMT NFs no statistical differences were found between the NF and the pure NaNO_3 ($p > 0.05$) at 450°C . Only in the case of adding Al_2O_3 NPs to the salt derives in a C_p enhancement in liquid state with slight significant differences ($p < 0.05$). Additionally, Fig. 7-b depicts the C_p variation in front of the pure NaNO_3 with the temperature. It can be seen that the mean values of the C_p variation of the three NFs decay with increasing the temperature (i.e., up to 34% in the case of MMT NFs, 30% for Al_2O_3 NFs and 27% for SiO_2 NFs, from 100 to 450°C) and they tend to even lower values at 450°C (i.e., -2% for SiO_2 NFs, 3% for MMT NFs and 12% for Al_2O_3 NFs). It is noticeable the high standard deviation for all the values of the three NFs.

Fig. 8 shows the C_p variation in a box-plot graph from 100°C to 450°C . Firstly, it can be observed that the C_p values for each NF show a high variability at 100°C evidenced by the difference between Q1 and Q3 quartiles, more evident in the case of Al_2O_3 (Fig. 8-b) and MMT NFs (Fig. 8-c). Similar trends are observed at higher temperatures with C_p values with positive and negative variations (high dispersion) although the C_p variation decreases with temperature while the NFs are solids ($T < 307^\circ\text{C}$). Once the NFs melted the C_p variation corresponding to the liquid state remains approximately constant ($T > 307^\circ\text{C}$). However, the high dispersion observed in the C_p values agrees with the opposing

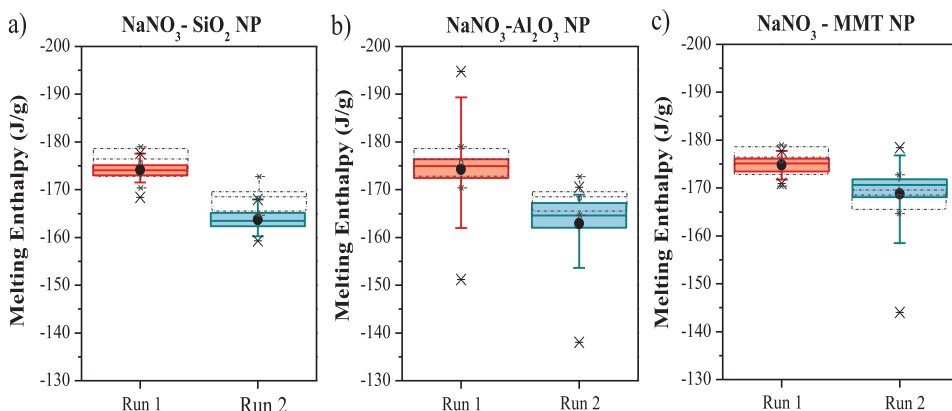


Fig. 5. Box-plot of the melting enthalpy values of the NFs over a population of N = 24. The results obtained during the first melting run (orange) and at the second melting run (blue) are also shown: a) NaNO₃- 1% wt. SiO₂ NFs, b) NaNO₃- 1% wt. Al₂O₃ NFs and c) NaNO₃-1% wt. MMT NFs. Grey dotted lines represent the statistical value of pure NaNO₃ with a statistical sampling of N = 12.

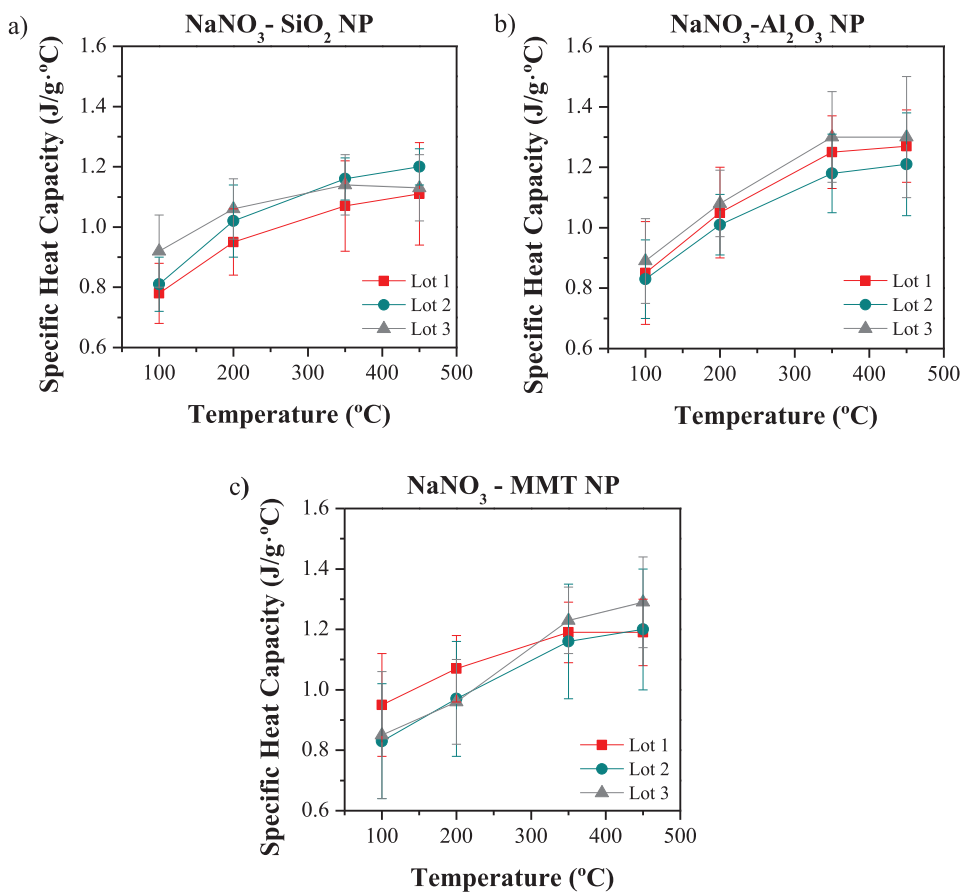


Fig. 6. Specific heat capacity of the NFs at selected temperatures in the range 100 °C to 450 °C for the three independent synthesized lots with a statistical sampling of N = 8 each lot. a) NaNO₃- 1% wt. SiO₂ NFs, b) NaNO₃- 1% wt. Al₂O₃ NFs and c) NaNO₃-1% wt. MMT NFs. Lots 1, 2 and 3 are represented by squares, circles and triangles, respectively.

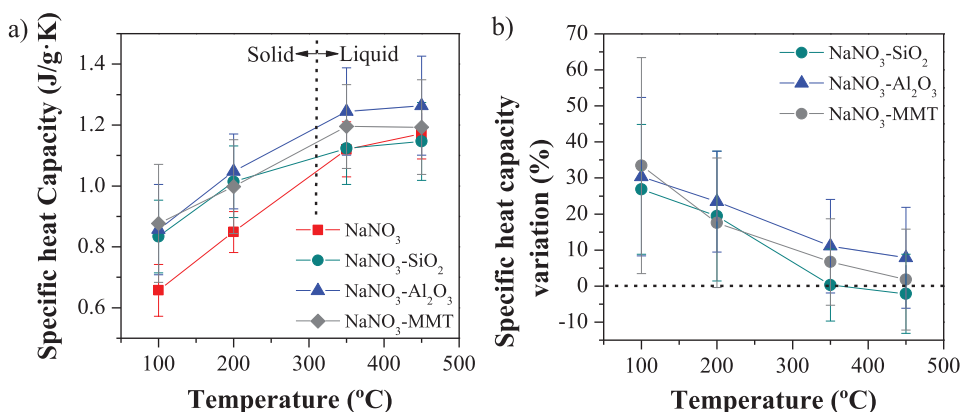


Fig. 7. a) Specific heat capacity mean values and b) specific heat capacity variation of the NFs at selected temperatures in the range 100 °C to 450 °C for a statistical sampling of N = 48 for NaNO₃- 1% wt. SiO₂ NFs (circle), NaNO₃- 1% wt. Al₂O₃ NFs (triangle), NaNO₃-1% wt. MMT NFs (rhomboidal) and pure NaNO₃ (squares) with only N = 24 measurements. Lots 1, 2 and 3 are represented by squares, circles, and triangles, respectively.

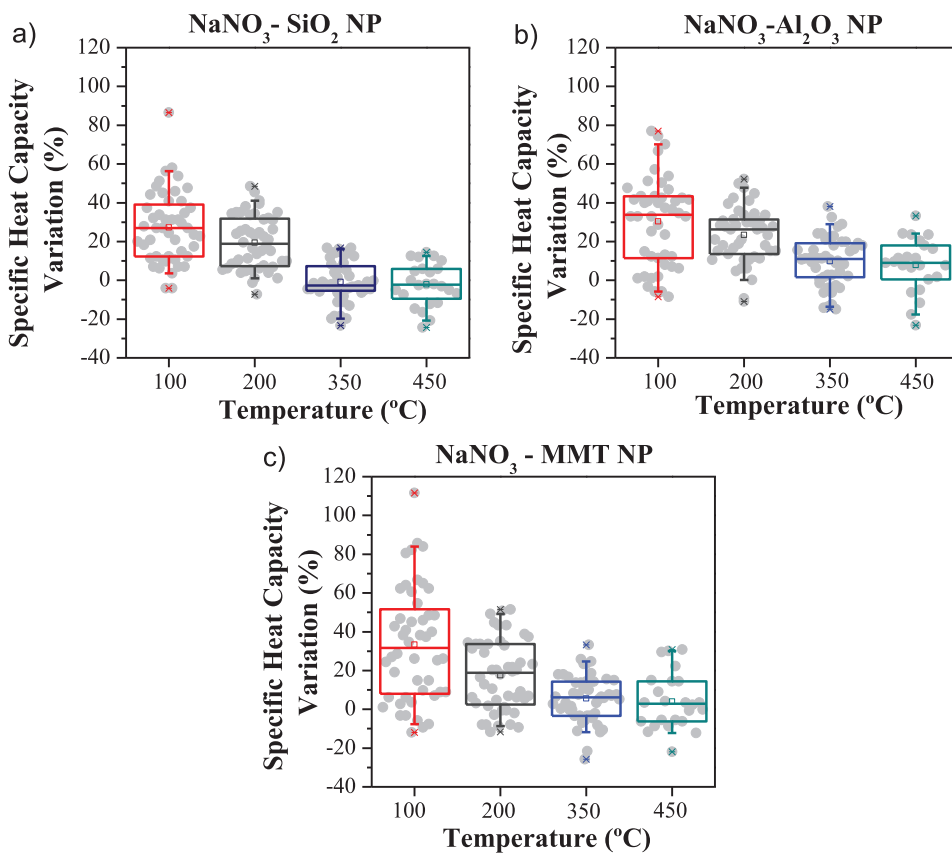


Fig. 8. Box-plot of the specific heat variation of the NFs at selected temperatures in the range 100 °C to 450 °C, over a population of N = 12. a) NaNO₃- 1% wt. SiO₂ NFs, b) NaNO₃- 1% wt. Al₂O₃ NFs and c) NaNO₃-1% wt. MMT NFs. Grey dots represent all the samples analysed per NF and temperature.

results already published [50,52,78–80] that show enhancements and decrements of C_p values for the same NF system.

One possible explanation to the high dispersion observed is the difficulty to obtain a representative NF sample because when a NF

is sampled, the samples under study probably have different concentrations of NP in their compositions.

For that reason, it is mandatory to perform a sample composition characterization in order to monitor the real NP wt% content

Table 4

Nanoparticle concentration obtained by ICP measurements for two samples of three independent synthesized lots of NaNO_3 - 1% wt. SiO_2 NFs, NaNO_3 - 1% wt. Al_2O_3 NFs and NaNO_3 - 1% wt. MMT NFs.

System	Lot 1	Lot 2	Lot 3
	% wt.		
NaNO_3 - SiO_2	0.71	0.75	0.66
	0.68	0.64	0.66
NaNO_3 - Al_2O_3	0.86	0.87	0.83
	0.77	1.04	0.89
NaNO_3 -MMT	0.45	0.45	0.48
	0.48	0.55	0.48

of each sample to ensure the proper sampling procedure along with the reproducibility.

Table 4 shows two repetitions of the ICP-AES measurements for each NF lot. In general, the concentration obtained is lower than the expected (1 wt%). Only one sample, Al_2O_3 NF lot 2, has 1 wt% NPs concentration. This fact indicates a low NP dispersion within the salt and/or NP agglomeration, or the loss of NPs during the NF synthesis procedure.

Consequently, a complementary characterization using ICP-AES is required to better describe the properties of NFs, and to be able to compare results under the same conditions.

On the other hand, there are not specific correlations between the slight differences of the NPs concentration and the C_p variation. The obtained results for each sub-sample from the synthesized lots, suggest that an additional phenomenon occurs in the thermal properties (i.e., thermal interfaces or layering phenomenon [5,22,81]). Therefore, based on these results, to determine the main C_p variation, the conventional DSC methodology may not be the most accurate method to understand the NFs performance. For this reason, more experiments are necessary to understand the mechanisms occurring in the NFs and their precise characterization.

4. Conclusions

A sampling study of ionic nanofluids with a wide sampling collection (84 samples) was performed. The nanofluids were based on NaNO_3 salt as a base fluid with three kinds of nanoparticles: SiO_2 , Al_2O_3 and montmorillonite (MMT) at 1% weight. The methodology used has allowed to measure enthalpy, melting temperature and C_p values and to obtain a reliable data collection.

The specific heat capacity decreases with temperature and is the property most influenced by the presence of nanoparticles, with variations between 80% and -20%. Furthermore, the nature of the nanoparticles showed an impact on the melting temperature behaviour with a slight decrease of the melting temperature in Al_2O_3 and MMT NPs. Despite of this, in the case of melting enthalpy, no significant differences were found by the addition of nanoparticles.

This study demonstrates the relevance of sampling for the evaluation of nanofluids and summarize some recommendations to present proper thermophysical values. The procedure proposed can be resumed in the following steps; (1) to obtain at least 2 independently synthesized samples, (2) from each independent sample, to obtain at least 3 sub-samples, (3) for each sub-sample perform at least 2 measurement repetitions (with the sample previously melted) and finally, (4) to perform statistical data treatment. This methodology is intended to facilitate the comparison between results and to obtain a representative value of the thermophysical properties of nanofluids.

According to this point, the significant differences regarding the C_p values after the sampling process can be explained due to the possible unsuitability of the DSC methodology to be used for mea-

suring thermophysical properties of NFs. This statistical treatment opens the door to explain the high dispersion of the results regarding the C_p in the literature. Nonetheless, further experiments are needed to deeply understand the mechanisms behind nanofluids for their correct characterization.

CRedit authorship contribution statement

A. Svobodova-Sedlackova: Conceptualization, Data curation, Investigation, Methodology, Visualization, Writing – original draft. **C. Barreneche:** Methodology, Writing – review & editing. **P. Gamallo:** Funding acquisition, Supervision, Writing – review & editing. **A. Inés Fernández:** Conceptualization, Funding acquisition, Methodology, Writing – review & editing.

Declaration of Competing Interest

The authors declare that they have no known competing financial interests or personal relationships that could have appeared to influence the work reported in this paper.

Acknowledgments

This work was partially funded by the Spanish Ministry of Science, Innovation and Universities with projects RTI2018-093849-B-C32, RTI2018-094757-B-I00 (MCIU/AEI/FEDER) and MDM-2017-0767. The authors would like to thank also the Catalan Government for the quality accreditation given to their research group (DIOPMA 2017 SGR 0118 and 2017 SGR 13). DIOPMA is certified agent TECNIO in the category of technology developers from the Government of Catalonia. A.S thanks to Generalitat de Catalunya, AGAUR, for her Grant FI-DGR 2018.

References

- [1] S. U. S. Choi, "Enhancing thermal conductivity of fluids with nanoparticles," *Am. Soc. Mech. Eng. Fluids Eng. Div. FED*, vol. 231, no. January 1995, pp. 99–105, 1995.
- [2] M. Awais, A.A. Bhuiyan, S. Salehin, M.M. Ehsan, B. Khan, M.H. Rahman, Synthesis, heat transport mechanisms and thermophysical properties of nanofluids: A critical overview, *Int. J. Thermofluids* 10 (2021) 100086, <https://doi.org/10.1016/j.ijft.2021.100086>.
- [3] S.A. Angayarkanni, J. Philip, Review on thermal properties of nanofluids: Recent developments, *Adv. Colloid Interface Sci.* 225 (2015) 146–176, <https://doi.org/10.1016/j.cis.2015.08.014>.
- [4] A.G.N. Sofiah, M. Samykano, A.K. Pandey, K. Kadirgama, K. Sharma, R. Saidur, Immense impact from small particles: Review on stability and thermophysical properties of nanofluids, *Sustain. Energy Technol. Assessments* 48 (5) (2021), <https://doi.org/10.1016/j.seta.2021.101635> 101635.
- [5] A. Svobodova-Sedlackova, C. Barreneche, G. Alonso, A.I. Fernandez, P. Gamallo, Effect of nanoparticles in molten salts – MD simulations and experimental study, *Renew. Energy* 152 (2020) 208–216, <https://doi.org/10.1016/j.renene.2020.01.046>.
- [6] K. Khanafer, K. Vafai, A review on the applications of nanofluids in solar energy field, *Renew. Energy* 123 (2018) 398–406, <https://doi.org/10.1016/j.renene.2018.01.097>.
- [7] T. Singh, M.A.A. Hussien, T. Al-Ansari, K. Saoud, G. McKay, Critical review of solar thermal resources in GCC and application of nanofluids for development of efficient and cost effective CSP technologies, *Renew. Sustain. Energy Rev.* 91 (February) (2018) 708–719, <https://doi.org/10.1016/j.rser.2018.03.050>.
- [8] A. Alirezaie, M.H. Hajmohammad, A. Alipour, Do nanofluids affect the future of heat transfer? A benchmark study on the efficiency of nanofluids, *Energy* 157 (2018), <https://doi.org/10.1016/j.energy.2018.05.060>.
- [9] A. Alashkar, M. Gadalla, Thermo-economic analysis of an integrated solar power generation system using nanofluids, *Appl. Energy* 191 (2017) 469–491, <https://doi.org/10.1016/j.apenergy.2017.01.084>.
- [10] H.A. Mohammed, H.B. Vuthaluru, S. Liu, Thermohydraulic and thermodynamics performance of hybrid nanofluids based parabolic trough solar collector equipped with wavy promoters, *Renew. Energy* 182 (2022) 401–426, <https://doi.org/10.1016/j.renene.2021.09.096>.
- [11] Z. Said, A.A. Hachicha, S. Aberoumand, B.A.A. Yousef, E.T. Sayed, E. Bellas, Recent advances on nanofluids for low to medium temperature solar collectors: energy, exergy, economic analysis and environmental impact, *Prog. Energy Combust. Sci.* 84 (2021) 100898, <https://doi.org/10.1016/j.pecc.2020.100898>.

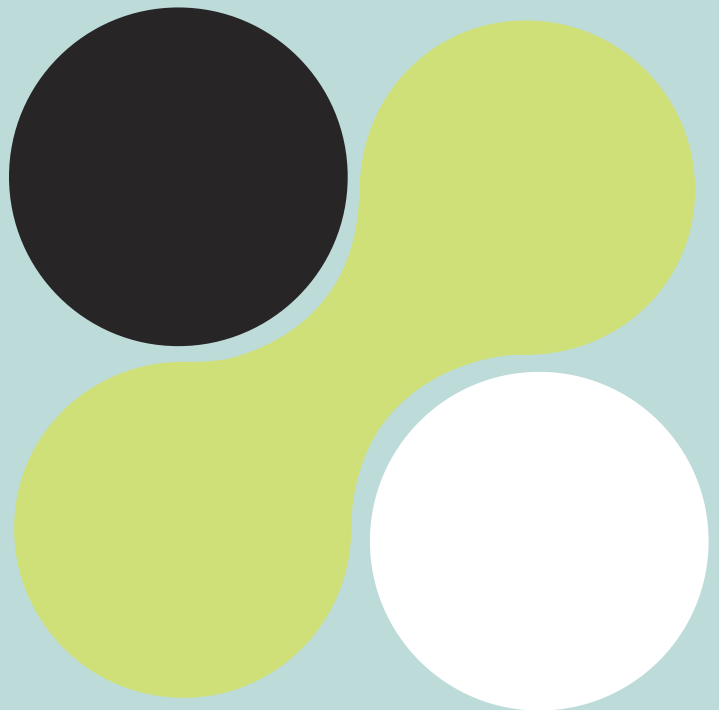
- [12] H.R. Allahyar, F. Hormozi, B. ZareNezhad, Experimental investigation on the thermal performance of a coiled heat exchanger using a new hybrid nanofluid, *Exp. Therm. Fluid Sci.* 76 (2016) 324–329, <https://doi.org/10.1016/j.exptthermfluidsci.2016.03.027>.
- [13] X. Han, S.J. Thrusz, Z. Zhang, G.C. Barber, H. Qu, Tribological characterization of ZnO nanofluids as fastener lubricants, *Wear* 468–469 (Dec 2021) 203592, <https://doi.org/10.1016/j.wear.2020.203592>.
- [14] K.R. Aglawe, R.K. Yadav, S.B. Thool, Preparation, applications and challenges of nanofluids in electronic cooling: A systematic review, *Mater. Today Proc.* 43 (2020) 366–372, <https://doi.org/10.1016/j.matpr.2020.11.679>.
- [15] M.B. Bigdeli, M. Fasano, A. Cardellini, E. Chiavazzo, P. Asinari, A review on the heat and mass transfer phenomena in nanofluid coolants with special focus on automotive applications, *Renew. Sustain. Energy Rev.* 60 (2016) 1615–1633, <https://doi.org/10.1016/j.rser.2016.03.027>.
- [16] V. Delavari, S.H. Hashemabadi, CFD simulation of heat transfer enhancement of Al₂O₃/water and Al₂O₃/ethylene glycol nanofluids in a car radiator, *Appl. Therm. Eng.* 73 (1) (2014) 380–390, <https://doi.org/10.1016/j.applthermaleng.2014.07.061>.
- [17] A. Siricharoenpanich, S. Wiriyasart, P. Naphon, "Study on the thermal dissipation performance of GPU cooling system with nanofluid as coolant", *Case Stud. Therm. Eng.* 25 (April 2021) 100904, <https://doi.org/10.1016/j.csite.2021.100904>.
- [18] V. Ghazanfari, M. Talebi, J. Khorsandi, R. Abdolahi, Thermal-hydraulic modeling of water/Al₂O₃ nanofluid as the coolant in annular fuels for a typical VVER-1000 core, *Prog. Nucl. Energy* 87 (2016) 67–73, <https://doi.org/10.1016/j.pnucene.2015.11.008>.
- [19] M. Jamshidmofid, A. Abbassi, M. Bahiraei, Efficacy of a novel graphene quantum dots nanofluid in a microchannel heat exchanger, *Appl. Therm. Eng.* 189 (September) (2021) 116673, <https://doi.org/10.1016/j.applthermaleng.2021.116673>.
- [20] D.P. Kulkarni, D.K. Das, R.S. Vajiha, Application of nanofluids in heating buildings and reducing pollution, *Appl. Energy* 86 (12) (2009) 2566–2573, <https://doi.org/10.1016/j.apenergy.2009.03.021>.
- [21] Y. Cao, S.M. Seyed Alizadeh, M.T. Fouladvand, A. Khan, A. Taghvaie Nakhjiri, Z. Heidari, R. Pelalak, T.A. Kurniawan, A.B. Albadarin, Mathematical modeling and numerical simulation of CO₂ capture using MDEA-based nanofluids in nanostructure membranes, *Process Saf. Environ. Prot.* 148 (2021) 1377–1385, <https://doi.org/10.1016/j.psep.2021.03.007>.
- [22] A. Svobodova-Sedlackova, A. Calderón, C. Barreneche, P. Gamallo, A.I. Fernández, Understanding the abnormal thermal behavior of nanofluids through infrared thermography and thermo - physical characterization, *Sci. Rep.* 0123456789 (2021) 1–10, <https://doi.org/10.1038/s41598-021-84292-9>.
- [23] M. Jamei, M. Karbasi, I. Adewale, M. Mosharaf-dehkordi, Specific heat capacity of molten salt-based nanofluids in solar thermal applications: A paradigm of two modern ensemble machine learning methods, *J. Mol. Liq.* 335 (2021), <https://doi.org/10.1016/j.molliq.2021.116434> 116434.
- [24] ASTM E1269-11(2018), Standard Test Method for Determining Specific Heat Capacity by Differential Scanning Calorimetry, West Conshohocken, PA, www.astm.org, 2018.
- [25] ASTM International, ASTM E2716, Standard Test Method for Determining Specific Heat Capacity by Sinusoidal Modulated Temperature Differential Scanning Calorimetry, PA, www.astm.org, West Conshohocken, 2014.
- [26] G. Ferrer, C. Barreneche, A. Solé, I. Martorell, L.F. Cabeza, New proposed methodology for specific heat capacity determination of materials for thermal energy storage (TES) by DSC, *J. Energy Storage* 11 (2017) 1–6, <https://doi.org/10.1016/j.est.2017.02.002>.
- [27] B. Dudda, D. Shin, Effect of nanoparticle dispersion on specific heat capacity of a binary nitrate salt eutectic for concentrated solar power applications, *Int. J. Therm. Sci.* 69 (2013) 37–42, <https://doi.org/10.1016/j.ijthermalsci.2013.02.003>.
- [28] H.Y. Ryu, Large enhancement of light extraction efficiency in AlGaIn-based nanorod ultraviolet light-emitting diode structures, *Nanoscale Res. Lett.* 9 (1) (2014) 1–7, <https://doi.org/10.1186/1556-276X-9-58>.
- [29] M. Chieruzzi, G.F. Cerritelli, A. Miliozzi, J.M. Kenny, L. Torre, Heat capacity of nanofluids for solar energy storage produced by dispersing oxide nanoparticles in nitrate salt mixture directly at high temperature, *Sol. Energy Mater. Sol. Cells* 167 (Dec 2017) 60–69, <https://doi.org/10.1016/j.solmat.2017.04.011>.
- [30] H. Tian et al., Enhanced specific heat capacity of binary chloride salt by dissolving magnesium for higher-temperature thermal energy storage and transfer, *J. Mater. Chem. A* 5 (28) (2017) 14811–14818, <https://doi.org/10.1039/c7ta04169a>.
- [31] D. Shin, D. Banerjee, Enhancement of specific heat capacity of high-temperature silica-nanofluids synthesized in alkali chloride salt eutectics for solar thermal-energy storage applications, *Int. J. Heat Mass Transf.* 54 (5–6) (2011) 1064–1070, <https://doi.org/10.1016/j.ijheatmasstransfer.2010.11.017>.
- [32] L.-d. Zhang, X. Chen, Y.-t. Wu, Y.-w. Lu, C.-f. Ma, Effect of nanoparticle dispersion on enhancing the specific heat capacity of quaternary nitrate for solar thermal energy storage application, *Sol. Energy Mater. Sol. Cells* 157 (2016) 808–813, <https://doi.org/10.1016/j.solmat.2016.07.046>.
- [33] M.X. Ho, C. Pan, Optimal concentration of alumina nanoparticles in molten hitec salt to maximize its specific heat capacity, *Int. J. Heat Mass Transf.* 70 (2014) 174–184, <https://doi.org/10.1016/j.ijheatmasstransfer.2013.10.078>.
- [34] C. Selvam, D. Mohan Lal, S. Harish, Thermal conductivity and specific heat capacity of water-ethylene glycol mixture-based nanofluids with graphene nanoplatelets, *J. Therm. Anal. Calorim.* 129 (2) (2017) 947–955, <https://doi.org/10.1007/s10973-017-6276-6>.
- [35] C.J. Ho, J.B. Huang, P.S. Tsai, Y.M. Yang, Water-based suspensions of Al₂O₃ nanoparticles and MEPCM particles on convection effectiveness in a circular tube, *Int. J. Therm. Sci.* 50 (5) (2011) 736–748, <https://doi.org/10.1016/j.ijthermalsci.2010.11.015>.
- [36] J. Choi, Y. Zhang, Numerical simulation of laminar forced convection heat transfer of Al₂O₃-water nanofluid in a pipe with return bend, *Int. J. Therm. Sci.* 55 (2012) 90–102, <https://doi.org/10.1016/j.ijthermalsci.2011.12.017>.
- [37] V. Leela Vinodhan, K.S. Sughanthi, K.S. Rajan, Convective heat transfer performance of CuO-water nanofluids in U-shaped minitube: Potential for improved energy recovery, *Energy Convers. Manag.* 118 (2016) 415–425, <https://doi.org/10.1016/j.enconman.2016.04.017>.
- [38] S. Akilu, A.T. Baheta, A.A. Minea, K.V. Sharma, Rheology and thermal conductivity of non-porous silica (SiO₂) in viscous glycerol and ethylene glycol based nanofluids, *Int. Commun. Heat Mass Transf.* 88 (Oct 2017) 245–253, <https://doi.org/10.1016/j.icheatmasstransfer.2017.08.001>.
- [39] S.M.S. Murshed, Simultaneous measurement of thermal conductivity, thermal diffusivity, and specific heat of nanofluids, *Heat Transf. Eng.* 33 (8) (2012) 722–731, <https://doi.org/10.1080/01457632.2011.635986>.
- [40] S.M.S. Murshed, Determination of effective specific heat of nanofluids, *J. Exp. Nanosci.* 6 (5) (2011) 539–546, <https://doi.org/10.1080/17458080.2010.498838>.
- [41] A.K. Starace, J.C. Gomez, J. Wang, S. Pradhan, G.C. Glatzmaier, Nanofluid heat capacities, *J. Appl. Phys.* 110 (12) (2011) 124323, <https://doi.org/10.1063/1.3672685>.
- [42] J.P. Vallejo, L. Ansia, J. Fal, J. Traciak, L. Lugo, Thermophysical, rheological and electrical properties of mono and hybrid TiB₂ / B₄C nano fluids based on a propylene glycol : water mixture, *Powder Technol.* 395 (2022) 391–399, <https://doi.org/10.1016/j.powtec.2021.09.074>.
- [43] M. Ghazvini, M.A. Akhavan-Behabadi, E. Rasouli, M. Raisee, Heat transfer properties of nanodiamond-engine oil nanofluid in laminar flow, *Heat Transf. Eng.* 33 (6) (2012) 525–532, <https://doi.org/10.1080/01457632.2012.624858>.
- [44] M. Saeedinia, M.A. Akhavan-Behabadi, P. Razi, Thermal and rheological characteristics of CuO-Base oil nanofluid flow inside a circular tube, *Int. Commun. Heat Mass Transf.* 39 (1) (2012) 152–159, <https://doi.org/10.1016/j.icheatmasstransfer.2011.08.001>.
- [45] M. Fakoor Pakdaman, M.A. Akhavan-Behabadi, P. Razi, An experimental investigation on thermo-physical properties and overall performance of MWCNT/heat transfer oil nanofluid flow inside vertical helically coiled tubes, *Exp. Therm. Fluid Sci.* 40 (2012) 103–111, <https://doi.org/10.1016/j.exptthermfluidsci.2012.02.005>.
- [46] K. Khanafer, F. Tavakkoli, K. Vafai, A. AlAmiri, A critical investigation of the anomalous behavior of molten salt-based nanofluids, *Int. Commun. Heat Mass Transf.* 69 (Oct 2015) 51–58, <https://doi.org/10.1016/j.icheatmasstransfer.2015.10.002>.
- [47] M. Chieruzzi, G.F. Cerritelli, A. Miliozzi, J.M. Kenny, Effect of nanoparticles on heat capacity of nanofluids based on molten salts as PCM for thermal energy storage, *Nanoscale Res. Lett.* 8 (1) (2013) 1–9, <https://doi.org/10.1186/1556-276X-8-448>.
- [48] Q. Xie, Q. Zhu, Y. Li, Thermal Storage Properties of Molten Nitrate Salt-Based Nanofluids with Graphene Nanoplatelets, *Nanoscale Res. Lett.* 11 (1) (2016) 306, <https://doi.org/10.1186/s11671-016-1519-1>.
- [49] H. Adun, I. Wole-Osho, E.C. Okonkwo, D. Kavaz, M. Dagbasi, A critical review of specific heat capacity of hybrid nanofluids for thermal energy applications, *J. Mol. Liq.* 340 (2021) 116890, <https://doi.org/10.1016/j.molliq.2021.116890>.
- [50] H. Riaz, S. Mesgari, N.A. Ahmed, R.A. Taylor, The effect of nanoparticle morphology on the specific heat of nanosalts, *Int. J. Heat Mass Transf.* 94 (2016) 254–261, <https://doi.org/10.1016/j.ijheatmasstransfer.2015.11.064>.
- [51] B. Dudda and D. Shin, "Imcece2012-87707 Investigation of Molten Salt Nanomaterial As Thermal Energy Storage in," pp. 1–6, 2012.
- [52] Z. Jiang et al., Novel key parameter for eutectic nitrates based nanofluids selection for concentrating solar power (CSP) system, *Appl. Energy* 235 (July 2019) 529–542, <https://doi.org/10.1016/j.apenergy.2018.10.114>.
- [53] N. Navarrete, L. Hernández, A. Vela, R. Mondragón, Influence of the production method on the thermophysical properties of high temperature molten salt-based nanofluids, *J. Mol. Liq.* 302 (2020) 112570, <https://doi.org/10.1016/j.molliq.2020.112570>.
- [54] U. Nithiyanantham, L. González-Fernández, Y. Grosu, A. Zaki, J.M. Igartua, A. Faik, Shape effect of Al₂O₃ nanoparticles on the thermophysical properties and viscosity of molten salt nanofluids for TES application at CSP plants, *Appl. Therm. Eng.* 169 (2020) 114942, <https://doi.org/10.1016/j.applthermaleng.2020.114942>.
- [55] B. Muñoz-Sánchez, J. Nieto-Maestre, I. Iparaguire-Torres, J.E. Juliá, A. García-Romero, Silica and alumina nano-enhanced molten salts for thermal energy storage: A comparison, *AIP Conf. Proc.* 1850 (June 2017), <https://doi.org/10.1063/1.4984439>.
- [56] A. Awad, H. Navarro, Y. Ding, D. Wen, Thermal-physical properties of nanoparticle-seeded nitrate molten salts, *Renew. Energy* 120 (2018) 275–288, <https://doi.org/10.1016/j.renene.2017.12.026>.
- [57] N. Navarrete, R. Mondragón, D. Wen, M.E. Navarro, Y. Ding, J.E. Juliá, Thermal energy storage of molten salt-based nanofluid containing nano-encapsulated metal alloy phase change materials, *Energy* 167 (2019) 912–920, <https://doi.org/10.1016/j.energy.2018.11.037>.

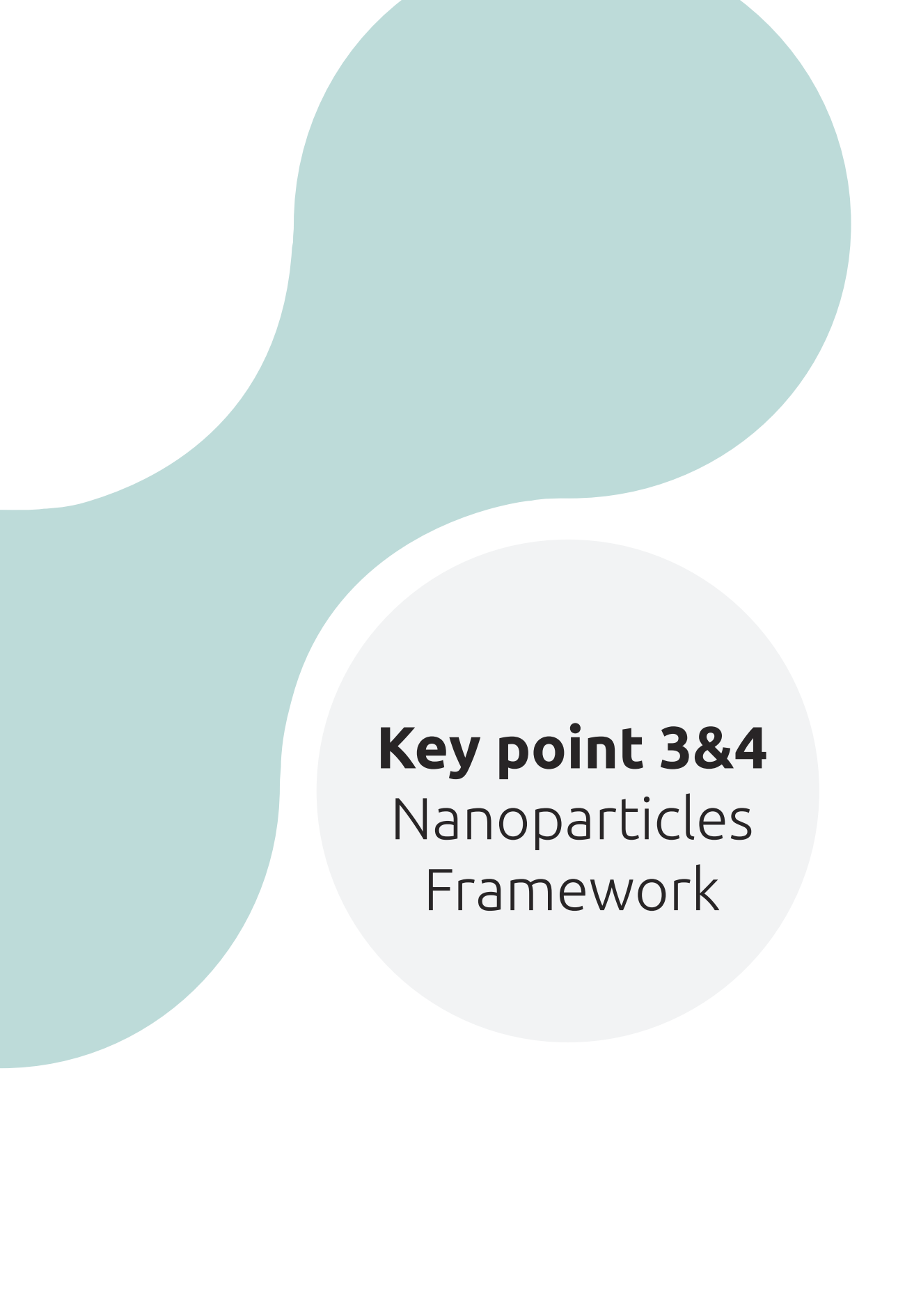
- [58] Y. Luo, G. Ran, N. Chen, C. Wang, Microstructure and morphology of Mo-based Tm₂O₃ composites synthesized by ball milling and sintering, *Adv. Powder Technol.* 28 (2) (2017) 658–664, <https://doi.org/10.1016/j.apt.2016.12.003>.
- [59] N. Navarrete, D. La Zara, A. Goulas, D. Valdesueiro, L. Hernández, J.R. van Ommen, R. Mondragón, Improved thermal energy storage of nanoencapsulated phase change materials by atomic layer deposition, *Solar Energy Materials and Solar Cells* 206 (2020) 110322, <https://doi.org/10.1016/j.solmat.2019.110322>.
- [60] N.A. Che Sidik, M. Mahmud Jamil, W.M.A. Aziz Japar, I. Muhammad Adamu, A review on preparation methods, stability and applications of hybrid nanofluids, *Renew. Sustain. Energy Rev.* 80 (May 2017) 1112–1122, <https://doi.org/10.1016/j.rser.2017.05.221>.
- [61] A.H. Pordanjani, S. Aghakhani, M. Afrand, M. Sharifpur, J.P. Meyer, H. Xu, H.M. Ali, N. Karimi, G. Cheraghian, Nanofluids: Physical phenomena, applications in thermal systems and the environment effects- a critical review, *J. Clean. Prod.* 320 (2021) 128573, <https://doi.org/10.1016/j.jclepro.2021.128573>.
- [62] N. Sezer, M.A. Atieh, M. Koc, A comprehensive review on synthesis, stability, thermophysical properties, and characterization of nanofluids, *Powder Technol.* 344 (2018) 404–431, <https://doi.org/10.1016/j.powtec.2018.12.016>.
- [63] "Standard Practice for Reducing Samples of Aggregate to Testing Size 1," *Astm C 702 - 9*, vol. 04, no. Reapproved, pp. 700–703, 2003.
- [64] D.R. Tobergte, S. Curtis, SODIUM NITRATE FOR HIGH TEMPERATURE LATENT HEAT STORAGE, *J. Chem. Inf. Model.* 53 (9) (2013) 1689–1699, <https://doi.org/10.1017/CBO9781107415324.004>.
- [65] R. Sabbah, A. Xu-Wu, J.S. Chickos, M.L.P. Leitão, M.V. Roux, L.A. Torres, Reference materials for calorimetry and differential thermal analysis, *Thermochim. Acta* 331 (2) (1999) 93–204, [https://doi.org/10.1016/s0040-6031\(99\)00009-x](https://doi.org/10.1016/s0040-6031(99)00009-x).
- [66] M. Zappa and M. Schubnell, "Measurement Uncertainty in Thermal Analysis," *METTLER TOLEDO Therm. Anal. Newsl.* 3/2020 Meas., 2020.
- [67] T. Hastie, R. Tibshirani, J. Friedman, *The Elements of Statistical Learning, Inference, and Prediction, Second Edi.* Springer, Data mining, 2009.
- [68] S. Lem, P. Onghena, L. Verschaffel, W. Van Dooren, The heuristic interpretation of box plots, *Learn. Instr.* 26 (2013) 22–35, <https://doi.org/10.1016/j.learninstruc.2013.01.001>.
- [69] M. Abd-Elghany, T.M. Klapötke, A review on differential scanning calorimetry technique and its importance in the field of energetic materials, *Phys. Sci. Rev.* 3 (4) (2018) 1–14, <https://doi.org/10.1515/psr-2017-0103>.
- [70] M. Chieruzzi, A. Miliozzi, T. Crescenzi, L. Torre, J.M. Kenny, A New Phase Change Material Based on Potassium Nitrate with Silica and Alumina Nanoparticles for Thermal Energy Storage, *Nanoscale Res Lett* 10 (1) (2015) 984, <https://doi.org/10.1186/s11671-015-0984-2>.
- [71] Y. Luo, X. Du, A. Awad, D. Wen, Thermal energy storage enhancement of a binary molten salt via in-situ produced nanoparticles, *Int. J. Heat Mass Transf.* 104 (2017) 658–664, <https://doi.org/10.1016/j.jheatmasstransfer.2016.09.004>.
- [72] M. Lasfargues, Q. Geng, H. Cao, Y. Ding, Mechanical dispersion of nanoparticles and its effect on the specific heat capacity of impure binary nitrate salt mixtures, *Nanomaterials* 5 (3) (2015) 1136–1146, <https://doi.org/10.3390/nano5031136>.
- [73] Y. Li, X. Chen, Y. Wu, Y. Lu, R. Zhi, X. Wang, C. Ma, Experimental study on the effect of SiO₂ nanoparticle dispersion on the thermophysical properties of binary nitrate molten salt, *Sol. Energy* 183 (2019) 776–781, <https://doi.org/10.1016/j.solener.2019.03.036>.
- [74] G. Qiao, M. Lasfargues, A. Alexiadis, Y. Ding, Simulation and experimental study of the specific heat capacity of molten salt based nanofluids, *Appl. Therm. Eng.* 111 (2017) 1517–1522, <https://doi.org/10.1016/j.applthermaleng.2016.07.159>.
- [75] P.D. Myers, T.E. Alam, R. Kamal, D.Y. Goswami, E. Stefanakos, Nitrate salts doped with CuO nanoparticles for thermal energy storage with improved heat transfer, *Appl. Energy* 165 (2016) 225–233, <https://doi.org/10.1016/j.apenergy.2015.11.045>.
- [76] T. Bauer, D. Laing, R. Tamme, Characterization of sodium nitrate as phase change material, *Int. J. Thermophys.* 33 (1) (2012) 91–104, <https://doi.org/10.1007/s10765-011-1113-9>.
- [77] B. Muñoz-Sánchez, J. Nieto-Maestre, G. Imbuluzqueta, I. Marañón, I. Iparraquirre-Torres, A. García-Romero, A precise method to measure the specific heat of solar salt-based nanofluids, *J. Therm. Anal. Calorim.* 129 (2) (2017) 905–914, <https://doi.org/10.1007/s10973-017-6272-x>.
- [78] I.M. Shahrul, I.M. Mahbulul, S.S. Khaleduzzaman, R. Saidur, M.F.M. Sabri, A comparative review on the specific heat of nanofluids for energy perspective, *Renew. Sustain. Energy Rev.* 38 (2014) 88–98, <https://doi.org/10.1016/j.rser.2014.05.081>.
- [79] X. Chen, Y.-t. Wu, L.-d. Zhang, X. Wang, C.-f. Ma, Experimental study on thermophysical properties of molten salt nanofluids prepared by high-temperature melting, *Sol. Energy Mater. Sol. Cells* 191 (2019) 209–217, <https://doi.org/10.1016/j.solmat.2018.11.003>.
- [80] M. Lasfargues, G. Stead, M. Amjad, Y. Ding, D. Wen, In situ production of copper oxide nanoparticles in a binary molten salt for concentrated solar power plant applications, *Mat. (Basel)* 10 (5) (2017) 1–10, <https://doi.org/10.3390/ma10050537>.
- [81] E. Leonardi, A. Floris, S. Bose, B. D'Aguzzano, Unified Description of the Specific Heat of Ionic Bulk Materials Containing Nanoparticles, *ACS Nano* 15 (1) (2021) 563–574, <https://doi.org/10.1021/acsnano.0c05892>.

08

Computational
approach to nitrate
salt-based nanofluids

Paper 4





Key point 3&4
Nanoparticles
Framework

8. Computational approach to nitrate salt-based nanofluids

MD Simulations and experimental study

8.1 Introduction

In the previous chapters, after analysing the data reported in the literature and the exhaustive sampling, it has been highlighted that some more complex processes/mechanisms govern the behaviour of nanofluids and, therefore, influence the observed properties.

In addition, trends regarding the effect of nanoparticles concentration and size and an evident influence between the fluid-particle interactions could be seen. Systems based on salts with metal oxide nanoparticles seem to have the most significant potential to reach high heat capacity values.

Therefore, thanks to the previous chapters, it has been possible to focus the investigation of nanofluids and to have a general idea of the effect of nanoparticles on thermophysical properties. Moreover, it has helped to identify the two key points that will be treated in this chapter. The two main issues that will be addressed are: (1) to determine clear trends in the effect of nanoparticles on the heat capacity of MSBNFs and (2) to study the mechanisms that modify the heat capacity of MSBNFs.

Simulation tools are helpful for this purpose. Therefore, this chapter has been approached through molecular dynamics (MD) simulations and experimental validation.

MD is a computer simulation technique in which atoms and molecules are allowed to interact over a period (trajectory). Therefore, MD is a computational tool to understand how things work on a detailed molecular level, ranging from electronic structures to the long-term phase behaviour of molecules. Molecules interact following Newton's laws of classical mechanics under the action of a force field (FF), which can consider intermolecular and intramolecular interactions. The system's trajectory is obtained by numerical integration using one of the available algorithms (verlet, frog jump, etc.).

This method allows us to get information of the system that would be analytically impossible or very complex to obtain, given the high number of atoms and interactions of which a system is composed.

The three main mechanisms proposed in the literature to explain capacity variation are discussed through MD simulations. In addition, this chapter offers trends on the effect of the concentration and size of nanoparticles validated both computationally and experimentally, giving reliability to the theoretical results.

8.1.1 Relevance

The relevance of this chapter lies in identifying the main mechanism involved in the modification of the heat capacity of MSBNFs through MD simulations, analyzing each of the mechanisms proposed in the literature.

In addition, not only the weight falls on the computational results, but the development of this chapter goes hand in hand with experimental results. Combining the two techniques allows us to validate the simulations and develop a theoretical framework with more robust results due to the high deviation of experimental results. Finally, this methodology also allows us to identify limitations and future challenges.

8.1.2 Objectives

The main objectives are:

- Study the mechanisms proposed in the literature through MD simulations.
- Compare thermophysical properties (i.e., heat capacity, melting temperature and density) of NSBNFs obtained by MD and experimentally.
- Identifies the main variables that modify the C_p of NSBNFs.
- And finally, outline a theoretical framework that allows advancing the research (**Key point 3 & 4**).

8.2 Paper 4

The complete study is published in the journal of Renewable Energy, entitled "Effect of nanoparticles in molten-salts- MD simulations and experimental study". The article is available online since the 17th of January 2020, and it was published on volume 152, as shown in **Figure 8.1**.

Besides, a related was presented at the: (1) "Iberian Meeting on Materials Science (CNMAT 2018) Congreso

Nacional de Materiales "(Salamanca, Spain, 2018). (2) Eurotherm Seminar n. 112: Advances in Thermal Energy Storage. (3) at the 1st International Conference on Nanofluids (ICNF) and the 2nd European Symposium on Nanofluids (ESNF) (castellón de la Plana, 2019). Finally, (4) at the CNIT 11 - Congreso Nacional e internacional de Termodinámica (Albacete, Spain, 2019), see **Appendix 3**.

Additionally, The MD codes it can be found in **Appendix 2**.

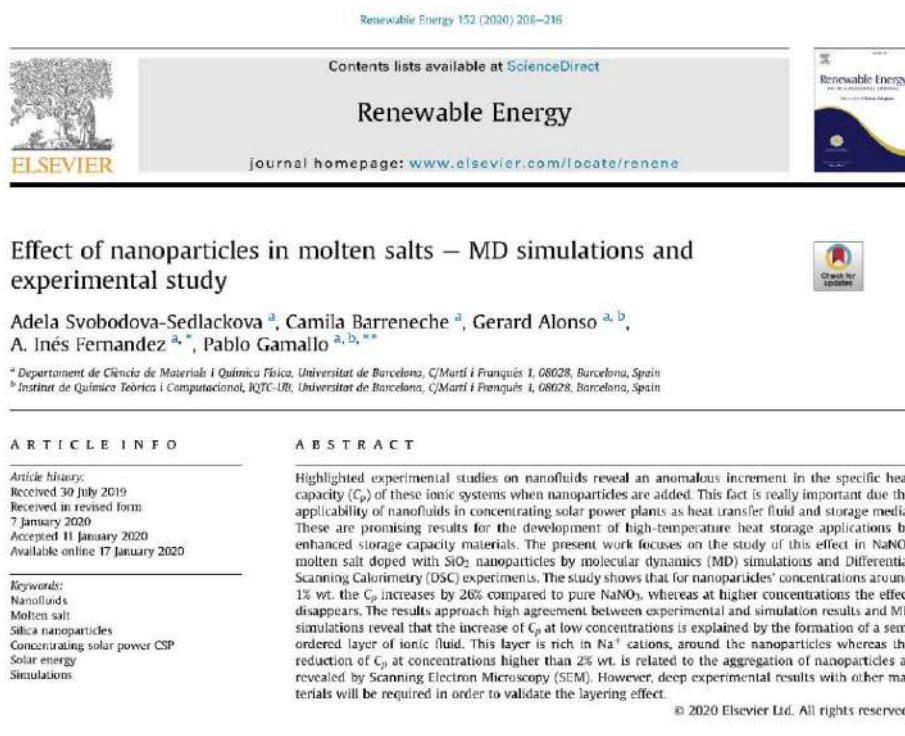


Figure 8.1. Article published in the Renewable Energy journal in 2020, entitled "Effect of nanoparticles in molten salts- MD simulations and experimental study" [1].

8.2.1 Graphical Abstract

Figure 8.2 summarizes the most relevant results.

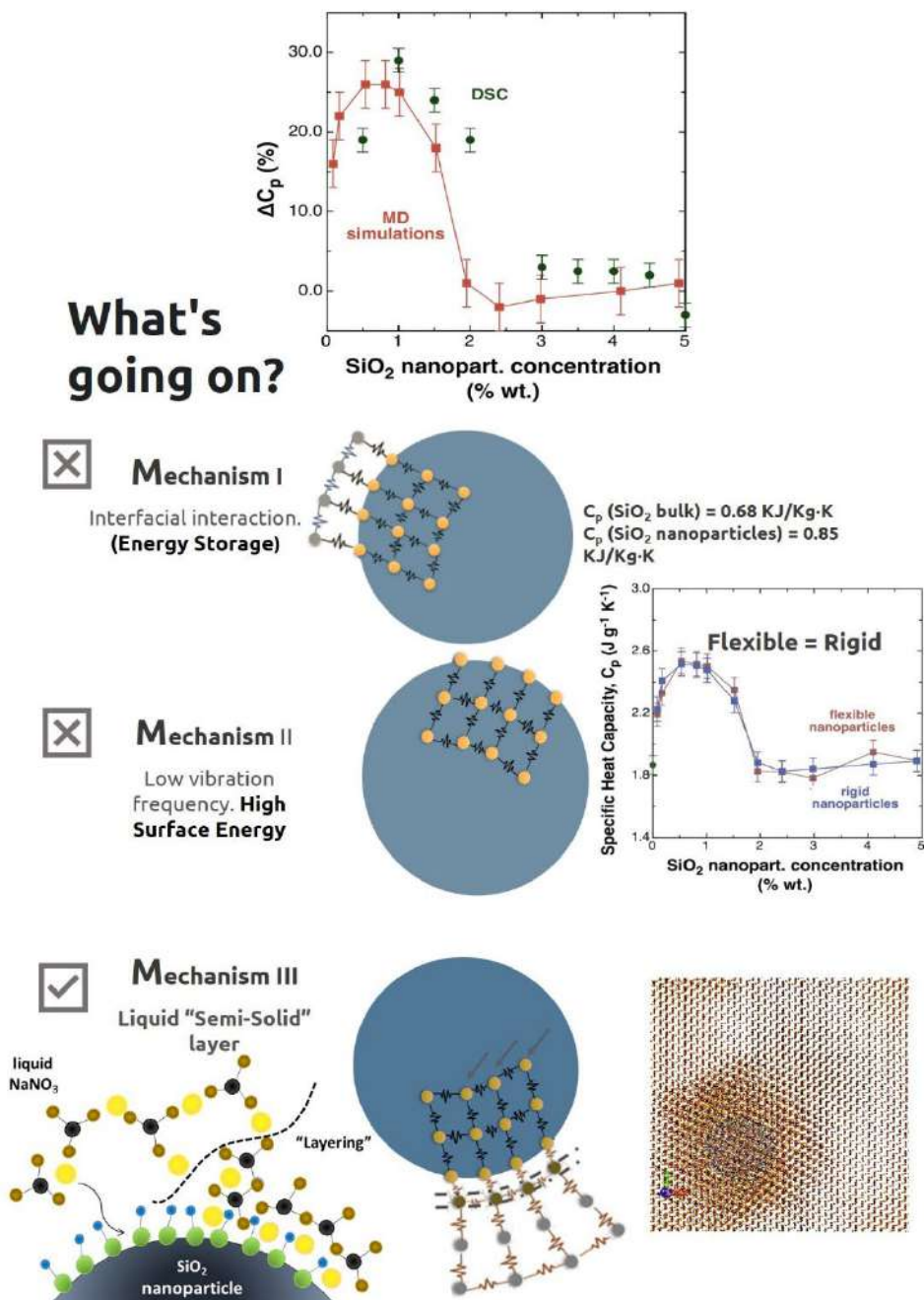


Figure 8.2. Graphical abstract of the article entitled "Effect of nanoparticles in molten salts- MD simulations and experimental study" [1].

8.2.2 Contribution to the state of the art

Key point 3
Nanoparticles

No clear tendencies about nanoparticles' effect. Literature suggests:

Maximum specific heat capacity enhancement around **1 wt. %** of nanoparticle concentration. Effect of nanoparticles **size, concentration, temperature.**

- ✓ MD simulations and experimental studies corroborate a nanoparticles' concentration dependency: a maximum of around 1 wt% was found with different nanoparticles sizes; 1nm (computational), 3 nm (computational), and 15-20 nm (experimental).
- ✓ Higher concentrations than [0.5-2] wt% nanoparticles tend to agglomerate and vanish specific heat capacity variation due to the lower specific surface area, **Figure 8.3**

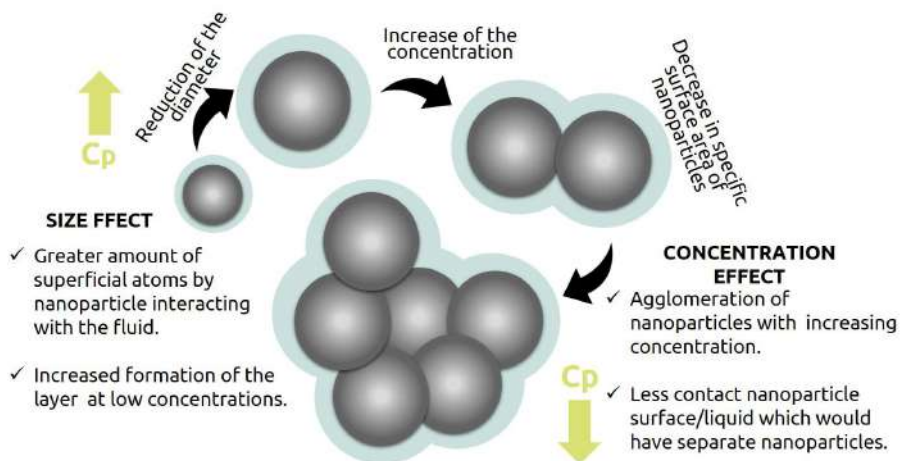


Figure 8.3. Scheme of the effect of nanoparticle concentrations and size on nanofluids specific heat capacity [1].

Key point 4 Framework

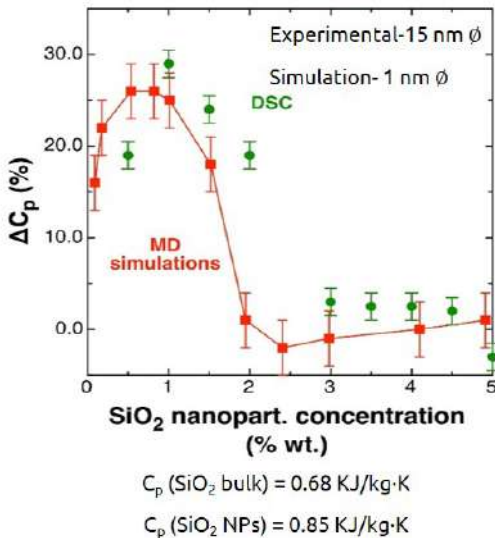
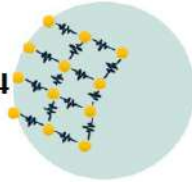
Lack of a robust theoretical framework to explain the abnormal thermal behaviour of nanofluids (focused on specific heat capacity).

Main proposed mechanism: Formation of a semi-solid layer and nanostructures in log-range terms with high specific surface areas.

There are no clear experimental demonstrations of the formation of nanostructured semi-solid layer and their properties.

- ✓ This study examines through MD simulations the three main proposed mechanism to explain the specific heat capacity enhancement:

Mechanism I



Mechanism I. The obtained C_p through MD simulations with nanoparticles of 1 nm, 3 nm and experimentally with NPs of 15 nm shows low differences between them, **Figure 8.4**. On the contrary, C_p determination of bulk SiO₂ and nanoparticles through DSC shows an enhancement of 25% with size reduction. Although these differences cannot totally explain the observed C_p modification and its concentration dependency. Therefore, the Mechanism I can not be the unique and main mechanism to explain the C_p enhancement.

Figure 8.4. Specific heat capacity variation as a function of nanoparticles concentration, obtained from MD simulations and DSC.

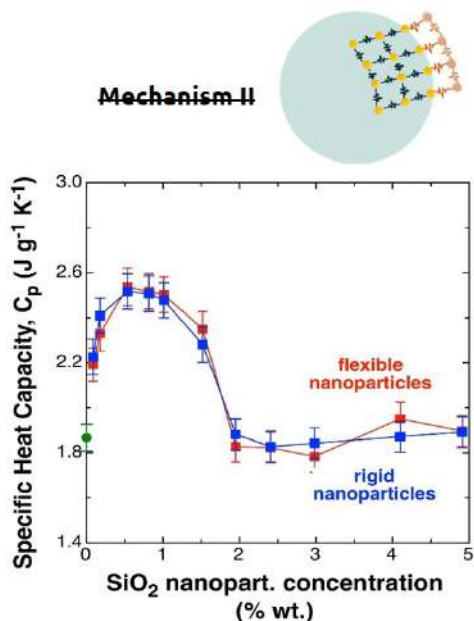


Figure 8.5. Specific heat capacity variation as a function of nanoparticles concentration for flexible and rigid nanoparticles.

Mechanism II. The specific heat capacity through MD simulations has been carried out in two modes with or without freezing the NPs atoms: rigid and flexible bodies, **Figure 8.5**. Both results show similar with low differences in the simulated Cp, indicating that Cp does not depend on the stiffness or flexibility of the nanoparticles. This fact points out that the shape or nature of the nanoparticles inside the fluid is not so relevant. Therefore, Mechanism II, which indicates an interfacial interaction and Mechanism II, which means low vibrational energy, can not explain the Cp enhancement totally.

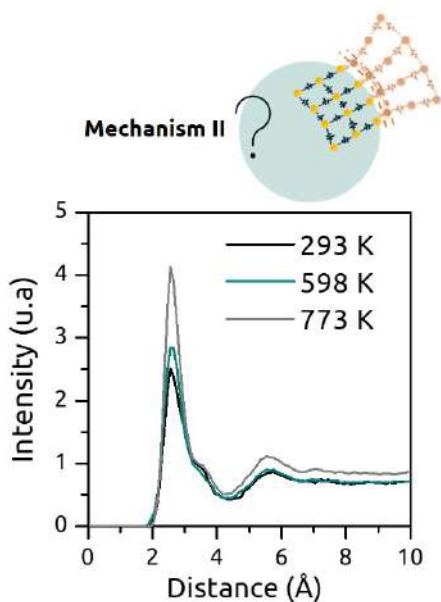


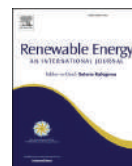
Figure 8.6. Radial pair distribution of Na-O atoms (O from the nanoparticle surface) at 293 K, 598 K, and 773 K.

Mechanism III. MD simulations show the formation of a thin ordered layer around the surface of the nanoparticles at low nanoparticles' concentration, **Figure 8.6**. The layer corresponds to a semi-solid state, and it is rich in Na⁺ cations with a thickness of around 1 Å. This fact confirms the existence of the layering phenomenon of Mechanism III.

- ✓ The results indicate that a single mechanism will not comprehensively explain the nanofluids' behaviour, but it will be a combination of effects. The most relevant result is the formation of the semi-solid layer around the surface of the nanoparticles. This phenomenon sets new challenges to achieve, starting with its experimental demonstration and obtaining its thermophysical properties to justify its effect on heat capacity. In addition, a remarkable fact is the contradictory results of the effect of temperature; the results presented here show an increase in C_p with temperature; however, this is not corroborated in many experimental results. This fact indicates that some puzzle pieces are missing, or another phenomena or interactions are not considered in the simulations (**Key point IV**).

8.2.3 Publication

The article is attached below (DOI: <https://doi.org/10.1016/j.renene.2020.01.046>).



Effect of nanoparticles in molten salts – MD simulations and experimental study

Adela Svobodova-Sedlackova^a, Camila Barreneche^a, Gerard Alonso^{a, b},
A. Inés Fernandez^{a, *}, Pablo Gamallo^{a, b, **}

^a Departament de Ciència de Materials i Química Física, Universitat de Barcelona, C/Martí i Franqués 1, 08028, Barcelona, Spain

^b Institut de Química Teòrica i Computacional, IQTC-UB, Universitat de Barcelona, C/Martí i Franqués 1, 08028, Barcelona, Spain



ARTICLE INFO

Article history:

Received 30 July 2019

Received in revised form

7 January 2020

Accepted 11 January 2020

Available online 17 January 2020

Keywords:

Nanofluids

Molten salt

Silica nanoparticles

Concentrating solar power CSP

Solar energy

Simulations

ABSTRACT

Highlighted experimental studies on nanofluids reveal an anomalous increment in the specific heat capacity (C_p) of these ionic systems when nanoparticles are added. This fact is really important due the applicability of nanofluids in concentrating solar power plants as heat transfer fluid and storage media. These are promising results for the development of high-temperature heat storage applications by enhanced storage capacity materials. The present work focuses on the study of this effect in NaNO_3 molten salt doped with SiO_2 nanoparticles by molecular dynamics (MD) simulations and Differential Scanning Calorimetry (DSC) experiments. The study shows that for nanoparticles' concentrations around 1% wt. the C_p increases by 26% compared to pure NaNO_3 , whereas at higher concentrations the effect disappears. The results approach high agreement between experimental and simulation results and MD simulations reveal that the increase of C_p at low concentrations is explained by the formation of a semi ordered layer of ionic fluid. This layer is rich in Na^+ cations, around the nanoparticles whereas the reduction of C_p at concentrations higher than 2% wt. is related to the aggregation of nanoparticles as revealed by Scanning Electron Microscopy (SEM). However, deep experimental results with other materials will be required in order to validate the layering effect.

© 2020 Elsevier Ltd. All rights reserved.

1. Introduction

Development, research and innovation in energy storage systems are indispensable for an energy transition to low carbon technologies, because they allow the full penetration of renewable energies in our energy system. Solar energy sources play an important role in the energy field, due to the great uncertainty over future energy supplies and to environmental issues. Concentrated solar power (CSP) plants are becoming one of the most massively implemented cost-efficient solar technology. The global world CSP capacity forecast to hit 10–22 GW by 2025. Thereby, all new CSP facilities that come online incorporate Thermal Storage (TES) systems. The main purpose of the thermal storage system is to mitigate renewable energy intermittency, to extend the power production period and to prevent possible black-outs of the CSP plant [1]. TES

used in CSP [2] plants store energy as sensible heat. For this purpose, molten salts are used as thermal energy storage medium or heat transfer fluid (HTF). The eutectic mixture of 60% sodium nitrate and 40% potassium nitrate known as Solar Salt [3], shows better thermal properties and a lower cost than mineral oils used as HTF. However, the main disadvantages are the low specific heat capacity (i.e., $C_p \sim 2 \text{ Jg}^{-1}\text{K}^{-1}$) and corrosion issues that may hinder the storage [4].

TES materials with enhanced thermal properties (e.g., high thermal stability and high C_p) are required to achieve high-energy efficiency in the CSP, since these materials could increase the operating range of the storage facilities, reduce the volume of storage tanks [1,5], and decrease the cost of solar power technology to compete with coal fired power plants in the near future [6]. Recent studies show that molten salts doped with low concentrations of nanoparticles produces a nanofluid with an unconventional C_p increment [7,8]. For these reasons, more investigations in the last years are focused on improving this key parameter and studying these nanofluids [9–15]. Most studied nanofluids showing this behavior are composed by silica, alumina or copper oxide

* Corresponding author.

** Corresponding author. Departament de Ciència de Materials i Química Física, Universitat de Barcelona, C/Martí i Franqués 1, 08028, Barcelona, Spain
E-mail address: ana_inesfernandez@ub.edu (A.I. Fernandez).

nanoparticles [16–21]. However, despite the C_p increment phenomenon observed in all these studies, there are great discrepancies among all of them, not only because of the different experimental conditions reported in the studies but also for the different theoretical models that could explain the effect [22,23]. Nowadays, there are three proposed mechanisms to explain that increment of C_p (Fig. 1). The first mechanism proposes that nanoparticles increase C_p due to the high surface energy per nanoparticle unit mass [24]. In fact, Lan et al. [25] argue through a theoretical model that a decrease of the nanoparticle size increases the C_p being a function of the nanoparticle's nominal diameter. The second mechanism suggests that the particle-liquid interface has an anomalous high resistance [24,26] which acts as a mechanism of thermal energy storage. Finally, the third mechanism considers the formation of a semi-solid structured layer (i.e., nano-layering) around the nanoparticles [27]. Although the C_p value for solids is commonly lower than for liquids, the presence of this semi-solid layer could enhance the C_p value of the nanofluid.

The two former mechanisms increase C_p since they increase the degrees of freedom of the system. However, mechanism three is not yet confirmed. The main scope of this paper is to understand the unconventional C_p increment. If this phenomenon is controlled, the use of nanofluids as HTF and TES media in CSP will mark a turning point in this technology. Therefore, the TES system, for example, will be more compacted and more efficient from an energetic point of view.

Therefore, the present study is focused on the effect in C_p values of the concentration and the size of silica nanoparticles in molten sodium nitrate salt. The computational and experimental results obtained aims to clarify the inconsistency and high variety of results reported in the literature and to find clear trends about the mechanisms that govern the C_p increase in nanofluids.

2. Methodology, systems and validation

2.1. Molecular dynamic simulations

Molecular Dynamics (MD) simulations were carried out with

Large-scale Atomic/Molecular Massively Parallel Simulator (LAMMPS) code [28]. The trajectory of each particle is obtained by integration of Newton's equations of motion with a 1 fs timestep, during 10^5 time steps for equilibration, and 10^5 time steps for production. The equilibration was performed in three consecutive steps: i) a thermal ramp to raise the temperature up to 773 K with the Langevin thermostat [29] (without barostat), ii) a thermal equilibration phase at the desired temperature with the same thermostat and iii) a pressure equilibration phase, with the Berendsen barostat [30] to achieve the pressure of 1 atm keeping the temperature constant. Once the equilibrium was reached, the system was time evolved with the isothermal-isobaric ensemble (NPT) using the Nosé-Hoover thermostat and barostat [31,32] with 0.1 ps and 1 ps of relaxation time, respectively.

Equation (1) describes the energy of the system, U_{pot} , that is calculated as a sum of internal or bonded terms, U_{bonded} , which describe the bonds, angles and rotations in a molecule and a sum of external or non-bonded terms, $U_{non-bonded}$, that account for interactions between non-bonded atoms.

$$U_{pot} = U_{bonded} + U_{non-bonded} \tag{1}$$

Thus, the bonded terms in Equation (2) represents the harmonic potentials shown in Equations (3)–(5),

$$U_{bonded} = U_{bond-stretch} + U_{angle-bending} + U_{improper} \tag{2}$$

$$U_{bond-stretch} = \sum_{i,j}^{1,2pairs} K_b^{ij} (b - b_0)^2 \tag{3}$$

$$U_{angle-bending} = \sum_{angles} K_\theta (\theta - \theta_0)^2 \tag{4}$$

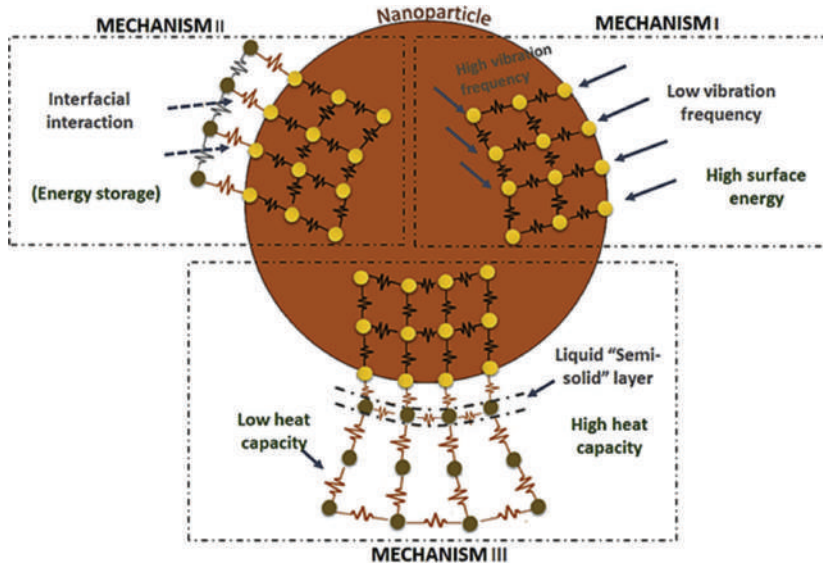


Fig. 1. Three proposed mechanisms as candidates to explain the unconventional C_p increment phenomenon in nanofluids. Adapted from Shin et al. [6].

$$U_{improper} = \sum_{improper} K_{imp}(\psi - \psi_0)^2 \quad (5)$$

where the former is the approximation to the energy of a bond as a function of the displacement from the ideal bond length, b_0 , and the force constant, K_b^{ij} , determines the strength of the bond. Both, ideal bond lengths and force constants are specific for each pair of bound atoms. The same kind of functions are used to describe the bending of an angle around its equilibrium value, θ_0 , and so on.

Equation (6) describes the non-bonded or intermolecular interactions. They were calculated using a Buckingham potential [33], Equation (7), for dispersion forces and a Coulomb potential [34], Equation (8), for electrostatic interactions.

$$U_{non-bonded} = U_{Buckingham} + U_{Coulomb} \quad (6)$$

$$U_{Buckingham} = \sum_i \sum_{j \neq i} A_{ij} e^{-r_{ij}/\rho_{ij}} - \frac{C_{ij}}{r_{ij}^6} \quad r_{ij} < r_c \quad (7)$$

$$U_{Coulomb} = \sum_i \sum_{j \neq i} \frac{q_i q_j}{\epsilon r_{ij}} \quad r_{ij} < r_c \quad (8)$$

where r_{ij} is the intermolecular distance, q_i , is the charge of i -species, r_c the cutoff distance and ρ_{ij} , A_{ij} and C_{ij} , are the force field corresponding parameters. Here, the dielectric function, ϵ , in Equation (8) is set to one since the solvent is treated explicitly in the simulations. The cutoff for both potentials was set to 11 Å and long-range interactions were accounted: i) with analytic tail corrections for the Buckingham potential, and ii) with the Particle-Particle/Particle-Mesh for the Coulomb potential.

The force field parameters to reproduce NaNO_3 were obtained from Jayaraman et al., [35] and the silica parameters were taken from Qiao and Emami et al. [24,36] NaNO_3 species were considered a flexible group and its intramolecular parameters (i.e., the N–O bond, the O–N–O angle and the O–N–O–O improper angle) are listed in Table 1, along with the whole set of intermolecular parameters. Otherwise, the silica nanoparticle was simulated as both rigid and flexible body to evaluate the effect of the vibration of nanoparticles in the calculation of nanofluids properties.

Two different simulation cells were built in this work from the NaNO_3 conventional cell obtained from Jayaraman et al., [35] with dimensions $5.07 \text{ \AA} \times 8.78 \text{ \AA} \times 16.82 \text{ \AA}$ and 12 NaNO_3 units. The first

one, did not contain any nanoparticle and it was created through a $(6 \times 4 \times 2)$ replication of the conventional cell to obtain 576 NaNO_3 units in a box of $30.42 \text{ \AA} \times 35.13 \text{ \AA} \times 33.64 \text{ \AA}$. This cell was used to obtain the heat capacity (C_p), density and crystallographic parameters of the pure NaNO_3 which were in good agreement with previous theoretical and experimental values reported in the literature [12,37–41]. The second one was a $(18 \times 12 \times 6)$ replication of the conventional cell to obtain 15552 NaNO_3 units in a box of $91.26 \text{ \AA} \times 105.38 \text{ \AA} \times 100.93 \text{ \AA}$, and it was large enough to contain different nanoparticle concentrations. Nanoparticles of different radii (i.e., from 5 Å to 15 Å) where added as follows: i) nanoparticles were created performing a spherical cut from the bulk structure of SiO_2 (α -quartz) and saturating the dangling oxygen atoms with hydrogen atoms; ii) nanoparticles are introduced in the simulation cell by deleting the NaNO_3 species inside spherical regions with radiuses similar to the nanoparticle radius; and iii) N nanoparticles were added in the N empty regions generated in the previous step.

The heat capacity (C_p) was obtained from MD simulations through the variation of enthalpy with temperature, Equation (9). To that end, different simulations ranging from 598 K to 773 K were performed to obtain the slope of the $\partial H/\partial T$ curve at the pressure of 1 atm. Also, the enthalpy was obtained directly with MD through Equation (10).

$$C_p = \left(\frac{\partial H}{\partial T} \right)_p \quad (9)$$

$$H = U + PV \quad (10)$$

2.2. Nanofluids synthesis

NaNO_3 used to manufacture the nanofluids was Sigma Aldrich, 99.995% and spherical silica nanoparticles of 5–15 nm of diameter (Sigma Aldrich, 99.5%). The synthesis of the nanofluids was carried out through the following steps (see Fig. 2):

- i) preparation of 40 gr of sample of sodium nitrate + nanoparticles with the respective percentage (w/w) of nanoparticles.
- ii) solvation in 30 mL of distilled water.
- iii) sonication during 6 min for a correct dispersion and homogenization of nanoparticles inside the salt.

Table 1
Force field parameters for NaNO_3 and SiO_2 nanoparticles.

Non-bonding parameters				
atom	q_i (e)	A_{ij} (kcal/mol) ^a	ρ_{ij} (Å)	C_{ij} (kcal/mol·Å ⁶)
Na	1	9778.060	0.3170	24.18
N	+0.95	33652.750	0.2646	259.10
O (in NaNO_3)	−0.65	62142.900	0.2392	259.40
O (in SiO_2)	−0.955209	15170.700	0.3860	617.24
Si	1.910418	72460.640	0.3510	14415.29
H	+0.4776	7194.197	0.2500	0
Bonding parameters				
N–O	$K_b^{\text{NO}} = 525.0 \text{ kcal mol}^{-1} \text{ \AA}^{-2}$		$b_0 = 1.2676 \text{ \AA}$	
O–N–O	$K_\theta = 105.0 \text{ kcal mol}^{-1} \text{ rad}^{-2}$		$\theta_0 = 120.0^\circ$	
O–N–O–O	$K_{imp} = 60.0 \text{ kcal mol}^{-1} \text{ rad}^{-2}$		$\psi_0 = 0.0^\circ$	
Si–O	$K_b^{\text{SiO}} = 285.0 \text{ kcal mol}^{-1} \text{ \AA}^{-2}$		$b_0 = 1.680 \text{ \AA}$	
O–H	$K_b^{\text{OH}} = 495.0 \text{ kcal mol}^{-1} \text{ \AA}^{-2}$		$b_0 = 0.945 \text{ \AA}$	
O–Si–O	$K_\theta = 100.0 \text{ kcal mol}^{-1} \text{ rad}^{-2}$		$\theta_0 = 109.5^\circ$	
Si–O–Si	$K_\theta = 100.0 \text{ kcal mol}^{-1} \text{ rad}^{-2}$		$\theta_0 = 149.0^\circ$	
Si–O–H	$K_\theta = 50.0 \text{ kcal mol}^{-1} \text{ rad}^{-2}$		$\theta_0 = 115.0^\circ$	

^a in the Buckingham potential the crossed terms are calculated as: $A_{ij} = (A_{ii}A_{jj})^{1/2}$, $C_{ij} = (C_{ii}C_{jj})^{1/2}$ and $1/\rho_{ij} = 1/\rho_{ii} + 1/\rho_{jj}$.

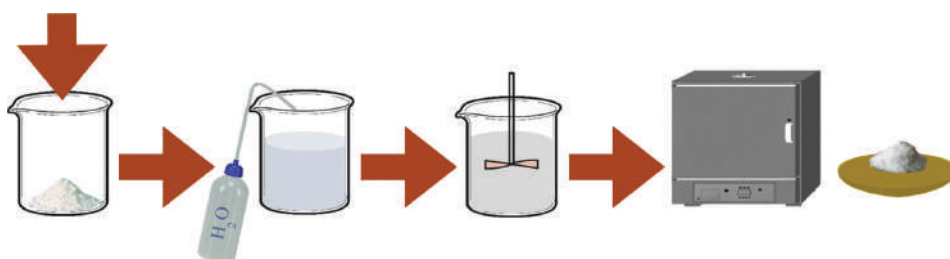


Fig. 2. 1-Step Nanofluid synthesis scheme.

- iv) drying in an oven at 105 °C until complete water evaporation and recrystallization of the material and,
- v) sampling and grinding in an Agatha mortar.

For the study of the concentration effect of nanoparticles in the system, NaNO₃ samples with [0.5–5] % wt. concentration of nanoparticles were prepared.

2.3. Nanofluids characterization

To observe the nanofluids morphology at solid state, the samples under study were characterized using a Scanning Electron Microscopy (ESEM Quanta 200 FEI) at 20 kW. The samples were coated with graphite and the measurements were performed in solid state under vacuum conditions.

X-Ray Powder Diffraction (Panalytical PRO MRD) was employed for the structural characterization. The measurements were performed in transmission geometry, with Cu K α radiation ($\lambda = 1.5418 \text{ \AA}$) and work power of 5 kV–40 mA, in a main angular range from 4 to 88°(2 θ) with a time step size of 0.026°(2 θ) and a measuring time of 148 s per step. Previously, the sample were ground in an Agatha mortar, and sandwiched between low transmission (polyester) films of 3.6 μm of thickness.

The C_p values were measured at 500 °C with the Differential Scanning Calorimetry from DSC 822e de Mettler Toledo with 50 mL/min of N₂ flow, using the methodology of the areas described by Ferrer et al. [42] A quartering method was employed to obtain representative samples. The amount of sample analyzed in a single experiment was around 10 mg within a 40 μl aluminum crucible. For each concentration of nanoparticles, three samples were analyzed to get an averaged C_p value with standard deviation of $\pm 2\%$.

3. Results and discussion

There are several studies that analyze different effects of introducing nanoparticles in molten salts (e.g., nanoparticle's size, shape, material composition and concentration) [7,12,43–45]. However, these studies report results that show a strong inconsistency among them. In general, most of these studies show the biggest increment in C_p when the concentration of nanoparticles is close to 1% wt., but with different sizes of nanoparticles, shapes and composition [13,38,46], indicating that the increase of C_p is inherent to the presence of nanoparticles in the molten salt base fluid and it is not due to the nanoparticles' nature. At the same time, some studies showed that the C_p improves with the size increment [16] while other studies observed the opposite [13]. Moreover, experiments at the same conditions [6,38], showed different C_p increments. These differences can be understood considering the extremely difficult task of sampling in nanofluids and obtaining a

good nanoparticle dispersion. On top of that, even computational studies using the same force field parameters [12,24] lead to different C_p values. Therefore, it is clear that these differences observed put some controversy about the thermal storage capacity of the nanofluids.

According to this, the present work is focused on comparing thermal capacities of NaNO₃ based nanofluids obtained by using Molecular Dynamics (MD) simulations and Differential Scanning Calorimetry (DSC) experiments. MD simulations have been carried out by means of LAMMPS code [28] with the force field and details previously described in the Methodology section. Just to remark, the force field used has been validated by calculating densities, cell parameters and heat capacities for NaNO₃ obtaining an agreement within 10% between experimental and theoretical values [35,39–41,47].

3.1. Thermophysical properties

In the MD study, spherical SiO₂ (α -quartz) nanoparticles of 1 nm of diameter are incorporated to NaNO₃ at different concentrations, [0–10%] wt. Fig. 3 shows the change in C_p as a function of the nanoparticles concentration until 5% since at higher concentrations C_p values are similar to those of 5%.

In a first stage, C_p increases until reaching a top value at 0.5% wt. of nanoparticles. Then, increasing the number of nanoparticles in the medium makes that the C_p value diminishes until recovering the pure NaNO₃ value. It is evident that the increase of C_p is only observed at a tiny interval of concentration of nanoparticles, losing the thermal effect as the number of nanoparticles increase within the fluid. The MD simulations have been carried out in two modes with or without freezing the atoms that form the nanoparticles (i.e., considering the nanoparticles as rigid or flexible bodies, respectively). As it is shown in Fig. 3, the small difference observed in simulated C_p results for flexible and rigid nanoparticles requires that C_p does not depend on the stiffness or flexibility of the nanoparticles. This fact points out that the shape or nature of the nanoparticles inside the fluid is not so important as suggested by Wang [48]. Nanofluids with more than 2% wt. nanoparticles exhibit a C_p fall even below the NaNO₃ bulk value but these results can be understood taking into account the associated errors in the measure.

Experimentally, samples with different concentrations of SiO₂ of 5–15 nm diameters were studied by DSC. As above-mentioned, the C_p values were determined using the method of the areas of Ferrer et al. [42] Considering the results plotted in Fig. 4, there is a proper consistency between experimental and computational increments. Indeed, there is a maximum C_p value, around the 1% wt. of nanoparticles concentration, which qualitatively agrees with MD values. The greatest value observed was $\Delta C_p = 29 \text{ J g}^{-1} \text{ K}^{-1} \pm 2\%$ respect to the NaNO₃ bulk value, comparable with the maximum increment

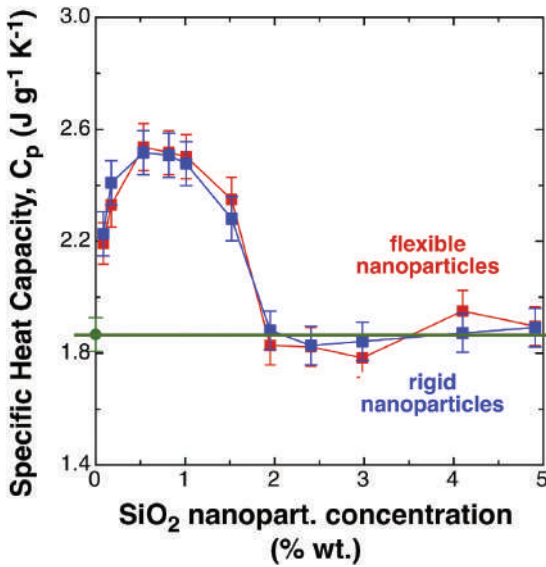


Fig. 3. Simulated specific heat capacities for pure NaNO_3 (\bullet), and for NaNO_3 dispersions of SiO_2 nanoparticles of 1 nm (\blacksquare) of diameter at different concentrations and at 773 K of temperature and 1 atm of pressure. Blue color stands for simulations performed considering nanoparticles as rigid entities (atoms kept fixed) whereas red color stands for nanoparticles where atoms are allowed to move during the simulations. (For interpretation of the references to color in this figure legend, the reader is referred to the Web version of this article.)

obtained through MD simulations $\Delta C_p = 26 \text{ J g}^{-1} \text{ K}^{-1} \pm 2\%$. These values are far from the hypothetical one coming from the law of mixtures described in Equation (11),

$$C_p = \frac{m_p C_{p,p} + m_f C_{p,f}}{m_p + m_f} \quad (11)$$

where m_p is the nanoparticle mass, m_f is the fluid mass and the $C_{p,p}$ and $C_{p,f}$ are the specific heat capacity of both nanoparticles and the fluid, respectively. Since specific heat capacities of α -quartz and pure NaNO_3 are $1.1 \text{ J g}^{-1} \text{ K}^{-1}$ and $1.8 \text{ J g}^{-1} \text{ K}^{-1}$ at 773 K respectively, the C_p value for the nanofluid is expected to be lower.

According to Fig. 4, extraordinary C_p values are obtained for nanoparticles concentrations below 2% wt. both computationally and experimentally. At higher concentrations, this effect is reversed until reaching the constant value predicted by Equation (11). Besides, to validate the tendency between the simulations (with nanoparticles of 1 nm) and the experimental values (with nanoparticles of 5–15 nm), simulations with flexible nanoparticles of 3 nm of nominal diameter were also performed at some concentrations. The obtained values show the same trend obtained for smaller nanoparticles (e.g., ΔC_p (%) = 26, 32 at 0.5% wt. with nanoparticles of 1 nm and 3 nm, respectively, and ΔC_p (%) = 26, 31 at 1% wt.) ensuring the validity of the results with the size of the nanoparticles. Therefore, even with the smallest nanoparticles simulated, the main trend of anomalous C_p increase is still captured by both methods (i.e., DSC and MD).

It is remarkable that DSC results depend strongly on some experimental parameters that must be controlled during the measurements. These are the mass analyzed, the heating rate, the temperature conditions to perform the analyses, and the sampling in order to ensure a homogenous material to be analyzed (i.e., the

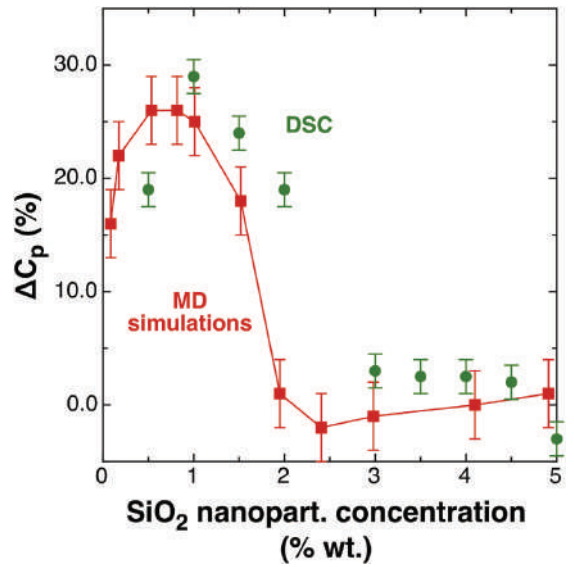


Fig. 4. Experimental DSC (\bullet) and MD (\blacksquare) ΔC_p for $\text{NaNO}_3 + \text{SiO}_2$ nanofluids as a function of the nanoparticle concentration and at 773 K and 1 atm. Flexible nanoparticles of 1 nm have been used in MD simulations and in the range of 5–15 nm in experimental samples.

same nanoparticle amount over the samples under study of each percentage). As previously commented, temperature is also a key factor to consider during the experiments because the nitrate decomposition. In the present study, the presence of nitrates has been scarce as determined by the UV–visible spectrum of the samples of the nanofluid after the thermal treatment. Thus, the low presence of nitrites during the experimental procedure validates using a non-reactive force field to describe the nanofluid during the simulations.

Once the experimental and the simulated C_p values agree, the analysis of MD simulations along with the use of other characterization techniques can help us to distinguish the proposed mechanisms that describe the increase in C_p as a function of nanoparticles concentration.

3.2. Structural characterization

Scanning electron microscopy (SEM) has been used to observe the samples under study. Fig. 5 shows several SEM images at different magnitudes and different nanoparticle concentrations.

As observed, the decreasing of C_p as the nanoparticle concentration increases is related to the agglomeration of the nanoparticles and the loose of effective area when nanoparticles become bigger. Some authors [17] reported the formation of substructures in the nanofluids, and they attributed the unconventional C_p increment phenomenon to these structures, to their high superficial energy, and the formation of agglomeration groups. Furthermore, other authors observed star like structures around the nanoparticles via SEM techniques [18,19]. According to SEM pictures shown in Fig. 5, agglomeration of nanoparticles in the NaNO_3 becomes more intense at higher concentrations. This process is easily observed in Fig. 5e) where the nanoparticle dispersion is reached and Fig. 5f) where the nanoparticles are highly agglomerated. Due to the presence of agglomeration of nanoparticles at higher concentrations it is expected the existence of a limiting

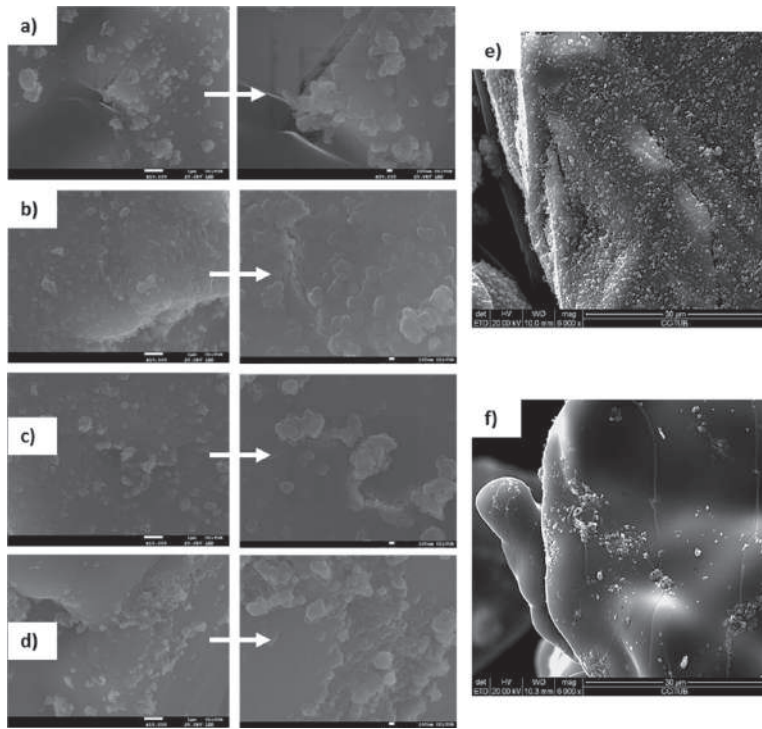


Fig. 5. Nanofluids SEM images at different concentrations of nanoparticles at 25 °C (left: x10.000 and right: x30.000): a) 1% wt. SiO₂; b) 2.5% wt. SiO₂; c) 5% wt. SiO₂; and d) 10% wt. SiO₂; e) nanoparticles dispersed in the salt surface, 5% wt. SiO₂, x6.000; f) nanoparticles agglomeration in the salt surface, 10% wt. SiO₂, x6.000.

diameter value of nanoparticle from which the thermal capacity effect disappears at all concentrations.

The main parameters that affect the C_p unconventional values based on the concentration changes and the nanoparticles size within the nanofluids are schematically described in Fig. 6.

In addition, the microstructure has been also studied via X-Ray

Powder Diffraction (XRD), to see a possible structural change in the synthesized nanofluids. To do this, new formulations of nanoparticles and NaNO₃ samples were prepared at the same nanoparticle concentration in order to analyze how these nanoparticles behave when NaNO₃ recrystallizes. The new formulation consists in a physical mixture. The samples were milled in an Agatha mortar

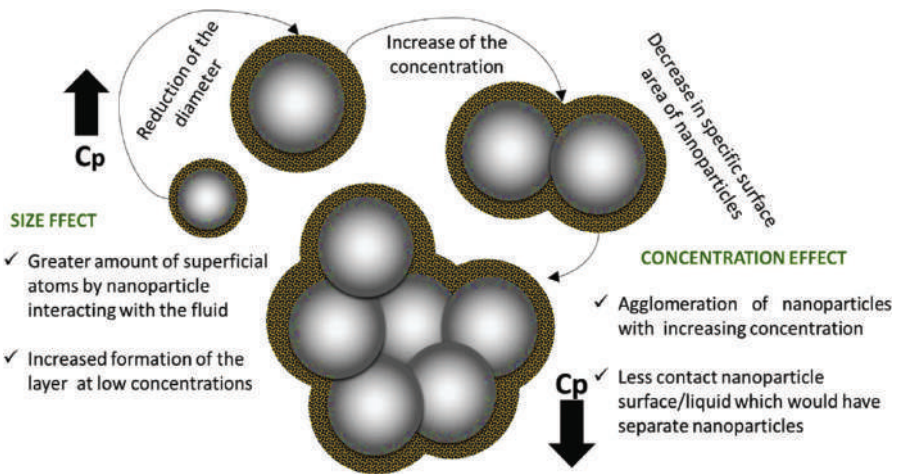


Fig. 6. Scheme of the main parameters that affect the C_p . Effect of the concentrations and the size of the nanoparticles in the nanofluids.

and placed between low absorption 3.6 μm films. Then, these samples were measured in transmission geometry. The diagrams obtained are shown in Fig. 7 where it is represented the main angular range between 10 and 35, $2\theta(^{\circ})$ of the NaNO_3 and silica nanoparticles (top) and the two formulations (i.e., namely mixture and synthesized, middle and bottom, respectively) containing 1%, 5% and 10% wt. of nanoparticles. The X-Ray powder diffraction diagrams showed that the higher the nanoparticle concentration, the

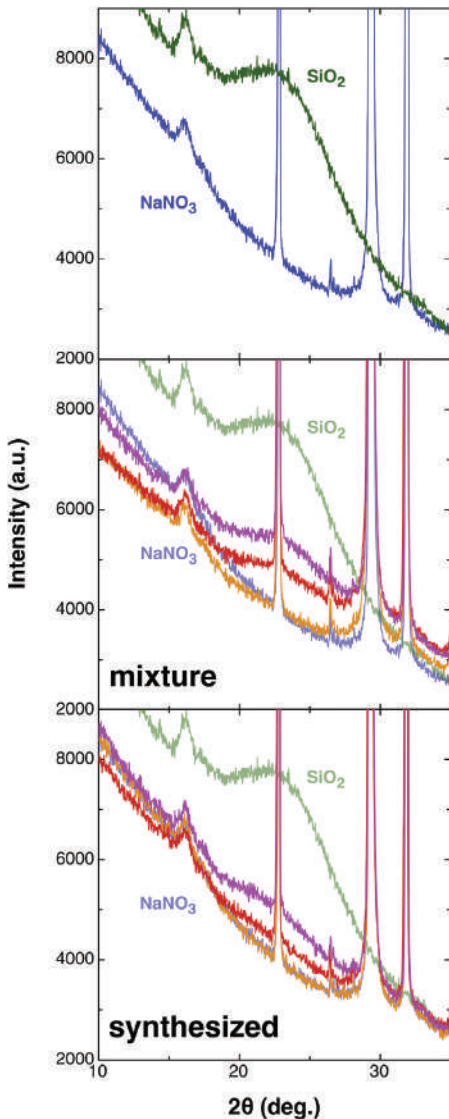


Fig. 7. X-Ray Powder Diffraction diagrams in the range 10–35 $2\theta(^{\circ})$ for SiO_2 nanoparticles (green) and NaNO_3 (blue) pure components (top), for the mixtures at different concentrations (middle) and for the synthesized nanofluids (bottom). The nanoparticles concentrations are 1% (orange), 5% (red) and 10% (pink) wt. In the middle and bottom diagrams the SiO_2 and NaNO_3 are represented with lower opacity to make comparison easier. (For interpretation of the references to color in this figure legend, the reader is referred to the Web version of this article.)

higher the presence of amorphous signal of the nanoparticles in both types of preparations. Nevertheless, when comparing the two methods, there are significant differences between them. In the case of the synthesized nanofluids, the amorphous phase has less presence than in the others. Therefore, in the case of the synthesized sample containing 1% wt. nanoparticles is not possible to identify the amorphous phase and it exhibits an almost identical diagram than the pure NaNO_3 sample. Both changes can be associated to the nanoparticles loss during the preparation process, or to a structural incorporation of up to 1% wt. of nanoparticles due to the possible effects of solubility, or to the formation of a new minor phase. These results show the importance of the methodology used to synthesize the nanofluids.

The analysis of MD simulations shows the formation of a thin ordered layer around the surface of the nanoparticles at low nanoparticles' concentration. Thus, Fig. 8 corresponds to simulation cell snapshots at equilibrium at different temperatures. At 273 K and 300 K, Fig. 8a) and 8b), respectively, NaNO_3 is a solid and even so, it is possible to observe the formation of the oriented layer around the nanoparticle surface. When the temperature is increased, the layer's radius grows, as shown in Fig. 8c) at 500K, a temperature close to the phase change of sodium nitrate (i.e., 581 K). Finally, Fig. 8d) shows the system in liquid state at 773 K. At this point, the layer is not evident due to the motion of the fluid. A zoom in the nanoparticle is depicted in Fig. 8e) where a fictional sphere is used to separate the nearest atoms to the surface. It is evident the presence of a higher number of Na^+ cations (yellow spheres) near the surface of the silica nanoparticle as drawn in the scheme of Fig. 8f).

In order to corroborate this fact, the radial pair distributions have been calculated and plot in Fig. 8g) where the pair distances between the Na^+ cations and the external oxygen atoms of SiO_2 nanoparticles are represented. The formation of a rich semi-solid layer in Na^+ cations around the external side of the nanoparticle is observed at a distance between 2.5 Å and 3 Å from the surface at all the temperatures explored and with a thickness of approximately 1 Å. This fact confirms the existence of the semi-solid layer mechanism at least at 1 nm nanoparticles. Fig. 8g) also shows the influence of the temperature in the semi-ordered layer. The Na^+ layer density increases as the temperature does, indicating that the layer formation of the liquid molecules in the solid-liquid interface is greater than in the solid state. Dubba et al., [16] reported the same relation with the temperature that shows opposite results to the ones obtained experimentally in different studies [20,38] who found bigger increments of C_p in solid state.

These results agree with the computational results of Xue et al., [26] who observed that the magnitude of the layering increases when the solid-liquid interaction strength increases, and results of Hu et al., [49] or Engelmann et al., [50] who obtained computationally the same trends for a different ionic system. They concluded that the ordering of the liquid layers is one possible mechanism to counterbalance the Kapitza resistance (interfacial thermal resistance). Also, Shin et al., [6] observed via SEM that the alkali salt material apparently has a higher density close to the nanoparticles. This fact also agrees with the layering phenomena observed computationally in Fig. 8.

4. Conclusions

The results shown in this study proves the existence of a limit nanoparticles concentration around 2% wt. for the C_p improvement of the NaNO_3 based nanofluid. Therefore, there is a range of concentrations between [0.2–2] % wt. where a C_p increment is obtained but the maximum increment is observed around 0.5–1 % wt. nanoparticles concentration. The computational results show the

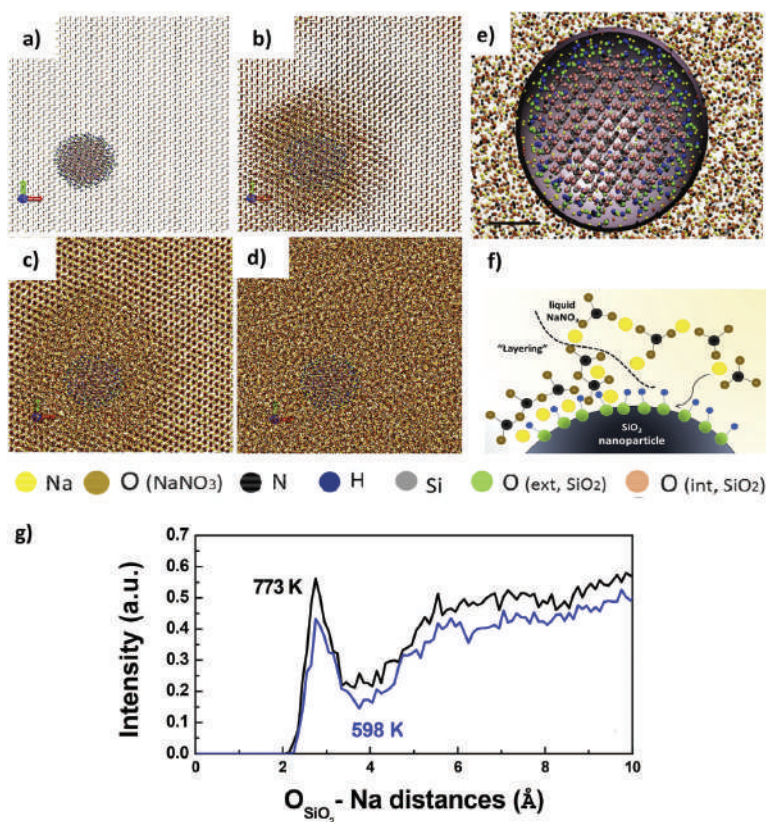


Fig. 8. MD snapshots of NaNO₃ and SiO₂ nanoparticles of 1 nm of diameter at different temperatures: a) 273 K, b) 300 K, c) 500 K and d) 773 K. e) Expanded snapshot at 773 K for the visualization of the NaNO₃ layer near the nanoparticle surface, f) representation of the nanoparticle surface and g) radial pair distribution of Na–O atoms (O from the nanoparticle surface) at 598 K and 773 K.

same trend than the experimental values obtained by DSC measurements with nanoparticles of 5–15 nm diameters.

Thereafter, the C_p values decrease until reaching the theoretical values of the mixture law when the nanoparticle concentration is higher than 2% wt. This fact is more promising because of the great discrepancy denoted in previous studies between the computational and experimental results or between different studies under the same experimental conditions, showing clear tendencies of the unconventional C_p increment phenomenon.

On the other hand, SEM images indicate nanoparticles agglomerations, and the agglomeration is emphasized when the nanoparticles concentration is higher than 5 % wt. This result matches with the decrease detected of the C_p values.

Moreover, analysis of the radial pair distribution shows the formation of a layer on the nanoparticles surface. This fact approaches the idea of describing the unconventional phenomenon and performance of the C_p . Therefore, the semi-solid layering mechanism is observed in MD simulation.

In summary, based on the results made known in this study the main mechanism to explain the unconventional C_p increment is the Mechanism III previously described: the layering of the liquid molecules around the nanoparticles surface. However, this phenomenon described computationally needs to be verified experimentally and therefore, deep information will be required from

properties analysis.

Authorship contributions

Adela Svobodova-Sedlackova: Conceptualization, Data curation, Formal analysis, Investigation, Methodology, Software, Validation, Visualization, Roles/Writing - original draft, Writing - review & editing.

A. Inés Fernandez: Conceptualization, Funding acquisition, Methodology, Project administration, Resources, Supervision, Writing - review & editing.

Pablo Gamallo: Conceptualization, Formal analysis, Funding acquisition, Methodology, Project administration, Resources, Writing - review & editing.

Camila Barreneche: Conceptualization, Formal analysis, Methodology, Resources, Roles/Writing - original draft, Writing - review & editing.

Gerard Alonso: Data curation, Methodology, Software, Roles/Writing - original draft.

Declaration of competing interest

The authors declare that they have no known competing financial interests or personal relationships that could have

appeared to influence the work reported in this paper.

Acknowledgements

The research leading to these results is partially funded by the Spanish government RTI2018-093849-B-C32, RTI2018-094757-B-I00, MDM-2017-0767, MCIU/AEI/FEDER, UE). The authors would like to thank the Catalan Government for the quality accreditation given to their research groups DIOPMA (2017 SGR 188) and CMSL (2017 SGR 13). A.S thanks to Generalitat de Catalunya for her Grant FI-DGR 2018, and G.A. acknowledges Universitat de Barcelona for his Grant APIF 2016. Finally, P.G. thanks Generalitat de Catalunya for his Serra Hünter Associate Professorship.

Appendix A. Supplementary data

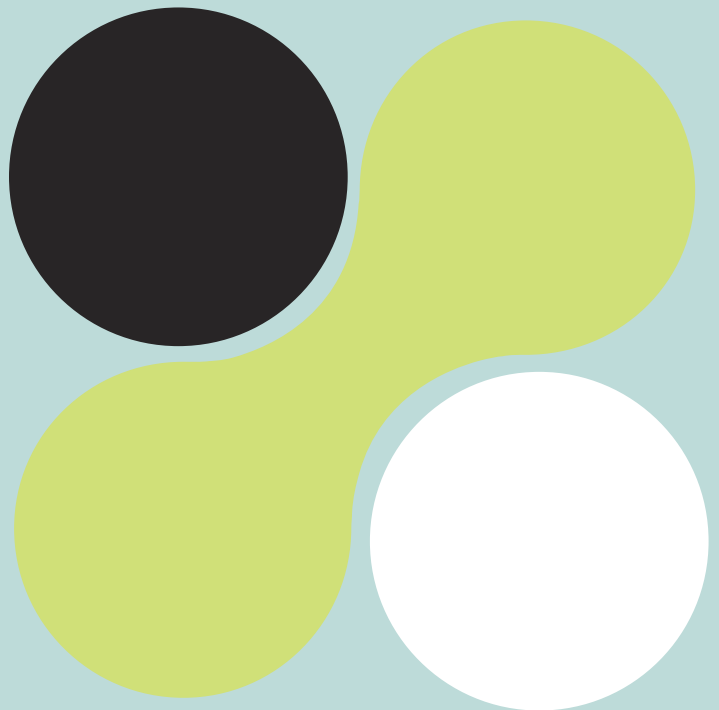
Supplementary data to this article can be found online at <https://doi.org/10.1016/j.renene.2020.01.046>.

References

- [1] U. Desideri, P.E. Campana, Analysis and comparison between a concentrating solar and a photovoltaic power plant, *Appl. Energy* 113 (2014) 422–433.
- [2] Y. Hou, R. Vidu, P. Stroeva, Solar energy storage methods, *Ind. Eng. Chem. Res.* 50 (2011) 8954–8964.
- [3] T. Bauer, et al., High-temperature molten salts for solar power application, in: *Molten Salts Chemistry*, Elsevier Inc., 2013, <https://doi.org/10.1016/B978-0-12-398538-5.00020-2>.
- [4] R.W. Bradshaw, N.P. Siegel, Molten nitrate salt development for thermal energy storage in parabolic trough solar power systems, in: *Proc. 2nd Int. Conf. Energy Sustain.*, 2008, pp. 631–637, <https://doi.org/10.1115/ES2008-54174>.
- [5] A. Alashkar, M. Gadalla, Thermo-economic analysis of an integrated solar power generation system using nanofluids, *Appl. Energy* 191 (2017) 469–491.
- [6] D. Shin, D. Banerjee, Enhancement of specific heat capacity of high-temperature silica-nanofluids synthesized in alkali chloride salt eutectics for solar thermal-energy storage applications, *Int. J. Heat Mass Transf.* 54 (2011) 1064–1070.
- [7] S.F. Ahmed, M. Khalid, W. Rashmi, A. Chan, K. Shahbaz, Recent progress in solar thermal energy storage using nanomaterials, *Renew. Sustain. Energy Rev.* 67 (2017) 450–460.
- [8] A. Awad, H. Navarro, Y. Ding, D. Wen, Thermal-physical properties of nanoparticle-seeded nitrate molten salts, *Renew. Energy* 120 (2018) 275–288.
- [9] Janz, G., Allen, C., Bansal, N., Murphy, R. & Tomkins, R. *Physical Properties Data Compilations Relevant to Energy Storage*.
- [10] P.D. Myers, T.E. Alam, R. Kamal, D.Y. Goswami, E. Stefanakos, Nitrate salts doped with CuO nanoparticles for thermal energy storage with improved heat transfer, *Appl. Energy* 165 (2016) 225–233.
- [11] R. Serrano-López, J. Fradera, S. Cuesta-López, Molten salts database for energy applications, *Chem. Eng. Process* (2013), <https://doi.org/10.1016/j.cep.2013.07.008>.
- [12] S.A. Angayarkanni, J. Philip, Review on thermal properties of nanofluids: recent developments, *Adv. Colloid Interface Sci.* 225 (2015) 146–176.
- [13] K. Khanafer, F. Tavakkoli, K. Vafai, A. AlAmiri, A critical investigation of the anomalous behavior of molten salt-based nanofluids, *Int. Commun. Heat Mass Transf.* 69 (2015) 51–58.
- [14] O. Mahian, A. Kianifar, S.A. Kalogirou, I. Pop, S. Wongwises, A review of the applications of nanofluids in solar energy, *Int. J. Heat Mass Transf.* 57 (2013) 582–594.
- [15] X. Wei, et al., Preparation and enhanced thermal conductivity of molten salt nanofluids with nearly unaltered viscosity, *Renew. Energy* 145 (2020) 2435–2444.
- [16] B. Dudda, D. Shin, Effect of nanoparticle dispersion on specific heat capacity of a binary nitrate salt eutectic for concentrated solar power applications, *Int. J. Therm. Sci.* 69 (2013) 37–42.
- [17] M.-C. Lu, C.-H. Huang, Specific heat capacity of molten salt-based alumina nanofluid, *Nanoscale Res. Lett.* 8 (2013) 292.
- [18] M. Chieruzzi, A. Miliozzi, T. Crescenzi, L. Torre, J.M. Kenny, A new phase change material based on potassium nitrate with silica and alumina nanoparticles for thermal energy storage, *Nanoscale Res. Lett.* 10 (2015) 984.
- [19] P.K. Madathil, et al., Preparation and characterization of molten salt based nanothermic fluids with enhanced thermal properties for solar thermal applications, *Appl. Therm. Eng.* 109 (2016) 901–905.
- [20] Y. Luo, X. Du, A. Awad, D. Wen, Thermal energy storage enhancement of a binary molten salt via in-situ produced nanoparticles, *Int. J. Heat Mass Transf.* 104 (2017) 658–664.
- [21] H. Tiznobaik, D. Shin, Enhanced specific heat capacity of high-temperature molten salt-based nanofluids, *Int. J. Heat Mass Transf.* 57 (2013) 542–548.
- [22] Y. Li, et al., Experimental study on the effect of SiO₂ nanoparticle dispersion on the thermophysical properties of binary nitrate molten salt, *Sol. Energy* 183 (2019) 776–781.
- [23] Y. Hu, Y. He, H. Gao, Z. Zhang, Forced convective heat transfer characteristics of solar salt-based SiO₂ nanofluids in solar energy applications, *Appl. Therm. Eng.* 155 (2019) 650–659.
- [24] G. Qiao, M. Lasfargues, A. Alexiadis, Y. Ding, Simulation and experimental study of the specific heat capacity of molten salt based nanofluids, *Appl. Therm. Eng.* 111 (2016) 1517–1522.
- [25] W. Lan, Z. Tan, S. Meng, D. Liang, L. Guanghai, Enhancement of molar heat capacity of nanostructured Al₂O₃, *J. Nanoparticle Res.* 3 (3) (2011) 483–487.
- [26] L. Xue, P. Koblinski, S.R. Phillpot, S.U.S. Choi, J.A. Eastman, Effect of liquid layering at the liquid-solid interface on thermal transport, *Int. J. Heat Mass Transf.* 47 (2004) 4277–4284.
- [27] L. Li, Y. Zhang, H. Ma, M. Yang, Molecular dynamics simulation of effect of liquid layering around the nanoparticle on the enhanced thermal conductivity of nanofluids, *J. Nanoparticle Res.* 12 (2010) 811–821.
- [28] S. Plimpton, Fast Parallel algorithms for short – range molecular dynamics, *J. Comput. Phys.* 117 (1995) 1–19.
- [29] T. Schneider, E. Stoll, Molecular-dynamics study of a three-dimensional one-component model for distortive phase transitions, *Phys. Rev. B Condens. Matter Mater. Phys.* 17 (1978).
- [30] H.J.C. Berendsen, et al., Molecular dynamics with coupling to an external bath, *J. Chem. Phys.* 3684 (1984).
- [31] G.J. Martyna, D.J. Tobias, M.L. Klein, Constant pressure molecular dynamics algorithms, *J. Chem. Phys.* 101 (1994) 4177–4189.
- [32] M. Parrinello, A. Rahman, Polymorphic transitions in single crystals : a new molecular dynamics method Polymorphic, *J. Appl. Phys.* 7182 (2012).
- [33] H. Sun, COMPASS: an ab initio force-field optimized for condensed-phase Applications s overview with details on alkane and benzene compounds, *J. Phys. Chem. B* 5647 (1998) 7338–7364.
- [34] R.W. Hockney, J.W. Eastwood, *Computer Simulation Using Particles*, McGraw-Hill International Book Co., 1989 c1981.
- [35] S. Jayaraman, A.P. Thompson, O.A. von Lilienfeld, E.J. Maginn, Molecular simulation of the thermal and transport properties of three alkali nitrate salts, *Ind. Eng. Chem. Res.* 49 (2010) 559–571.
- [36] S.V. Patwardhan, et al., Chemistry of Aqueous Silica Nanoparticle Surfaces and the Mechanism of Selective Peptide Adsorption, 2012, <https://doi.org/10.1021/ja211307u>.
- [37] K. Khanafer, F. Tavakkoli, K. Vafai, A. AlAmiri, A critical investigation of the anomalous behavior of molten salt-based nanofluids, *Int. Commun. Heat Mass Transf.* 69 (2015) 51–58.
- [38] M. Chieruzzi, G.F. Cerretti, A. Miliozzi, J.M. Kenny, Effect of nanoparticles on heat capacity of nanofluids based on molten salts as PCM for thermal energy storage, *Nanoscale Res. Lett.* 8 (2013) 448.
- [39] Y. Takahashi, R. Sakamoto, M. Kamimoto, Heat capacities and latent heats of LiNO₃, NaNO₃, and KNO₃, *Int. J. Thermophys.* 9 (1988) 1081–1090.
- [40] T. Bauer, D. Laing, R. Tamme, Characterization of sodium nitrate as phase change material, *Int. J. Thermophys.* 33 (2012) 91–104.
- [41] K. Ichikawa, T. Matsumoto, Heat capacities of lithium, sodium, potassium, rubidium, and caesium nitrates in the solid and liquid states, *Bull. Chem. Soc. Jpn.* 56 (1983) 2093–2100.
- [42] G. Ferrer, C. Barreneche, A. Solé, I. Martorell, L.F. Cabeza, New proposed methodology for specific heat capacity determination of materials for thermal energy storage (TES) by DSC, *J. Energy Storage* 11 (2017) 1–6.
- [43] V. Sridhara, L.N. Satapathy, Al₂O₃-based nanofluids: a review, *Nanoscale Res. Lett.* 6 (2011) 1–16.
- [44] J. Philip, P.D. Shima, Thermal properties of nanofluids, *Adv. Colloid Interface Sci.* 183–184 (2012) 30–45.
- [45] W. Rashmi, M. Khalid, S.S. Ong, R. Saidur, Preparation, thermo-physical properties and heat transfer enhancement of nanofluids, *Mater. Res. Express* 1 (2014).
- [46] Q. Xie, Q. Zhu, Y. Li, Thermal storage properties of molten nitrate salt-based nanofluids with graphene nanoplatelets, *Nanoscale Res. Lett.* 11 (2016) 306.
- [47] T. Jirji, J. Rogez, C. Bergman, J.C. Mathieu, Thermodynamic study of the condensed phases of NaNO₃, KNO₃ and CsNO₃ and their transitions, *Thermochim. Acta* 266 (1995) 147–161.
- [48] B.-X. Wang, L.-P. Zhou, X.-F. Peng, Surface and size effects on the specific heat capacity of nanoparticles, *Int. J. Thermophys.* 27 (2006) 139–151.
- [49] Y. Hu, Y. He, Z. Zhang, D. Wen, Enhanced heat capacity of binary nitrate eutectic salt-silica nanofluid for solar energy storage, *Sol. Energy Mater. Sol. Cells* 192 (2019) 94–102.
- [50] S. Engelmann, R. Hentschke, Specific heat capacity enhancement studied in silica doped potassium nitrate via molecular dynamics simulation, *Sci. Rep.* 9 (2019) 1–14.

Abnormal specific heat capacity in nitrate salt-based nanofluids

Paper 5





Key point 4
Framework

9. Abnormal specific heat capacity in nitrate salt-based nanofluids

Understanding the thermophysical properties of nanofluids

9.1 Introduction

Molecular dynamics simulations have helped to identify the layering phenomenon as one of the main mechanisms involved in the variation of NSBNFs heat capacity. Nevertheless, it also indicates that the behaviour of nanofluids will probably be given by the combination of various mechanisms at the same time. An optimal nanoparticles concentration of 1wt% was also confirmed, where C_p presented a maximum increase of

around 30%, as suggested by the statistical literature analysis in **Chapter 7**. The optimal concentration is given by a homogeneous nanoparticle's dispersion, favouring higher specific surfaces areas and lower intramolecular forces that prevent agglomeration.

In **Chapter 7**, a significant standard deviation that MSBNFs present in heat capacity under the same measurement and synthesis conditions was already seen. Therefore, despite the computational results, several variables, such as the effect of temperature, nanoparti-

cles size, and dispersion of results, disagree with the phenomenon's observed experimentally. These factors, together with the strong influence that the fluid-particle interaction seems to have, these factors make a new scenario that has not been considered in the investigation until now.

The new research focus is on the possibility of chemical interactions between the fluid medium and the nanoparticles surface may play a fundamental role in the nanofluids behaviour.

Recently, some studies, such as the one carried out by R. Mondragón et al., [1], demonstrate the interaction between nanoparticles and molten salt through an ionic exchange on the surface of the nanoparticles. This fact implies a reactive system. The computational methods used in **Chapter 8** (through the integration of Newton's equations) cannot study the formation or bond-breaking since they do not contemplate excited or reactive states. Therefore, they would not be considering counts all system variables.

In a view of these results, in this chapter, a series of novel experiments have been designed, focused on giving a new vision of the nanofluids behav-

iour, encompassing the advances reported in the literature to take a step forward in developing an increasingly robust theoretical framework and contribute to **Key point IV**.

9.1.1 Relevance

The relevance of this chapter lies in the originality of the experiments carried out based on infrared thermography and on the thermal study of a higher amount of sample than that used in conventional calorimetry equipment. It offers a new point of view of the behaviour of nanofluids. Thanks to the methodology used, it will be possible to answer some of the main questions raised in the literature and specifically to the models proposed by Sin, D. and Banerjee, D, Tiznobaik, H., or Dudda described in section **5.4.1.2**

9.1.2 Objectives

The main objectives of this chapter are the followings:

- Demonstrates experimentally the nanostructure's formation and the layering phenomenon.
- Understand the reasons for the high dispersion of specific heat capacity values.
- Contribute to the description of the phenomenon involved in the specific heat modification; therefore, to the **key point IV**.

9.2 Paper 5

The complete study is published in the Scientific Reports journal, entitled "Understanding the abnormal thermal behaviour of nanofluids through infrared thermography and thermophysical characterization". The article is available online in the Nature Portfolio since

the 1st of March 2021, and it was published on volume 152, as shown in **Figure 9.1**.

Besides, a related work (see **Appendix 3**) was presented at the 15th international virtual conference on energy storage "Enerstock 2021".

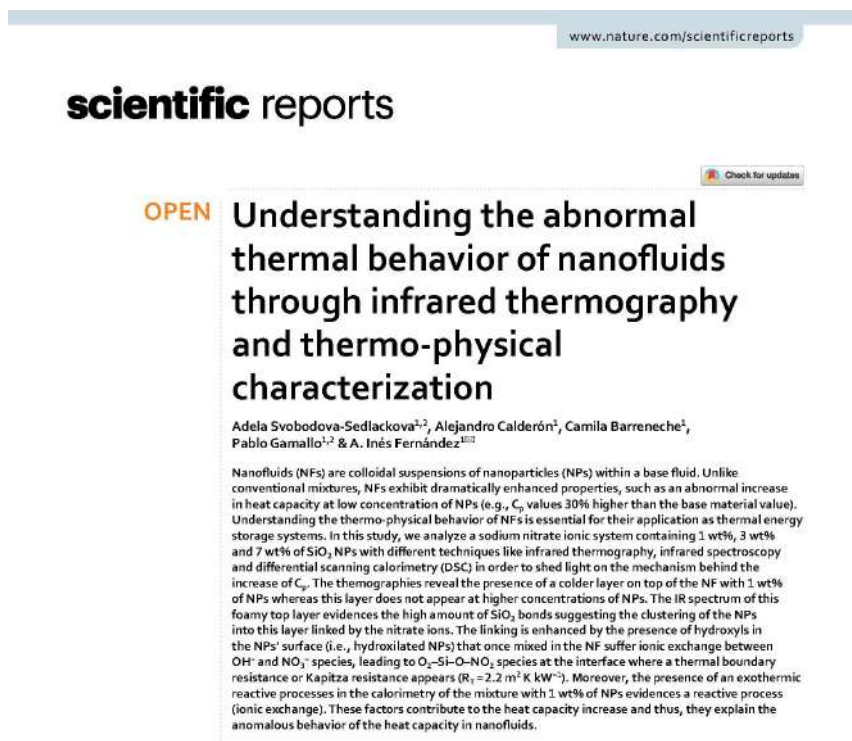


Figure 9.1. Article published in the Scientific Reports journal in 2021, entitled "Understanding the abnormal thermal behaviour of nanofluids through Infrared thermography and thermophysical characterization" [2].

9.2.1 Graphical Abstract

Figure 9.2 summarizes the most relevant results.

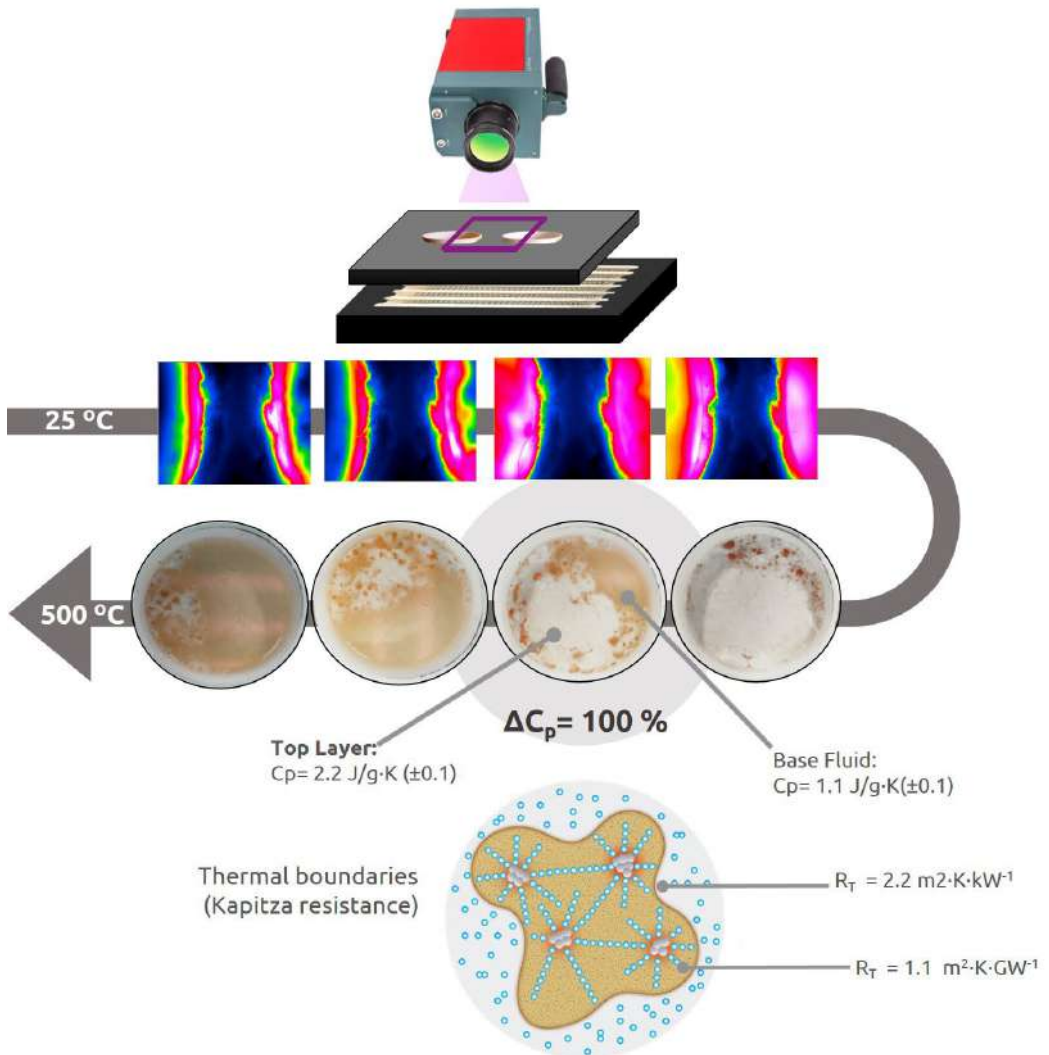


Figure 9.2. Graphical Abstract of the article entitled "Understanding the abnormal thermal behaviour of nanofluids through Infrared thermography and thermo-physical characterization" [2].

9.2.2 Contribution to the state of the art

Key point 4 Framework

Lack of a robust theoretical framework to explain the abnormal thermal behaviour of nanofluids (focused on specific heat capacity).

Main proposed mechanism: Formation of a semi-solid layer and nanostructures in log-range terms with high specific surface areas.

There are no clear experimental demonstrations of the formation of nanostructured semi-solid layer and their properties.

- ✓ Through infrared thermography has observed the formation of lower temperature surfaces after the melting temperature of NaNO_3 (308°C) remained stable until around 450°C , from which its fusion began, **Figure 9.3**.
- ✓ The low-temperature regions correspond to the semi-solid phase formation on the surface of the nanoparticles after fusion. The characterization of this new biphasic system showed us that the surface was composed of nanostructures with high specific surfaces areas and the base mainly by pure sodium nitrate.
- ✓ Optimal dispersion and nanoparticles concentration generate a pattern that, in the first order, causes the ordering of fluid atoms on the surface of the nanoparticles (layering phenomenon) and forms long-term nanostructures.

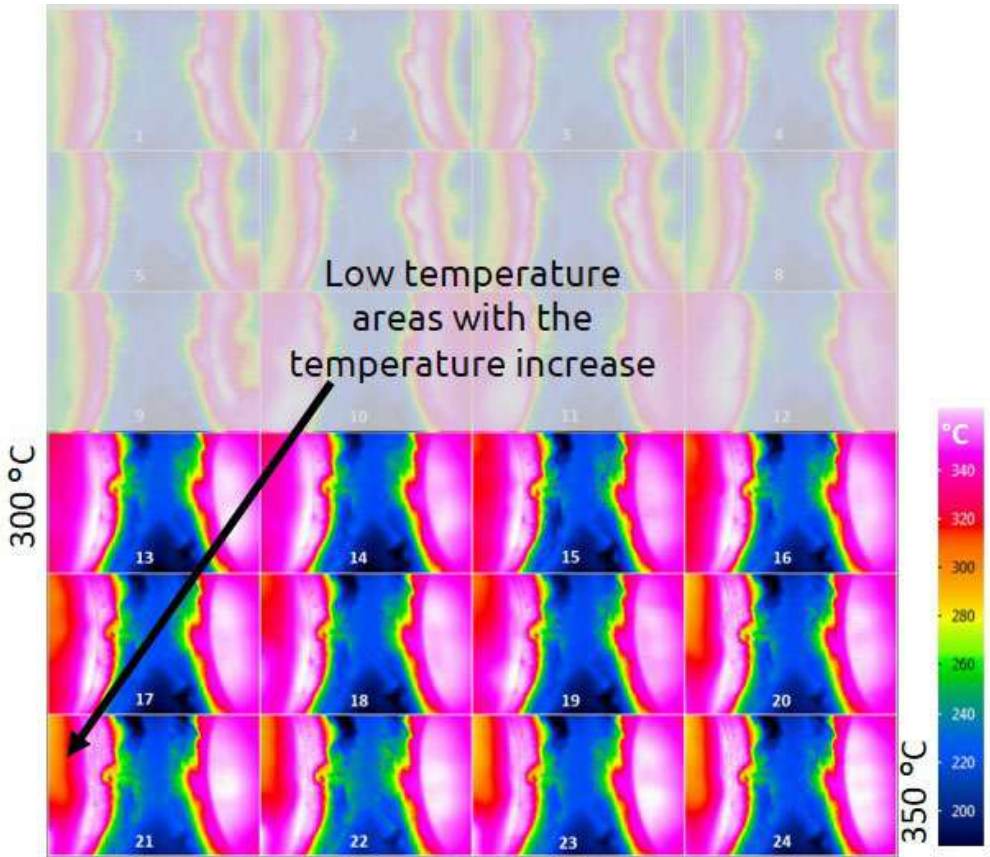


Figure 9.3. Infrared thermography's during the heating process of the nanofluid sample, NF (left, $\text{NaNO}_3 + 1 \text{ wt\% SiO}_2$) and the fluid sample (right, NaNO_3).

- ✓ The heat capacity of the nanostructure turned out to be 100% higher than the rest of the fluid. In addition, both through thermographic data and MD, values of thermal resistances were obtained, which have a relevant impact on the thermal behaviour and heat capacity, **Figure 9.4**.
- ✓ These nanostructures turned out to be highly dependent on the amount of sample and nanoparticles concentration and dispersion, explaining the high dispersion observed in the sampling study of **section 7.3** and in the literature.

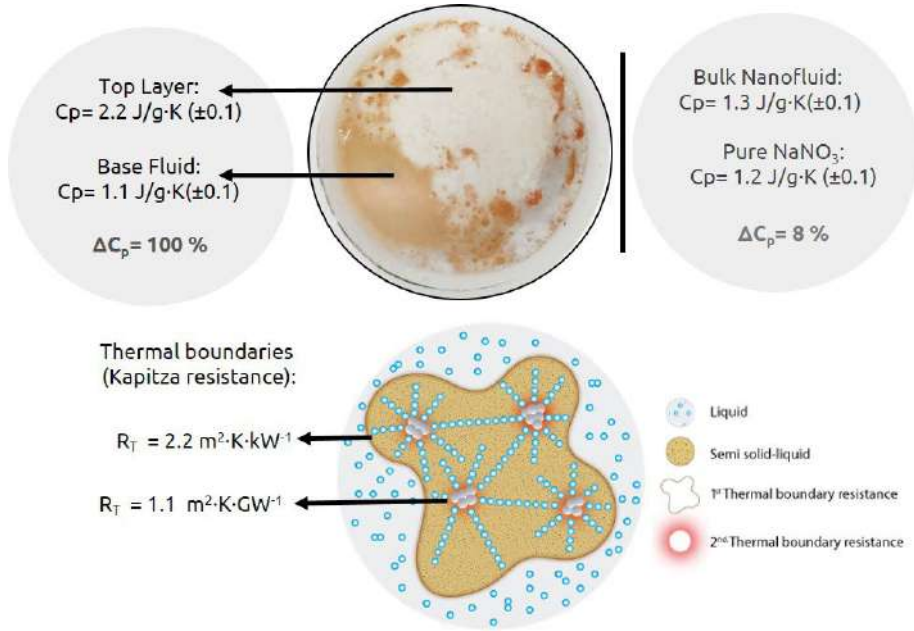


Figure 9.4. Specific heat capacity of Foamy-like white semisolid layer on top of NF sample and schematic representation of nanofluid phases and interphases.

- ✓ The experimental findings demonstrate the layering phenomenon and the formation of nanostructures for the first time. In addition, it solves one of the main limitations of the proposed mathematical theories: the non-availability of their thermal-physical values.

Through the obtained values of the formed layer can be validate the proposed **equation 6.5 (section 5.4.1.2)** by Dudda and Shin [83] in 2013 to predict nanofluids specific heat capacity:

$$C_{p,nf} = \frac{m_s \cdot C_{p,s} + m_{bf} \cdot C_{p,bf} + m_{ns} \cdot C_{p,ns}}{m_s + m_{nf} + m_{ns}} \quad (6.5)$$

If the specific heat of SiO₂ nanoparticles, NaNO₃ and foamy-like layer are: $C_{p,s} = 0.85 \frac{\text{kJ}}{\text{kg}\cdot\text{K}}$, $C_{p,bf} = 1.2 \frac{\text{kJ}}{\text{kg}\cdot\text{K}}$, $C_{p,ns} = 2.2 \frac{\text{kJ}}{\text{kg}\cdot\text{K}}$ respectively. And the weight of the nanoparticles is 1 wt% and of the foamy-like layer is between 30-40 wt%. Therefore, the average NMSBNF heat capacity is between the range:

$C_{p,nf} = 1.49\text{-}1.59 \text{ kJ}\cdot\text{kg}^{-1}\cdot\text{K}^{-1}$ that represents an increase between 24.2-32.5% in front of the pure NaNO_3 .

The average heat capacity increase is accordingly with the computational results of **Chapter 8**, and the average values obtained through the sampling procedure in **Chapter 7**.

- ✓ This study offers a step forward in describing a theoretical framework for the variation of heat capacity and, therefore, contributes to the key point III.
 - The formation of the foamy-like layer takes us back to the article results in chapter 8. The article synthesised nanofluids based on $\text{NaNO}_3 + 1 \text{ wt\%}$ of SiO_2 nanoparticles by the two-step method and a physical mixture of the two components. X-ray powder diffraction measurements were performed under weight control. Structural differences could be observed: the samples obtained through a physical mixture presented a higher amorphous signal and a shift to low angles of the peaks of the samples by the two-step method (wet method).
 - After observing in this chapter, the foamy-like layer formation with samples obtained with the conventional two-step method, the same test was carried out with the physical mixture samples; these did not form any layer on their surface and behaved thermally in a similar way to pure NaNO_3 . In addition, the foamy-like layer of the layer, the nanofluid and the NaNO_3 structural parameters were determined using the Fullprof software, as shown in **Table 9.1**. A slight tendency to increase the cell parameters can be observed in the foamy-like layer.

Table 9.1. Structural cell parameters of foamy-like layer, NaNO₃-1 wt% SiO₂ nanofluid and pure NaNO₃ after thermal treatment of 500°C.

	a (Å)	b(Å)	c(Å)	alfa	beta	gama	symmetry	volume (Å ³)
Foamy-like layer	5.0775	5.0775	16.8541	90	90	120	Hexag.	376.3
NaNO ₃ -1 wt% SiO ₂	5.0699	5.0699	16.836	90	90	120	Hexag.	374.78
NaNO ₃	5.0715	5.0715	16.8329	90	90	120	Hexag.	374.94

- ✓ This result indicates that the synthesis method, precisely the wet method, greatly modifies the final nanofluids' properties and influence the foamy-like layer formation, as indicated in the literature (section 2.2.3). Furthermore, these preliminary results open the doors to further research and advance on the development of a theoretical framework (**Key point IV**).

9.2.3 Publication

The article is attached below (DOI: <https://doi-org/10.1038/s41598-021-84292-9>).



OPEN

Understanding the abnormal thermal behavior of nanofluids through infrared thermography and thermo-physical characterization

Adela Svobodova-Sedlackova^{1,2}, Alejandro Calderón¹, Camila Barreneche¹, Pablo Gamallo^{1,2} & A. Inés Fernández^{1✉}

Nanofluids (NFs) are colloidal suspensions of nanoparticles (NPs) within a base fluid. Unlike conventional mixtures, NFs exhibit dramatically enhanced properties, such as an abnormal increase in heat capacity at low concentration of NPs (e.g., C_p values 30% higher than the base material value). Understanding the thermo-physical behavior of NFs is essential for their application as thermal energy storage systems. In this study, we analyze a sodium nitrate ionic system containing 1 wt%, 3 wt% and 7 wt% of SiO₂ NPs with different techniques like infrared thermography, infrared spectroscopy and differential scanning calorimetry (DSC) in order to shed light on the mechanism behind the increase of C_p . The thermographies reveal the presence of a colder layer on top of the NF with 1 wt% of NPs whereas this layer does not appear at higher concentrations of NPs. The IR spectrum of this foamy top layer evidences the high amount of SiO₂ bonds suggesting the clustering of the NPs into this layer linked by the nitrate ions. The linking is enhanced by the presence of hydroxyls in the NPs' surface (i.e., hydroxylated NPs) that once mixed in the NF suffer ionic exchange between OH⁻ and NO₃⁻ species, leading to O₂-Si-O-NO₂ species at the interface where a thermal boundary resistance or Kapitza resistance appears ($R_T = 2.2 \text{ m}^2 \text{ K kW}^{-1}$). Moreover, the presence of an exothermic reactive processes in the calorimetry of the mixture with 1 wt% of NPs evidences a reactive process (ionic exchange). These factors contribute to the heat capacity increase and thus, they explain the anomalous behavior of the heat capacity in nanofluids.

Energy storage systems are key technologies for achieving the transition to renewable energies. Such systems allow to improve energy efficiency making renewable energy more viable¹. An example of this is the great advances made in the efficiency of solar energy by using thermal energy storage (TES) systems. At present, more than 70% of concentrated solar power (CSP) projects have integrated TES systems², and such power plants reached an installed capacity of 4.5 GW at the end of 2019³. Due to the importance of the storage systems for the viability of CSP technology, it is necessary to keep on improving them by increasing both their energy efficiency and their capacity of continuously generating electricity, without forgetting their competitiveness from an economic point of view.

Materials science and technology are essential to meet these improvements. Nanoscience has made great strides forward in the field of energy storage and retrieval. Nanofluids (NFs) are a promising option for a wide variety of techniques in the future, including TES systems^{4,5}. NFs are a colloidal suspension of nanoparticles (NPs) within a base fluid. Unlike conventional mixtures of different components, NFs exhibit dramatically enhanced properties, such as an abnormal increase in heat capacity⁶ at low concentration of NPs (e.g., C_p values 30% higher than the base material value)⁷. According to this, the use of materials as NFs in TES systems allows increasing the CSP plant's efficiency as well as reducing the costs associated to the thermal storage process. Precisely, the energy density of a material is the product of its specific heat, C_p , and its density. Therefore, an increase in C_p of

¹Departament de Ciència de Materials i Química Física, Universitat de Barcelona, C/Martí i Franqués 1, 08028 Barcelona, Spain. ²Institut de Química Teòrica i Computacional, IQTCUB, Universitat de Barcelona, C/Martí i Franqués 1, 08028 Barcelona, Spain. ✉email: ana_inesfernandez@ub.edu

a TES material leads to a proportional increase in the energy density, which also means a decrease in the size of the storage tanks required, hence allowing more efficient and compact systems.

Despite the great potential of NFs, we are still far away from understanding fundamental questions concerning them as simply the NF stability⁸. Moreover, it does not help the discrepancies observed in experimental and simulated values of some thermo-physical properties (e.g., C_p) of NFs already published^{9,10}. Thus, there is no a clear explanation for the observed phenomena like the increase in heat capacity observed at low concentration of nanoparticles, although several hypotheses are available^{11–13}. Literature suggests that Infrared Thermography (IRT) technique it is a very useful technique to study the thermal behavior of NFs and it has been successfully applied to the study of vaporization and wettability of NFs^{14–16}. This work, therefore, tries to provide an explanation of the anomalous increase in C_p of sodium nitrate NFs containing one of the commonly used NPs: silicon dioxide. To this end, high-resolution IR is used as it allows observing the thermal behavior of NFs, together with Fourier-transform infrared spectroscopy (FT-IR) combined with differential scanning calorimetry (DSC), which allows to characterize the physico-chemical properties of the NFs.

Infrared thermography and Kapitza resistance. Infrared thermography allows the study of heat transfer in NFs and their thermal behavior. The Stefan-Boltzmann law establishes that the total energy radiated by a material, E , is directly proportional to the fourth power of its temperature, via the Eq. (1):

$$E = \varepsilon \cdot \sigma \cdot T_e^4 \quad (1)$$

where $\sigma = 5,67 \cdot 10^{-8} \frac{W}{m^2 \cdot K^4}$ is the Boltzmann constant of proportionality, T_e is the effective temperature (absolute temperature of the surface) and ε is the emissivity of the material.

The thermographies for the NF and the base fluid obtained from a high-resolution infrared camera are shown in Fig. 1, where different images (1–24) were taken at different times (every 15 min). For each image, the left-hand side corresponds to the NF (i.e., sodium nitrate with 1 wt% of SiO₂) in the set-up and the right-hand side corresponds to the base fluid (i.e., pure sodium nitrate), represented as (F). Both samples are always subjected to the same heating by means of electrical resistances, so the temperature profile observed in each sample is related to the thermal behavior of each of them. Temperature of samples is controlled directly by thermocouples and indirectly, inferred from the thermographies although the maximum temperature that camera can measure is 340 °C. The experimental device used for obtaining the thermographies has been developed by the University of Barcelona (see Methodology section).

As it can be inferred from the thermographies, heating takes place in various stages:

- Stage 1: from images (2) to (8), a very similar temperature profile is observed for both samples, with the fluid (F) and the NF reaching approximately 292 °C ± 5 °C and 295 °C ± 6 °C, respectively, in (8).
- Stage 2: starting at image (9), the fluid (right) begins to melt (320 °C ± 4 °C), while the NF (left) is at a lower temperature (306 °C ± 4 °C) and still solid.
- Stage 3: from images (10) to (14), the phase transition is completed in both samples and therefore, at the end of this stage, both are in liquid phase with a similar temperature: approximately 355 °C ± 3 °C and 337 °C ± 10 °C for F and NF, respectively. It is worth noting that the NF has a less homogeneous temperature. The melting of the NF requires a higher temperature than the one for melting the pure salt. This behavior is just the opposite to what should be expected for a non-pure species according to classical theories¹⁷.
- Stage 4: from image (15) to (24) domains at lower temperature appear in the NF sample, despite the increase in heat flow. At this point, a foamy-like white layer appears on top of the NF sample (Fig. 2). The foamy-like white layer is formed from the beginning of the melting process (~308 °C) (Fig. 2a) and it persists up to approximately 450–500 °C, at which temperature the layer melts (Fig. 2d). The presence of this top foamy layer (i.e., new phase) corresponds with the lower temperature regions observed in the thermographs in Fig. 1, images (15) to (24), i.e., stage 4. Furthermore, the formation of the new phase generates additional interphases in the system (e.g., liquid–solid interphase) that produce thermal boundary resistance or Kapitza resistance (R_T)^{18,19} (i.e., a sudden change in temperature between foamy top layer and the bulk fluid). It is possible to obtain the Kapitza resistance from the variation of temperature between the foamy top layer and the bulk liquid fluid (ΔT) and the heat flux crossing the interface (q) since $R_T = \Delta T/q$. An accurate exploration of the thermographies in which the top layer is present (stage 4) show an average difference in temperature of 55.8 ± 3 °C between the fluid and the foamy semisolid layer in the NF sample. According to the power of heat communicated to the samples (112.01 W) and the interface area between the top layer and the fluid (i.e., almost the crucible's area 44.18 cm²), the resulting interfacial thermal resistance is $R_T = 2.2 \text{ m}^2 \text{ K kW}^{-1}$.

The anomalous behavior observed in the thermographs shown in Fig. 1 (variation of the melting parameters and a decrease in the thermal radiation from the surface as the thermal flow increases), and the evidence offered by Fig. 2 (formation of a semisolid foamy layer), indicate that in order to analyze and understand the abnormal behavior of NFs it is necessary to perform a detailed thermo-physical characterization of both the top foamy layer and the bulk fluid. The characterization has been focused on the NF sample with 1 wt% SiO₂ NPs because at this concentration it is observed the presence of the semisolid top phase. Once the foamy layer is formed both phases are separated, cooled down to room temperature and then, characterized using FT-IR and DSC techniques.

Physicochemical characterization of NFs. The FT-IR characterization allows to identify the principal functional groups present in the samples. Figure 3 shows the FT-IR spectra of the foamy semisolid layer when it

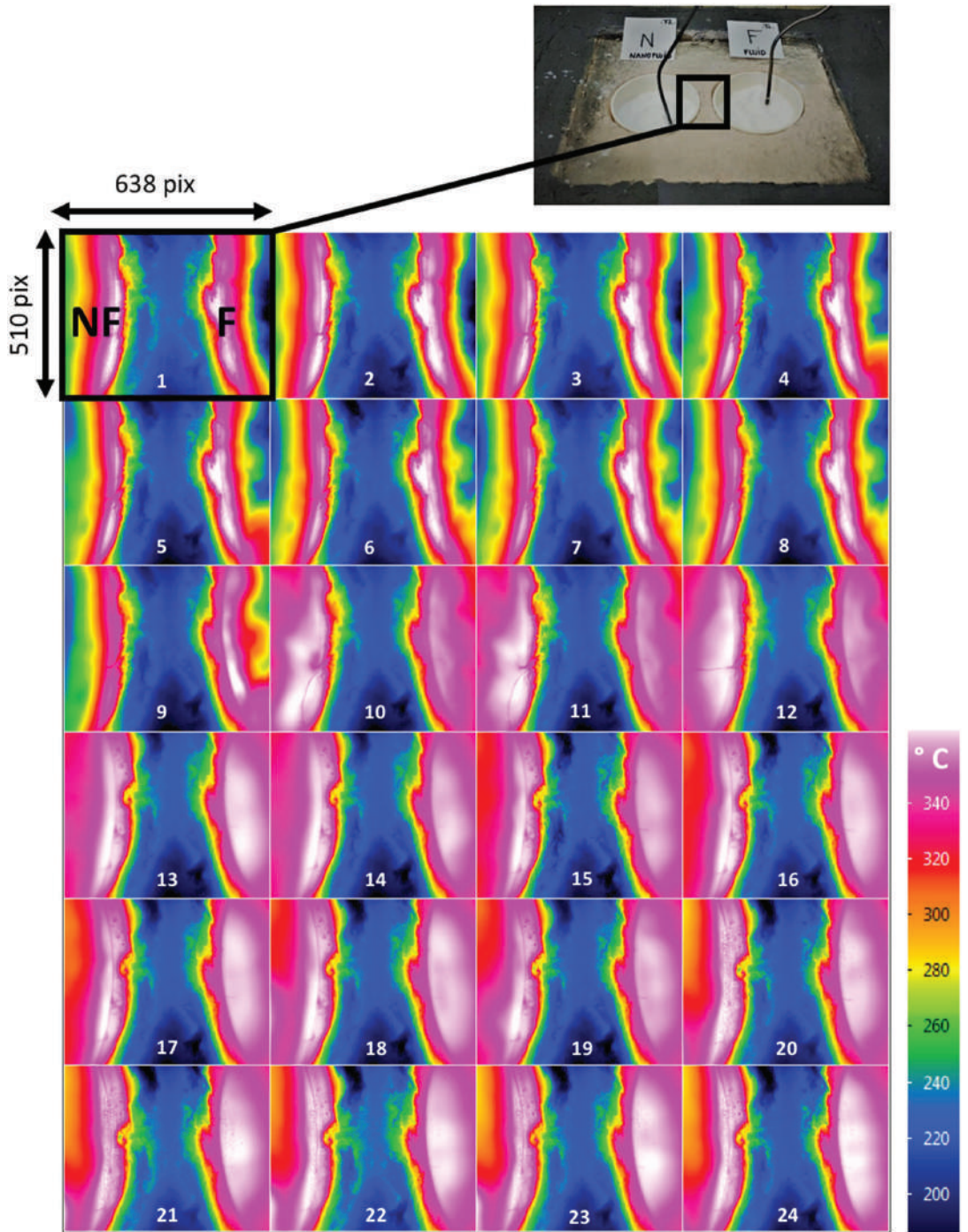


Figure 1. Infrared thermographies during the heating process of the nanofluid sample, NF (left, $\text{NaNO}_3 + 1 \text{ wt\% SiO}_2$) and the fluid sample F (right, NaNO_3). The electrical power communicated to both samples is the same along the experiment.

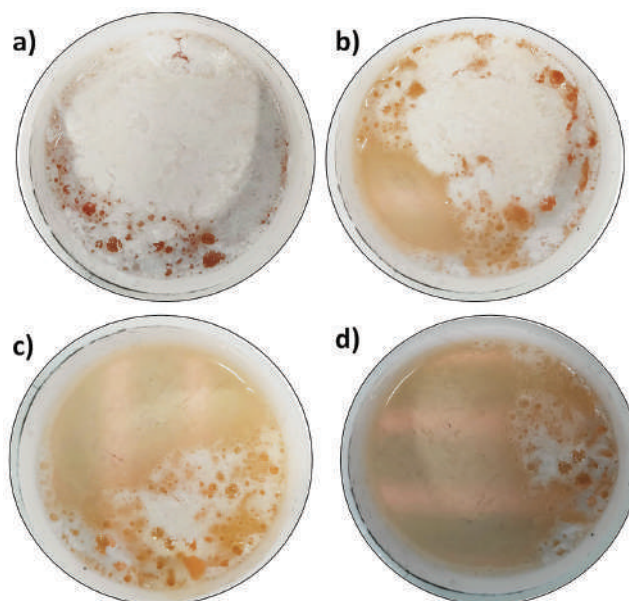


Figure 2. NF sample with 1 wt% of NPs at different temperatures, from 300 °C (a) to 450 °C (d). It is evident the formation of the foamy-like white semisolid layer on top of the sample that is colder than the liquid phase as it can be seen in Fig. 1, left hand side of images (15) to (24).

is formed (M1) when it is heated (M2) and when it melts (M3). Moreover, M4 corresponds to the FT-IR spectrum of the entire NF once melted.

The analysis of the spectra has been done focusing on eleven bands (Fig. 3). The bands (1), (3) and (7) are characteristic of sodium nitrate and they are observed in all the series. Concretely, in M1 they correspond to the out-of-plane N=O bond bending (1789 cm^{-1}), the symmetrical bending of NO_3^- (1352 cm^{-1}) and the asymmetric stretching of NO_3^- (836 cm^{-1}), respectively^{20,21}. It is notorious the slight blue shift of band (3) compared to the value for pure nitrate (1338 cm^{-1}) and the red shift that it suffers as the top layer melts. Moreover, the width of a band is characteristic of the crystallinity of the material²², so the band is progressively narrowed from M4 to M1, indicating an increasing of crystallinity, with the greatest degree in M1, which corresponds to the formation of the foamy semisolid top layer. Moreover, band (7), the asymmetric NO_3^- stretching mode, is also sensitive to the transition from the semisolid state (M1) to the liquid phase (M3 at 829 cm^{-1}) with a slight red shift during the melting process²². Obviously, these facts are produced by an alteration in the force constant and the dipole moment of the NO_3^- vibrational group, indicating that the sodium nitrate environment has been altered.

The characteristic bands of silicon dioxide have been also identified²³. Band (5) is associated to the asymmetric stretching of SiO_x (1085 cm^{-1} for $x=2$)²⁴. In the samples, it is observed a broadening and a blue shift of band (5) from M1 (1081 cm^{-1}) to M4 (1089 cm^{-1}). Band (6) is the symmetric stretching of SiO_4 only present in M1 (972 cm^{-1}) and M2 (952 cm^{-1}) and band (9) corresponds to the Si-O-Si symmetric stretching mode (724 cm^{-1})^{25,26} and band (11) corresponds to the symmetric bending mode of SiO_4 (462 cm^{-1})^{24,27}. Band (11) exhibits a rapid and considerable decrease from M1 (semisolid) to M4 (melting). According to Ref.²⁹, the maximum intensity observed when the foamy top layer is formed owe to the adsorption of nitrate ions on the nanoparticle surface confirming an ionic exchange process between hydroxylated nanoparticles ($\text{O}_2\text{-Si-OH}$) and sodium nitrate generating silica modified units like $\text{O}_2\text{-Si-O-NO}_2$ (i.e., $\text{O}_2\text{-Si-NO}_3$) and OH^- in the medium. This fact produces the formation of high specific-surface-area (SSA) silica layer modes that develop on the dissolving glass particles²⁵ (see Fig. 4). It is worth noting that, taken together, the vibrational bands at 1385 cm^{-1} , 870 cm^{-1} and 715 cm^{-1} , which were weaker in M4, indicate the interfacial precipitation of crystalline Na^+ cationic species²⁸. Obviously, the new spatial ordering of the species causes the enhancement of the specific heat.

According to Ref.²⁸, bands (3), (7) and (9) are associated to the low-frequency region by means of the so-called non-bridging oxygens (NBOs), due to such effects as vibrations of Si-O units, where the negative charge is electrostatically compensated by cationic species, in this case by Na^+ cations²⁸. This implies a lower reactivity. These bands disappeared during the melting of the surface layer (M3), implying there was diffusion of Na^+ cations into the liquid²⁹. Other additional bands were found: at 555 cm^{-1} (line 10), due to Si-O-Si asymmetric bending mode; while the signals at 815 cm^{-1} and 802 cm^{-1} (line 8), were associated with the O-Si-O bending mode for M1, and with Si-O-Si in the formed layer of SiO_2 ²⁴, in sample M2. Finally, in both samples, in the region of

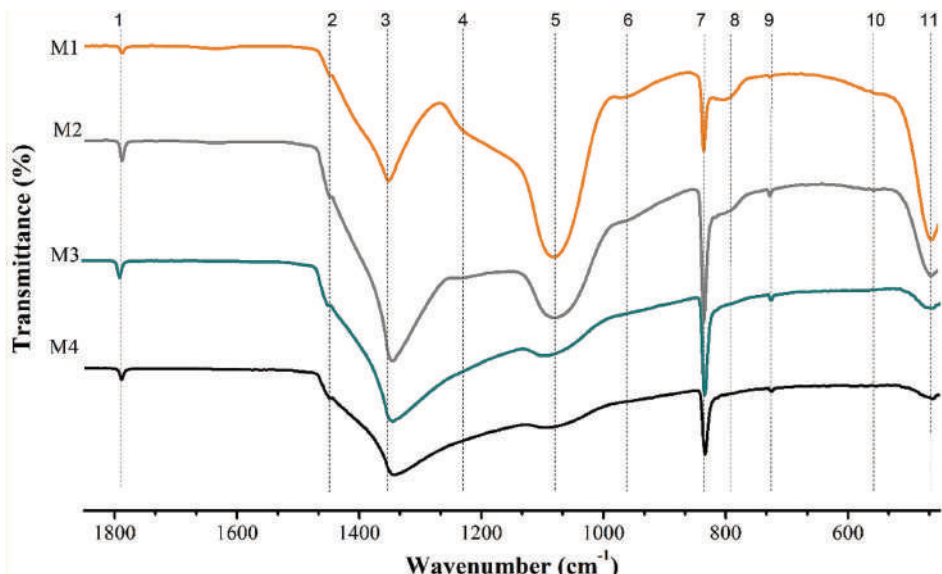


Figure 3. FT-IR spectra of the foamy semisolid top layer (M1, M2 and M3) along with the bulk melted NF with a 1 wt% concentration in NPs. M1 to M3 corresponds to the evolution of the top layer with temperature, from 300 to 450 °C. M4 corresponds to the spectrum of the entire NF once melted. The analyzed bands are identified by a number from 1 to 11. The 100% of transmittance for each spectrum is the base line at high wave numbers.

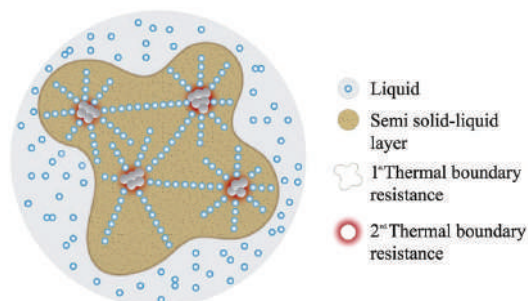


Figure 4. Schematic representation of nanofluid phases and interphases.

1220 cm^{-1} (line 4), we identified the asymmetric stretching vibration of the surface component of Si–O–Si due to the formation of an interfacial SSA silica layer^{17,19}.

Calorimetric study. After confirming the ionic exchange between the fluid and the nanoparticles, a detailed thermophysical characterization is essential to study the thermal behavior of the samples.

Figure 5a shows the heat flow absorbed as a function of temperature for the foamy top layer and for the bulk NF with a concentration of 1 wt% of NPs. The endothermic peak corresponds to the phase change (i.e., the enthalpy of melting). The top layer formed on the surface of the NF shows a broadening of the melting peak, compared to the bulk fluid sample. Consequently, the foamy top layer exhibits a greater enthalpy than the bulk fluid (i.e., -180.4 J g^{-1} and -154.5 J g^{-1} , respectively). Therefore, there is an alteration of the thermal behavior between the phase formed at the surface and the rest of the system, consistent with the results determined using FT-IR.

The effect of the NPs' concentration in the formation of the foamy top layer has been studied by means of isothermal measurements at 400 °C, to analyze the absorbed heat at this temperature. Figure 5b shows the heat flow absorbed (endothermic peaks) as a function of time at 400 °C for concentrations of NPs of 1, 3 and 7 wt%. The results show variations in the heat absorbed. At the maximum concentration of nanoparticles (7 wt%) the same behavior was observed as in the case of the base fluid without NPs. In contrast, as the concentration of NPs decreased, it took longer times for the system to reach thermal equilibrium compared to pure NaNO_3 . The

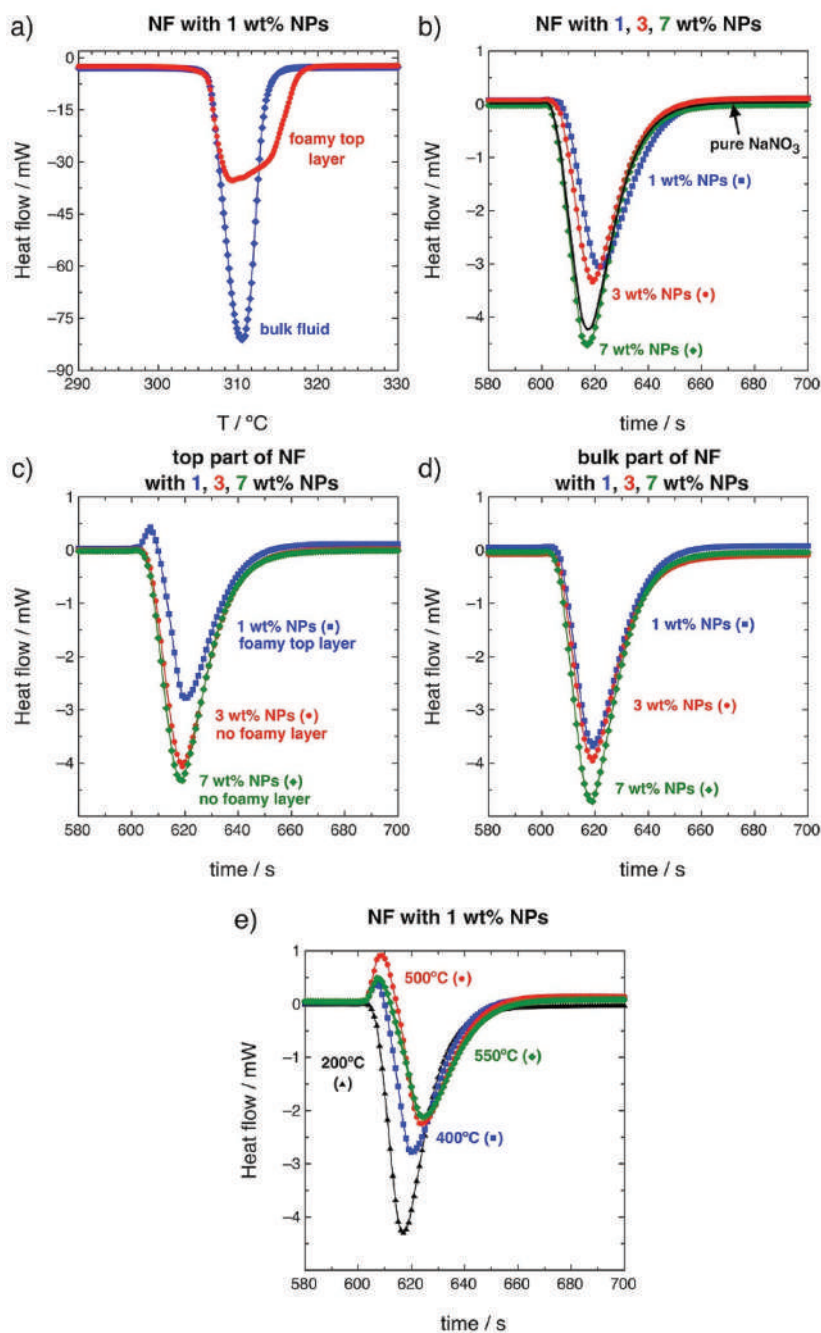


Figure 5. (a) Enthalpy of melting of the NF with 1 wt% of NPs: bulk fluid (blue rhombohedras) and foamy top layer (red circles). (b) Sensible heat at 400 °C for NFs with 1 wt% (blue squares), 3 wt% (red circles) and 7 wt% (green rhombohedras) of NPs along with the values for pure NaNO₃ (black line). (c) Sensible heat at 400 °C of the top part of the NFs with 1 wt% (blue squares), 3 wt% (red circles) and 7 wt% (green rhombohedras) of NPs. The NF with 1 wt% of NPs is the only sample that exhibits the foamy top layer. (d) Sensible heat at 400 °C of the bulk fluid part of the NFs with 1 wt% (blue squares), 3 wt% (red circles) and 7 wt% (green rhombohedras) of NPs. (e) Temperature evolution of the foamy top layer's sensible heat from 200 to 550 °C (NF with 1 wt% of NPs).

isothermal analysis has been also done for the foamy top layer (Fig. 5c) and for the bulk fluid (Fig. 5d) of the NFs. However, the foamy top layer is only formed in the NF with 1 wt% of NPs although for NFs with 3 wt% and 7 wt% the analysis has been also done but for samples of the non foamy top part of the NF. As it can be inferred from Fig. 5c, the NF with 1 wt% of NPs is the only sample that showed an exothermic peak of 1.70 J g^{-1} in the isothermal calorimetry. This exothermic peak indicates the ionic exchange and reordering in the interphase NP and fluid that derives in the foamy semisolid top layer (Fig. 2). This top layer phase was not observed at higher NP concentrations as evidenced by the profiles observed in Fig. 5c. According to the literature, the increase in C_p depends strongly on the concentration of NPs reaching a maximum at around 1 wt%³¹ so it is straightforward that the increase of the C_p value comes from the foamy semisolid top layer. The nitrate-nitrite decomposition has been discarded for this peak since it is a process that occurs in a tiny extent at 400°C and to the fact that the peak only appears at 1 wt% of NPs and it should appear for all the samples.

The isothermal analysis of the foamy top layer has been done at different temperatures (Fig. 5e) showing that at temperatures higher than 500°C the exothermic peak begins to decay. This temperature corresponds to the melting and blending of the foamy layer with the rest of the fluid.

The presence of the Si-NO₃ bonds in the top layer increase the crystallinity of the system and consequently, the top layer melting point is higher than that of NaNO₃. The measurement of the heat capacity has been carried out on the 1 wt% SiO₂ NF as a whole and also split the system in two parts (i.e., the foamy top layer and the bulk fluid) at 350°C . The C_p values obtained are $2.2 \pm 0.1 \text{ J g}^{-1} \text{ K}^{-1}$ for the foamy top layer and $1.1 \pm 0.1 \text{ J g}^{-1} \text{ K}^{-1}$ for the bulk fluid, really close to the value for pure NaNO₃ (i.e., $1.2 \pm 0.1 \text{ J g}^{-1} \text{ K}^{-1}$). The C_p value of the foamy top layer represents a $100 \pm 10\%$ of increasing with respect to the bulk phase. In the case of the C_p for the entire sample of NaNO₃ + 1 wt% SiO₂, a value of $1.3 \pm 0.1 \text{ J g}^{-1} \text{ K}^{-1}$ was obtained, which represents an increase of the nanofluid value over the pure NaNO₃ value of approximately $9.1 \pm 0.9\%$. These findings also support the presence of Si-O-NO₂ bonds that built the islands of NPs connected by sodium nitrate on the foamy top layer and the presence of simply NaNO₃ in the bulk phase of the NF.

Given the coexistence of phases up to approximately 450°C , we have calculated C_p for mixtures of the whole system using the calorimetric data. The law of mixtures can be expressed by the following Eq. (2):¹⁷

$$C_{p,\text{mixture}} = \sum_i C_{p_i} \cdot x_i = C_{p_i} \cdot \left(\frac{n_i}{n_t} \right) \quad (2)$$

where for the i -species is defined the mole fraction (x_i), the specific heat capacity (c_{p_i}) and the number of moles (n_i) whereas n_t stands for the total number of moles of all the species in the system. In the case under study, the components of C_p are those formed by the foamy top layer (tl) and the bulk fluid (bf), Eq. (3):

$$C_{p,\text{mixture}} = \sum_i C_{p_i} \cdot \left(\frac{n_i}{n_t} \right) = C_{p_{tl}} \cdot \left(\frac{n_{tl}}{n_t} \right) + C_{p_{bf}} \cdot \left(\frac{n_{bf}}{n_t} \right) \quad (3)$$

where: $n_{tl} = x \cdot n(\text{SiO}_2) + y \cdot n(\text{NaNO}_3)$; $n_{bf} = (1-x) \cdot n(\text{SiO}_2) + (1-y) \cdot n(\text{NaNO}_3)$, with x being the fraction of SiO₂ and y , that of NaNO₃. By solving this equation, together with the law of conservation of mass and the constrain that the SiO₂ is localized in the top layer (i.e., in the bulk fluid, $1-x \rightarrow 0$) the value of the molar mass of the foamy top layer ($M = \sum_i M_i \cdot x_i$) of approximately 83 g mol^{-1} . From this, we can derive a relationship between density ($\rho_i = \frac{n_i \cdot M_i}{V_i}$), the molar mass (\bar{M}) and the volume of the top layer formed (V_{tl}): $V \propto 2 \cdot V_{tl}$ and therefore: $\rho_{tl} \propto \frac{1}{2 \cdot V_{tl}} \rightarrow \rho_{tl} \propto \frac{2}{V}$.

Therefore, the interphases formed in the system will be highly dependent on the amount of material to be analyzed. This dependence makes it difficult to carry out the measurements using conventional calorimetry equipment, since it uses small amounts of samples, of the order of 10–20 mg, which do not favor the formation of the surface layer or its identification due to the resolution of the equipment.

Heat capacity: discussion. Heat capacity is a property that is well defined for gases and solids, but it lacks for a robust theory that describes the heat capacity of liquids^{8,27}. It is therefore an extremely complex task to describe this property in NFs, where an extra difficulty comes from the presence of interphase effects.

Based on the classical view, NFs can be understood as fluids confined at the nano-scale³³, in which a large number liquid-solid interfaces (LSIs) originate between the NPs surfaces and the fluid medium, where the heat transport properties become special and complex. When heat flows through the interphases between dissimilar media, a discontinuity in temperature occurs that is proportional to the thermal boundary resistance, or Kapitza resistance, due to the acoustic mismatch between the media in contact³⁴, as observed in the thermographs we obtained (see Fig. 1). Therefore, at the interphases generated due to the formation of the foamy top layer, the phonon distribution function is disturbed by interfacial dispersion. One of the effects that this phenomenon provokes in measurements taken with calorimetry equipment is the variation in the thermal resistance of the material, therefore requiring longer times to reach thermal equilibrium, as can be observed in our calorimetric results. The concentration, size and dispersion of the NPs is of great importance for the formation of LSIs. This is because by reducing the system to the nanoscale, the effects of quantum confinement come into play. Such states are generated by nanostructured surfaces, causing a change in the occurrence of surface phonon modes³⁵. Furthermore, liquid–solid interactions introduce stratification into the liquid near solid surfaces^{8,31}. This is corroborated by the FT-IR results showing a higher degree of crystallization of the atoms in the liquid in the presence of NPs. The distribution of atoms in the liquid around solid surfaces is highly influenced by the nano-pattern formed by the distribution of NPs within the liquid. This distribution affects the adsorption characteristics of the surfaces, favoring—or not—the rearrangement of the liquid¹⁹. Thus, with a low concentration of NPs and high dispersion, (preventing agglomeration), a nano-pattern is generated which favors the formation of vibrational

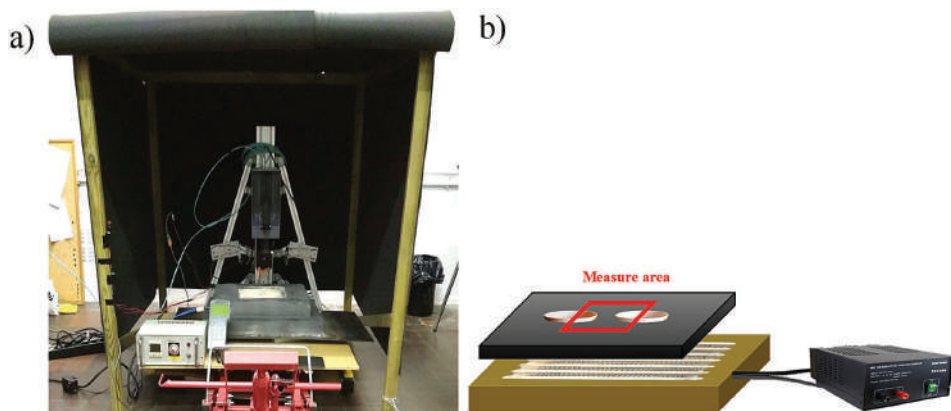


Figure 6. (a) Measurement system and (b) oven schematic representation and measurement area.

bands in surface modes (high SSA SiO_2). This is dependent on the formation of the surface layer and the degree of liquid–solid coupling.

To understand the effect that these phenomena have on thermodynamic properties such as heat capacity, we can consider its increase as being attributed to the entropic contribution resulting from the multiple micro-regions of high SSA formed in the surface layer. These micro-regions cause an increase in the number of degrees of freedom of the system and in the vibrational entropy of the surfaces, which leads to an increase in C_p . A schematic representation of the NF system is represented in Fig. 4. There are depicted the formation of the semi solid–liquid surface layer due to the atoms rearrangement around the nanoparticles surface and the two formed thermal boundaries: nanoparticles–surface layer–liquid.

Conclusions

This study demonstrates experimentally for the first time the main phenomena involved in the abnormal increase of C_p in NFs. It provides a more detailed and unified vision and explanation of this phenomenon that has been studied considerably over recent years. Using infrared thermography, we established that there are regions which exhibit high temperature gradients. These gradients stem from the formation of LSIs with high-energy vibrational modes. The presence of these new interphases is due to exothermic processes linked to the reactivity between the ionic medium and the nanoparticulate oxide. The formation of LSIs directly influences the increase in the heat capacity of the system, increasing the number of degrees of freedom and the vibrational entropy of the surfaces. Furthermore, the dependency we found between the weight of sample analyzed and the volume of the surface layer that is formed can explain the large deviations between the published results of calorimetric values.

The results obtained in this study open the doors to the possibility of optimizing NFs, with the possibility of being able to design systems with the required C_p for different applications. In addition to radically changing the way we understand NFs, and specifically their applicability, this study also represents a step forward towards being able to scale them up.

Materials and methods

Materials. Sodium nitrate (Sigma Aldrich, 99.995%) and silicon oxide NPs between 5 and 15 nm in diameter (Sigma-Aldrich, 99.5%) were used. The NFs formulated for this study contained 1 wt%, 3 wt% and 7 wt% NPs by weight.

Synthesis. To synthesize the materials the standard 1-step method was used, as it is the most straightforward and one of the most widely used for the synthesis of NFs³⁷. The method consisted of: (1) preparation of 50 g of sample; (2) dissolution of this in 30 ml of distilled water; (3) 10 min of sonication for correct dispersion and homogenization of the NPs throughout the base material; (4) evaporation of the solvent in an oven at 105 °C, until all the water had evaporated and the material recrystallized; and finally, (5) extraction of the sample and milling in an agate mortar.

Design and construction of the oven. *Materials.* Different materials were used to build the oven structure, including: a kaowool blanket, glass wool, refractory cement, refractory plates for resistances and high-temperature paint. For the electrical part we used a Kanthal A1 filament, a power supply, fans and five type K thermocouples. Samples were heated in sintered alumina crucibles.

Measurement system. The complete measurement system is shown in Fig. 6. It consisted of the following parts: the infrared camera, the oven, the control and measurement system, and the temperature output. There was also a ventilation and safety system. Finally, a black box was used to isolate the system from its surroundings.

Infrared characterization. A high-resolution infrared camera (InfraTec GmbH) with IRBIS 3.1 professional software (www.infratec.eu) was used to obtain the infrared thermography images. The camera's thermal resolution is 25 mK with an image resolution of $1,289 \times 1,024$ infrared pixels². The area sampled was 510×638 pixels² during 5.5 h per experiment. The thermographies were taken every 15 min lasting 40 s at a rate of 1,000 frames every 10 s (i.e., a total of 88,000 frames per experiment). The error associated to the temperature measure was obtained averaging 100 consecutive frames.

The first measurements were taken at room temperature (approximately 20 °C). Then, a heating gradient of 1 °C min⁻¹ was applied, up to approximately 340 °C (maximum camera temperature).

Thermal characterization. The values of the heat capacity and enthalpy of the system were obtained at temperatures between 200 °C and 360 °C, with a differential scanning calorimeter (DSC 822e Star3+, from Mettler Toledo). A constant flow of 50 mL min⁻¹ of nitrogen was applied to preserve an inert atmosphere. The method described by Ferrer et al.³⁸ was used to calculate C_p . The amount of sample analyzed was 10 mg, performed in 100 µL aluminum crucibles. These crucibles were used for safety reasons (i.e., to prevent the fluid from rising up the walls of the crucible due to capillary action). Finally, each value was given as the mean of measurements from 20 independent samples (20 replicates) with the associated standard deviation.

Characterization of chemical structure and composition. FT-IR spectroscopy with attenuated total reflectance sampling, FT-IR ATR (Spectrum Two™, PerkinElmer) was used to determine the chemical composition of the samples. The instrumental error was 4 cm⁻¹, and for each composition three independent samples were analyzed.

Received: 22 September 2020; Accepted: 5 February 2021

Published online: 01 March 2021

References

- Wagner, S. J. & Rubin, E. S. Economic implications of thermal energy storage for concentrated solar thermal power. *Renew. Energy* **61**, 81–95 (2014).
- Palacios, A., Barreneche, C., Navarro, M. E. & Ding, Y. Thermal energy storage technologies for concentrated solar power—a review from a materials perspective. *Renew. Energy* **156**, 1244–1265 (2020).
- Renewables 2019 Analysis and forecast to 2024*. (IEA, International Energy Agency, 2019).
- Singh, N. & Khullar, V. Efficient volumetric absorption solar thermal platforms employing thermally stable—solar selective nanofluids engineered from used engine oil. *Sci. Rep.* **9**, 1–12 (2019).
- Bocquet, L. Nanofluidics coming of age. *Nat. Mater.* **19**, 254–256 (2020).
- Zhu, D., Wang, L., Yu, W. & Xie, H. Intriguingly high thermal conductivity increment for CuO nanowires contained nanofluids with low viscosity. *Sci. Rep.* **8**, 1–12 (2018).
- Sezer, N., Atieh, M. A. & Koc, M. A comprehensive review on synthesis, stability, thermophysical properties, and characterization of nanofluids. *Powder Technol.* **344**, 404–431 (2018).
- Hassanloo, H., Sadeghzadeh, S. & Ahmadi, R. A new approach to dispersing and stabilizing graphene in aqueous nanofluids of enhanced efficiency of energy-systems. *Sci. Rep.* **10**, 1–11 (2020).
- Shahru, I. M., Mahbulul, I. M., Khaleduzzaman, S. S., Saidur, R. & Sabri, M. F. M. A comparative review on the specific heat of nanofluids for energy perspective. *Renew. Sustain. Energy Rev.* **38**, 88–98 (2014).
- Verma, S. K. & Tiwari, A. K. Progress of nanofluid application in solar collectors: a review. *Energy Convers. Manag.* **100**, 324–346 (2015).
- Sui, J., Zheng, L., Zhang, X., Chen, Y. & Cheng, Z. A novel equivalent agglomeration model for heat conduction enhancement in nanofluids. *Sci. Rep.* **6**, 1–9 (2016).
- Carrillo-Berdugo, I. et al. Interface-inspired formulation and molecular-level perspectives on heat conduction and energy storage of nanofluids. *Sci. Rep.* **9**, 1–13 (2019).
- Engelmann, S. & Hentschke, R. Specific heat capacity enhancement studied in silica doped potassium nitrate via molecular dynamics simulation. *Sci. Rep.* **9**, 1–14 (2019).
- Wang, X. J., Li, X. F., Xu, Y. H. & Zhu, D. S. Thermal energy storage characteristics of Cu-H₂O nanofluids. *Energy* **78**, 212–217 (2014).
- Jackson, R. G. et al. Effect of surface wettability on carbon nanotube water-based nanofluid droplet impingement heat transfer. *J. Phys. Conf. Ser.* **525** (2014).
- Zaaroura, I. et al. Evaporation of nanofluid sessile drops: Infrared and acoustic methods to track the dynamic deposition of copper oxide nanoparticles. *Int. J. Heat Mass Transf.* **127**, 1168–1177 (2018).
- Teja, A. S. Simple method for the calculation of heat capacities of liquid mixtures. *J. Chem. Eng. Data* **28**, 83–85 (1983).
- Barrat, J. & Chiaruttini, F. Kapitza resistance at the liquid—solid interface. *Mol. Phys.* **101**, 1605–1610 (2003).
- Issa, K. M. & Mohamad, A. A. Lowering liquid-solid interfacial thermal resistance with nanopatterned surfaces. *Phys. Rev. E Stat Nonlinear Soft Matter Phys.* **85**, 3–7 (2012).
- Hernández-Paredes, J., Glossman-Mitnik, D., Esparza-Ponce, H. E., Alvarez-Ramos, M. E. & Duarte-Moller, A. Band structure, optical properties and infrared spectrum of glycine-sodium nitrate crystal. *J. Mol. Struct.* **875**, 295–301 (2008).
- Trivedi, M. K. & Dahryn Trivedi, A. B. Spectroscopic characterization of disodium hydrogen orthophosphate and sodium nitrate after biofield treatment. *J. Chromatogr. Sep. Tech.* **06** (2015).
- Wu, F. M., Wang, X. W., Pang, S. F. & Zhang, Y. H. Measuring hygroscopicity of internally mixed NaNO₃ and glutaric acid particles by vacuum FTIR. *Spectrochim. Acta A Mol. Biomol. Spectrosc.* **219**, 104–109 (2019).
- Ram, S. Electronic Raman and fluorescence spectroscopic studies of Eu³⁺-doped A₂SO₄ · xH₂O sulphates. *J. Raman Spectrosc.* **18**, 537–548 (1987).
- Hollenstein, C. et al. Silicon oxide particle formation in RF plasmas investigated by infrared absorption spectroscopy and mass spectrometry. *J. Phys. D. Appl. Phys.* **31**, 74–84 (1998).
- Kansal, I. et al. Structure, biodegradation behavior and cytotoxicity of alkali-containing alkaline-earth phosphosilicate glasses. *Mater. Sci. Eng. C* **44**, 159–165 (2014).
- Zheng, Z., Li, Y., Zhang, Z. & Ma, X. The impacts of sodium nitrate on hydration and microstructure of Portland cement and the leaching behavior of Sr²⁺. *J. Hazard. Mater.* **388** (2020).
- Feifel, S. C. & Lisdaf, F. Silica nanoparticles for the layer-by-layer assembly of fully electro-active cytochrome c multilayers. *J. Nanobiotechnology* **9**, 59 (2011).

28. Lusvardi, G., Malavasi, G., Menabue, L., Aina, V. & Morterra, C. Fluoride-containing bioactive glasses: surface reactivity in simulated body fluids solutions. *Acta Biomater.* **5**, 3548–3562 (2009).
29. Mondragón, R., Juliá, J. E., Cabedo, L. & Navarrete, N. On the relationship between the specific heat enhancement of salt-based nanofluids and the ionic exchange capacity of nanoparticles. *Sci. Rep.* **8**, 1–12 (2018).
30. Nandasiri, M. I. *et al.* Increased thermal conductivity in metal-organic heat carrier nanofluids. *Sci. Rep.* **6**, 2–9 (2016).
31. Svobodova-Sedlackova, A., Barreneche, C., Alonso, G., Fernandez, A. I. & Gamallo, P. Effect of nanoparticles in molten salts—MD simulations and experimental study. *Renew. Energy* **152**, 208–216 (2020).
32. Bolmatov, D., Brazhkin, V. V. & Trachenko, K. The phonon theory of liquid thermodynamics. 1–6 (2012) <https://doi.org/10.1038/srep00421>.
33. Alosious, S., Kannam, S. K., Sathian, S. P. & Todd, B. D. Prediction of Kapitza resistance at fluid-solid interfaces. *J. Chem. Phys.* **151**, 194502 (2019).
34. Meilakhs, A. P., Semak, B. V. & Model, D. M. Calculation of Kapitza resistance with kinetic equation. (2019).
35. Ashby, M. F., Ferreira, P. J. & Schodek, D. L. *Nanomaterials, Nanotechnologies and Design. An Introduction for Engineers and Architects* (Butterworth-Heinemann, Oxford, 2009). <https://doi.org/10.1016/B978-0-7506-8149-0.X0001-3>.
36. Wasan, D. T. & Nikolov, A. D. Spreading of nanofluids on solids. *Lett. Nat.* **423**, 156–159 (2003).
37. Navarrete, N., Hernández, L., Vela, A. & Mondragón, R. Influence of the production method on the thermophysical properties of high temperature molten salt-based nanofluids. *J. Mol. Liq.* **302**, 112570 (2020).
38. Ferrer, G., Barreneche, C., Solé, A., Martorell, I. & Cabeza, L. F. New proposed methodology for specific heat capacity determination of materials for thermal energy storage (TES) by DSC. *J. Energy Storage* **11**, 1–6 (2017).

Acknowledgements

The research leading to these results is partially funded by the Spanish government RTI2018-093849-B-C32, RTI2018-094757-BI00, MDM-2017-0767, MCIU/AEI/FEDER, UE and MAT2016-75823-R. The authors would like to thank the Catalan Government for the quality accreditation given to their research groups DIOPMA (2017 SGR 118) and CMSL (2017 SGR 13). A.S thanks to Generalitat de Catalunya for her Grant FI-DGR 2018. Finally, P.G. thanks Generalitat de Catalunya for his Serra Hünter Associate Professorship.

Author contributions

A.S and A.C designed the experiments and device development. A.S performed the experiments and data analysis. A.I.F, C.B and P.G oversaw the research project. All authors discussed the results. Finally, all authors have supervised the final version of this manuscript.

Competing interests

The authors declare no competing interests.

Additional information

Correspondence and requests for materials should be addressed to A.I.F.

Reprints and permissions information is available at www.nature.com/reprints.

Publisher's note Springer Nature remains neutral with regard to jurisdictional claims in published maps and institutional affiliations.

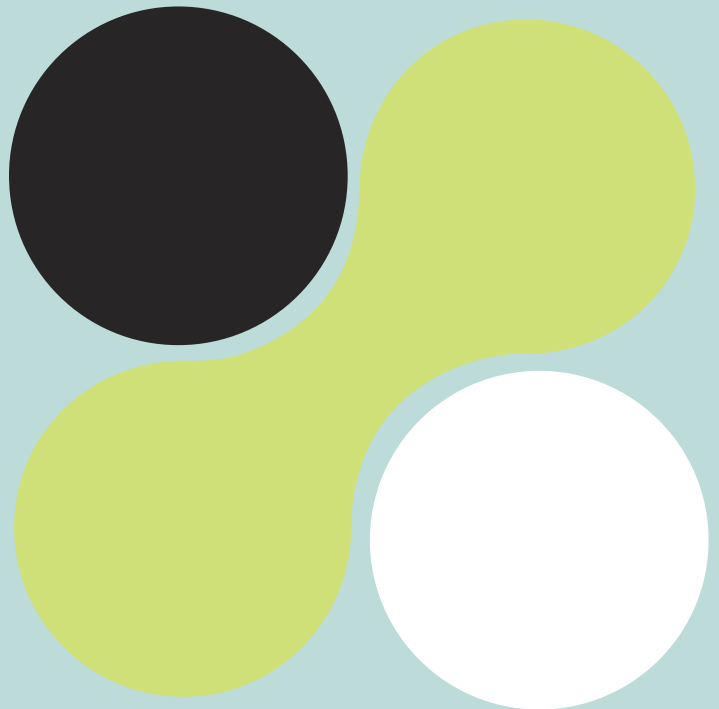


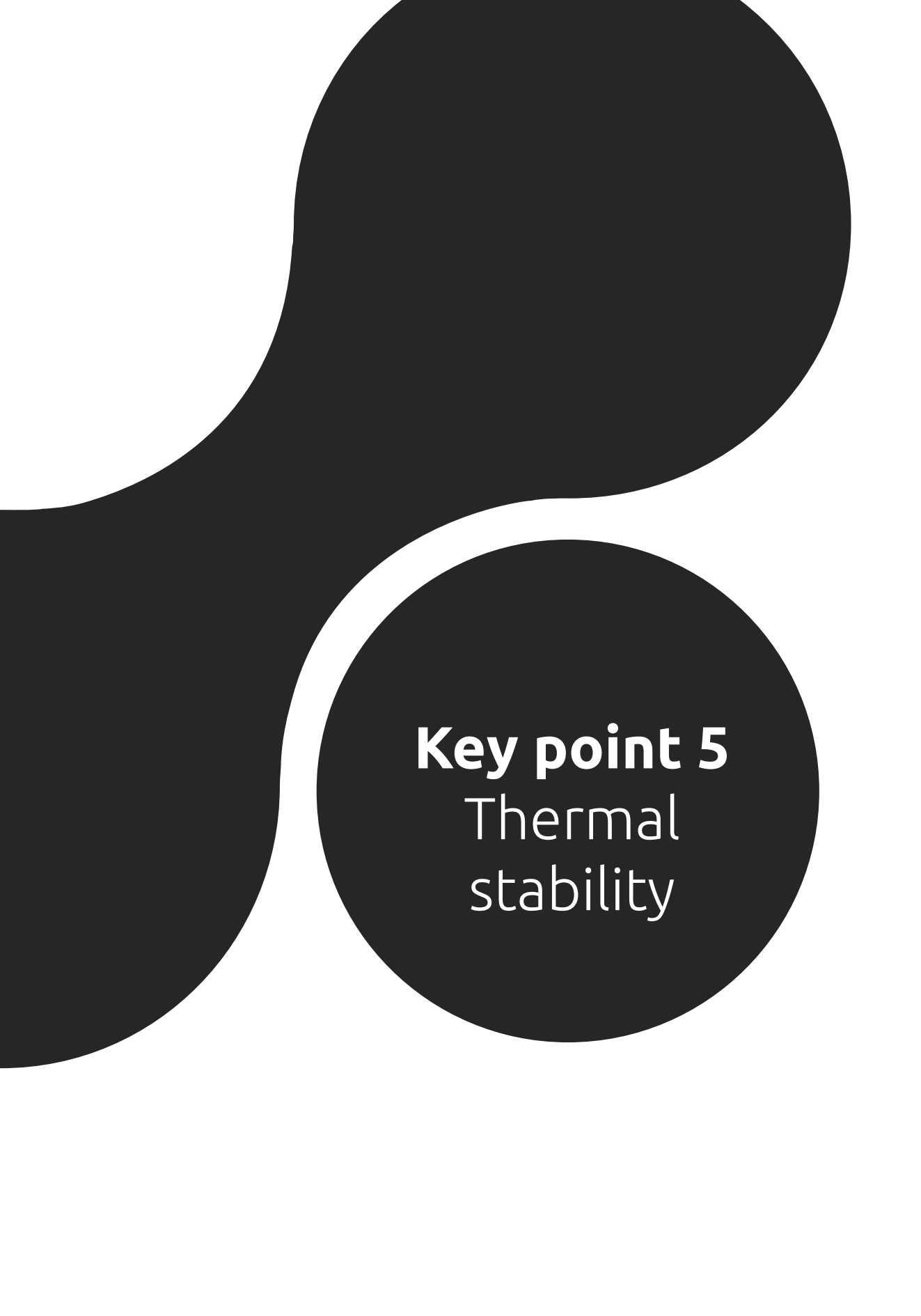
Open Access This article is licensed under a Creative Commons Attribution 4.0 International License, which permits use, sharing, adaptation, distribution and reproduction in any medium or format, as long as you give appropriate credit to the original author(s) and the source, provide a link to the Creative Commons licence, and indicate if changes were made. The images or other third party material in this article are included in the article's Creative Commons licence, unless indicated otherwise in a credit line to the material. If material is not included in the article's Creative Commons licence and your intended use is not permitted by statutory regulation or exceeds the permitted use, you will need to obtain permission directly from the copyright holder. To view a copy of this licence, visit <http://creativecommons.org/licenses/by/4.0/>.

© The Author(s) 2021

Thermal stability of
nitrate salt-based
nanofluids

Paper 6





Key point 5
Thermal
stability

10. Thermal stability of nitrate salt-based nanofluids

A relevant parameter in CSP TES systems

10.1 Introduction

Throughout the previous chapters, it has been possible to deepen fundamental questions related to the behaviour of nanofluids based on molten salts, especially in the phenomena that control the modification of the specific heat capacity. Instead, this chapter will focus on the thermal stability of MSBNFs for its application in thermal storage systems for CSP.

Previously, some of the parameters related to the TES material that influence storage efficiency were described. Some of these parameters are:

1. High operational temperature range: Low melting/solidification temperature and high-temperature stability.
2. High and uniform Specific Heat capacity with temperature.
3. High thermal conductivity (quick changing-discharging cycles).
4. Minimal supercooling.
5. Low price and widely available.
6. High thermal, chemical and cyclic stability.
7. Non-flammable, non-toxic, non-corrosive, and low vapour pressure.

Apart from knowing the thermophysical properties of MSBNFs, to assess their impact and suitability as TES medium, it is essential to study their working temperature ranges.

These parameters have been addressed on a study that evaluates the

thermal stability of NSBNFs with different types of nanoparticles. As in the previous chapters, the selection of these salts is made to reduce the number of variables of the system.

One of the main limitations of nitrate salts is their low stability temperature, causing decomposition to nitrites which causes damage to system components. Therefore, the effect of nanoparticles on the nitrite's formation in the temperature range between room temperature and 500 °C is evaluated. Secondly, through a thermogravimetric study, the effect of nanoparticles on the decomposition kinetics is evaluated up to high temperatures (900°C).

10.1.1 Relevance

The relevance of the study presented in this chapter lies in evaluating critical parameters for implementing MSBNFs in TES systems for CSP. With nanofluids thermally stable and operating in higher temperature ranges, the efficiency of the Rankine cycle can be increased and, therefore, the general efficiency of the storage system. On the

other hand, one of the most relevant points for advancing the research is to dispose of reliable thermophysical values **in-service**, since the literature offers poor information. Therefore, this chapter tries to provide more objective values for the industry and contributes to **key point V**.

10.1.2 Objectives

The main objectives of this chapter are the following:

- Study the effect of different types of nanoparticles with 1 wt% on the formation of nitrites.
- Determination of the thermal stability of NSBNFs with different types of nanoparticles with 1 wt%.
- Study of the effect of nanoparticles on decomposition kinetics.

10.2 Paper 6

The complete study is accepted in the journal of Nanomaterials from MPDI group, entitled “*Effect of nanoparticles on the thermal stability and reaction kinetics in ionic nanofluids*” since 17th May 2022, as shown in **Figure 10.1**.

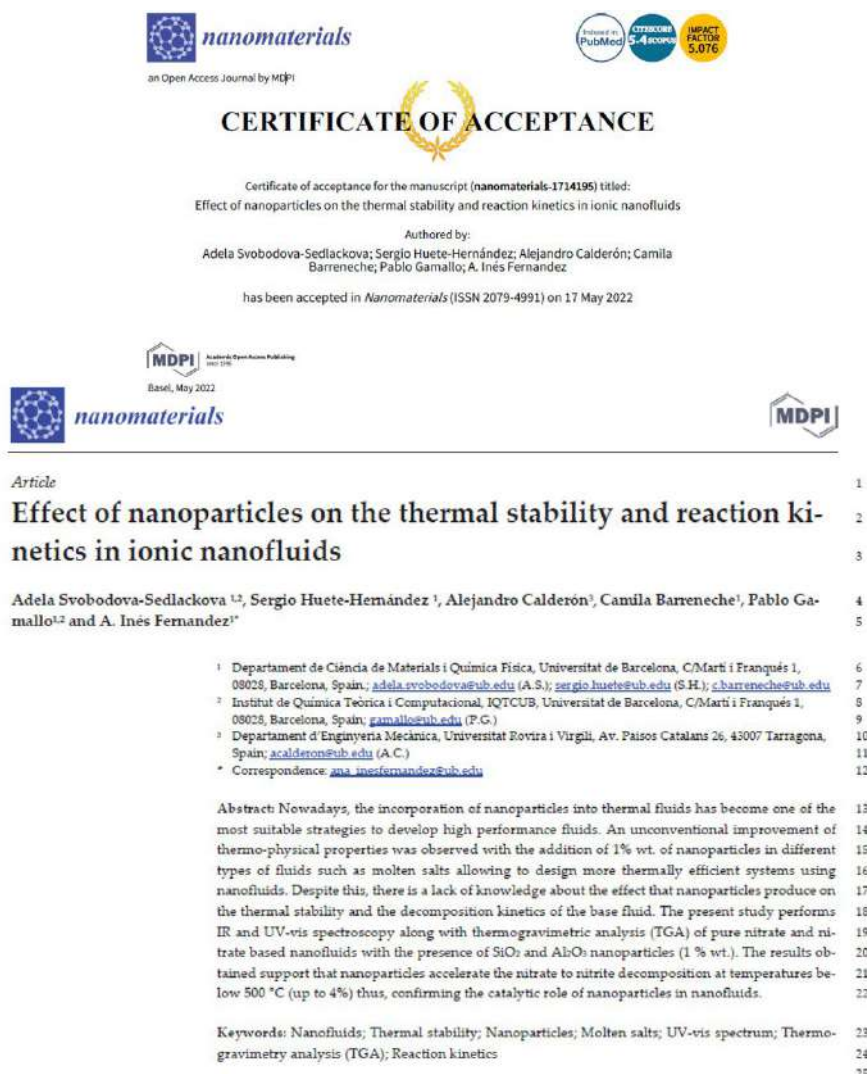


Figure 10.1. Article accepted in nanomaterials journal (MPDI), entitled “*Effect of nanoparticles on the thermal stability and reaction kinetics in ionic nanofluids*”.

10.2.1 Graphical Abstract

Figure 10.2 summarizes the most relevant results.

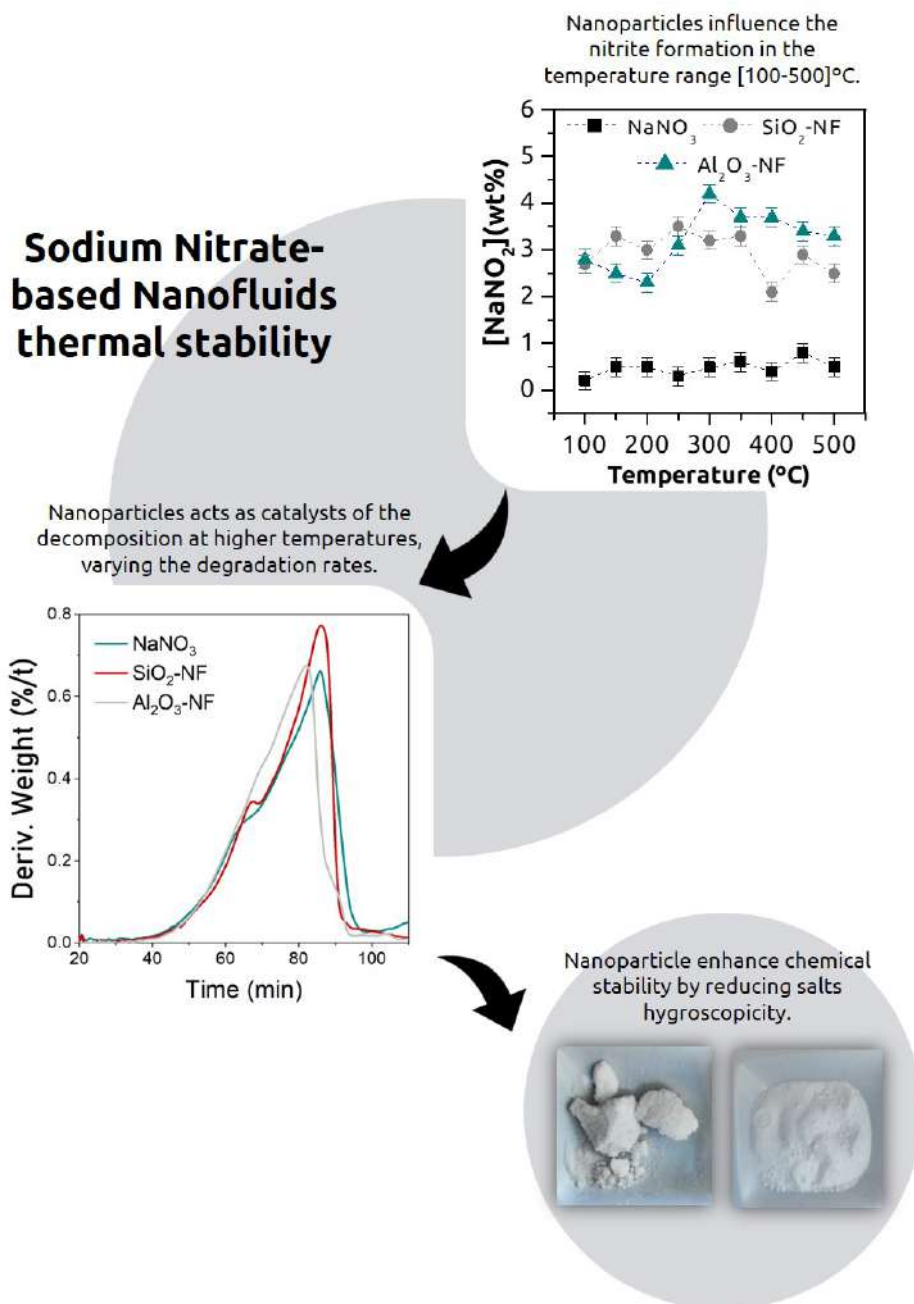


Figure 10.2. Graphical Abstract of the article entitled “Effect of nanoparticles on the thermal stability and reaction kinetic of nitrate molten salt-based nanofluids”.

10.2.2 Contribution to the state of the art

Key point 5 Thermal stability

There are no clear trends in the effect of nanoparticles on the thermal stability of MSBNFs.

Lack of information on the stability of the properties under working conditions in CSP.

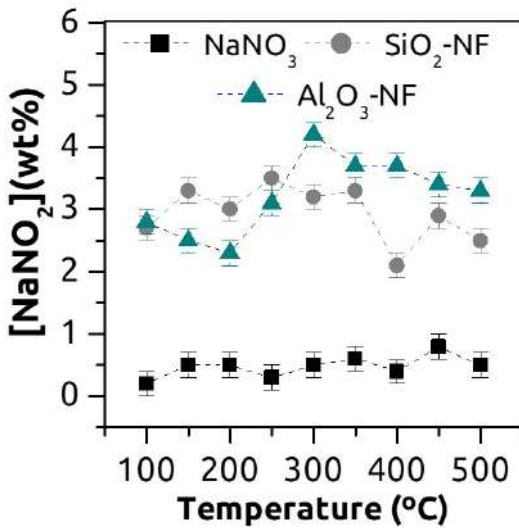


Figure 10.3. Nitrite concentration as a function of temperature for pure NaNO_3 and Nitrate-based nanofluids with 1 wt% of SiO_2 and Al_2O_3 nanoparticles.

- ✓ Through UV-Vis and FTIR spectroscopy, the nitrite concentration was monitored from room temperature to 500°C. NSBNFs between this temperature range show the more significant nitrites formation, up to 4% in front of pure sodium nitrate (up to 0.8%), **Figure 10.3**. Already, the results indicate an influence in the chemical degradation due to the nature of the nanoparticles, the more alkaline NPs, the greater variation in absorbance for the temperature range.

- ✓ SiO_2 and Al_2O_3 nanoparticles increase nanofluids' thermal stability above 600°C before starting to decompose. In addition, with Al_2O_3 nanoparticles, weight loss at 900°C was about 6% lower than NaNO_3 , **Figure 10.4**.

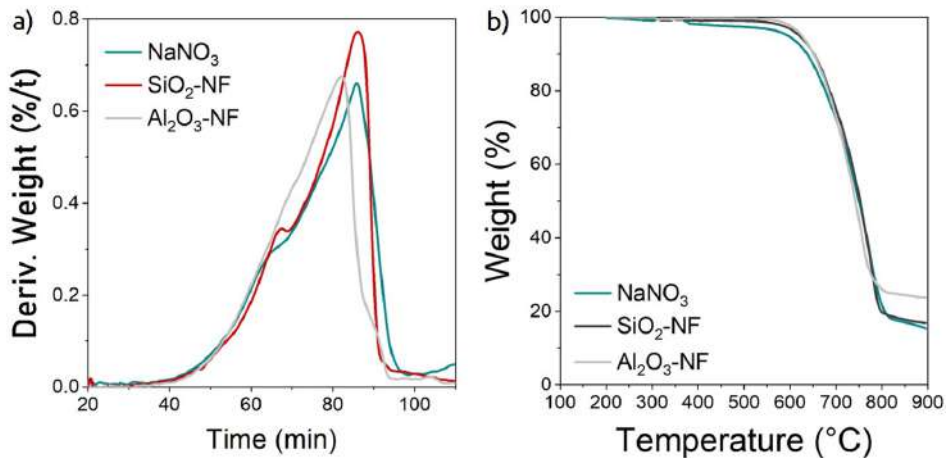


Figure 10.4. TGA measurement from 100 to 900°C of NaNO₃, and NaNO₃/SiO₂, NaNO₃/Al₂O₃ NFs with 1 wt% of NPs: a) weight loss as a function of temperature and, b) weight derivative as a function of time.

- ✓ The presence of nanoparticles alters the decomposition stages. First, SiO₂ and Al₂O₃ nanoparticles reduce the decomposition temperatures of NaNO₃-NaNO₂-Na₂O₂ up to 7°C. Even so, the reactions involved were accelerated by the presence of nanoparticles. Particularly, SiO₂ NPs accelerate the reactions more than Al₂O₃ NPs. Second, the final decomposition to Na₂O occurs at higher temperatures (up to 14 °C) than pure NaNO₃.
- ✓ The presence of nanoparticles helps to prevent humidity absorption, contributing to its higher chemical stability with lower hygroscopicity.
- ✓ Given these results, the nanoparticles act as a catalyst for the reactions. However, at temperatures above 500°C, nanofluids exhibit higher thermal stability than pure NaNO₃ despite the slight increase in nitrite concentration. Therefore, the results contribute to **key point V**, offering reliable nanofluids' thermal stability data.

10.2.3 Publication

The article is attached below.

Effect of nanoparticles on the thermal stability and reaction kinetics in ionic nanofluids

Adela Svobodova-Sedlackova^{1,2}, Sergio Huete-Hernández¹, Alejandro Calderón³, Camila Barreneche¹, Pablo Gamallo^{1,2} and A. Inés Fernández*

¹ Departament de Ciència de Materials i Química Física, Universitat de Barcelona, C/Martí i Franqués 1, 08028, Barcelona, Spain; adela.svobodova@ub.edu (A.S.); sergio.huete@ub.edu (S.H.); c.barreneche@ub.edu

² Institut de Química Teòrica i Computacional, IQTCUB, Universitat de Barcelona, C/Martí i Franqués 1, 08028, Barcelona, Spain; gamallo@ub.edu (P.G.)

³ Departament d'Enginyeria Mecànica, Universitat Rovira i Virgili, Av. Paisos Catalans 26, 43007 Tarragona, Spain; acalderon@ub.edu (A.C.)

* Correspondence: ana_inesfernandez@ub.edu

Abstract: Nowadays, the incorporation of nanoparticles into thermal fluids has become one of the most suitable strategies to develop high performance fluids. An unconventional improvement of thermo-physical properties was observed with the addition of 1% wt. of nanoparticles in different types of fluids such as molten salts allowing to design more thermally efficient systems using nanofluids. Despite this, there is a lack of knowledge about the effect that nanoparticles produce on the thermal stability and the decomposition kinetics of the base fluid. The present study performs IR and UV-vis spectroscopy along with thermogravimetric analysis (TGA) of pure nitrate and nitrate based nanofluids with the presence of SiO₂ and Al₂O₃ nanoparticles (1 % wt.). The results obtained support that nanoparticles accelerate the nitrate to nitrite decomposition at temperatures below 500 °C (up to 4%) thus, confirming the catalytic role of nanoparticles in nanofluids.

Keywords: Nanofluids; Thermal stability; Nanoparticles; Molten salts; UV-vis spectrum; Thermogravimetry analysis (TGA); Reaction kinetics

Citation: Lastname, F.; Lastname, F.;

Lastname, F. Title. *Nanomaterials*

2022, 12, x.

<https://doi.org/10.3390/xxxxx>

Academic Editor: Firstname Lastname

Received: date

Accepted: date

Published: date

Publisher's Note: MDPI stays neutral with regard to jurisdictional claims in published maps and institutional affiliations.



Copyright: © 2022 by the authors. Submitted for possible open access publication under the terms and conditions of the Creative Commons Attribution (CC BY) license (<https://creativecommons.org/licenses/by/4.0/>).

1. Introduction

The incorporation of suspended nanoparticles (NPs) into a fluid has become a suitable strategy for improving the thermo-physical properties of fluids. This concept, defined as a nanofluid (NF), was first introduced in 1995 by Choi et al. [1], who showed that the thermal conductivity of water and ethylene glycol increased by adding Al₂O₃ or CuO NPs. Since then, many efforts have been devoted to the development of NFs and also to the understanding of some exceptional properties exhibited by them [2,3]. More precisely, one of the aspects that attracted the scientific interest is the abnormal improvement of the specific heat capacity (C_p) observed in NFs. Thus, a large number of publications indicate C_p increments up to 40% when low concentrations of NPs are incorporated into the fluid [4], around 1% wt. According to this and to the fact that material's energy density is determined by the product of C_p and the fluid density, the heat capacity becomes one of the most relevant design parameters in industrial applications allowing to reach more compact and effective heat transfer systems using NFs. Consequently, NFs open the door to the next generation of heat transfer fluids (HTF) with better thermal performance than the traditional fluids such as water, oils, molten salts or ethylene glycol, solving their relatively poor heat transfer characteristics. In the last years, NFs have been incorporated in many applications such as solar energy [5][6], geothermal [7], heat exchange [7], oil recovery [8,9], lubricants [10], [11], refrigeration [12], desalination [13] or CO₂ capture [14], among others.

Specifically, the incorporation of NFs as a thermal energy storage (TES) medium in concentrate solar power (CSP) plants would improve the storage efficiency and thus, it may contribute to the possibility of reducing the volume of the storage tanks, involving an important material cost reduction [15–17]. Molten salts and particularly, solar salt (*i.e.*, a eutectic mixture of sodium and potassium nitrate) was the most commercially used TES material in CSP plants. Molten salt-based NFs are widely studied in the literature [18]–[21], showing a high C_p enhancement. For example, Y. Huang et al., [22] report C_p enhancements up to 168% after adding MgO NPs into the solar salt. However, the majority of publications report C_p enhancements up to 30% adding NPs at different concentrations into molten salts systems like $\text{Li}_2\text{CO}_3/\text{K}_2\text{CO}_3 + 1\%$ wt. SiO_2 [23], $\text{NaNO}_3/\text{KNO}_3 + 0.8\%$ wt. Al_2O_3 [24], $\text{KNO}_3/\text{NaNO}_2/\text{NaNO}_3 + 0.07\%$ wt. Al_2O_3 [25], $\text{NaNO}_3 + 1\%$ wt. SiO_2 [26] and $\text{Ca}(\text{NO}_3)_2/\text{KNO}_3/\text{NaNO}_3/\text{LiNO}_3 + 0.5\%$ wt. SiO_2 [27], among others. Nevertheless, some studies show just the opposite trend [28]–[30]. It is the case of the studies carried out by Q. Xie et al., [31], M. A. Hassan et al., [32] or M. C. Lu et al., [33], in which a decrease in C_p was reported by the addition of NPs in molten salts. Hence, there are no clear trends regarding the effect of C_p enhancement due to the addition of nanoparticles in the heat transfer fluid.

Moreover, another relevant parameter for the implementation of NFs in industrial applications is their thermal stability (*i.e.*, solar salts for TES in CSP stations work between 250°C - 400°C). Pramod et al., [34] demonstrated that NPs in molten salts help to improve their thermal stability. Contrarily, no significant changes were observed by P. Myers et al., [35] and P. Andreu-Cabedo et al., [36] adding CuO or SiO_2 NPs into molten salts, respectively. The thermal stability of solar salts (eutectic mixture of NaNO_3 (60%)- KNO_3 (40%)) is directly related to the nitrate-nitrite conversion; therefore, more precise experiments are needed to understand the effect of NPs on the kinetics of the thermal decomposition. Likewise, monitoring the decomposition rate of nitrates (*i.e.*, nitrites formation) is essential to control the NF's stability as the nitrite formation contributes to salt decomposition and to increase corrosion rates in the storage systems. This aspect is very relevant due to the high corrosion caused by salts in the metallic components of CSP facilities [29–31].

This work aims at studying the effect of introducing NPs in the sodium nitrate salt thermal stability. For this propose, IR and UV spectroscopic techniques have been used for determining the nitrite concentration in aqueous solution in the temperature range from 100°C to 500°C. Furthermore, thermogravimetric analysis was performed to study the weight loss, temperature decomposition and reaction kinetics through representative samples of two types of NaNO_3 based NFs ($\text{NaNO}_3 + 1\%$ wt. SiO_2 and $\text{NaNO}_3 + 1\%$ wt. Al_2O_3) in the same range of temperatures for evaluating the degree of nitrites formation and the temperature stability of the samples. Other techniques like electron microscopy were also used for characterizing the NPs.

2. Materials and Methods

2.1. Nanofluids sample's preparation

NaNO_3 used to synthesize the NFs was Sigma Aldrich (99.995%), spherical SiO_2 and Al_2O_3 NPs of 5–15 nm and 13 nm, respectively, of nominal diameter (both Sigma Aldrich, 99.5%). The synthesis of the NFs were carried out through the following six steps (described in Figure 1): (1) weighting of NaNO_3 and 1% of NPs (wt./wt.); (2) dissolving the mixture in 20 mL of distilled water; (3) sonicating during 20 minutes for a correct dispersion and homogenization of NPs in the solution; (4) drying in an oven at 105°C until complete water evaporation and salt recrystallization; (5) grinding in an Agatha mortar; and (6) obtaining a representative sample by following the quartering standard methodology [40] with a hand-made riffle-splitter suitable for tiny amounts of sample.

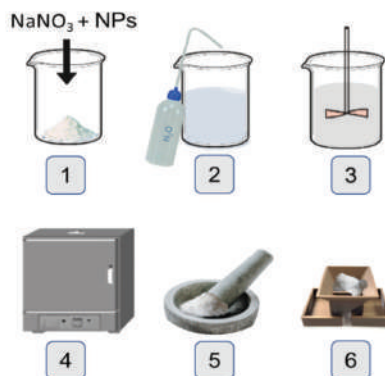


Figure 1. Schematic representation of the two-step nanofluid synthesis.

2.2. Transmission electron microscopy

A transmission electron microscope (TEM) JEOL JEM 2100 (JEOL, JAPAN) was employed to characterize the NPs. To proceed, NPs were dispersed in ethanol and sonicated by ultrasonic bath to avoid agglomeration.

2.3. UV-Spectroscopy

An UV-Vis Spectrophotometer Shimadzu UV-1280 (Shimadzu, Japan) was employed to measure the absorbance and quantify the nitrites ion concentration (i.e., $[\text{NO}_2^-]$). The absorbance measurements were performed in the wavelength range between 230 to 600 nm. For this purpose, 10 independent samples were synthesized for each type of NP into pure sodium nitrate. First, each sample was subjected to different thermal treatments in a furnace at room temperature and then, heated at intervals of 50°C from in a temperature range between 50°C and 500°C. For each temperature, the sample was left in the furnace for around 30 minutes to ensure a homogeneous temperature of the sample. Subsequently, the samples were cooled into liquid nitrogen to freeze the structure at each temperature. After the thermal treatment, 0.3 M solutions were prepared by dissolving the samples in deionized water. Moreover, 0.3 M sodium nitrate samples with different concentrations of sodium nitrite (2.5%, 5%, 12.5% and 25% and 100% wt.) were prepared for the nitrite calibration. The measurement uncertainty in the absorbance values was ± 0.001 in arbitrary units.

2.4. Thermogravimetric analysis

To perform the thermogravimetric and differential thermogravimetric analysis (TG/DTG), a Q-600 SDT TA Instruments (TA instruments, United States) was used. Measurements were conducted from 30°C to 900°C at a heating rate of 10°C·min⁻¹ in air atmosphere with a gas flow of 100 mL·min⁻¹. Each sample was prepared in standard aluminum crucibles with around 11 mg wt. Uncertainties were 0.5°C for temperature, 1% for weight loss and 0.01% for mass.

2.5. pH

A pH and ion-meter GLP 22 of Crison (Crison Instruments, Spain) was employed to measure the pH of the samples at room temperature ($29.5 \pm 0.2^\circ\text{C}$) with an uncertainty of 1%.

2.6. FT-IR Spectroscopy

Fourier Transform Infrared Spectroscopy with Attenuated Total Reflectance (FT-IR ATR) technique with a spectrometer TwoTM by PerkinElmer (PerkinElmer, United States) was used to determine the chemical composition. The instrumental error associated to the measure was 4 cm^{-1} .

3. Results

3.1. Nanoparticle's characterization

The size and the concentration of the NPs are important parameters that govern the NF performance [33,34]. The characterization of the nanoparticles has been done through pure samples electronic microscopy. Thus, Figure 2 shows TEM images of the SiO_2 and Al_2O_3 NPs. The silicon oxide NPs exhibit a higher degree of sintering forming agglomerates of even more than one micrometer (Figure 2a,b). The SiO_2 nanoparticles length and width were around: $(12 \times 25)\text{ nm}^2$. On the contrary, alumina NPs have a nominal diameter in the range $10.8 - 12.3\text{ nm}$ (Figure 2c,d).

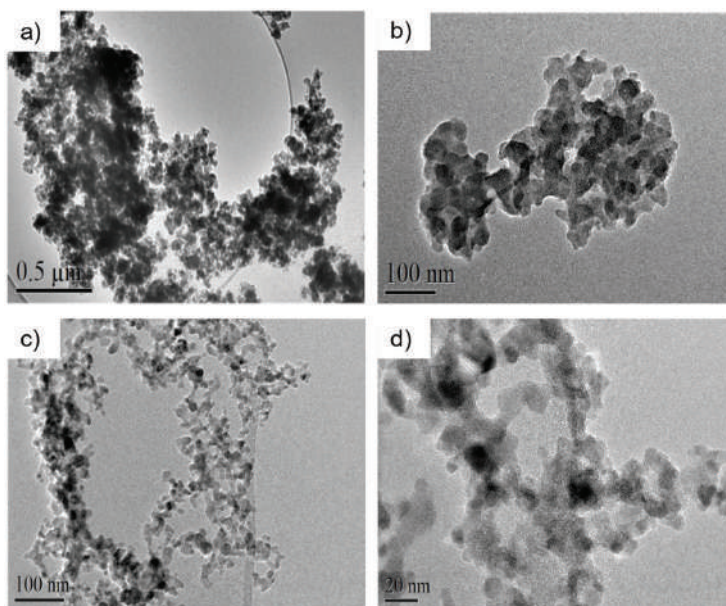


Figure 2. TEM images at different magnifications for SiO_2 , a-b), and Al_2O_3 nanoparticles, c-d).

3.2. Nitrite determination

Indirect methods based on UV and visible spectroscopy allow quantifying the nitrite concentration with an excellent limit of detection [35,36]. The UV-Vis absorption spectra were performed to $\text{NaNO}_3/\text{NaNO}_2$ mixtures samples for $0.3\ \text{M}$ (in deionized water) at 2.5%, 5%, 12.5% and 25% wt. in NaNO_2 concentration. Figure 3. The characteristic absorption peaks for $[\text{NO}_2^-]$ and $[\text{NO}_3^-]$ ions were found at $354\ \text{nm}$ and $300\ \text{nm}$, respectively [36,37]. The most interesting result is the increase observed in the nitrite peak as the concentration increases from 2.5% to 25% wt., Figure 3a. The absorbance of nitrite peaks as a

function of concentration (Figure 3b) exhibits a perfect linear trend with $R=0.99782$, $a=0.19999 \pm 0.01013$ (intersection) and $b=0.0706 \pm 0.00165$ (slope) with a good accuracy, $\sigma = \pm 0.2$.

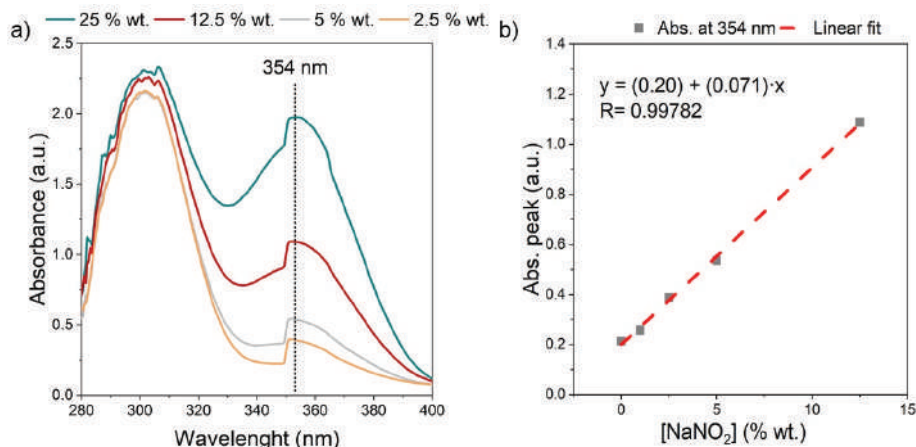


Figure 3. UV-vis spectra of 0.3M sodium nitrate-nitrite solutions: a) evolution of nitrite peak with the concentration of NaNO₂, from 2.5 to 25% wt. in NaNO₃ solution, b) linear relationship between light absorption and the concentration of nitrites at wavelength of 354 nm.

Samples exposed to different thermal treatments, from room temperature to 500°C and then, cooled in liquid N₂ to freeze the structure at each temperature. Figure 4 shows the temperature evolution of the UV-Vis spectrum of pure 0.3 M NaNO₃ (Figure 4a), 0.3 M NaNO₃/SiO₂ NF (Figure 4b), and 0.3 M NaNO₃/Al₂O₃ NF (Figure 4c). Moreover, for each spectrum the absorbance intensity at 354 nm was determined (grey line). For the pure NaNO₃ and the two formulated NFs an intensity difference in the nitrite peak with temperature was observed. Thus, Table 1 summarizes all the absorbance intensities at 354 nm as a function of the temperature. Additionally, for each value, the predicted NaNO₂ concentration was determined by the linear fit of Figure 3b. Both formulated NFs show a slight increase in the concentration of NaNO₂ (absorbance of 0.378 and 0.434 for SiO₂ and Al₂O₃ NPs at 1% wt. at 50°C) in front of the pure NaNO₃ (absorbance of 0.232 at 50°C) caused by the presence of NPs. Therefore, the NPs modify the reaction kinetics of NaNO₃ decomposition in the temperature range explored. Moreover, Al₂O₃ NPs accelerate the nitrate-nitrite conversion even more than the SiO₂ NPs. This fact indicates that the nature of the NPs influences the chemical degradation of NFs; thus, the more alkaline NPs (Al₂O₃ > SiO₂) the greater variation in absorbance for the temperature range. However, it is remarkable that the maximum concentration of NaNO₂ was around 300°C for the two NFs. Despite this, it is noteworthy that the maximum NaNO₂ concentration was less than $4 \pm 0.2\%$ for the two NFs and less than $0.8 \pm 0.2\%$ for the pure NaNO₃, Figure 5.

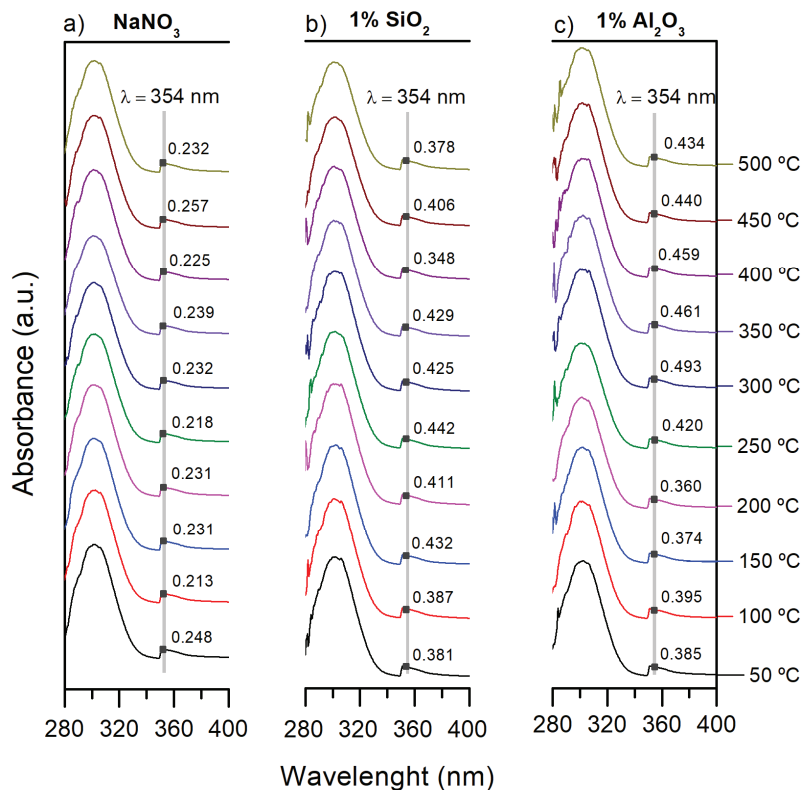


Figure 4. UV-vis absorption spectra of samples after the thermal treatment from 50°C to 500°C: a) pure 0.3M NaNO₃, b) 0.3M NaNO₃/SiO₂ NF (1% wt.) and c) 0.3M NaNO₃/Al₂O₃ NF (1% wt.).

Table 1. Nitrite concentration (% wt.) in pure 0.3M NaNO₃, 0.3M NaNO₃/SiO₂ NF (1% wt.) and 0.3M NaNO₃/Al₂O₃ NF (1% wt.) derived from the absorbance (arbitrary units) at 354 nm as a function of temperature from 100°C to 500°C.

Sample	NaNO ₃		NaNO ₃ /SiO ₂ NF		NaNO ₃ /Al ₂ O ₃ NF	
	Abs. at 354 nm a.u ± 0.001	[NaNO ₂] % wt. ± 0.2	Abs. at 354 nm a.u ± 0.001	[NaNO ₂] % wt. ± 0.2	Abs. at 354 nm a.u ± 0.001	[NaNO ₂] % wt. ± 0.2
Temperature (°C)						
100	0.213	0.2	0.387	2.6	0.395	2.7
150	0.231	0.4	0.432	3.3	0.374	2.5
200	0.232	0.5	0.411	3.0	0.360	2.3
250	0.218	0.3	0.442	3.4	0.420	3.1
300	0.232	0.5	0.425	3.2	0.493	4.1
350	0.239	0.5	0.429	3.2	0.461	3.7
400	0.225	0.4	0.348	2.1	0.459	3.6
450	0.257	0.8	0.406	2.9	0.440	3.4
500	0.232	0.5	0.378	2.5	0.434	3.3

193

194
195

196

197
198
199

200
201

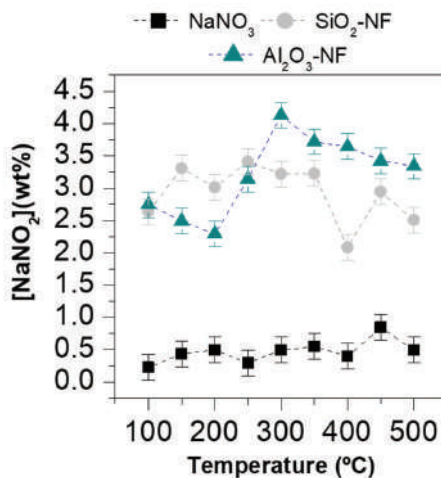


Figure 5. Nitrite concentration [NaNO₂] as a function of temperature from 100°C to 500°C for pure 0.3M NaNO₃ (black symbols), 0.3M NaNO₃/SiO₂NF (1% wt.) (grey symbols) and 0.3M NaNO₃/Al₂O₃ NF (1% wt.) (green symbols).

Nonetheless, the nitrite concentration in aqueous solution is strongly pH dependent. At pH values higher than 5 (pH > 5), the literature suggests that the UV absorbance have good linearity with nitrite concentration [46]. To corroborate the adjustment and then, the nitrite concentration, the pH was measured for all the samples of Table 1 and the results are summarized in Table 2. The pH values were in the range 5-7. Furthermore, with the addition of both NPs, the acidity of the NFs slightly decreases (i.e., the pH increases). Since the pH of the dissolution of nitrite was 7.08 ± 0.01, the increase of pH in the two formulated NFs was in accordance with the increase of NaNO₂ concentration in the samples obtained from the linear fit in Table 1.

Table 2. pH values at room temperature for pure 0.3M NaNO₃, 0.3M NaNO₃/SiO₂ NF (1% wt.) and 0.3M NaNO₃/Al₂O₃ NF (1% wt.) at different thermal treatments from 50 to 500°C.

Thermal treatment (°C)	NaNO ₃ pH ± 0.01	NaNO ₃ /SiO ₂ NF pH ± 0.01	NaNO ₃ /Al ₂ O ₃ NF pH ± 0.01
50	5.76	5.52	6.08
100	5.83	6.25	6.18
150	5.92	5.73	6.17
200	5.77	5.51	6.34
250	5.78	5.98	6.31
300	5.99	6.03	6.52
350	5.78	6.42	6.84
400	6.08	6.67	6.74
450	5.88	6.88	6.81
500	5.93	6.96	6.69

202
203
204
205
206
207
208
209
210
211
212
213
214
215
216
217
218
219

To corroborate and validate the nitrite formation, FT-IR spectroscopy was employed to determine the chemical composition of the samples. The FT-IR spectra for pure NaNO_3 and the two NFs after thermal treatments at 50°C and 500°C , are shown in Figure 6. There are several vibrational bands that allow to identify the NaNO_3 - NaNO_2 conversion, three of them are: (1) the relative intensity of the band at 825 cm^{-1} corresponding to the bending mode ν_2 of NO_2^- . The relative intensity of this mode decreases with the increase of $[\text{NO}_2^-]$ also observing a slight shift of the mode frequency from 835 cm^{-1} to 825 cm^{-1} . (2) Modification of the band contour of the ν_4 mode, 725 cm^{-1} , that corresponds to the asymmetric in-plane bending mode. This band begins to appear as the $[\text{NO}_3^-]$ decrease for $x=0.6 \left(\frac{[\text{NO}_2^-]}{[\text{NO}_3^-]}\right)$ and exhibits a slight shift from 725 cm^{-1} to 715 cm^{-1} . (3) The narrowing of the band located around 1358 cm^{-1} , corresponding to the asymmetric stretching mode of $[\text{NO}_3^-]$, and the presence of the band at 1271 cm^{-1} , corresponding to one of the fundamental vibrational modes of NaNO_2 , ν_3 [39,40]. Nonetheless, at low $[\text{NO}_2^-]$ concentrations, band (3) is the only that can monitor the evolution of nitrite concentration [38]. Figure 5 shows the 3 bands: (1) $\sim 1358\text{ cm}^{-1}$, (2) $\sim 1270\text{ cm}^{-1}$, and (3) $\sim 1100\text{ cm}^{-1}$. All the samples, except for NaNO_3 , show the presence of the tiny band (2) and a slight broadening of the band (1) as temperature increases. The relative intensity of the band (2) is increased in the NFs samples, indicating a high nitrite formation in comparison to pure NaNO_3 . The low intensity of this band agrees with the low $[\text{NO}_2^-]$ concentrations determined in Table 1. Additionally, the presence of the band (3) in the NaNO_3 sample at 500°C , is a good indicator of the presence of low $[\text{NO}_2^-]$ concentrations, between $x=0.1/0.2$ [41-43]. In the NFs spectra this band appears with higher intensity corroborating the $[\text{NO}_2^-]$ formation. Nonetheless, in the case of SiO_2 NFs, this band overlaps with the asymmetric stretching of SiO_2 , causing a higher band intensity.

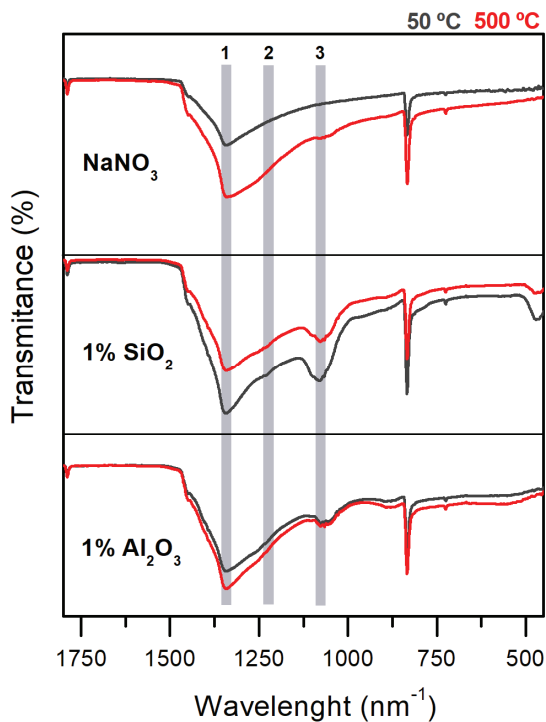


Figure 6. FT-IR spectra of NaNO_3 and $\text{NaNO}_3/\text{SiO}_2$, $\text{NaNO}_3/\text{Al}_2\text{O}_3$ NFs with 1% wt. of NPs after thermal treatment at 50°C and 500°C . Band (1) correspond to asymmetric stretching mode of NO_3^- , and bands (2)-(3) corresponds to fundamental vibration bands of NO_2^- .

3.3. Nanofluids reaction kinetics and decomposition

The increase of NaNO_2 concentration in the NFs indicates a change in the reaction kinetics of NaNO_3 decomposition. To study the effect of the NPs in the decomposition of NaNO_3 , the sample weight loss and derivative weight over time from 100°C to 900°C were evaluated in Figure 7. In the temperature range between 100 – 500°C , Figure 7a), no significant weight loss was observed for pure NaNO_3 and $\text{NaNO}_3/\text{SiO}_2$, $\text{NaNO}_3/\text{Al}_2\text{O}_3$ NFs. The maximum weight loss was 2.5% in the case of pure NaNO_3 and lower than 1% for the two formulated NFs. Hence, NFs were slightly more stable than the pure NaNO_3 . On the other hand, due to the limit of detection (1%) in the weight loss, it is not possible to identify the low NaNO_3 - NaNO_2 conversion determined in Table 1. Conversely, the NFs samples did not show any relevant change in the temperature range sampled, and they start to decompose around 600°C , as previously suggested for pure NaNO_3 [52]. It is remarkable that after the total decomposition, $\approx 800^\circ\text{C}$, the weight loss of Al_2O_3 -NF was lower than SiO_2 NF and pure NaNO_3 .

Figure 7b), shows the derivative of the weight ($d(\%/t)$), as a function of time. The derivative of weight loss gives information of the reaction kinetics. Dissimilar behaviours were identified. Two main peaks were observed for the three samples, approximately between 278 – 699°C (around 60 min.) and at 730 – 775°C (between 80–86 min.), respectively. On the other hand, a third peak was observed for the Al_2O_3 NF sample over 795°C (around 90 min.) The principal decomposition peak (around 80 min.) shows a variation in time and temperature. Consequently, a variation in the reaction kinetics and the thermal stability of the salt (*i.e.*, the equilibrium constants and the activation energy) are modified with the addition of Al_2O_3 and SiO_2 NPs. Table 3 summarizes all the main identified temperature peaks and the associated weight loss.

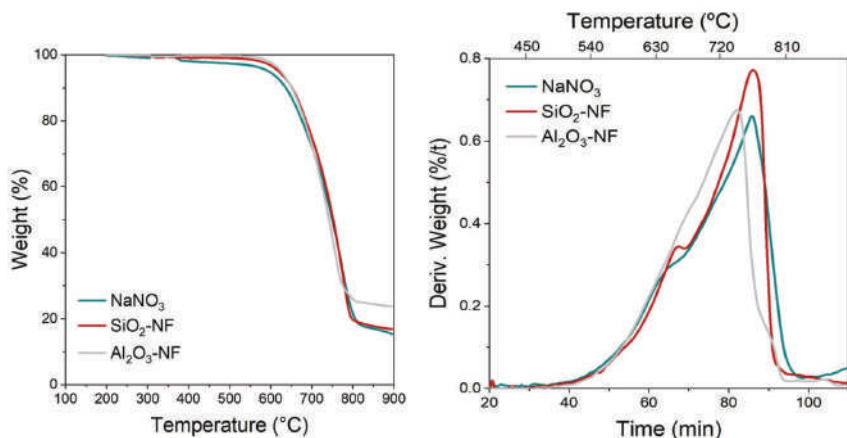
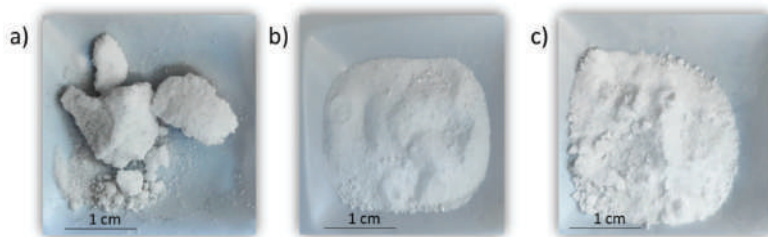


Figure 7. TGA measurement from 100 to 900°C of NaNO_3 , and $\text{NaNO}_3/\text{SiO}_2$, $\text{NaNO}_3/\text{Al}_2\text{O}_3$ NFs with 1% wt. of NPs: a) weight loss as a function of temperature and, b) weight derivative as a function of time and temperature.

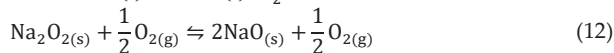
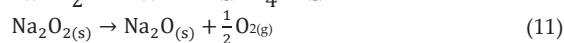
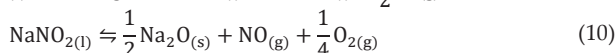
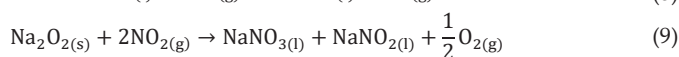
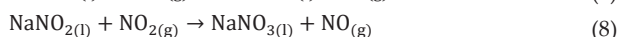
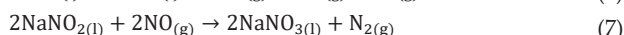
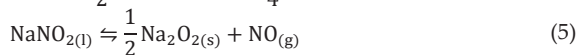
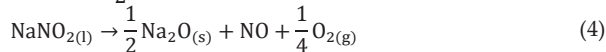
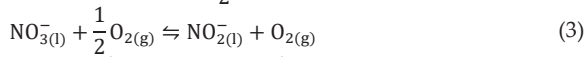
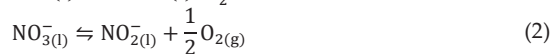
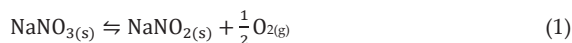
The lowest weight loss before the beginning of the decomposition above 600°C can be explained by the lower hygroscopicity of NFs; the NPs help to reduce the moisture absorption. Figure 8 illustrates the change that experiments sodium nitrate after one year of exposure at room temperature when it is pure (a) and in presence of SiO_2 (b) and Al_2O_3 (c) NPs. Pure NaNO_3 showed more aggregates than sodium nitrate with the presence of NPs due to moisture absorption. This behaviour is a relevant finding on the point of view of molten salts application because their high hygroscopicity in contact with environment increases the damage of metal compounds present in the plant [45,46]. Thus, this effect is reduced considerably with the presence of NPs.

Table 3. Temperature and weight loss obtained by TGA measurements of pure NaNO₃ and NaNO₃ with SiO₂ and Al₂O₃ NFs at 1% wt

Sample	NaNO ₃	SiO ₂	Al ₂ O ₃
Mass (mg) ± 0.01	13.74	14.27	14.55
First peak temperature (°C) ± 0.5	678.7	681.1	698.9
Weight loss at first peak (%) ± 1	18	20	27
Second peak temperature (°C) ± 0.5	774.8	775.2	755.0
Weight loss at second peak (%) ± 1	62	62	45
Third peak temperature (°C) ± 0.5	-	-	794.5
Weight loss at third peak (%) ± 1	-	-	3
Total weight loss between 507-840 °C (%) ± 1	80	81	75

**Figure 8.** Effect of moisture on physical properties (water absorption) of a) pure NaNO₃, b) NaNO₃/SiO₂ NPs (1% wt.) and c) NaNO₃/Al₂O₃ NPs (1% wt.).

To better understand the thermal decomposition and to relate the TGA profiles to the possible reactions involved, the deconvolution of the TGA peaks have been statistically performed by a Gaussian fit [55]. A total of fifteen reactions have been taken into consideration corresponding all to nitrate-nitrite conversions and to sodium oxides decompositions:



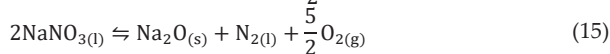
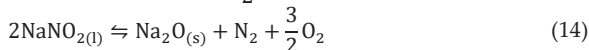


Figure 9 shows the TGA peak deconvolution and the cumulative fit peak (grey dotted line) for pure NaNO₃ (Figure 9a), for SiO₂ NF (Figure 9b) and AlO₃ NF (Figure 9c). All the Gaussian models (cumulative fit peak) show a good fitting (i.e., R² = 0.996, 0.998 and 0.999 for pure NaNO₃, SiO₂ and Al₂O₃ NFs, respectively). Moreover, Table 3 summarizes the parameters of the deconvoluted peaks and also the reactions that contribute to each of them.

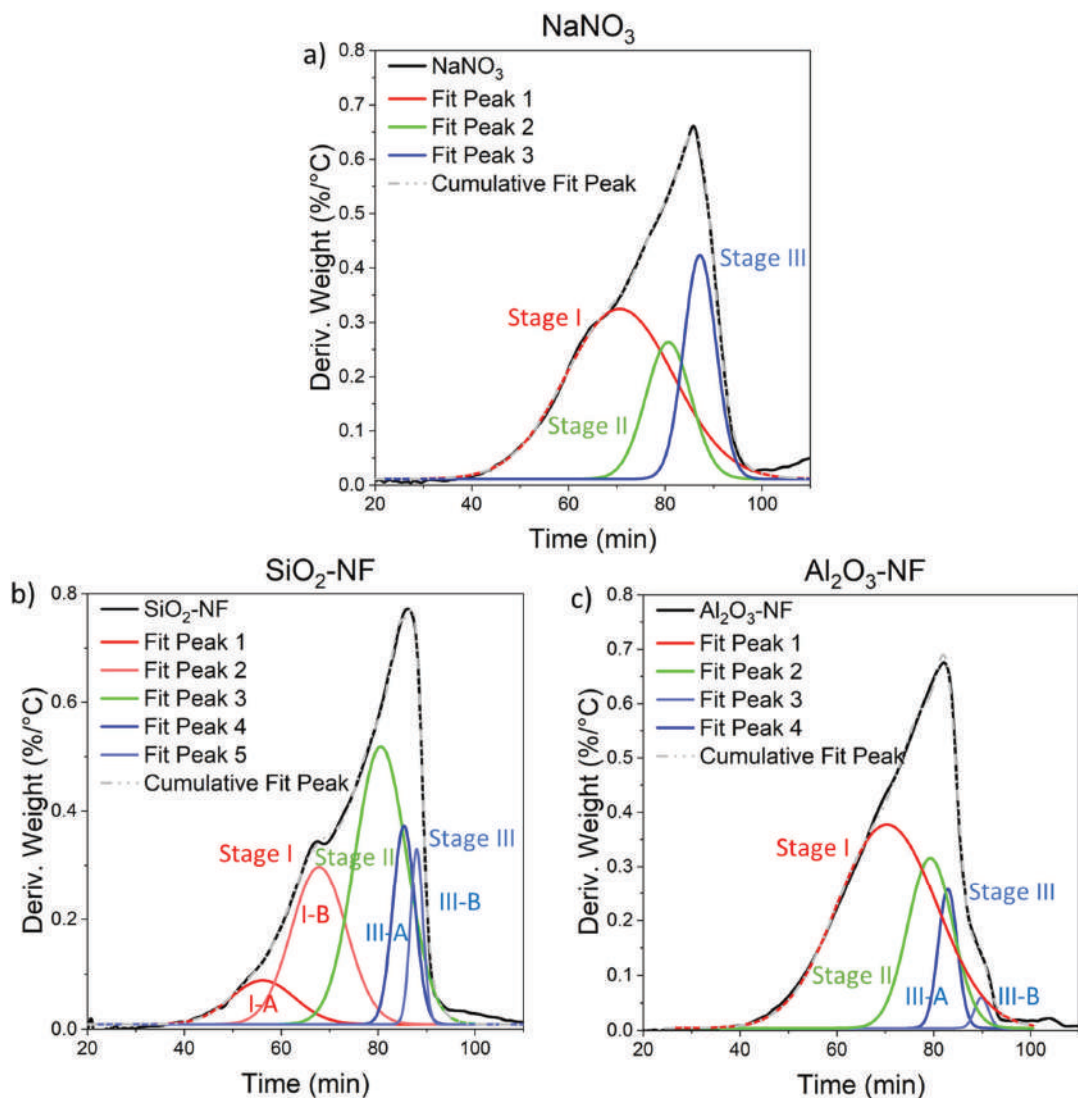


Figure 9. Non-linear peak deconvolution fit of the TGA weight derivative over time for a) NaNO₃, b) NaNO₃/SiO₂ NF (1% wt.) and c) NaNO₃/Al₂O₃ NF (1% wt.).

306
307
308
309
310
311
312

313
314

Table 4. Gaussian non-linear fit parameters and the predominant reactions involved of the deconvoluted peaks for NaNO₃, NaNO₃/SiO₂ NF (1% wt.) and NaNO₃/Al₂O₃ NF (1% wt.)

315
316

Stage	Step	Fit max. Peak	NaNO ₃	NaNO ₃ /SiO ₂ NF	NaNO ₃ /Al ₂ O ₃ NF	Reactive processes
			value ± std. dev.	value ± std. dev.	value ± std. dev.	
Stage I	I-A	Peak	Peak 1			
		Time (min.)	-	56.2 ± 0.5	-	
		Temp. (°C)	-	625.8 ± 0.5	-	NaNO _{3(s)} ⇌ NaNO _{2(s)} + $\frac{1}{2}$ O _{2(g)} (1)
	I-B	Peak	Peak 1	Peak 2	Peak 1	
		Time (min.)	70.56 ± 0.06	67.80 ± 0.06	70.34 ± 0.03	NO _{3(l)} ⇌ NO _{2(l)} + $\frac{1}{2}$ O _{2(g)} (2)
		Temp. (°C)	697.3 ± 0.5	683.0 ± 0.5	695.7 ± 0.5	NO _{3(l)} + $\frac{1}{2}$ O _{2(g)} ⇌ NO _{2(l)} + O _{2(g)} (3)
Stage II		Peak	Peak 2	Peak 3	Peak 2	NaNO _{2(l)} → $\frac{1}{2}$ Na ₂ O _(s) + NO + $\frac{1}{4}$ O _{2(g)} (4)
		Time (min.)	80.66 ± 0.15	80.55 ± 0.07	79.28 ± 0.05	NaNO _{2(l)} ⇌ $\frac{1}{2}$ Na ₂ O _{2(s)} + NO _(g) (5)
		Temp. (°C)	747.9 ± 0.5	747.0 ± 0.5	740.5 ± 0.5	2NaNO _{3(l)} → Na ₂ O _(l) + NO _{2(g)} + NO _(g) + O _{2(g)} (6)
		Time (min.)				2NaNO _{2(l)} + 2NO _(g) → 2NaNO _{3(l)} + N _{2(g)} (7)
		Temp. (°C)				NaNO _{2(l)} + NO _{2(g)} → NaNO _{3(l)} + NO _(g) (8)
						Na ₂ O _{2(s)} + 2NO _{2(g)} → NaNO _{3(l)} + NaNO _{2(l)} + $\frac{1}{2}$ O _{2(g)} (9)
Stage III	III-A	Peak	Peak 3	Peak 4	Peak 3	
		Time (min.)	87.17 ± 0.04	85.32 ± 0.05	82.876 ± 0.009	
		Temp. (°C)	781.2 ± 0.5	771.4 ± 0.5	758.9 ± 0.5	Na ₂ O _{2(s)} → Na ₂ O _(s) + $\frac{1}{2}$ O _{2(g)} (11)
	III-B	Peak		Peak 5	Peak 4	
		Time (min.)	-	87.966 ± 0.008	89.86 ± 0.03	Na ₂ O _{2(s)} + $\frac{1}{2}$ O _{2(g)} ⇌ 2NaO _(s) + $\frac{1}{2}$ O _{2(g)} (12)
		Temp. (°C)	-	785.4 ± 0.5	795.2 ± 0.5	Na ₂ O _{2(s)} ⇌ Na ₂ O _(s) + $\frac{1}{2}$ O _{2(g)} (13)
					2NaNO _{2(l)} ⇌ Na ₂ O _(s) + N ₂ + $\frac{3}{2}$ O _{2(g)} (14)	
					2NaNO _{3(l)} ⇌ Na ₂ O _(s) + N _{2(l)} + $\frac{5}{2}$ O _{2(g)} (15)	

Three main stages were identified in the peak deconvolution of NaNO_3 in Figure 9a. The decomposition of NaNO_3 has been well studied in the literature [48-52] and, it is known that at high temperatures as a result of its decomposition, nitrite and sodium oxides species coexist. Moreover, the decomposition process of nitrate salt can be subdivided into several stages that occur simultaneously and/or consecutively.

Stage I: The first identified stage corresponds to the solid-state reaction of formation of NaNO_2 , above the melting temperature to 450°C , according to eq. (1). The equilibrium of this reversible reaction depends on the temperature and, above $600\text{-}730^\circ\text{C}$, the backward reaction with oxygen is slower than the decomposition [56], eq. (2). In Stage I-B occurs the oxidation-decomposition processes, eqs. (2-3). This peak reaches the maximum value at $697.3 \pm 0.5^\circ\text{C}$ (at a velocity of $9.88 \pm 0.01^\circ\text{C}/\text{min}$) for pure NaNO_3 . Noticeably, the same peak for SiO_2 NF (Figure 9b) and for Al_2O_3 NF (Figure 9c) appears shifted at lower temperatures (i.e., $-14.3 \pm 0.7^\circ\text{C}$ and $-1.6 \pm 0.7^\circ\text{C}$, respectively). Furthermore, the addition of SiO_2 NPs make that the single peak decomposes into two peaks (I-A and I-B), varying the decomposition kinetics of eqs. (1-3). Specifically, an initial decomposition stage appears, Stage I-A, with a maximum at $625.8 \pm 0.5^\circ\text{C}$, with highest reaction kinetics ($11.1 \pm 0.1^\circ\text{C}/\text{min}$). Therefore, the addition of NPs drives to an acceleration of decomposition at lower temperatures than pure NaNO_3 (Table 3).

Stage II: In the intermediate stage, from 450°C to 700°C , the first-order liquid-liquid reaction occurs, the reverse reaction in the melt sodium nitrite to form sodium nitrate (oxidation-decomposition) eq. (2). This reverse equation is possible due to the formation of NaO_2 or Na_2O_2 as intermediates during the decomposition of sodium nitrite, eqs. (4-10). When the equilibrium of eq. (2) was displaced to the decomposition, the formation of O_2 and NO is favoured. Therefore, the eq. (4) becomes the most kinetically and energy-favoured reaction [57]. A single peak was identified for the three samples in this stage. The maximum of this stage for NaNO_3 occurs at $747.9 \pm 0.5^\circ\text{C}$. A decrease of temperature was observed only with Al_2O_3 NPs ($-9.4 \pm 0.5^\circ\text{C}$). Therefore, the presence of Al_2O_3 NPs drives to a NaNO_2 decomposition, eqs. (4-10), at lower temperatures.

Stage III: Finally, above 700°C a reaction of NaNO_2 and direct decomposition of NaNO_3 occurs with the formation of Na_2O and release of nitrogen oxides [56], eqs. (11-15). In the case of pure NaNO_3 the reaction occurs with a single step, stage III-A, with a maximum at $781.2 \pm 0.5^\circ\text{C}$. The presence of this peak confirms that Na_2O_2 and/or NaO_2 are formed as intermediates for the formation of Na_2O , eqs. (11-15), [61]. In contrast, the decomposition to Na_2O for NFs follow two steps: III-A and III-B described by parallel reactions. The initial decomposition stage for NFs, III-A, starts at lower temperature than the pure NaNO_3 (and at lower times). The peak temperature decreases $-9.8 \pm 0.7^\circ\text{C}$ and $-22.3 \pm 0.7^\circ\text{C}$ with SiO_2 and Al_2O_3 NPs, respectively, in comparison to pure NaNO_3 . Contrarily, in the final reaction process, III-B, the maximum peak temperature increases $+4.2 \pm 0.7^\circ\text{C}$ with SiO_2 NPs and $13.9 \pm 0.7^\circ\text{C}$ with Al_2O_3 NPs.

Consequently, the presence of NPs produces an acceleration of the decomposition of nitrates through the sequence $\text{NaNO}_3\text{-NaNO}_2\text{-Na}_2\text{O}_2$, and a shift to high temperatures in the formation of Na_2O . Despite the final decomposition occurs at higher temperatures, it occurs at lower times. Accordingly, the NFs need higher temperatures and lower times to decompose than the pure salt confirming the role of NPs as catalysts of decomposition reactions.

Moreover, some authors described a chemical reaction between NaNO_3 and NPs, generating new intermediate species like Na_2SiO_3 [54,55]. To corroborate the reactivity between the NPs and NaNO_3 , the final product of the two NFs after the thermal treatment (after stage III, 850°C) was analysed by FT-IR. Figure 10, shows the comparison between FT-IR spectra at 500°C and 850°C , for the two NFs. The identified bands at the regions (1), (2), (3) and (4), indicate the formation of new species. In the case of presence of Al_2O_3 NPs, these bands indicated the formation of species like NaAlO_2 [64]. Similarly, the presence of SiO_2 NPs favours the formation of NaSiO_2 . The bands in the region (1) and (4) indicate the mixed formation of NaSiO_2 and Na_2SiO_3 [65]. This fact can explain the variation in decomposition rates and temperatures, as demonstrated by the study carried out by Y. Hoshino et al. [50], with the addition of several oxides at the μm scale into NaNO_3 .

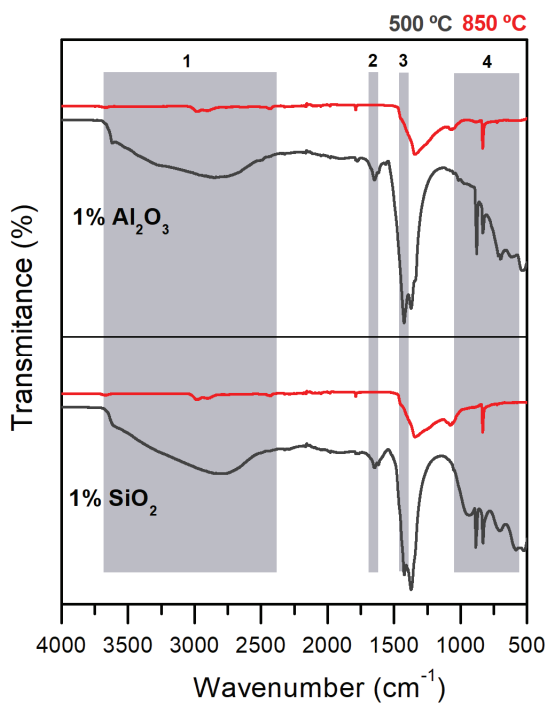


Figure 10. FT-IR spectra for (top) $\text{NaNO}_3/\text{Al}_2\text{O}_3$ NF (1% wt.) and (bottom) $\text{NaNO}_3/\text{SiO}_2$ NF (1% wt.) after thermal treatment at 500°C and 850°C .

5. Conclusions

The effect of the incorporation of nanoparticles on the thermal stability of NaNO_3 was investigated in this study. Through UV-Vis spectroscopy and thermogravimetric analysis, NaNO_2 concentration and decomposition were studied for pure NaNO_3 and two NaNO_3 -based nanofluids formulated with 1% wt. of SiO_2 and Al_2O_3 nanoparticles, respectively. Three key findings were achieved:

1. Detection of higher nitrite concentration (up to 4% wt.) than pure NaNO_3 (up to 0.8 % wt.), due to the presence of nanoparticles in the temperature range from 50°C to 500°C . Al_2O_3 nanoparticles cause a higher nitrate-nitrite conversion than SiO_2 nanoparticles.

2. The presence of nanoparticles increases thermal stability to over 600°C before starting to decompose. In addition, with Al₂O₃ nanoparticles, weight loss at 900°C was about 6% lower than NaNO₃.
3. Three main reaction stages were identified in the NaNO₃ decomposition in accordance with the literature. These decomposition stages are altered by the presence of nanoparticles. First, SiO₂ and Al₂O₃ nanoparticles reduce the decomposition temperatures of NaNO₃-NaNO₂-Na₂O₂ up to 7°C. Even so, the reactions involved were accelerated by the presence of nanoparticles. Particularly, SiO₂ NPs accelerate the reactions more than Al₂O₃ NPs. Second, the final decomposition to Na₂O occurs at higher temperatures (up to 14°C) than pure NaNO₃. Nonetheless, the final decomposition takes place in shorter times.

In view of these results, the nanoparticles act as catalyst for the reactions. However, at temperatures above 500°C, nanofluids exhibit higher thermal stability than pure NaNO₃ despite the slight increase in nitrite concentration. To conclude, this study demonstrates the adequacy of the use of UV-Vis absorption and deconvolution of the TGA signal to study nitrite concentration and reaction kinetics.

Author Contributions: Conceptualization, A.S., P.G. and A.I.F.; methodology, A.S., S.H. and P.G.; formal analysis, A.S.; investigation, A.S.; resources, P.G., C.B. and A.I.F.; data curation, S.H., A.C. and A.S.; writing—original draft preparation, A.S.; writing—review and editing, A.C., P.G., C.B. and A.I.F.; visualization, A.S.; supervision, P.G. and A.I.F.; funding acquisition, P.G. and A.I.F. All authors have read and agreed to the published version of the manuscript.

Funding: This research was partially funded by the Spanish government RTI2018-093849-B-C32, RTI2018-094757-BI00, MDM-2017-0767, MCIU/AEI/FEDER, UE/DIOPMA is a certified agent TECNIO in the category of technology developers from the Government of Catalonia. The authors would like to thank the Catalan Government for the quality accreditation given to their research groups DIOPMA (2017 SGR 118) and CMSL (2017 SGR 13). A.S. thanks to Generalitat de Catalunya and AGAUR for her Grant FI-DGR 2018 and S.H. is grateful to the Generalitat de Catalunya and the Universitat de Barcelona for the research grant, APIF-DGR 2018. Finally, P.G. thanks Generalitat de Catalunya for his Serra Hünter Associate Professorship.

Conflicts of Interest: The authors declare no conflict of interest. The funders had no role in the design of the study; in the collection, analyses, or interpretation of data; in the writing of the manuscript, or in the decision to publish the results.

References

- [1] S. U. S. Choi, S. Li, and J. A. Eastman, "Measuring thermal conductivity of fluids containing oxide nanoparticles," *J. Heat Transfer*, vol. 121, no. 2, pp. 280–289, 1999, doi: 10.1115/1.2825978.
- [2] M. Awais, A. A. Bhuiyan, S. Salehin, M. M. Ehsan, B. Khan, and M. H. Rahman, "Synthesis, heat transport mechanisms and thermophysical properties of nanofluids: A critical overview," *Int. J. Thermofluids*, vol. 10, p. 100086, 2021, doi: 10.1016/j.ijft.2021.100086.
- [3] M. J. Assael, K. D. Antoniadis, W. A. Wakeham, and X. Zhang, "Potential applications of nanofluids for heat transfer," *Int. J. Heat Mass Transf.*, vol. 138, pp. 597–607, 2019, doi: 10.1016/j.ijheatmasstransfer.2019.04.086.
- [4] E. Cuce, P. M. Cuce, T. Guclu, and A. B. Besir, "On the use of nanofluids in solar energy applications," *J. Therm. Sci.*, vol. 29, no. 3, pp. 513–534, 2020, doi: 10.1007/s11630-020-1269-3.
- [5] Q. Xiong, A. Hajjar, B. Alshuraiaan, M. Izadi, S. Altnji, and S. A. Shehzad, "State-of-the-art review of nanofluids in solar collectors: A review based on the type of the dispersed nanoparticles," *J. Clean. Prod.*, vol. 310, no. March, p. 127528, 2021, doi: 10.1016/j.jclepro.2021.127528.
- [6] H. M. R. Gonçalves *et al.*, "Nanofluid Based on Glucose-Derived Carbon Dots Functionalized with [Bmim]Cl for the Next Generation of Smart Windows," *Adv. Sustain. Syst.*, vol. 3, no. 7, pp. 1–10, 2019, doi: 10.1002/adsu.201900047.

- [7] R. Du, D. D. Jiang, Y. Wang, and K. Wei Shah, "An experimental investigation of CuO/water nanofluid heat transfer in geothermal heat exchanger," *Energy Build.*, vol. 227, p. 110402, 2020, doi: 10.1016/j.enbuild.2020.110402. 446-447
- [8] H. Eltoum, Y. L. Yang, and J. R. Hou, "The effect of nanoparticles on reservoir wettability alteration: a critical review," *Pet. Sci.*, vol. 18, no. 1, pp. 136–153, 2021, doi: 10.1007/s12182-020-00496-0. 448-449
- [9] F. Yakasai, M. Z. Jaafar, S. Bandyopadhyay, and A. Agi, "Current developments and future outlook in nanofluid flooding: A comprehensive review of various parameters influencing oil recovery mechanisms," *J. Ind. Eng. Chem.*, vol. 93, pp. 138–162, 2021, doi: 10.1016/j.jiec.2020.10.017. 450-452
- [10] X. Han, S. J. Thrush, Z. Zhang, G. C. Barber, and H. Qu, "Tribological characterization of ZnO nanofluids as fastener lubricants," *Wear*, vol. 468–469, no. December 2020, p. 203592, 2021, doi: 10.1016/j.wear.2020.203592. 453-454
- [11] M. Hemmat Esfe, M. Bahiraei, and A. Mir, "Application of conventional and hybrid nanofluids in different machining processes: A critical review," *Adv. Colloid Interface Sci.*, vol. 282, p. 102199, 2020, doi: 10.1016/j.cis.2020.102199. 455-456
- [12] G. Yıldız, Ü. Ağbulut, and A. E. Gürel, "A review of stability, thermophysical properties and impact of using nanofluids on the performance of refrigeration systems," *Int. J. Refrig.*, vol. 129, pp. 342–364, 2021, doi: 10.1016/j.ijrefrig.2021.05.016. 457-458
- [13] H. B. Parmar *et al.*, "Nanofluids improve energy efficiency of membrane distillation," *Nano Energy*, vol. 88, no. May, p. 106235, 2021, doi: 10.1016/j.nanoen.2021.106235. 459-460
- [14] W. Yu, T. Wang, A. H. A. Park, and M. Fang, "Review of liquid nano-absorbents for enhanced CO₂ capture," *Nanoscale*, vol. 11, no. 37, pp. 17137–17156, 2019, doi: 10.1039/c9nr05089b. 461-462
- [15] G. Peiró, J. Gasia, L. Miró, C. Prieto, and L. F. Cabeza, "Influence of the heat transfer fluid in a CSP plant molten salts charging process," *Renew. Energy*, vol. 113, pp. 148–158, 2017, doi: 10.1016/j.renene.2017.05.083. 463-464
- [16] A. Wahab, A. Hassan, M. Arslan, H. Babar, and M. Usman, "Solar energy systems – Potential of nanofluids," *J. Mol. Liq.*, vol. 289, 2019, doi: 10.1016/j.molliq.2019.111049. 465-466
- [17] T. Singh, M. A. A. Hussien, T. Al-Ansari, K. Saoud, and G. McKay, "Critical review of solar thermal resources in GCC and application of nanofluids for development of efficient and cost effective CSP technologies," *Renew. Sustain. Energy Rev.*, vol. 91, no. February, pp. 708–719, 2018, doi: 10.1016/j.rser.2018.03.050. 467-469
- [18] Y. Hu, Y. He, Z. Zhang, and D. Wen, "Enhanced heat capacity of binary nitrate eutectic salt-silica nanofluid for solar energy storage," *Sol. Energy Mater. Sol. Cells*, vol. 192, no. July 2018, pp. 94–102, 2019, doi: 10.1016/j.solmat.2018.12.019. 470-471
- [19] U. Nithiyantham, Y. Grosu, L. González-Fernández, A. Zaki, J. M. Igartua, and A. Faik, "Development of molten nitrate salt based nanofluids for thermal energy storage application: High thermal performance and long storage components lifetime," *SOLARPACES 2018 Int. Conf. Conc. Sol. Power Chem. Energy Syst.*, vol. 2126, p. 200025, 2019, doi: 10.1063/1.5117740. 472-474
- [20] W. Wang, Z. Wu, B. Li, and B. Sundén, "A review on molten-salt-based and ionic-liquid-based nanofluids for medium-to-high temperature heat transfer," *J. Therm. Anal. Calorim.*, vol. 136, no. 3, pp. 1037–1051, 2019, doi: 10.1007/s10973-018-7765-y. 475-476
- [21] B. Muñoz-Sánchez, J. Nieto-Maestre, I. Iparraguirre-Torres, A. García-Romero, and J. M. Sala-Lizarraga, "Molten salt-based nanofluids as efficient heat transfer and storage materials at high temperatures. An overview of the literature," *Renew. Sustain. Energy Rev.*, vol. 82, no. November 2017, pp. 3924–3945, 2018, doi: 10.1016/j.rser.2017.10.080. 477-479
- [22] Y. Huang, X. Cheng, Y. Li, G. Yu, K. Xu, and G. Li, "Effect of in-situ synthesized nano-MgO on thermal properties of NaNO₃-KNO₃," *Sol. Energy*, vol. 160, no. December 2017, pp. 208–215, 2018, doi: 10.1016/j.solener.2017.11.077. 480-481
- [23] D. Shin and D. Banerjee, "Enhanced specific heat capacity of nanomaterials synthesized by dispersing silica nanoparticles in eutectic mixtures," *J. Heat Transfer*, vol. 135, no. 3, pp. 1–8, 2013, doi: 10.1115/1.4005163. 482-483
- [24] M. Schuller, Q. Shao, and T. Lalk, "Experimental investigation of the specific heat of a nitrate-alumina nanofluid for solar thermal energy storage systems," *Int. J. Therm. Sci.*, vol. 91, pp. 142–145, 2015, doi: 10.1016/j.ijthermalsci.2015.01.012. 484-485
- [25] M. X. Ho and C. Pan, "Optimal concentration of alumina nanoparticles in molten hitec salt to maximize its specific heat capacity," *Int. J. Heat Mass Transf.*, vol. 70, pp. 174–184, 2014, doi: 10.1016/j.ijheatmasstransfer.2013.10.078. 486-487

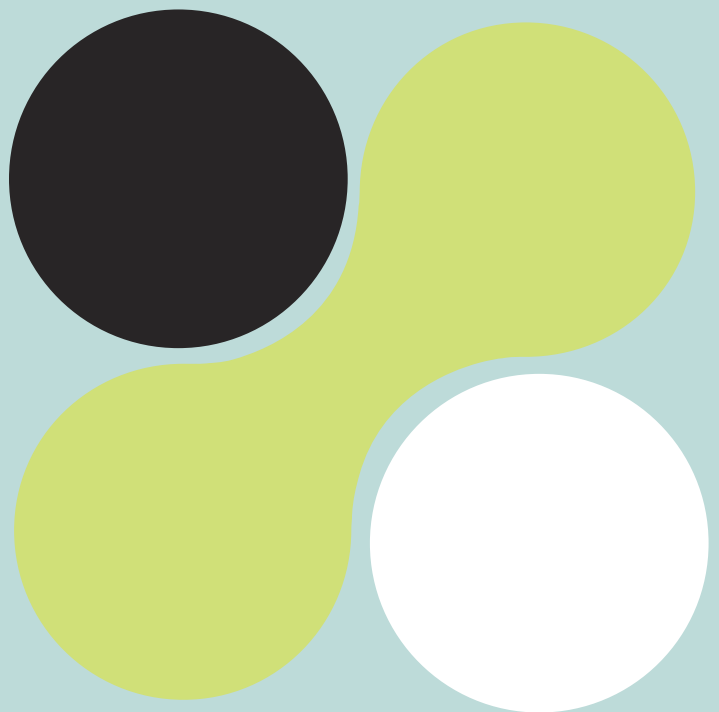
- [26] A. Svobodova-Sedlackova, C. Barreneche, G. Alonso, A. I. Fernandez, and P. Gamallo, "Effect of nanoparticles in molten salts – MD simulations and experimental study," *Renew. Energy*, vol. 152, pp. 208–216, 2020, doi: 10.1016/j.renene.2020.01.046. 488–489
- [27] X. Chen, Y. ting Wu, L. di Zhang, X. Wang, and C. fang Ma, "Experimental study on thermophysical properties of molten salt nanofluids prepared by high-temperature melting," *Sol. Energy Mater. Sol. Cells*, vol. 191, no. December 2017, pp. 209–217, 2019, doi: 10.1016/j.solmat.2018.11.003. 490–492
- [28] B. Dudda and D. Shin, "Imece2012-87707 Investigation of Molten Salt Nanomaterial As Thermal Energy Storage in," pp. 1–6, 2012. 493–494
- [29] A. Awad, H. Navarro, Y. Ding, and D. Wen, "Thermal-physical properties of nanoparticle-seeded nitrate molten salts," *Renew. Energy*, vol. 120, pp. 275–288, 2018, doi: 10.1016/j.renene.2017.12.026. 495–496
- [30] Q. He, S. Wang, M. Tong, and Y. Liu, "Experimental study on thermophysical properties of nanofluids as phase-change material (PCM) in low temperature cool storage," *Energy Convers. Manag.*, vol. 64, pp. 199–205, 2012, doi: 10.1016/j.enconman.2012.04.010. 497–499
- [31] Q. Xie, Q. Zhu, and Y. Li, "Thermal storage properties of molten nitrate salt-based nanofluids with graphene nanoplatelets," *Nanoscale Res. Lett.*, vol. 11, no. 1, p. 306, 2016, doi: 10.1186/s11671-016-1519-1. 500–501
- [32] M. A. Hassan and D. Banerjee, "A soft computing approach for estimating the specific heat capacity of molten salt-based nanofluids," *J. Mol. Liq.*, vol. 281, pp. 365–375, 2019, doi: 10.1016/j.molliq.2019.02.106. 502–503
- [33] M. C. Lu and C. H. Huang, "Specific heat capacity of molten salt-based alumina nanofluid," *Nanoscale Res. Lett.*, vol. 8, no. 1, pp. 1–7, 2013, doi: 10.1186/1556-276X-8-292. 504–505
- [34] K. Pramod *et al.*, "Preparation and characterization of molten salt based nanothermic fluids with enhanced thermal properties for solar thermal applications," *Appl. Therm. Eng.*, vol. 109, pp. 901–905, 2016, doi: 10.1016/j.applthermaleng.2016.04.102. 506–507
- [35] P. D. Myers, T. E. Alam, R. Kamal, D. Y. Goswami, and E. Stefanakos, "Nitrate salts doped with CuO nanoparticles for thermal energy storage with improved heat transfer," *Appl. Energy*, vol. 165, pp. 225–233, 2016, doi: 10.1016/j.apenergy.2015.11.045. 508–510
- [36] P. Andreu-Cabedo, R. Mondragon, L. Hernandez, R. Martinez-Cuenca, L. Cabedo, and J. Julia, "Increment of specific heat capacity of solar salt with SiO₂ nanoparticles," *Nanoscale Res. Lett.*, vol. 9, no. 1, p. 582, 2014, doi: 10.1186/1556-276X-9-582. 511–512
- [37] M. Sarvghad, T. A. Steinberg, and G. Will, "Corrosion of stainless steel 316 in eutectic molten salts for thermal energy storage," *Sol. Energy*, vol. 172, no. November 2017, pp. 198–203, 2018, doi: 10.1016/j.solener.2018.03.053. 513–514
- [38] S. Guillot *et al.*, "Corrosion effects between molten salts and thermal storage material for concentrated solar power plants," *Appl. Energy*, vol. 94, pp. 174–181, 2012, doi: 10.1016/j.apenergy.2011.12.057. 515–516
- [39] C. Prieto, R. Osuna, A. I. Fernández, and L. F. Cabeza, "Thermal storage in a MW scale . Molten salt solar thermal pilot facility: Plant description and commissioning experiences," *Renew. Energy*, vol. 99, pp. 852–866, 2016, doi: 10.1016/j.renene.2016.07.053. 517–519
- [40] "Standard Practice for Reducing Samples of Aggregate to Testing Size 1," *Astm C 702 - 9*, vol. 04, no. Reapproved, pp. 700–703, 2003. 520–521
- [41] L. H. Kumar, S. N. Kazi, H. H. Masjuki, and M. N. M. Zubir, "A review of recent advances in green nanofluids and their application in thermal systems," *Chem. Eng. J.*, vol. 429, no. September 2021, p. 132321, 2022, doi: 10.1016/j.cej.2021.132321. 522–523
- [42] H. A. Aljaerani, M. Samykano, R. Saidur, A. K. Pandey, and K. Kadirgama, "Nanoparticles as molten salts thermophysical properties enhancer for concentrated solar power: A critical review," *J. Energy Storage*, vol. 44, no. PA, p. 103280, 2021, doi: 10.1016/j.est.2021.103280. 524–526
- [43] A. C. Edwards, P. S. Hooda, and Y. Cook, "Determination of nitrate in water containing dissolved organic carbon by ultraviolet spectroscopy," *Int. J. Environ. Anal. Chem.*, vol. 80, no. 1, pp. 49–59, 2001, doi: 10.1080/03067310108044385. 527–528
- [44] H. Wang, A. Ju, and L. Wang, "Ultraviolet Spectroscopic Detection of Nitrate and Nitrite in Seawater Simultaneously Based 529

- on Partial Least Squares," *Molecules*, vol. 26, no. 12, p. 3685, 2021, doi: 10.3390/molecules26123685. 530
- [45] D. M. Dong *et al.*, "Determination of nitrite using UV absorption spectra based on multiple linear regression," *Asian J. Chem.*, 531
vol. 25, no. 4, pp. 2273–2277, 2013, doi: 10.14233/ajchem.2013.13840. 532
- [46] E. Riordan, N. Minogue, D. Healy, P. O'Driscoll, and J. R. Sodeau, "Spectroscopic and optimization modeling study of nitrous 533
acid in aqueous solution," *J. Phys. Chem. A*, vol. 109, no. 5, pp. 779–786, 2005, doi: 10.1021/jp040269v. 534
- [47] T. M. Hammad, "Infrared absorption spectra studies in (NaNO₃-NaNO₂) system," *Ann. der Phys.*, vol. 11, no. 6, pp. 435–441, 535
2002, doi: 10.1002/1521-3889(200206)11:6<435::AID-ANDP435>3.0.CO;2-2. 536
- [48] L. Wen-Jui, S. Min-yi, Y. Chin-hui, and L. Yuan-Pern, "Infrared absorption of cyclic - and trans - NaNO₂ and KNO₂ in solid 537
argon," *J. Chem. Phys.*, vol. 935, no. September 1995, 1998. 538
- [49] R. W. Berg, D. H. Kerridge, and P. H. Larsen, "NaNO₂ + NaNO₃ phase diagram: New data from DSC and Raman 539
spectroscopy," *ournal Chem. Eng. Data*, no. 51, pp. 34–39, 2006. 540
- [50] Y. Hoshino, T. Utsunomiya, and O. Abe, "The thermal decomposition of sodium nitrate and the effects of several oxides on 541
the decomposition," *Bull. Chem. Soc. Jpn.*, vol. 54, pp. 1385–1391, 1981, doi: 10.1246/bcsj.54.1385. 542
- [51] Y. Sato, K. Gesi, and Y. Takagi, "Study of the Phase Transition in NaNO₂ by Polarized Infrared radiation," *J. Phys. Soc. Soc.*, 543
vol. 16, no. 11, 1961. 544
- [52] T. Bauer, D. Laing, and R. Tamme, "Characterization of sodium nitrate as phase change material," *Int. J. Thermophys.*, vol. 33, 545
no. 1, pp. 91–104, 2012, doi: 10.1007/s10765-011-1113-9. 546
- [53] W.-D. Steinmann, "Thermal energy storage systems for concentrating solar power plants," in *Concentrating Solar Power 547
Technology*, 2nd ed., Elsevier Ltd., 2021, pp. 399–440. 548
- [54] A. Ibrahim, H. Peng, A. Riaz, M. Abdul Basit, U. Rashid, and A. Basit, "Molten salts in the light of corrosion mitigation 549
strategies and embedded with nanoparticles to enhance the thermophysical properties for CSP plants," *Sol. Energy Mater. Sol. 550
Cells*, vol. 219, no. August 2020, p. 110768, 2021, doi: 10.1016/j.solmat.2020.110768. 551
- [55] M. hui Zhang, X. Chen, and H. Dong, "A study on multistep thermal decomposition behavior and kinetics of magnesium 552
nitrate hydrate," *Thermochim. Acta*, vol. 701, no. May, p. 178951, 2021, doi: 10.1016/j.tca.2021.178951. 553
- [56] D. A. Nissen and D. E. Meeker, "Nitrate/Nitrite Chemistry in NaNO₃-KNO₃ Melts," *Inorg. Chem.*, vol. 22, no. 5, pp. 716–721, 554
1983, doi: 10.1021/ic00147a004. 555
- [57] S. and E. L. I. S. Freeman, "The Kinetics of the thermal decomposition of sodium nitrate and of the reaction between sodium 556
nitrite and oxygen," *J. Phys. Chem.*, vol. 60, no. 13, pp. 1487–1493, 1956. 557
- [58] V. A. Sötz, A. Bonk, J. Forstner, and T. Bauer, "Microkinetics of the reaction NO₃ ⇌ NO₂ + 0.5 O₂ in molten sodium nitrate 558
and potassium nitrate salt," *Thermochim. Acta*, vol. 678, no. 3, p. 178301, 2019, doi: 10.1016/j.tca.2019.178301. 559
- [59] C. Villada, A. Bonk, T. Bauer, and F. Bolívar, "High-temperature stability of nitrate/nitrite molten salt mixtures under 560
different atmospheres," *Appl. Energy*, vol. 226, no. January 2017, pp. 107–115, 2018, doi: 10.1016/j.apenergy.2018.05.101. 561
- [60] K. H. Stern, "High temperature properties and decomposition of inorganic salts part 3, nitrates and nitrites," *J. Phys. Chem. 562
Ref. Data*, vol. 1, no. 3, pp. 747–772, 1972, doi: 10.1063/1.3253104. 563
- [61] W. M. Jacobs *et al.*, "The thermal decomposition of sodium nitrate," *Inorg. Phys. Theor.*, pp. 2–5, 1959. 564
- [62] A. Svobodova-Sedlackova, A. Calderón, C. Barreneche, P. Gamallo, and A. I. Fernández, "Understanding the abnormal 565
thermal behavior of nanofluids through infrared thermography and thermo - physical characterization," *Sci. Rep.*, no. 566
0123456789, pp. 1–10, 2021, doi: 10.1038/s41598-021-84292-9. 567
- [63] R. Mondragón, J. E. Juliá, L. Cabedo, and N. Navarrete, "On the relationship between the specific heat enhancement of salt- 568
based nanofluids and the ionic exchange capacity of nanoparticles," *Sci. Rep.*, vol. 8, no. 1, pp. 1–12, 2018, doi: 10.1038/s41598- 569
018-25945-0. 570
- [64] B. Li *et al.*, "Calcined sodium silicate as an efficient and benign heterogeneous catalyst for the transesterification of natural 571

- lecithin to L- α -glycerophosphocholine," *Green Process. Synth.*, vol. 8, no. 1, pp. 78–84, 2019, doi: 10.1515/gps-2017-0190. 572
- [65] S. K. Cherikkallinmel, A. Gopalakrishnan, Z. Yaakob, R. M. Ramakrishnan, S. Sugunan, and B. N. Narayanan, "Sodium 573
aluminate from waste aluminium source as catalyst for the transesterification of Jatropha oil," *RSC Adv.*, vol. 5, no. 57, pp. 574
46290–46294, 2015, doi: 10.1039/c5ra05982h. 575
576

New approach
to nanofluids
characterization

Small angle X-ray scattering



The image features a minimalist design with overlapping circles in a dark grey color. A white, irregular path winds through the composition, connecting different areas. The text is centered within one of the circles.

Key point 6
Characterization

11. New approach to nanofluids characterization

Small angle X-ray Scattering (SAXS), an unconventional technique for characterizing nanofluids

11.1 Introduction

This chapter arises from the need of having alternative characterization techniques for nanofluids and to be able to evaluate the behaviour of nanoparticles within the base fluid, in addition to being able to carry out experiments at higher temperatures, as we could see in **Chapter 5, section 5.5**.

Therefore, studying new techniques and methodologies to characterize nanomaterials has many advantages. First, it allows us to obtain detailed information about the system and secondly, it can help us develop more versatile techniques. For this reason, this

chapter analyses the feasibility of carrying out Small Angle X-Ray Scattering (SAXS) measurements in the existing facilities in the Centres Científics i Tecnològics de la Universitat de Barcelona (CCiT-UB) in the X-Ray Diffraction department. Furthermore, implementing this technique can provide high versatility to the conventional XRD equipment, allowing not only to determine the composition and structural parameters but also morphological ones such as particle size, shape, specific area or molecular weights with the same equipment and samples preparation.

This chapter is divided in two parts; the first is focused on the feasibility study of the implementation of the SAXS

technique, and the second is on the analysis of nanofluids using SAXS measurement as a function of temperature.

11.1.1 Relevance

The relevance of this chapter lies in the evaluation of a new feature to the CCIT-UB and to provide further versatility to the diffractometers available in the X-ray diffraction laboratory. But mainly, the application of this technique for the characterization of nanofluids allows obtaining both structural and morphological information at temperatures above ambient, which is one of the main limitations of conventional techniques. Therefore, the final relevance of this chapter is contributing to **key point VI** with original data and to presenting SAXS as a suitable technique to nanofluids characterization.

11.1.2 Objectives

The main objectives of this chapter are:

PART A:

- Study the feasibility of performing SAXS experiments on the PANalytical X'Pert PRO MPD TT2 diffractometer in the CCIT-UB.
- Validation of SAXS measurements.

PART B:

- SAXS experiments of NSBNFs samples with temperature.
- Evolution of the nanoparticle's distribution and specific areas with temperature.

11.2 What is SAXS?

Small Angle X-ray scattering (SAXS) is a helpful technique for the structural characterisation of nanomaterials. SAXS is a technique that measures the intensities of X-rays scattered by a sample as a function of the scattering angle, as depicted in **Figure 11.1**. Through a mathematical treatment of the scattering profiles, a comprehensive collection of information about the structure and materials properties can be obtained, such as nanoparticle size and distribution, particle shape, particle structure, specific surface area, agglomeration behaviour of nanoparticles, pore size distribution or liquid crystalline phases or characteristics distances of partially ordered materials among others. The technique allows colloidal suspensions and nanomaterials but tolerates solid objects, powders, or gels, and they may be amorphous, crystalline or semi-crystalline. The measurement limit ranged

from 1 to above 100 nm, and concentration ranges between 0.1 wt% to 99.9 wt%. Therefore, a SAXS signal is observed in materials with structural features on the length scale of nanometers [2].

The SAXS method is precise, non-destructive, and typically requires minimal sample preparation. SAXS signal is achieved by analysing the elastic scattering behaviour of X-rays when travelling through the material, recording their scattering at small angles (typically $0.1 - 10^\circ 2\theta$). According to Bragg's law, larger structures can be determined with the scattering angle decrease. At very small angles, the shape of the scattering is the so-called Guinier region. The Guinier region allows determining the radius of gyration (R_g ,

which represents the average particle radius) of any distinct structures on this length scale. At higher angles, if a diluted system of relatively identical particles is considered, one might be able to see broad peaks that would also give information on the shape of the particles. In a system of strongly interacting particles, Bragg peaks may be observed, which will obscure single-particle information but give structural information. At higher angles, in the Porod region, the shape of the curve is suitable for obtaining information on the surface-to-volume ratio of the scattering objects and the dimensions of the scattering particles [2,3], as shown in **Figure 11.2**. Moreover, SAXS allows the determination of more parameters like a particle's interaction or molecular weights.

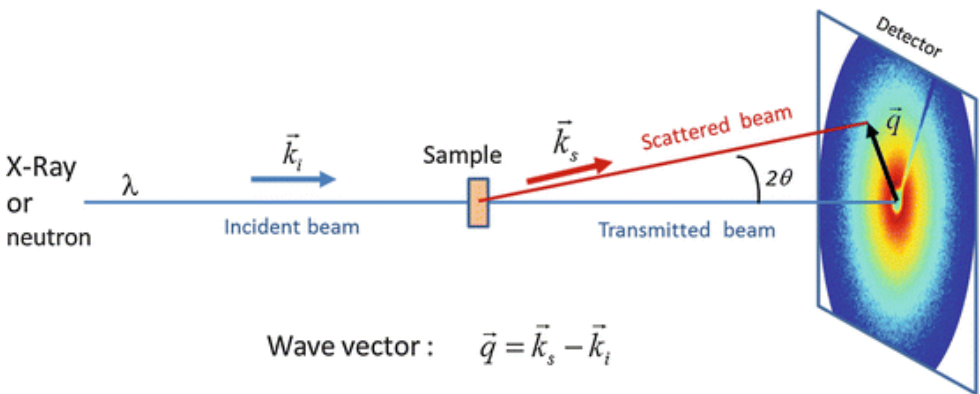


Figure 11.1. X-Ray beam in SAXS configuration [1].

11.3 Small angle X-ray scattering (SAXS) experiments in the diffractometer PANalytical X'Pert PRO MPD TT2 of the CCiT-UB

Dedicated laboratory instruments are commercially available for SAXS measurements. Besides, synchrotron SAXS measurements can also be performed, with the same applications but with higher performance.

Both cases have clear limitations; in the first case, much space is required in the laboratory and a significant economic investment. Likewise, to carry out experiences in synchrotron facilities, the available beam time is limited and/or

expensive. In addition, a previous pre-characterization of the samples is required to use this type of installation efficiently. Hence, the possibility to provide and develop in-house laboratory SAXS instruments in a quite standard X-ray diffractometer have clear advantages.

J. Bolze et al., [1] developed a methodology to perform optimal SAXS measurements in a multi-functional laboratory goniometer with pre-aligned x-ray modules. Therefore, in addition to responding to the need of many laboratories, they give greater versatility to conventional goniometers.

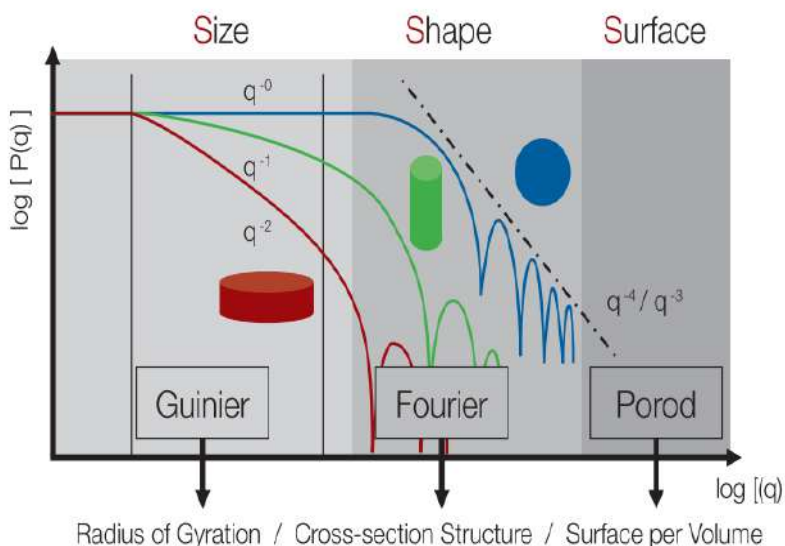


Figure 11.2. Guinier and Porod Plot [1].

This chapter assesses the feasibility of carrying out SAXS measurements in the Panalytical X'Pert PRO MPD *TT2* equipment located in the X-ray Diffraction laboratory of the CCI-UB for its subsequent application in the characterization of nanofluids. To do this, firstly will be selected the most appropriate geometry and optics to obtain useful SAXS measurements.

Second, using powder PANalytical nanocrystalline calibration standards and the EASYSAXS software will validate the results obtained with the X'Pert PRO MPD *TT2* diffractometer. Finally, preliminary measurements of nanofluids will be carried out to assess the suitability of this technique for this type of systems.

11.3.1 PANalytical X'Pert PRO MPD *TT2* characteristics

The PANalytical X'Pert PRO MPD *TT2* is a diffractometer with a vertical goniometer in θ/θ geometry of 240 mm radius and a smallest step size of 0.001 $^\circ 2\theta$, with a PreFix system [4].

A metal-ceramic, sealed Cu X-ray tube with a long fine focus (dimensions $12 \times 0.4 \text{ mm}^2$) is mounted on the omega arm of the goniometer. It usually operates at 1.8 kW, at 40 kV-45 mA.

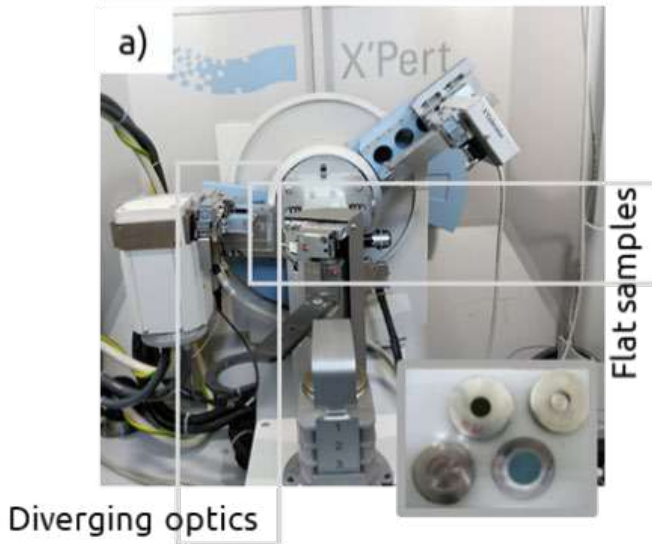
Typically, the *TT2* diffractometer can work in two configurations: (1) in Bragg-Brentano geometry with Ni filtered $K\alpha_{1-2}$ Cu radiation and (2) with a focalizing elliptic mirror primary optic providing monochromatized $K\alpha_{1-2}$ Cu radiation.

Moreover, the diffractometer can work both in reflection and transmission configuration. Usually Bragg-Brentano for reflection, **Figure 11.3-a**), and the mirror for transmission configurations, either with flats samples, sandwiched between low-absorbing thin films of polyester (*mylar*) or polyamide (*Kapton*), **Figure 11.3-b**) and **b**) or in capillary **Figure 11.3-c**..

11.3.2 SAXS geometry

Likewise, the diffractometer has the potential to work in SAXS geometry. The most successful SAXS configurations appears to be the focalizing mirror in capillary transmission geometry. The mirror incorporates a device to reduce the dispersion of the incident beam, as seen in **Figure 11.3-b** and **c**.

Bragg- Brentano Geometry



Transmission Geometry

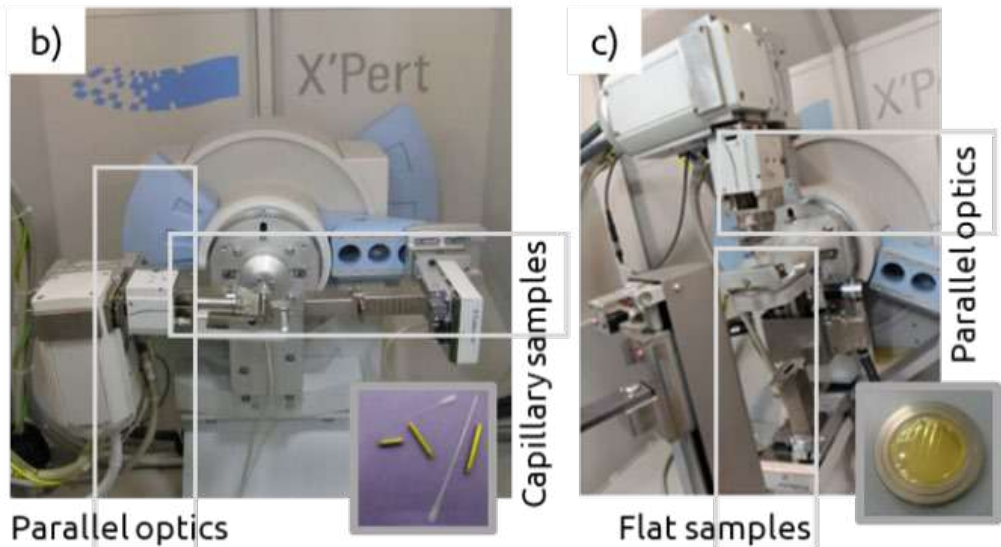


Figure 11.3. PANalytical X'Pert PRO MPD 772 configurations [4]; a) Bragg-Brentano geometry (reflection geometry), b) transmission geometry with capillary sample holder, and c) transmission geometry with flat transparent sample holder.

11.3.2.1 SAXS technical requirements

The instrumental requirements for performing SAXS measurements are challenging, as indicated by J. Bolze et al., [5]. One of the main requirements is that the intensity of the X-rays scattered by the sample must be measured as a function of the 2θ angle very close to the direct beam with $2\theta_{\min} < 0.1^\circ$ ($q_{\min} < 0.08 \text{ nm}^{-1}$). On the other hand, an intense but strongly collimated X-ray beam is required and must minimize any sources of parasitic scattering to achieve sufficient sensitivity. For this reason, the positioning and mechanical stability of the different optical components and prefix systems are crucial for an optimal fit. To work on the SAXS geometry, this will be a limiting parameter for implementing the technique in this diffractometer.

It is also essential to use a detector with high linearity, a high dynamic range, negligible intrinsic noise and a high spatial resolution to allow good low-angle resolution. In addition, to obtain high sensitivity, the beam path should be under vacuum; generating a beam vacuum path can avoid residual parasitic scattering from the air and consequently decrease the background level.

According to the positioning and stability requirement to obtain a very narrow beam, the configuration that presents the best values is the horizontal configuration with capillary samples. However, the alignment of the mirror and x-ray tube in the vertical configuration should be examined. This configuration shows centring deviations and instabilities mainly caused by using the extension arm in the refracted beam. Although negligible for conventional analysis, these slight deviations are critical for SAXS experiences.

11.3.2.2 SAXS configuration with parallel optics and capillary sample holder

The configuration to perform SAXS measurements in the PANalytical X'Pert PRO MPD TT2 diffractometer is shown in **Figure 11.4**.

Incident beam: On the side closest to the X-ray tube, an **incident divergence slit (1)** can be incorporated (these can be of different angular openings: $1/2^\circ$, $1/4^\circ$, $1/8^\circ$, $1/16^\circ$, $1/32^\circ$) that modify the height of the beam. Next, there is an opening to insert a **beam attenuator (2)**. Next the mirror **(3)** and the anti-scattering device.

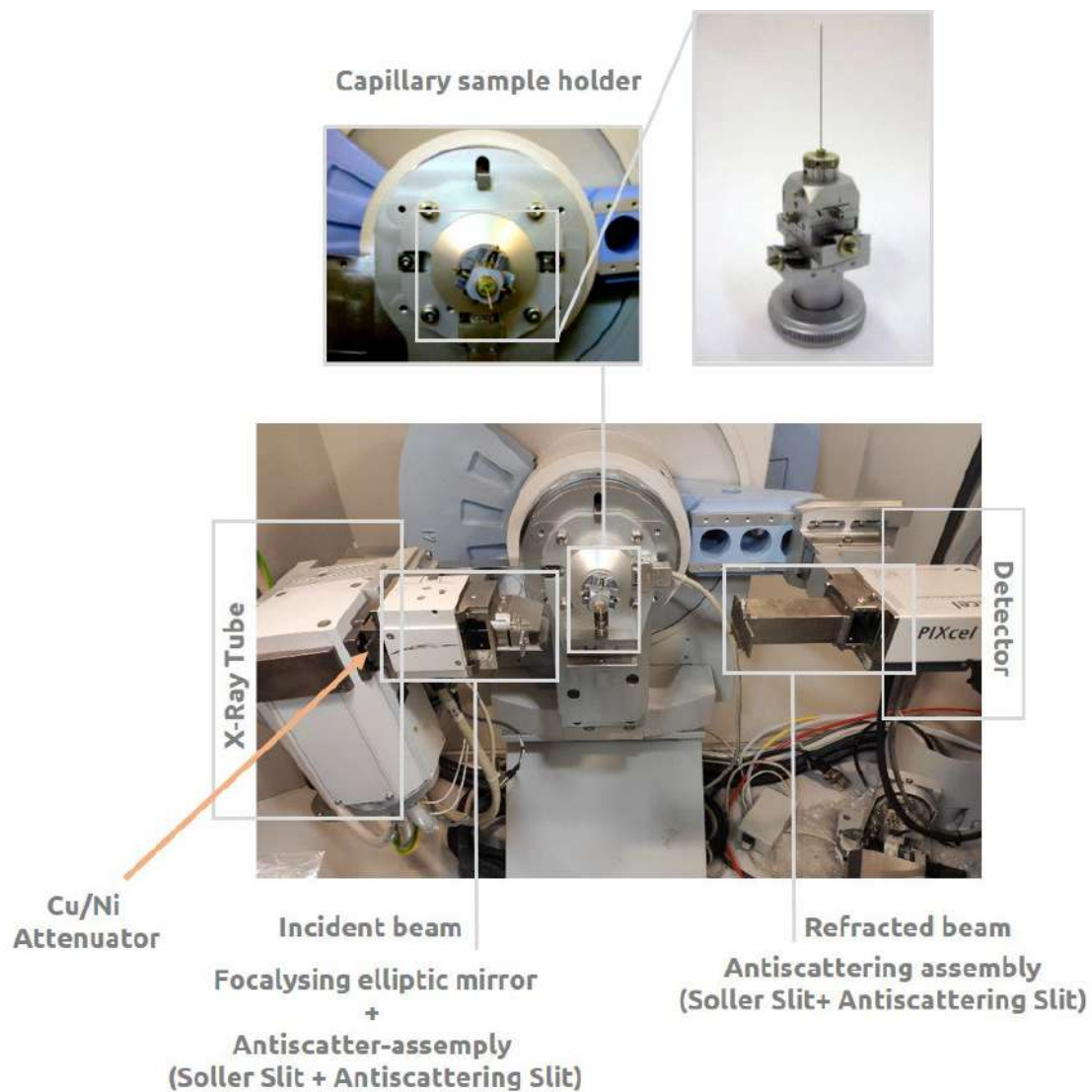


Figure 11.4. PANalytical X'Pert PRO MPD 772, with parallel optics configuration.

In the anti-scattering device, we find the following elements (from closer to farther from the X-ray tube): **(4) Soller slits** (reduce the effects of axial divergence) that can be of 0.01, 0.02 and 0.04 radians. **(5) Anti-scatter slit** (usually with the same opening than the divergence slit. **(6) Metal plate with a lip**, which reduces the signal due to air diffusion. **(7) beam-stop** placed after the capillary sample, which prevents the incident beam signal from reaching the detector.

Sample stage: sample holder platform in **rotating capillaries (8)**. The capillaries must be poorly absorbent and generally have a diameter of less than 2 mm. Those available are 8.5 cm long cylindrical glass tubes with a linear absorption coefficient for copper radiation of 97.4 cm^{-1} .

Scattered beam: first, there is an opening for an **anti-scatter slit (9)**, followed by an opening for **soller slit (10)**. Finally, there is the **detector (11)**; this equipment has a high-resolution PIXcel detector.

The SAXS configuration of the **Figure 11.4** consists of the following elements:

(1): Molybdenum divergent slit; $DS=1/32$ SAXS. **(2):** 0.2mm/Ni 0.02 mm attenuator. **(3):** Parallel optics mirror. **(4):**

No incident soller-slit (SS). **(5):** Anti-scatter incident slit $ASS=1/8$. **(6):** No metal plate with lip. **(7):** No beam stop. **(8):** Capillary stage. **(9):** Anti-scatter diffracted slit $ASS=0.1 \text{ mm}$. **(10):** No Diffracted DSS. **(11)** PIXcel detector.

11.3.3 SAXS measurements validation

11.3.3.1 Prefix system alignment

Before performing SAXS measurements, it is necessary to check the alignment of the optics with the X-ray tube.

The instrumental conditions of the diffractometer presented a SAXS peak shape service with a good peak position centration of 0.002° 2Theta, and good centration of the mirror assembly of 0.0007° 2Theta. These positioning values are suitable for making SAXS measurements.

11.3.3.2 Measurement program and samples preparation

After having the diffractometer in the SAXS geometry and checking the alignment of the optics, it remains to specify the measurement program. The SAXS measurements will be carried out under the following conditions with the X'Pert Data Collector program.

The measurement will be done with the detector in the receiving slit mode with an active length of 0.05 mm; a continuous scan is performed in the range of -0.115 to -5.005 $^{\circ}2\theta$ with a step size 0.010 $^{\circ}$ and a counting time of 1.5 seconds.

The attenuator is necessary for the range between -0.115 - 0.05 $^{\circ}2\theta$, to avoid saturation of the detector when the incident beam is almost parallel to the sample. Another crucial aspect of obtaining high-quality SAXS measurements is sample preparation.

0.3 mm diameter glass capillaries will be generally used. But if we work with highly absorbent samples, we will have to reduce the capillary radius; it is always advisable to determine these values to guarantee the quality of the measurement. Therefore, to obtain quality SAXS measurements, the absorption factor of the sample must be small. The optimal width of the sample will depend on the linear absorption coefficient of the sample, as show in **eq.11.1** [1]:

$$d_{opt}(cm) = \frac{1}{\mu} \quad (11.1)$$

Finally, background subtraction is an essential part of SAXS data processing, so the blank measurement must always be performed for each experiment and whenever the configuration

is modified, which can cause misalignment. Therefore, the blank (background) will be performed with an empty capillary with the same characteristics as the problem sample.

11.3.3.3 Easy SAXS software

Data processing is carried out using the specific PANalytical software (www.malvernpanalytical.com).

EasySAXS is a program licensed from Malvern Panalytical to process SAXS data. It is an advanced, user-friendly program that offers comprehensive data analysis to obtain structural and dimensional information, nanoparticles' shape, and specific areas at the nanoscale. The software includes data reduction, Guinier and Porod analysis, particle and pore size distributions, calculation of the pair distance distribution, least-squares fitting and model simulations.

11.3.3.4 Patterns

There are three calibration standards of nanoparticulate materials provided by PANalytical:

ZNO 41705 / TiO₂ 11210 / TiO₂ 41508

Following, the patterns characterization was performed.

11.3.3.5 EasySAXS characterization

The patterns analysis using EasySaxs software is shown in **Figure 11.6**. They

offer the size distribution per volume, the most frequent radius, the average radius, the relative standard deviation and the surface-to-volume ratio.

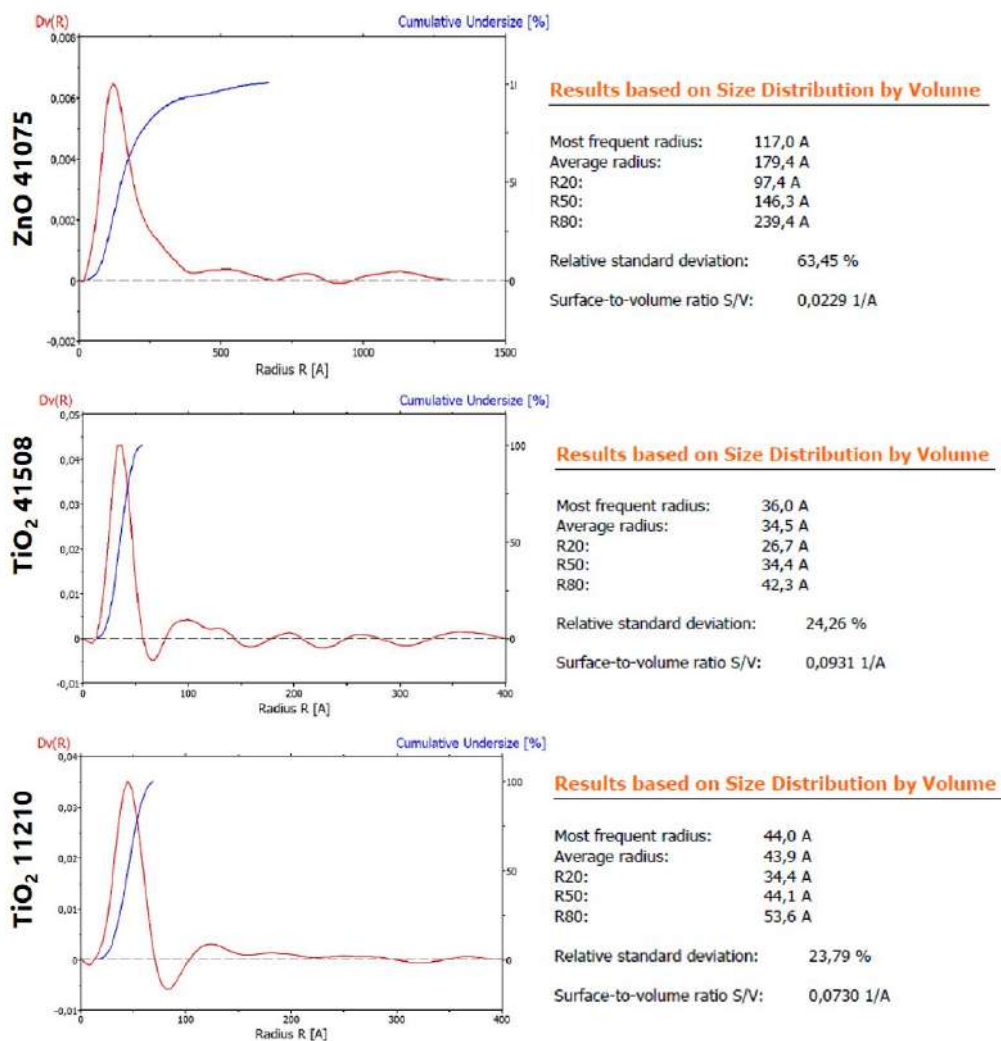


Figure 11.5. EasySaxs results for ZnO 41075, TiO₂ 41508, and TiO₂ 11210 patterns.

11.3.3.5.1 Phase and microstructural analysis

High statistics, high resolution Cu K α_1 powder XRD data have been obtained

in the PANalytical X'Pert PRO MPD *alpha1* diffractometer of the CCiT-UB. $2\theta/\theta$ scans from 4 to 145 $^\circ 2\theta$, step size 0.026 and a measuring time of 300 sec-

onds per step. The phase and micro-structure analysis of ZnO 41075, TiO₂ 41508 and TiO₂ 11210 patterns was fitted by Rietveld method using the TOPAS V6 software.

The fitted phases and their LVol-IB (that represents the crystal size), R-Bragg, space group and density crystal determination is shown in **Figure 11.7**, **Figure 11.8** and **Figure 11.9**, respectively. A good fit was obtained from the Rietveld analysis of the pattern

ZnO 41075, as depicted in **Figure 11-6**. Stephen's correction for anisotropic broadening has been applied.

The obtained residuals from the refinement were 6.42% for R_{wp} and 1.65% for R_{exp} , and 3.88% for GOF. This pattern presents two main phases: ZnO (57.51%) with an average crystallite size of 35.5 nm and hydrozincite (42.49%) with an average size of 70 nm.

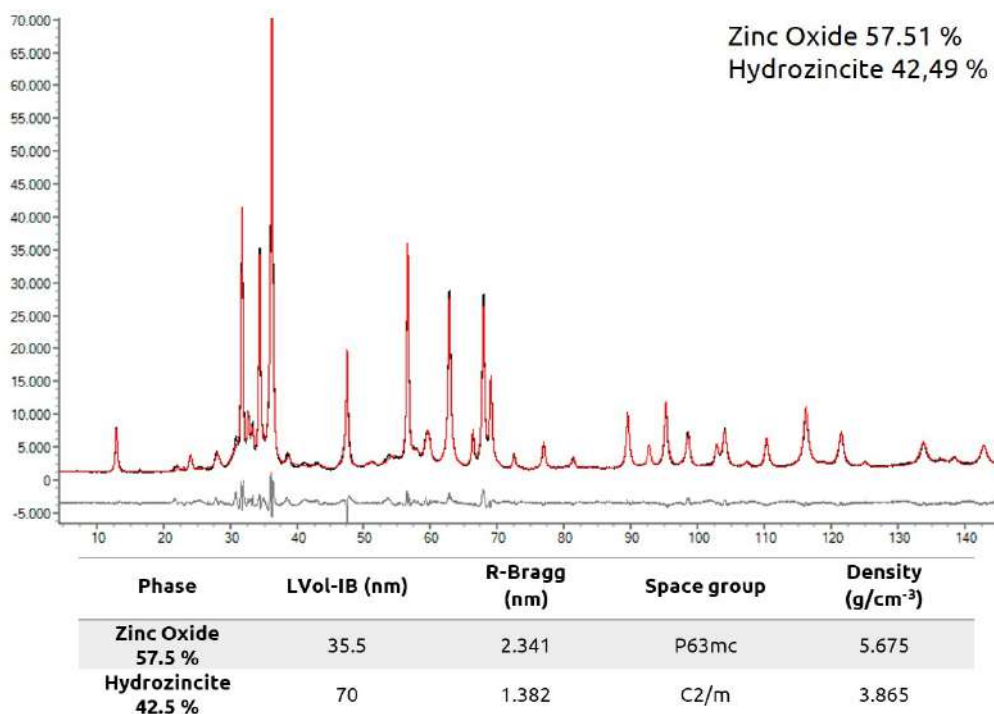


Figure 11.6. Phase and microstructural fit of ZnO 41075 pattern.

The ZnO phase turns out to have little chemical stability; therefore, the presence of the hydrozincite phase ($Zn_5(CO_3)_2(OH)_6$) may have formed (or increased its percentage) due to contact with the environment. Then, as a recommendation, careful handling and storage of patterns are mandatory.

The two TiO_2 standards, TiO_2 41508 and TiO_2 11210, present the Anatase structure as the main phase, as can be seen in the profile fits of **Figure 11-7** and **Figure 11-8**, respectively. Both patterns offer a good fit. As for the ZnO pattern, the Stephens correction has been applied for the anisotropic

broadening in both TiO_2 patterns. The obtained residuals from the pattern TiO_2 41508 refinements were 1.59% for R_{wp} and 1.32% for R_{exp} , and 1.20% for GOF. The main anatase phase (94.65%) has an average crystallite size of 12.86 nm. However, it is remarkable that the minor Rutile phase has a significantly larger crystallite size than anatase, with an average of 30.5 nm. On the contrary, the residuals from the refinement of the pattern TiO_2 11210 were 1.71% for R_{wp} , 1.32% for R_{exp} , and 1.27% for GOF. The main anatase phase (95.53%) has an average crystallite size of 11.49.

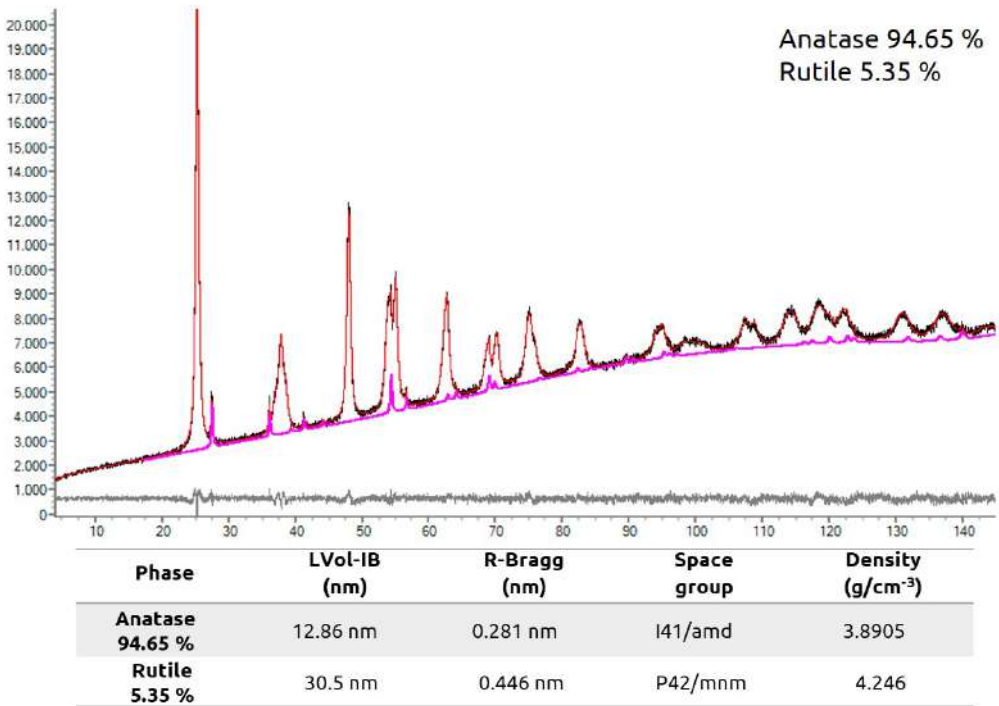


Figure 11.7. Phase and microstructural fit of TiO_2 41508 pattern.

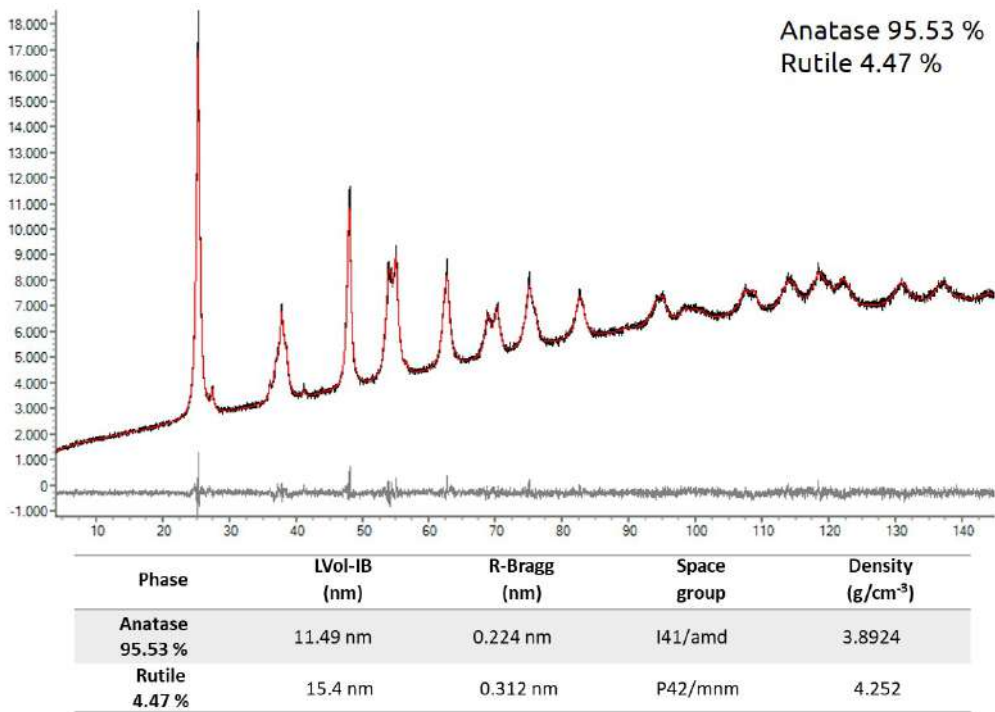


Figure 11.8. Phase and microstructural fit of TiO₂ 11210 pattern.

11.3.3.5.2 TEM

Figure 11.10. The average particles size and form were tabulated in Table 11.1.

TEM images of ZnO 41075, TiO₂ 41508 and TiO₂ 11210 patterns are shown in

Table 11.1. Patterns Average particles size (nm) and form.

Sample	Average size (nm)	Nanoparticles' form
ZnO 41075	Two main sizes distribution: (1) 30-32 nm (2) ~60 nm	Lamellar and spherical nanoparticles. Nanoparticles' agglomeration.
TiO ₂ 11210	Primary size distribution: 9-12 nm Minoritarian (elongated): ~50 nm	Majoritarian spherical and minor cluster of elongated nanoparticles. High nanoparticles' agglomeration.
TiO ₂ 41508	Primary size distribution: 13-15 nm Minoritarian (elongated): ~50 nm	Spherical and elongated nanoparticles. High nanoparticles' agglomeration.

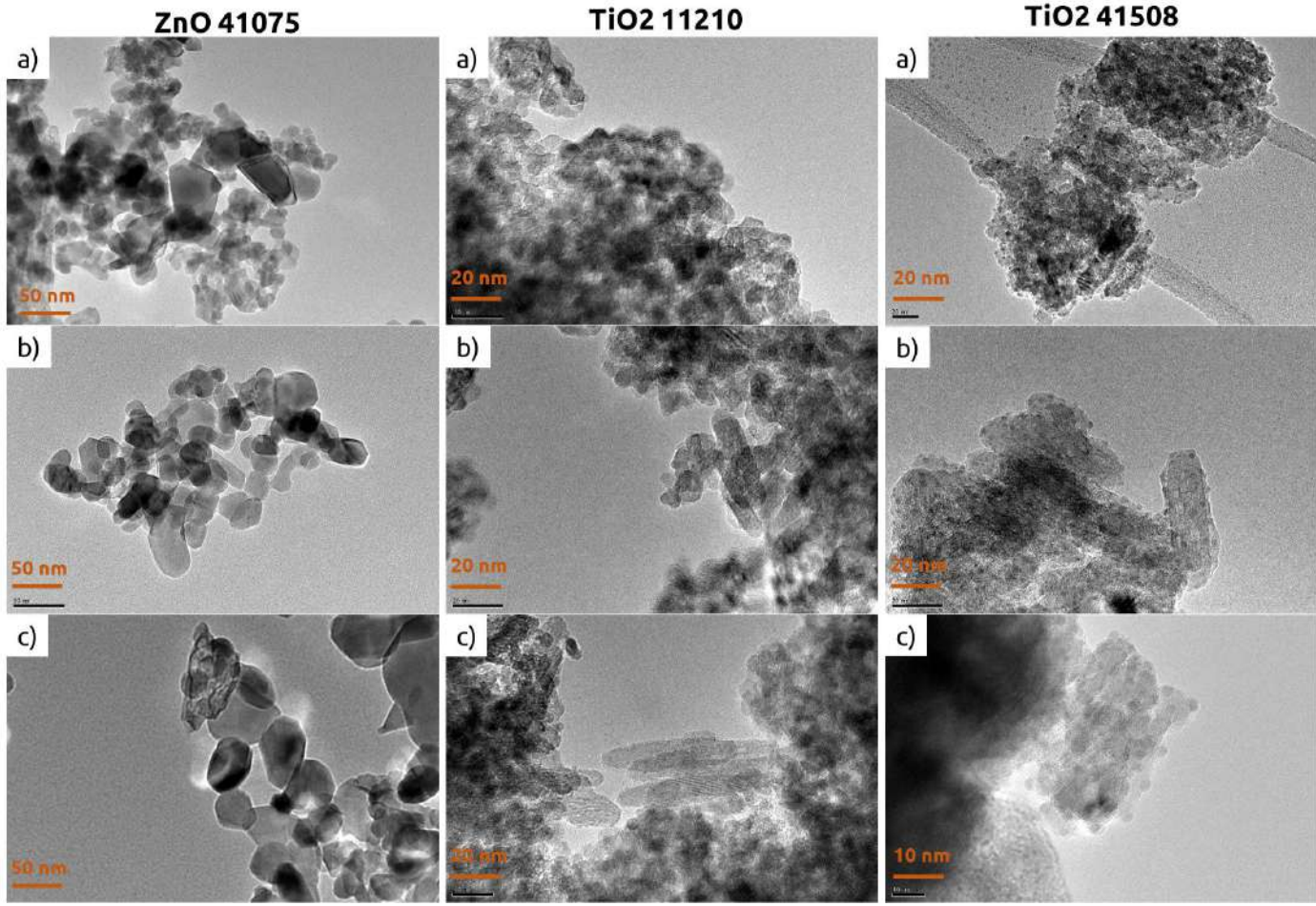


Figure 11.9. TEM images.

11.3.3.5.3 Brunauer-Emmett-Teller
(BET)-Specific Surface Area

The BET specific area analysis of the patterns is shown in **Table 11.2**, where the specific area, pore volume and pore size values are tabulated.

Table 11.2. SAXS patterns BET analysis.

Sample	BET surface area (m ² /g)	Pore volume (cm ³ /g)	Pore Size (Å)
ZnO 41075	19.3893	0.010237	21.1184
TiO ₂ 41508	122.3376	0.064736	21.1664
TiO ₂ 11210	149.5506	0.078722	21.0557

11.3.3.6 Results summary and patterns validation

Table 11.3 summarizes all the patterns characterizations.

Table 11.3. Patterns characterization results summary by BET, SAXS, TEM, Rietveld, and PANalytical references values.

		ZnO 41075	TiO ₂ 41508	TiO ₂ 11210
BET	Surface Area (m ² /g)	19.3893	122.3376	149.5506
	S/V (Å ⁻¹)	0.0229	0.0730	0.0931
SAXS	Surface area (m ² /g)	46.67	187.63	239.18
	Most frequent radius (nm)	11.7	3.60	4.40
	Average radius (nm)	17.94	3.45 (6.9)	4.39
	Morphology	Lamellar/spherical	-	-
TEM	Morphology	Lamellar/spherical	Mainly spherical	Spherical/elongated
	Average diameter	30-32	6-15	8-12
Rietveld Fit	LVol-IB* (nm)	35.5	12.86	11.49
	Density* g/cm ³	4.906	3.8905	3.8924
PANalytical REF VALUES	S/V (Å ⁻¹)	0.0226	-	0.0736
	Most frequent radius (nm)	11.7	-	4.40
	Average radius (nm)	20.12	-	4.38

11.3.4 Conclusions

According to the results summarized in **Table 11.3** the morphology and size values obtained through SAXS in the PANalytical X'Pert PRO MPD q/q equipment agree with TEM and Rietveld characterizations.

In addition, the results show excellent reproducibility compared to those provided by PANalytical.

The specific surface area presents differences between the SAXS and BET techniques. This variation may be caused by the high agglomeration of the nanoparticles observed by TEM (accentuated with the decrease in particle size). This agglomeration causes a reduction in the specific area of the samples and can explain the observed differences.

Considering the results, the feasibility of performing high-resolution SAXS measurements on the PANalytical X'Pert PRO MPD q/q diffractometer is shown, considering the instrumental limitations and possibilities.

11.4 SAXS for MSBNFs characterization

This section will evaluate the usefulness of the SAXS technique in molten salt-based nanofluids. The available

bibliography for nanofluids is collected in the following **Table 11.4**. Currently, the literature does not offer any results using this technique for salt-based systems.

Table 11.4. Summary of published articles about nanofluids characterization by SAXS technique.

Title	System	Year	REF
Application of SAXS to the study of particle-size-dependent thermal conductivity in silica nanofluids	SiO ₂ -Water	2008	[6]
Particle shape effects on thermophysical properties of alumina nanofluids	EG/H ₂ O-Al ₂ O ₃	2009	[7]
Thermal Transport in Nanofluids: Boiling heat transfer	-	2011	[8]
An investigation of silicon carbide-water nanofluid for heat transfer applications	SiC-water	2009	[9]
Systematical study of multi-walled carbon nanotube nanofluids based disposed transformer oil	MWCNT-Oil	2020	[10]
Experimental evidence for the significant role of initial cluster size and liquid confinement on thermophysical properties of magnetic nanofluids under applied magnetic field	Oleic acid-Fe ₃ O ₄	2018	[11]
Investigation of particle size distribution and aggregate structure of various ferrofluids by small angle scattering experiments	Fe ₃ O ₄ -organic fluid	1999	[12]
Adsorption of poly (acrylic acid) onto the surface of titanium dioxide and the colloidal stability of aqueous suspension	TiO-acrylic acid	2005	[13]
Aggregation and settling in aqueous polydisperse alumina nanoparticle suspensions	Al ₂ O ₃ -water	2012	[14]
Preparation of metal oxide nanoparticles of different sizes and morphologies, their characterization using small angle X-ray scattering and study of thermal properties	CuO/Fe ₃ O ₄ -water	2014	[15]
Amphiphile-based nanofluids for the removal of styrene/acrylate coatings: Cleaning of stucco decoration in the Uaxactun archeological site (Guatemala)	Amphiphile-based nanofluid	2015	[16]
The phase diagram of colloidal silica-PNIPAm core-shell nanogels	Silica-PNIPAm	2020	[17]
A novel Nanodiamond based Ionanofluid: Experimental and mathematical study of thermal properties	nanodiamond-ionic liquid	2018	[18]
Structural, thermodiffusive and thermoelectric properties of maghemite nanoparticles dispersed in ethylammonium nitrate	maghemite-ethylammonium nitrate	2020	[19]

11.4.1 Methodology and samples preparation

NaNO₃ samples with 1 wt% of SiO₂ nanoparticles are used with the methodology and sample preparation developed in **section 7.3**. SiO₂ nanoparticles were previously characterized by TEM in **Chapter 10**, where an average particle size of 20-30 nm and spherical geometry was determined.

In this characterization, a new variable is added. The measurements will be carried out under temperature control. However, a cryostat is available for the capillary configuration, with a maximum service temperature of 500K. The cryostat is mounted on the capillary stage and is cooled with nitrogen.

11.4.2 Results

Figure 11-10 depicts the scattering curves obtained from SiO₂ nanofluids in the temperature range between 20°C -227°C, where $\Delta\rho = \rho_1 - \rho_2$ and ρ_1 is the SiO₂-NaNO₃ nanofluid and ρ_2 is the NaNO₃-capillary subtracted matrix. Then, to obtain the scattering from the particles alone, one must subtract the scattering of the matrix material, **eq. 11.2 [1]**:

$$\Delta I(q) = I_{S,exp}(q) - I_{M,exp}(q) \quad (11.2)$$

A pronounced peak around 0.3 nm⁻¹ was observed for all the temperatures. This peak generally is attributed to the particles align themselves into a highly ordered and periodic (i.e., crystalline) arrangement and corresponds to the Bragg peak. The position of its maximum (q_{peak}) indicates the distance (d_{bragg}) between the aligned particles by using Bragg's law (**eq.11.3**). All temperatures show the same d_{bragg} above 25.70 nm.

$$d_{bragg} = \frac{2 \cdot \pi}{q_{peak}} \quad (11.3)$$

As seen previously, it is possible to determine the nanoparticles main shape with the Guinier plot. **Figure 11-11**, shows a double logarithmic plot of $\ln(\Delta I(q))$ vs $\ln(q)$. If the initial slope is 0, -1 or -2 indicates globular, cylindrical or lamellar shape, respectively. If the slope is steeper than -3/-4, indicates that the particles are larger than the resolution limit and the Porod region is the only part of the form factor that can be observed. The sample slope is around -3 at 20°C, indicating that the sample is above the resolution limit and the shape is not easily determine. Therefore, complementary techniques such as TEM are essential for complete characterization. On the contrary, the

slope tends to decrease with temperature indicating a possible deagglomeration of the particles.

Since a modification of the nanoparticles is not expected, the most relevant parameters for nanofluids are the size distribution and the specific area as a function of temperature. **Figure 11-12** shows the results obtained using the NMSBNF's EasySAXS software at 20°C, 90°C, 120°C and 227°C. A variation of the size distribution with temperature can be observed. In addition, as determined in Figure 7.12, the maximum values of the radii are at the resolution limit.

A low intensity values at 20°C and 90°C was observed for all temperatures at

small q-values, this behaviour is typical for repulsive interaction, which corresponds to aggregation phenomena of the particles.

For the sample at 20°C the most frequent radius is 14.30 nm and at 90°C, over 16.92 nm, that is according to the average particles size obtained by TEM. Likewise, at 90°C the distribution becomes narrower, indicating the decrease of nanoparticles agglomeration obtaining a more homogeneous nanoparticles' dispersion in the salts.

However, the negatives values can indicate and inhomogeneous particles or changes in the particles contrast as when the contrast of one region is smaller than the matrix system.

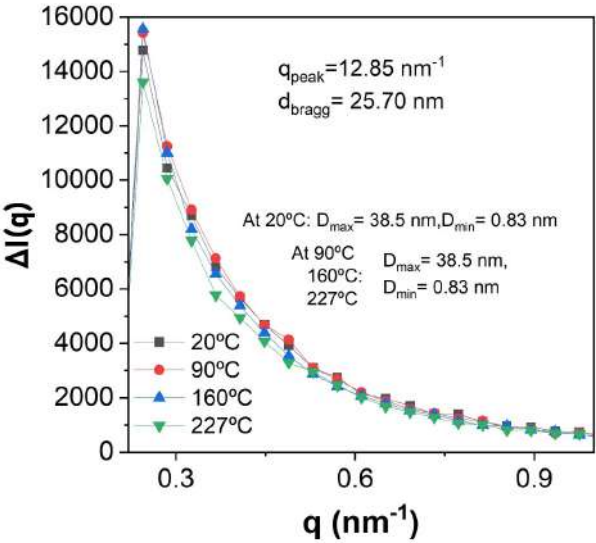


Figure 11.10. NSBNF-1 wt% SiO₂ nanoparticles scattering curves as a function of temperature.

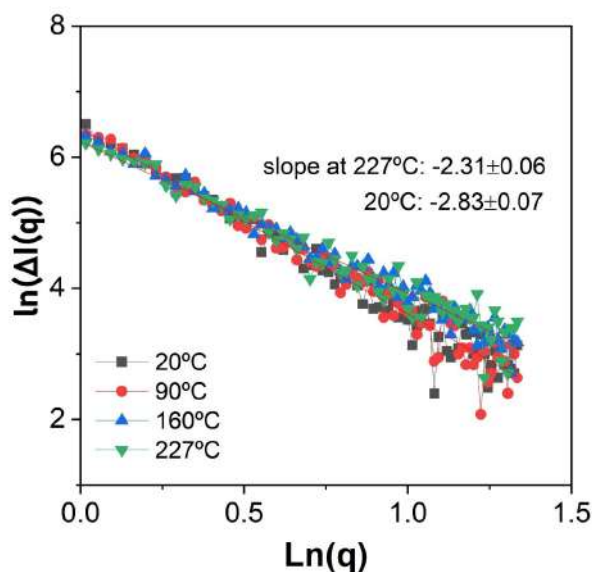
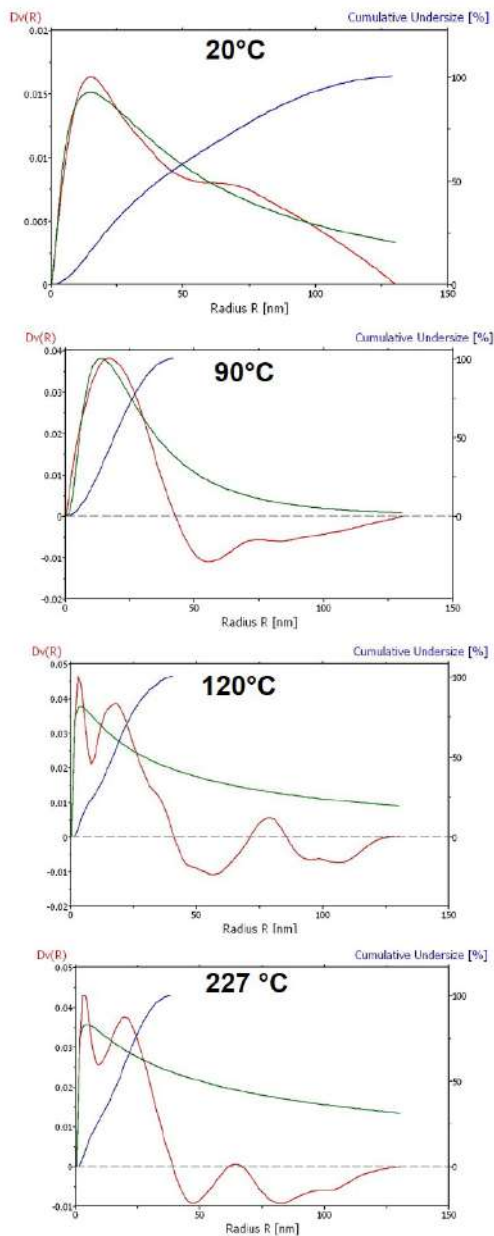


Figure 11.11. Nanoparticles form factor.

At higher temperatures, 160°C and 227°C, the volume distributions show a dissimilar behaviour. For both temperatures a narrow particles distribution of small radius of 2.60 nm are observed, smaller than the nanoparticles average size, indicating the presence of another phase/structure. At the same time the average radius at both temperatures agrees with the size distribution at lowest temperatures. Moreover, the distributions go to negatives values due to the excluded volume caused by the hard-sphere effect, and shows a second maximum at larger distances, that is attributed to the shell of next-neighbouring particles which increase the density above

bulk level due to the locally increased particle concentration, typical for liquid-phase state. Therefore, the negatives values correspond to smaller electron densities than the bulk.

Finally, the surface-area-to-volume is the surface per amount of area per unit volume of an object. According to the table of the **Figure 11-12** S/V values increases with the increases of temperature from approximately 0.13 nm⁻¹ (20°C) to 0.33 nm⁻¹ (227°C). Furthermore, the variation of this parameter can be attributed by the prevalence of smaller size distributions.



Temperature (°C)	Most frequent radius (nm)	Average radius (nm)	Relative standard deviation (%)	Surface-to-volume ratio (1/nm)
20	14.30	47.15	66.01	0.1300
90	16.90	19.13	47.39	0.2289
160	2.60	16.70	57.59	0.3390
227	2.60	16.64	55.52	0.3312

Figure 11.12. Radial distribution per volume at a function of temperature and surface-to-volume values of NMSBNF- 1wt% SiO₂ nanoparticles.

11.4.3 Contribution to the state of the art

A graphic consisting of a teal rounded rectangle. On the left side, there is a dark grey circle with a white border. Inside the circle, the text "Key point 6" is written in white, bold font, and "Characterization" is written below it in a smaller white font. To the right of the circle, the text "Lack of techniques to characterize MSBNs in a liquid state at high temperature." is written in a dark grey font.

Key point 6
Characterization

Lack of techniques to characterize MSBNs in a liquid state at high temperature.

- ✓ This technique shows a high potential to characterize nanofluids and obtain relevant information about their thermal behaviour. In addition, if combined with a higher temperature cryostat, it would offer the possibility of distribution sizes and specific areas in a liquid state and at working temperatures in CSP. In addition, it not only serves to characterize nanoparticles but by working with contrast differences, the formation of new phases, structures or another phenomenon's can be identified.
- ✓ One of the most relevant results is the presence of a predominant distribution of small radius. This phenomenon could coincide with the formation of nanostructures around the nanoparticles, as proposed by the literature described in **section 5.4.1.1**. Besides, it agrees with the results of **Chapter 9**, where nanostructures with higher density and specific area than bulk were formed.

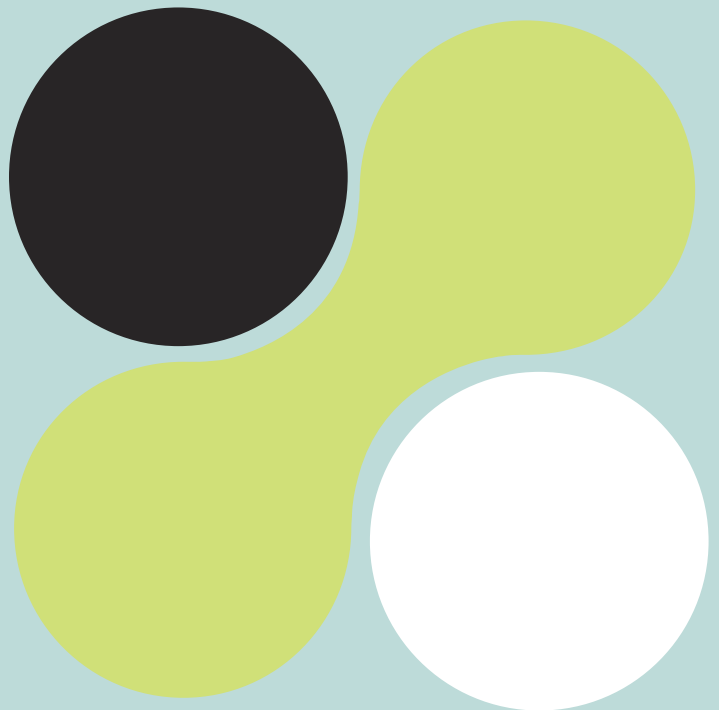
- ✓ Therefore, this chapter contributes directly to **Key point VI** by offering a methodology to characterize nanofluids with temperature and presenting original and complementary data to advance nanofluids research.

- ✓ Finally, it should be mentioned that these are preliminary results, and need to be confirmed since the subtraction of the matrix can only be carried out directly when the sample and the matrix present similar transmittance values $T_s=T_m$. Different corrections must be applied for the correct data treatment according to **eq. 11.4** [1] if the transmittance values are dissimilar. The experimental scattering curves must be scaled by their respective transmittance values taking in account the dark-count rate of the detector, $I_{dc}(q)$. Therefore, the transmittance values of the samples should be previously determined for a correct data treatment.

$$\Delta I(q) = \frac{I_{S,exp}(q) - I_{dc}(q)}{T_S} - \frac{I_{M,exp}(q) - I_{dc}(q)}{T_M} \quad (11.4)$$

12

Results summary



12. Results summary

Following, the main results are summarized.

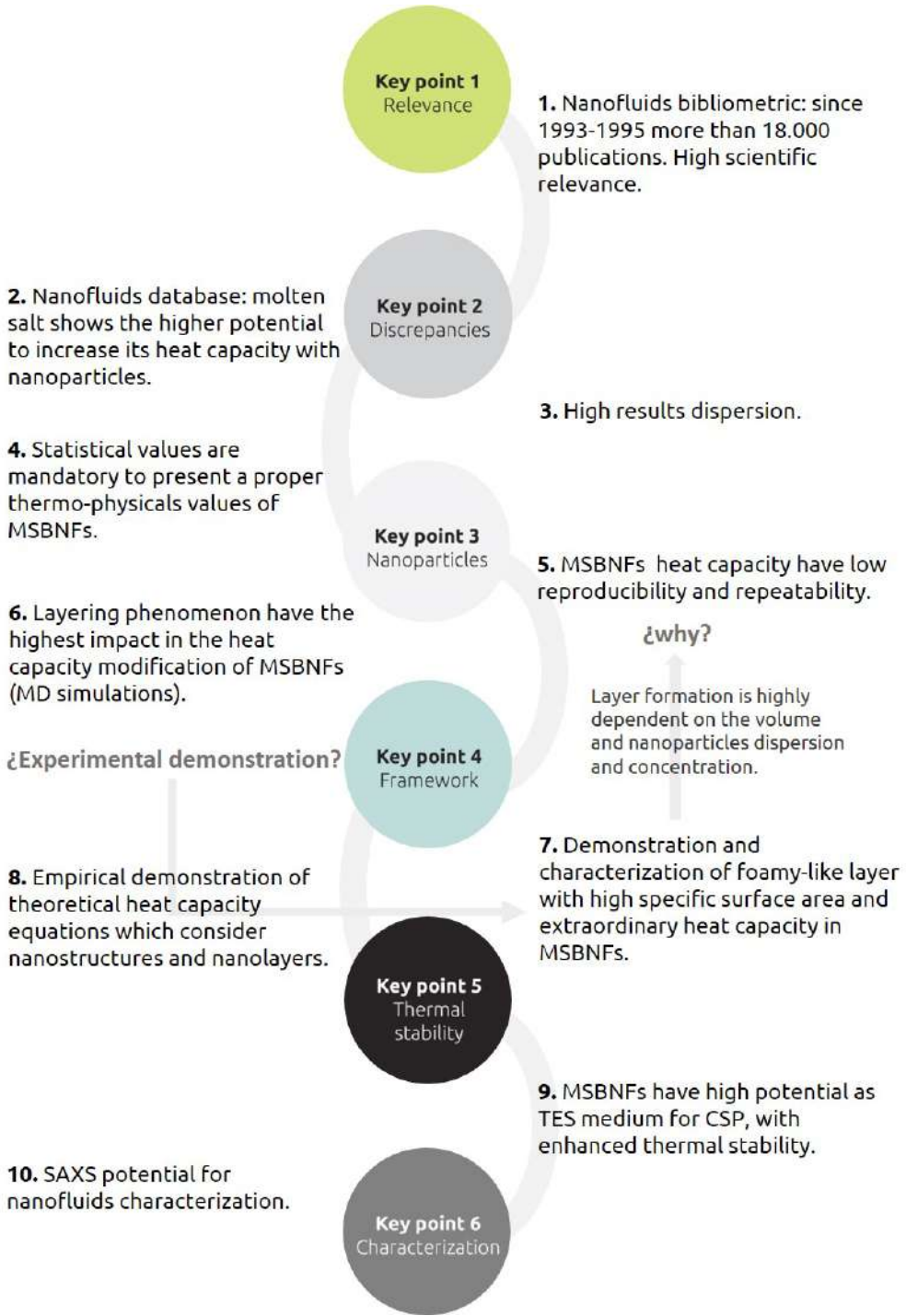
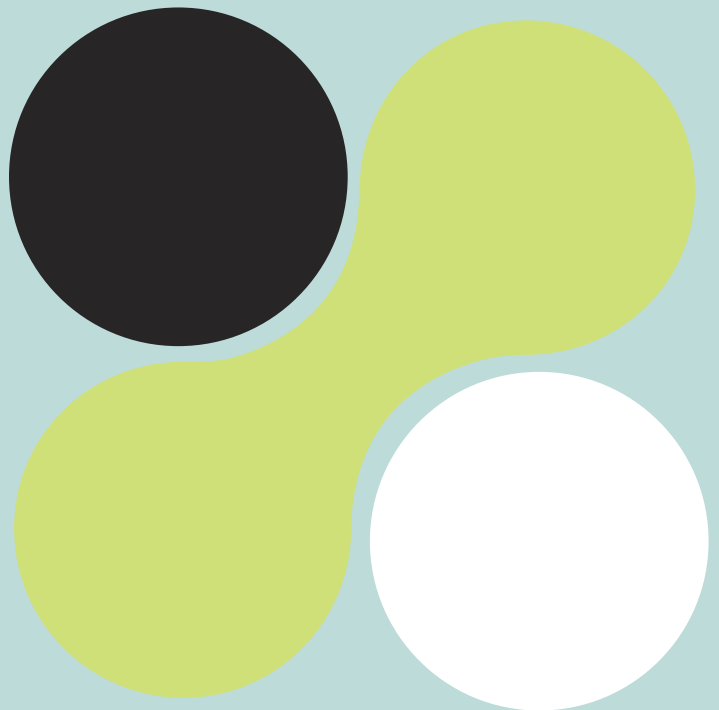


Figure 12.1. Results summary.

13

Conclusions and future work



13. Conclusions and future work

13.1 General conclusions

In this thesis, results regarding the behaviour of nanofluids based on nitrate salts, their state of the art, and their potential as a thermal storage fluid, and above all, the identification of the fundamental mechanisms that contribute to the heat capacity modification were presented.

The main conclusions derived from the PhD thesis are listed below:

- i. Nitrate salt-based nanofluids are bi-phasic systems due to the reactivity between the nanoparticles and the ionic medium, forming a "foamy-like" phase. This phase comprises nanostructures with a high specific area and high heat capacity (100% greater than pure sodium nitrate) and a melting temperature of around 450 °C.
- ii. The formation of the foamy-like phase demonstrates the liquid layering experimentally around the surface of the nanoparticles in the first order and the formation of nanostructures in a long range. Furthermore, the thermal characterization of nanostructures has made it possible to validate the equations proposed in the literature for predicting the heat capacity of nanofluids, offering an advance in the development of a theoretical framework.

- iii. The formation of the foamy-like phase and, therefore, the increase in heat capacity is greatly influenced by the combination of sample quantity, concentration and dispersion of the nanoparticles and the preparation method.
- iv. The nanofluids characterization by conventional techniques such as difference scanning calorimetry (DSC) is limited due to the difficulty of obtaining a representative sample with the optimal concentration and, more importantly, with a homogeneous dispersion of the nanoparticles. This difficulty is reflected in the heat capacity results obtained after the sampling study, where the increase in C_p for the same sample collections varied between -20 to 80%. At the same time, this ΔC_p deviation justifies the results published in the literature, which indicates that the source of error is given by the lack of an adequate methodology to characterize nanofluids and obtain a representative sample.
- v. Due to the low reproducibility of results due to the dependencies mentioned above and the difficulty obtaining representative samples, it is essential to present data with good statistics. Nevertheless, not only limited to statistical values but to follows a standard methodology and a detailed description of the methodological procedures to facilitate the comparison between results. From chapter 7, the proposal of a measurement methodology for DSC is derived:
 1. Synthesize at least two independent samples to minimize the error associated with the synthesis method.
 2. Obtain at least three sub-samples from each sample using standard quartering methodologies.
 3. Prior to characterization, pre-melt the samples.
 4. For each property to be analysed, carry out at least 2 repetitions per sample.
 5. Finally, perform the appropriate statistical treatment.
- vi. Based on the thermophysical properties, molten salt-based nanofluids have a high potential to be used as heat transfer media in thermal storage systems for CSP. Thanks to its increased heat capacity, it would allow the reduction of the volume of thermal storage tanks, directly impacting the reduction of storage costs and the environmen-

tal impacts of the use of salts. Despite the nanofluids potential in TES systems, due to the high cost of nanoparticles and the difficulty of synthesizing nanofluids on a large scale and at a low cost, numerous challenges and obstacles have been overcome by the scientific community to bring nanofluids closer to the industry.

Accordingly, three main considerations are summarized:

- i. Despite enhancing the efficiency of TES systems by using nanofluids, the nanofluids synthesis production cost and specifically the costs associated with the nanoparticle production should decrease considerably to obtain economic benefits in the substitution of the TES medium. Therefore, the increased TES material cost must be balanced by the cost reduction of the overall TES system due to the reduction of the storage tank volume and expanding its lifespan.
- ii. The use of nanoparticles carries environmental and health risks, so the next step is to consider this aspect in evaluating sustainability issues.
- iii. Finally, one of the main points is that if salt-based nanofluids be-

have as a biphasic system, their applicability to storage systems in a two-tank configuration might be reconsidered, which brings us to introduce this aspect in the design of new storage configurations.

13.2 Future work

All research opens new paths, new challenges, and objectives. Several future works and proposals are derived from this thesis, which are summarized in the following four points:

- i. Research for more sustainable and economical nanofluids. One of the main factors that modify the heat capacity is the high specific area of the nanoparticles. Based on this idea, it is proposed to search for other systems with a high specific area.
- ii. In the thesis, a foamy-like phase with exceptional thermal properties has been identified. For this reason, it is proposed to study new synthesis routes to obtain materials with the structure and properties of the layer.
- iii. The formation of a biphasic system may inspire new configurations of TES tanks for CSP, such as the study of nanofluids in thermocline configuration.

- iv. The research carried out at the University of Birmingham shows the potential of nanofluids to reduce corrosion rates. Hence, studying the corrosion of nanofluids is essential for applying nanofluids in CSP plants and increasing the useful life of metallic components in contact with salts.
- v. Finally, essential future work is the study of the environmental impact and the study of routes to incorporate nanofluids in a circular economy.

Re.

References



References

Chapter 1

- [1] Delbeke, J., Runge-Metzger, A., Slingenberg, Y., and Werksman, J. 2015. The Paris agreement. United Nations, *Towards a Climate-Neutral Europe: Curbing the Trend*, pp. 24–45. doi: 10.4324/9789276082569-2.
- [2] Yoichi, K. and Keiichi, Y. 1997. *Environment, energy, and economy: Strategies for sustainability*, The United. Tokio-New York-Paris: United Nations University Press.
- [3] Bp. and Looney, B. 2021. Statistical Review of World Energy 2021, *bp Review World Energy data*, vol. 70, pp. 8–20.
- [4] International Energy Agency. 2021. Global Energy Review 2021, *Global Energy Review 2020*, pp. 1–36. [Online]. Available: <https://iea.blob.core.windows.net/assets/d0031107-401d-4a2f-a48b-9eed19457335/GlobalEnergyReview2021.pdf>
- [5] Henner, D. and REN21. 2017. *Ren21- renewables 2021 global status report*, 2021st ed. Paris: REN21 Secretariat. [Online]. Available: [https://abdn.pure.elsevier.com/en/en/researchoutput/ren21\(5d1212f6-d863-45f7-8979-5f68a61e380e\).html](https://abdn.pure.elsevier.com/en/en/researchoutput/ren21(5d1212f6-d863-45f7-8979-5f68a61e380e).html)
- [6] Murdock, H. E. 2019. *Renewables 2019 Global Status Report Collaborative*, vol. 105, no. July. [Online]. Available: <http://www.ren21.net/gsr-2019/pages/foreword/foreword/>
- [7] Wagner, S. J. and Rubin, E. S. 2014. Economic implications of thermal energy storage for concentrated solar thermal power, *Renewable Energy*, vol. 61, pp.

- 81–95. doi: 10.1016/j.renene.2012.08.013.
- [8] Islam, M. T., Huda, N., Abdullah, A. B., and Saidur, R. 2018. A comprehensive review of state-of-the-art concentrating solar power (CSP) technologies: Current status and research trends, *Renewable and Sustainable Energy Reviews*, vol. 91, no. November 2017, pp. 987–1018. doi: 10.1016/j.rser.2018.04.097.
- [9]. 2019. *Renewables 2019 Analysis and forecast to 2024*. IEA, International Energy Agency.
- [10] Achkari, O. and El Fadar, A. 2020. Latest developments on TES and CSP technologies – Energy and environmental issues, applications and research trends, *Applied Thermal Engineering*, vol. 167, no. August 2019, p. 114806. doi: 10.1016/j.applthermaleng.2019.114806.
- [11] Peterseim, J. H., White, S., Tadros, A., and Hellwig, U. 2013. Concentrated solar power hybrid plants, which technologies are best suited for hybridisation?, *Renewable Energy*, vol. 57, pp. 520–532. doi: 10.1016/j.renene.2013.02.014.
- [12] Crespo, L. 2021. *The long-term market potential of concentrating solar power systems*, 2nd ed. Elsevier Ltd. doi: 10.1016/b978-0-12-819970-1.00004-9.
- [13] Peiró, G., Gasia, J., Miró, L., Prieto, C., and Cabeza, L. F. 2017. Influence of the heat transfer fluid in a CSP plant molten salts charging process, *Renewable Energy*, vol. 113, pp. 148–158. doi: 10.1016/j.renene.2017.05.083.
- [14] Report, T. 2014. *The Economic and Reliability Benefits of CSP with Thermal Energy Storage : Literature Review and Research Needs*.
- [15] Prieto, C., Osuna, R., Fernández, A. I., and Cabeza, L. F. 2016. Thermal storage in a MW scale . Molten salt solar thermal pilot facility: Plant description and commissioning experiences, *Renewable Energy*, vol. 99, pp. 852–866. doi: 10.1016/j.renene.2016.07.053.
- [16] Prieto, C., Osuna, R., Fernández, A. I., and Cabeza, L. F. 2016. Molten salt facilities, lessons learnt at pilot plant scale to guarantee commercial plants; heat losses evaluation and correction, *Renewable Energy*, vol. 94, pp. 175–185. doi: 10.1016/j.renene.2016.03.039.
- [17] Mostafavi, S. S., Taylor, R. A., Nithyanandam, K., and Shafiei, A. 2017. Annual comparative performance and cost analysis of high temperature , sensible thermal energy storage systems integrated with a concentrated solar power plant, *Solar Energy*, vol. 153, pp. 153–172. doi: 10.1016/j.solener.2017.05.044.
- [18] Jacob, R., Belusko, M., Fernández, A. I., Cabeza, L. F., Saman, W., and Bruno, F. 2016. Embodied energy and cost of high temperature thermal energy storage systems for use with concentrated solar power plants, *Applied Energy*, vol. 180, pp. 586–597. doi: 10.1016/j.apenergy.2016.08.027.
- [19] Wahab, A., Hassan, A., Arslan, M., Babar, H., and Usman, M. 2019. Solar energy

systems – Potential of nanofluids, *Journal of Molecular Liquids*, vol. 289. doi: 10.1016/j.molliq.2019.111049.

- [20] Cuce,E.,Cuce,P. M.,Guclu,T.,and Besir,A. B. 2020.On the use of nanofluids in solar energy applications, *Journal of Thermal Science*, vol. 29, no. 3, pp. 513–534. doi: 10.1007/s11630-020-1269-3.

Chapter 2

- [1] Choi,S. U. S. 1995.Enhancing thermal conductivity of fluids with nanoparticles, *American Society of Mechanical Engineers, Fluids Engineering Division (Publication) FED*, vol. 231, no. January 1995, pp. 99–105.
- [2] Buongiorno,J. 2006.Convective transport in nanofluids, *Journal of Heat Transfer*, vol. 128, no. 3, pp. 240–250. doi: 10.1115/1.2150834.
- [3] Eastman,J. A.,Choi,S. U. S.,Li,S.,Yu,W.,and Thompson,L. J. 2001.Anomalously increased effective thermal conductivities of ethylene glycol-based nanofluids containing copper nanoparticles, *Applied Physics Letters*, vol. 78, no. 6, pp. 718–720. doi: 10.1063/1.1341218.
- [4] Choi,S. U. S.,Li,S.,and Eastman,J. A. 1999.Measuring thermal conductivity of fluids containing oxide nanoparticles, *Journal of Heat Transfer*, vol. 121, no. 2, pp. 280–289. doi: 10.1115/1.2825978.
- [5] Khanafer,K.,Vafai,K.,and Lightstone,M. 2003.Buoyancy-driven heat transfer enhancement in a two-dimensional enclosure utilizing nanofluids, *International Journal of Heat and Mass Transfer*, vol. 46, no. 19, pp. 3639–3653. doi: 10.1016/S0017-9310(03)00156-X.
- [6] Choi,S. U. S. and Eastman,J. A. 1995.Enhancing Thermal Conductivity of Fluids with Nanoparticles, in *De-velopments and Applications of Non-Newtonian Flows*, ASME., vol. FED-Vol. 2, New York, pp. 99–105.
- [7] Taylor,R. *et al.* 2013.Small particles, big impacts: A review of the diverse applications of nanofluids, *Journal of Applied Physics*, vol. 113, no. 1. doi: 10.1063/1.4754271.
- [8] Masuda,H.,Ebata,A.,Teramae,K.,and Hishinuma,N. 1993.Alteration of Thermal Conductivity and Viscosity of Liquid by Dispersing Ultra-Fine Particles. Dispersion of Al₂O₃, SiO₂ and TiO₂ Ultra-Fine Particles., *Netsu Bussei*, vol. 7, no. 4, pp. 227–233. doi: 10.2963/jjtp.7.227.
- [9] Hiroshi A., Tsukasaki Y.,Y. S. and T. A. 1978.Magnetic Properties of Ferromagnetic Ultrafine Particles Prepared By Vacuum, *Journal of Crystal Growth*, vol. 45, pp. 495–500.

- [10] Hamilton, R. L. and Crosser, O. K. 1962. Thermal conductivity of heterogeneous two-component systems, *Industrial and Engineering Chemistry Fundamentals*, vol. 1, no. 3, pp. 187–191. doi: 10.1021/i160003a005.
- [11] Hemmat Esfe, M., Esfandeh, S., and Kamyab, M. H. 2020. History and introduction, in *Hybrid Nanofluids for Convection Heat Transfer*, INC, pp. 1–48. doi: 10.1016/b978-0-12-819280-1.00001-x.
- [12] Zhu, D., Wang, L., Yu, W., and Xie, H. 2018. Intriguingly high thermal conductivity increment for CuO nanowires contained nanofluids with low viscosity, *Scientific Reports*, vol. 8, no. 1, pp. 1–12. doi: 10.1038/s41598-018-23174-z.
- [13] Wang, B. X., Zhou, L. P., Peng, X. F., Du, X. Z., and Yang, Y. P. 2010. On the specific heat capacity of CuO nanofluid, *Advances in Mechanical Engineering*, vol. 2010, no. January. doi: 10.1155/2010/172085.
- [14] Andreu-Cabedo, P., Mondragon, R., Hernandez, L., Martinez-Cuenca, R., Cabedo, L., and Julia, J. 2014. Increment of specific heat capacity of solar salt with SiO₂ nanoparticles, *Nanoscale Research Letters*, vol. 9, no. 1, p. 582. doi: 10.1186/1556-276X-9-582.
- [15] Seo, J. and Shin, D. 2014. Enhancement of specific heat of ternary nitrate (LiNO₃-NaNO₃-KNO₃) salt by doping with SiO₂ nanoparticles for solar thermal energy storage, *Micro and Nano Letters*, vol. 9, no. 11, pp. 817–820. doi: 10.1049/mnl.2014.0407.
- [16] Sridhara, V. and Satapathy, L. N. 2011. Al₂O₃-based nanofluids: A review, *Nanoscale Research Letters*, vol. 6, no. 1, pp. 1–16. doi: 10.1186/1556-276X-6-456.
- [17] Elias, M. M. *et al.* 2014. Experimental investigation on the thermo-physical properties of Al₂O₃ nanoparticles suspended in car radiator coolant, *International Communications in Heat and Mass Transfer*, vol. 54, pp. 48–53. doi: 10.1016/j.icheatmasstransfer.2014.03.005.
- [18] Yang, L. and Hu, Y. 2017. Toward TiO₂ Nanofluids—Part 1: Preparation and Properties, *Nanoscale Research Letters*, vol. 12, pp. 1–21. doi: 10.1186/s11671-017-2184-8.
- [19] Shao, X. F. *et al.* 2017. Solidification behavior of hybrid TiO₂ nanofluids containing nanotubes and nanoplatelets for cold thermal energy storage, *Applied Thermal Engineering*, vol. 117, pp. 427–436. doi: 10.1016/j.applthermaleng.2017.02.045.
- [20] Han, X., Thrush, S. J., Zhang, Z., Barber, G. C., and Qu, H. 2021. Tribological characterization of ZnO nanofluids as fastener lubricants, *Wear*, vol. 468–469, no. December 2020, p. 203592. doi: 10.1016/j.wear.2020.203592.
- [21] K.S., S., V., L. V., and K.S., R. 2016. ZnO–propylene glycol–water nanofluids with improved properties for potential applications in renewable energy and

- thermal management, *Colloids and Surfaces A: Physicochemical and Engineering Aspects*, vol. 506, pp. 63–73. doi: 10.1016/j.colsurfa.2016.06.007.
- [22] Mohammadfam, Y., Zeinali Heris, S., and Khazini, L. 2020. Experimental Investigation of Fe₃O₄/hydraulic oil magnetic nanofluids rheological properties and performance in the presence of magnetic field, *Tribology International*, vol. 142, no. July 2019, p. 105995. doi: 10.1016/j.triboint.2019.105995.
- [23] Kumar, L. H., Kazi, S. N., Masjuki, H. H., and Zubir, M. N. M. 2022. A review of recent advances in green nanofluids and their application in thermal systems, *Chemical Engineering Journal*, vol. 429, no. September 2021, p. 132321. doi: 10.1016/j.cej.2021.132321.
- [24] Sen, S., Moazzen, E., Aryal, S., Segre, C. U., and Timofeeva, E. V. 2015. Engineering nanofluid electrodes: controlling rheology and electrochemical activity of γ -Fe₂O₃ nanoparticles, *Journal of Nanoparticle Research*, vol. 17, no. 11, pp. 1–10. doi: 10.1007/s11051-015-3242-8.
- [25] Abbasian Arani, A., Aberoumand, H., Aberoumand, S., Jafari Moghaddam, A., and Dastanian, M. 2016. An empirical investigation on thermal characteristics and pressure drop of Ag-oil nanofluid in concentric annular tube, *Heat and Mass Transfer/Waerme- und Stoffuebertragung*, vol. 52, no. 8, pp. 1693–1706. doi: 10.1007/s00231-015-1686-0.
- [26] Walshe, J., Amarandei, G., Ahmed, H., McCormack, S., and Doran, J. 2019. Development of poly-vinyl alcohol stabilized silver nanofluids for solar thermal applications, *Solar Energy Materials and Solar Cells*, vol. 201, no. June, p. 110085. doi: 10.1016/j.solmat.2019.110085.
- [27] Li, Q., Yu, Y., Liu, Y., Liu, C., and Lin, L. 2017. Thermal properties of the mixed n-octadecane/Cu nanoparticle nanofluids during phase transition: A molecular dynamics study, *Materials*, vol. 10, no. 1. doi: 10.3390/ma10010038.
- [28] Gunjo, D. G., Jena, S. R., Mahanta, P., and Robi, P. S. 2018. Melting enhancement of a latent heat storage with dispersed Cu, CuO and Al₂O₃ nanoparticles for solar thermal application, *Renewable Energy*, vol. 121, pp. 652–665. doi: 10.1016/j.renene.2018.01.013.
- [29] Hong, K. S., Hong, T. K., and Yang, H. S. 2006. Thermal conductivity of Fe nanofluids depending on the cluster size of nanoparticles, *Applied Physics Letters*, vol. 88, no. 3, pp. 1–3. doi: 10.1063/1.2166199.
- [30] Lee, S. W., Park, S. D., Kang, S., Bang, I. C., and Kim, J. H. 2011. Investigation of viscosity and thermal conductivity of SiC nanofluids for heat transfer applications, *International Journal of Heat and Mass Transfer*, vol. 54, no. 1–3, pp. 433–438. doi: 10.1016/j.ijheatmasstransfer.2010.09.026.
- [31] Li, X., Zou, C., Zhou, L., and Qi, A. 2016. Experimental study on the thermo-physical

- properties of diathermic oil based SiC nanofluids for high temperature applications, *International Journal of Heat and Mass Transfer*, vol. 97, pp. 631–637. doi: 10.1016/j.ijheatmasstransfer.2016.02.056.
- [32] Wozniak, M., Rutkowski, P., and Kata, D. 2016. Rheological properties and thermal conductivity of AlN–poly(propylene glycol) suspensions, *Heat and Mass Transfer/Waerme- und Stoffuebertragung*, vol. 52, no. 1, pp. 103–112. doi: 10.1007/s00231-015-1597-0.
- [33] Akhavan-Behabadi, M. A., Pakdaman, M. F., and Ghazvini, M. 2012. Experimental investigation on the convective heat transfer of nanofluid flow inside vertical helically coiled tubes under uniform wall temperature condition, *International Communications in Heat and Mass Transfer*, vol. 39, no. 4, pp. 556–564. doi: 10.1016/j.icheatmasstransfer.2012.02.008.
- [34] Shahrul, I. M., Mahbulul, I. M., Khaleduzzaman, S. S., Saidur, R., and Sabri, M. F. M. 2014. A comparative review on the specific heat of nanofluids for energy perspective, *Renewable and Sustainable Energy Reviews*, vol. 38, pp. 88–98. doi: 10.1016/j.rser.2014.05.081.
- [35] Yu, W., Xie, H., Li, Y., Chen, L., and Wang, Q. 2011. Experimental investigation on the thermal transport properties of ethylene glycol based nanofluids containing low volume concentration diamond nanoparticles, *Colloids and Surfaces A: Physicochemical and Engineering Aspects*, vol. 380, no. 1–3, pp. 1–5. doi: 10.1016/j.colsurfa.2010.11.020.
- [36] Starace, A. K., Gomez, J. C., Wang, J., Pradhan, S., and Glatzmaier, G. C. 2011. Nanofluid heat capacities, *Journal of Applied Physics*, vol. 110, no. 12. doi: 10.1063/1.3672685.
- [37] Fakoor Pakdaman, M., Akhavan-Behabadi, M. A., and Razi, P. 2012. An experimental investigation on thermo-physical properties and overall performance of MWCNT/heat transfer oil nanofluid flow inside vertical helically coiled tubes, *Experimental Thermal and Fluid Science*, vol. 40, pp. 103–111. doi: 10.1016/j.expthermflusci.2012.02.005.
- [38] Hamdy, E., Ebrahim, S., Abulfotuh, F., and Soliman, M. 2017. Effect of multi-walled carbon nanotubes on thermal properties of nitrate molten salts, *Proceedings of 2016 International Renewable and Sustainable Energy Conference, IRSEC 2016*, pp. 317–320. doi: 10.1109/IRSEC.2016.7983997.
- [39] Hajatzadeh, A. et al. 2021. Nanofluids: Physical phenomena, applications in thermal systems and the environment effects- a critical review, *Journal of Cleaner Production*, vol. 320, no. July, p. 128573. doi: 10.1016/j.jclepro.2021.128573.
- [40] Nair, V., Taylor, P. R., and Parekh, A. D. 2016. Nanorefrigerants: A comprehensive review on its past, present and future, *International Journal of Refrigeration*, vol. 67, pp. 290–307. doi: 10.1016/j.ijrefrig.2016.01.011.

- [41] Aljaerani,H. A.,Samykan,M.,Saidur,R.,Pandey,A. K.,and Kadirgama,K. 2021.Nanoparticles as molten salts thermophysical properties enhancer for concentrated solar power: A critical review, *Journal of Energy Storage*, vol. 44, no. PA, p. 103280. doi: 10.1016/j.est.2021.103280.
- [42] Sezer,N.,Atieh,M. A.,and Koç,M. 2019.A comprehensive review on synthesis, stability, thermophysical properties, and characterization of nanofluids, *Powder Technology*, vol. 344, pp. 404–431. doi: 10.1016/j.powtec.2018.12.016.
- [43] Yıldız,G.,Ağbulut,Ü.,and Gürel,A. E. 2021.A review of stability, thermophysical properties and impact of using nanofluids on the performance of refrigeration systems, *International Journal of Refrigeration*, vol. 129, pp. 342–364. doi: 10.1016/j.ijrefrig.2021.05.016.
- [44] Paul,G.,Chopkar,M.,Manna,I.,and Das,P. K. 2010.Techniques for measuring the thermal conductivity of nanofluids: A review, *Renewable and Sustainable Energy Reviews*, vol. 14, no. 7, pp. 1913–1924. doi: 10.1016/j.rser.2010.03.017.
- [45] Ding,Y.,Alias,H.,Wen,D.,and Williams,R. A. 2006.Heat transfer of aqueous suspensions of carbon nanotubes (CNT nanofluids), *International Journal of Heat and Mass Transfer*, vol. 49, no. 1–2, pp. 240–250. doi: 10.1016/j.ijheatmasstransfer.2005.07.009.
- [46] Navarrete,N.,Mondragón,R.,Wen,D.,Navarro,M. E.,Ding,Y.,and Juliá,J. E. 2019.Thermal energy storage of molten salt –based nanofluid containing nano-encapsulated metal alloy phase change materials, *Energy*, vol. 167, pp. 912–920. doi: 10.1016/j.energy.2018.11.037.
- [47] Akilu,S.,Baheta,A. T.,Minea,A. A.,and Sharma,K. V. 2017.Rheology and thermal conductivity of non-porous silica (SiO₂) in viscous glycerol and ethylene glycol based nanofluids, *International Communications in Heat and Mass Transfer*, vol. 88, no. October, pp. 245–253. doi: 10.1016/j.icheatmasstransfer.2017.08.001.
- [48] Myers,P. D.,Alam,T. E.,Kamal,R.,Goswami,D. Y.,and Stefanakos,E. 2016.Nitrate salts doped with CuO nanoparticles for thermal energy storage with improved heat transfer, *Applied Energy*, vol. 165, pp. 225–233. doi: 10.1016/j.apenergy.2015.11.045.
- [49] Hameed,A. *et al.* 2019.Experimental investigation on synthesis, characterization, stability, thermo-physical properties and rheological behavior of MWCNTs-kapok seed oil based nanofluid, *Journal of Molecular Liquids*, vol. 277, pp. 812–824. doi: 10.1016/j.molliq.2019.01.012.
- [50] Li,X.,Chen,Y.,Cheng,Z.,Jia,L.,Mo,S.,and Liu,Z. 2014.Ultrahigh specific surface area of graphene for eliminating subcooling of water, *Applied Energy*, vol. 130, pp. 824–829. doi: 10.1016/j.apenergy.2014.02.032.
- [51] Chandrasekar,M.,Suresh,S.,and Senthilkumar,T. 2012.Mechanisms proposed through experimental investigations on thermophysical properties and forced

- convective heat transfer characteristics of various nanofluids - A review, *Renewable and Sustainable Energy Reviews*, vol. 16, no. 6, pp. 3917–3938. doi: 10.1016/j.rser.2012.03.013.
- [52] Alawi, O. A., Sidik, N. A. C., Xian, H. W., Kean, T. H., and Kazi, S. N. 2018. Thermal conductivity and viscosity models of metallic oxides nanofluids, *International Journal of Heat and Mass Transfer*, vol. 116, pp. 1314–1325. doi: 10.1016/j.ijheatmasstransfer.2017.09.133.
- [53] Seo, J. and Shin, D. 2016. Size effect of nanoparticle on specific heat in a ternary nitrate (LiNO₃-NaNO₃-KNO₃) salt eutectic for thermal energy storage, *Applied Thermal Engineering*, vol. 102, pp. 144–148. doi: 10.1016/j.applthermaleng.2016.03.134.
- [54] Chon, C. H., Kihm, K. D., Lee, S. P., and Choi, S. U. S. 2005. Empirical correlation finding the role of temperature and particle size for nanofluid (Al₂O₃) thermal conductivity enhancement, *Applied Physics Letters*, vol. 87, no. 15, pp. 1–3. doi: 10.1063/1.2093936.
- [55] Timofeeva, E. V. *et al.* 2007. Thermal conductivity and particle agglomeration in alumina nanofluids: Experiment and theory, *Physical Review E - Statistical, Nonlinear, and Soft Matter Physics*, vol. 76, no. 6, pp. 28–39. doi: 10.1103/PhysRevE.76.061203.
- [56] Godson, L., Raja, B., Lal, D. M., and Wongwises, S. 2010. Experimental investigation on the thermal conductivity and viscosity of silver-deionized water nanofluid, *Experimental Heat Transfer*, vol. 23, no. 4, pp. 317–332. doi: 10.1080/08916150903564796.
- [57] Esfahani, N. N., Toghraie, D., and Afrand, M. 2018. A new correlation for predicting the thermal conductivity of ZnO–Ag (50%–50%)/water hybrid nanofluid: An experimental study, *Powder Technology*, vol. 323, pp. 367–373. doi: 10.1016/j.powtec.2017.10.025.
- [58] Sharma, P., Baek, I. H., Cho, T., Park, S., and Lee, K. B. 2011. Enhancement of thermal conductivity of ethylene glycol based silver nanofluids, *Powder Technology*, vol. 208, no. 1, pp. 7–19. doi: 10.1016/j.powtec.2010.11.016.
- [59] Esfe, M. H., Esfandeh, S., Afrand, M., Rejvani, M., and Rostamian, S. H. 2018. Experimental evaluation, new correlation proposing and ANN modeling of thermal properties of EG based hybrid nanofluid containing ZnO-DWCNT nanoparticles for internal combustion engines applications, *Applied Thermal Engineering*, vol. 133, pp. 452–463. doi: 10.1016/j.applthermaleng.2017.11.131.
- [60] Yu, W. and Xie, H. 2012. A Review on Nanofluids: Preparation, Stability Mechanisms, and Applications, vol. 2012. doi: 10.1155/2012/435873.
- [61] Dudda, B. and Shin, D. 2013. Effect of nanoparticle dispersion on specific heat

- capacity of a binary nitrate salt eutectic for concentrated solar power applications, *International Journal of Thermal Sciences*, vol. 69, pp. 37–42. doi: 10.1016/j.ijthermalsci.2013.02.003.
- [62] Muñoz-Sánchez, B., Nieto-Maestre, J., Iparraguirre-Torres, I., Julià, J. E., and García-Romero, A. 2017. Silica and alumina nano-enhanced molten salts for thermal energy storage: A comparison, *AIP Conference Proceedings*, vol. 1850, no. June. doi: 10.1063/1.4984439.
- [63] Luo, Y., Ran, G., Chen, N., and Wang, C. 2017. Microstructure and morphology of Mo-based Tm_2O_3 composites synthesized by ball milling and sintering, *Advanced Powder Technology*, vol. 28, no. 2, pp. 658–664. doi: 10.1016/j.apt.2016.12.003.
- [64] Shin, D. and Banerjee, D. 2015. Enhanced thermal properties of SiO_2 nanocomposite for solar thermal energy storage applications, *International Journal of Heat and Mass Transfer*, vol. 84, pp. 898–902. doi: 10.1016/j.ijheatmasstransfer.2015.01.100.
- [65] Jo, B. and Banerjee, D. 2015. Enhanced specific heat capacity of molten salt-based carbon nanotubes nanomaterials, *Journal of Heat Transfer*, vol. 137, no. 9, pp. 1–7. doi: 10.1115/1.4030226.
- [66] Xie, H., Wang, J., Xi, T., Liu, Y., and Ai, F. 2002. Dependence of the thermal conductivity on nanoparticle-fluid mixture on the base fluid, *Journal of Materials Science Letters*, vol. 21, no. 19, pp. 1469–1471. doi: 10.1023/A:1020060324472.
- [67] Hemmat Esfe, M., Afrand, M., Karimipour, A., Yan, W. M., and Sina, N. 2015. An experimental study on thermal conductivity of MgO nanoparticles suspended in a binary mixture of water and ethylene glycol, *International Communications in Heat and Mass Transfer*, vol. 67, pp. 173–175. doi: 10.1016/j.icheatmasstransfer.2015.07.009.
- [68] Ahmadi, M. H., Mirlohi, A., Alhuyi Nazari, M., and Ghasempour, R. 2018. A review of thermal conductivity of various nanofluids, *Journal of Molecular Liquids*, vol. 265, pp. 181–188. doi: 10.1016/j.molliq.2018.05.124.
- [69] Hemmat Esfe, M., Esfandeh, S., Saedodin, S., and Rostamian, H. 2017. Experimental evaluation, sensitivity analysis and ANN modeling of thermal conductivity of ZnO -MWCNT/EG-water hybrid nanofluid for engineering applications, *Applied Thermal Engineering*, vol. 125, pp. 673–685. doi: 10.1016/j.applthermaleng.2017.06.077.
- [70] Chieruzzi, M., Cerritelli, G. F., Miliozzi, A., and Kenny, J. M. 2013. Effect of nanoparticles on heat capacity of nanofluids based on molten salts as PCM for thermal energy storage, *Nanoscale Research Letters*, vol. 8, no. 1, pp. 1–9. doi: 10.1186/1556-276X-8-448.

- [71] Jiang,Z. *et al.* 2019.Novel key parameter for eutectic nitrates based nanofluids selection for concentrating solar power (CSP) system, *Applied Energy*, vol. 235, no. July 2018, pp. 529–542. doi: 10.1016/j.apenergy.2018.10.114.
- [72] Vajjha,R. S. and Das,D. K. 2012.A review and analysis on influence of temperature and concentration of nanofluids on thermophysical properties, heat transfer and pumping power, *International Journal of Heat and Mass Transfer*, vol. 55, no. 15–16, pp. 4063–4078. doi: 10.1016/j.ijheatmasstransfer.2012.03.048.
- [73] Garg,J. *et al.* 2008.Enhanced thermal conductivity and viscosity of copper nanoparticles in ethylene glycol nanofluid, *Journal of Applied Physics*, vol. 103, no. 7. doi: 10.1063/1.2902483.
- [74] Pastoriza-Gallego,M. J.,Casanova,C.,Legido,J. L.,and Piñeiro,M. M. 2011.CuO in water nanofluid: Influence of particle size and polydispersity on volumetric behaviour and viscosity, *Fluid Phase Equilibria*, vol. 300, no. 1–2, pp. 188–196. doi: 10.1016/j.fluid.2010.10.015.
- [75] Prasher,R.,Song,D.,Wang,J.,and Phelan,P. 2006.Measurements of nanofluid viscosity and its implications for thermal applications, *Applied Physics Letters*, vol. 89, no. 13, pp. 87–90. doi: 10.1063/1.2356113.
- [76] Pastoriza-Gallego,M. J.,Casanova,C.,Páramo,R.,Barb s,B.,Legido,J. L.,and Piñeiro,M. M. 2009.A study on stability and thermophysical properties (density and viscosity) of Al₂O₃ in water nanofluid, *Journal of Applied Physics*, vol. 106, no. 6. doi: 10.1063/1.3187732.
- [77] Nguyen,C. T. *et al.* 2007.Temperature and particle-size dependent viscosity data for water-based nanofluids - Hysteresis phenomenon, *International Journal of Heat and Fluid Flow*, vol. 28, no. 6, pp. 1492–1506. doi: 10.1016/j.ijheatfluidflow.2007.02.004.
- [78] Verma,S. K. and Tiwari,A. K. 2015.Progress of nanofluid application in solar collectors: A review, *Energy Conversion and Management*, vol. 100, pp. 324–346. doi: 10.1016/j.enconman.2015.04.071.
- [79] Zhu,H.,Li,C.,Wu,D.,Zhang,C.,and Yin,Y. 2010.Preparation, characterization, viscosity and thermal conductivity of CaCO₃ aqueous nanofluids, *Science China Technological Sciences*, vol. 53, no. 2, pp. 360–368. doi: 10.1007/s11431-010-0032-5.
- [80] Lee,J. H. *et al.* 2008.Effective viscosities and thermal conductivities of aqueous nanofluids containing low volume concentrations of Al₂O₃ nanoparticles, *International Journal of Heat and Mass Transfer*, vol. 51, no. 11–12, pp. 2651–2656. doi: 10.1016/j.ijheatmasstransfer.2007.10.026.
- [81] Chandrasekar,M.,Suresh,S.,and Chandra Bose,A. 2010.Experimental investigations and theoretical determination of thermal conductivity and

- viscosity of Al₂O₃/water nanofluid, *Experimental Thermal and Fluid Science*, vol. 34, no. 2, pp. 210–216. doi: 10.1016/j.expthermflusci.2009.10.022.
- [82] Timofeeva, E. V., Yu, W., France, D. M., Singh, D., and Routbort, J. L. 2011. Base fluid and temperature effects on the heat transfer characteristics of SiC in ethylene glycol/H₂O and H₂O nanofluids, *Journal of Applied Physics*, vol. 109, no. 1. doi: 10.1063/1.3524274.
- [83] Turgut, A., Tavman, I., Chirtoc, M., Schuchmann, H. P., Sauter, C., and Tavman, S. 2009. Thermal conductivity and viscosity measurements of water-based TiO₂ nanofluids, *International Journal of Thermophysics*, vol. 30, no. 4, pp. 1213–1226. doi: 10.1007/s10765-009-0594-2.
- [84] Yu, W., Xie, H., Li, Y., and Chen, L. 2011. Experimental investigation on thermal conductivity and viscosity of aluminum nitride nanofluid, *Particuology*, vol. 9, no. 2, pp. 187–191. doi: 10.1016/j.partic.2010.05.014.
- [85] Schmidt, A. J. *et al.* 2008. Experimental investigation of nanofluid shear and longitudinal viscosities, *Applied Physics Letters*, vol. 92, no. 24. doi: 10.1063/1.2945799.
- [86] Kole, M. and Dey, T. K. 2011. Effect of aggregation on the viscosity of copper oxide-gear oil nanofluids, *International Journal of Thermal Sciences*, vol. 50, no. 9, pp. 1741–1747. doi: 10.1016/j.ijthermalsci.2011.03.027.
- [87] Chevalier, J., Tillement, O., and Ayela, F. 2007. Rheological properties of nanofluids flowing through microchannels, *Applied Physics Letters*, vol. 91, no. 23, pp. 1–4. doi: 10.1063/1.2821117.
- [88] Nelson, I. C., Banerjee, D., and Ponnappan, R. 2009. Flow loop experiments using polyalphaolefin nanofluids, *Journal of Thermophysics and Heat Transfer*, vol. 23, no. 4, pp. 752–761. doi: 10.2514/1.31033.
- [89] Navarrete, N., Hernández, L., Vela, A., and Mondragón, R. 2020. Influence of the production method on the thermophysical properties of high temperature molten salt-based nanofluids, *Journal of Molecular Liquids*, vol. 302, p. 112570. doi: 10.1016/j.molliq.2020.112570.
- [90] Schuller, M., Shao, Q., and Lalk, T. 2015. Experimental investigation of the specific heat of a nitrate-alumina nanofluid for solar thermal energy storage systems, *International Journal of Thermal Sciences*, vol. 91, pp. 142–145. doi: 10.1016/j.ijthermalsci.2015.01.012.
- [91] Xie, Q., Zhu, Q., and Li, Y. 2016. Thermal Storage Properties of Molten Nitrate Salt-Based Nanofluids with Graphene Nanoplatelets, *Nanoscale Research Letters*, vol. 11, no. 1, pp. 1–7. doi: 10.1186/s11671-016-1519-1.
- [92] Choi, J. and Zhang, Y. 2012. Numerical simulation of laminar forced convection heat transfer of Al₂O₃-water nanofluid in a pipe with return bend, *International Journal of Thermal Sciences*, vol. 55, pp. 90–102. doi:

10.1016/j.ijthermalsci.2011.12.017.

- [93] Dudda,B. and Shin,D. 2012.Imece2012-87707 Investigation of Molten Salt Nanomaterial As Thermal Energy Storage in, pp. 1–6.
- [94] Lu,M. C. and Huang,C. H. 2013.Specific heat capacity of molten salt-based alumina nanofluid, *Nanoscale Research Letters*, vol. 8, no. 1, pp. 1–7. doi: 10.1186/1556-276X-8-292.
- [95] Chieruzzi,M.,Miliozzi,A.,Crescenzi,T.,Torre,L.,and Kenny,J. M. 2015.A New Phase Change Material Based on Potassium Nitrate with Silica and Alumina Nanoparticles for Thermal Energy Storage, *Nanoscale Research Letters*, vol. 10, no. 1. doi: 10.1186/s11671-015-0984-2.
- [96] He,Q.,Wang,S.,Tong,M.,and Liu,Y. 2012.Experimental study on thermophysical properties of nanofluids as phase-change material (PCM) in low temperature cool storage, *Energy Conversion and Management*, vol. 64, pp. 199–205. doi: 10.1016/j.enconman.2012.04.010.
- [97] Bock Choon Pak,Y. I. C. 2013.Hydrodynamic and Heat Transfer Study of Dispersed Fluids With Submicron Metallic Oxide, *Experimental Heat Transfer : A Journal of , Thermal Energy Transport , Storage , and Conversion*, no. January 2013, pp. 37–41.
- [98] Zhou,S. Q. and Ni,R. 2008.Measurement of the specific heat capacity of water-based Al₂ O₃ nanofluid, *Applied Physics Letters*, vol. 92, no. 9, pp. 2006–2009. doi: 10.1063/1.2890431.
- [99] Vajjha,R. S. and Das,D. K. 2009.Specific heat measurement of three nanofluids and development of new correlations, *Journal of Heat Transfer*, vol. 131, no. 7, pp. 1–7. doi: 10.1115/1.3090813.
- [100] Riazi,H.,Mesgari,S.,Ahmed,N. A.,and Taylor,R. A. 2016.The effect of nanoparticle morphology on the specific heat of nanosalts, *International Journal of Heat and Mass Transfer*, vol. 94, pp. 254–261. doi: 10.1016/j.ijheatmasstransfer.2015.11.064.
- [101] Ryu,H. Y. 2014.Large enhancement of light extraction efficiency in AlGaN-based nanorod ultraviolet light-emitting diode structures, *Nanoscale Research Letters*, vol. 9, no. 1, pp. 1–7. doi: 10.1186/1556-276X-9-58.
- [102] Huang,Y.,Cheng,X.,Li,Y.,Yu,G.,Xu,K.,and Li,G. 2018.Effect of in-situ synthesized nano-MgO on thermal properties of NaNO₃-KNO₃, *Solar Energy*, vol. 160, no. December 2017, pp. 208–215. doi: 10.1016/j.solener.2017.11.077.
- [103] Murshed,S. M. S. and Nieto De Castro,C. A. 2014.Superior thermal features of carbon nanotubes-based nanofluids - A review, *Renewable and Sustainable Energy Reviews*, vol. 37, pp. 155–167. doi: 10.1016/j.rser.2014.05.017.
- [104] Liu,Y. and Yang,Y. 2017.Investigation of specific heat and latent heat

- enhancement in hydrate salt based TiO₂ nanofluid phase change material, *Applied Thermal Engineering*, vol. 124, pp. 533–538. doi: 10.1016/j.applthermaleng.2017.05.150.
- [105] Liu, J., Wang, F., Zhang, L., Fang, X., and Zhang, Z. 2014. Thermodynamic properties and thermal stability of ionic liquid-based nanofluids containing graphene as advanced heat transfer fluids for medium-to-high-temperature applications, *Renewable Energy*, vol. 63, pp. 519–523. doi: 10.1016/j.renene.2013.10.002.
- [106] Lee, J. and Mudawar, I. 2007. Assessment of the effectiveness of nanofluids for single-phase and two-phase heat transfer in micro-channels, *International Journal of Heat and Mass Transfer*, vol. 50, no. 3–4, pp. 452–463. doi: 10.1016/j.ijheatmasstransfer.2006.08.001.
- [107] Murshed, S. M. S., Leong, K. C., and Yang, C. 2006. Determination of the effective thermal diffusivity of nanofluids by the double hot-wire technique, *Journal of Physics D: Applied Physics*, vol. 39, no. 24, pp. 5316–5322. doi: 10.1088/0022-3727/39/24/033.
- [108] Eastman, J. A., Phillpot, S. R., Choi, S. U. S., and Keblinski, P. 2004. Thermal transport in nanofluids, *Annual Review of Materials Research*, vol. 34, pp. 219–246. doi: 10.1146/annurev.matsci.34.052803.090621.
- [109] Xuan, Y. and Li, Q. 2003. Investigation on convective heat transfer and flow features of nanofluids, *Journal of Heat Transfer*, vol. 125, no. 1, pp. 151–155. doi: 10.1115/1.1532008.
- [110] Khodadadi, J. M. and Hosseinizadeh, S. F. 2007. Nanoparticle-enhanced phase change materials (NEPCM) with great potential for improved thermal energy storage, *International Communications in Heat and Mass Transfer*, vol. 34, no. 5, pp. 534–543. doi: 10.1016/j.icheatmasstransfer.2007.02.005.
- [111] Pantzali, M. N., Kanaris, A. G., Antoniadis, K. D., Mouza, A. A., and Paras, S. V. 2009. Effect of nanofluids on the performance of a miniature plate heat exchanger with modulated surface, *International Journal of Heat and Fluid Flow*, vol. 30, no. 4, pp. 691–699. doi: 10.1016/j.ijheatfluidflow.2009.02.005.
- [112] Dudda, B. and Shin, D. 2013. Effect of nanoparticle dispersion on specific heat capacity of a binary nitrate salt eutectic for concentrated solar power applications, *International Journal of Thermal Sciences*, vol. 69, pp. 37–42. doi: 10.1016/j.ijthermalsci.2013.02.003.
- [113] Lasfargues, M., Bell, A., and Ding, Y. 2016. In situ production of titanium dioxide nanoparticles in molten salt phase for thermal energy storage and heat-transfer fluid applications, *Journal of Nanoparticle Research*, vol. 18, no. 6, pp. 1–11. doi: 10.1007/s11051-016-3460-8.
- [114] Awad, A., Navarro, H., Ding, Y., and Wen, D. 2018. Thermal-physical properties of nanoparticle-seeded nitrate molten salts, *Renewable Energy*, vol. 120, pp. 275–

288. doi: 10.1016/j.renene.2017.12.026.

- [115] Lasfargues, M., Geng, Q., Cao, H., and Ding, Y. 2015. Mechanical dispersion of nanoparticles and its effect on the specific heat capacity of impure binary nitrate salt mixtures, *Nanomaterials*, vol. 5, no. 3, pp. 1136–1146. doi: 10.3390/nano5031136.
- [116] Shin, D. and Banerjee, D. 2013. Enhanced specific heat capacity of nanomaterials synthesized by dispersing silica nanoparticles in eutectic mixtures, *Journal of Heat Transfer*, vol. 135, no. 3, pp. 1–8. doi: 10.1115/1.4005163.
- [117] Tiznobaik, H., Banerjee, D., and Shin, D. 2015. Effect of formation of “long range” secondary dendritic nanostructures in molten salt nanofluids on the values of specific heat capacity, *International Journal of Heat and Mass Transfer*, vol. 91, pp. 342–346. doi: 10.1016/j.ijheatmasstransfer.2015.05.072.
- [118] Toghyani, S., Baniasadi, E., and Afshari, E. 2016. Thermodynamic analysis and optimization of an integrated Rankine power cycle and nano-fluid based parabolic trough solar collector, *Energy Conversion and Management*, vol. 121, pp. 93–104. doi: 10.1016/j.enconman.2016.05.029.
- [119] Timofeeva, E. V., Routbort, J. L., and Singh, D. 2009. Particle shape effects on thermophysical properties of alumina nanofluids, *Journal of Applied Physics*, vol. 106, no. 1. doi: 10.1063/1.3155999.
- [120] Maji, N. C. and Chakraborty, J. 2020. Explaining the disparity in nanofluid results: Role of morphology, material, and state of aggregation of colloidal particles, *International Journal of Heat and Mass Transfer*, vol. 156. doi: 10.1016/j.ijheatmasstransfer.2020.119709.
- [121] Ibrahim, A., Peng, H., Riaz, A., Abdul Basit, M., Rashid, U., and Basit, A. 2021. Molten salts in the light of corrosion mitigation strategies and embedded with nanoparticles to enhance the thermophysical properties for CSP plants, *Solar Energy Materials and Solar Cells*, vol. 219, no. August 2020, p. 110768. doi: 10.1016/j.solmat.2020.110768.
- [122] Grosu, Y., Nithiyantham, U., Zaki, A., and Faik, A. 2018. A simple method for the inhibition of the corrosion of carbon steel by molten nitrate salt for thermal storage in concentrating solar power applications, *npj Materials Degradation*, vol. 2, no. 1, pp. 1–8. doi: 10.1038/s41529-018-0055-0.
- [123] Eltoun, H., Yang, Y. L., and Hou, J. R. 2021. The effect of nanoparticles on reservoir wettability alteration: a critical review, *Petroleum Science*, vol. 18, no. 1, pp. 136–153. doi: 10.1007/s12182-020-00496-0.
- [124] Jackson, R. G. *et al.* 2014. Effect of surface wettability on carbon nanotube water-based nanofluid droplet impingement heat transfer, *Journal of Physics: Conference Series*, vol. 525, no. 1. doi: 10.1088/1742-6596/525/1/012024.
- [125] Choi, T. J., Jang, S. P., and Kedzierski, M. A. 2018. Effect of surfactants on the

- stability and solar thermal absorption characteristics of water-based nanofluids with multi-walled carbon nanotubes, *International Journal of Heat and Mass Transfer*, vol. 122, pp. 483–490. doi: 10.1016/j.ijheatmasstransfer.2018.01.141.
- [126] Singh,N. and Khullar,V. 2019.Efficient Volumetric Absorption Solar Thermal Platforms Employing Thermally Stable - Solar Selective Nanofluids Engineered from Used Engine Oil, *Scientific Reports*, vol. 9, no. 1, pp. 1–12. doi: 10.1038/s41598-019-47126-3.
- [127] Tlili,I.,Bhatti,M. M.,Mustafa,S.,and Barzinjy,A. A. 2019.Macroscopic modeling for convection of Hybrid nanofluid with magnetic effects, *Physica A*, vol. 534, p. 122136. doi: 10.1016/j.physa.2019.122136.
- [128] Glory,J.,Bonetti,M.,Helezen,M.,Mayne-L'Hermite,M.,and Reynaud,C. 2008.Thermal and electrical conductivities of water-based nanofluids prepared with long multiwalled carbon nanotubes, *Journal of Applied Physics*, vol. 103, no. 9. doi: 10.1063/1.2908229.
- [129] Vallejo,J. P.,Ansia,L.,Fal,J.,Traciak,J.,and Lugo,L. 2022.Thermophysical , rheological and electrical properties of mono and hybrid TiB₂ / B₄C nano fl uids based on a propylene glycol : water mixture, *Powder Technology*, vol. 395, pp. 391–399. doi: 10.1016/j.powtec.2021.09.074.
- [130] Teng,T. P. and Hung,Y. H. 2014.Estimation and experimental study of the density and specific heat for alumina nanofluid, *Journal of Experimental Nanoscience*, vol. 9, no. 7, pp. 707–718. doi: 10.1080/17458080.2012.696219.
- [131] Wang,B.-X.,Zhou,L.-P.,and Peng,X.-F. 2006.Surface and Size Effects on the Specific Heat Capacity of Nanoparticles, *International Journal of Thermophysics*, vol. 27, no. 1, pp. 139–151. doi: 10.1007/s10765-006-0022-9.
- [132] Beck,M. P.,Yuan,Y.,Warrier,P.,and Teja,A. S. 2009.The effect of particle size on the thermal conductivity of alumina nanofluids, *Journal of Nanoparticle Research*, vol. 11, no. 5, pp. 1129–1136. doi: 10.1007/s11051-008-9500-2.
- [133] Li,C. H. and Peterson,G. P. 2007.The effect of particle size on the effective thermal conductivity of Al₂O₃-water nanofluids, *Journal of Applied Physics*, vol. 101, no. 4. doi: 10.1063/1.2436472.
- [134] Ho,M. X. and Pan,C. 2014.Optimal concentration of alumina nanoparticles in molten hitec salt to maximize its specific heat capacity, *International Journal of Heat and Mass Transfer*, vol. 70, pp. 174–184. doi: 10.1016/j.ijheatmasstransfer.2013.10.078.
- [135] Masoud Hosseini,S.,Vafajoo,L.,Ghasemi,E.,and Salman,B. H. 2016.Experimental investigation the effect of nanoparticle concentration on the rheological behavior of paraffin-based nickel ferrofluid, *International Journal of Heat and Mass Transfer*, vol. 93, pp. 228–234. doi:

10.1016/j.ijheatmasstransfer.2015.09.082.

- [136] Giwa,S. O.,Sharifpur,M.,Goodarzi,M.,Alsulami,H.,and Meyer,J. P. 2021.Influence of base fluid, temperature, and concentration on the thermophysical properties of hybrid nanofluids of alumina–ferrofluid: experimental data, modeling through enhanced ANN, ANFIS, and curve fitting, *Journal of Thermal Analysis and Calorimetry*, vol. 143, no. 6, pp. 4149–4167. doi: 10.1007/s10973-020-09372-w.
- [137] Anagnostopoulos,A.,Palacios,A.,Navarrete,N.,Navarro,M. E.,Hernandez,L.,and Ding,Y. 2019.Effect of temperature on the internal structure of solar salt-SiO₂, *SOLARPACES 2018: International Conference on Concentrating Solar Power and Chemical Energy Systems*, vol. 2126, no. July, p. 200003. doi: 10.1063/1.5117718.
- [138] Wang,Z. L.,Tang,D. W.,Liu,S.,Zheng,X. H.,and Araki,N. 2007.Thermal-conductivity and thermal-diffusivity measurements of nanofluids by 3ω method and mechanism analysis of heat transport, *International Journal of Thermophysics*, vol. 28, no. 4, pp. 1255–1268. doi: 10.1007/s10765-007-0254-3.
- [139] Amrollahi,A.,Hamidi,A. A.,and Rashidi,A. M. 2008.The effects of temperature, volume fraction and vibration time on the thermo-physical properties of a carbon nanotube suspension (carbon nanofluid), *Nanotechnology*, vol. 19, no. 31. doi: 10.1088/0957-4484/19/31/315701.
- [140] Xian-Ju,W. and Xin-Fang,L. 2009.Influence of pH on Nanofluids' Viscosity and Thermal Conductivity, *Chinese Physics Letters*, vol. 26, no. 5, p. 056601. doi: 10.1088/0256-307x/26/5/056601.
- [141] Sahooli,M. and Sabbaghi,S. 2013.CuO Nanofluids: The Synthesis and Investigation of Stability and Thermal Conductivity, *Journal of Nanofluids*, vol. 1, no. 2, pp. 155–160. doi: 10.1166/jon.2012.1014.
- [142] Yıldız,G.,Ağbulut,Ü.,and Gürel,A. E. 2021.A review of stability, thermophysical properties and impact of using nanofluids on the performance of refrigeration systems, *International Journal of Refrigeration*, vol. 129, pp. 342–364. doi: 10.1016/j.ijrefrig.2021.05.016.
- [143] Sofiah,A. G. N.,Samykan,M.,Pandey,A. K.,Kadrigama,K.,Sharma,K.,and Saidur,R. 2021.Immense impact from small particles: Review on stability and thermophysical properties of nanofluids, *Sustainable Energy Technologies and Assessments*, vol. 48, no. 5, p. 101635. doi: 10.1016/j.seta.2021.101635.
- [144] Ma,B.,Shin,D.,and Banerjee,D. 2021.One-step synthesis of molten salt nanofluid for thermal energy storage application – a comprehensive analysis on thermophysical property, corrosion behavior, and economic benefit, *Journal of Energy Storage*, vol. 35, no. September 2020, p. 102278. doi: 10.1016/j.est.2021.102278.

- [145] Babita, Sharma, S. K., and Gupta, S. M. 2016. Preparation and evaluation of stable nanofluids for heat transfer application: A review, *Experimental Thermal and Fluid Science*, vol. 79, pp. 202–212. doi: 10.1016/j.expthermflusci.2016.06.029.
- [146] Che Sidik, N. A., Mahmud Jamil, M., Aziz Japar, W. M. A., and Muhammad Adamu, I. 2017. A review on preparation methods, stability and applications of hybrid nanofluids, *Renewable and Sustainable Energy Reviews*, vol. 80, no. May, pp. 1112–1122. doi: 10.1016/j.rser.2017.05.221.
- [147] Awais, M., Bhuiyan, A. A., Salehin, S., Ehsan, M. M., Khan, B., and Rahman, M. H. 2021. Synthesis, heat transport mechanisms and thermophysical properties of nanofluids: A critical overview, *International Journal of Thermofluids*, vol. 10, p. 100086. doi: 10.1016/j.ijft.2021.100086.
- [148] Jo, B. and Banerjee, D. 2014. Enhanced specific heat capacity of molten salt-based nanomaterials: Effects of nanoparticle dispersion and solvent material, *Acta Materialia*, vol. 75, pp. 80–91. doi: 10.1016/j.actamat.2014.05.005.
- [149] Muñoz-Sánchez, B., Nieto-Maestre, J., Iparraguirre-Torres, I., García-Romero, A., and Sala-Lizarraga, J. M. 2018. Molten salt-based nanofluids as efficient heat transfer and storage materials at high temperatures. An overview of the literature, *Renewable and Sustainable Energy Reviews*, vol. 82, no. November 2017, pp. 3924–3945. doi: 10.1016/j.rser.2017.10.080.
- [150] Pordanjani, A. H. et al. 2021. Nanofluids: Physical phenomena, applications in thermal systems and the environment effects- a critical review, *Journal of Cleaner Production*, vol. 320, no. August, p. 128573. doi: 10.1016/j.jclepro.2021.128573.
- [151] Moita, A., Moreira, A., and Pereira, J. 2021. Nanofluids for the next generation thermal management of electronics: A review, *Symmetry*, vol. 13, no. 8. doi: 10.3390/sym13081362.
- [152] Kumaresan, V. and Velraj, R. 2012. Experimental investigation of the thermophysical properties of water-ethylene glycol mixture based CNT nanofluids, *Thermochimica Acta*, vol. 545, pp. 180–186. doi: 10.1016/j.tca.2012.07.017.
- [153] Flemban, T. et al. 2022. Physicochemical Properties of Nanofluids Produced from Oxidized Nanoparticles Synthesized in a Liquid by Pulsed Laser Ablation, *Lasers in Manufacturing and Materials Processing*. doi: 10.1007/s40516-021-00160-4.
- [154] Raj Sha, M. M., Correya, A. A., Nampoore, V. P. N., and Mujeeb, A. 2021. Laser ablated silicon nanoparticles with selected solvents: A comparison of thermal diffusivity under different concentrations, *Optik*, vol. 247, no. June, p. 167881. doi: 10.1016/j.ijleo.2021.167881.
- [155] Lo, C. H., Tsung, T. T., and Lin, H. M. 2007. Preparation of silver nanofluid by the submerged arc nanoparticle synthesis system (SANSS), *Journal of Alloys and*

- Compounds*, vol. 434–435, no. SPEC. ISS., pp. 659–662. doi: 10.1016/j.jallcom.2006.08.217.
- [156] Kao, M. J., Lo, C. H., Tsung, T. T., Wu, Y. Y., Jwo, C. S., and Lin, H. M. 2007. Copper-oxide brake nanofluid manufactured using arc-submerged nanoparticle synthesis system, *Journal of Alloys and Compounds*, vol. 434–435, no. SPEC. ISS., pp. 672–674. doi: 10.1016/j.jallcom.2006.08.305.
- [157] Chang, H., Chen, X. Q., Jwo, C. S., and Chen, S. L. 2009. Electrostatic and sterical stabilization of CuO nanofluid prepared by vacuum arc spray nanofluid synthesis system (ASNSS), *Materials Transactions*, vol. 50, no. 8, pp. 2098–2103. doi: 10.2320/matertrans.M2009129.
- [158] Chang, H. and Liu, M. K. 2007. Fabrication and process analysis of anatase type TiO₂ nanofluid by an arc spray nanofluid synthesis system, *Journal of Crystal Growth*, vol. 304, no. 1, pp. 244–252. doi: 10.1016/j.jcrysgr.2007.02.009.
- [159] Sreeju, N., Rufus, A., and Philip, D. 2016. Microwave-assisted rapid synthesis of copper nanoparticles with exceptional stability and their multifaceted applications, *Journal of Molecular Liquids*, vol. 221, pp. 1008–1021. doi: 10.1016/j.molliq.2016.06.080.
- [160] Yadav, N., Chaturvedi, V. K., and Yadav, R. R. 2020. Microwave assisted green synthesis and characterization of bimetallic Au/Pt nanofluids, *AIP Conference Proceedings*, vol. 2265, no. November. doi: 10.1063/5.0017109.
- [161] Nguyen, M. T., Kim, J. H., and Kim, J. C. 2018. Formation of different Cu nanopowders and stability of Cu fluids produced by electrical explosion of wire in liquid, *Archives of Metallurgy and Materials*, vol. 63, no. 3, pp. 1453–1457. doi: 10.24425/123827.
- [162] Fe, E. *et al.* 2021. Synthesis, Characterization and Filtration Properties of Ecofriendly Fe₃O₄ Nanoparticles Derived from Olive Leaves Extract, *Materials*, vol. 14, no. 4306.
- [163] Ni, Z. *et al.* 2021. Facile synthesis of copper(I) oxide nanochains and the photo-thermal conversion performance of its nanofluids, *Coatings*, vol. 11, no. 7. doi: 10.3390/coatings11070749.
- [164] Fuskele, V. and Sarviya, R. M. 2017. Recent developments in Nanoparticles Synthesis, Preparation and Stability of Nanofluids, *Materials Today: Proceedings*, vol. 4, no. 2, pp. 4049–4060. doi: 10.1016/j.matpr.2017.02.307.
- [165] Ali, N., Bahman, A. M., Aljuwayhel, N. F., Ebrahim, S. A., Mukherjee, S., and Alsayegh, A. 2021. Carbon-based nanofluids and their advances towards heat transfer applications—a review, *Nanomaterials*, vol. 11, no. 6. doi: 10.3390/nano11061628.
- [166] Sezer, N., Atieh, M. A., and Koc, M. 2018. A comprehensive review on synthesis, stability, thermophysical properties, and characterization of nanofluids,

- Powder Technology*, vol. 344, pp. 404–431. doi: 10.1016/j.powtec.2018.12.016.
- [167] Devendiran, D. K. and Amirtham, V. A. 2016. A review on preparation, characterization, properties and applications of nanofluids, *Renewable and Sustainable Energy Reviews*, vol. 60, pp. 21–40. doi: 10.1016/j.rser.2016.01.055.
- [168] Muñoz-Sánchez, B., Nieto-Maestre, J., Iparraguirre-Torres, I., Sánchez-García, J. A., Julia, J. E., and García-Romero, A. 2016. The influence of mixing water on the thermophysical properties of nanofluids based on solar salt and silica nanoparticles, *AIP Conference Proceedings*, vol. 1734, no. May 2016. doi: 10.1063/1.4949129.
- [169] Sandhya, M., Ramasamy, D., Sudhakar, K., Kadirgama, K., and Harun, W. S. W. 2021. Ultrasonication an intensifying tool for preparation of stable nanofluids and study the time influence on distinct properties of graphene nanofluids – A systematic overview, *Ultrasonics Sonochemistry*, vol. 73. doi: 10.1016/j.ultsonch.2021.105479.
- [170] Pordanjani, A. H. *et al.* 2021. Nanofluids: Physical phenomena, applications in thermal systems and the environment effects- a critical review, *Journal of Cleaner Production*, vol. 320, no. February 2020, p. 128573. doi: 10.1016/j.jclepro.2021.128573.
- [171] Kumaran, K. 2021. A comprehensive review on the application of nanofluids in the machining process, *The International Journal of Advanced Manufacturing Technology*, vol. 47. doi: <https://doi.org/10.1007/s00170-021-07316-8>.
- [172] Hemmat Esfe, M., Bahiraei, M., and Mir, A. 2020. Application of conventional and hybrid nanofluids in different machining processes: A critical review, *Advances in Colloid and Interface Science*, vol. 282, p. 102199. doi: 10.1016/j.cis.2020.102199.
- [173] Xian, H. W., Sidik, N. A. C., and Najafi, G. 2019. Recent state of nanofluid in automobile cooling systems, *Journal of Thermal Analysis and Calorimetry*, vol. 135, no. 2, pp. 981–1008. doi: 10.1007/s10973-018-7477-3.
- [174] Delavari, V. and Hashemabadi, S. H. 2014. CFD simulation of heat transfer enhancement of Al₂O₃/water and Al₂O₃/ethylene glycol nanofluids in a car radiator, *Applied Thermal Engineering*, vol. 73, no. 1, pp. 380–390. doi: 10.1016/j.applthermaleng.2014.07.061.
- [175] Kumar, A. and Subudhi, S. 2019. Preparation, characterization and heat transfer analysis of nanofluids used for engine cooling, *Applied Thermal Engineering*, vol. 160, no. June, p. 114092. doi: 10.1016/j.applthermaleng.2019.114092.
- [176] Harikrishnan, S., Roseline, A. A., and Kalaiselvam, S. 2013. Preparation and thermophysical properties of water-glycerol mixture-based CuO nanofluids as PCM for cooling applications, *IEEE Transactions on Nanotechnology*, vol. 12, no. 4, pp. 629–635. doi: 10.1109/TNANO.2013.2265753.

- [177] Bretado-de los Rios, M. S., Rivera-Solorio, C. I., and Nigam, K. D. P. 2021. An overview of sustainability of heat exchangers and solar thermal applications with nanofluids: A review, *Renewable and Sustainable Energy Reviews*, vol. 142, no. March, p. 110855. doi: 10.1016/j.rser.2021.110855.
- [178] Aglawe, K. R., Yadav, R. K., and Thool, S. B. 2020. Preparation, applications and challenges of nanofluids in electronic cooling: A systematic review, *Materials Today: Proceedings*, vol. 43, pp. 366–372. doi: 10.1016/j.matpr.2020.11.679.
- [179] Soheli, M. R., Saidur, R., Khaleduzzaman, S. S., and Ibrahim, T. A. 2015. Cooling performance investigation of electronics cooling system using Al₂O₃-H₂O nanofluid, *International Communications in Heat and Mass Transfer*, vol. 65, pp. 89–93. doi: 10.1016/j.icheatmasstransfer.2015.04.015.
- [180] Zhou, R., Fu, S., Li, H., Yuan, D., Tang, B., and Zhou, G. 2019. Experimental study on thermal performance of copper nanofluids in a miniature heat pipe fabricated by wire electrical discharge machining, *Applied Thermal Engineering*, vol. 160, no. June, p. 113989. doi: 10.1016/j.applthermaleng.2019.113989.
- [181] Ghorabae, H., Emami, M. R. S., Moosakazemi, F., Karimi, N., Cheraghian, G., and Afrand, M. 2021. The use of nanofluids in thermosyphon heat pipe: A comprehensive review, *Powder Technology*, vol. 394, pp. 250–269. doi: 10.1016/j.powtec.2021.08.045.
- [182] Ren, Q. 2019. Enhancement of nanoparticle-phase change material melting performance using a sinusoidal heat pipe, *Energy Conversion and Management*, vol. 180, no. November 2018, pp. 784–795. doi: 10.1016/j.enconman.2018.11.033.
- [183] Mohammed, H. A., Vuthaluru, H. B., and Liu, S. 2022. Thermohydraulic and thermodynamics performance of hybrid nanofluids based parabolic trough solar collector equipped with wavy promoters, *Renewable Energy*, vol. 182, pp. 401–426. doi: 10.1016/j.renene.2021.09.096.
- [184] Ahmed, S. F., Khalid, M., Rashmi, W., Chan, A., and Shahbaz, K. 2017. Recent progress in solar thermal energy storage using nanomaterials, *Renewable and Sustainable Energy Reviews*, vol. 67, pp. 450–460. doi: 10.1016/j.rser.2016.09.034.
- [185] Mahian, O., Kianifar, A., Kalogirou, S. A., Pop, I., and Wongwises, S. 2013. A review of the applications of nanofluids in solar energy, *International Journal of Heat and Mass Transfer*, vol. 57, no. 2, pp. 582–594. doi: 10.1016/j.ijheatmasstransfer.2012.10.037.
- [186] Rubbi, F., Das, L., Habib, K., Aslfattahi, N., Saidur, R., and Rahman, M. T. 2021. State-of-the-art review on water-based nanofluids for low temperature solar thermal collector application, *Solar Energy Materials and Solar Cells*, vol. 230, no. February, p. 111220. doi: 10.1016/j.solmat.2021.111220.

- [187] Abbas,N. *et al.* 2019.Applications of nanofluids in photovoltaic thermal systems: A review of recent advances, *Physica A: Statistical Mechanics and its Applications*, vol. 536, p. 122513. doi: 10.1016/j.physa.2019.122513.
- [188] Jamei,M.,Karbasi,M.,Adewale,I.,and Mosharaf-dehkordi,M. 2021.Specific heat capacity of molten salt-based nanofluids in solar thermal applications: A paradigm of two modern ensemble machine learning methods, *Journal of Molecular Liquids*, vol. 335, p. 116434. doi: 10.1016/j.molliq.2021.116434.
- [189] Hafs,H.,Zaaoumi,A.,Ansari,O.,Bah,A.,Asbik,M.,and Malha,M. 2019.Effect of the Nanofluid (Brackish water/Al₂O₃) on the Passive Solar Still Desalination Performance with Heat Storage System, *Proceedings of the 10th International Conference on Electronics, Computers and Artificial Intelligence, ECAI 2018*, pp. 1–6. doi: 10.1109/ECAI.2018.8678956.
- [190] Liu,C. *et al.* 2021.Recent advances of nanofluids in micro/nano scale energy transportation, *Renewable and Sustainable Energy Reviews*, vol. 149, no. July 2020, p. 111346. doi: 10.1016/j.rser.2021.111346.
- [191] Islam,M. R.,Shabani,B.,and Rosengarten,G. 2017.Electrical and Thermal Conductivities of 50/50 Water-ethylene Glycol Based TiO₂ Nanofluids to be Used as Coolants in PEM Fuel Cells, *Energy Procedia*, vol. 110, no. December 2016, pp. 101–108. doi: 10.1016/j.egypro.2017.03.113.
- [192] Ramezanizadeh,M.,Alhuyi Nazari,M.,Hossein Ahmadi,M.,and Chen,L. 2019.A review on the approaches applied for cooling fuel cells, *International Journal of Heat and Mass Transfer*, vol. 139, pp. 517–525. doi: 10.1016/j.ijheatmasstransfer.2019.05.032.
- [193] Sayuti,M.,Erh,O. M.,Sarhan,A. A. D.,and Hamdi,M. 2014.Investigation on the morphology of the machined surface in end milling of aerospace AL6061-T6 for novel uses of SiO₂ nanolubrication system, *Journal of Cleaner Production*, vol. 66, pp. 655–663. doi: 10.1016/j.jclepro.2013.11.058.
- [194] Du,R.,Jiang,D. D.,Wang,Y.,and Wei Shah,K. 2020.An experimental investigation of CuO/water nanofluid heat transfer in geothermal heat exchanger, *Energy and Buildings*, vol. 227, p. 110402. doi: 10.1016/j.enbuild.2020.110402.
- [195] Yakasai,F.,Jaafar,M. Z.,Bandyopadhyay,S.,and Agi,A. 2021.Current developments and future outlook in nanofluid flooding: A comprehensive review of various parameters influencing oil recovery mechanisms, *Journal of Industrial and Engineering Chemistry*, vol. 93, pp. 138–162. doi: 10.1016/j.jiec.2020.10.017.
- [196] Panchal,H.,Patel,H.,Patel,J.,and Shah,M. 2021.A systematic review on nanotechnology in enhanced oil recovery, *Petroleum Research*, vol. 6, no. 3, pp. 204–212. doi: 10.1016/j.ptlrs.2021.03.003.
- [197] Ghazanfari,V.,Talebi,M.,Khorsandi,J.,and Abdolahi,R. 2016.Thermal-hydraulic

- modeling of water/Al₂O₃ nanofluid as the coolant in annular fuels for a typical VVER-1000 core, *Progress in Nuclear Energy*, vol. 87, pp. 67–73. doi: 10.1016/j.pnucene.2015.11.008.
- [198] Kulkarni, D. P., Das, D. K., and Vajjha, R. S. 2009. Application of nanofluids in heating buildings and reducing pollution, *Applied Energy*, vol. 86, no. 12, pp. 2566–2573. doi: 10.1016/j.apenergy.2009.03.021.
- [199] Elsaid, K., Olabi, A. G., Wilberforce, T., Abdelkareem, M. A., and Sayed, E. T. 2021. Environmental impacts of nanofluids: A review, *Science of the Total Environment*, vol. 763. doi: 10.1016/j.scitotenv.2020.144202.

Chapter 5

- [1] Calderón, A., Barreneche, C., Prieto, C., Segarra, M., and Fernández, A. I. 2021. Concentrating Solar Power Technologies: A Bibliometric Study of Past, Present and Future Trends in Concentrating Solar Power Research, *Frontiers in Mechanical Engineering*, vol. 7, no. June, pp. 1–22. doi: 10.3389/fmech.2021.682592.
- [2] Hou, Y., Vidu, R., and Stroeve, P. 2011. Solar Energy Storage Methods, *Industrial & Engineering Chemistry Research*, vol. 50, no. 15, pp. 8954–8964. doi: 10.1021/ie2003413.
- [3] Palacios, A., Barreneche, C., Navarro, M. E., and Ding, Y. 2020. Thermal energy storage technologies for concentrated solar power – A review from a materials perspective, *Renewable Energy*, vol. 156, pp. 1244–1265. doi: 10.1016/j.renene.2019.10.127.
- [4] Mostafavi Tehrani, S. S., Taylor, R. A., Nithyanandam, K., and Shafiei Ghazani, A. 2017. Annual comparative performance and cost analysis of high temperature, sensible thermal energy storage systems integrated with a concentrated solar power plant, *Solar Energy*, vol. 153, pp. 153–172. doi: 10.1016/j.solener.2017.05.044.
- [5] Achkari, O. and El Fadar, A. 2020. Latest developments on TES and CSP technologies – Energy and environmental issues, applications and research trends, *Applied Thermal Engineering*, vol. 167, no. October 2018, p. 114806. doi: 10.1016/j.applthermaleng.2019.114806.
- [6] Prieto, C., Osuna, R., Fernández, A. I., and Cabeza, L. F. 2016. Thermal storage in a MW scale . Molten salt solar thermal pilot facility: Plant description and commissioning experiences, *Renewable Energy*, vol. 99, pp. 852–866. doi: 10.1016/j.renene.2016.07.053.
- [7] Mohan, G., Venkataraman, M. B., and Coventry, J. 2019. Sensible energy storage options for concentrating solar power plants operating above 600 °C, *Renewable and Sustainable Energy Reviews*, vol. 107, no. January, pp. 319–337. doi: 10.1016/j.rser.2019.01.062.

- [8] Ibrahim,A.,Peng,H.,Riaz,A.,Abdul Basit,M.,Rashid,U.,and Basit,A. 2021.Molten salts in the light of corrosion mitigation strategies and embedded with nanoparticles to enhance the thermophysical properties for CSP plants, *Solar Energy Materials and Solar Cells*, vol. 219, no. September 2020, p. 110768. doi: 10.1016/j.solmat.2020.110768.
- [9] Gasia,J.,Miró,L.,and Cabeza,L. F. 2017.Review on system and materials requirements for high temperature thermal energy storage. Part 1: General requirements, *Renewable and Sustainable Energy Reviews*, vol. 75, no. May 2016, pp. 1320–1338. doi: 10.1016/j.rser.2016.11.119.
- [10] Jacob,R.,Belusko,M.,Fernández,A. I.,Cabeza,L. F.,Saman,W.,and Bruno,F. 2016.Embodied energy and cost of high temperature thermal energy storage systems for use with concentrated solar power plants, *Applied Energy*, vol. 180, pp. 586–597. doi: 10.1016/j.apenergy.2016.08.027.
- [11] Alashkar,A. and Gadalla,M. 2017.Thermo-economic analysis of an integrated solar power generation system using nanofluids, *Applied Energy*, vol. 191, pp. 469–491. doi: 10.1016/j.apenergy.2017.01.084.
- [12] Kwak,H.,Shin,D.,and Banerjee,D. 2010.Enhanced sensible heat capacity of molten salt and conventional Heat Transfer Fluid Based Nanofluid for Solar Thermal Energy, no. 979, pp. 1–5.
- [13] Chieruzzi,M.,Cerritelli,G. F.,Miliozzi,A.,and Kenny,J. M. 2013.Effect of nanoparticles on heat capacity of nanofluids based on molten salts as PCM for thermal energy storage, *Nanoscale Research Letters*, vol. 8, no. 1, pp. 1–9. doi: 10.1186/1556-276X-8-448.
- [14] Shin,D. and Banerjee,D. 2011.Enhanced specific heat of silica nanofluid, *Journal of Heat Transfer*, vol. 133, no. 2, pp. 1–4. doi: 10.1115/1.4002600.
- [15] Tiznobaik,H. and Shin,D. 2013.Enhanced specific heat capacity of high-temperature molten salt-based nanofluids, *International Journal of Heat and Mass Transfer*, vol. 57, no. 2, pp. 542–548. doi: 10.1016/j.ijheatmasstransfer.2012.10.062.
- [16] De Castro,C. A. N. *et al.* 2010.Thermal properties of ionic liquids and loNanoFluids of imidazolium and pyrrolidinium liquids, *Journal of Chemical and Engineering Data*, vol. 55, no. 2, pp. 653–661. doi: 10.1021/jc900648p.
- [17] Dudda,B. and Shin,D. 2013.Effect of nanoparticle dispersion on specific heat capacity of a binary nitrate salt eutectic for concentrated solar power applications, *International Journal of Thermal Sciences*, vol. 69, pp. 37–42. doi: 10.1016/j.ijthermalsci.2013.02.003.
- [18] Aljaerani,H. A.,Samyano,M.,Saidur,R.,Pandey,A. K.,and Kadirgama,K. 2021.Nanoparticles as molten salts thermophysical properties enhancer for concentrated solar power: A critical review, *Journal of Energy Storage*, vol. 44, no. PA, p. 103280. doi: 10.1016/j.est.2021.103280.
- [19] Grosu,Y.,Nithiyantham,U.,González-Fernández,L.,and Faik,A. 2019.Preparation and characterization of nanofluids based on molten salts with enhanced thermophysical properties for thermal energy storage at concentrate solar power, *SOLARPACES 2018: International Conference on*

Concentrating Solar Power and Chemical Energy Systems, vol. 2126, p. 200021. doi: 10.1063/1.5117736.

- [20] Riazi,H.,Mesgari,S.,Ahmed,N. A.,and Taylor,R. A. 2016.The effect of nanoparticle morphology on the specific heat of nanosalts, *International Journal of Heat and Mass Transfer*, vol. 94, pp. 254–261. doi: 10.1016/j.ijheatmasstransfer.2015.11.064.
- [21] Ryu,H. Y. 2014.Large enhancement of light extraction efficiency in AlGaIn-based nanorod ultraviolet light-emitting diode structures, *Nanoscale Research Letters*, vol. 9, no. 1, pp. 1–7. doi: 10.1186/1556-276X-9-58.
- [22] Jiang,Z. *et al.* 2019.Novel key parameter for eutectic nitrates based nanofluids selection for concentrating solar power (CSP) system, *Applied Energy*, vol. 235, no. July 2018, pp. 529–542. doi: 10.1016/j.apenergy.2018.10.114.
- [23] Huang,Y.,Cheng,X.,Li,Y.,Yu,G.,Xu,K.,and Li,G. 2018.Effect of in-situ synthesized nano-MgO on thermal properties of NaNO₃-KNO₃, *Solar Energy*, vol. 160, no. December 2017, pp. 208–215. doi: 10.1016/j.solener.2017.11.077.
- [24] Awad,A.,Navarro,H.,Ding,Y.,and Wen,D. 2018.Thermal-physical properties of nanoparticle-seeded nitrate molten salts, *Renewable Energy*, vol. 120, pp. 275–288. doi: 10.1016/j.renene.2017.12.026.
- [25] Chieruzzi,M.,Cerritelli,G. F.,Miliozzi,A.,Kenny,J. M.,and Torre,L. 2017.Heat capacity of nanofluids for solar energy storage produced by dispersing oxide nanoparticles in nitrate salt mixture directly at high temperature, *Solar Energy Materials and Solar Cells*, vol. 167, no. December 2016, pp. 60–69. doi: 10.1016/j.solmat.2017.04.011.
- [26] Chieruzzi,M.,Miliozzi,A.,Crescenzi,T.,Torre,L.,and Kenny,J. M. 2015.A New Phase Change Material Based on Potassium Nitrate with Silica and Alumina Nanoparticles for Thermal Energy Storage, *Nanoscale Res Lett*, vol. 10, no. 1, p. 984. doi: 10.1186/s11671-015-0984-2.
- [27] Luo,Y.,Du,X.,Awad,A.,and Wen,D. 2017.Thermal energy storage enhancement of a binary molten salt via in-situ produced nanoparticles, *International Journal of Heat and Mass Transfer*, vol. 104, pp. 658–664. doi: 10.1016/j.ijheatmasstransfer.2016.09.004.
- [28] Xie,Q.,Zhu,Q.,and Li,Y. 2016.Thermal storage properties of molten nitrate salt-based nanofluids with graphene nanoplatelets., *Nanoscale research letters*, vol. 11, no. 1, p. 306. doi: 10.1186/s11671-016-1519-1.
- [29] Xie,Q.,Zhu,Q.,and Li,Y. 2016.Thermal Storage Properties of Molten Nitrate Salt-Based Nanofluids with Graphene Nanoplatelets., *Nanoscale research letters*, vol. 11, no. 1, p. 306. doi: 10.1186/s11671-016-1519-1.
- [30] Lasfargues,M.,Geng,Q.,Cao,H.,and Ding,Y. 2015.Mechanical dispersion of nanoparticles and its effect on the specific heat capacity of impure binary nitrate salt mixtures, *Nanomaterials*, vol. 5, no. 3, pp. 1136–1146. doi: 10.3390/nano5031136.
- [31] Li,Y. *et al.* 2019.Experimental study on the effect of SiO₂ nanoparticle dispersion on the thermophysical properties of binary nitrate molten salt, *Solar Energy*, vol. 183, no. December 2018, pp. 776–781. doi:

10.1016/j.solener.2019.03.036.

- [32] Awad,A.,Navarro,H.,Ding,Y.,and Wen,D. 2018.Thermal-physical properties of nanoparticle-seeded nitrate molten salts, *Renewable Energy*, vol. 120, pp. 275–288. doi: 10.1016/j.renene.2017.12.026.
- [33] Qiao,G.,Lasfargues,M.,Alexiadis,A.,and Ding,Y. 2017.Simulation and experimental study of the specific heat capacity of molten salt based nanofluids, *Applied Thermal Engineering*, vol. 111, pp. 1517–1522. doi: 10.1016/j.applthermaleng.2016.07.159.
- [34] Myers,P. D.,Alam,T. E.,Kamal,R.,Goswami,D. Y.,and Stefanakos,E. 2016.Nitrate salts doped with CuO nanoparticles for thermal energy storage with improved heat transfer, *Applied Energy*, vol. 165, pp. 225–233. doi: 10.1016/j.apenergy.2015.11.045.
- [35] Pramod,K. *et al.* 2016.Preparation and characterization of molten salt based nanothermic fluids with enhanced thermal properties for solar thermal applications, *Applied Thermal Engineering*, vol. 109, pp. 901–905. doi: 10.1016/j.applthermaleng.2016.04.102.
- [36] Myers,P. D.,Alam,T. E.,Kamal,R.,Goswami,D. Y.,and Stefanakos,E. 2016.Nitrate salts doped with CuO nanoparticles for thermal energy storage with improved heat transfer, *Applied Energy*, vol. 165, pp. 225–233. doi: 10.1016/j.apenergy.2015.11.045.
- [37] Andreu-Cabedo,P.,Mondragon,R.,Hernandez,L.,Martinez-Cuenca,R.,Cabedo,L.,and Julia,J. 2014.Increment of specific heat capacity of solar salt with SiO₂ nanoparticles, *Nanoscale Research Letters*, vol. 9, no. 1, p. 582. doi: 10.1186/1556-276X-9-582.
- [38] Sang,L.,Ai,W.,Liu,T.,Wu,Y.,and Ma,C. 2019.Insights into the specific heat capacity enhancement of ternary carbonate nanofluids with SiO₂ nanoparticles: the effect of change in the composition ratio, *RSC Advances*, vol. 9, no. 10, pp. 5288–5294. doi: 10.1039/c8ra10318f.
- [39] Shahrul,I. M.,Mahbulul,I. M.,Khaleduzzaman,S. S.,Saidur,R.,and Sabri,M. F. M. 2014.A comparative review on the specific heat of nanofluids for energy perspective, *Renewable and Sustainable Energy Reviews*, vol. 38, pp. 88–98. doi: 10.1016/j.rser.2014.05.081.
- [40] Jiang,Z.,Palacios,A.,Lei,X.,Navarro,M. E.,Qiao,G.,and Mura,E. 2019.Novel key parameter for eutectic nitrates based nanofluids selection for concentrating solar power (CSP) systems, *Applied Energy*, vol. 235, no. November 2018, pp. 529–542. doi: 10.1016/j.apenergy.2018.10.114.
- [41] Navarrete,N.,Mondragón,R.,Wen,D.,Navarro,M. E.,Ding,Y.,and Juliá,J. E. 2019.Thermal energy storage of molten salt –based nanofluid containing nano-encapsulated metal alloy phase change materials, *Energy*, vol. 167, pp. 912–920. doi: 10.1016/j.energy.2018.11.037.
- [42] Said,Z.,Hachicha,A. A.,Aberoumand,S.,Yousef,B. A. A.,Sayed,E. T.,and Bellos,E. 2021.Recent advances on nanofluids for low to medium temperature solar collectors: energy, exergy, economic analysis and environmental impact, *Progress in Energy and Combustion Science*, vol. 84. doi:

10.1016/j.pecs.2020.100898.

- [43] Fernández,A. G.,Muñoz-Sánchez,B.,Nieto-Maestre,J.,and García-Romero,A. 2019.High temperature corrosion behavior on molten nitrate salt-based nanofluids for CSP plants, *Renewable Energy*, vol. 130, pp. 902–909. doi: 10.1016/j.renene.2018.07.018.
- [44] Piquot,J.,Nithiyantham,U.,Grosu,Y.,and Faik,A. 2019.Spray-graphitization as a protection method against corrosion by molten nitrate salts and molten salts based nanofluids for thermal energy storage applications, *Solar Energy Materials and Solar Cells*, vol. 200, no. June, p. 110024. doi: 10.1016/j.solmat.2019.110024.
- [45] Nithiyantham,U.,Grosu,Y.,González-Fernández,L.,Zaki,A.,Igartua,J. M.,and Faik,A. 2019.Corrosion aspects of molten nitrate salt-based nanofluids for thermal energy storage applications, *Solar Energy*, vol. 189, no. June, pp. 219–227. doi: 10.1016/j.solener.2019.07.050.
- [46] Jo,B. and Banerjee,D. 2015.Effect of dispersion homogeneity on specific heat capacity enhancement of molten salt nanomaterials using carbon nanotubes, *Journal of Solar Energy Engineering, Transactions of the ASME*, vol. 137, no. 1, pp. 1–9. doi: 10.1115/1.4028144.
- [47] Jo,B. and Banerjee,D. 2015.Enhanced specific heat capacity of molten salt-based carbon nanotubes nanomaterials, *Journal of Heat Transfer*, vol. 137, no. 9, pp. 1–7. doi: 10.1115/1.4030226.
- [48] Kim,H. J. and Jo,B. 2018.Anomalous increase in specific heat of binary molten salt-based graphite nanofluids for thermal energy storage, *Applied Sciences (Switzerland)*, vol. 8, no. 8. doi: 10.3390/app8081305.
- [49] Jo,B. and Banerjee,D. 2015.Effect of solvent on specific heat capacity enhancement of binary molten salt-based carbon nanotube nanomaterials for thermal energy storage, *International Journal of Thermal Sciences*, vol. 98, pp. 219–227. doi: 10.1016/j.ijthermalsci.2015.07.020.
- [50] Shahsavar,A.,Salimpour,M. R.,Saghafian,M.,and Shafii,M. B. 2015.An experimental study on the effect of ultrasonication on thermal conductivity of ferrofluid loaded with carbon nanotubes, *Thermochimica Acta*, vol. 617, pp. 102–110. doi: 10.1016/j.tca.2015.08.025.
- [51] Sandhya,M.,Ramasamy,D.,Sudhakar,K.,Kadrigama,K.,and Harun,W. S. W. 2021.Ultrasonication an intensifying tool for preparation of stable nanofluids and study the time influence on distinct properties of graphene nanofluids – A systematic overview, *Ultrasonics Sonochemistry*, vol. 73. doi: 10.1016/j.ultsonch.2021.105479.
- [52] Bakthavatchalam,B.,Habib,K.,Saidur,R.,Saha,B. B.,and Irshad,K. 2020.Comprehensive study on nanofluid and ionanofluid for heat transfer enhancement: A review on current and future perspective, *Journal of Molecular Liquids*, vol. 305, p. 112787. doi: 10.1016/j.molliq.2020.112787.
- [53] Yu,W.,Xie,H.,Li,Y.,Chen,L.,and Wang,Q. 2011.Experimental investigation on the thermal transport properties of ethylene glycol based nanofluids containing low volume concentration diamond nanoparticles, *Colloids and Surfaces A*:

Physicochemical and Engineering Aspects, vol. 380, no. 1–3, pp. 1–5. doi: 10.1016/j.colsurfa.2010.11.020.

- [54] Habibzadeh,S.,Kazemi-Beydokhti,A.,Khodadadi,A. A.,Mortazavi,Y.,Omanovic,S.,and Shariat-Niassar,M. 2010.Stability and thermal conductivity of nanofluids of tin dioxide synthesized via microwave-induced combustion route, *Chemical Engineering Journal*, vol. 156, no. 2, pp. 471–478. doi: 10.1016/j.cej.2009.11.007.
- [55] Alashkar,A. and Gadalla,M. 2017.Thermo-economic analysis of an integrated solar power generation system using nanofluids, *Applied Energy*, vol. 191, pp. 469–491. doi: 10.1016/j.apenergy.2017.01.084.
- [56] Shin,D.,Tiznobaik,H.,and Banerjee,D. 2014.Specific heat mechanism of molten salt nanofluids, *Applied Physics Letters*, vol. 104, no. 12. doi: 10.1063/1.4868254.
- [57] Shin,D. and Banerjee,D. 2011.Enhancement of specific heat capacity of high-temperature silica-nanofluids synthesized in alkali chloride salt eutectics for solar thermal-energy storage applications, *International Journal of Heat and Mass Transfer*, vol. 54, no. 5–6, pp. 1064–1070. doi: 10.1016/j.ijheatmasstransfer.2010.11.017.
- [58] Lan,W.,Tan,Z.,Meng,S.,Liang,D.,and Guanghai,L. 2011.Enhancement of molar heat capacity of nanostructured Al₂O₃, *Journal of Nanoparticle Research 3*; vol. 3, no. 4, pp. 483–487. doi: 10.1179/1743294411Y.0000000076.
- [59] Wang,B.-X.,Zhou,L.-P.,and Peng,X.-F. 2006.Surface and Size Effects on the Specific Heat Capacity of Nanoparticles, *International Journal of Thermophysics*, vol. 27, no. 1, pp. 139–151. doi: 10.1007/s10765-006-0022-9.
- [60] Avramov,I. and Michailov,M. 2008.Specific heat of nanocrystals, *Journal of Physics Condensed Matter*, vol. 20, no. 29. doi: 10.1088/0953-8984/20/29/295224.
- [61] Shin,D. and Banerjee,D. 2011.Enhancement of specific heat capacity of high-temperature silica-nanofluids synthesized in alkali chloride salt eutectics for solar thermal-energy storage applications, *International Journal of Heat and Mass Transfer*, vol. 54, no. 5–6, pp. 1064–1070. doi: 10.1016/j.ijheatmasstransfer.2010.11.017.
- [62] Xue,L.,Kebinski,P.,Phillpot,S. R.,Choi,S. U. S.,and Eastman,J. A. 2004.Effect of liquid layering at the liquid-solid interface on thermal transport, *International Journal of Heat and Mass Transfer*, vol. 47, no. 19–20, pp. 4277–4284. doi: 10.1016/j.ijheatmasstransfer.2004.05.016.
- [63] Lu,M.-C. and Huang,C.-H. 2013.Specific heat capacity of molten salt-based alumina nanofluid., *Nanoscale research letters*, vol. 8, no. 1, p. 292. doi: 10.1186/1556-276X-8-292.
- [64] Li,L.,Zhang,Y.,Ma,H.,and Yang,M. 2010.Molecular dynamics simulation of effect of liquid layering around the nanoparticle on the enhanced thermal conductivity of nanofluids, *Journal of Nanoparticle Research*, vol. 12, no. 3, pp. 811–821. doi: 10.1007/s11051-009-9728-5.
- [65] Oh,S. H.,Kauffmann,Y.,Scheu,C.,Kaplan,W. D.,and Rühle,M. 2005.Ordered

- liquid aluminum at the interface with sapphire, *Science*, vol. 310, no. 5748, pp. 661–663. doi: 10.1126/science.1118611.
- [66] Yu, C. J., Richter, A. G., Datta, A., Durbin, M. K., and Dutta, P. 2000. Molecular layering in a liquid on a solid substrate: An X-ray reflectivity study, *Physica B: Condensed Matter*, vol. 283, no. 1–3, pp. 27–31. doi: 10.1016/S0921-4526(99)01885-2.
- [67] Song, W., Lu, Y., Wu, Y., and Ma, C. 2018. Effect of SiO₂ nanoparticles on specific heat capacity of low-melting-point eutectic quaternary nitrate salt, *Solar Energy Materials and Solar Cells*, vol. 179, no. August 2017, pp. 66–71. doi: 10.1016/j.solmat.2018.01.014.
- [68] Tiznobaik, H., Banerjee, D., and Shin, D. 2015. Effect of formation of “long range” secondary dendritic nanostructures in molten salt nanofluids on the values of specific heat capacity, *International Journal of Heat and Mass Transfer*, vol. 91, pp. 342–346. doi: 10.1016/j.ijheatmasstransfer.2015.05.072.
- [69] Rizvi, S. M. M. and Shin, D. 2020. Mechanism of heat capacity enhancement in molten salt nanofluids, *International Journal of Heat and Mass Transfer*, vol. 161. doi: 10.1016/j.ijheatmasstransfer.2020.120260.
- [70] Jo, B. and Banerjee, D. 2014. Enhanced specific heat capacity of molten salt-based nanomaterials: Effects of nanoparticle dispersion and solvent material, *Acta Materialia*, vol. 75, pp. 80–91. doi: 10.1016/j.actamat.2014.05.005.
- [71] Yedhu Krishnan, R., Manikandan, S., Suganthi, K. S., Leela Vinodhan, V., and Rajan, K. S. 2016. Novel copper - Propylene glycol nanofluid as efficient thermic fluid for potential application in discharge cycle of thermal energy storage, *Energy*, vol. 107, pp. 482–492. doi: 10.1016/j.energy.2016.04.047.
- [72] Vinod, S. and Philip, J. 2018. Experimental evidence for the significant role of initial cluster size and liquid confinement on thermo-physical properties of magnetic nanofluids under applied magnetic field, *Journal of Molecular Liquids*, vol. 257, pp. 1–11. doi: 10.1016/j.molliq.2018.02.086.
- [73] Jung, S. and Banerjee, D. 2011. A simple analytical model for specific heat of nanofluid with tube shaped and disc shaped nanoparticles, *ASME/JSME 2011 8th Thermal Engineering Joint Conference, AJTEC 2011*, pp. 1–6. doi: 10.1115/ajtec2011-44372.
- [74] Wang, B. X., Zhou, L. P., Peng, X. F., Du, X. Z., and Yang, Y. P. 2010. On the specific heat capacity of CuO nanofluid, *Advances in Mechanical Engineering*, vol. 2010. doi: 10.1155/2010/172085.
- [75] Yimin, X. and Wilfried, R. 2000. Conceptions for heat transfer correlation of nanofluids, *International Journal of Heat and Mass Transfer*, vol. 43, no. 4, pp. 3701–3707. doi: 10.1016/j.aej.2017.01.005.
- [76] O’Hanley, H., Buongiorno, J., McKrell, T., and Hu, L. W. 2012. Measurement and model validation of nanofluid specific heat capacity with differential scanning calorimetry, *Advances in Mechanical Engineering*, vol. 2012. doi: 10.1155/2012/181079.
- [77] Dudda, B. and Shin, D. 2013. Effect of nanoparticle dispersion on specific heat capacity of a binary nitrate salt eutectic for concentrated solar power

applications, *International Journal of Thermal Sciences*, vol. 69, pp. 37–42. doi: 10.1016/j.ijthermalsci.2013.02.003.

- [78] Tiznobaik,H. and Shin,D. 2013.Experimental validation of enhanced heat capacity of ionic liquid-based nanomaterial, *Applied Physics Letters*, vol. 102, no. 17, pp. 1–4. doi: 10.1063/1.4801645.

Chapter 6

- [1] Belter,C. W. 2015.Bibliometric indicators: Opportunities and limits, *Journal of the Medical Library Association*, vol. 103, no. 4, pp. 219–221. doi: 10.3163/1536-5050.103.4.014.
- [2] Rameshchandra,R. and Toshniwal,P. 2017.Analysis of Bibliometric term in Web of Science, *International Research Journal*, vol. 01, no. 32, pp. 78–83.
- [3] Szomszor,M. *et al.* 2021.Interpreting Bibliometric Data, *Frontiers in Research Metrics and Analytics*, vol. 5, no. February, pp. 1–20. doi: 10.3389/frma.2020.628703.
- [4] Adams,J.,Pendlebury,D.,and Szomszor,M. 2020.Global Research Report-The value of bibliometric databases: Data-intensive studies beyond search and discovery, p. 16.
- [5] Jang,S. P. and Choi,S. U. S. 2004.Role of Brownian motion in the enhanced thermal conductivity of nanofluids, *Applied Physics Letters*, vol. 84, no. 21, pp. 4316–4318. doi: 10.1063/1.1756684.
- [6] Yu,W. and Choi,S. U. S. 2004.The role of interfacial layers in the enhanced thermal conductivity of nanofluids: A renovated Hamilton-Crosser model, *Journal of Nanoparticle Research*, vol. 6, no. 4, pp. 355–361. doi: 10.1007/s11051-004-2601-7.

Chapter 7

- [1] Svobodova-Sedlackova,A.,Barreneche,C.,Gamallo,P.,and Inés Fernández,A. 2021.Novel sampling procedure and statistical analysis for the thermal characterization of ionic nanofluids, *Journal of Molecular Liquids*, vol. 347, p. 118316. doi: 10.1016/j.molliq.2021.118316.

Chapter 8

- [1] Svobodova-Sedlackova,A.,Barreneche,C.,Alonso,G.,Fernandez,A. I.,and Gamallo,P. 2020.Effect of nanoparticles in molten salts – MD simulations and experimental study, *Renewable Energy*, vol. 152, pp. 208–216. doi: 10.1016/j.renene.2020.01.046.

Chapter 9

- [1] Mondragón,R.,Juliá,J. E.,Cabedo,L.,and Navarrete,N. 2018.On the relationship between the specific heat enhancement of salt-based nanofluids and the ionic exchange capacity of nanoparticles, *Scientific Reports*, vol. 8, no. 1, pp. 1–12. doi: 10.1038/s41598-018-25945-0.
- [2] Svobodova-Sedlackova,A.,Calderón,A.,Barreneche,C.,Gamallo,P.,and Fernández,A. I. 2021.Understanding the abnormal thermal behavior of nanofluids through infrared thermography and thermo - physical characterization, *Scientific Reports*, no. 0123456789, pp. 1–10. doi: 10.1038/s41598-021-84292-9.

Chapter 11

- [1] Parr,A. 2013.The SAXS Guide.
- [2] Braun,D.,Cherdron,H.,Rehahn,M.,Ritter,H.,and Voit,B. 2013.*Polymer synthesis: Theory and practice: Fundamentals, methods, experiments, fifth edition*. doi: 10.1007/978-3-642-28980-4.
- [3] Angayarkanni,S. A. and Philip,J. 2015.Review on thermal properties of nanofluids: Recent developments, *Advances in Colloid and Interface Science*, vol. 225, pp. 146–176. doi: 10.1016/j.cis.2015.08.014.
- [4] Alcob,X.,Barcelona,G.,and Alcobé,X. 2007.Calibratges instrumentals de difraccòmetres de raigs x de pols.
- [5] Bolze,J.,Kogan,V.,Beckers,D.,and Fransen,M. 2018.High-performance small- and wide-angle X-ray scattering (SAXS/WAXS) experiments on a multi-functional laboratory goniometer platform with easily exchangeable X-ray modules, *Review of Scientific Instruments*, vol. 89, no. 8. doi: 10.1063/1.5041949.
- [6] Chen,G.,Yu,W.,Singh,D.,Cookson,D.,and Routbort,J. 2008.Application of SAXS

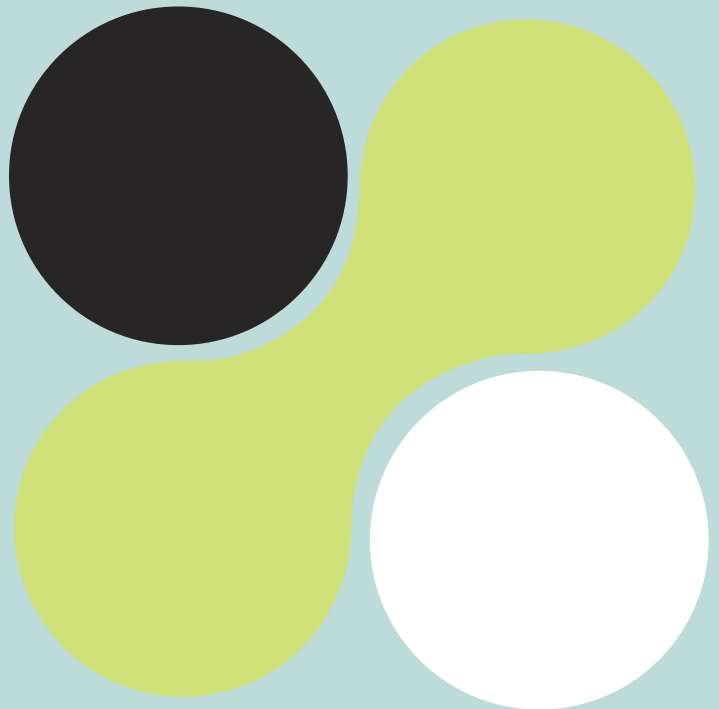
- to the study of particle-size-dependent thermal conductivity in silica nanofluids, *Journal of Nanoparticle Research*, vol. 10, no. 7, pp. 1109–1114. doi: 10.1007/s11051-007-9347-y.
- [7] Timofeeva, E. V., Routbort, J. L., and Singh, D. 2009. Particle shape effects on thermophysical properties of alumina nanofluids, *Journal of Applied Physics*, vol. 106, no. 1. doi: 10.1063/1.3155999.
- [8] Witharana, S. 2011. Thermal Transport in Nanofluids : Boiling heat transfer.
- [9] Singh, D. *et al.* 2009. An investigation of silicon carbide-water nanofluid for heat transfer applications, *Journal of Applied Physics*, vol. 105, no. 6. doi: 10.1063/1.3082094.
- [10] Suhaimi, N. S. *et al.* 2020. Systematical study of multi-walled carbon nanotube nanofluids based disposed transformer oil, *Scientific Reports*, vol. 10, no. 1, pp. 1–8. doi: 10.1038/s41598-020-77810-8.
- [11] Vinod, S. and Philip, J. 2018. Experimental evidence for the significant role of initial cluster size and liquid confinement on thermo-physical properties of magnetic nanofluids under applied magnetic field, *Journal of Molecular Liquids*, vol. 257, pp. 1–11. doi: 10.1016/j.molliq.2018.02.086.
- [12] Eberbeck, D. and Bläsing, J. 1999. Investigation of particle size distribution and aggregate structure of various ferrofluids by small-angle scattering experiments, *Journal of Applied Crystallography*, vol. 32, no. 2, pp. 273–280. doi: 10.1107/S0021889898012539.
- [13] Liu, F., Xiao, H., and Li, Y. 2005. Adsorption of poly(acrylic acid) onto the surface of titanium dioxide and the colloidal stability of aqueous suspension, *Journal of Colloid and Interface Science*, vol. 281, no. 1, pp. 155–163. doi: 10.1016/j.jcis.2004.08.075.
- [14] Witharana, S., Hodges, C., Xu, D., Lai, X., and Ding, Y. 2012. Aggregation and settling in aqueous polydisperse alumina nanoparticle suspensions, *Journal of Nanoparticle Research*, vol. 14, no. 5. doi: 10.1007/s11051-012-0851-3.
- [15] Gopinath, S. and Philip, J. 2014. Preparation of metal oxide nanoparticles of different sizes and morphologies, their characterization using small angle X-ray scattering and study of thermal properties, *Materials Chemistry and Physics*, vol. 145, no. 1–2, pp. 213–221. doi: 10.1016/j.matchemphys.2014.02.005.
- [16] Baglioni, M., Jáidar Benavides, Y., Desprat-Drapela, A., and Giorgi, R. 2015. Amphiphile-based nanofluids for the removal of styrene/acrylate coatings: Cleaning of stucco decoration in the Uaxactun archeological site (Guatemala), *Journal of Cultural Heritage*, vol. 16, no. 6, pp. 862–868. doi: 10.1016/j.culher.2015.03.008.
- [17] Frenzel, L., Lehmkuhler, F., Koof, M., Lokteva, I., and Grübel, G. 2020. The phase diagram of colloidal silica-PNIPAm core-shell nanogels, *Soft Matter*, vol. 16, no.

2, pp. 466–475. doi: 10.1039/c9sm01884k.

- [18] Jorjani,S.,Mozaffarian,M.,and Pazuki,G. 2018.A novel Nanodiamond based loNanofluid: Experimental and mathematical study of thermal properties, *Journal of Molecular Liquids*, vol. 271, pp. 211–219. doi: 10.1016/j.molliq.2018.08.116.
- [19] Bhattacharya,K. *et al.* 2020.Structural, thermodiffusive and thermoelectric properties of maghemite nanoparticles dispersed in ethylammonium nitrate, *ChemEngineering*, vol. 4, no. 1, pp. 1–25. doi: 10.3390/chemengineering4010005.

A1

Appendix 1



Appendix 1

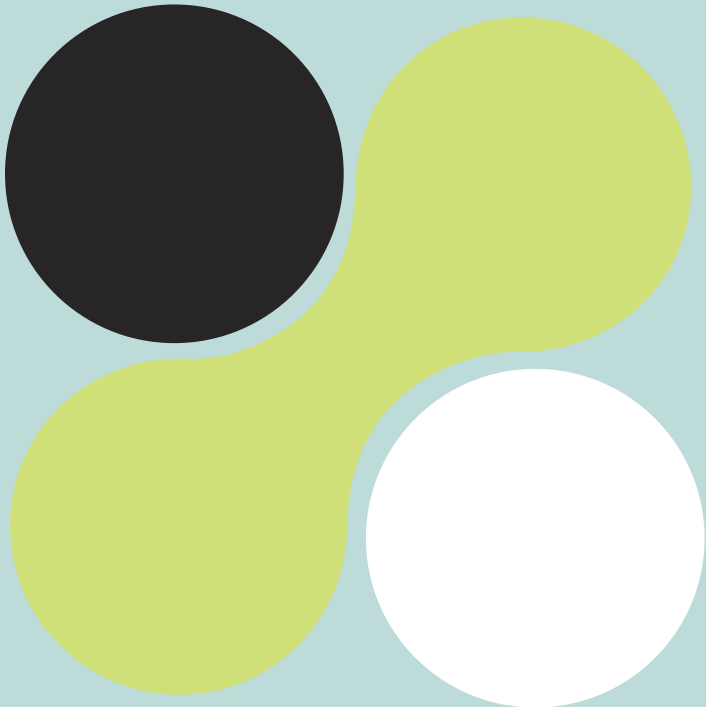
15.1 Database values

The link below is linked to a supplementary file with nanofluids' specific heat capacity, thermal conductivity, and viscosity database.

Link: http://www.diopma.org/supp/nsbnf/supp_file_1.pdf

A2

Appendix 2



Appendix 2

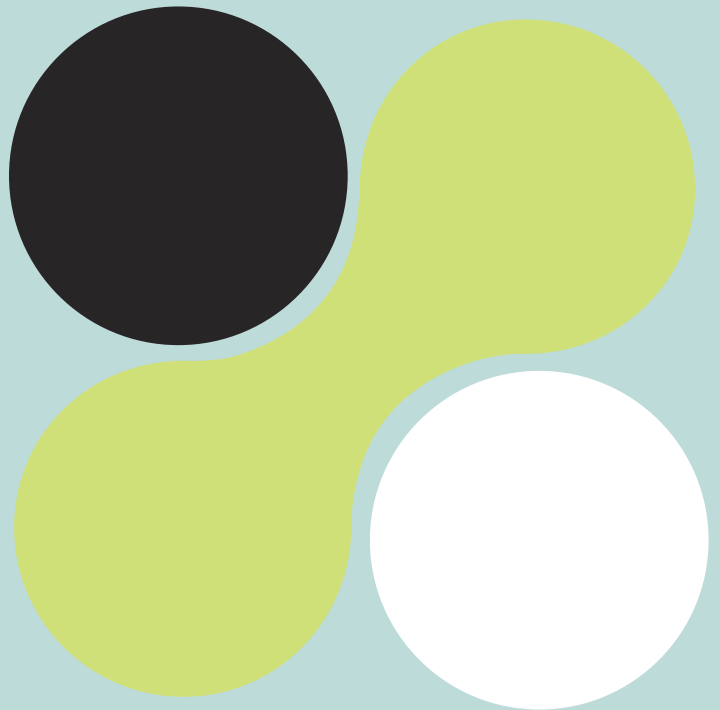
16.1 MD simulations – LAMMPS codes

The link below is linked to a supplementary file with LAMMPS codes.

Link: http://www.diopma.org/supp/nsbnf/supp_file_2.pdf

A3

Appendix 3



Appendix 3

17.1 Contributions in conferences

- **Title:** Effect of SiO₂ nanoparticles on molten salt used as heat storage medium: MD simulations and experimental characterization.
 - **Conference:** I Iberian Meeting on Materials Science (CNMAT 2018) XV Congreso Nacional de Materiales.
 - **Type of contribution:** Oral presentation
 - **Authors:** Svobodova, A.; Barreneche, C.; Gamallo, P.; Fernández, A. I.
 - **Scope:** International
 - **Country:** Salamanca-SPAIN
 - **Year:** 2018



Certificate of Oral Presentation

In recognition of presentation of the paper entitled:

**Effect of SiO₂ nanoparticles on molten salt used as heat storage medium:
MD simulations and experimental characterization**

This certificate is awarded to:

Sra. Adela Svobodova

Dra. Camila Barreneche

Dr. Pablo Gamallo

Dra. Ana I. Fernández

Figure A3.17-1. Certificate of oral presentation at I Iberian Meeting on Materials Science (CNMAT 2018) and XV Congreso Nacional de Materiales.

- **Title:** Can Molecular Simulations Help Industrial Processes?
 - **Conference:** 2nd International Vigo Meeting on Advanced Computational Chemistry
 - **Type of contribution:** Oral presentation
 - **Authors:** Svobodova, A.; Gamallo, P.
 - **Scope:** International
 - **Country:** Vigo-SPAIN
 - **Year:** 2019
-

- **Title:** Nanofluids: MD Simulations and Thermo-Chemical Study
 - **Conference:** Eurotherm Seminar n. 112: Advances in Thermal Energy Storage
 - **Type of contribution:** Oral presentation
 - **Authors:** Svobodova-Sedlackova, A.; Barreneche, C.; Alonso, G.; Gamallo, P.; Ines Fernandez, A.
 - **Scope:** International
 - **Country:** Lleida- ESPAÑA
 - **Year:** 2019
-



Eurotherm Seminar #112
Advances in Thermal Energy Storage



ADELA SVOBODOVA SEDLACKOVA

attended the

Eurotherm Seminar #112

Advances in Thermal Energy Storage

held in Lleida on 15-17 May 2019

Prof. Dr. Luisa F. Cabeza
Universitat de Lleida (Spain)
Co-chair of the Scientific Committee

Figure A3.17-2. Certificate of oral presentation at Eurotherm Seminar #112. Advances in Thermal Energy Storage.

- **Title:** From MD Simulations to experimental study: Molten salt based nanofluids.
 - **Conference:** 1st International Conference on Nanofluids (ICNF2019) 2nd European Symposium on Nanofluids (ESNF2019)
 - **Type of contribution:** Oral presentation
 - **Authors:** A. Svobodova-Sedlackova, C. Barreneche, Alonso, G, P. Gamallo and A. Ines Fernandez
 - **Scope:** International
 - **Country:** Catellón de la Plana- SPAIN
 - **Year:** 2019



Figure A3.17-3. Certificate of oral presentation at 1st International Conference on Nanofluids (ICNF2019) and 2nd European Symposium on Nanofluids (ESNF2019).

- **Title:** Molecular dynamic simulation of NaNO₃ nanofluid validated by thermochemical and thermophysical characterization.
 - **Conference:** CNIT 11 - Congreso Nacional e internacional de Termodinámica.
 - **Type of contribution:** Oral presentation
 - **Authors:** A. Svobodova, P. Gamallo, A.I. Fernández, C. Barreneche
 - **Scope:** International
 - **Country:** Albacete- SPAIN
 - **Year:** 2019
 - **Publication:** Proceeding CNIT 11 - Congreso Nacional e internacional de Termodinámica 2019 **ISBN:** 978-84-09-11635-5
-
- **Title:** Nanofluids study through infrared thermography and physico-chemical characterization.
 - **Conference:** ENERSTOCK. 15th International Virtual Conference on Energy Storage.
 - **Type of contribution:** Oral presentation
 - **Authors:** A. Svobodova, A. Calderón, C. Barreneche, P. Gamallo, A.I. Fernández
 - **Scope:** International
 - **Country:** Virtual- Slovenia
 - **Year:** 2021
 - **Publication:** Proceeding Enerstock 2021- **ISBN** 978-961-6104-49-4
-



Figure A3.17-4. Certificate of oral presentation at Enerstock 2021. 15th International Virtual Conference on Energy Storage.

- **Title:** Thermophysical properties of nanofluids: a sampling study.
 - **Conference:** 3rd European Symposium on Nanofluids (ESNF) in the frame of COST CIG action NanoConvex.
 - **Type of contribution:** Oral presentation
 - **Authors:** A. Svobodova, C. Barreneche, P. Gamallo, A.I. Fernández,
 - **Scope:** International
 - **Country:** Virtual - Romania
 - **Year:** 2021

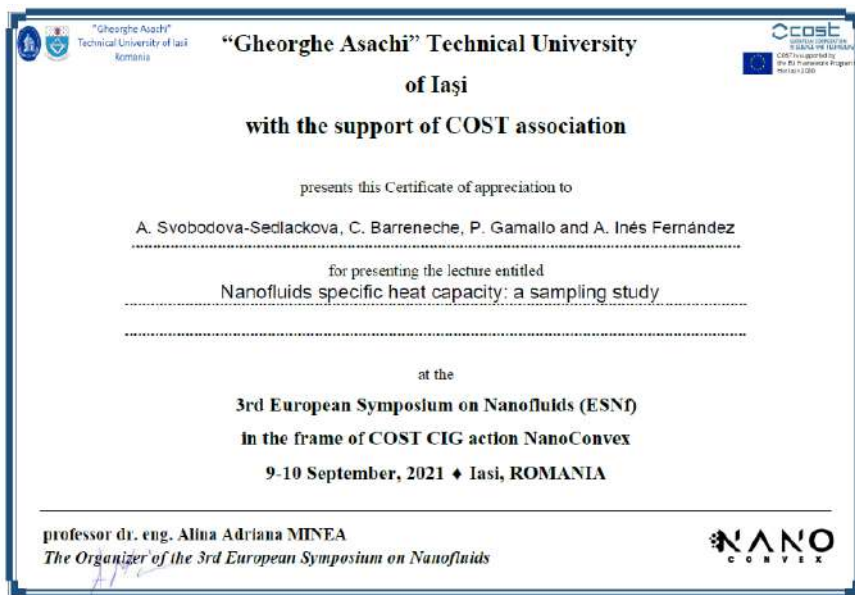


Figure A3.17-5. Certificate of oral presentation at 3rd European Symposium on Nanofluids (ESNF) in the frame of COST CIG action NanoConvex.

- **Title:** Nanofluids specific heat capacity: A sampling study.
 - **Conference:** SolarPACES 2020, the online conference on Concentrating Solar Power and Chemical Energy Systems.
 - **Type of contribution:** Poster presentation
 - **Authors:** A. Svobodova, C. Barreneche, P. Gamallo, A.I. Fernández,
 - **Scope:** International
 - **Country:** Virtual - Germany
 - **Year:** 2021

CERTIFICATE OF ATTENDANCE

This is to certify that

Ms. Adela Svobodova Sedlackova

attended SolarPACES 2021, the online conference on
Concentrating Solar Power and Chemical Energy Systems
on September 27 – October 1, 2021.

Freiburg, Germany, October 1, 2021

 **Conexio-PSE GmbH**
Emmy-Noether-Str. 2
79110 Freiburg, Germany
Tel. +49 (0) 761 769918-20
www.conexio-pse.de

SolarPACES Organizing Team

Figure A3.17-6. Certificate of oral poster presentation at the SolarPACES 2021, the online conferences on Concentrating Solar Power and Chemical Energy Systems.

17.2 Contributions in training schools

- **Title:** Molecular Dynamics Simulations Applied to Industrial Processes
 - **School:** Computational Modeling of Materials
 - **Type of contribution:** Oral presentation
 - **Authors:** A. Svobodova, P. Gamallo
 - **Scope:** International
 - **Country:** Sofia-BULGARY
 - **Year:** 2017



Faculty of Chemistry and Pharmacy
University of Sofia



Certificate of Attendance

This is to certify that

Adela Svobodova
University of Barcelona, Spain

participated in "Computational Modeling of Materials" School, 04–05 December, 2017

with oral presentation
"Molecular Dynamics Simulations Applied to Industrial Processes"



Figure A3.17-7. Certificate of oral presentation at the Computational Modeling of Materials school.

- **Title:** Molecular Dynamics Tool for TES Materials.
 - **School:** Materials for thermal energy storage - material selection, optimization & characterization
 - **Type of contribution:** Oral presentation
 - **Authors:** Svobodova, A.; Barreneche, C.; Alongo, G. Fernández, A. I., Gamallo, P.
 - **Scope:** International
 - **Country:** Barcelona-SPAIN
 - **Year:** 2019
-



This certifies that

Adela Svobodova

from

Universitat de Barcelona

**Participated in the
Training School: Materials for Thermal
Energy Storage – Material Selection,
Optimization & Characterization**

held in Barcelona, Spain, 20-21 May 2019

Signed:

Chair: Dr. Ana Inés Fernández, Universitat de Barcelona



Figure A3.17-8. Certificate of participation in the Materials for thermal energy storage- Materials selection, optimization & characterization school.

17.3 Contribution in WorkShops

- **Title:** Materials development and characterization

Type of contribution: Oral presentation

Authors: Svobodova, A.

WorkShop: WorkShop interno anual de la Red Española de almacenamiento de energía térmica- Red TES.

Carácter: Internacional

Country: Lleida- ESPAÑA

Year: 2019

- **Title:** Materials development and characterization

Type of contribution: Oral presentation

Authors: Svobodova, A.

WorkShop: WorkShop interno anual de la Red Española de almacenamiento de energía térmica- Red TES.

Carácter: National

Country: Virtual

Year: 2020

- **Title:** Materials development and characterization

Type of contribution: Oral presentation

Authors: Svobodova, A.

WorkShop: WorkShop interno anual de la Red Española de almacenamiento de energía térmica- Red TES.

Carácter: National

Country: Virtual

Year: 2021

17.4 Participation in COST Action



Subject | Participation in NANOUP TAKE COST Action CA15119

Castellón de la Plana (Spain), 8th October 2020

Dr. Leonor Hernández, as professor of the Mechanical Engineering and Building Department at University Jaume I and Action Chair of the project NANOUP TAKE Overcoming Barriers to Nanofluids Market Uptake (COST Action CA15119),

CONFIRM

That Ms. Adela Svobodova Sedlackova has been participant member of this COST Action (CA15119 - Overcoming Barriers to Nanofluids Market Uptake - NANOUP TAKE) from 1st May 2016 to 30th April 2020 (<http://www.nanouptake.eu/> and <https://www.cost.eu/actions/CA15119/#tabs|Name:overview>).

Signed:



Dr. Leonor Hernández
Chair COST Action CA15119
E-mail: lhernand@uji.es

17.5 International collaborations



From Professor Yulong Ding of University of Birmingham

March 11, 2019

To whom it may concern

Dear Madam/Sir,

From 15 January to 14 February 2019, Adela Svobodova (PhD student from Universitat de Barcelona) was working and visiting us at University of Birmingham (United Kingdom) with a short term scientific mission (STSM) of the Nanouptake Cost ACTION (No. CA151119). During this period, she characterized nanofluids we developed previously in a corrosion test.

I confirm the information she explained and reported in the STSM final report is correct and we worked together to obtain the report results during the time she was here visiting us at University of Birmingham (UK).

We thank Ms. Svobodova for the work performed and we hope to continue strength collaboration between our both institutions.

Yours truly,

A handwritten signature in black ink, appearing to be 'Y. Ding', written over a light blue grid background.

Professor Yulong Ding
Founding J. Chamberlain Chair of Chemical Engineering
Royal Academy of Engineering - Highview Power Storage Chair of Energy Storage
Founding Director of Birmingham Centre for Energy Storage
University of Birmingham
Edgbaston, Birmingham B15 2TT
UK

17.6 Other publications derived from the PhD thesis

One scientific publication is derived from the research carried out during the stay in the Birmingham Center for Energy Storage group with Professor Yulong Ding of the University of Birmingham. The research analysed solar salt based-nanofluids' thermal stability and thermophysical properties (melting temperature, enthalpy, heat capacity, thermal conductivity, and viscosity) based on solar salts after a 90-day corrosion test at 500°C in contact with different metal alloys. The corrosion test was carried out with four alloys commonly used in the CSP industry: AISI-304H, AISI 316L, AISI 1045 and INCONEL 600.

Therefore, the research analyses the most relevant properties for implementing nanofluids in CSP, their reliability over cycles and their compatibility with different metals. The results obtained from this test show that nanofluids as presented as suitable thermal fluids with improved and stable thermo-physical properties over time in working CSP conditions. Furthermore, the presence of nanoparticles in molten salts reduces the percentage of corrosion products, reducing the corrosion rates. Finally, it is shown that the 316L metal alloy has the best compatibility with nanofluids in working conditions. **Figure A3-9** shows a summary of the main results.

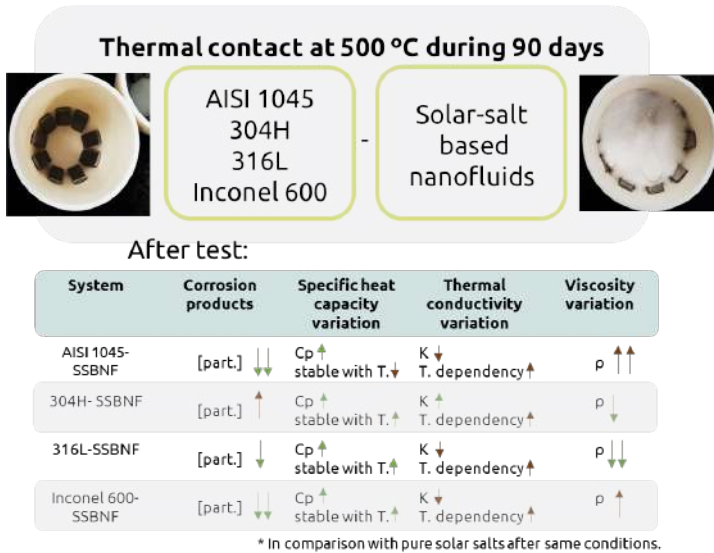


Figure A3-9. Graphical abstract of the main results obtained in the Birmingham Centre for Energy Storage.

